frontiers

RESEARCH TOPICS

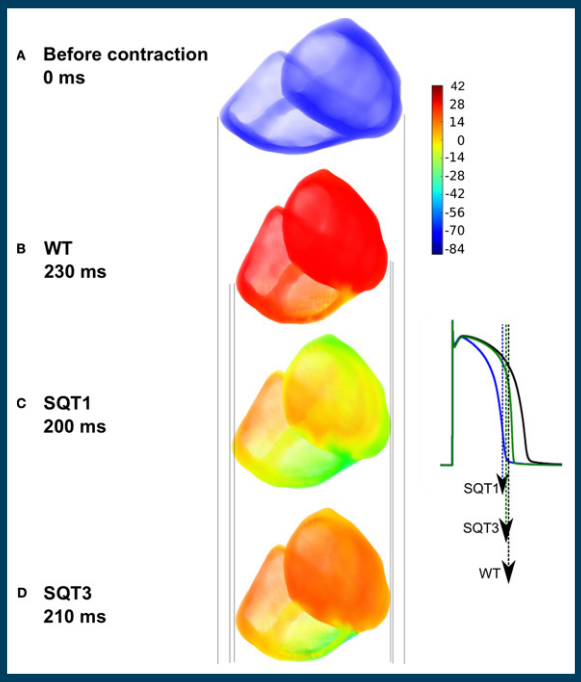

SUDDEN ARRHYTHMIC DEATH: FROM BASIC SCIENCE TO CLINICAL PRACTICE

Topic Editors
Ian N. Sabir, Christopher L.-H. Huang and Gareth D. Matthews

frontiers in PHYSIOLOGY

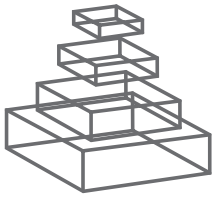

frontiers

ISSN 1664-8714
ISBN 978-2-88919-269-4
DOI 10.3389/978-2-88919-269-4

ABOUT FRONTIERS

Frontiers is more than just an open-access publisher of scholarly articles: it is a pioneering approach to the world of academia, radically improving the way scholarly research is managed. The grand vision of Frontiers is a world where all people have an equal opportunity to seek, share and generate knowledge. Frontiers provides immediate and permanent online open access to all its publications, but this alone is not enough to realize our grand goals.

FRONTIERS JOURNAL SERIES

The Frontiers Journal Series is a multi-tier and interdisciplinary set of open-access, online journals, promising a paradigm shift from the current review, selection and dissemination processes in academic publishing.
All Frontiers journals are driven by researchers for researchers; therefore, they constitute a service to the scholarly community. At the same time, the Frontiers Journal Series operates on a revolutionary invention, the tiered publishing system, initially addressing specific communities of scholars, and gradually climbing up to broader public understanding, thus serving the interests of the lay society, too.

DEDICATION TO QUALITY

Each Frontiers article is a landmark of the highest quality, thanks to genuinely collaborative interactions between authors and review editors, who include some of the world's best academicians. Research must be certified by peers before entering a stream of knowledge that may eventually reach the public - and shape society; therefore, Frontiers only applies the most rigorous and unbiased reviews.
Frontiers revolutionizes research publishing by freely delivering the most outstanding research, evaluated with no bias from both the academic and social point of view.
By applying the most advanced information technologies, Frontiers is catapulting scholarly publishing into a new generation.

WHAT ARE FRONTIERS RESEARCH TOPICS?

Frontiers Research Topics are very popular trademarks of the Frontiers Journals Series: they are collections of at least ten articles, all centered on a particular subject. With their unique mix of varied contributions from Original Research to Review Articles, Frontiers Research Topics unify the most influential researchers, the latest key findings and historical advances in a hot research area!
Find out more on how to host your own Frontiers Research Topic or contribute to one as an author by contacting the Frontiers Editorial Office: researchtopics@frontiersin.org

SUDDEN ARRHYTHMIC DEATH: FROM BASIC SCIENCE TO CLINICAL PRACTICE

Topic Editors:
Ian N. Sabir, King's College London, United Kingdom
Christopher L.-H. Huang, University of Cambridge, United Kingdom
Gareth D. Matthews, University of Cambridge, United Kingdom

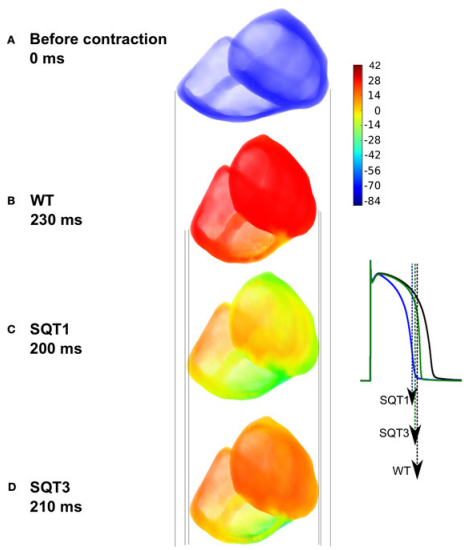

Electromechanical activation patterns in a 3D model before (A) and during contraction (B-D) in wild-type (B) human ventricles and ventricles containing mutations causing short QT syndromes types 1 (C) and 3 (D) (SQT1 and 3) showing maximum deformation at 230 ms at the onset (B) and at 200 (C) and 210 ms when repolarisation is already well advanced (D). Colour bar: coding of membrane potentials (-86 to 42 mV). Stretch-activated channel currents included in these models.
Figure taken from: Adeniran I, Hancox JC and Zhang H (2013) In silico investigation of the short QT syndrome, using human ventricle models incorporating electromechanical coupling. *Front. Physiol.* 4:166. doi: 10.3389/fphys.2013.00166

With upwards of 4.5 million deaths worldwide each year, and more than one tenth of these occurring in those with no previously documented heart disease, sudden arrhythmic death (SAD) is both a major public health burden and a highly emotive issue for society at large. Recent years have witnessed a marked expansion in our knowledge of the physiology underlying SAD, both in the context of hereditary and acquired cardiac disorders. Thanks largely to work in genetically modified animals, the growth in our understanding of mechanisms underlying arrhythmia in the hereditary channelopathies has been particularly marked.

Our growing knowledge of the fundamental mechanisms underlying SAD has so far failed to spur substantial developments in clinical practice. Despite a large body of work in both humans and animals, it remains impossible to confidently identify those at high risk of SAD, making pre-emptive therapy a challenge. What is more, with the thankful exception of the implantable cardioverter-defibrillators and pharmacological agents in very specific situations, there has been depressingly little progress in finding new and effective therapies.

This Research Topic aims to go some way towards bridging the gap between advances in basic science and the development and delivery of new therapies. It brings together original research contributions and review articles from key opinion leaders in the field, focusing on the direct clinical implications of the basic science research now and in the future.

Table of Contents

frontiers in PHYSIOLOGY

EDITORIAL
published: 25 November 2013
doi: 10.3389/fphys.2013.00339

Sudden arrhythmic death: from basic science to clinical practice

Ian N. Sabir[1], Gareth D. K. Matthews[2] and Christopher L.-H. Huang[2,3]*

[1] *The Rayne Institute, St. Thomas' Hospital, London, UK*
[2] *Physiological Laboratory, University of Cambridge, Cambridge, UK*
[3] *Department of Biochemistry, University of Cambridge, Cambridge, UK*
**Correspondence: clh11@cam.ac.uk*

Edited by:
Ruben Coronel, Academic Medical Center, Netherlands

Keywords: sudden cardiac death, ventricular arrhythmia, ion channels, action potentials, conduction velocity, re-entrant substrate, Brugada Syndrome, catecholaminergic polymorphic ventricular tachycardia

Sudden cardiac death refers to unexpected death attributable to a cardiac cause occurring within 1 h of the onset of symptoms (NICE, 2006). It often results from cardiac arrhythmias and is a major worldwide cause of morbidity and mortality. Arrhythmias account for 180,000 to 250,000 deaths per year in the United States and ∼70,000 deaths per year in the United Kingdom (NICE, 2006; Chugh et al., 2008). These commonly present as ventricular fibrillation often preceded by ventricular tachycardia (Turakhia and Tseng, 2007). Cardiac arrhythmias most frequently result from underlying ischaemic heart disease (Behr et al., 2003). However, ∼4% may arise from ion channel abnormalities (Tung et al., 1994; Martin et al., 2012) with their own implications for management (Martin et al., 2011). In all events, cardiac arrhythmias follow disruption of the normal cell excitation and recovery sequence propagating through successive cardiac regions. A sequence of reviews and original articles in *Frontiers in Cardiac Electrophysiology* together survey genetic, biophysical, physiological and modeling studies bearing upon mechanisms of and possible translational implications for ventricular arrhythmia and sudden cardiac death, referring to other arrhythmic situations, particularly atrial fibrillation, where these throw light upon fundamental mechanisms.

Kapur and Macrae (2013) review *developmental events* regulating appearance of molecules and structures underlying normal automaticity and conduction responsible for atrial rhythm, providing a necessary background for normal ventricular activation. Jagu et al. (2013) then outline and illustrate outcomes of *genetic studies* of biochemical processes underlying relationships between genetic background and protein expression whose alterations lead to arrhythmic tendency. Ion channel expression depends upon a sequence of processes beginning with DNA *transcription* into mRNA and its regulation by promoter sites. Persistence of the resulting mRNA then depends upon its stability and the presence or absence of mRNA splicing. *Translation* from mRNA into protein is potentially regulated by microRNAs and alternative translation phenomena. Finally, *expression* of synthesized protein depends upon its assembly, post-translational modification and trafficking to its normal membrane site.

Nielsen et al. (2013) further explore uncertainties in *relationships between genetic change and their functional consequences* specifically for Brugada Syndrome (BrS). This condition is associated with hundreds of variants in 17 genes, most commonly with *SCN5A* mutations implicating cardiac voltage-gated sodium channels. However, ∼70% of BrS cases cannot currently be explained genetically. Clarification of these relationships would enhance genetic risk stratification taking advantage of multi-gene Next Generation Sequencing. However, Gütter et al. (2013) throw biophysical light on uncertainties in the relationship between genetic and functional properties: voltage-clamp investigations revealed that only one out of three mutant channels associated with clinical long QT syndrome type 3 (LQT3) and three out of six mutant channels associated with BrS showed functional abnormalities in a series of N-terminal, human hNav1.5, mutations.

Nevertheless Nielsen et al. (2013) associate more severe BrS disease phenotypes with large as opposed to small reductions in I_{Na}, whose most obvious *biophysical effect* is to reduce action potential conduction velocity, producing potentially pro-arrhythmic *re-entrant substrate*. King et al. (2013) review factors affecting cardiac conduction velocity. The underlying local circuit current flows between myocytes depend upon not only on fast Na^+ current, but also axial resistance and cellular excitability. These could alter with impaired Na^+ channel and gap junction function, and altered tissue geometry following fibrotic change accompanying pathophysiological processes. Such *substrate* may accompany arrhythmic situations particularly with the *triggering* events typically associated with disrupted Ca^{2+} homeostasis exemplified by the altered sarcoplasmic reticular Ca^{2+} release through RyR2-Ca^{2+} release channels in catecholaminergic polymorphic ventricular tachycardia. Zhang et al. (2013) summarize recent studies associating *RyR2* abnormalities with atrial in addition to ventricular arrhythmias. They further point out that homozygotic *RyR2-P2328S* hearts show reduced conduction velocities potentially generating arrhythmic substrate, in addition to delayed afterdepolarization and ectopic action potential firing.

Computational studies permit biophysical information to be compiled into theoretical reconstructions of *in vivo physiological changes* resulting from a primary loss or gain of function. Thus, carbon monoxide (CO) is produced by a number of different mammalian tissues and exerts significant cardiovascular effects. Computational studies (Trenor et al., 2013) relate known changes in CO-induced alterations in ventricular slowly-inactivating ranolazine-sensitive late Na^+, and Ca^{2+}, channel, activity, to potentially pro-arrhythmic after-depolarization-like rhythm disturbances illustrating important elements of their underlying causes. Computational studies also illuminate *in vivo*

physiological outcomes even where primary experimental systems are not available. Adeniran et al. (2013) apply these to the relatively rare, but well-defined clinical short QT syndrome, associated with accelerated ventricular repolarization, arrhythmias and sudden cardiac death. Few experimental SQT1 and SQT3 models, involving altered K^+ or Ca^{2+} channel function are currently available. Nevertheless, application of the ten Tusscher and Panfilov (TP) human ventricular single cell model allowed *in silico* exploration of the consequences of this condition for Ca^{2+} release and mechanical output. Combined with cable theory, this further yielded whole organ functional reconstructions. This provided testable predictions implicating stretch-activated current in contractile function. Finally, an original contribution by Finlay et al. (2013) then successfully apply a modeling approach based on one-dimensional cable theory to describe human restitution dynamics incorporating both conduction velocity restitution and action potential restitution, for the first time in man.

Finally, discussions of possible *clinical translational developments* begin with problems and methodologies associated with diagnosis of sudden cardiac death risk. Vyas and Lambiase (2013) evaluate currently available *screening strategies* for sudden cardiac death risk in sudden arrhythmic death syndrome families, looking forward to roles for molecular autopsy and genetic testing, and potential future applications of stem cell-based diagnostic strategies. The first of two preliminary *clinical studies* report findings relating to sphingolipid levels as novel markers for early detection of human myocardial ischaemic injury predisposing to malignant ventricular arrhythmias (Egom et al., 2013). A report in chronic kidney disease patients, in which both early repolarization and sudden cardiac death are common, nevertheless did not associate early repolarization with increased 1-year mortality or entry onto dialysis programs (Hajhosseiny et al., 2013).

This collection of articles thus overviews current knowledge bearing on experimental studies of sudden cardiac death and its associated arrhythmias, and possible translational insights concerning clinical prevention and management.

REFERENCES

Adeniran, I., Hancox, J. C., and Zhang, H. (2013). *In silico* investigation of the short QT syndrome, using human ventricle models incorporating electromechanical coupling. *Front. Physiol.* 4:166. doi: 10.3389/fphys.2013.00166

Behr, E., Wood, D. A., Wright, M., Syrris, P., Sheppard, M. N., Casey, A., et al. (2003). Sudden Arrhythmic Death Syndrome Steering Group. Cardiological assessment of first-degree relatives in sudden arrhythmic death syndrome. *Lancet* 362, 1457–1459.

Chugh, S. S., Reinier, K., Teodorescu, C., Evanado, A., Kehr, E., Al Samara, M., et al. (2008). Epidemiology of sudden cardiac death: clinical and research implications. *Prog. Cardiovasc. Dis.* 51, 213–228. doi: 10.1016/j.pcad.2008.06.003

Egom, E. E., Mamas, M. A., Chacko, S., Stringer, S. E., Charlton-Menys, V., El-Omar, M., et al. (2013). Serum sphingolipids level as a novel potential marker for early detection of human myocardial ischaemic injury. *Front. Physiol.* 4:130. doi: 10.3389/fphys.2013.00130

Finlay, M. C., Xu, L., Taggart, P., Hanson, B., and Lambiase, P. D. (2013). Bridging the gap between computation and clinical biology: validation of cable theory in humans. *Front. Physiol.* 4:213. doi: 10.3389/fphys.2013.00213

Gütter, C., Benndorf, K., and Zimmer, T. (2013). Characterization of N-terminally mutated cardiac Na^+ channels associated with long QT syndrome 3 and Brugada syndrome. *Front. Physiol.* 4:153. doi: 10.3389/fphys.2013.00153

Hajhosseiny, R., Rajani, R., Khavandi, K., Sebag, F. A., Mashayekhi, S., Wright, M., et al. (2013). The prevalence of electrocardiographic early repolarization in an adult cohort with chronic kidney disease and its impact upon all-cause mortality and progression to dialysis. *Front. Physiol.* 4:127. doi: 10.3389/fphys.2013.00127

Jagu, B., Charpentier, F., and Toumaniantz, G. (2013). Identifying potential functional impact of mutations and polymorphisms: linking heart failure, increased risk of arrhythmias and sudden cardiac death. *Front. Physiol.* 4:254. doi: 10.3389/fphys.2013.00254

Kapur, S., and Macrae, C. A. (2013). The developmental basis of adult arrhythmia: atrial fibrillation as a paradigm. *Front. Physiol.* 4:221. doi: 10.3389/fphys.2013.00221

King, J. H., Huang, C. L.-H., and Fraser, J. A. (2013). Determinants of myocardial conduction velocity: implications for arrhythmogenesis. *Front. Physiol.* 4:154. doi: 10.3389/fphys.2013.00154

Martin, C. A., Huang, C. L.-H., and Matthews, G. D. (2011). Recent developments in the management of patients at risk for sudden cardiac death. *Postgrad. Med.* 123, 84–94. doi: 10.3810/pgm.2011.03.2266

Martin, C. A., Matthews, G. D., and Huang, C. L.-H. (2012). Sudden cardiac death and inherited channelopathy: the basic electrophysiology of the myocyte and myocardium in ion channel disease. *Heart* 98, 536–543. doi: 10.1136/heartjnl-2011-300953

National Institute for Health and Clinical Excellence (NICE). (2006). *Arrhythmia - implantable cardioverter defibrillators (ICDs) (review)*. London: Technical Appraisals. TA95. Available online at: http://guidance.nice.org.uk/TA95.

Nielsen, M. W., Holst, A. G., Olesen, S. P., and Olesen, M. S. (2013). The genetic component of Brugada syndrome. *Front. Physiol.* 4:179. doi: 10.3389/fphys.2013.00179

Trenor, B., Cardona, K., Saiz, J., Rajamani, S., Belardinelli, L., and Giles, W. R. (2013). Carbon monoxide effects on human ventricle action potential assessed by mathematical simulations. *Front. Physiol.* 4:282. doi: 10.3389/fphys.2013.00282

Tung, R. T., Shen, W. K., Hammill, S. C., and Gersh, B. J. (1994). Idiopathic ventricular fibrillation in out-of-hospital cardiac arrest survivors. *Pacing Clin. Electrophysiol.* 17, 1405–1412. doi: 10.1111/j.1540-8159.1994.tb02460.x

Turakhia, M., and Tseng, Z. H. (2007). Sudden cardiac death: epidemiology, mechanisms, and therapy. *Curr. Probl. Cardiol.* 32, 501–546. doi: 10.1016/j.cpcardiol.2007.05.002

Vyas, V., and Lambiase, P. D. (2013). The investigation of sudden arrhythmic death syndrome (SADS)-the current approach to family screening and the future role of genomics and stem cell technology. *Front. Physiol.* 4:199. doi: 10.3389/fphys.2013.00199

Zhang, Y., Matthews, G. D., Lei, M., and Huang, C. L.-H. (2013), Abnormal Ca^{2+} homeostasis, atrial arrhythmogenesis, and sinus node dysfunction in murine hearts modeling RyR2 modification. *Front. Physiol.* 4:150. doi: 10.3389/fphys.2013.00150

Received: 30 October 2013; accepted: 03 November 2013; published online: 25 November 2013.

*Citation: Sabir IN, Matthews GDK and Huang CL-H (2013) Sudden arrhythmic death: from basic science to clinical practice. Front. Physiol. **4**:339. doi: 10.3389/fphys.2013.00339*

This article was submitted to Cardiac Electrophysiology, a section of the journal Frontiers in Physiology.

frontiers in
PHYSIOLOGY

REVIEW ARTICLE
published: 12 September 2013
doi: 10.3389/fphys.2013.00221

The developmental basis of adult arrhythmia: atrial fibrillation as a paradigm

Sunil Kapur and Calum A. MacRae*

Medicine, Cardiovascular Division, Brigham and Women's Hospital and Harvard Medical School, Boston, MA, USA

Edited by:
Ian N. Sabir, King's College London, UK

Reviewed by:
Bas Boukens, Academic Medical Center, Netherlands
Gareth D. K. Matthews, University of Cambridge, UK
Christopher Huang, University of Cambridge, UK

****Correspondence:***
Calum A. MacRae, Brigham and Women's Hospital, 75 Francis Street, Boston, MA 02115, USA
e-mail: camacrae@bics.bwh.harvard.edu

Normal cardiac rhythm is one of the most fundamental physiologic phenomena, emerging early in the establishment of the vertebrate body plan. The developmental pathways underlying the patterning and maintenance of stable cardiac electrophysiology must be extremely robust, but are only now beginning to be unraveled. The step-wise emergence of automaticity, AV delay and sequential conduction are each tightly regulated and perturbations of these patterning events is now known to play an integral role in pediatric and adult cardiac arrhythmias. Electrophysiologic patterning within individual cardiac chambers is subject to exquisite control and is influenced by early physiology superimposed on the underlying gene networks that regulate cardiogenesis. As additional cell populations migrate to the developing heart these too bring further complexity to the organ, as it adapts to the dynamic requirements of a growing organism. A comprehensive understanding of the developmental basis of normal rhythm will inform not only the mechanisms of inherited arrhythmias, but also the differential regional propensities of the adult heart to acquired arrhythmias. In this review we use atrial fibrillation as a generalizable example where the various factors are perhaps best understood.

Keywords: arrhythmia, developmental biology, genetics, electrophysiology, remodeling

INTRODUCTION

Atrial fibrillation (AF) is the most common cardiac arrhythmia (Go et al., 2001) and is associated with substantial morbidity and mortality even in paroxysmal forms (Benjamin et al., 1998). AF is a central phenotype at the nexus of a broad spectrum of cardiovascular syndromes including; hypertension, congestive heart failure (CHF), and thromboembolism. AF is typically associated with different forms of structural heart disease, ischemic or other cardiomyopathies and systemic disorders, so that the mechanism of the arrhythmia has been variously attributed to elevated atrial pressures, chronic atrial fibrosis or inflammatory stimuli (Nattel et al., 2000). However, not unlike many other common clinical arrhythmic phenotypes, it has proven remarkably difficult to discriminate primary from secondary phenomena in the causal chain. In the last few years a confluence of basic and translational research has begun to define a role for a primary underlying diathesis in many, if not all, forms of AF (Ellinor et al., 2008; Postma et al., 2009). In this review we will summarize recent data in this area, highlighting developmental aspects of the biology of AF and the relationship to downstream biology including ventricular dysfunction that predisposes to other arrhythmias and to sudden death. We will focus on the importance of exploring the basis of arrhythmias using approaches that not only encompass all of the native biological context, but that also allow the characterization of the very earliest and most upstream pathophysiologic events.

A PRIMARY DIATHESIS

While the mechanism of sustained AF is unclear, many potential factors have been proposed. Three models have been considered for nearly 100 years (Garrey, 1924), though the precise relationship of each of these conceptual frameworks to human AF is still an area of investigation. The focal mechanism theory with fibrillatory conduction stands on the notion that AF is provoked by the rapid firing of single or multiple ectopic foci (Waldo, 2003), and also suggests a role for continued ectopic firing in the maintenance of AF. This theory has gained recent support from clinical observations (Haissaguerre et al., 1998). The single circuit re-entry theory of AF assumes the presence of a single dominant reentry circuit—a "mother rotor" with the fragmentation of emanating waves in the heterogeneous electrical substrate of normal atrial tissue. The multiple wavelet theory of AF assumes the presence of multiple reentry circuits with randomly propagating wavefronts that must find receptive tissue in order to persist. Shortening of the refractory period of atrial myocytes and slowing of conduction velocities—central features of the electrical remodeling seen with AF—both may help to stabilize the arrhythmia by decreasing circuit size (Ausma et al., 2001). Clearly these three mechanistic models are not mutually exclusive and each may be applicable to certain subgroups of AF patients or may coexist in a single subject at various stages in the pathogenesis of AF (Patton et al., 2005).

There are numerous animal models of AF, each of which capture some aspects of the underlying biology (Milan and MacRae, 2005). However, most AF models, if not all, require some continued extrinsic stimulus for the maintenance of the arrhythmia. The extrinsic stimuli may include vagal stimulation, continuous atrial pacing, or combinations of different manipulations. Irrespective of the stimulus, on withdrawal there is almost always

reversion to normal sinus rhythm, usually within hours. Together these observations suggest that the spontaneous paroxysmal or persistent AF observed in susceptible humans is the result of a fundamental predisposition to the arrhythmia upon which acquired or environmental factors are layered. While a large number of experimental studies have explored the mechanisms of both the onset and maintenance of the arrhythmia over the last few decades, there remains little understanding of the biologic basis of this presumed underlying primary diathesis. A fundamental premise of this review is that each of the known mechanisms operant in later stages of AF may be influenced by developmental pathways, such that this apparently late onset arrhythmia may be conditioned by intrinsic differences in the excitability of the pulmonic veins, the coupling patterns of atrial myocytes, the electrophysiologic properties of individual cardiomyocytes or any other contributory factor determined during the earliest stages of cardiogenesis.

Further evidence in support of a primary predisposition to AF has emerged from studies of the genetics of different forms of the arrhythmia. Traditionally, AF has not been considered a genetic condition. However, a number of recent studies have demonstrated that some forms of the arrhythmia, and in particular lone AF, have a substantial genetic basis (Ellinor et al., 2005, 2008; Sinner et al., 2011). These findings raise the possibility that, in at least a subset of AF, susceptibility to the arrhythmia is a function of intrinsic biologic differences in the hearts of affected individuals.

Together, these data supporting an intrinsic predisposition toward AF infer that our understanding of the arrhythmia is likely to benefit from exploration of the developmental biology of atrial electrophysiology. This approach is particularly powerful in the context where the known effects of the arrhythmia itself on atrial physiology and cell biology-so called atrial remodeling-obscure the distinction between cause and effect. The opportunity to define the earliest events in AF, before these have been contaminated by environmental modifiers or the remodeling associated with even short-lived episodes of the arrhythmia itself, offers the opportunity for unique insights into the potential biologic mechanisms of spontaneous or sustained arrhythmia, as well as the complex links between this "benign" atrial disorder and CHF or stroke.

MODERN CLINICAL INSIGHTS

Seminal clinical studies by Haissaguerre et al. (1998) demonstrated that in a subset of paroxysmal AF may be initiated by repetitive rapid electrical activity originating from the pulmonary veins (PVs), and that ablation of such foci might "eliminate" paroxysmal forms of the arrhythmia. Post-mortem anatomical studies showed that PV myocardial sleeves were present in 100% of patients with AF, whereas similar muscle tissue was observed in only 85% of those without AF (Hassink et al., 2003). In addition, patients with AF had significantly longer muscle sleeves with considerably thicker PV myocardial tissue. In some instances arrhythmogenicity could only be localized to these areas of thickening (Guerra et al., 2003). While in most cases the electrical origins of paroxysmal AF are found in the myocardial sleeves clothing the pulmonary veins (Nattel, 2003), additional sites for ectopic automaticity are increasingly recognized. For example, triggered and automatic activity can be induced in the muscle sleeves of the canine coronary sinus, but not in the atrial cells. Other investigators have noted that other venous sites, such as the superior vena cava and the vein of Marshall, can also serve as the origin of rapid ectopy driving AF. It is known that the thoracic veins activate at shorter activation cycle lengths than the atria during sustained AF in dogs (Wu et al., 2001). These findings suggest that rapid activity from thoracic veins might be responsible for the perpetuation of non-paroxysmal AF (Chen et al., 2002a). Compatible with this hypothesis, many clinical studies have shown that RF ablation or isolation of thoracic veins may result in the elimination at least for some time of chronic AF in humans. These human data suggest that AF may be the result of perturbation of pathways that normally suppress automaticity in veins connecting to the atria or prevent conduction of electrical impulses from the veins to the atria.

PATTERNING THE ATRIUM AND ITS BOUNDARIES

THE ATRIA FORM FROM DISTINCTIVE POPULATIONS OF CARDIOMYOCYTES

The four-chambered mammalian heart develops from a simple linear tube. Embryologic studies have shown that the complicated looping process of the heart tube brings together the essential parts of the sino-atrial and primary ring myocardium which are the embryonic precursors of definitive conduction system (van den Berg et al., 2009). The myocardium of the original heart tube is only part of the eventual heart, as further myocardium is subsequently added to its poles. A hallmark feature of the primary myocardium is the expression of connexins (Cx) 30.2 and 45, which form low-conductance gap-junction channels. The transcriptional repressor genes Tbx2 and Tbx3 maintain the phenotype of primary myocardium (Habets et al., 2002). In contrast, chamber myocardium, as it is specified, expresses Cx40 and Cx43, which form high-conductance gap-junction channels, and the α-subunit of the sodium channels Nav 1.5, encoded by *Scn5a*, providing the atrial compartment with the excitability necessary for high conduction velocities. During atrial septation the pulmonary orifice is positioned in the left atrium, and the smooth-walled dorsal atrial wall forms from cardiac precursor cells recruited from the pulmonary mesenchyme, which express the transcription factors Nkx2-5 and Isl1 (Mommersteeg et al., 2007a; Snarr et al., 2007). As organogenesis progresses the pulmonary venous component becomes incorporated into the roof of the left atrium, such that each of the four PVs, with short myocardial sleeves of various lengths, opens at a corner of the atrial back wall. This integration of venous and atrial cells appears to be the result of highly conserved guidance cues paralleling those in the central and peripheral nervous systems. From the outset, the so-called pulmonary myocardium expresses *Cx40* as observed in working myocardium, although it does not express *Nppa*, the gene encoding atrial natriuretic peptide. The myocardium that is added at the systemic part of the venous pole, or sinus venosus myocardium, is derived from Nkx2-5-negative, Isl1-negative, and Tbx18-positive mesenchymal cardiac precursors (Christoffels et al., 2006). This sinus

venosus myocardium starts to form at day 9.5 of mouse development and initially is Cx40-negative, but expresses the pacemaker channel Hcn4 and the transcriptional repressor Tbx3 (Hoogaars et al., 2004). Ultimately, the sinus myocardium matures into atrial working myocardium, with the exception of the region where the sinus node is formed, which remains Tbx3-positive, Nkx2-5-negative, Cx40-negative, and Hcn4-positive. Notably, these data suggest that distinctive cardiomyocyte populations with discrete automaticity and excitability, as well as coupling characteristics are determined at the boundaries of the cardiac chambers under the regulation of combinatorial patterns of transcription factor expression. Thus, several regions, including the orifice of the coronary sinus, the terminal crest, and the lower rim of the right atrium, are functionally distinct from the remainder of the atrium and represent the core physiologic and anatomical substrate for specific atrial arrhythmias. These same myocardial regions are often involved in structural congenital heart disease, explaining to some extent the frequent occurrence of atrial flutter and AF in these disorders. Whether this heterogeneity extends into the chamber myocardium remains to be seen, but the very same signaling pathways are deployed in the complex patterning of neurogenesis suggesting this is likely.

OTHER CELL TYPES CONTRIBUTE TO ATRIAL PHYSIOLOGY

Embryological evidence also supports the participation of other cell types in genesis of normal atria. Among these are cells with features of specialized conduction system within PV myocardium. Investigators have noted the presence of spontaneously depolarizing cells in the PVs of dogs (Chen et al., 2000). Recently, "P cells," normally found in the AV and SA node, have also been localized to the PVs (Perez-Lugones et al., 2003; Wit and Boyden, 2007). These were found in substantially greater numbers near the atrial ostia. The same study also identified Purkinje and transitional cells in PVs. The current belief is that spontaneous depolarization in P cells may lead to the production of electrical impulses that are propagated to the left atrium through Purkinje-like cells (Chen and Yeh, 2003).

Studies have also demonstrated that cells with gene expression features consistent with developing cardiac conduction system could be found in PVs prior to birth (Jongbloed et al., 2004). In a CCS-lacZ transgenic line, LacZ positive cardiomyocytes were observed in the PVs (Rentschler et al., 2001). The heterogeneous presence of CCS-lacZ expression was also noted in other tissue involved in atrial arrhythmias, including Bachmann's bundle (Perez-Lugones et al., 2003).

The situation is further complicated by the identification of cells resembling the so-called interstitial cells of Cajal in the muscular pulmonary venous sleeves from at least some human subjects (Morel et al., 2008). Although their exact function is unclear, correlation with phenotypically similar cells in the gut, as well as direct observations, leave little doubt that these cells are capable of providing a pacemaking function (Thuneberg, 1982; Sanders, 1996). Unlike the situation in the heart, or in the renal tract (Gosling and Dixon, 1972), the interstitial cells within the gut are not grouped together into "nodes," but rather intermingle with the myocytes in the intestinal wall. Similarly, the interstitial cells in the PVs appear to comingle with the myocytes making up venous sleeves. Their potential pacemaking function is demonstrated by their reactivity with HCN4, a marker for the hyperpolarization-activated and cyclic nucleotide-sensitive ionic current.

Recent seminal work has defined pigmented cells within the murine heart, though their function remains unknown (Mjaatvedt et al., 2005). Interestingly, dermal melanocytes and melanoma lines do express voltage-dependent currents and under conditions of increased oxidative stress some ionic currents are modified to promote cellular excitability (Levin et al., 2009). The melanin synthesis enzyme dopachrome tautomerase (Dct) contributes to, but is not required for, melanin synthesis in dermal melanocytes by catalyzing the conversion of L-dopachrome to 5,6-dihydroxyindole-2-carboxylic acid which is thought be an intermediate in the eumelanin synthesis pathway. Furthermore, Dct is important for intracellular calcium regulation; in fact, eumelanin binds calcium with an affinity similar to calmodulin (Bush and Simon, 2007). Studies have shown a unique Dct-expressing cell population within murine and human hearts is specifically located around the pulmonary veins, atria, and atrioventricular canal. Adult mice lacking Dct displayed normal cardiac development but an increased susceptibility to atrial arrhythmias. Cultured primary cardiac melanocyte-like cells were excitable, and those lacking Dct displayed prolonged repolarization with early afterdepolarizations. Furthermore, mice with mutations in the tyrosine kinase receptor Kit lacked cardiac melanocyte-like cells and did not develop atrial arrhythmias in the absence of Dct. These data suggest that dysfunction of melanocyte-like cells in the atrium and pulmonary veins may contribute to atrial arrhythmias (Levin et al., 2009).

Neuronal contributions to the final developmental cellular biology of the atria are complex. The intrinsic nervous system of the heart is incompletely characterized and its role in AF remains largely speculative (Huang et al., 1996). However, there is no doubt that these cells and the associated autonomic ganglia play a central role in the control of atrial excitability later in life (Verrier and Antzelevitch, 2004). The emerging links between autonomic innervation and AF with therapeutic manipulation through radiofrequency ablation, both of cardiac and renal plexuses, suggest that there is much still to be learned (Pokushalov et al., 2012).

SPECIFICATION OF CELLULAR FUNCTION

Foci of abnormal automaticity are the result of either (1) an abnormal pacemaker discharging spontaneously in the absence of an initiating stimulation or (2) automatic activity triggered by an initiating stimulus related to oscillating after-depolarization or early after-depolarization. The venous-atrial boundary is also a potential nidus for abnormal electrical activity (Postma et al., 2009). Structurally, the transition from atrial to venous walls is gradual as the left atrial myocardial sleeves overlap with smooth muscle of the venous myocardium (Ho et al., 1999). The muscle fibers in pulmonary veins are usually orientated perpendicularly to the blood flow. Such an arrangement, together with increased anisotropy due to ageing-induced fibrosis, may facilitate re-entry

within the pulmonary veins. Further, the cellular properties of PV cardiomyocytes, such as shorter action potential and lower phase-0 upstroke velocities than in the left atrium, favor re-entry (Ehrlich et al., 2003). Quantitative mapping analysis of the left atrial-PV ostium junction indicates impulse conduction block or delay at sites noted for the presence of connective tissue barriers. The fact that connective tissue septae separating myocyte tissue islands are much more common in the PVs as compared with the atria may contribute to the role of PV ectopy in arrhythmogenesis (Hamabe et al., 2003).

Beyond the ectopic development of pacemaker cells, perturbation of the electrophysiologic specification of PV cardiomyocytes may occur leading to intrinsic abnormalities of automaticity. Normal PV myocytes may display spontaneous phase 4 depolarizations, along with slowed phase 0 rates, both characteristic features of pacemaker cells in the SA node (Chen et al., 2000). The PV myocyte membranes have a much lower density of I_{K1}-channels as compared with typical atrial tissue (Chen et al., 2001). SA nodal cells also have a characteristic I_f-current, whose presence was recently demonstrated within PV myocytes (Chen et al., 2001), allowing for pacemaker behavior in PV cells. Another possibly important finding was the presence of I_{Ca2+-t}-channels within PV myocytes (Chen et al., 2004). The Ca^{2+}-current from these channels has been shown to aid in the production of spontaneous depolarizations by causing the release of Ca^{2+} from the sarcoplasmic reticulum at low voltages (−60 mV), facilitating pacemaker activity. These channels may also increase the plateau phase of action potentials, raising the possibility of EADs. Application of nickel, a rather non-specific inhibitor of I_{Ca2+-t}-channels, to PV tissue drastically reduced both triggered activity and automaticity in PV myocytes (Huser et al., 2000).

As noted, there is quite extensive innervation of the PVs and atria (Gardner and O'Rahilly, 1976). Functionally, heart rate variability analyses note that sympathovagal imbalance is present before the onset of paroxysmal AF episodes. The importance of autonomic innervation is further supported by animal experiments and recent clinical studies showing that vagal denervation enhances the efficacy of circumferential pulmonary vein ablation in preventing AF recurrence (Pokushalov et al., 2012). ANS activation facilitates early afterdepolarization and triggered activity by simultaneously prolonging the intracellular calcium [Ca(i)] transient (sympathetic effect) and shortening the action potential duration (parasympathetic effect) (Chen and Tan, 2007). Beyond the immediate functional implications, it is possible that autonomic innervation has trophic effects on cardiac development (Postma et al., 2009).

PATTERNING OF CELLULAR CONNECTIONS

An interesting potential connection between left-right asymmetry and AF has recently emerged though studies of developmental biology and the human genetics of AF. Left-right asymmetric morphogenesis is initiated in the presomitic embryo and is mediated through the Nodal signaling pathway a major downstream effector of which is the Pitx2 homeobox gene (Hamada et al., 2002). One isoform of this protein, Pitx2c, is required for left–right patterning of the visceral organs, including the atria and systemic venous return of the heart (Franco and Campione, 2003). Human genetic studies have identified sequence variants on chromosome 4q25, close to the *Pitx2* gene that are strongly associated with increased risk for AF, making this a likely candidate for the predisposition to AF at this locus (Gudbjartsson et al., 2007). PITX2 is known to act in cardiac development by directing asymmetric morphogenesis of the heart (Gudbjartsson et al., 2007). Knockout models of PITX2 in mice have been shown to derepress the normal inhibition of sinoatrial node formation in the left atrium (Mommersteeg et al., 2007b). PITX2 was also demonstrated to be necessary for the development of the pulmonary myocardium (Mommersteeg et al., 2007a). Pitx2c-deficient mice do not develop a pulmonary myocardial sleeve because they fail to form the initial pulmonary myocardial cells (Mommersteeg et al., 2007a).

From the outset, pulmonary myocardium expresses the transcription factor Nkx2-5 and its target gap-junction gene Cx40. Notably, when Nkx2-5 protein levels were lowered experimentally, the pulmonary myocardium transitioned to a Cx40-negative, Hcn4-positive phenotype, resembling sinoatrial nodal-like cells. Thus, under a reduced dose of a single transcription factor, Nkx2-5, the pulmonary myocardium converts more easily into a nodal phenotype, suggesting that subtle genetic variation between individuals in Nkx2-5 dosage could be an important contributing trigger to the development of AF (Postma et al., 2009). Indeed, some mutations in Nkx2-5 are suggested to be linked to AF (Gutierrez-Roelens et al., 2006), though much as with the Pitx2 story, the formal causal connection with human disease is not complete. Taken together, variations in the regulatory sequences of transcription factors specifying the final physiologic characteristics of cardiomyocytes throughout the entire cardiac anlagen are prime candidates for further research into the underlying cause of AF.

Other developmental pathways have also been implicated in the patterning of cardiomyocyte connections including the Wnt family of developmental signaling molecules. These secreted proteins regulate crucial aspects of development, including cell-fate specification, proliferation, survival, migration, and adhesion (Nusse, 2005). The effects of canonical Wnt/β-catenin signaling on cardiac neural crest cells may be mediated by both the transcriptional upregulation and functional activation of *Pitx2* (Malekar et al., 2010). Again the picture that is emerging is one of complex and coordinated specification of cellular physiology and cellular connectivity, with the potential for additional functional remodeling during development and beyond. Extensive systems-level studies will be necessary to define the gene networks and the functional inputs responsible for the final atrial phenotypes in health and disease (Brundel et al., 2002).

PERPETUATION OF AF: INTRINSIC DIFFERENCES IN PV AND ATRIAL SUBSTRATE

While an active focus may be needed to initiate AF, re-entrant circuits are needed to maintain it. Persistent AF is characterized by the presence of re-entry pathways. Shorter refractory periods facilitate the maintenance of AF by increasing the prospect for re-entry. Cardiomyocytes of PVs exhibit varying refractory

periods that may lend themselves well to the development of AF (Jais et al., 2002; Tada et al., 2002), but the electrophysiologic basis of these altered refractory periods in the PV is not fully accounted for. PV cell membranes exhibit an increased I_{Ks}- and I_{Kr}-current densities, as well as reduced I_{Ca2+}-currents, when compared to neighboring left atrial myocytes (Ehrlich et al., 2003). In addition, the cognate channel proteins were present at greater concentrations within PV myocytes (Melnyk et al., 2005). These observations suggest that individuals with inherited variations in PV myocyte channel protein expression or function may be predisposed to AF.

There is robust genetic evidence that primary gain-of function mutations in ion channels can mediate increased I_{Ks}, resulting in familial AF (Chen et al., 2003a). From a four-generation family with AF, the investigators were able to map the disease locus to a 12-megabase region on the short arm of chromosome 11. The KCNQ1 gene was located within this region and sequencing of the gene revealed a serine to glycine missense mutation at position 140 (S140G) in affected family members. The S140G mutation is located in the first transmembrane-spanning segment at the outer edges of the voltage-sensing domain and far from the pore-forming region of the potassium channel structure (Schenzer et al., 2005). Unlike the mutations in KCNQ1 associated with the long QT syndrome, which typically result in a loss of channel function, the S140G mutation resulted in a gain of channel function. In cultured cells, expression of the S140G mutant channel resulted in dramatically enhanced potassium channel currents and markedly altered potassium channel gating kinetics, changes that would be predicted to reduce the probability of fibrillatory conduction. These findings, and the abnormal prolongation of ventricular repolarization observed in these same individuals, suggest that there may be disparate effects of the gain of function mutations on atrial and ventricular physiology, possibly through differential interactions with distinct partner proteins or through other unknown mechanisms. In addition, both sympathetic and vagal stimulation may cause reductions in effective refractory period (ERP) (Takei et al., 1991) and thus influence the maintenance of AF. Acetycholine activates I_{KACH}-channels via G-protein second messengers, resulting again in decreased ERP and action potential duration (APD) (Ohmoto-Sekine et al., 1999). It is postulated that norepinephrine lowers ERP by activating IP3 and diacyl glycerol leading to an initial influx of Ca^{2+}. Finally, I_{KH}, an inward K^+-conductance current, has also shown to be increased under both sympathetic and parasympathetic stimulation (Ehrlich et al., 2004).

Cell coupling also may play a role in the propensity to AF. PVs exhibit a reduced density of connexin-40 (Cx-40) within their myocardial sleeves as compared with adjoining left atrial tissue (Verheule et al., 2002). The implied decreased electrical coupling of cardiocytes would result in lowered conduction velocity, promoting AF maintenance. Further support for a role of connexins in AF comes from mice lacking Cx-40 which have been shown to have both conduction block and increased AF development (van Rijen et al., 2001). The existing human data are, however, somewhat less convincing with only occasional reports of somatic mutation in the connexin genes and no definitive evidence of heritable defects in cell-cell coupling in AF (Gollob et al., 2006). While common genetic variation in the connexin genes may modulate electrical coupling between atrial and PV myocytes, a role for such variation in human AF remains unproven.

Primary structural differences in the PV and atrial cellular architecture may also sustain re-entry through effects on conduction velocity. Anisotropic conduction is highly dependent on the nature of the connections at specific cell boundaries (Sano et al., 1959). Conduction delays occur in the left superior PV and have been correlated with myocyte fiber orientation (Hocini et al., 2002; Hamabe et al., 2003). Similarly, discrete effects on myocardial architecture (structural and functional) may cause the disorganized propagation of an impulse to neighboring tissue, resulting in chaotic rather than focal, linear conduction (de Bakker et al., 2002). Connective tissue differences may also contribute to the primary electrophysiologic substrate in AF but are often among the most obvious differences in atria remodeled by chronic AF (Spach and Dolber, 1986; Hassink et al., 2003). Physiologic connective tissue barriers are seen in PVs and are associated with impulse conduction block or delay (Hamabe et al., 2003).

These structural differences may have some developmental underpinnings. For example, it has been noted that transgenic mice with increased levels of TGF-β1 had increased baseline connective tissue within their atria and were consequently predisposed to AF development (Verheule et al., 2004). Numerous Mendelian cardiac and vascular diseases associated with AF are now known to result from inherited perturbations of TGF-β signaling and it is certainly conceivable that subtle variation in these same pathways during PV angiogenesis and atrial patterning may contribute to abnormal myocyte networks that sustain AF.

PERPETUATION OF AF: ATRIAL REMODELING

"Atrial remodeling" is a concept which by the presence of AF affects the structure and function of the atria in a manner that favors the maintenance of the arrhythmia (Wijffels et al., 1995). How does the development of this remodeling perpetuate AF and perhaps more importantly is some element of the propensity to atrial remodeling a core component of the intrinsic predisposition toward AF? Studies have noted slowing of impulse conduction and reduced ERP in atrial cells after AF (Gaspo et al., 1997). Atrial tachycardia has been shown to reduce ERP primarily through a decrease in the I_{Ca2+-L}–current of myocytes. In addition, sustained fibrillation has also been associated with structural changes such as myocyte hypertrophy, myocyte death, and atrial stretch (Aime-Sempe et al., 1999), which act in concert to reduce conduction velocity. Both electrophysiological and structural changes of the atria are thought to be involved in the development of chronic AF, and so the theory that "AF begets AF" has been introduced. If this concept is dissected further, then one notes that PVs are the primary source for ectopic foci during AF. Therefore, it is likely that the arrhythmogenic activity of PVs may be an important cause of "atrial remodeling." Thomas et al. showed that the "Star" model for radio-frequency ablation, where

PVs are electrically isolated, resulted in "reverse atrial remodeling" in patients with AF (Thomas et al., 2003). The study found that atrial size and function was restored after surgery. In addition, structural changes in the atria after remodeling, such as stretch, may also result in increased PV activity. Atrial stretch leads to increased intra-atrial pressure causing a rise in the rate and spatio-temporal organization of electrical waves originating in the PVs (Kalifa et al., 2003). Rapid atrial pacing (RAP) has also been shown to reduce ERP and APD within PV myocytes. RAP reduces the density of I_{Ca2+-L}-and I_{To}-currents, both involved in the plateau phase of action potentials (Chen et al., 2001). The same study found that PV myocytes had increased I_f-currents after RAP. These changes imply that electrical and structural remodeling increase the likelihood of ectopic PV automaticity and AF maintenance and provide a potential mechanism by which atrial remodeling might take place.

The process of remodeling itself may be an intrinsic part of cardiac development. Early plasticity has numerous evolutionary advantages and is observed in many tissues (even exploiting pathways already implicated in cardiac arrhythmias) (Salinas and Price, 2005), though whether it operates in the heart remains an open question. These existing questions suggest that the exploration of developmental electrophysiology is likely to have a significant impact on our understanding of disease biology in adult arrhythmias and sudden death.

MODULATION OF AF: DISEASE STATES

Given the proposed role of developmental factors in AF, it is likely that many of the disease states associated with AF also act at this level. To date few studies have explored these relationships. For example, there is a strong reciprocal epidemiologic relationship between heart failure and AF that is unexplained (Wang et al., 2003). Some forms of heart failure are known to result from changes in the dynamics of calcium handling in cardiomyocytes and similar effects have been associated with increased automaticity in cells within the PVs (Honjo et al., 2003), but no direct mechanistic connections have yet been made between these two common syndromes. The syndrome of tachycardia-related cardiomyopathy that is seen in AF might be interpreted as a shared common diathesis to AF and heart failure, since the very presence of sustained AF suggests a primary abnormality of myocardium. Whether in some instances this reflects a shared aberrant remodeling response is not known, but as functional imaging tools improve these hypotheses can be directly tested.

Similarly, thyroid hormone signaling, can also be connected with acute effects on triggered activity in the myocardial sleeves of the PVs (Chen et al., 2002b), but the role of chronic subclinical thyroid imbalance during cardiogenesis not known. Inflammatory cells are critical for the tissue remodeling that takes place during development, but while there are clear effects on AF in later life, the role of these same pathways in patterning atrial biology is just beginning to emerge (Rudolph et al., 2010; Issac et al., 2007). Fundamental relationships between metabolic abnormalities, including obesity, and AF are also recognized. Indeed, metabolic abnormalities are emerging as some of the most rapid changes seen in atrial remodeling (Nattel, 2004). The intrinsic differences in metabolic response seen in AF, and the relationship with obesity, suggest that there may be both inherited and acquired components to this aspect of the AF diathesis ranging from distinctive regulation of core body temperature to biases in substrate utilization (Chen et al., 2003b). Finally, transgenerational differences in autonomic reactivity have been documented in several species. The role of early physiology in patterning these differences is emerging, and the extensive innervation of PVs by sympathetic and parasympathetic nerves makes a role for these effects in AF plausible, but there are no data that directly address this hypothesis (Gardner and O'Rahilly, 1976).

Finally, the link between AF and stroke is multifaceted with AF predicting an increased risk not only of thromboembolic stroke, but also of hemorrhagic stroke even in those who are not on any anticoagulant therapies. This connection has no clear mechanistic basis, but the increasingly recognized role of endocardial signals in cardiac development proposes at least one potential connection, a shared upstream endocardial abnormality.

CONCLUSION

AF is a highly complex disease with numerous contributing factors. In this review, we have briefly summarized the data suggesting a significant role for developmental factors in the genesis of the underlying diathesis to this common arrhythmia. We anticipate that the study of the developmental basis of adult onset arrhythmic disorders will complement existing approaches to the biology, diagnosis, and therapy of these clinically important syndromes.

FUNDING SOURCES

NIH, Harvard Stem Cell Institute, Leducq Foundation

REFERENCES

Aime-Sempe, C., Folliguet, T., Rucker-Martin, C., Krajewska, M., Krajewska, S., Heimburger, M., et al. (1999). Myocardial cell death in fibrillating and dilated human right atria. *J. Am. Coll. Cardiol.* 34, 1577–1586. doi: 10.1016/S0735-1097(99)00382-4

Ausma, J., Litjens, N., Lenders, M. H., Duimel, H., Mast, F., Wouters, L., et al. (2001). Time course of atrial fibrillation-induced cellular structural remodeling in atria of the goat. *J. Mol. Cell. Cardiol.* 33, 2083–2094. doi: 10.1006/jmcc.2001.1472

Benjamin, E. J., Wolf, P. A., D'Agostino, R. B., Silbershatz, H., Kannel, W. B., and Levy, D. (1998). Impact of atrial fibrillation on the risk of death: the framingham heart study. *Circulation* 98, 946–952. doi: 10.1161/01.CIR.98.10.946

Brundel, B. J., Henning, R. H., Kampinga, H. H., Van Gelder, I. C., and Crijns, H. J. (2002). Molecular mechanisms of remodeling in human atrial fibrillation. *Cardiovasc. Res.* 54, 315–324. doi: 10.1016/S0008-6363(02)00222-5

Bush, W. D., and Simon, J. D. (2007). Quantification of Ca(2+) binding to melanin supports the hypothesis that melanosomes serve a functional role in regulating calcium homeostasis. *Pigment Cell Res.* 20, 134–139. doi: 10.1111/j.1600-0749.2007.00362.x

Chen, P. S., and Tan, A. Y. (2007). Autonomic nerve activity and atrial fibrillation. *Heart Rhythm* 4(Suppl. 3), S61–S64. doi: 10.1016/j.hrthm.2006.12.006

Chen, P. S., Wu, T. J., Hwang, C., Zhou, S., Okuyama, Y., Hamabe, A., et al. (2002a). Thoracic veins and

the mechanisms of non-paroxysmal atrial fibrillation. *Cardiovasc. Res.* 54, 295–301. doi: 10.1016/S0008-6363(01)00554-5

Chen, Y. C., Chen, S. A., Chen, Y. J., Chang, M. S., Chan, P., and Lin, C. I. (2002b). Effects of thyroid hormone on the arrhythmogenic activity of pulmonary vein cardiomyocytes. *J. Am. Coll. Cardiol.* 39, 366–372. doi: 10.1016/S0735-1097(01)01731-4

Chen, S. A., and Yeh, H. I. (2003). Specialized conduction cells in human pulmonary veins: fact and controversy. *J. Cardiovasc. Electrophysiol.* 14, 810–811. doi: 10.1046/j.1540-8167.2003.03259.x

Chen, Y. H., Xu, S. J., Bendahhou, S., Wang, X. L., Wang, Y., Xu, W. Y., et al. (2003a). KCNQ1 gain-of-function mutation in familial atrial fibrillation. *Science* 299, 251–254. doi: 10.1126/science.1077771

Chen, Y. J., Chen, Y. C., Chan, P., Lin, C. I., and Chen, S. A. (2003b). Temperature regulates the arrhythmogenic activity of pulmonary vein cardiomyocytes. *J. Biomed. Sci.* 10, 535–543. doi: 10.1007/BF02256115

Chen, Y. C., Chen, S. A., Chen, Y. J., Tai, C. T., Chan, P., and Lin, C. I. (2004). T-type calcium current in electrical activity of cardiomyocytes isolated from rabbit pulmonary vein. *J. Cardiovasc. Electrophysiol.* 15, 567–571. doi: 10.1046/j.1540-8167.2004.03399.x

Chen, Y. J., Chen, S. A., Chang, M. S., and Lin, C. I. (2000). Arrhythmogenic activity of cardiac muscle in pulmonary veins of the dog: implication for the genesis of atrial fibrillation. *Cardiovasc. Res.* 48, 265–273. doi: 10.1016/S0008-6363(00)00179-6

Chen, Y. J., Chen, S. A., Chen, Y. C., Yeh, H. I., Chan, P., Chang, M. S., et al. (2001). Effects of rapid atrial pacing on the arrhythmogenic activity of single cardiomyocytes from pulmonary veins: implication in initiation of atrial fibrillation. *Circulation* 104, 2849–2854. doi: 10.1161/hc4801.099736

Christoffels, V. M., Mommersteeg, M. T., Trowe, M. O., Prall, O. W., de Gier-de Vries, C., Soufan, A. T., et al. (2006). Formation of the venous pole of the heart from an Nkx2-5-negative precursor population requires Tbx18. *Circ. Res.* 98, 1555–1563. doi: 10.1161/01.RES.0000227571.84189.65

de Bakker, J. M., Ho, S. Y., and Hocini, M. (2002). Basic and clinical electrophysiology of pulmonary vein ectopy. *Cardiovasc. Res.* 54, 287–294. doi: 10.1016/S0008-6363(01)00532-6

Ehrlich, J. R., Cha, T. J., Zhang, L., Chartier, D., Melnyk, P., Hohnloser, S. H., et al. (2003). Cellular electrophysiology of canine pulmonary vein cardiomyocytes: action potential and ionic current properties. *J. Physiol.* 551(Pt 3), 801–813. doi: 10.1113/jphysiol.2003.046417

Ehrlich, J. R., Cha, T. J., Zhang, L., Chartier, D., Villeneuve, L., Hebert, T. E., et al. (2004). Characterization of a hyperpolarization-activated time-dependent potassium current in canine cardiomyocytes from pulmonary vein myocardial sleeves and left atrium. *J. Physiol.* 557(Pt 2), 583–597. doi: 10.1113/jphysiol.2004.061119

Ellinor, P. T., Yi, B. A., and MacRae, C. A. (2008). Genetics of atrial fibrillation. *Med. Clin. North Am.* 92, 41–51. doi: 10.1016/j.mcna.2007.09.005

Ellinor, P. T., Yoerger, D. M., Ruskin, J. N., and MacRae, C. A. (2005). Familial aggregation in lone atrial fibrillation. *Hum. Genet.* 118, 179–184. doi: 10.1007/s00439-005-0034-8

Franco, D., and Campione, M. (2003). The role of Pitx2 during cardiac development. Linking left-right signaling and congenital heart diseases. *Trends Cardiovasc. Med.* 13, 157–163. doi: 10.1016/S1050-1738(03)00039-2

Gardner, E., and O'Rahilly, R. (1976). The nerve supply and conducting system of the human heart at the end of the embryonic period proper. *J. Anat.* 121(Pt 3), 571–587.

Garrey, W. (1924). Auricular fibrillation. *Physiol. Rev.* 4, 215–250.

Gaspo, R., Bosch, R. F., Bou-Abboud, E., and Nattel, S. (1997). Tachycardia-induced changes in Na+ current in a chronic dog model of atrial fibrillation. *Circ. Res.* 81, 1045–1052. doi: 10.1161/01.RES.81.6.1045

Go, A. S., Hylek, E. M., Phillips, K. A., Chang, Y., Henault, L. E., Selby, J. V., et al. (2001). Prevalence of diagnosed atrial fibrillation in adults: national implications for rhythm management and stroke prevention: the AnTicoagulation and Risk Factors in Atrial Fibrillation (ATRIA) Study. *JAMA* 285, 2370–2375. doi: 10.1001/jama.285.18.2370

Gollob, M. H., Jones, D. L., Krahn, A. D., Danis, L., Gong, X. Q., Shao, Q., et al. (2006). Somatic mutations in the connexin 40 gene (GJA5) in atrial fibrillation. *N. Engl. J. Med.* 354, 2677–2688. doi: 10.1056/NEJMoa052800

Gosling, J. A., and Dixon, J. S. (1972). Structural evidence in support of an urinary tract pacemaker. *Br. J. Urol.* 44, 550–560. doi: 10.1111/j.1464-410X.1972.tb10122.x

Gudbjartsson, D. F., Arnar, D. O., Helgadottir, A., Gretarsdottir, S., Holm, H., Sigurdsson, A., et al. (2007). Variants conferring risk of atrial fibrillation on chromosome 4q25. *Nature* 448, 353–357. doi: 10.1038/nature06007

Guerra, P. G., Thibault, B., Dubuc, M., Talajic, M., Roy, D., Crepeau, J., et al. (2003). Identification of atrial tissue in pulmonary veins using intravascular ultrasound. *J. Am. Soc. Echocardiogr.* 16, 982–987. doi: 10.1016/S0894-7317(03)00421-8

Gutierrez-Roelens, I., De Roy, L., Ovaert, C., Sluysmans, T., Devriendt, K., Brunner, H. G., et al. (2006). A novel CSX/NKX2-5 mutation causes autosomal-dominant AV block: are atrial fibrillation and syncopes part of the phenotype. *Eur. J. Hum. Genet.* 14, 1313–1316. doi: 10.1038/sj.ejhg.5201702

Habets, P. E., Moorman, A. F., Clout, D. E., van Roon, M. A., Lingbeek, M., van Lohuizen, M., et al. (2002). Cooperative action of Tbx2 and Nkx2.5 inhibits ANF expression in the atrioventricular canal: implications for cardiac chamber formation. *Genes Dev.* 16, 1234–1246. doi: 10.1101/gad.222902

Haissaguerre, M., Jais, P., Shah, D. C., Takahashi, A., Hocini, M., Quiniou, G., et al. (1998). Spontaneous initiation of atrial fibrillation by ectopic beats originating in the pulmonary veins. *N. Engl. J. Med.* 339, 659–666. doi: 10.1056/NEJM199809033391003

Hamabe, A., Okuyama, Y., Miyauchi, Y., Zhou, S., Pak, H. N., Karagueuzian, H. S., et al. (2003). Correlation between anatomy and electrical activation in canine pulmonary veins. *Circulation* 107, 1550–1555. doi: 10.1161/01.CIR.0000056765.97013.5E

Hamada, H., Meno, C., Watanabe, D., and Saijoh, Y. (2002). Establishment of vertebrate left-right asymmetry. *Nat. Rev. Genet.* 3, 103–113. doi: 10.1038/nrg732

Hassink, R. J., Aretz, H. T., Ruskin, J., and Keane, D. (2003). Morphology of atrial myocardium in human pulmonary veins: a postmortem analysis in patients with and without atrial fibrillation. *J. Am. Coll. Cardiol.* 42, 1108–1114. doi: 10.1016/S0735-1097(03)00918-5

Ho, S. Y., Sanchez-Quintana, D., Cabrera, J. A., and Anderson, R. H. (1999). Anatomy of the left atrium: implications for radiofrequency ablation of atrial fibrillation. *J. Cardiovasc. Electrophysiol.* 10, 1525–1533.

Hocini, M., Ho, S. Y., Kawara, T., Linnenbank, A. C., Potse, M., Shah, D., et al. (2002). Electrical conduction in canine pulmonary veins: electrophysiological and anatomic correlation. *Circulation* 105, 2442–2448. doi: 10.1161/01.CIR.0000016062.80020.11

Honjo, H., Boyett, M. R., Niwa, R., Inada, S., Yamamoto, M., Mitsui, K., et al. (2003). Pacing-induced spontaneous activity in myocardial sleeves of pulmonary veins after treatment with ryanodine. *Circulation* 107, 1937–1943. doi: 10.1161/01.CIR.0000062645.38670.BD

Hoogaars, W. M., Tessari, A., Moorman, A. F., de Boer, P. A., Hagoort, J., Soufan, A. T., et al. (2004). The transcriptional repressor Tbx3 delineates the developing central conduction system of the heart. *Cardiovasc. Res.* 62, 489–499. doi: 10.1016/j.cardiores.2004.01.030

Huang, M. H., Friend, D. S., Sunday, M. E., Singh, K., Haley, K., Austen, K. F., et al. (1996). An intrinsic adrenergic system in mammalian heart. *J. Clin. Invest.* 98, 1298–1303. doi: 10.1172/JCI118916

Huser, J., Blatter, L. A., and Lipsius, S. L. (2000). Intracellular Ca2+ release contributes to automaticity in cat atrial pacemaker cells. *J. Physiol.* 524(Pt 2), 415–422. doi: 10.1111/j.1469-7793.2000.00415.x

Issac, T. T., Dokainish, H., and Lakkis, N. M. (2007). Role of inflammation in initiation and perpetuation of atrial fibrillation: a systematic review of the published data. *J. Am. Coll. Cardiol.* 50, 2021–2028. doi: 10.1016/j.jacc.2007.06.054

Jais, P., Hocini, M., Macle, L., Choi, K. J., Deisenhofer, I., Weerasooriya, R., et al. (2002). Distinctive electrophysiological properties of pulmonary veins in patients with atrial fibrillation. *Circulation* 106, 2479–2485. doi: 10.1161/01.CIR.0000036744.39782.9F

Jongbloed, M. R., Schalij, M. J., Poelmann, R. E., Blom, N. A., Fekkes, M. L., Wang, Z., et al. (2004). Embryonic conduction tissue: a spatial correlation with adult arrhythmogenic areas. *J. Cardiovasc. Electrophysiol.* 15, 349–355. doi: 10.1046/j.1540-8167.2004.03487.x

Kalifa, J., Jalife, J., Zaitsev, A. V., Bagwe, S., Warren, M., Moreno, J., et al. (2003). Intra-atrial pressure increases rate and organization of waves emanating from the superior pulmonary veins during atrial fibrillation. *Circulation* 108, 668–671. doi: 10.1161/01.CIR.0000086979.39843.7B

Levin, M. D., Lu, M. M., Petrenko, N. B., Hawkins, B. J., Gupta, T. H., Lang, D., et al. (2009). Melanocyte-like cells in the heart and pulmonary veins contribute to atrial arrhythmia triggers. *J. Clin. Invest.* 119, 3420–3436.

Malekar, P., Hagenmueller, M., Anyanwu, A., Buss, S., Streit, M. R., Weiss, C. S., et al. (2010). Wnt signaling is critical for maladaptive cardiac hypertrophy and accelerates myocardial remodeling. *Hypertension* 55, 939–945. doi: 10.1161/HYPERTENSIONAHA.109.141127

Melnyk, P., Ehrlich, J. R., Pourrier, M., Villeneuve, L., Cha, T. J., and Nattel, S. (2005). Comparison of ion channel distribution and expression in cardiomyocytes of canine pulmonary veins versus left atrium. *Cardiovasc. Res.* 65, 104–116. doi: 10.1016/j.cardiores.2004.08.014

Milan, D. J., and MacRae, C. A. (2005). Animal models for arrhythmias. *Cardiovasc. Res.* 67, 426–437. doi: 10.1016/j.cardiores.2005.06.012

Mjaatvedt, C. H., Kern, C. B., Norris, R. A., Fairey, S., and Cave, C. L. (2005). Normal distribution of melanocytes in the mouse heart. *Anat. Rec. A Discov. Mol. Cell Evol. Biol.* 285, 748–757. doi: 10.1002/ar.a.20210

Mommersteeg, M. T., Brown, N. A., Prall, O. W., de Gier-de Vries, C., Harvey, R. P., Moorman, A. F., et al. (2007a). Pitx2c and Nkx2-5 are required for the formation and identity of the pulmonary myocardium. *Circ. Res.* 101, 902–909. doi: 10.1161/CIRCRESAHA.107.161182

Mommersteeg, M. T., Hoogaars, W. M., Prall, O. W., de Gier-de Vries, C., Wiese, C., Clout, D. E., et al. (2007b). Molecular pathway for the localized formation of the sinoatrial node. *Circ. Res.* 100, 354–362. doi: 10.1161/01.RES.0000258019.74591.b3

Morel, E., Meyronet, D., Thivolet-Bejuy, F., and Chevalier, P. (2008). Identification and distribution of interstitial Cajal cells in human pulmonary veins. *Heart Rhythm* 5, 1063–1067. doi: 10.1016/j.hrthm.2008.03.057

Nattel, S. (2003). Basic electrophysiology of the pulmonary veins and their role in atrial fibrillation: precipitators, perpetuators, and perplexers. *J. Cardiovasc. Electrophysiol.* 14, 1372–1375. doi: 10.1046/j.1540-8167.2003.03445.x

Nattel, S. (2004). Is atrial remodeling a viable target for prevention of atrial fibrillation recurrence. *J. Cardiovasc. Electrophysiol.* 15, 885–886. doi: 10.1046/j.1540-8167.2004.04325.x

Nattel, S., Li, D., and Yue, L. (2000). Basic mechanisms of atrial fibrillation–very new insights into very old ideas. *Annu. Rev. Physiol.* 62, 51–77. doi: 10.1146/annurev.physiol.62.1.51

Nusse, R. (2005). Wnt signaling in disease and in development. *Cell Res.* 15, 28–32. doi: 10.1038/sj.cr.7290260

Ohmoto-Sekine, Y., Uemura, H., Tamagawa, M., and Nakaya, H. (1999). Inhibitory effects of aprindine on the delayed rectifier K+ current and the muscarinic acetylcholine receptor-operated K+ current in guinea-pig atrial cells. *Br. J. Pharmacol.* 126, 751–761. doi: 10.1038/sj.bjp.0702334

Patton, K. K., Zacks, E. S., Chang, J. Y., Shea, M. A., Ruskin, J. N., Macrae, C. A., et al. (2005). Clinical subtypes of lone atrial fibrillation. *Pacing Clin. Electrophysiol.* 28, 630–638. doi: 10.1111/j.1540-8159.2005.00161.x

Perez-Lugones, A., McMahon, J. T., Ratliff, N. B., Saliba, W. I., Schweikert, R. A., Marrouche, N. F., et al. (2003). Evidence of specialized conduction cells in human pulmonary veins of patients with atrial fibrillation. *J. Cardiovasc. Electrophysiol.* 14, 803–809. doi: 10.1046/j.1540-8167.2003.03075.x

Pokushalov, E., Romanov, A., Corbucci, G., Artyomenko, S., Baranova, V., Turov, A., et al. (2012). A randomized comparison of pulmonary vein isolation with versus without concomitant renal artery denervation in patients with refractory symptomatic atrial fibrillation and resistant hypertension. *J. Am. Coll. Cardiol.* 60, 1163–1170. doi: 10.1016/j.jacc.2012.05.036

Postma, A. V., Dekker, L. R., Soufan, A. T., and Moorman, A. F. (2009). Developmental and genetic aspects of atrial fibrillation. *Trends Cardiovasc. Med.* 19, 123–130. doi: 10.1016/j.tcm.2009.07.003

Rentschler, S., Vaidya, D. M., Tamaddon, H., Degenhardt, K., Sassoon, D., Morley, G. E., et al. (2001). Visualization and functional characterization of the developing murine cardiac conduction system. *Development* 128, 1785–1792.

Rudolph, V., Andrie, R. P., Rudolph, T. K., Friedrichs, K., Klinke, A., Hirsch-Hoffmann, B., et al. (2010). Myeloperoxidase acts as a profibrotic mediator of atrial fibrillation. *Nat. Med.*16, 470–474. doi: 10.1038/nm.2124

Salinas, P. C., and Price, S. R. (2005). Cadherins and catenins in synapse development. *Curr. Opin. Neurobiol.* 15, 73–80. doi: 10.1016/j.conb.2005.01.001

Sanders, K. M. (1996). A case for interstitial cells of Cajal as pacemakers and mediators of neurotransmission in the gastrointestinal tract. *Gastroenterology* 111, 492–515. doi: 10.1053/gast.1996.v111.pm8690216

Sano, T., Takayama, N., and Shimamoto, T. (1959). Directional difference of conduction velocity in the cardiac ventricular syncytium studied by microelectrodes. *Circ. Res.* 7, 262–267. doi: 10.1161/01.RES.7.2.262

Schenzer, A., Friedrich, T., Pusch, M., Saftig, P., Jentsch, T. J., Grotzinger, J., et al. (2005). Molecular determinants of KCNQ (Kv7) K+ channel sensitivity to the anticonvulsant retigabine. *J. Neurosci.* 25, 5051–5060. doi: 10.1523/JNEUROSCI.0128-05.2005

Sinner, M. F., Ellinor, P. T., Meitinger, T., Benjamin, E. J., and Kaab, S. (2011). Genome-wide association studies of atrial fibrillation: past, present, and future. *Cardiovasc. Res.* 89, 701–709. doi: 10.1093/cvr/cvr001

Snarr, B. S., O'Neal, J. L., Chintalapudi, M. R., Wirrig, E. E., Phelps, A. L., Kubalak, S. W., et al. (2007). Isl1 expression at the venous pole identifies a novel role for the second heart field in cardiac development. *Circ. Res.* 101, 971–974. doi: 10.1161/CIRCRESAHA.107.162206

Spach, M. S., and Dolber, P. C. (1986). Relating extracellular potentials and their derivatives to anisotropic propagation at a microscopic level in human cardiac muscle. Evidence for electrical uncoupling of side-to-side fiber connections with increasing age. *Circ. Res.* 58, 356–371. doi: 10.1161/01.RES.58.3.356

Tada, H., Oral, H., Ozaydin, M., Greenstein, R., Pelosi, F. Jr., Knight, B. P., et al. (2002). Response of pulmonary vein potentials to premature stimulation. *J. Cardiovasc. Electrophysiol.* 13, 33–37. doi: 10.1046/j.1540-8167.2002.00033.x

Takei, M., Furukawa, Y., Narita, M., Ren, L. M., Karasawa, Y., Murakami, M., et al. (1991). Synergistic nonuniform shortening of atrial refractory period induced by autonomic stimulation. *Am. J. Physiol.* 261(6 Pt 2), H1988–H1993.

Thomas, L., Boyd, A., Thomas, S. P., Schiller, N. B., and Ross, D. L. (2003). Atrial structural remodelling and restoration of atrial contraction after linear ablation for atrial fibrillation. *Eur. Heart J.* 24, 1942–1951. doi: 10.1016/j.ehj.2003.08.018

Thuneberg, L. (1982). Interstitial cells of Cajal: intestinal pacemaker cells. *Adv. Anat. Embryol. Cell Biol.* 71, 1–130. doi: 10.1007/978-3-642-68417-3_1

van den Berg, G., Abu-Issa, R., de Boer, B. A., Hutson, M. R., de Boer, P. A., Soufan, A. T., et al. (2009). A caudal proliferating growth center contributes to both poles of the forming heart tube. *Circ. Res.* 104, 179–188. doi: 10.1161/CIRCRESAHA.108.185843

van Rijen, H. V., van Veen, T. A., van Kempen, M. J., Wilms-Schopman, F. J., Potse, M., Krueger, O., et al. (2001). Impaired conduction in the bundle branches of mouse hearts lacking the gap junction protein connexin40. *Circulation* 103, 1591–1598. doi: 10.1161/01.CIR.103.11.1591

Verheule, S., Sato, T., Everett, T. 4th., Engle, S. K., Otten, D., Rubart-von der Lohe, M., et al. (2004). Increased vulnerability to atrial fibrillation in transgenic mice with selective atrial fibrosis caused by overexpression of TGF-beta1. *Circ. Res.* 94, 1458–1465. doi: 10.1161/01.RES.0000129579.59664.9d

Verheule, S., Wilson, E. E., Arora, R., Engle, S. K., Scott, L. R., and Olgin, J. E. (2002). Tissue structure and connexin expression of canine pulmonary veins. *Cardiovasc. Res.* 55, 727–738. doi: 10.1016/S0008-6363(02)00490-X

Verrier, R. L., and Antzelevitch, C. (2004). Autonomic aspects of arrhythmogenesis: the enduring and the new. *Curr. Opin. Cardiol.* 19, 2–11. doi: 10.1097/00001573-200401000-00003

Waldo, A. L. (2003). Mechanisms of atrial fibrillation. *J. Cardiovasc. Electrophysiol.* 14(Suppl. 12), S267–S274. doi: 10.1046/j.1540-8167.2003.90401.x

Wang, T. J., Larson, M. G., Levy, D., Vasan, R. S., Leip, E. P., Wolf, P. A., et al. (2003). Temporal relations of atrial fibrillation and congestive heart failure and their joint influence on mortality: the framingham heart study. *Circulation*

107, 2920–2925. doi: 10.1161/01.CIR.0000072767.89944.6E

Wijffels, M. C., Kirchhof, C. J., Dorland, R., and Allessie, M. A. (1995). Atrial fibrillation begets atrial fibrillation. A study in awake chronically instrumented goats. *Circulation* 92, 1954–1968. doi: 10.1161/01.CIR.92.7.1954

Wit, A. L., and Boyden, P. A. (2007). Triggered activity and atrial fibrillation. *Heart Rhythm* 4(Suppl. 3), S17–S23. doi: 10.1016/j.hrthm.2006.12.021

Wu, T. J., Ong, J. J., Chang, C. M., Doshi, R. N., Yashima, M., Huang, H. L., et al. (2001). Pulmonary veins and ligament of Marshall as sources of rapid activations in a canine model of sustained atrial fibrillation. *Circulation* 103, 1157–1163. doi: 10.1161/01.CIR.103.8.1157

Conflict of Interest Statement: The authors declare that the research was conducted in the absence of any commercial or financial relationships that could be construed as a potential conflict of interest.

Received: 28 May 2013; accepted: 02 August 2013; published online: 12 September 2013.
Citation: Kapur S and MacRae CA (2013) The developmental basis of adult arrhythmia: atrial fibrillation as a paradigm. Front. Physiol. ***4****:221. doi: 10.3389/fphys.2013.00221*
This article was submitted to Cardiac Electrophysiology, a section of the journal Frontiers in Physiology.

frontiers in
PHYSIOLOGY

REVIEW ARTICLE
published: 20 September 2013
doi: 10.3389/fphys.2013.00254

Identifying potential functional impact of mutations and polymorphisms: linking heart failure, increased risk of arrhythmias and sudden cardiac death

Benoît Jagu*[1,2,3]*, Flavien Charpentier*[1,2,3] *and Gilles Toumaniantz*[1,2,3]*

[1] *INSERM, UMR1087, l'institut du thorax, IRS-UN, Nantes, France*
[2] *CNRS, UMR6291, Nantes, France*
[3] *Faculté de Médecine, Université de Nantes, Nantes, France*

Edited by:
Christopher Huang, University of Cambridge, UK

Reviewed by:
Thomas Hund, Ohio State University, USA
Christopher Huang, University of Cambridge, UK

****Correspondence:***
Gilles Toumaniantz, INSERM, UMR1087, CNRS UMR6291, l'Institut du Thorax, IRT-UN, 8 quai Moncousu, BP 70721, 44007 Nantes Cedex 1, France
e-mail: gilles.toumaniantz@inserm.fr

Researchers and clinicians have discovered several important concepts regarding the mechanisms responsible for increased risk of arrhythmias, heart failure, and sudden cardiac death. One major step in defining the molecular basis of normal and abnormal cardiac electrical behavior has been the identification of single mutations that greatly increase the risk for arrhythmias and sudden cardiac death by changing channel-gating characteristics. Indeed, mutations in several genes encoding ion channels, such as SCN5A, which encodes the major cardiac Na^+ channel, have emerged as the basis for a variety of inherited cardiac arrhythmias such as long QT syndrome, Brugada syndrome, progressive cardiac conduction disorder, sinus node dysfunction, or sudden infant death syndrome. In addition, genes encoding ion channel accessory proteins, like anchoring or chaperone proteins, which modify the expression, the regulation of endocytosis, and the degradation of ion channel a-subunits have also been reported as susceptibility genes for arrhythmic syndromes. The regulation of ion channel protein expression also depends on a fine-tuned balance among different other mechanisms, such as gene transcription, RNA processing, post-transcriptional control of gene expression by miRNA, protein synthesis, assembly and post-translational modification and trafficking. The aim of this review is to inventory, through the description of few representative examples, the role of these different biogenic mechanisms in arrhythmogenesis, HF and SCD in order to help the researcher to identify all the processes that could lead to arrhythmias. Identification of novel targets for drug intervention should result from further understanding of these fundamental mechanisms.

Keywords: arrhythmia, sudden cardiac death, cardiac ionic channel, regulation, biogenic properties

INTRODUCTION

Annually, more than 300,000 cases of sudden cardiac death (SCD) occur in the United States, representing a major public health concern (George, 2013). SCD mainly results from severe ventricular arrhythmias, ventricular fibrillation being the most common underlying arrhythmia. These arrhythmias can be the result of a variety of structural changes of the heart or ion channel dysfunctions sometimes through an altered expression. During the last decade, researchers and clinicians have discovered important concepts by elucidating the mechanisms responsible for rare monogenic arrhythmic disorders, so called channelopathies (Martin et al., 2012; George, 2013). Indeed, one major step in defining the molecular basis of normal and abnormal cardiac electrical behavior has been the identification of single mutations that greatly increase the risk for arrhythmias, cardiomyopathies, and SCD (for review see Basso et al., 2011; McNally et al., 2013). Significant technological advances in the study of the genetics of sudden cardiac death have taken place in the last decade (Brion et al., 2010). The vast majority of the mutations identified so far are located in the coding regions of gene encoding ion channel subunits or regulatory proteins and significantly affect the biophysical properties (gating, ion permeation) or the membrane expression of key ion channels. Mouse models of related cardiac arrhythmias, which recapitulate for most of them the clinical phenotypes of the patients, have helped us to elucidate the pathophysiological relevance of these mechanisms (Derangeon et al., 2013; Remme, 2013a). However, patients carrying these mutations remain rare. Heart failure (HF), a syndrome caused by significant impairments in cardiac function, is the leading cause of hospitalization in people older than 65 years in developed countries. HF is a classical situation where the risk of arrhythmias is increased, contributes substantially to morbidity and is responsible for SCD, which represents a large proportion of all deaths in these patients (Janse, 2004; Martin et al., 2011). In HF, and in other cardiac diseases, arrhythmias have been shown to be secondary to electrical remodeling i.e., altered expression of ion channels (Nattel et al., 2010), studied mainly at the mRNA level, although post-transcriptional processes could also be involved (for review see, Zorio et al., 2009; Kim, 2013).

Because of the magnitude of the SCD issue, the opportunities for a real public health impact are significant. SCD is a major health problem and constitutes one of the most important unsolved challenges. Recent medical progresses have had a remarkable impact on SCD in patients at high risk because of advanced heart disease or because they are affected by monogenic arrhythmias (for review, see Martin et al., 2011). However, the majority of victims do not fall into these high-risk groups. Particularly, a significant number of previously healthy young people have died suddenly and unexpectedly, due to genetic heart disorders, either structural cardiomyopathies or arrhythmogenic abnormalities (Brion et al., 2010; Cross et al., 2011). The risk of fatal arrhythmias may be modulated by genetically determined variants in key pathways and may become manifest in the face of environmental triggers such as myocardial ischemia, drugs, or HF (Anvari et al., 2001; Hu et al., 2007a,b; Mittleman and Mostofsky, 2011; Amin et al., 2013). Abnormalities in plasma membrane ion channel function are central to arrhythmogenesis. Recent studies have provided valuable information on how the ion channel expression level, localization, and biophysical properties are regulated, but also revealed that our understanding of the underlying mechanisms is still limited (Harkcom and Abbott, 2010; Ravens and Wettwer, 2011; Rook et al., 2012). Currently, the research should no longer be restricted to study mRNA expression (in acquired cardiac diseases) or biophysical processes (in channelopathies). Although many studies have focused on cell surface expression of mutant channels, it becomes essential to expand our fields of investigation to all the molecular processes responsible for the biogenic properties such as RNA processing, translation and trafficking to understand these fundamental mechanisms. Indeed, incorrect processing causes many diseases. This review focuses on examples chosen to illustrate processes that may account for the malfunction of mutant cardiac channel, allowing to identify novel targets for drug intervention.

GENE TRANSCRIPTION AND RNA PROCESSING

GENE TRANSCRIPTION AND PROMOTER OR OPEN-READING-FRAME POLYMORPHISMS

In the last decade, researchers would elucidate inherited arrhythmic disorders by a monogenic approach. But this concept was enable to explain the incomplete penetrance of arrhythmic disorders and the overlap syndromes. These limitations are typically observed in SCN5A-related channelopathies (Remme and Wilde, 2008). The SCN5A gene encodes a voltage-sensitive sodium channel mainly expressed in the cardiac muscle: Nav1.5. Numerous mutations in SCN5A gene have been associated with different rare arrhythmic syndromes, such as type 3 long QT syndrome (LQT3), Brugada syndrome (BrS), cardiac conduction disorders, sick sinus syndrome, atrial standstill and overlap syndromes (Rook et al., 2012). A good example of overlap syndrome is the disease associated with the SCN5A 1795insD mutation. Patients carrying this mutation exhibit bradycardia, conduction disease, LQT3, and Brugada syndromes (Bezzina et al., 1999). Remme and co-workers generated a knock-in mouse carrying the mouse equivalent (1798insD) of the human SCN5A-1795insD mutation and confirmed that a single SCN5A mutation may indeed be sufficient to cause the overlap syndrome (Remme et al., 2006). However, other factors may modify and modulate this clinical phenotype (Remme et al., 2009; Scicluna et al., 2011). These factors, such as the age, gender, drug therapy, associated disease, oligogenic factors, or the genetic background of the patient may explain the diversity of phenotypes observed for the same mutation. The predictive power of autonomic dysregulation and markers such as lipid levels, hypertension, diabetes, and smoking is quite low in subclinical heart disease, the population in which the majority of SCD occur. Thus, it should be considered that a genetic element such as a single nucleotide polymorphism (SNP) could minimize or exacerbate the effect of mutations and must be considered as a functional genetic element. Although the identification of genetic modifiers of disease severity in genetically inherited arrhythmias is rare (Scicluna et al., 2008), the understanding of these diseases will be improved by bioinformatics approaches to identify previously unknown functional genetic elements and to examine their contributions to arrhythmia susceptibility (Arking et al., 2004; Brion et al., 2010; Arking and Sotoodehnia, 2012).

The first level of regulation to study in the "gene to function" relationship remains the level of gene expression that is directly associated with the activity of its promoter region, which plays a central role in the regulation of transcription. In 2006, Bezzina and collaborators identified a set of 6 polymorphisms in near-complete linkage disequilibrium in SCN5A gene promoter region. This variant haplotype, found in about 25% of Asian subjects and absent in whites and blacks, induces a marked reduction of reporter activity in cardiomyocytes (Bezzina et al., 2006). The relationship between SCN5A promoter haplotype and conduction velocity, was analyzed in a cohort of Japanese patients with Brugada syndrome without SCN5A mutations and of Japanese control subjects. This study showed that the variant haplotype was associated with slowed conduction in normal subjects and exacerbated conduction slowing in those with Brugada syndrome. This study provides evidence that genetically determined variable Nav1.5 transcription occurs in the human heart and is associated with variable conduction velocity, an important contributor to arrhythmia susceptibility.

In the same way, Park and collaborators have studied the role of SCN5A promoter variants and DNA methylation by using a family-based approach in predicting phenotype severity in a large kindred with a heterozygous loss-of-function SCN5A mutation (Park et al., 2012). Affected patients exhibited a mixed phenotype of Brugada Syndrome and atrioventricular conduction disease and a marked variation in phenotype severity. During systematic survey of the SCN5A promoter region, they have identified 2 SNP in complete linkage disequilibrium. These promoter variants were significantly associated with disease severity (mild vs. severe phenotype). On the contrary, the analysis of genome-wide DNA methylation profiles did not support a role for the methylation of SCN5A-related genes. This study suggests that the presence of specific promoter variants increase the risk of a severe phenotype in heterozygous carriers of an SCN5A loss-of-function mutation.

These promoter implications on arrhythmogenesis were also confirmed by *in vitro* studies. For instance, Yang and collaborators have identified DNA variants in the proximal promoter region of SCN5A and determined their frequency in 1121 subjects.

Interestingly, this population consisted of 88 Brugada syndrome patients with no mutation in SCN5A coding region, and 1033 anonymized subjects from various ethnicities (Yang et al., 2007). Variant promoter activity was assayed in CHO cells and neonatal cardiomyocytes by transient transfection of promoter–reporter constructs. *In vitro* functional analysis identified four variants with significantly reduced reporter activity, up to 62.8% in CHO cells and 55% in cardiomyocytes. The authors concluded that the SCN5A core promoter includes multiple DNA polymorphisms with altered *in vitro* activity, further supporting the concept of interindividual variability in transcription of this gene.

An association between promoter variants and increased arrhythmic risk has also been found for other genes, such as GJA5, which encodes connexin 40. Two closely linked polymorphisms in the promoter of Cx40 gene (−44G→A, rs35594137, and +71A→G, rs11552588) were suggested to decrease Cx40 promoter activity and to be linked to atrial standstill, when expressed homozygously and cosegregating with an SCN5A loss-of-function mutation (Groenewegen et al., 2003), or increased risk of atrial fibrillation (Firouzi et al., 2004). However, Wirka and collaborators have shown more recently that the Cx40 promoter rs35594137 SNP was not associated with altered Cx40 mRNA levels in atria (Wirka et al., 2011). This observation underscores the difficulty of such studies in terms of understanding the molecular basis of cardiac arrhythmias: identifying a SNP in a promoter region is not sufficient, *in vivo* functional validation is necessary. In addition, the authors have identified another common SNP (rs10465885), which alters the configuration of one TATA box of an alternative Cx40 promoter. A promoter-luciferase assay in cultured murine cardiomyocytes demonstrated reduced activity of the promoter containing the minor allele of this SNP. It was strongly associated with Cx40 mRNA expression and displayed strong and consistent allelic expression imbalance in human atrial tissue. It was also associated with early-onset atrial fibrillation.

Several studies have shown an association between angiotensinogen (AGT) promoter polymorphisms and hypertension. For instance, the A-6G and A-20C polymorphisms in the promoter region of AGT gene are associated, respectively, to decreased and increased risks of hypertension (Watkins et al., 2010; Gu et al., 2011). Hypertension is a risk factor for left ventricular hypertrophy, which is a powerful predictor of morbidity and mortality from myocardial infarction, stroke, and congestive heart failure (Rasmussen-Torvik et al., 2005). In the same way, Chen and collaborators have described that the promoter polymorphism G-6A is also associated with non-familial sick sinus syndrome (Chen et al., 2012). This syndrome, including profound sinus bradycardia, sinus arrest, sino-atrial exit block, and tachy-bradycardia, is a group of abnormal heart rhythms presumably caused by a malfunction of the sinus node (Dobrzynski et al., 2007). By *in vitro* approaches, Chen and co-workers have confirmed that nucleotide G at position −6 modulates the binding affinity with nuclear factors and yields a lower transcriptional activity than nucleotide A. The authors concluded that this promoter polymorphism might contribute to non-familial sick sinus syndrome susceptibility.

It should be noted that the vast majority of the mutations identified so far in the context of arrhythmic diseases are located in the coding regions of genes encoding cardiac ion channels or accessory ion channel subunits. These genetic elements can cause life-threatening arrhythmias and sudden death in heterozygous mutation carriers as it has been extensively described for the congenital long QT or Brugada syndromes (for recent review Amin et al., 2013; Remme, 2013b). The application of the same kind of genotype-phenotype relationship between promoter variants and cardiac arrhythmias is a major and critical challenge. Indeed, potential demographic, environmental, and genetic factors in conjunction with a mutation, may modify the phenotype for pathology, and thereby determine, at least partially, the large variability in disease severity.

In this context, some authors have examined the input of promoter mutations under pathological conditions. A deletion/insertion polymorphism (4G/5G) within the gene encoding the plasminogen activator inhibitor 1(PAI-1), has been proposed as a coronary risk factor (Iwai et al., 1998; Margaglione et al., 1998). Indeed, a study performed in healthy people showed that the group with a first-degree relative who had suffered from a coronary ischemic episode had a higher number of homozygotes for the deleted allele (4G/4G) of the PAI-1 gene (Margaglione et al., 1998). Moreover, the 4G/4G and 4G/5G haplotypes have been associated with a faster onset of acute coronary syndromes after the first angina pain (Iwai et al., 1998). Variability of the PAI-1 4G/5G genotype contributes to the variability in circulating PAI-1 levels, with the 4G/4G genotype being associated with higher PAI-1 plasma levels. In this context, Anvari and collaborators have tested the hypothesis that the 4G/4G genotype could promote ischemia-associated malignant ventricular arrhythmias based on the onset of transient coronary ischemic events. They have determined the PAI-1 4G/5G genotypes, as well as PAI-1 antigen levels in 2 groups of patients with coronary artery disease (CAD): one without malignant arrhythmias and one with a history of SCD (Anvari et al., 2001). They revealed a significant association between the 4G allele and the risk for malignant arrhythmias, with greatest risk in subjects possessing the 4G/4G genotype. They also demonstrated that a genetically determined prothrombotic/antifibrinolytic state in patients with CAD may serve as a marker of the severity of the disease, as observed by higher PAI-1 levels in the group of SCD survivors.

In Brugada syndrome, loss-of-function SCN5A mutations have been identified as causative in 20% of cases (Calloe et al., 2013; Remme, 2013b). However, some authors have also examined the input of SCN5A mutations under ischemic conditions. In this context, Antzelevitch and collaborators have enrolled 19 patients developing VF during acute myocardial infarction (AMI) in order to search for possible complications due to SCN5A mutations under ischemic conditions (Hu et al., 2007a,b; Oliva et al., 2009). Among the cohort of 19 patients, one missense mutation (G400A) in SCN5A was detected in a conserved region. An H558R polymorphism was detected on the same allele. Unlike the other 18 patients, who each developed 1–2 VF episodes during AMI, the G400A mutation carrier developed 6 episodes of VT/VF within the first 12 h. This mutation induced a marked decrease in sodium peak current. So they have described the first sodium channel mutation to be associated with the development of an arrhythmic storm during acute ischemia. These

findings also suggest that a loss-of-function mutation in SCN5A may predispose to ischemia-induced arrhythmic storm.

These two examples suggest that a genetic variant could serve as a marker of arrhythmic risk in the context of common cardiac diseases.

GENE TRANSCRIPTION AND mRNA STABILITY

During transcription, the RNA-polymerase generates long strands of RNA that contain untranslated 5′ and 3′ regions, multiple exons (amino acid encoding RNA sequences) and introns. It should be noted that the functions of non-coding RNA sequences are presently incompletely understood. Regulating the expression of ion channels at the cell surface begins at the level of gene transcription and **mRNA stability**. Thus, pathogenic nucleotide substitutions, deletions, and insertions can affect mRNA synthesis and stability, thereby altering the amount of mRNA available for subsequent protein generation. The 3′- and 5′-UTRs are important in controlling mRNA stability, cellular and subcellular localization, and translation activation or repression (Matoulkova et al., 2012).

Mutations in the human ether-a-go-go-related gene (hERG) result in type 2 long QT syndrome (LQT2). More than 30% of the LQT2 mutations result in premature termination codons. The hERG gene encodes a K^+ channel that contributes to the repolarization of the cardiac action potential. Gong and collaborators have described that hERG mRNA transcripts that contain premature termination codon mutations are rapidly degraded by nonsense-mediated mRNA decay (NMD) (Gong et al., 2007). The NMD is an evolutionarily conserved RNA surveillance mechanism that recognizes and eliminates transcripts containing Premature Termination Codons (PTC). This process is increasingly recognized as a mechanism for reducing mRNA levels in a variety of human diseases (Nagy and Maquat, 1998; Maquat, 2004; Chang et al., 2007). Gong and collaborators investigated 2 nonsense mutations, W1001X and R1014X, in the C-terminal region of the hERG channel. The primary consequence of the W1001X and R1014X mutations was the degradation of mutant mRNA by NMD. In parallel, the two mutations produced truncated hERG channel proteins and reduced hERG current amplitude. More interestingly, the R1014X mutation also caused a dominant-negative effect on the wild-type hERG channel, which is expected to result in a severe clinical phenotype. Thus, these LQT2 nonsense mutations cause a decrease in mutant mRNA levels by NMD rather than a production of truncated proteins suggesting that the degradation of hERG mutant mRNA by nonsense-mediated mRNA decay is also a significant mechanism in LQT2 patients (Gong et al., 2007). The same mechanism was also described in the pathogenesis of the hERG P926AfsX14 frameshift mutation, which is associated with a severe phenotype (Zarraga et al., 2011).

More recently, Stump and collaborators described another mechanism for the origin of long QT syndrome in which hERG transcripts containing the Q81X nonsense mutation escaped NMD by the reinitiation of translation, resulting in the generation of N-terminally truncated channels. Because the N-terminus of hERG contains several essential regions that contribute to the maintenance of slow channel deactivation, these isoforms exhibited decreased tail current density, accelerated deactivation kinetics, reduced resurgent outward current and co-assembled with wild-type hERG to form heteromeric channels with altered gating properties. The authors present this reinitiation of translation as a new mechanism of hERG channel dysfunction in LQT2 (Stump et al., 2012), in which mRNA stability modulation may induce biophysical changes that contribute to the development of the pathology.

ALTERNATIVE SPLICING

In the post genomic era, it became clear that the number of genes in eukaryotic genomes does not reflect the biological complexity of corresponding organisms. The number of functionally distinct protein isoforms encoded by eukaryotic genes may at least partially explain this lack of correlation. To explain this diversity, it is essential to consider *alternative splicing* as a common eukaryotic process. Normal mRNA splicing can vary for a single gene product, thereby generating multiple transcripts with different coding regions and/or differing translation efficiencies (Kornblihtt et al., 2013). Many splicing variants associated with Nav1.5 and hERG channels have been reported (respectively Shang et al., 2007 and Farrelly et al., 2003). However, the Nav1.5 channel was chosen to illustrate this topic in view of its multiplicity of splicing processes.

In general, SCN5A mRNA is derived from 28 different exons (**Figure 1**). Exons 2–28 contain the protein-coding sequence, exon 1, and part of exon 2 further encode the 5′-untranslated region (5′-UTR), whereas exon 28 also contains the 3′-UTR. Multiple SCN5A mRNA variants have been detected in the mammalian heart, most of which are generated by alternative splicing and apparently evolutionary conserved mechanisms (Schroeter et al., 2010). Many studies correlated altered action potential morphology and increased arrhythmia vulnerability with changes in the Nav1.5 expression level and/or sodium current (I_{Na}) density. Such changes have been frequently reported in common cardiac diseases such as HF (Borlak and Thum, 2003; Valdivia et al., 2005; Shang et al., 2007).

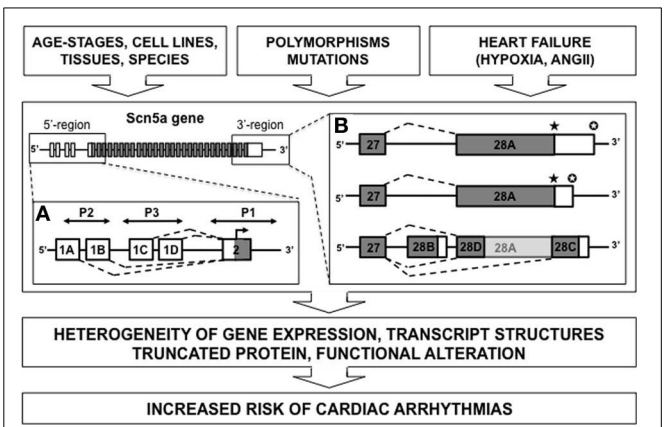

FIGURE 1 | Diagram depicting alternative splicing for SCN5A gene. Multiples mRNA variants were described for the 5′ or 3′-untranslated regions (respectively **A** and **B**) (white rectangle, untranslated region; gray rectangle, translated region; *P*, promoter element; ★, stop codon; ✪, polyadenylation site).

Polymorphisms in the 5′-sequence adjacent to the SCN5A gene have been linked to cardiac arrhythmias. Shang and collaborators have identified three alternative 5′-splice variants (1A, 1B, and 1C) of the untranslated exon 1 in the murine SCN5A mRNA (Shang and Dudley, 2005). Consistent with playing a regulatory role in Na^+ current, the splice variants differ in relative abundance during development, with a prominent up-regulation of exon 1C in an adult compared with a fetal heart. These 5′-UTRs for SCN5A gene show multiple "Transcription Start Sites" (TSSs). Previously, nine potential TSSs have been identified in rat muscle (Sheng et al., 1994), then three other TSSs have been noted in the human SCN5A gene in sequences preceding the exon 1A (Yang et al., 2004) and finally Shang and collaborators have positioned two other TSSs associated with exon 1C (Shang and Dudley, 2005). Adding the possibility of more complex regulation, the total identified promoter region contained consensus-binding sites for several transcription factors that may be functionally significant. These results suggest the possibility of complex transcriptional and translational regulation of the cardiac sodium channel. Moreover, the SCN5A promoter region is large and complex including repressor elements, tissue-specific promoter elements, and three untranslated exon 1 variants. For instance, the presence of an upstream open reading frame in the human SCN5A transcript containing exon 1D-derived sequences was recently identified. This sequence almost completely abolished translation of Nav1.5 (Van Stuijvenberg et al., 2010). One can easily imagine the pathological consequences of such a complexity.

Many other alternative splicing processes were characterized for this gene (Rook et al., 2012). Among these, there is a splice form in coding region, which is associated with development, knowledge that exceeds the investigation field of arrhythmias.

Nav1.5 possesses a central pore-forming α-subunit, comprising four repeat domains (D1–D4), each composed of six membrane-spanning segments (S1–S6). A major type of alternative splicing of voltage-gated sodium channel genes involves inclusion of two alternative exons 6 (5′ genomic and the 3′ genomic) encoding the D1:S3 segment and the D1:S3/S4 extracellular linker. In developmentally regulated D1:S3 splicing of Nav1.5, there are 31 nucleotide differences between the 5′-exon ("neonatal") and the 3′-exon ("adult") forms, resulting in 7 amino acid differences in D1:S3-S3/S4 linker region. Onkal and collaborators (2008) have realized an electrophysiological comparison of "neonatal" and "adult" isoforms. They have observed that the "neonatal" isoform exhibited significant functional differences with the "adult" form. The neonatal isoform presents a shift of steady-state activation toward less negative voltages; it shows a shift of steady-state inactivation toward more negative voltages; has much slower activation and inactivation kinetics; it is associated with significantly greater Na^+ influx; it shows a stronger voltage dependence of time to peak and recovers from inactivation significantly more slowly (Onkal et al., 2008). In the same time, the authors also tried to determine the critical involvement of a lysine residue in this "neonatal" form. Indeed, they have observed that the K211D mutagenesis in "neonatal" Nav1.5 resulted in a strong shift from the "neonatal" back to the "adult" electrophysiological phenotype. By this approach, they concluded that the negative aspartate ("adult") to positive lysine ("neonatal") substitution was primarily responsible for the effects of D1:S3 splicing on Nav1.5 biophysical characteristics (Onkal et al., 2008). Compared to the "adult," for example, the "neonatal" channel was associated with a larger inward current (Na^+) during each opening of the channel. In overall conclusion, the authors have stated that electrophysiological characteristics of "neonatal" Nav1.5 are highly likely to have a number of significant pathophysiological as well as physiological consequences. Following this characterization, pathological implications have been attributed to this neonatal form. It was effectively observed that "neonatal" Nav1.5 is a novel marker with significant clinical potential for management of metastatic breast cancer (Onkal and Djamgoz, 2009; Chioni et al., 2010).

Splicing processes within the coding region can also generate truncated forms of Nav1.5. Dudley and collaborators published an interesting example of abnormal Nav1.5 splicing regulation in human HF. This pathological splicing contributes to a reduction in current of a magnitude likely to contribute to the arrhythmic risk in this condition (Shang et al., 2007; Gao et al., 2011). Theses authors have observed that HF results in an increase in two SCN5A mRNA variants, designated Exon 28C (39 bp) and Exon 28D (114 bp). Compared with the full-length Nav1.5 messenger, these variants are shorter and encode prematurely truncated, non-functional Na^+ channel proteins missing the last part of intramembrane domain IV, from the S3 (for exon 28C) or S4 (exon 28D) segments to the C terminus. The physiological significance of truncations in exon 28 was tested by making a gene-targeted mouse model with a nonsense mutation in this exon between the truncations caused by the E28C and E28D variants. Experiments performed on cardiomyocytes differentiated from embryonic stem cells carrying this mutation at the heterozygous state showed a significant reduction in cardiac Na+ current and conduction velocity (Shang et al., 2007).

But what is the mechanism behind this pathological splicing? During HF, the splicing factors LUC7L3 and RBM25 are up regulated (Choudhary and Dudley, 2002). These proteins are able to bind to the canonical sequence in exon 28 near the splicing sites of SCN5A variants Exon 28C and Exon 28D. This observation has significant pathological implications because the authors also observed that two common features present in HF, Angiotensin II and hypoxia, were able to induce these splicing factors (Gao et al., 2011). This observation was consistent with clinical data suggesting that renin-angiotensin system inhibition and revascularization have antiarrhythmic effects (Moro et al., 2010). This mechanism of splicing does not appear to be tissue restricted but can explain other clinical implications as previously described for cancer (Onkal and Djamgoz, 2009; Chioni et al., 2010).

Are these complex alternative splicing processes characteristic of SCN5A gene or more generally widespread among ion channels? Houtman and collaborators published mapping for two genes encoding the inward rectifier current, KCNJ2 (Kir2.1) and KCNJ12 (Kir2.2) in dog (Houtman et al., 2012). Defective inward rectifier current may lead, amongst other features, to severe cardiac arrhythmias in mouse and man such as ventricular arrhythmias and atrial fibrillation (Anumonwo and Lopatin, 2010). By Race PCR, Houtman and collaborators demonstrated the status

of KCNJ2 as a "two exon" gene with a complete Open reading Frame (ORF) in the second exon and only one transcription initiation site was mapped. However, they described four differential transcription termination sites found downstream of two consensus polyadenylation signals. KCNJ12 gene was found to comprise three exons, with its ORF located in the third exon. Only one transcription initiation and one termination site were found for this channel. In addition, the canine KCNJ2 and KCNJ12 gene structures were conserved amongst other vertebrates. Contrary to what has been described for SCN5A, no alternative splicing was observed for KCNJ2 and KCNJ12 genes (Houtman et al., 2012).

Such investigations may be extended to other channels. Thus, mutations in two mutually exclusive exons of the gene encoding the human cardiac L-type calcium channel ($Ca_V1.2$) were identified in patients with Timothy syndrome (TS) who exhibit prolonged QT interval and lethal cardiac arrhythmias. Splawski and collaborators have discovered that TS was associated with two $Ca_V1.2$ mutations, G406R and G402S. They are located in alternatively spliced exon 8A, encoding transmembrane segment S6 of domain I (Splawski et al., 2005). The spliced form of $Ca_V1.2$ containing exon 8 is highly expressed in heart and brain, accounting for approximately 80% of $Ca_V1.2$ mRNAs. G406R and G402S cause reduced channel inactivation, resulting in maintained depolarizing L-type calcium currents. These data indicate that gain-of-function mutations of $Ca_V1.2$ exons 8 and 8A cause TS. In contrast, the loss-of-function mutations of $Ca_V1.2$ channel in patients with Brugada syndrome produce short QT interval that could result in sudden cardiac death (Liao and Soong, 2010). Furthermore, recent reports revealed a linkage of $Ca_V1.2$ channel polymorphism with multiple central nervous system disorders including bipolar disorder, depression, and schizophrenia.

Nevertheless, the channels are not the only cases of genetic variability affecting gene splicing described to date. Thus, Refaat and collaborators have worked on the prevalence of mutations in the RNA splicing protein RBM20 in a large cohort of patients with dilated cardiomyopathy (DCM) (Refaat et al., 2011). The coding region and splice junctions of RBM20 were screened in subjects with DCM. Following this research, 2 common polymorphisms in this splice factor, rs942077 and rs35141404, were genotyped in all subjects. Although mutations in RBM20 were observed in approximately 3% of pathological subjects, no differences in survival, transplantation rate, and frequency of ICD therapy in mutation carriers were observed. Despite this apparently negative result, such studies should be generalized and extended to all the proteins involved directly or indirectly in the mechanism of splicing.

TRANSLATIONAL CONTROL BY miRNA AND ALTERNATIVE TRANSLATION

Improving our knowledge on molecular mechanisms of cardiac arrhythmias will also necessitate gaining knowledge on post-transcriptional mRNA regulation.

TRANSLATIONAL CONTROL BY miRNA

Noncoding RNA sequences, with incompletely understood function, appear to be involved in the post-transcriptional regulation by microRNAs (miRNA). The complexity of this regulation is still not completely understood and should represent a novel concept about combination of basic research and clinical application.

MiRNAs are small noncoding RNAs that regulate the expression of target 1) by a direct degradation of their target mRNA following a near-perfect hybridization, but this case is rare or 2) by binding to sequence that include the 3′ untranslated region (3′-UTR) of newly synthesized mRNA transcripts by a block of translation (**Figure 2**). The human genome is estimated to encode more than 1000 miRNAs, which are either transcribed as stand-alone transcripts, often encoding several miRNAs, or generated by the processing of protein coding gene introns. The miRNAs typically exert their inhibitory effects on several mRNAs, which often encode proteins that govern the same biologic process or several components of a molecular pathway.

Although published studies focusing on miRNAs and cardiac excitability are still sparse, recent articles have highlighted the role of miRNAs in cardiac rhythm through regulation of key ion channels, transporters, and cellular proteins in arrhythmogenic conditions (Kim, 2013). The available data from experimental studies demonstrate that miRNAs regulate numerous properties of cardiac excitability including conduction, repolarization, automaticity, Ca^{2+} handling, spatial heterogeneity, and apoptosis and fibrosis. To illustrate this post-transcriptional process, we have chosen to discuss about two suitable examples.

Drawnel and collaborators have described an interesting mutual antagonism between inositol 1,4,5′-triphosphate receptor II (IP_3RII) calcium channel and miRNA-133a. This antagonism regulates calcium signals and cardiac hypertrophy (Drawnel et al.,

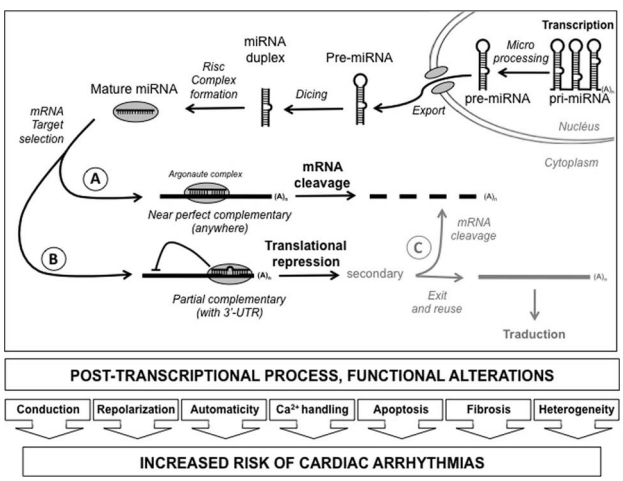

FIGURE 2 | Diagram depicting post-transcriptional process by miRNA. After their transcription, the pri-miRNA were matured in pre-miRNA and exported to cytoplasm. After digestion by dicer and Risc complex formation, the mRNA target selection can take place depending on the quality of the match. When the complementary is near perfect, throughout the length of the mRNA, cleavage of the messenger will take place leading to its degradation **(A)**. However, if the setting is only partial, usually in the 3′-untranslated region, a translational repression can take place without any degradation on the messenger **(B)**. Secondarily, it is possible for the cell to remove the inhibition and to reuse either definitively destroy the messenger **(C)** [*3′-UTR*: 3′-untranslated region; $(A)_n$: polyadenylation tail].

2012). Indeed, IP_3RII expression is increased in hypertrophic failing human myocardium. The ectopic calcium released from these receptors induces pro-hypertrophic gene expression and may promote arrhythmias. Drawnel and collaborators have investigated the mechanisms that produce up regulation of IP3RII during hypertrophic cardiomyocyte remodeling. This study clearly delineates an anti-hypertrophic role for miR133a that is intrinsic to the ventricular myocyte by maintaining low basal IP3RII expression. The authors have observed that decreased expression of miR-133a allows IP3RII expression to increase, thereby promoting hypertrophy. This maintains an appropriate level of myocyte growth until the balance between miR-133a and IP3RII is perturbed by pathological stimuli that elicit calcium signals. The authors have also described a deleterious positive feedback loop. Indeed, an increase in calcium signals sustains repression of miR-133a, providing a powerful driving force for pathological remodeling. In a relevant manner, other pro-hypertrophic positive feedback loops have been identified involving miRNAs and the signaling pathways that regulate their expression. This is the case for miR-1–dependent modulation of insulin-like growth factor-1 signaling (Elia et al., 2009) and miR-199b–mediated regulation of dual-specificity tyrosine phosphorylation-regulated kinase 1a (Dyrk1a), the NFAT negative regulatory kinase (da Costa Martins et al., 2010). When taken together, these studies indicate that several reciprocal regulatory loops may be active within the myocardium under pro-hypertrophic conditions. The potential clinical implications are interesting. Indeed, miR-133a activity *in vivo* is sufficient to mediate pathological cardiac growth. In particular, infusion of miR-133a antagomir (a miRNA blocker) is sufficient to induce hypertrophic remodeling in adult mice (Carè et al., 2007). However, things remain to be clarified as other authors have observed that miR-133a maintains cardiac function via anti-apoptotic and anti-fibrotic effects within the adult myocardium (Matkovich et al., 2010). But this observation does not take away the relevance of this mode of regulation in our arrhythmia issue.

To illustrate the cardiovascular consequences of this post-transcriptional regulation, we will focus on Friedreich ataxia (FRDA), which is an autosomal recessive neurodegenerative disease arising from mutations in both alleles of the frataxin gene (FXN). In approximately 97% of cases the mutant alleles have an expansion of a GAA trinucleotide repeat in intron 1 of FXN that reduces the amount of frataxin available to assist with mitochondrial iron efflux and increases sensitivity to oxidative stress, resulting in cell damage and death due to excess production of free radicals (Cossee et al., 1997; Wong et al., 1999). As well as the neurological features of the disease, a large proportion of FRDA patients develop cardiac abnormalities of cardiac structure or function. Indeed, heart failure and cardiac arrhythmias are thought to be the most important causes of death in FRDA (De Michele et al., 1996).

Kelly and collaborators have used a tag SNP approach to investigate the association of genetic variability in three important genes of the Renin–Angiotensin–Aldosterone system (RAAS) with measures of cardiac phenotype severity in FRDA (Kelly et al., 2011). The genes selected for investigation were AGTR1, which encodes AT1R, the predominant angiotensin-II receptor in the cardiovascular system, and the ACE and ACE2 genes, which encode the converting enzymes directly involved in the production and degradation of angiotensin-II. On the basis of this investigation, the authors have identified rs5186, a SNP in AGTR1, as a potential modifier of the cardiac phenotype in a large population of FRDA patients. The rs5186 SNP is a functional A/C polymorphism that occurs in the target sequence of a regulatory microRNA, miR-155, in the 3′ untranslated region of AGTR1 (Martin et al., 2007). However, the rs5186 C allele interrupts base-pair complementarily between miR-155 and the cis-regulatory target site, decreasing the ability of miR-155 to bind, thereby increasing the expression of AT1R (Kelly et al., 2011). The unexpected and intriguing finding of this study was that the C allele of rs5186 was more common in this cohort of FRDA patients than in a healthy control population. Further investigation of the prevalence and cardiovascular effects of rs5186 in other large FRDA populations is required, but it appears that this polymorphism should present a protective effect, resulting in increased survival. Indeed, the prohypertrophic cardiac effects assigned to this polymorphism, confer a survival advantage for FRDA patients that present this SNP. Future studies have to assess the activity of miR-155 in FRDA patients, as it is the likely mechanism by which rs5186 modifies the cardiac phenotype, but these observations underline the importance of this mode of regulation in cardiovascular remodeling. Despite many recent article withdrawals, the current literature on miRNAs is rich and alterations of this mode of post-transcriptional regulation need to be systematically studied in our investigations of arrhythmia mechanisms.

ALTERNATIVE TRANSLATION

Another molecular mechanism potentially allowing a single mRNA to produce several proteins is alternative translation (for review, see Kochetov, 2008).

It is widely established that an eukaryotic mRNA typically contains one translation start site and encodes a single functional protein product. In mammalian translation systems the consensus sequence is "GCCRCCAUGG" in positions near the start AUG codon (Kozak, 2005). However, it is now well-documented that a single mRNA may code for multiple proteins based on utilization of alternative initiation codons. "Non-AUG codons," as well as the classical AUG start codon, should be jointly considered in mechanisms for translation of mRNAs. These "non-AUG codons" are represented by the codons CUG, GUG, UUG, AUA, and ACG. These alternative Translation Initiation Sites (aTIS) give new opportunities to the cell for their protein synthesis by increasing the number of functionally novel protein isoforms encoded by genes, which present non-AUG codons. However, open-reading frames started from alternative start codons can commonly be located in different positions. The proteins resulting from these aTIS can be unrelated. Nevertheless, in most cases, the "non-AUG codons" respect the main ORF and lead to the synthesis of either N-end truncated or N-end extended isoforms of the CDS-encoded protein, commonly rather small. At the sight of this new knowledge, polymorphisms or mutations located within or downstream of the canonical ATG codon of candidate sequences should be studied with renewed interest.

It is well-established that the N-end segment of proteins frequently contains secretory signals. Thus, these isoforms can differ in the protein N-end segment and may be delivered to different compartments and present different subcellular localizations. In this context, this process takes all its full meaning for channel trafficking. One should nevertheless be cautious about any rapid conclusion. Indeed, channels have the added complexity of possessing several transmembrane spanning domains with numerous signal sequences, not restricted to the amino terminal, to be targeted to plasma membrane. For example, Lu and collaborators have described that multiple topogenic determinants cooperate during Kv1.3 voltage-gated K^+ channel translocation. Only the transmembrane segment S2 likely functions as the initial signal sequence to determine Kv1.3 N-terminus topology (Tu et al., 2000). Thus, the changes in the N-terminus portion of a given channel by aTIS cannot always explain alone the channel trafficking defect. So in this context, aTIS identification must be taken into account with caution on an individual basis according to the considered channel.

Numerous mammalian regulatory proteins utilize aTIS as critical regulators that control distinct biological functions like metabolism, intracellular signal transduction, transcription and gene expression, growth mechanisms, and related cellular functions (Kochetov, 2008). And the number of experimentally verified examples of alternative translation is growing rapidly.

Nevertheless, it should be noted that alternative translation initiation is a rare process in mammalian mRNA. In this context, bioinformatics evaluations of 5′-UTR sequences of mammalian mRNAs will represent a critical opportunity to characterize new aTIS in mRNA sequences that have been experimentally involved in pathologies. In the field of ion channels, a computational analysis of aTIS performed by Wegrzyn and collaborators a few years ago suggested that the calcium channel γ8 ancillary subunit (CACNG8) contains at least one alternative initiation site (Wegrzyn et al., 2008). This protein was recently identified as a regulator of the main human heart L-type calcium channel, $Ca_V1.2$ (Yang et al., 2011). Other genes involved in cardiovascular functions, such as the Vascular Endothelial Growth Factor (VEGF) have also been shown to contain aTIS (Wegrzyn et al., 2008). The ability to define aTIS through computational analyses can be of high importance for genomic analyses to provide full predictions of translated mammalian and human gene products required for cellular functions in health and disease. Whether aTIS plays a role in cardiac electrical activity and more broadly in cardiovascular physiopathology remains an open question.

POST-TRANSLATIONAL MODIFICATIONS AND TRAFFICKING

A recent bibliography reflects quite well this mode of regulation. Post-translational modification of cardiac ion channels is a cellular mechanism for maintaining the rhythmicity of the heartbeat. Therefore, several studies have made it clear that extensive post-translational modifications may modulate cardiac channel expression levels, localization, and gating.

The glycosylation is one of the most common post-translational modifications. The Nav1.5 protein harbors multiple evolutionary conserved amino acid motifs for N-glycosylation in its extracellular domain. Although the precise molecular composition of the N-glycans in cardiomyocytes and their attachment sites have not been determined yet, their presences in cardiac Nav1.5 and impact on channel gating have been recognized. Thus, Zang and collaborators have described that glycosylation influences voltage-dependent gating of cardiac and skeletal muscle sodium channels (Zhang et al., 1999). The contribution of sugar residues to channel gating was examined in transfected cells pretreated with various glycosidase and enzyme inhibitors to deglycosylate channel proteins. Pretreating transfected cells caused depolarizing shifts of steady-state activation of hH1a (human isoform of Nav1.5). These data clearly suggested that glycosylation differentially regulates sodium channel function in heart and skeletal muscle myocytes. The same observation was done for the adult rat ventricular myocytes (Stocker and Bennett, 2006). In this context, Johnson and collaborators have described interesting observations on the glycosylation of β-1 subunit of voltage-gated sodium channels (Nav) (Johnson et al., 2004). Nav are composed of a pore-forming alpha subunit and often one to several modulating beta subunits. The fully sialylated ß1 subunit induces a uniform hyperpolarizing shift in steady state and kinetic gating of the cardiac and two neuronal alpha subunit isoforms. Moreover, Johnson and collaborators have observed that under conditions of reduced sialylation, the ß1-induced gating effect was eliminated. These observations are consistent with the fact that the mutation of ß1 N-glycosylation sites abolished all effects of ß1 on channel gating. Thus, as it has been shown that glycosylation could differ according to the location within the heart tissue (Montpetit et al., 2009) and as electrical remodeling in cardiac disease is usually ascribed to altered expression and distribution of ion channel proteins such as Nav1.5, the location of any mutation in these consensus sites of modification should be considered as probable causes of arrhythmia occurrence.

This type of argument can obviously be extended to other channels. Chandrasekhar has recently described that an essential regulatory subunit of the cardiac I_{Ks} potassium channel complex, KCNE1, is glycosylated at threonine-7 *in vivo* (Chandrasekhar et al., 2011). Mutations that prevent glycosylation at this amino acid result in I_{Ks} channel complexes that are unable to efficiently traffic to the plasma membrane. Indeed, examination of these mutants revealed that complexes that lack N-terminal glycans adjacent to the N-terminus were functionally similar to wild type (WT), but had significantly reduced cell surface expression. Thus, mutations on threonine-7 directly suppress the O-glycosylation site and have a dramatic effect on biogenesis and anterograde trafficking of the protein complex, yielding unglycosylated and mono-N-glycosylated complexes that are trafficking defective and compromised, respectively. These observations provide a cellular mechanism for a KCNE1 mutation on threonine-7 that may be associated with cardiac arrhythmias.

The glycosylation is a critical regulation, but other types of post-translational modifications are not to be neglected, such as phosphorylation. In this context, Nav1.5 and ß-adrenergic receptors colocalize to caveolin domains that participate in membrane trafficking. Yarbrough and collaborators have shown that under stimulation of beta-adrenergic receptors, a mechanism involving the alpha subunit of the stimulatory heterotrimeric G-protein,

Galpha(s), promotes the presentation of cardiac sodium channels associated with caveolar membranes to the sarcolemma, leading to an increase in sodium current amplitude (Yarbrough et al., 2002). In addition, Zhou and collaborators have demonstrated that the activation of cAMP-dependent protein kinase (protein kinase A) secondary to the stimulation of beta-adrenergic receptors can potentiate I_{Na} by two processes: a fast saturable and a slow unsaturable component. The fast component involves direct channel phosphorylation events regulating the kinetics and voltage dependence of channel gating, while the slow component of PKA-dependent I_{Na} potentiation is due to enhanced trafficking and insertion of additional functional channels into the membrane. It should be noted that the I-II cytoplasmic interdomain linker loop is critical for this effect (Zhou et al., 2000). However, other critical sites have been characterized. The I-II interdomain linker of the channel contains 3 sites with the RXR motif known to mediate retention of proteins in the endoplasmic reticulum. The PKA-mediated increase in Na^+ current was completely abolished when all 3 sites were eliminated (Zhou et al., 2002). These results demonstrate that both phosphorylation and the presence of putative ER retention signals are required for the PKA-mediated increase in cardiac Na^+ current. These observations may have important physiological consequences for the increase in cardiac conduction velocity observed with sympathetic stimulation and the genesis of re-entrant arrhythmias in ischemic myocardium. Herren and collaborators focussed on the molecular and functional aspects of Na^+ channel phosphorylation, which is potentiated in heart failure and has been causally linked to cardiac arrhythmias (Herren et al., 2013).

The oxidation/nitrosylation is also one of the critical and ubiquitous post-translational modification systems for the regulation of cardiac ion channels (for reviews Gonzalez et al., 2009; Herren et al., 2013). S-nitrosylation consists of the addition of a nitric oxyde (NO) group to the thiol moiety of a cysteine residue. Several ion channels are reportedly redox responsive. For example, Xu and collaborators have explored the mechanism of NO action on the cardiac calcium release channel, of the sarcoplasmic reticulum, the type 2 ryanodine receptor (Xu et al., 1998). They have described that the S-nitrosylation led to progressive channel activation, which was reversed by denitrosylation. In contrast, its oxidation had no effect. So this channel can differentiate nitrosative from oxidative signals. The authors suggest that NO and related molecules may regulate excitation-contraction coupling through discrete mechanisms. On the one hand, they can inhibit the L-type channel via cGMP; on the other hand, they sensitize the muscle to Ca^{2+}-induced Ca^{2+} release. So the cardiac ion channels subserving excitation-contraction coupling are potentially regulated by S- nitrosylation. In the same way, the sodium channel is rich in cysteine and the metabolic state is also intimately coupled to sodium current. However, this process appears to have tissue specificity. Indeed, a full S-nitrosylation motif of the acid base type is found in the Nav of sensory neurons, but only partial in the heart (Li et al., 1998). As for the ryanodine receptor, it is possible that beside S-nitrosylation, Nav channels could be regulated also by cysteine oxidation (Evans and Bielefeldt, 2000). Ueda and collaborators have described an association of this post-translational regulation with inherited long QT syndrome (Ueda et al., 2008). They have identified a missense mutation by direct sequencing of the gene encoding alpha1-syntrophin (SNTA1), a member of the dystrophin-associated proteins normally serving as a scaffold protein for the neuronal nitric oxide synthase (nNOS) and the plasmalemmal calcium pump PMCA, an interaction that results in inhibition of NO production. The SNTA1 is also known to associate with Nav1.5. Syntrophin mutation results in a disruption of the PMCA-NOS1 complex and favors interaction of NOS1 with the Na^+ channel. Release of PMCA increases NOS1 activity promoting S-nitrosylation of Nav1.5 and thereby increasing late Na^+ currents at the origin of LQTS-susceptibility.

Another interesting mechanism is the potential dominant-negative effect due to a heterozygous expression of a mutated form. Type 2 long QT syndrome involves mutations in the human ether a-go-go–related gene (hERG or KCNH2) (Keller et al., 2005), which encodes Kv11.1 channel. Kv11.1 channel current, because of its unique slow activation and deactivation gating kinetics relative to its rapid kinetics of inactivation and recovery from inactivation, plays a significant role in late repolarization in the mammalian heart. As T421M, a mutation in the S1 transmembrane spanning domain of Kv11.1, was identified in a resuscitated patient, Balijepalli and co-authors have assessed its biophysical, protein trafficking, and pharmacological consequences in adult rat ventricular myocytes (Balijepalli et al., 2012). The T421M mutation markedly altered the voltage dependence and kinetics of both Kv11.1 activation and deactivation but had minimal effects on the rates of inactivation and recovery from inactivation. Furthermore, interestingly, for coexpressed wild-type and T421M-Kv11.1 channels, different dominant-negative interactions govern protein trafficking and ion channel gating, and these are likely to be reflected in the clinical phenotype.

Malfunction may also result from defects in the multiprotein machinery specialized in channel membrane targeting. In this context, Wu and collaborators have described MOG1, a small protein that is highly conserved from yeast to human, as a critical co-factor for Nav1.5. This protein, expressed in both atrial and ventricular tissues with predominant localization at the intercalated discs, can modulate the function of Nav1.5 (Wu et al., 2008). MOG1, which interacts physically with Nav1.5, increases sodium current density by an increase in the number and/or availability of Nav1.5 on cell surface. In addition to increased trafficking of Nav1.5 to the plasma membrane, MOG1 may reduce the turnover of Nav1.5 localized on the plasma membrane.

Thus, genetic mutations in MOG1 may affect the expression and function of Nav1.5, leading to Brugada syndrome or other types of lethal arrhythmias. Indeed, Kattygnarath and collaborators have reported by genetic screening that the MOG1 missense mutation E83D could affect Nav1.5 activity and provide molecular and clinical evidence that this MOG1 loss-of-function mutation is linked to Brugada syndrome physiopathology (Kattygnarath et al., 2011). As expected, this mutant exerted a dominant-negative effect on wild-type MOG1 and reduced Nav1.5 channel trafficking to the cell surface. Similarly, Olesen and collaborators have screened MOG1 for variants in 197 young patients with lone atrial fibrillation and 23 patients with Brugada syndrome and identified a novel nonsense variant mediating a

premature stop codon, p.E61X (Olesen et al., 2011). Their heterologous expression data on p.E61X mutant showed MOG1 loss of function. This mutant completely failed to increase the sodium channel current compared to wild-type MOG1. Nevertheless, this variant seemed to have a higher frequency in patients compared to control subjects but the difference was not statistically significant. Also in this context, Chakrabarti and collaborators have recently hypothesized that MOG1 can serve as a therapeutic target for sodium channelopathies. They have observed that this co-factor can enhance plasma membranes trafficking of mutant sodium channels and rescue the reduced sodium current associated with Nav1.5 mutations leading defects in trafficking (Chakrabarti et al., 2013). These results indicate that MOG1 could also be a potential Brugada syndrome modifier gene and could explain part of the variable penetrance of the pathology. MOG1 is not the only example of modulation of trafficking for Nav1.5 by a chaperone protein. For example, Ishikawa and collaborators have found that two missense mutations in the gene encoding the sarcolemmal membrane-associated protein (SLMAP), Val269Ile and Glu710Ala, affect Nav1.5 membrane surface expression (Ishikawa et al., 2012). These mutations in SLMAP, which ultimately reduce Nav1.5 current, may cause Brugada syndrome via modulating the intracellular trafficking of Nav1.5.

These defaults of trafficking caused by mutations have been described for many other cardiac ion channels, including KCNQ1 potassium channel, Sato and collaborators have investigated the functional alterations caused by 2 KCNQ1 mutations, a deletion (delV595) and a frameshift (P631fs/19), which were identified in patients with autosomal-recessive LQTS not accompanied by hearing loss (Sato et al., 2009). Functional analyses showed that both mutations impaired cell surface expression due to trafficking defects. The mutations severely affected outward potassium current. It was found that delV595 impaired the binding and assembly of KCNQ1 subunits, whereas the P631fs/19 mutant channel was retained in endoplasmic reticulum due to the newly added 19-amino acid sequence containing two retention motifs (R(633)GR and R(646)LR. In the same manner, a channel may present multiple kinds of abnormalities. Limberg and collaborators have identified two novel heterozygous KCNJ2 mutations (p.N318S, p.W322C) located in the C-terminus of the Kir2.1 potassium channel subunit in a large set of patients with congenital long-QT syndrome (Limberg et al., 2013). While the N318S mutants regularly reached the plasma membrane, W322C mutants primarily resided in late endosomes. The co-expression of N318S or W322C with wild-type Kir2.1 reduced current amplitudes by 20–25% due to defective channel trafficking (W322C) or gating (N318S). Thus, understanding the dynamics of cardiac channel surface expression and their potential trafficking abnormality has become even more essential.

CONCLUSIONS

Thus, at the sight of the multiplicity of mechanisms regulating ion channel protein expression, such as gene transcription, RNA processing, post-transcriptional control of gene expression by miRNA, protein synthesis, assembly and post-translational modification and trafficking, polymorphisms possibly affecting these mechanisms should be investigated in our work of understanding new processes at the origin of arrhythmogenesis, not only as phenotype modulators of genetically-inherited arrhythmias, but also as putative a arrhythmic substrates in more common diseases such as cardiac hypertrophy and heart failure.

REFERENCES

Amin, A. S., Pinto, Y. M., and Wilde, A. A. (2013). Long QT syndrome: beyond the causal mutation. *J. Physiol.* doi: 10.1113/jphysiol.2013.254920. [Epub ahead of print].

Anumonwo, J. M., and Lopatin, A. N. (2010). Cardiac strong inward rectifier potassium channels. *J. Mol. Cell. Cardiol.* 48, 45–54. doi: 10.1016/j.yjmcc.2009.08.013

Anvari, A., Schuster, E., Gottsauner-Wolf, M., Wojta, J., and Huber, K. (2001). PAI-I 4G/5G polymorphism and sudden cardiac death in patients with coronary artery disease. *Thromb. Res.* 103, 103–107. doi: 10.1016/S0049-3848(01)00277-8

Arking, D. E., Chugh, S. S., Chakravarti, A., and Spooner, P. M. (2004). Genomics in sudden cardiac death. *Circ. Res.* 94, 712–723. doi: 10.1161/01.RES.0000123861.16082.95

Arking, D. E., and Sotoodehnia, N. (2012). The genetics of sudden cardiac death. *Annu. Rev. Genomics Hum. Genet.* 13, 223–239. doi: 10.1146/annurev-genom-090711-163841

Balijepalli, S. Y., Lim, E., Concannon, S. P., Chew, C. L., Holzem, K. E., Tester, D. J., et al. (2012). Mechanism of loss of Kv11.1 K+ current in mutant T421M-Kv11.1-expressing rat ventricular myocytes: interaction of trafficking and gating. *Circulation* 126, 2809–2818. doi: 10.1161/CIRCULATIONAHA.112.118018

Basso, C., Bauce, B., Corrado, D., and Thiene, G. (2011). Pathophysiology of arrhythmogenic cardiomyopathy. *Nat. Rev. Cardiol.* 9, 223–233. doi: 10.1038/nrcardio.2011.173

Bezzina, C., Veldkamp, M. W., van Den Berg, M. P., Postma, A. V., Rook, M. B., Viersma, J. W., et al. (1999). A single Na(+) channel mutation causing both long-QT and Brugada syndromes. *Circ. Res.* 85, 1206–1213. doi: 10.1161/01.RES.85.12.1206

Bezzina, C. R., Shimizu, W., Yang, P., Koopmann, T. T., Tanck, M. W., Miyamoto, Y., et al. (2006). Common sodium channel promoter haplotype in asian subjects underlies variability in cardiac conduction. *Circulation* 113, 338–344. doi: 10.1161/CIRCULATIONAHA.105.580811

Borlak, J., and Thum, T. (2003). Hallmarks of ion channel gene expression in end-stage heart failure. *FASEB J.* 17, 1592–1608. doi: 10.1096/fj.02-0889com

Brion, M., Quintela, I., Sobrino, B., Torres, M., Allegue, C., and Carracedo, A. (2010). New technologies in the genetic approach to sudden cardiac death in the young. *Forensic Sci. Int.* 203, 15–24. doi: 10.1016/j.forsciint.2010.07.015

Calloe, K., Refaat, M. M., Grubb, S., Wojciak, J., Campagna, J., Thomsen, N. M., et al. (2013). Characterization and mechanisms of action of novel NaV1.5 channel mutations associated with Brugada syndrome. *Circ. Arrhythm. Electrophysiol.* 6, 177–184. doi: 10.1161/CIRCEP.112.974220

Carè, A., Catalucci, D., Felicetti, F., Bonci, D., Addario, A., Gallo, P., et al. (2007). MicroRNA-133 controls cardiac hypertrophy. *Nat. Med.* 13, 613–618. doi: 10.1038/nm1582

Chakrabarti, S., Wu, X., Yang, Z., Wu, L., Yong, S. L., Zhang, C., et al. (2013). MOG1 rescues defective trafficking of Nav1.5 mutations in brugada syndrome and sick sinus syndrome. *Circ Arrhythm. Electrophysiol.* 6, 392–401. doi: 10.1161/CIRCEP.111.000206

Chandrasekhar, K. D., Lvov, A., Terrenoire, C., Gao, G. Y., Kass, R. S., and Kobertz, W. R. (2011). O-glycosylation of the cardiac I(Ks) complex. *J. Physiol.* 589(Pt 15), 3721–3730.

Chang, Y. F., Imam, J. S., and Wilkinson, M. F. (2007). The nonsense-mediated decay RNA surveillance pathway. *Annu. Rev. Biochem.* 76, 51–74. doi: 10.1146/annurev.biochem.76.050106.093909

Chen, J.-Y., Liou, Y.-M., Wu, H.-D. I., Lin, K.-H., and Chang, K.-C. (2012). Promoter polymorphism G-6A, which modulates angiotensinogen gene expression, is associated with non-familial sick sinus syndrome. *PLoS ONE* 7:e29951. doi: 10.1371/journal.pone.0029951

Chioni, A. M., Shao, D., Grose, R., and Djamgoz, M. B. (2010). Protein kinase A and regulation of neonatal Nav1.5 expression in human breast cancer cells: activity-dependent positive feedback and cellular migration. *Int. J. Biochem. Cell. Biol.* 42, 346–358. doi: 10.1016/j.biocel.2009.11.021

Choudhary, G., and Dudley, S. C. Jr. (2002). Heart failure, oxidative stress, and ion channel modulation. *Congest. Heart Fail.* 8, 148–155. doi: 10.1111/j.1527-5299.2002.00716.x

Cossee, M., Schmitt, M., Campuzano, V., Reutenauer, L., Moutou, C., Mandel, J. L., et al. (1997). Evolution of the Friedreich's ataxia trinucleotide repeat expansion: founder effect and premutations. *Proc. Natl. Acad. Sci. U.S.A.* 94, 7452–7457. doi: 10.1073/pnas.94.14.7452

Cross, B. J., Estes, N. A. 3rd., and Link, M. S. (2011). Sudden cardiac death in young athletes and nonathletes. *Curr. Opin. Crit. Care* 17, 328–334. doi: 10.1097/MCC.0b013e328348bf84

da Costa Martins, P. A., Salic, K., Gladka, M. M., Armand, A.-S., Leptidis, S., el Azzouzi, H., et al. (2010). MicroRNA-199b targets the nuclear kinase Dyrk1a in an auto-amplification loop promoting calcineurin/NFAT signalling. *Nat. Cell Biol.* 12, 1220–1227. doi: 10.1038/ncb2126

De Michele, G., Perrone, F., Filla, A., Mirante, E., Giordano, M., De Placido, S., et al. (1996). Age of onset, sex, and cardiomyopathy as predictors of disability and survival in Friedreich's disease: a retrospective study on 119 patients. *Neurology* 5, 1260–1264. doi: 10.1212/WNL.47.5.1260

Derangeon, M., Montnach, J., Baró, I., and Charpentier, F. (2013). Mouse models of SCN5A-related cardiac arrhythmias. *Front. Physiol.* 3:210. doi: 10.3389/fphys.2012.00210

Dobrzynski, H., Boyett, M. R., and Anderson, R. H. (2007). New insights into pacemaker activity: promoting understanding of sick sinus syndrome. *Circulation* 115, 1921–1932. doi: 10.1161/CIRCULATIONAHA.106.616011

Drawnel, F. M., Wachten, D., Molkentin, J. D., Maillet, M., Aronsen, J. M., Swift, F., et al. (2012). Mutual antagonism between IP(3)RII and miRNA-133a regulates calcium signals and cardiac hypertrophy. *J. Cell. Biol.* 199, 783–798. doi: 10.1083/jcb.201111095

Elia, L., Contu, R., Quintavalle, M., Varrone, F., Chimenti, C., Russo, M. A., et al. (2009). Reciprocal regulation of microRNA-1 and insulin-like growth factor-1 signal transduction cascade in cardiac and skeletal muscle in physiological and pathological conditions. *Circulation* 120, 2377–2385. doi: 10.1161/CIRCULATIONAHA.109.879429

Evans, J. R., and Bielefeldt, K. (2000). Regulation of sodium currents through oxidation and reduction of thiol residues. *Neuroscience* 101, 229–236. doi: 10.1016/S0306-4522(00)00367-5

Farrelly, A. M., Ro, S., Callaghan, B. P., Khoyi, M. A., Fleming, N., Horowitz, B., et al. (2003). Expression and function of KCNH2 (HERG) in the human jejunum. *Am. J. Physiol. Gastrointest. Liver Physiol.* 284, G883–G895.

Firouzi, M., Ramanna, H., Kok, B., Jongsma, H. J., Koeleman, B. P., Doevendans, P. A., et al. (2004). Association of human connexin40 gene polymorphisms with atrial vulnerability as a risk factor for idiopathic atrial fibrillation. *Circ. Res.* 95, e29–e33. doi: 10.1161/01.RES.0000141134.64811.0a

Gao, G., Xie, A., Huang, S. C., Zhou, A., Zhang, J., Herman, A. M., et al. (2011). Role of RBM25/LUC7L3 in abnormal cardiac sodium channel splicing regulation in human heart failure. *Circulation* 124, 1124–1131. doi: 10.1161/CIRCULATIONAHA.111.044495

George, A. L. Jr. (2013). Molecular and genetic basis of sudden cardiac death. *J. Clin. Invest.* 123, 75–83. doi: 10.1172/JCI62928

Gong, Q., Zhang, L., Vincent, G. M., Horne, B. D., and Zhou, Z. (2007). Nonsense mutations in hERG cause a decrease in mutant mRNA transcripts by nonsense-mediated mRNA decay in human long-QT syndrome. *Circulation* 116, 17–24. doi: 10.1161/CIRCULATIONAHA.107.708818

Gonzalez, D. R., Treuer, A., Sun, Q. A., Stamler, J. S., and Hare, J. M. (2009). S-Nitrosylation of cardiac ion channels. *J. Cardiovasc. Pharmacol.* 54, 188–195. doi: 10.1097/FJC.0b013e3181b72c9f

Groenewegen, W. A., Firouzi, M., Bezzina, C. R., Vliex, S., van Langen, I. M., Sandkuijl, L., et al. (2003). A cardiac sodium channel mutation cosegregates with a rare connexin40 genotype in familial atrial standstill. *Circ. Res.* 92, 14–22. doi: 10.1161/01.RES.0000050585.07097.D7

Gu, W., Liu, J., Niu, Q., Wang, H., Lou, Y., Liu, K., et al. (2011). A-6G and A-20C polymorphisms in the angiotensinogen promoter and hypertension risk in Chinese: a meta-analysis. *PLoS ONE* 6:e29489. doi: 10.1371/journal.pone.0029489

Harkcom, W. T., and Abbott, G. W. (2010). Emerging concepts in the pharmacogenomics of arrhythmias: ion channel trafficking. *Expert Rev. Cardiovasc. Ther.* 8, 1161–1173. doi: 10.1586/erc.10.89

Herren, A. W., Bers, D. M., and Grandi, E. (2013). Post-translational modifications of the cardiac NA channel: contribution of CaMKII-dependent phosphorylation to acquired arrhythmias. *Am. J. Physiol. Heart Circ. Physiol.* 305, H431–H445. doi: 10.1152/ajpheart.00306.2013

Houtman, M. J., Takanari, H., Kok, B. G., van Eck, M., Montagne, D. R., Vos, M. A., et al. (2012). Experimental mapping of the canine KCNJ2 and KCNJ12 gene structures and functional analysis of the canine K(IR)2.2 ion channel. *Front. Physiol.* 3:9. doi: 10.3389/fphys.2012.00009

Hu, D., Viskin, S., Oliva, A., Carrier, T., Cordeiro, J. M., Barajas-Martinez, H., et al. (2007a). Novel mutation in the SCN5A gene associated with arrhythmic storm development during acute myocardial infarction. *Heart Rhythm.* 4, 1072–1080. doi: 10.1016/j.hrthm.2007.03.040

Hu, D., Viskin, S., Oliva, A., Cordeiro, J. M., Guerchicoff, A., Pollevick, G. D., et al. (2007b). Genetic predisposition and cellular basis for ischemia-induced ST-segment changes and arrhythmias. *J. Electrocardiol.* 40(6 Suppl.), S26–S29. doi: 10.1016/j.jelectrocard.2007.05.019

Ishikawa, T., Sato, A., Marcou, C. A., Tester, D. J., Ackerman, M. J., Crotti, L., et al. (2012). A novel disease gene for Brugada syndrome: sarcolemmal membrane-associated protein gene mutations impair intracellular trafficking of hNav1.5. *Circ. Arrhythm. Electrophysiol.* 5, 1098–1107. doi: 10.1161/CIRCEP.111.969972

Iwai, N., Shimoike, H., Nakamura, Y., Tamaki, S., and Kinoshita, M. (1998). The 4G/5G polymorphism of the plasminogen activator inhibitor gene is associated with the time course of the progression to acute coronary syndromes. *Atherosclerosis* 136, 109–114. doi: 10.1016/S0021-9150(97)00191-3

Janse, M. J. (2004). Electrophysiological changes in heart failure and their relationship to arrhythmogenesis. *Cardiovasc. Res.* 61, 208–217. doi: 10.1016/j.cardiores.2003.11.018

Johnson, D., Montpetit, M. L., Stocker, P. J., and Bennett, E. S. (2004). The sialic acid component of the beta1 subunit modulates voltage-gated sodium channel function. *J. Biol. Chem.* 279, 44303–44310. doi: 10.1074/jbc.M408900200

Kattygnarath, D., Maugenre, S., Neyroud, N., Balse, E., Ichai, C., Denjoy, I., et al. (2011). MOG1: a new susceptibility gene for Brugada syndrome. *Circ. Cardiovasc. Genet.* 4, 261–268. doi: 10.1161/CIRCGENETICS.110.959130

Keller, S. H., Platoshyn, O., and Yuan, J. X. (2005). Long QT syndrome-associated I593R mutation in HERG potassium channel activates ER stress pathways. *Cell Biochem. Biophys.* 43, 365–377. doi: 10.1385/CBB:43, 3:365

Kelly, M., Bagnall, R. D., Peverill, R. E., Donelan, L., Corben, L., Delatycki, M. B., et al. (2011). A polymorphic miR-155 binding site in AGTR1 is associated with cardiac hypertrophy in Friedreich ataxia. *J. Mol. Cell. Cardiol.* 51, 848–854. doi: 10.1016/j.yjmcc.2011.07.001

Kim, G. H. (2013). MicroRNA regulation of cardiac conduction and arrhythmias. *Transl. Res.* 161, 381–392. doi: 10.1016/j.trsl.2012.12.004

Kochetov, A. V. (2008). Alternative translation start sites and hidden coding potential of eukaryotic mRNAs. *Bioessays* 30, 683–691. doi: 10.1002/bies.20771

Kornblihtt, A. R., Schor, I. E., Alló, M., Dujardin, G., Petrillo, E., and Muñoz, M. J. (2013). Alternative splicing: a pivotal step between eukaryotic transcription and translation. *Nat. Rev. Mol. Cell Biol.* 14, 153–165. doi: 10.1038/nrm3525

Kozak, M. (2005). Regulation of translation via mRNA structure in prokaryotes and eukaryotes. *Gene* 361, 13–37. doi: 10.1016/j.gene.2005.06.037

Li, Z., Chapleau, M. W., Bates, J. N., Bielefeldt, K., Lee, H. C., and Abboud, F. M. (1998). Nitric oxide as an autocrine regulator of sodium currents in baroreceptor neurons. *Neuron* 20, 1039–1049. doi: 10.1016/S0896-6273(00)80484-5

Liao, P., and Soong, T. W. (2010). CaV1.2 channelopathies: from arrhythmias to autism, bipolar disorder, and immunodeficiency. *Pflugers Arch.* 460, 353–359. doi: 10.1007/s00424-009-0753-0

Limberg, M. M., Zumhagen, S., Netter, M. F., Coffey, A. J., Grace, A., Rogers, J., et al. (2013). Non dominant-negative KCNJ2 gene mutations leading to Andersen-Tawil syndrome with an isolated cardiac phenotype.

Basic Res. Cardiol. 108, 353. doi: 10.1007/s00395-013-0353-1

Maquat, L. E. (2004). Nonsense-mediated mRNA decay: splicing, translation and mRNP dynamics. *Nat. Rev. Mol. Cell Biol.* 5, 89–99. doi: 10.1038/nrm1310

Margaglione, M., Cappucci, G., Colaizzio, D., Giuliani, N., Vecchione, G., Grandone, E., et al. (1998). The PAI-1 gene locus 4G/5G polymorphism is associated with a family history of coronary artery disease. *Arterioscler. Thromb. Vasc. Biol.* 18, 152–156. doi: 10.1161/01.ATV.18.2.152

Martin, C. A., Huang, C. L., and Matthews, G. D. (2011). Recent developments in the management of patients at risk for sudden cardiac death. *Postgrad. Med.* 123, 84–94. doi: 10.3810/pgm.2011.03.2266

Martin, C. A., Matthews, G. D., and Huang, C. L. (2012). Sudden cardiac death and inherited channelopathy: the basic electrophysiology of the myocyte and myocardium in ion channel disease. *Heart* 98, 536–543. doi: 10.1136/heartjnl-2011-300953

Martin, M. M., Buckenberger, J. A., Jiang, J., Malana, G. E., Nuovo, G. J., Chotani, M., et al. (2007). The human angiotensin II type 1 receptor +1166 A/C polymorphism attenuates microrna-155 binding. *J. Biol. Chem.* 282, 24262–24269. doi: 10.1074/jbc.M701050200

Matkovich, S. J., Wang, W., Tu, Y., Eschenbacher, W. H., Dorn, L. E., Condorelli, G., et al. (2010). MicroRNA-133a protects against myocardial fibrosis and modulates electrical repolarization without affecting hypertrophy in pressure-overloaded adult hearts. *Circ. Res.* 106, 166–175. doi: 10.1161/CIRCRESAHA.109.202176

Matoulkova, E., Michalova, E., Vojtesek, B., and Hrstka, R. (2012). The role of the 3′ untranslated region in post-transcriptional regulation of protein expression in mammalian cells. *RNA Biol.* 9, 563–576. doi: 10.4161/rna.20231

McNally, E. M., Golbus, J. R., and Puckelwartz, M. J. (2013). Genetic mutations and mechanisms in dilated cardiomyopathy. *J. Clin. Invest.* 123, 19–26. doi: 10.1172/JCI62862

Mittleman, M. A., and Mostofsky, E. (2011). Physical, psychological and chemical triggers of acute cardiovascular events: preventive strategies. *Circulation* 124, 346–354. doi: 10.1161/CIRCULATIONAHA.110.968776

Montpetit, M. L., Stocker, P. J., Schwetz, T. A., Harper, J. M., Norring, S. A., Schaffer, L., et al. (2009). Regulated and aberrant glycosylation modulate cardiac electrical signaling. *Proc. Natl. Acad. Sci. U.S.A.* 106, 16517–16522. doi: 10.1073/pnas.0905414106

Moro, C., Hernandez-Madrid, A., and Matia, R. (2010). Non-antiarrhythmic drugs to prevent atrial fibrillation. *Am. J. Cardiovasc. Drugs* 10, 165–173. doi: 10.2165/11537270-000000000-00000

Nagy, E., and Maquat, L. E. (1998). A rule for termination-codon position within intron-containing genes: when nonsense affects RNA abundance. *Trends Biochem. Sci.* 23, 198–199. doi: 10.1016/S0968-0004(98)01208-0

Nattel, S., Frelin, Y., Gaborit, N., Louault, C., and Demolombe, S. (2010). Ion-channel mRNA-expression profiling: insights into cardiac remodeling and arrhythmic substrates. *J. Mol. Cell Cardiol.* 48, 96–105. doi: 10.1016/j.yjmcc.2009.07.016

Olesen, M. S., Jensen, N. F., Holst, A. G., Nielsen, J. B., Tfelt-Hansen, J., Jespersen, T., et al. (2011). A novel nonsense variant in Nav1.5 cofactor MOG1 eliminates its sodium current increasing effect and may increase the risk of arrhythmias. *Can. J. Cardiol.* 27, 523.e17–523.e23. doi: 10.1016/j.cjca.2011.01.003

Oliva, A., Hu, D., Viskin, S., Carrier, T., Cordeiro, J. M., Barajas-Martinez, H., et al. (2009). SCN5A mutation associated with acute myocardial infarction. *Leg. Med. (Tokyo)* 11(Suppl. 1), S206–S209. doi: 10.1016/j.legalmed.2009.02.044

Onkal, R., and Djamgoz, M. B. (2009). Molecular pharmacology of voltage-gated sodium channel expression in metastatic disease: clinical potential of neonatal Nav1.5 in breast cancer. *Eur. J. Pharmacol.* 625, 206–219. doi: 10.1016/j.ejphar.2009.08.040

Onkal, R., Mattis, J. H., Fraser, S. P., Diss, J. K., Shao, D., Okuse, K., et al. (2008). Alternative splicing of Nav1.5: an electrophysiological comparison of 'neonatal' and 'adult' isoforms and critical involvement of a lysine residue. *J. Cell Physiol.* 216, 716–726. doi: 10.1002/jcp.21451

Park, J. K., Martin, L. J., Zhang, X., Jegga, A. G., and Benson, D. W. (2012). Genetic variants in SCN5A promoter are associated with arrhythmia phenotype severity in patients with heterozygous loss-of-function mutation. *Heart Rhythm* 9, 1090–1096. doi: 10.1016/j.hrthm.2012.02.023

Rasmussen-Torvik, L. J., North, K. E., Gu, C. C., Lewis, C. E., Wilk, J. B., Chakravarti, A., et al. (2005). A population association study of angiotensinogen polymorphisms and haplotypes with left ventricular phenotypes. *Hypertension* 46, 1294–1299. doi: 10.1161/01.HYP.0000192653.17209.84

Ravens, U., and Wettwer, E. (2011). Ultra-rapid delayed rectifier channels: molecular basis and therapeutic implications. *Cardiovasc. Res.* 89, 776–785. doi: 10.1093/cvr/cvq398

Refaat, M. M., Lubitz, S. A., Makino, S., Islam, Z., Frangiskakis, J. M., Mehdi, H., et al. (2011). Genetic variation in the alternative splicing regulator RBM20 is associated with dilated cardiomyopathy. *Heart Rhythm* 9, 390–396. doi: 10.1016/j.hrthm.2011.10.016

Remme, C. A. (2013a). Transgenic models of cardiac arrhythmias and sudden death. *Front. Physiol.* 4:60. doi: 10.3389/fphys.2013.00060

Remme, C. A. (2013b). Cardiac sodium channelopathy associated with SCN5A mutations: electrophysiological, molecular and genetic aspects. *J. Physiol.* doi: 10.1113/jphysiol.2013.256461. [Epub ahead of print].

Remme, C. A., Scicluna, B. P., Verkerk, A. O., Amin, A. S., van Brunschot, S., Beekman, L., et al. (2009). Genetically determined differences in sodium current characteristics modulate conduction disease severity in mice with cardiac sodium channelopathy. *Circ. Res.* 104, 1283–1292. doi: 10.1161/CIRCRESAHA.109.194423

Remme, C. A., Verkerk, A. O., Nuyens, D., van Ginneken, A. C., van Brunschot, S., Belterman, C. N., et al. (2006). Overlap syndrome of cardiac sodium channel disease in mice carrying the equivalent mutation of human SCN5A-1795insD. *Circulation* 114, 2584–2594. doi: 10.1161/CIRCULATIONAHA.106.653949

Remme, C. A., and Wilde, A. A. M. (2008). SCN5A overlap syndromes: no end to disease complexity? *Europace* 10, 1253–1255. doi: 10.1093/europace/eun267

Rook, M. B., Evers, M. M., Vos, M. A., and Bierhuizen, M. F. (2012). Biology of cardiac sodium channel Nav1.5 expression. *Cardiovasc. Res.* 93, 12–23. doi: 10.1093/cvr/cvr252

Sato, A., Arimura, T., Makita, N., Ishikawa, T., Aizawa, Y., Ushinohama, H., et al. (2009). Novel mechanisms of trafficking defect caused by KCNQ1 mutations found in long QT syndrome. *J. Biol. Chem.* 284, 35122–35133. doi: 10.1074/jbc.M109.017293

Schroeter, A., Walzik, S., Blechschmidt, S., Haufe, V., Benndorf, K., and Zimmer, T. (2010). Structure and function of splice variants of the cardiac voltage-gated sodium channel Nav1.5. *J. Mol. Cell Cardiol.* 49, 16–24. doi: 10.1016/j.yjmcc.2010.04.004

Scicluna, B. P., Tanck, M. W., Remme, C. A., Beekman, L., Coronel, R., Wilde, A. A., and Bezzina, C. R. (2011). Quantitative trait loci for electrocardiographic parameters and arrhythmia in the mouse. *J. Mol. Cell. Cardiol.* 50, 380–389. doi: 10.1016/j.yjmcc.2010.09.009

Scicluna, B. P., Wilde, A. A., and Bezzina, C. R. (2008). The primary arrhythmia syndromes: same mutation, different manifestations. Are we starting to understand why? *J. Cardiovasc. Electrophysiol.* 19, 445–452. doi: 10.1111/j.1540-8167.2007.01073.x

Shang, L. L., and Dudley, S. C. Jr. (2005). Tandem promoters and developmentally regulated 5′- and 3′-mRNA untranslated regions of the mouse SCN5A cardiac sodium channel. *J. Biol. Chem.* 280, 933–40. doi: 10.1074/jbc.M409977200

Shang, L. L., Pfahnl, A. E., Sanyal, S., Jiao, Z., Allen, J., Banach, K., et al. (2007). Human heart failure is associated with abnormal C-terminal splicing variants in the cardiac sodium channel. *Circ. Res.* 101, 1146–1154. doi: 10.1161/CIRCRESAHA.107.152918

Sheng, Z. H., Zhang, H., Barchi, R. L., and Kallen, R. G. (1994). Molecular cloning and functional analysis of the promoter of rat skeletal muscle voltage-sensitive sodium channel subtype 2 (rSkM2): evidence for muscle-specific nuclear protein binding to the core promoter. *DNA Cell Biol.* 13, 9–23. doi: 10.1089/dna.1994.13.9

Splawski, I., Timothy, K. W., Decher, N., Kumar, P., Sachse, F. B., Beggs, A. H., et al. (2005). Severe arrhythmia disorder caused by cardiac L-type calcium channel mutations. *Proc. Natl. Acad. Sci. U.S.A.* 102, 8089–8096. doi: 10.1073/pnas.0502506102

Stocker, P. J., and Bennett, E. S. (2006). Differential sialylation modulates voltage-gated Na+ channel gating throughout the developing myocardium. *J. Gen. Physiol.* 127, 253–265. doi: 10.1085/jgp.200509423

Stump, M. R., Gong, Q., Packer, J. D., and Zhou, Z. (2012). Early LQT2 nonsense mutation generates N-terminally truncated hERG channels with altered gating properties by the reinitiation of translation. *J. Mol. Cell Cardiol.* 53, 725–733. doi: 10.1016/j.yjmcc.2012.08.021

Tu, L., Wang, J., Helm, A., Skach, W. R., and Deutsch, C. (2000). Transmembrane biogenesis of Kv1.3. *Biochemistry* 39, 824–836. doi: 10.1021/bi991740r

Ueda, K., Valdivia, C., Medeiros-Domingo, A., Tester, D. J., Vatta, M., Farrugia, G., et al. (2008). Syntrophin mutation associated with long QT syndrome through activation of the nNOS-SCN5A macromolecular complex. *Proc. Natl. Acad. Sci. U.S.A.* 105, 9355–9360. doi: 10.1073/pnas.0801294105

Valdivia, C. R., Chu, W. W., Pu, J., Foell, J. D., Haworth, R. A., Wolff, M. R., et al. (2005). Increased late sodium current in myocytes from a canine heart failure model and from failing human heart. *J. Mol. Cell Cardiol.* 38, 475–483. doi: 10.1016/j.yjmcc.2004.12.012

Van Stuijvenberg, L., Yildirim, C., Kok, B. G. J. M., Van Veen, T. A. B., Varro, A., Winckels, S. K. G., et al. (2010). Alternative promoter usage and splicing of the human SCN5A gene contribute to transcript heterogeneity. *DNA Cell Biol.* 29, 577–587. doi: 10.1089/dna.2009.0999

Watkins, W. S., Rohrwasser, A., Peiffer, A., Leppert, M. F., Lalouel, J. M., and Jorde, L. B. (2010). AGT genetic variation, plasma AGT, and blood pressure: an analysis of the Utah Genetic Reference Project pedigrees. *Am. J. Hypertens.* 23, 917–923. doi: 10.1038/ajh.2010.83

Wegrzyn, J. L., Drudge, T. M., Valafar, F., and Hook, V. (2008). Bioinformatic analyses of mammalian 5′-UTR sequence properties of mRNAs predicts alternative translation initiation sites. *BMC Bioinformatics* 9:232. doi: 10.1186/1471-2105-9-232

Wirka, R. C., Gore, S., Van Wagoner, D. R., Arking, D. E., Lubitz, S. A., Lunetta, K. L., et al. (2011). A common connexin-40 gene promoter variant affects connexin-40 expression in human atria and is associated with atrial fibrillation. *Circ. Arrhythm. Electrophysiol.* 4, 87–93. doi: 10.1161/CIRCEP.110.959726

Wong, A., Yang, J., Cavadini, P., Gellera, C., Lonnerdal, B., Taroni, F., et al. (1999). The Friedreich's ataxia mutation confers cellular sensitivity to oxidant stress which is rescued by chelators of iron and calcium and inhibitors of apoptosis. *Hum. Mol. Genet.* 8, 425–430. doi: 10.1093/hmg/8.3.425

Wu, L., Yong, S. L., Fan, C., Ni, Y., Yoo, S., Zhang, T., et al. (2008). Identification of a new co-factor, MOG1, required for the full function of cardiac sodium channel Nav 1.5. *J. Biol. Chem.* 283, 6968–6978. doi: 10.1074/jbc.M709721200

Xu, L., Eu, J. P., Meissner, G., and Stamler, J. S. (1998). Activation of the cardiac calcium release channel (ryanodine receptor) by poly-S-nitrosylation. *Science* 279, 234–237. doi: 10.1126/science.279.5348.234

Yang, L., Katchman, A., Morrow, J. P., Doshi, D., and Marx, S. O. (2011). Cardiac L-type calcium channel (Cav1.2) associates with gamma subunits. *FASEB J.* 25, 928–936. doi: 10.1096/fj.10-172353

Yang, P., Koopmann, T. T., Pfeufer, A., Jalilzadeh, S., Schulze-Bahr, E., Kääb, S., et al. (2007). Polymorphisms in the cardiac sodium channel promoter displaying variant *in vitro* expression activity. *Eur. J. Hum. Genet.* 16, 350–357. doi: 10.1038/sj.ejhg.5201952

Yang, P., Kupershmidt, S., and Roden, D. M. (2004). Cloning and initial characterization of the human cardiac sodium channel (SCN5A) promoter. *Cardiovasc. Res.* 61, 56–65. doi: 10.1016/j.cardiores.2003.09.030

Yarbrough, T. L., Lu, T., Lee, H. C., and Shibata, E. F. (2002). Localization of cardiac sodium channels in caveolin-rich membrane domains: regulation of sodium current amplitude. *Circ. Res.* 90, 443–449. doi: 10.1161/hh0402.105177

Zarraga, I. G., Zhang, L., Stump, M. R., Gong, Q., Vincent, G. M., and Zhou, Z. (2011). Nonsense-mediated mRNA decay caused by a frameshift mutation in a large kindred of type 2 long QT syndrome. *Heart Rhythm* 8, 1200–1206. doi: 10.1016/j.hrthm.2011.03.039

Zhang, Y., Hartmann, H. A., and Satin, J. (1999). Glycosylation influences voltage-dependent gating of cardiac and skeletal muscle sodium channels. *J. Membr. Biol.* 171, 195–207. doi: 10.1007/s002329900571

Zhou, J., Shin, H. G., Yi, J., Shen, W., Williams, C. P., and Murray, K. T. (2002). Phosphorylation and putative ER retention signals are required for protein kinase A-mediated potentiation of cardiac sodium current. *Circ. Res.* 91, 540–546. doi: 10.1161/01.RES.0000033598.00903.27

Zhou, J., Yi, J., Hu, N., George, A. L. Jr., and Murray, K. T. (2000). Activation of protein kinase A modulates trafficking of the human cardiac sodium channel in Xenopus oocytes. *Circ. Res.* 87, 33–38. doi: 10.1161/01.RES.87.1.33

Zorio, E., Medina, P., Rueda, J., Millán, J. M., Arnau, M. A., Beneyto, M., et al. (2009). Insights into the role of microRNAs in cardiac diseases: from biological signalling to therapeutic targets. *Cardiovasc. Hematol. Agents Med. Chem.* 7, 82–90. doi: 10.2174/187152509787047676

Conflict of Interest Statement: The authors declare that the research was conducted in the absence of any commercial or financial relationships that could be construed as a potential conflict of interest.

Received: 07 May 2013; accepted: 29 August 2013; published online: 20 September 2013.

*Citation: Jagu B, Charpentier F and Toumaniantz G (2013) Identifying potential functional impact of mutations and polymorphisms: linking heart failure, increased risk of arrhythmias and sudden cardiac death. Front. Physiol. **4**:254. doi: 10.3389/fphys.2013.00254*

This article was submitted to Cardiac Electrophysiology, a section of the journal Frontiers in Physiology.

frontiers in
PHYSIOLOGY

REVIEW ARTICLE
published: 15 July 2013
doi: 10.3389/fphys.2013.00179

The genetic component of Brugada syndrome

Morten W. Nielsen[1,2], Anders G. Holst[1,2], Søren-Peter Olesen[1] and Morten S. Olesen[1,2]*

[1] *The Danish National Research Foundation Centre for Cardiac Arrhythmia, Copenhagen, Denmark*
[2] *Department of Cardiology, Laboratory for Molecular Cardiology, The Heart Centre, Rigshospitalet, University of Copenhagen, Copenhagen, Denmark*

Edited by:
Ian N. Sabir, King's College London, UK

Reviewed by:
Ruben Coronel, Academic Medical Center, Netherlands
James H. King, University of Cambridge, UK

****Correspondence:***
Morten S. Olesen, Department of Cardiology, Laboratory for Molecular Cardiology, Section 9312, Copenhagen University Hospital, Rigshospitalet, Juliane Mariesvej 20, Copenhagen Ø, 2100, Denmark
e-mail: morten.salling.olesen@gmail.com

Brugada syndrome (BrS) is a clinical entity first described in 1992. BrS is characterized by ST-segment elevations in the right precordial leads and susceptibility to ventricular arrhythmias and sudden cardiac death. It affects young subjects, predominantly males, with structurally normal hearts. The prevalence varies with ethnicity ranging from 1:2,000 to 1:100,000 in different parts of the world. Today, hundreds of variants in 17 genes have been associated with BrS of which mutations in *SCN5A*, coding for the cardiac voltage-gated sodium channel, accounts for the vast majority. Despite this, approximately 70% of BrS cases cannot be explained genetically with the current knowledge. Moreover, the monogenic role of some of the variants previously described as being associated with BrS has been questioned by their occurrence in about 4% (1:23) of the general population as found in NHLBI GO Exome Sequencing Project (ESP) currently including approximately 6500 individuals. If we add the variants described in the five newest identified genes associated with BrS, they appear at an even higher prevalence in the ESP (1:21). The current standard treatment of BrS is an implantable cardioverter-defibrillator (ICD). The risk stratification and indications for ICD treatment are based on the ECG and on the clinical and family history. In this review we discuss the genetic basis of BrS.

Keywords: Brugada syndrome, genetics, Exome Sequencing Project, mutation, treatment

INTRODUCTION

The Brugada syndrome (BrS) was first described as a clinical entity in 1992 (Brugada and Brugada, 1992). It is inherited in an autosomal dominant manner (Antzelevitch et al., 2005). BrS has traditionally been viewed as a consequence of comprised electrical function without structural abnormalities, although the latter has been reported (Coronel et al., 2005; Frustaci et al., 2005; Nademanee et al., 2011; Duthoit et al., 2012).

BrS is characterized by an ST-segment elevation in the right precordial ECG leads V_1–V_3. The most descriptive ECG changes have been described at consensus conferences, endorsed by Heart Rhythm Society (HRS) and European Heart Rhythm Association (EHRA) over the last decade (Antzelevitch et al., 2005). In a consensus report from 2012, two specific ECG patterns are found to be descriptive (Bayés de Luna et al., 2012).

The BrS ECG pattern is characterized by a coved type ST-segment elevation $\geq$2 mm followed by a negative T wave in at least one of the right precordial leads (V_1–V_3) in the presence or absence of a sodium channel-blocking agent (type 1 ECG). BrS is diagnosed when this is seen in conjunction with one of the following: ventricular tachycardia/fibrillation (VF/VT), a family history of sudden cardiac death (SCD) <45 years old, coved-type ECGs in family members, inducibility of VT with programmed electrical stimulation (PES), syncope or nocturnal agonal respiration (Antzelevitch et al., 2005).

Patients with BrS have an increased risk of SCD secondary to VT/VF (Antzelevitch et al., 2005). Different cohorts have reported different risk of developing VT/VF (Brugada et al., 2002; Priori et al., 2002; Eckardt et al., 2005). In the most updated and largest BrS population so far, the cardiac event rate per year was 0.5% in asymptomatic patients, 1.9% in patients with syncope and 7.7% in patients with aborted SCD. The median age of diagnosis was 45 $\pm$ 10 years (Probst et al., 2010). In general, men are affected 8–10 fold more often than women, probably due to gender differences in the expression of certain cardiac ion channels (Antzelevitch, 2006). Approximately 20% of Brugada patients also develop supraventricular arrhythmias with atrial fibrillation accounting for most of the cases (Antzelevitch et al., 2005).

The syndrome is estimated to be responsible for 4% of all sudden deaths (SD) and 20% of SD's among patients with structurally normal hearts. The prevalence is ranging between 1:2,000 and 1:100,000 (Hermida et al., 2000; Letsas et al., 2007; Gallagher et al., 2008; Sinner et al., 2009; Holst et al., 2012a) in different countries, and it is the most common cause of death, besides accidents, in men under 40 years in some parts of the world, e.g., in Thailand (Antzelevitch et al., 2005). The syndrome is probably underestimated due to the fact that the characteristic ECG-pattern often is dynamic and concealed and by the fact, that there are several differential diagnoses associated with elevated ST-segments in right precordial leads (Brugada et al., 2009). The characteristic ECG pattern can in some cases be unmasked by administration of sodium channel-blockers, by febrile state or by vasotonic agents. Indeed sodium channel blockers such as flecainide are used in the diagnosis of BrS (Antzelevitch et al., 2005).

Experimental studies have provided some understanding of the pathophysiological basis of the two main clinical characteristics; elevated coved ST-segment in V_1–V_3 and the increased risk of VT/VF (Yan and Antzelevitch, 1999). However, a consensus concerning the exact mechanism has not been established and there is

an ongoing dispute as to whether BrS is a repolarization disorder, a depolarization disorder, or maybe both (Meregalli et al., 2005; Hoogendijk et al., 2010; Wilde et al., 2010). The central mechanism underlying the ECG pattern and arrhythmias, according to the repolarization hypothesis, is a more prominent transmural voltage-gradient in the early repolarization phase due to a more prominent I_{to} current in the epicardium compared to the endocardium of the right ventricle (Meregalli et al., 2005). Thus, in the epicardium, in the face of reduced sodium current, increased potassium current or reduced calcium current, complete loss of the phase 2 dome can occur. If this appears at some epicardial sites but not at others and a further heterogeneity between the epicardium and the endocardium occur, the result is an epicardial and transmural dispersion of repolarisation, respectively. This could lead to the development of a re-entry loop and premature beats already in the phase 2 of the on-going action potential (AP) that could further trigger VT/VF (Meregalli et al., 2005).

The reason why ST-segment elevation occurs in right precordial leads, and not left, has been suggested to be due to a more prominent I_{to} in the right ventricle than in the left (Di Diego et al., 1996). Accordingly, this current is believed to have a central role in BrS pathogenesis. This hypothesis has been tested by Calloe et al. (2009), who demonstrated that an I_{to} activator recapitulated the electrographic and arrhythmic manifestations of BrS.

The depolarization theory states that the substrate for the ECG changes and susceptibility of VT/VF is a slowing of conduction caused both by fibrosis in right ventricular outflow tract (RVOT) and a decreased I_{Na}. This decrease in conduction velocity is more prominent in RVOT compared to the rest of the right ventricle which gives rise to the substrate for ECG changes and re-entry arrhythmias (Meregalli et al., 2005).

Recently Hoogendijk et al. stated that none of the proposed mechanism so far described has been irrefutably demonstrated in BrS patients. Therefore they suggested a unifying explanation, the so-called current-to-load mismatch. This hypothesis states that current-to-load mismatch caused by structural and functional abnormality could explain the ST-segment elevation and susceptibility to arrhythmias (Hoogendijk et al., 2010).

GENETIC BASIS OF BrS

To date, 17 genes have been associated with BrS or BrS ECG phenotype (**Table 1**). *SCN5A* was the first gene to be associated with BrS and still represents the major gene in BrS pathogenesis. The individual genes associated with BrS are described in detail in the following.

BrS1 IS ASSOCIATED WITH MUTATIONS IN SCN5A

The *SCN5A* gene encodes the α-subunit of the voltage-dependent cardiac sodium channel, $Na_v1.5$ (Gellens et al., 1992). Mutations in this gene in association with BrS were first described in 1998 by Chen et al. (1998). Since then more than 300 mutations in this gene have been associated with BrS.

Functional studies of many different mutations in the gene have been performed and they all lead to a reduction in net sodium current due to one or more of following reasons (Antzelevitch et al., 2005); (1) reduced current density due to failure of the sodium channel to express or defect trafficking of the channel (Baroudi et al., 2001; Valdivia et al., 2004; Pfahnl et al., 2007), (2) a shift in the voltage- and time-dependence of sodium channel current activation, inactivation or reactivation (Keller et al., 2005; Hsueh et al., 2009; Calloe et al., 2013), or (3) entry of the sodium channel into an intermediate state of inactivation from which it recovers relatively slower than normal (Bezzina

Table 1 | Mutations in genes associated with Brugada syndrome.

BrS subtype	Gene name	Gene product	Ionic current	Functional effect	References	Incidence, %
BrS1	*SCN5A*	$Na_v1.5$	I_{Na}	Loss-of-function	Chen et al., 1998	11–24 Kapplinger et al., 2010
BrS2	*GPD1-L*	G3PD1L	I_{Na}	Loss-of-function	London et al., 2007	Rare Antzelevitch and Nof, 2008
BrS3	*CACNA1C*	$Ca_v1.2$	I_{Ca-L}	Loss-of-function	Antzelevitch et al., 2007	6–7 Antzelevitch and Nof, 2008
BrS4	*CACNB2*	$Ca_vβ2$	I_{Ca-L}	Loss-of-function	Antzelevitch et al., 2007	4–5 Antzelevitch and Nof, 2008
BrS5	*SCN1B*	$Na_vβ1$	I_{Na}	Loss-of-function	Watanabe et al., 2008	1–2 Antzelevitch and Nof, 2008
BrS6	*KCNE3*	MiRP2	I_{to}/I_{Ks}	Gain-of-function	Delpón et al., 2008	<1 Antzelevitch and Nof, 2008
BrS7	*SCN3B*	$Na_vβ3$	I_{Na}	Loss-of-function	Hu et al., 2009	Probably rare
BrS8	*KCNH2*	hERG1	I_{Kr}	Loss-of-function	Itoh et al., 2009; Verkerk et al., 2005	Probably rare
BrS9	*KCNJ8*	Kir6.1	I_{KATP}	Gain-of-function	Medeiros-Domingo et al., 2010	Probably rare
BrS10	*CACNA2D1*	$Ca_vα_2δ$-1	I_{Ca-L}	Not available	Burashnikov et al., 2010	Probably rare
BrS11	*RANGRF*	MOG1	I_{Na}	Loss-of- function	Kattygnarath et al., 2011	Probably rare
BrS12	*KCNE5*	MiRP4	I_{to}/I_{Ks}	Gain-of-function	Ohno et al., 2011	Probably rare
BrS13	*KCND3*	$K_v4.3$	I_{to}	Gain-of-function	Giudicessi et al., 2011	Probably rare
BrS14	*HCN4*	HCN4	I_f	Not available	Crotti et al., 2012	Probably rare
BrS15	*SLMAP*	SLMAP	I_{Na}	Loss-of-function	Ishikawa et al., 2012	Probably rare
BrS16	*TRMP4*	TRMP4	NSC_{Ca}	Both	Liu et al., 2013	6*
BrS17	*SCN2B*	$Na_vβ2$	I_{Na}	Loss-of-function	Riuró et al., 2013	Probably rare

Subtypes listed chronologically.

*NSC_{Ca}, Calcium activated Non-Selective Cation channel. *6% of original cohort consisting of 248 BrS cases.*

et al., 1999; Veldkamp et al., 2000; Chiang et al., 2009). A number of knock-out mouse models support the central role of *SCN5A* in the pathogenesis of BrS (Killeen et al., 2008; Derangeon et al., 2012). Heterozygous knock-out mice have been shown to have compromised conduction velocity, impaired AV conduction and QRS prolongation. Furthermore during programmed ventricular electrical pacing two thirds of the mice developed ventricular tachyarrhythmias (Derangeon et al., 2012).

The arrhythmic potential of mutations in *SCN5A* is also emphasized by its involvement in other arrhythmic diseases such as LQTS, BrS, SIDS, cardiomyopathy and AF. Various *SCN5A* mutations are known to present with mixed phenotypes, a presentation known as cardiac sodium channel overlap syndrome (Darbar et al., 2008; Remme et al., 2008; Olesen et al., 2012a). This really emphasises the complexity of *SCN5A* gene mutations in BrS.

See supplementary Tables S1–S5 for a complete overview of all mutations in *SCN5A* associated with BrS.

BrS2 IS ASSOCIATED WITH MUTATIONS IN GPD1L (SEE TABLE 2)

Weiss et al. (2002), linked a locus, close to but distinct from the *SCN5A* locus, to BrS in a large Italian family (Weiss et al., 2002). London et al. (2007) characterized the locus to be the glycerol-3-phosphat dehydrogenase 1-like, *GPD1-L* gene. There is 84% homology with the Glycerol-3-phosphate dehydrogenase protein, GPD, a dimer involved in the glycerol phosphate shuttle that transfers electrons from cytosolic NADH to the mitochondrial transport chain. The GPD1-L protein is highly expressed in the heart and is concentrated in the membrane fraction. London et al. found that an A280V mutation from a BrS patient in *GPD1-L* was linked to a 48% decrease in inward Na^+ current and a marked decrease in surface expression of $Na_v1.5$ (London et al., 2007).

A mechanism by which *GPD1-L* mutations could affect $Na_v1.5$ has been studied since by Liu et al. (2009). They, on the basis of the homology between *GPD* and *GPD1-L*, investigated whether the *GPD1-L*, as *GPD*, is involved in NAD-dependent energy metabolism and thereby, whether NAD(H) could regulate $Na_v1.5$. Indeed they found that A280V-GPD1-L increased $[NADH]_i$ and that this increase in $[NADH]_i$ reduced I_{Na}. This suggests a link between metabolism and I_{Na}.

BrS3 IS ASSOCIATED WITH MUTATIONS IN CACNA1C (SEE TABLE 2)

This gene encodes the α-subunit of the human L-type voltage-gated calcium channel, $Ca_v1.2$ (Takimoto et al., 1997). Antzelevitch et al. (2007) identified an association between mutations in *CACNA1C* and BrS. In a Brugada cohort they found two missense mutations in two probands, G490R and A39V. The ECG of the affected patients revealed short QT interval. Both mutations occurred in highly conserved regions of the $Ca_v1.2$ protein and both mutations led to a major loss-of-function in calcium channel activity. The loss-of-function caused by the A39V mutation was found to be caused by a trafficking defect (Antzelevitch et al., 2007).

BrS4 IS ASSOCIATED WITH MUTATIONS IN CACNB2B (SEE TABLE 2)

This gene encodes the β-subunit of $Ca_v1.2$, $Ca_vβ2$, which is involved in regulation of the gating process of I_{Ca-L}, in increasing the I_{Ca-L} and in modulation of I_{Ca-L} trafficking (Cornet et al., 2002; Catterall et al., 2005; Hedley et al., 2009).

Antzelevitch et al. (2007) identified a mutation in *CACNB2b* (S481L) in one proband with BrS as well as short QT. The S481L mutation was present in all 6 phenotype-positive and absent in all 4 phenotype-negative family members. The I_{Ca-L} was found to be reduced markedly. Hedley et al. (2009) suggested that the pathogenic mechanism for this mutation could be interference of the stimulatory role of $Ca_vβ2$ on I_{Ca-L}, by the fact that the mutation is localized close to the $Ca_v1.2$ binding domain.

In 2009, Cordeiro et al. associated a novel mutation in *CACNB2b* with BrS. They detected a missense mutation in *CACNB2b,* T11I. They found that the mutation led to an accelerated inactivation of the L-type Ca^{2+} channel. This change of kinetics resulted in a reduced depolarizing current contributing to the plateau phase of the epicardial AP (Cordeiro et al., 2009). Since, Burashnikov et al. (2010) have revealed additional mutations in *CACNB2b* (see **Table 2**).

BrS5 IS ASSOCIATED WITH MUTATIONS IN SCN1B (SEE TABLE 2)

The gene encodes the β1-subunit of $Na_v1.5$, $Na_vβ1$, which is translated into to isoforms; β1 and β1b. Functions attributed to the β-subunit include an increase in $Na_v1.5$ expression at the cell surface, modulation of channel gating and voltage dependence, and a role in cell adhesion and recruitment of cytosolic proteins such as Ankyrin-G (Isom, 2001; Watanabe et al., 2008).

The association of mutations in *SCN1B* with BrS was first identified by Watanabe et al. (2008). They screened 282 probands with BrS and 44 patients with conduction disease. They identified one mutation (W179X (β1b)) in *SCN1B* in a patient with BrS ECG phenotype. The mutated form of *SCN1B* was not able to increase I_{Na} as normal. Recently, Holst *et al.* added further evidence for an association between mutations in *SCN1B* and BrS. Two mutations in two probands in *SCN1Bb* (H162P and R214Q) were identified from a cohort of 42 *SCN5A*-negative BrS patients. However, R214Q was also found in ESP; H162P was not (Holst et al., 2012b; Olesen et al., 2012b). Hu et al. (2012) investigated the functional consequence of the R214Q variant. When co-expressed with WT-*SCN5A* the mutant *SCN1Bb* induced a significant decrease in peak sodium current compared to WT-*SCN1Bb*. Interestingly, when co-expressed with WT-*KCND3*, the variant induced a greater I_{to}, suggesting a combined loss of function of sodium channel current and gain of function of transient outward potassium current in BrS pathogenesis.

BrS6 IS ASSOCIATED WITH MUTATIONS IN KCNE3 (SEE TABLE 2)

This gene encodes the protein MiRP2, one of five homologous β-subunits (*KCNE1-5*) of voltage gated potassium ion channels (Abbott et al., 2001; Hedley et al., 2009). The potassium channel complex, Kv:KCNE, is a heterohexameric structure consisting of four α-subunits and two *KCNE* peptides. The functional role of *KCNE* peptides, in general, is modulation of several potassium currents in the heart, for instance I_{to} and I_{Ks}(Delpón et al., 2008). The association of mutations in *KCNE3* with BrS was identified by Delpón et al. (2008). They screened 105 probands with BrS and found a R99H missense mutation in one individual who were highly symptomatic with one aborted cardiac

Table 2 | Mutations in genes associated with BrS2-BrS17.

Subtype	Gene	Ionic current	Amino acid substitution	Functional effect	References
BrS2	*GPD1L*	I_{Na}	A280V	Loss-of-function	London et al., 2007
BrS3	*CACNA1C*	I_{Ca-L}	A39V	Loss-of-function	Antzelevitch et al., 2007
			G490R	Loss-of-function	Antzelevitch et al., 2007
			E1115K	Loss-of-function	Burashnikov et al., 2010
			R1880Q	Loss-of-function	Burashnikov et al., 2010
			V2014I	Loss-of-function	Burashnikov et al., 2010
			D2130N	Loss-of-function	Burashnikov et al., 2010
BrS4	*CACNB2*	I_{Ca-L}	S481L	Loss-of-function	Antzelevitch et al., 2007
			T11I	Loss-of-function	Cordeiro et al., 2009
			S143F	Loss-of-function	Burashnikov et al., 2010
			L399F	Loss-of-function	Burashnikov et al., 2010
			T450I	Loss-of-function	Burashnikov et al., 2010
			D538E	Loss-of-function	Burashnikov et al., 2010
			V340I	Not available	Crotti et al., 2012
			E499D	Not available	Crotti et al., 2012
BrS5	*SCN1B*	I_{Na}	W179X	Loss-of-function	Watanabe et al., 2008
			R214Q	Loss-of-function	Holst et al., 2012b; Hu et al., 2012
			H162P	Not available	Holst et al., 2012b
			Q204R	Not available	Crotti et al., 2012
BrS6	*KCNE3*	I_{to}/I_{Ks}	R99H	Gain-of-function	Delpón et al., 2008
BrS7	*SCN3B*	I_{to}/I_{Ks}	L10P	Loss-of-function	Hu et al., 2009
			V110I	Loss-of-function	Ishikawa et al., 2013
BrS8	*KCNH2*	I_{Kr}	G873S	Gain-of-function	Verkerk et al., 2005
			N985S	Gain-of-function	Verkerk et al., 2005
			R1135H	Gain-of-function	Itoh et al., 2009
BrS9	*KCNJ8*	I_{KATP}	S422L	Gain-of-function	Medeiros-Domingo et al., 2010
BrS10	*CACNA2D1*	I_{Ca-L}	D550Y	Not available	Burashnikov et al., 2010
			S709N	Not available	Burashnikov et al., 2010
			Q917H	Not available	Burashnikov et al., 2010
BrS11	*RANGRF*	I_{Na}	E83D	Loss-of-function	Kattygnarath et al., 2011
BrS12	*KCNE5*	I_{to}/I_{Ks}	Y81H	Gain-of-function	Ohno et al., 2011
			D92E; E93X	Gain-of-function	Ohno et al., 2011
BrS13	*KCND3*	I_{to}	L450F	Gain-of-function	Giudicessi et al., 2011
			G600R	Gain-of-function	Giudicessi et al., 2011
BrS14	HCN4	I_f	S841L	Not available	Crotti et al., 2012
BrS15	*SLMAP*	I_{Na}	V269I	Loss-of-function	Ishikawa et al., 2012
			E710A	Loss-of-function	Ishikawa et al., 2012
BrS16	*TRPM4*	NSC_{Ca}	R144W	Not available	Liu et al., 2013
			A432T	Gain-of-function	Liu et al., 2013, 2010
			G555R	Not available	Liu et al., 2013
			G582S	Not available	Liu et al., 2013
			F773I	Not available	Liu et al., 2013
			P779R	Loss-of-function	Liu et al., 2013
			T873I	Gain-of-function	Liu et al., 2013
BrS17	*SCN2B*	I_{Na}	D211G	Loss-of-function	Riuró et al., 2013

arrest and numerous appropriate shocks after ICD implantation. The family of this individual was examined and they found that 4/4 phenotype-positive and 0/3 phenotype-negative family members had the mutation. Co-transfection of R99H-*KCNE3* with *KCNQ1* produced no alteration in current magnitude or kinetics. Co-expressed with WT $K_v4.3$, I_{to} channel, the mutation had a gain-of-function effect leading to an increase in peak current and an accelerated inactivation of I_{to}. Overall, the mutation led to a significant increase in total charge carried by I_{to}.

BrS7 IS ASSOCIATED WITH MUTATIONS IN SCN3B (SEE TABLE 2)

This gene encodes the β3-subunit of the cardiac sodium channel, $Na_v\beta3$ (Morgan et al., 2000). The functional attribution of $Na_v\beta3$ is modulation of the channel gating of $Na_v1.5$, similar to the β1-subunit, although with different kinetics (Morgan et al., 2000).

The association of *SCN3B* with BrS have been identified by Hu et al. (2009). They found a missense mutation (L10P) in an individual with BrS. The mutation led to a decrease in peak sodium current density, accelerated inactivation, and slowed reactivation compared to wild type. The L10P mutation has also been associated with lone atrial fibrillation (AF) suggesting an overlap in phenotypes (Olesen et al., 2011b). Recently, Ishikawa *et al.* reported another novel *SCN3B* mutation, V110I, in three of 178 unrelated Japanese BrS patients. (Ishikawa et al., 2013) The mutation was absent in 480 Japanese controls and displayed a loss-of-function effect due to impaired cell surface expression of Nav1.5.

BrS8 IS ASSOCIATED WITH MUTATIONS IN KCNH2 (SEE TABLE 2)

The α-subunit of the rapid delayed rectifier channel (hERG1) is encoded by *KCNH2*. Verkerk et al. in 2005, identified two mutations (G873S and N985S) in two unrelated *SCN5A*-negative BrS patients. Functional investigation revealed an increase in the rectifying current, namely an increase in peak current during phase 0 and phase 1 of the ventricular AP. Through computer simulations this gain-of-function in I_{Kr} enhanced the susceptibility of loss of AP dome in right ventricular subepicardial myocytes, which is characteristic of BrS. G873S, however, was found in 2 of 500 unrelated Han Chinese controls suggesting that the variant has only a modifying role or is an innocent bystander. Further support for this interpretation is the fact that the glycine at position 873 is not conserved between human, mouse and rat (Verkerk et al., 2005). For this reason, they were not denoted as the first to associate mutations in *KCNH2* with BrS. In 2009, Itoh et al., as the "first", identified a mutation (R1135H) in *KCNH2* in a 34-year old man with Brugada-type ECG and short QT interval. The mutation displayed a gain-of-function effect on I_{Kr}(Itoh et al., 2009). Subsequently, Wilders and Verkerk, demonstrated, through computer simulations, that R1135H had the same consequence on AP as G873S and N985S (Wilders and Verkerk, 2010).

BrS9 IS ASSOCIATED WITH MUTATIONS IN KCNJ8 (SEE TABLE 2)

This gene encodes the cardiac K_{ATP} channel, Kir6.1. The Kir6.1 channel facilitates a non-voltage-gated inwardly rectifying potassium current, leading to a shortening of the AP duration under conditions of metabolic stress (Delaney et al., 2012).

Medeiros-Domingo et al. (2010) found a mutation (S422L) in *KCNJ8* in a patient with a flecainide induced type 1 ECG pattern. Electrophysiological the mutation displayed a gain-of-function consequence on K_{ATP}. Subsequently, Barajas-Martínez et al. (2012) identified the same mutation in three other BrS patients. When *KCNJ8*-S422L was co-expressed with the wild type regulatory SUR2A, it showed a twofold gain-of-function on $I_{K,ATP}$. Furthermore, the mutant channel displayed a reduced sensitivity to ATP, pointing to incomplete closing of the channel under normoxic conditions.

BrS10 IS ASSOCIATED WITH MUTATIONS IN CACNA2D1 (SEE TABLE 2)

CACNA2D1 encodes the $\alpha_2\delta$-subunit of the voltage-dependent calcium channel and has been found to share similar functional properties with $Ca_v\beta2$ (Gurnett et al., 1996; Hobom et al., 2000). Burashnikov *et al.* identified three different missense mutations in *CACNA2D1* (S709N, D550Y and Q917H) in three BrS patients from a cohort consisting of 205 patients with BrS, short QT, idiopathic ventricular fibrillation (IVF) and early repolarisation syndrome. However, in two of the three patients, additional mutations in genes recognized as being associated with BrS were identified. Unfortunately, the authors did not investigate the electrophysiological consequence of the three missense mutations. New mutations in *CACNB2b* and *CACNA1C* were also detected in this cohort (see **Table 2**) (Burashnikov et al., 2010).

BrS11 IS ASSOCIATED WITH MUTATIONS IN RANGRF (SEE TABLE 2)

Kattygnarath et al. (2011) reported the gene *RANGRF*, encoding MOG1 (a protein important for the trafficking of *SCN5A* to the cell membrane), as a new BrS gene. They identified a missense mutation E83D in a BrS patient that dominant-negatively compromised the sodium current. The mutation was not found in 281 control subjects. Olesen et al. identified another MOG1 variant, E61X, in both AF patients and healthy controls indicating that a person may have complete loss of one MOG1 allele without having any signs of disease (Olesen et al., 2011a). Genetic variants that compromise the MOG1 protein are therefore more likely to increase the susceptibility of BrS, rather than to be the major genetic susceptibility variant.

BrS12 IS ASSOCIATED WITH MUTATIONS IN KCNE5 (SEE TABLE 2)

This gene encodes one of the regulatory β-subunits of the I_{to}/I_{Ks} channels mentioned under BrS6. In 2011, Ohno et al. identified two novel variants (Y81H and D92E;E93X) in *KCNE5* in a Japanese cohort consisting of 205 patients with BrS or IVF (Ohno et al., 2011). Three probands comprised the Y81H variant, one the D92E;E93X variant. In 300 unrelated healthy Japanese controls, Y81H was identified in 3 women, and D92E; E93X was absent. All four probands were symptomatic and received an ICD. When co-expressed with *KCND3* (α-subunit of I_{to}), the mutant channels significantly increased I_{to} compared to wild type, displaying a gain-of-function effect. Stimulation study revealed that the two variants induced altered ventricular AP profiles. This could provide the likelihood of a proarrhythmic substrate. Another interesting notion drawn by the authors is that *KCNE5* is located on chromosome X. This could in part explain the gender

difference seen in prevalence. Indeed, the male phenotype in the study by Ohno et al. was more severe.

BrS13 IS ASSOCIATED WITH MUTATIONS IN KCND3 (SEE TABLE 2)

KCND3 encodes the α-subunit of I_{to}, $K_v4.3$, a voltage-gated potassium channel expressed in heart. In 2011, two novel mutations (L450F and G600R) were identified in two unrelated BrS patients (Giudicessi et al., 2011). Both mutations were absent in 1560 reference alleles. Co-expression of $K_v4.3$ mutants with KChIP2-WT revealed a significant increase in I_{to} current density compared with WT-$K_v4.3$. Moreover, the two mutations induced loss of AP dome in RV epicardial myocytes, demonstrated by computer simulations, providing the arrhythmic substrate for BrS phenotype (Giudicessi et al., 2011).

BrS14 IS ASSOCIATED WITH MUTATIONS IN HCN4 (SEE TABLE 2)

HCN4 encodes the hyperpolarisation-activated cyclic nucleotide-gated channel 4 which is a pacemaker channel responsible for the funny current (I_f). Mutations in this gene has formerly been associated with sinus node dysfunction (Ueda et al., 2004). Recently, Crotti *et al.* identified a mutation (S841L) in *HCN4* in one proband of 129 unrelated BrS patients (Crotti et al., 2012). The mutation was absent in ≥1400 ethnicity matched reference alleles and in publicly available databases. The functional effect of this mutation has not been assessed and therefore, before drawing any conclusion in BrS pathogenesis, this gene has to be investigated more thoroughly.

BrS15 IS ASSOCIATED WITH MUTATIONS IN SLMAP (SEE TABLE 2)

SLMAP encodes the sarcolemmal membrane-associated protein, a component of T-tubules and sarcoplasmic reticulum which is involved in excitation-contraction coupling in cardiomyocytes (Ishikawa et al., 2012). Ventricular arrhythmias have previously been linked to mutations in proteins involved in excitation-contraction coupling (Priori et al., 2001). Ishikawa et al. (2012) recently reported two mutations (V269I and E710A) in 190 unrelated BrS patients. In cell lines the two mutations were shown to reduce cell surface expression of $Na_v1.5$ resulting in decreased peak sodium current density. In line with this, the investigators demonstrated that silencing the two *SLMAP* mutants rescued the decreased surface expression of $Na_v1.5$.

BrS16 IS ASSOCIATED WITH MUTATIONS IN TRPM4 (SEE TABLE 2)

The *TRPM4* gene encodes the transient receptor potential melastatin protein number 4 which is a calcium-activated non-selective cation channel (NSC_{Ca}) that mediates transport of monovalent cations across membranes, thereby depolarizing the membrane. Mutations in this gene have been associated with cardiac conduction blocks (Kruse et al., 2009; Liu et al., 2010; Stallmeyer et al., 2012) and recently, Liu et al. (2013) associated mutations in *TRPM4* with BrS. In 248 BrS cases, the investigators identified 7 mutations absent in approximately 14,000 control alleles. Functional characterization of selected mutations revealed both a decrease in *TRPM4* expression (P779R) and an increase in expression (T873I) suggesting that both loss- and gain-of-function mutations in this gene may lead to BrS.

BrS17 IS ASSOCIATED WITH MUTATIONS IN SCN2B (SEE TABLE 2)

The *SCN2B* gene encodes the β2-subunit of the cardiac sodium channel. The association of *SCN2B* with BrS have just recently been identified by Riuró et al. (2013). They found a missense mutation (A211G) in an individual with BrS. The mutation was absent in 500 control alleles and available databases. The mutation led to a significant reduction in sodium current density when co-expressed with $Na_v1.5$ compared to wild type. This reduction was shown to be due to a reduced $Na_v1.5$ cell surface expression (Riuró et al., 2013).

BIOINFORMATIC RE-EVALUATION OF VARIANTS

With the recently published exome data from the NHLBI GO Exome Sequencing Project (ESP), knowledge regarding genetic variation in the general population have become available [Exome Variant Server, NHLBI GO (ESP)]. In ESP, next-generation sequencing has been carried out for all protein-coding regions in approximately 6500 persons from different population studies. Risgaard et al. (2013) have, by using these data, found a high genotype prevalence of 1:23 in the ESP of genetic variants in twelve genes (*SCN5A, GPD1L, CACNA1C, CACNB2, SCN1B, KCNE3, SCN3B, KCNH2, CACNA2D1, MOG1, KCND3,* and *KCNJ8*) previously associated with BrS. This is a very high prevalence compared to the prevalence of BrS in the general population ranging between 1:2,000 and 1:100,000 (Hermida et al., 2000; Letsas et al., 2007; Gallagher et al., 2008; Sinner et al., 2009; Holst et al., 2012a). Moreover, in a synergistic use of prediction analysis using ≥3 prediction tools, 47% of the variants found in ESP were predicted pathogenic compared to 75% of the variants not found in ESP ($p < 0.0001$). These data definitely questions the pathogenic role of some of the previously BrS-associated variants. A limitation in the study is that there are no clinical data on the persons in ESP. However, Refsgaard et al. have recently conducted a number of studies that indicate, that the exome database is indeed representative for genetic variation in healthy subject (Refsgaard et al., 2012; Andreasen et al., 2013a,b). Moreover, none of the studies in ESP specifically included patients with channelopathies and at least two studies excluded such patients (Refsgaard et al., 2012).

We investigated the prevalence in ESP of the genes not investigated by Risgaard et al. (2013), BrS subtypes 12 and 14-17. The *KCNE5, SCN2B* and *SLMAP* mutations were not found in ESP. The *HCN4* mutation (S841L) was found in 3 out of 4289 European American (EA) individuals. The *TRPM4* mutation R144W was present in 1 of 2199 Afro-American (AA) individuals, A432T in 9 of 4291 AA, and G582S in 9 of 4291 EA. The rest of the *TRPM4* mutations were not present in ESP [Exome Variant Server, NHLBI GO (ESP)]. If we add the variants found in the five newest identified genes associated with BrS, this corresponds to an even higher genotype prevalence of 1:21 (296:6258) in ESP.

TREATMENT

IMPLANTABLE CARDIOVERTER DEFIBRILLATOR—ICD

ICD is the only widely accepted treatment of BrS thus far (Brugada et al., 1999, 2000). In 2003, a second consensus conference was held which focused on risk stratifications and

approaches to therapy (Antzelevitch et al., 2005). This consensus report stated the recommendations for ICD implantation.

Sarkozy et al. (2007) studied the effectiveness of ICD treatment in a retrospective study. 47 high risk Brugada patients (mean age: 44 ± 15 years) with ICD were included. During a mean follow-up of 47.5 months, seven patients had appropriate shocks for potentially life-threatening ventricular arrhythmias. However, seventeen patients received inappropriate shocks due to shocks for sinus tachycardia and atrial arrhythmias, which is common in Brugada patients.

A multicenter study by Sacher et al. (2006) showed the same pattern. In 220 BrS patients with ICD (mean follow up >3 years) 8% experienced appropriate shocks and 20% inappropriate shocks. Overall, complications occurred in 28% of the patients.

In a just published article, Miyazaki et al. (2013) also investigated the prevalence of ICD-related complications. In 41 BrS patients and during a median follow-up of 76 months, 15 patients (37%) experienced adverse effects after ICD implantation. This includes complications in 8 (20%) and inappropriate shocks in 10 (24%). Appropriate shocks were detected in 5 patients (12%), (please keep in mind that some patients experience more than one adverse effect). In a nationwide study by Holst et al. (2012a), 26% experienced appropriate shocks and 8% experienced inappropriate shocks during a median follow-up of 47 months in 35 definite BrS patients. The difference in rate of appropriate and inappropriate shocks compared to the three other studies could be due to a more severe phenotype of patients included and due to difference in ICD discrimination algorithms as suggested by Holst et al. (2012a).

A pharmacological approach with fewer complications is obviously desirable and there is a growing effort to define such a safe and efficient treatment for this specific syndrome.

PHARMACOLOGICAL THERAPY

Loss-of-function mutations are responsible for the vast majority of BrS incidents. This makes it more difficult in regard to a pharmacological therapy as it is difficult to compensate for the missing allele. However some substances may be beneficial. The objective is to rebalance the inward and outward currents during the AP and thereby restoring electrical homogeneity (Brugada et al., 2009).

The prominent I_{to} in the right ventricle is thought to have a central role in the pathogenesis of BrS, so a drug like quinidine that inhibits I_{to} (Imaizumi and Giles, 1987) has been suggested to have a therapeutic value in BrS (Yan and Antzelevitch, 1999).

Hermida et al. (2004) observed that hydroquinidine therapy prevented VT/VF inducibility in 22 out of 29 asymptomatic patients with BrS and inducible arrhythmia, as well as VT/VF recurrence in four BrS patients with multiple ICD shocks.Belhassen et al. (2004) reported that quinidine bisulfate prevented VF induction in 22 of 25 BrS patients. All 25 patients had inducible VF before treatment. However, administration of quinidine was associated with a 36% incidence of side-effects that resolved after drug discontinuation. In general, disadvantages of oral quinidine include gastrointestinal side-effects, as observed by Belhassen et al. (2004), and proarrhythmic side-effects (QT prolongation), as observed by Hermida et al. (2004). The latter is probably due to a quinidine block of I_{Kr} and I_{Ks}, however this side effect is rare (Antzelevitch and Nof, 2008). In a recent study by Márquez et al. (2012) the authors investigate the long-term efficacy of low doses quinidine on malignant arrhythmias in BrS patients. A total of twenty patients, of whom seventeen patients had an ICD, were included. In all but three cases, quinidine effectively suppressed arrhythmic events corresponding to an efficacy of quinidine on 85%. All patients tolerated the medication well.

Taken together the data suggest that preventive treatment by quinidine may be an alternative or complimentary strategy to ICD in BrS patients, both in the short and long term. A more I_{to} selective compound that does not permeate the blood-brain-barrier would in theory be the optimal treatment. For other possible beneficial agents please see Márquez et al. (2007) and Minoura et al. (2013).

DISCUSSION AND PERSPECTIVES

Presently over 300 mutations in 17 genes have been associated with BrS or BrS ECG phenotype, in contrast to 5 years ago where only mutations in the *SCNA5* gene were associated with BrS. The knowledge about BrS associated mutations is therefore rapidly increasing and this could potentially make genetic screening important in future. The intention would be to use this knowledge in risk stratification, as some asymptomatic BrS patients have an appreciable risk of arrhythmia (Probst et al., 2010). The rapidly declining cost of multi-gene screening by Next Generation Sequencing adds to the rationale. A study by Meregalli et al. (2009) reveal an association between the type of *SCN5A* mutation and the clinical severity. They compared groups having either missense mutations or mutations leading to premature truncation of the protein. They found that the disease phenotype was more severe in the patients with large I_{Na} reduction than in those with small I_{Na} reduction (truncation versus missense), as evidenced by larger proportions of patients with syncope and SCD. Sommariva et al. (2013) recently demonstrated that *SCN5A* mutation carriers had a significantly increased risk of major arrhythmic event compared with non-carriers in a BrS cohort. In addition they established an association of five polymorphisms with major arrhythmic event.Crotti et al. (2012) recently conducted a comprehensive mutational analysis of twelve BrS genes in a large BrS cohort. They did not detect any significant difference in mutation yield between those patients with definite BrS and those patients only displaying a type 1 ECG pattern. On this basis, the authors argue that genetic testing should additionally be conducted in patients displaying only type 1 ECG pattern. Secondly, they demonstrated that inclusion of the minor BrS susceptibility genes (genes other than *SCN5A*) in genetic testing, only minimally affected the sensitivity of the test. Therefore, these genes should only be screened under special circumstances.

These data may show some promise for the use of genetic data in risk stratification regarding clinical outcome in BrS patients. However, the scientific community is increasingly focusing on separating genetic noise from true pathogenic mutations. Risgaard et al. (2013) reported a high prevalence (1:23) of previously BrS-associated variants in ESP. If we added the variants described in the five newest identified genes associated with BrS, they appeared at an even higher prevalence in the ESP (1:21).

These data definitely questions the pathogenic role of some of the previously BrS-associated variants. With regard to deletions and insertions in *SCN5A* (Tables S1–S5) these are more likely susceptibility mutations, as also evidenced by their lack of presence in ESP.

In a HRS/EHRA consensus document, screening is recommended in family members and relatives following the identification of a BrS-causative mutation in an index case (Ackerman et al., 2011). If the clinician should perform risk stratifications based on genetic screening it is important that variants being associated with BrS are truly pathogenic. An index patient with definite BrS but a false-positive variant might have another true pathogenic variant that is not found. This could lead to misdiagnosis of family members with clinical consequences.

Another important motive for identifying the important susceptibility mutations by genetically screening BrS patients could be the tailoring of specific drugs to specific mutations as personal medicine. Presently, the rationale behind the pharmacological approach is to rebalance the inward and outward currents during the AP, regardless of the underlying mutation. Maybe in the future, it could be possible to treat the different BrS types (1–17) differently, according to their mutational consequences, although the disease entity is so small that the drugs will most likely not be developed for this indication in the first case. For instance, in the study done by Liu et al. (2009), they found that the NADH-induced decrease in I_{Na} could be antagonized by externally or internally applied NAD^+. This result suggests that drugs that increase the availability of NAD^+ may be a future treatment strategy for BrS2. Teng et al. (2009) found that a *SCN5A* non-sense mutation (W822X) associated with BrS effectively could be suppressed by read-through enhancing agents, thereby restoring the expression of normal length sodium channels. This holds promising for all non-sense mutations associated with BrS. Chakrabarti et al. (2013) recently showed that overexpression of *MOG1* effectively rescued the trafficking defect and the impaired plasma membrane expression of $Na_v1.5$ caused by the mutations D1275N and G1743, respectively. These data suggests that MOG1-enabled trafficking of Nav1.5 to plasma membrane may serve as a novel therapy for BrS patients with loss-of-function mutations in Nav1.5.

Even though over 300 mutations in 17 genes have been associated with BrS, approximately 70% of BrS incidents cannot be explained genetically at present. The causes may have to be found in epigenetic regulation or in other mechanisms than ion channel mutations. For instance methylation of promoters or mutations in microRNA binding sites as is has been shown for LQTS1 (Amin et al., 2012).

There is a need for an alternative strategy to ICD therapy. Firstly, because ICD treatment is prohibitively expensive in many parts of the world (Brugada et al., 2009). This is the case in Thailand where the prevalence is exceptionally high. Secondly, the high incidence of side-effects/complications associated with ICD (Sacher et al., 2006; Sarkozy et al., 2007; Miyazaki et al., 2013). And thirdly, BrS has been linked to sudden death infant syndrome (Van Norstrand et al., 2007) and ICD therapy in children is challenging in general. The high risk of complications reported in adults is likely to be worse in children (Antzelevitch and Nof, 2008).

The incentive for developing a good pharmacological paradigm is evident. Quinidine is yet the best alternative to ICD and has proven effective in small case series. However, a clear need exists for a large randomized clinical controlled trial to assess the effectiveness of quinidine in BrS patients.

ACKNOWLEDGMENTS

The study was supported by grants from "The John and Birthe Meyer Foundation.", The Arvid Nilsson Foundation, the Director Ib Henriksens Foundation, The Villadsen Family Foundation and The Stock Broker Henry Hansen and Wife Karla Hansen, born Westergaard, Grant.

SUPPLEMENTARY MATERIAL

The Supplementary Material for this article can be found online at: http://www.frontiersin.org/Cardiac_Electrophysiology_/10.3389/fphys.2013.00179/abstract

REFERENCES

Abbott, G. W., Butler, M. H., Bendahhou, S., Dalakas, M. C., Ptacek, L. J., and Goldstein, S. A. (2001). MiRP2 forms potassium channels in skeletal muscle with Kv3.4 and is associated with periodic paralysis. *Cell* 104, 217–231. doi: 10.1016/S0092-8674(01)00207-0

Ackerman, M. J., Priori, S. G., Willems, S., Berul, C., Brugada, R., Calkins, H., et al. (2011). HRS/EHRA expert consensus statement on the state of genetic testing for the channelopathies and cardiomyopathies this document was developed as a partnership between the Heart Rhythm Society (HRS) and the European Heart Rhythm Association (EHRA). *Heart Rhythm* 8, 1308–1339. doi: 10.1016/j.hrthm.2011.05.020

Amin, A. S., Giudicessi, J. R., Tijsen, A. J., Spanjaart, A. M., Reckman, Y. J., Klemens, C. A., et al. (2012). Variants in the 3' untranslated region of the KCNQ1-encoded Kv7.1 potassium channel modify disease severity in patients with type 1 long QT syndrome in an allele-specific manner. *Eur. Heart J.* 33, 714–723. doi: 10.1093/eurheartj/ehr473

Andreasen, C., Nielsen, J. B., Refsgaard, L., Holst, A. G., Christensen, A. H., Andreasen, L., et al. (2013a). New population-based exome data are questioning the pathogenicity of previously cardiomyopathy-associated genetic variants. *Eur. J. Hum. Genet.* doi: 10.1038/ejhg.2012.283. [Epub ahead of print].

Andreasen, C., Refsgaard, L., Nielsen, J. B., Sajadieh, A., Winkel, B. G., Tfelt-Hansen, J., et al. (2013b). Mutations in genes encoding cardiac ion channels previously associated with sudden infant death syndrome (SIDS) are present with high frequency in new exome data. *Can. J. Cardiol.* doi: 10.1016/j.cjca.2012.12.002. [Epub ahead of print].

Antzelevitch, C. (2006). Brugada syndrome. *Pacing Clin. Electrophysiol.* 29, 1130–1159. doi: 10.1111/j.1540-8159.2006.00507.x

Antzelevitch, C., Brugada, P., Borggrefe, M., Brugada, J., Brugada, R., Corrado, D., et al. (2005). Brugada syndrome: report of the second consensus conference: endorsed by the Heart Rhythm Society and the European Heart Rhythm Association. *Circulation* 111, 659–670. doi: 10.1161/01.CIR.0000152479.54298.51

Antzelevitch, C., and Nof, E. (2008). Brugada syndrome: recent advances and controversies. *Curr. Cardiol. Rep.* 10, 376–383. doi: 10.1007/s11886-008-0060-y

Antzelevitch, C., Pollevick, G. D., Cordeiro, J. M., Casis, O., Sanguinetti, M. C., Aizawa, Y., et al. (2007). Loss-of-function mutations in the cardiac calcium channel underlie a new clinical entity characterized by ST-segment elevation, short QT intervals, and sudden cardiac death. *Circulation* 115, 442–449. doi: 10.1161/CIRCULATIONAHA.106.668392

Barajas-Martínez, H., Hu, D., Ferrer, T., Onetti, C. G., Wu, Y., Burashnikov, E., et al. (2012). Molecular genetic and functional association of Brugada and early repolarization syndromes with S422L missense mutation in KCNJ8. *Heart Rhythm* 9, 548–555. doi: 10.1016/j.hrthm.2011.10.035

Baroudi, G., Pouliot, V., Denjoy, I., Guicheney, P., Shrier, A., and Chahine, M. (2001). Novel mechanism for Brugada syndrome: defective surface localization of an SCN5A mutant (R1432G). *Circ. Res.* 88, E78–E83. doi: 10.1161/hh1201.093270

Bayés de Luna, A., Brugada, J., Baranchuk, A., Borggrefe, M., Breithardt, G., Goldwasser, D., et al. (2012). Current electrocardiographic criteria for diagnosis of Brugada pattern: a consensus report. *J. Electrocardiol.* 45, 433–442. doi: 10.1016/j.jelectrocard.2012.06.004

Belhassen, B., Glick, A., and Viskin, S. (2004). Efficacy of quinidine in high-risk patients with Brugada syndrome. *Circulation* 110, 1731–1737. doi: 10.1161/01.CIR.0000143159.30585.90

Bezzina, C., Veldkamp, M. W., van Den Berg, M. P., Postma, A. V., Rook, M. B., Viersma, J. W., et al. (1999). A single Na(+) channel mutation causing both long-QT and Brugada syndromes. *Circ. Res.* 85, 1206–1213. doi: 10.1161/01.RES.85.12.1206

Brugada, J., Brugada, R., Antzelevitch, C., Towbin, J., Nademanee, K., and Brugada, P. (2002). Long-term follow-up of individuals with the electrocardiographic pattern of right bundle-branch block and ST-segment elevation in precordial leads V1 to V3. *Circulation* 105, 73–78. doi: 10.1161/hc0102.101354

Brugada, J., Brugada, R., and Brugada, P. (2000). Pharmacological and device approach to therapy of inherited cardiac diseases associated with cardiac arrhythmias and sudden death. *J. Electrocardiol.* 33(Suppl.), 41–47. doi: 10.1054/jelc.2000.20322

Brugada, P., Benito, B., Brugada, R., and Brugada, J. (2009). Brugada syndrome: update 2009. *Hellenic J. Cardiol.* 50, 352–372.

Brugada, P., and Brugada, J. (1992). Right bundle branch block, persistent ST segment elevation and sudden cardiac death: a distinct clinical and electrocardiographic syndrome. A multicenter report. *J. Am. Coll. Cardiol.* 20, 1391–1396. doi: 10.1016/0735-1097(92)90253-J

Brugada, P., Brugada, R., Brugada, J., and Geelen, P. (1999). Use of the prophylactic implantable cardioverter defibrillator for patients with normal hearts. *Am. J. Cardiol.* 83, 98D–100D. doi: 10.1016/S0002-9149(98)01009-1

Burashnikov, E., Pfeiffer, R., Barajas-Martinez, H., Delpón, E., Hu, D., Desai, M., et al. (2010). Mutations in the cardiac L-type calcium channel associated with inherited J-wave syndromes and sudden cardiac death. *Heart Rhythm* 7, 1872–1882. doi: 10.1016/j.hrthm.2010.08.026

Calloe, K., Cordeiro, J. M., Di Diego, J. M., Hansen, R. S., Grunnet, M., Olesen, S. P., et al. (2009). A transient outward potassium current activator recapitulates the electrocardiographic manifestations of Brugada syndrome. *Cardiovasc. Res.* 81, 686–694. doi: 10.1093/cvr/cvn339

Calloe, K., Refaat, M. M., Grubb, S., Wojciak, J., Campagna, J., Thomsen, N. M., et al. (2013). Characterization and mechanisms of action of novel NaV1.5 channel mutations associated with Brugada syndrome. *Circ. Arrhythm. Electrophysiol.* 6, 177–184. doi: 10.1161/CIRCEP.112.974220

Catterall, W. A., Perez-Reyes, E., Snutch, T. P., and Striessnig, J. (2005). International union of pharmacology. Xlviii. Nomenclature and structure-function relationships of voltage-gated calcium channels. *Pharmacol. Rev.* 57, 411–425. doi: 10.1124/pr.57.4.5

Chakrabarti, S., Wu, X., Yang, Z., Wu, L., Yong, S. L., Zhang, C., et al. (2013). MOG1 rescues defective trafficking of Nav1.5 mutations in Brugada syndrome and sick sinus syndrome. *Circ. Arrhythm. Electrophysiol.* 6, 392–401. doi: 10.1161/CIRCEP.111.000206

Chen, Q., Kirsch, G. E., Zhang, D., Brugada, R., Brugada, J., Brugada, P., et al. (1998). Genetic basis and molecular mechanism for idiopathic ventricular fibrillation. *Nature* 392, 293–296. doi: 10.1038/32675

Chiang, K.-C., Lai, L.-P., and Shieh, R.-C. (2009). Characterization of a novel Nav1.5 channel mutation, A551T, associated with Brugada syndrome. *J. Biomed. Sci.* 16, 76. doi: 10.1186/1423-0127-16-76

Cordeiro, J. M., Marieb, M., Pfeiffer, R., Calloe, K., Burashnikov, E., and Antzelevitch, C. (2009). Accelerated inactivation of the L-type calcium current due to a mutation in CACNB2b underlies Brugada syndrome. *J. Mol. Cell. Cardiol.* 46, 695–703. doi: 10.1016/j.yjmcc.2009.01.014

Cornet, V., Bichet, D., Sandoz, G., Marty, I., Brocard, J., Bourinet, E., et al. (2002). Multiple determinants in voltage-dependent P/Q calcium channels control their retention in the endoplasmic reticulum. *Eur. J. Neurosci.* 16, 883–895. doi: 10.1046/j.1460-9568.2002.02168.x

Coronel, R., Casini, S., Koopmann, T. T., Wilms-Schopman, F. J. G., Verkerk, A. O., de Groot, J. R., et al. (2005). Right ventricular fibrosis and conduction delay in a patient with clinical signs of Brugada syndrome: a combined electrophysiological, genetic, histopathologic, and computational study. *Circulation* 112, 2769–2777. doi: 10.1161/CIRCULATIONAHA.105.532614

Crotti, L., Marcou, C. A., Tester, D. J., Castelletti, S., Giudicessi, J. R., Torchio, M., et al. (2012). Spectrum and prevalence of mutations involving BrS1- through BrS12-susceptibility genes in a cohort of unrelated patients referred for Brugada syndrome genetic testing: implications for genetic testing. *J. Am. Coll. Cardiol.* 60, 1410–1418. doi: 10.1016/j.jacc.2012.04.037

Darbar, D., Kannankeril, P. J., Donahue, B. S., Kucera, G., Stubblefield, T., Haines, J. L., et al. (2008). Cardiac sodium channel (SCN5A) variants associated with atrial fibrillation. *Circulation* 117, 1927–1935. doi: 10.1161/CIRCULATIONAHA.107.757955

Delaney, J. T., Muhammad, R., Blair, M. A., Kor, K., Fish, F. A., Roden, D. M., et al. (2012). A KCNJ8 mutation associated with early repolarization and atrial fibrillation. *Europace* 14, 1428–1432. doi: 10.1093/europace/eus150

Delpón, E., Cordeiro, J. M., Núñez, L., Thomsen, P. E. B., Guerchicoff, A., Pollevick, G. D., et al. (2008). Functional effects of KCNE3 mutation and its role in the development of Brugada syndrome. *Circ. Arrhythm. Electrophysiol.* 1, 209–218. doi: 10.1161/CIRCEP.107.748103

Derangeon, M., Montnach, J., Baró, I., and Charpentier, F. (2012). Mouse models of SCN5A-related cardiac arrhythmias. *Front. Physiol.* 3:210. doi: 10.3389/fphys.2012.00210

Di Diego, J. M., Sun, Z. Q., and Antzelevitch, C. (1996). I(to) and action potential notch are smaller in left vs. right canine ventricular epicardium. *Am. J. Physiol.* 271, H548–H561.

Duthoit, G., Fressart, V., Hidden-Lucet, F., Simon, F., Kattygnarath, D., Charron, P., et al. (2012). Brugada ECG pattern: a physiopathological prospective study based on clinical, electrophysiological, angiographic, and genetic findings. *Front. Physiol.* 3:474. doi: 10.3389/fphys.2012.00474

Eckardt, L., Probst, V., Smits, J. P. P., Bahr, E. S., Wolpert, C., Schimpf, R., et al. (2005). Long-term prognosis of individuals with right precordial ST-segment-elevation Brugada syndrome. *Circulation* 111, 257–263. doi: 10.1161/01.CIR.0000153267.21278.8D

Exome Variant Server, NHLBI GO Exome Sequencing Project (ESP). Seattle, WA. Available online at: http://evs.gs.washington.edu/EVS/ [Accessed February 1, 2013].

Frustaci, A., Priori, S. G., Pieroni, M., Chimenti, C., Napolitano, C., Rivolta, I., et al. (2005). Cardiac histological substrate in patients with clinical phenotype of Brugada syndrome. *Circulation* 112, 3680–3687. doi: 10.1161/CIRCULATIONAHA.105.520999

Gallagher, M. M., Forleo, G. B., Behr, E. R., Magliano, G., De Luca, L., Morgia, V., et al. (2008). Prevalence and significance of Brugada-type ECG in 12,012 apparently healthy European subjects. *Int. J. Cardiol.* 130, 44–48. doi: 10.1016/j.ijcard.2007.07.159

Gellens, M. E., George, A. L. Jr., Chen, L. Q., Chahine, M., Horn, R., and Kallen R. G. (1992). Primary structure and functional expression of the human cardiac tetrodotoxin-insensitive voltage-dependent sodium channel. *Proc. Natl. Acad. Sci. U.S.A.* 89, 554–558. doi: 10.1073/pnas.89.2.554

Giudicessi, J. R., Ye, D., Tester, D. J., Crotti, L., Mugione, A., Nesterenko, V. V., et al. (2011). Transient outward current (I(to)) gain-of-function mutations in the KCND3-encoded Kv4.3 potassium channel and Brugada syndrome. *Heart Rhythm* 8, 1024–1032. doi: 10.1016/j.hrthm.2011.02.021

Gurnett, C. A., De Waard, M., and Campbell, K. P. (1996). Dual function of the voltage-dependent Ca2+ channel alpha 2 delta subunit in current stimulation and subunit interaction. *Neuron* 16, 431–440. doi: 10.1016/S0896-6273(00)80061-6

Hedley, P. L., Jørgensen, P., Schlamowitz, S., Moolman-Smook, J., Kanters, J. K., Corfield, V. A., et al. (2009). The genetic basis of Brugada syndrome: a mutation update.

Hum. Mutat. 30, 1256–1266. doi: 10.1002/humu.21066

Hermida, J. S., Lemoine, J. L., Aoun, F. B., Jarry, G., Rey, J. L., and Quiret, J. C. (2000). Prevalence of the brugada syndrome in an apparently healthy population. *Am. J. Cardiol.* 86, 91–94. doi: 10.1016/S0002-9149(00)00835-3

Hermida, J.-S., Denjoy, I., Clerc, J., Extramiana, F., Jarry, G., Milliez, P., et al. (2004). Hydroquinidine therapy in Brugada syndrome. *J. Am. Coll. Cardiol.* 43, 1853–1860. doi: 10.1016/j.jacc.2003.12.046

Hobom, M., Dai, S., Marais, E., Lacinova, L., Hofmann, F., and Klugbauer, N. (2000). Neuronal distribution and functional characterization of the calcium channel alpha2delta-2 subunit. *Eur. J. Neurosci.* 12, 1217–1226. doi: 10.1046/j.1460-9568.2000.01009.x

Holst, A. G., Jensen, H. K., Eschen, O., Henriksen, F. L., Kanters, J., Bundgaard, H., et al. (2012a). Low disease prevalence and inappropriate implantable cardioverter defibrillator shock rate in Brugada syndrome: a nationwide study. *Europace* 14, 1025–1029. doi: 10.1093/europace/eus002

Holst, A. G., Saber, S., Houshmand, M., Zaklyazminskaya, E. V., Wang, Y., Jensen, H. K., et al. (2012b). Sodium current and potassium transient outward current genes in Brugada syndrome: screening and bioinformatics. *Can. J. Cardiol.* 28, 196–200. doi: 10.1016/j.cjca.2011.11.011

Hoogendijk, M. G., Opthof, T., Postema, P. G., Wilde, A. A. M., de Bakker, J. M. T., and Coronel, R. (2010). The Brugada ECG pattern: a marker of channelopathy, structural heart disease, or neither? Toward a unifying mechanism of the Brugada syndrome. *Circ. Arrhythm. Electrophysiol.* 3, 283–290. doi: 10.1161/CIRCEP.110.937029

Hsueh, C.-H., Chen, W.-P., Lin, J.-L., Tsai, C.-T., Liu, Y.-B., Juang, J.-M., et al. (2009). Distinct functional defect of three novel Brugada syndrome related cardiac sodium channel mutations. *J. Biomed. Sci.* 16, 23. doi: 10.1186/1423-0127-16-23

Hu, D., Barajas-Martinez, H., Burashnikov, E., Springer, M., Wu, Y., Varro, A., et al. (2009). A mutation in the beta 3 subunit of the cardiac sodium channel associated with Brugada ECG phenotype. *Circ. Cardiovasc. Genet.* 2, 270–278. doi: 10.1161/CIRCGENETICS.108.829192

Hu, D., Barajas-Martínez, H., Medeiros-Domingo, A., Crotti, L., Veltmann, C., Schimpf, R., et al. (2012). A novel rare variant in SCN1Bb linked to Brugada syndrome and SIDS by combined modulation of Na(v)1.5 and K(v)4.3 channel currents. *Heart Rhythm* 9, 760–769. doi: 10.1016/j.hrthm.2011.12.006

Imaizumi, Y., and Giles, W. R. (1987). Quinidine-induced inhibition of transient outward current in cardiac muscle. *Am. J. Physiol.* 253, H704–H708.

Ishikawa, T., Sato, A., Marcou, C. A., Tester, D. J., Ackerman, M. J., Crotti, L., et al. (2012). A novel disease gene for Brugada syndrome: sarcolemmal membrane-associated protein gene mutations impair intracellular trafficking of hNav1.5. *Circ. Arrhythm. Electrophysiol.* 5, 1098–1107. doi: 10.1161/CIRCEP.111.969972

Ishikawa, T., Takahashi, N., Ohno, S., Sakurada, H., Nakamura, K., On, Y. K., et al. (2013). Novel SCN3B mutation associated with Brugada syndrome affects intracellular trafficking and function of Nav1.5. *Circ. J.* 77, 959–967.

Isom, L. L. (2001). Sodium channel beta subunits: anything but auxiliary. *Neuroscientist* 7, 42–54. doi: 10.1177/107385840100700108

Itoh, H., Sakaguchi, T., Ashihara, T., Ding, W.-G., Nagaoka, I., Oka, Y., et al. (2009). A novel KCNH2 mutation as a modifier for short QT interval. *Int. J. Cardiol.* 137, 83–85. doi: 10.1016/j.ijcard.2008.05.050

Kapplinger, J. D., Tester, D. J., Alders, M., Benito, B., Berthet, M., Brugada, J., et al. (2010). An international compendium of mutations in the SCN5A-encoded cardiac sodium channel in patients referred for Brugada syndrome genetic testing. *Heart Rhythm* 7, 33–46. doi: 10.1016/j.hrthm.2009.09.069

Kattygnarath, D., Maugenre, S., Neyroud, N., Balse, E., Ichai, C., Denjoy, I., et al. (2011). MOG1: a new susceptibility gene for Brugada syndrome. *Circ. Cardiovasc. Genet.* 4, 261–268. doi: 10.1161/CIRCGENETICS.110.959130

Keller, D. I., Rougier, J.-S., Kucera, J. P., Benammar, N., Fressart, V., Guicheney, P., et al. (2005). Brugada syndrome and fever: genetic and molecular characterization of patients carrying SCN5A mutations. *Cardiovasc. Res.* 67, 510–519. doi: 10.1016/j.cardiores.2005.03.024

Killeen, M. J., Thomas, G., Sabir, I. N., Grace, A. A., and Huang, C. L.-H. (2008). Mouse models of human arrhythmia syndromes. *Acta Physiol. (Oxf).* 192, 455–469. doi: 10.1111/j.1748-1716.2007.01822.x

Kruse, M., Schulze-Bahr, E., Corfield, V., Beckmann, A., Stallmeyer, B., Kurtbay, G., et al. (2009). Impaired endocytosis of the ion channel TRPM4 is associated with human progressive familial heart block type I. *J. Clin. Invest.* 119, 2737–2744. doi: 10.1172/JCI38292

Letsas, K. P., Gavrielatos, G., Efremidis, M., Kounas, S. P., Filippatos, G. S., Sideris, A., et al. (2007). Prevalence of Brugada sign in a Greek tertiary hospital population. *Europace* 9, 1077–1080. doi: 10.1093/europace/eum221

Liu, H., Chatel, S., Simard, C., Syam, N., Salle, L., Probst, V., et al. (2013). Molecular genetics and functional anomalies in a series of 248 Brugada cases with 11 mutations in the TRPM4 channel. *PLoS ONE* 8:e54131. doi: 10.1371/journal.pone.0054131

Liu, H., El Zein, L., Kruse, M., Guinamard, R., Beckmann, A., Bozio, A., et al. (2010). Gain-of-function mutations in TRPM4 cause autosomal dominant isolated cardiac conduction disease. *Circ. Cardiovasc. Genet.* 3, 374–385. doi: 10.1161/CIRCGENETICS.109.930867

Liu, M., Sanyal, S., Gao, G., Gurung, I. S., Zhu, X., Gaconnet, G., et al. (2009). Cardiac Na+ current regulation by pyridine nucleotides. *Circ. Res.* 105, 737–745. doi: 10.1161/CIRCRESAHA.109.197277

London, B., Michalec, M., Mehdi, H., Zhu, X., Kerchner, L., Sanyal, S., et al. (2007). Mutation in glycerol-3-phosphate dehydrogenase 1 like gene (GPD1-L) decreases cardiac Na+ current and causes inherited arrhythmias. *Circulation* 116, 2260–2268. doi: 10.1161/CIRCULATIONAHA.107.703330

Márquez, M. F., Bonny, A., Hernández-Castillo, E., De Sisti, A., Gómez-Flores, J., Nava, S., et al. (2012). Long-term efficacy of low doses of quinidine on malignant arrhythmias in Brugada syndrome with an implantable cardioverter-defibrillator: a case series and literature review. *Heart Rhythm* 9, 1995–2000. doi: 10.1016/j.hrthm.2012.08.027

Márquez, M. F., Salica, G., Hermosillo, A. G., Pastelín, G., Gómez-Flores, J., Nava, S., et al. (2007). Ionic basis of pharmacological therapy in Brugada syndrome. *J. Cardiovasc. Electrophysiol.* 18, 234–240. doi: 10.1111/j.1540-8167.2006.00681.x

Medeiros-Domingo, A., Tan, B.-H., Crotti, L., Tester, D. J., Eckhardt, L., Cuoretti, A., et al. (2010). Gain-of-function mutation S422L in the KCNJ8-encoded cardiac K(ATP) channel Kir6.1 as a pathogenic substrate for J-wave syndromes. *Heart Rhythm* 7, 1466–1471. doi: 10.1016/j.hrthm.2010.06.016

Meregalli, P. G., Tan, H. L., Probst, V., Koopmann, T. T., Tanck, M. W., Bhuiyan, Z. A., et al. (2009). Type of SCN5A mutation determines clinical severity and degree of conduction slowing in loss-of-function sodium channelopathies. *Heart Rhythm* 6, 341–348. doi: 10.1016/j.hrthm.2008.11.009

Meregalli, P. G., Wilde, A. A. M., and Tan, H. L. (2005). Pathophysiological mechanisms of Brugada syndrome: depolarization disorder, repolarization disorder, or more? *Cardiovasc. Res.* 67, 367–378. doi: 10.1016/j.cardiores.2005.03.005

Minoura, Y., Panama, B. K., Nesterenko, V. V., Betzenhauser, M., Barajas-Martínez, H., Hu, D., et al. (2013). Effect of wenxin keli and quinidine to suppress arrhythmogenesis in an experimental model of Brugada syndrome. *Heart Rhythm.* 10, 1054–1062. doi: 10.1016/j.hrthm.2013.03.011

Miyazaki, S., Uchiyama, T., Komatsu, Y., Taniguchi, H., Kusa, S., Nakamura, H., et al. (2013). Long-term complications of implantable defibrillator therapy in Brugada syndrome. *Am. J. Cardiol.* 111, 1448–1451. doi: 10.1016/j.amjcard.2013.01.295

Morgan, K., Stevens, E. B., Shah, B., Cox, P. J., Dixon, A. K., Lee, K., et al. (2000). beta 3: an additional auxiliary subunit of the voltage-sensitive sodium channel that modulates channel gating with distinct kinetics. *Proc. Natl. Acad. Sci. U.S.A.* 97, 2308–2313. doi: 10.1073/pnas.030362197

Nademanee, K., Veerakul, G., Chandanamattha, P., Chaothawee, L., Ariyachaipanich, A., Jirasirirojanakorn, K., et al. (2011). Prevention of ventricular fibrillation episodes in Brugada syndrome by catheter ablation over the anterior right ventricular outflow tract epicardium. *Circulation* 123, 1270–1279. doi: 10.1161/CIRCULATIONAHA.110.972612

Ohno, S., Zankov, D. P., Ding, W.-G., Itoh, H., Makiyama, T., Doi, T., et al. (2011). KCNE5 (KCNE1L) variants are novel modulators of Brugada syndrome and idiopathic ventricular fibrillation. *Circ. Arrhythm.*

Electrophysiol. 4, 352–361. doi: 10.1161/CIRCEP.110.959619

Olesen, M. S., Jensen, N. F., Holst, A. G., Nielsen, J. B., Tfelt-Hansen, J., Jespersen, T., et al. (2011a). A novel nonsense variant in Nav1.5 cofactor MOG1 eliminates its sodium current increasing effect and may increase the risk of arrhythmias. *Can. J. Cardiol.* 27, 523.e17–23. doi: 10.1016/j.cjca.2011.01.003

Olesen, M. S., Jespersen, T., Nielsen, J. B., Liang, B., Møller, D. V., Hedley, P., et al. (2011b). Mutations in sodium channel β-subunit SCN3B are associated with early-onset lone atrial fibrillation. *Cardiovasc. Res.* 89, 786–793. doi: 10.1093/cvr/cvq348

Olesen, M. S., Yuan, L., Liang, B., Holst, A. G., Nielsen, N., Nielsen, J. B., et al. (2012a). High prevalence of long QT syndrome associated SCN5A variants in patients with early-onset lone atrial fibrillation. *Circ. Cardiovasc. Genet.* Available online at: http://www.ncbi.nlm.nih.gov/pubmed/22685113 [Accessed August 1, 2012]. 5, 450–459. doi: 10.1161/CIRCGENETICS.111.962597

Olesen, M. S., Holst, A. G., Svendsen, J. H., Haunsø, S., and Tfelt-Hansen, J. (2012b). SCN1Bb R214Q found in 3 patients: 1 with Brugada syndrome and 2 with lone atrial fibrillation. *Heart Rhythm Off. J. Heart Rhythm Soc.* 9, 770–773. doi: 10.1016/j.hrthm.2011.12.005

Pfahnl, A. E., Viswanathan, P. C., Weiss, R., Shang, L. L., Sanyal, S., Shusterman, V., et al. (2007). A sodium channel pore mutation causing Brugada syndrome. *Heart Rhythm* 4, 46–53. doi: 10.1016/j.hrthm.2006.09.031

Priori, S. G., Napolitano, C., Gasparini, M., Pappone, C., Della Bella, P., Giordano, U., et al. (2002). Natural history of Brugada syndrome: insights for risk stratification and management. *Circulation* 105, 1342–1347. doi: 10.1161/hc1102.105288

Priori, S. G., Napolitano, C., Tiso, N., Memmi, M., Vignati, G., Bloise, R., et al. (2001). Mutations in the cardiac ryanodine receptor gene (hRyR2) underlie catecholaminergic polymorphic ventricular tachycardia. *Circulation* 103, 196–200. doi: 10.1161/01.CIR.103.2.196

Probst, V., Veltmann, C., Eckardt, L., Meregalli, P. G., Gaita, F., Tan, H. L., et al. (2010). Long-term prognosis of patients diagnosed with Brugada syndrome: Results from the FINGER Brugada Syndrome Registry. *Circulation* 121, 635–643. doi: 10.1161/CIRCULATIONAHA.109.887026

Refsgaard, L., Holst, A. G., Sadjadieh, G., HaunsØ, S., Nielsen, J. B., and Olesen, M. S. (2012). High prevalence of genetic variants previously associated with LQT syndrome in new exome data. *Eur. J. Hum. Genet.* 20, 905–908. doi: 10.1038/ejhg.2012.23

Remme, C. A., Wilde, A. A. M., and Bezzina, C. R. (2008). Cardiac sodium channel overlap syndromes: different faces of SCN5A mutations. *Trends Cardiovasc. Med.* 18, 78–87. doi: 10.1016/j.tcm.2008.01.002

Risgaard, B., Jabbari, R., Refsgaard, L., Holst, A. G., Haunsø, S., Sadjadieh, A., et al. (2013). High prevalence of genetic variants previously associated with Brugada Syndrome in new exome data. *Clin. Genet.* doi: 10.1111/cge.12126. [Epub ahead of print].

Riuró, H., Beltran-Alvarez, P., Tarradas, A., Selga, E., Campuzano, O., Vergés, M., et al. (2013). A missense mutation in the sodium channel β2 subunit reveals SCN2B as a new candidate gene for Brugada syndrome. *Hum. Mutat.* 34, 961–966. doi: 10.1002/humu.22328

Sacher, F., Probst, V., Iesaka, Y., Jacon, P., Laborderie, J., Mizon-Gérard, F., et al. (2006). Outcome after implantation of a cardioverter-defibrillator in patients with Brugada syndrome: a multicenter study. *Circulation* 114, 2317–2324. doi: 10.1161/CIRCULATIONAHA.106.628537

Sarkozy, A., Boussy, T., Kourgiannides, G., Chierchia, G.-B., Richter, S., De Potter, T., et al. (2007). Long-term follow-up of primary prophylactic implantable cardioverter-defibrillator therapy in Brugada syndrome. *Eur. Heart J.* 28, 334–344. doi: 10.1093/eurheartj/ehl450

Sinner, M. F., Pfeufer, A., Perz, S., Schulze-Bahr, E., Mönnig, G., Eckardt, L., et al. (2009). Spontaneous Brugada electrocardiogram patterns are rare in the German general population: results from the KORA study. *Europace* 11, 1338–1344. doi: 10.1093/europace/eup205

Sommariva, E., Pappone, C., Martinelli Boneschi, F., Di Resta, C., Rosaria Carbone, M., Salvi, E., et al. (2013). Genetics can contribute to the prognosis of Brugada syndrome: a pilot model for risk stratification. *Eur. J. Hum. Genet.* doi: 10.1038/ejhg.2012.289. [Epub ahead of print].

Stallmeyer, B., Zumhagen, S., Denjoy, I., Duthoit, G., Hébert, J.-L., Ferrer, X., et al. (2012). Mutational spectrum in the Ca(2+)–activated cation channel gene TRPM4 in patients with cardiac conductance disturbances. *Hum. Mutat.* 33, 109–117. doi: 10.1002/humu.21599

Takimoto, K., Li, D., Nerbonne, J. M., and Levitan, E. S. (1997). Distribution, splicing and glucocorticoid-induced expression of cardiac alpha 1C and alpha 1D voltage-gated Ca2+ channel mRNAs. *J. Mol. Cell. Cardiol.* 29, 3035–3042. doi: 10.1006/jmcc.1997.0532

Teng, S., Gao, L., Paajanen, V., Pu, J., and Fan, Z. (2009). Readthrough of nonsense mutation W822X in the SCN5A gene can effectively restore expression of cardiac Na+ channels. *Cardiovasc. Res.* 83, 473–480. doi: 10.1093/cvr/cvp116

Ueda, K., Nakamura, K., Hayashi, T., Inagaki, N., Takahashi, M., Arimura, T., et al. (2004). Functional characterization of a trafficking-defective HCN4 mutation, D553N, associated with cardiac arrhythmia. *J. Biol. Chem.* 279, 27194–27198. doi: 10.1074/jbc.M311953200

Valdivia, C. R., Tester, D. J., Rok, B. A., Porter, C.-B. J., Munger, T. M., Jahangir, A., et al. (2004). A trafficking defective, Brugada syndrome-causing SCN5A mutation rescued by drugs. *Cardiovasc. Res.* 62, 53–62. doi: 10.1016/j.cardiores.2004.01.022

Van Norstrand, D. W., Valdivia, C. R., Tester, D. J., Ueda, K., London, B., Makielski, J. C., et al. (2007). Molecular and functional characterization of novel glycerol-3-phosphate dehydrogenase 1 like gene (GPD1-L) mutations in sudden infant death syndrome. *Circulation* 116, 2253–2259. doi: 10.1161/CIRCULATIONAHA.107.704627

Veldkamp, M. W., Viswanathan, P. C., Bezzina, C., Baartscheer, A., Wilde, A. A., and Balser, J. R. (2000). Two distinct congenital arrhythmias evoked by a multidysfunctional Na(+) channel. *Circ. Res.* 86, E91–E97. doi: 10.1161/01.RES.86.9.e91

Verkerk, A. O., Wilders, R., Schulze-Bahr, E., Beekman, L., Bhuiyan, Z. A., Bertrand, J., et al. (2005). Role of sequence variations in the human ether-a-go-go-related gene (HERG, KCNH2) in the Brugada syndrome. *Cardiovasc. Res.* 68, 441–453. doi: 10.1016/j.cardiores.2005.06.027

Watanabe, H., Koopmann, T. T., Le Scouarnec, S., Yang, T., Ingram, C. R., Schott, J.-J., et al. (2008). Sodium channel β1 subunit mutations associated with Brugada syndrome and cardiac conduction disease in humans. *J. Clin. Invest.* 118, 2260–2268. doi: 10.1172/JCI33891

Weiss, R., Barmada, M. M., Nguyen, T., Seibel, J. S., Cavlovich, D., Kornblit, C. A., et al. (2002). Clinical and molecular heterogeneity in the Brugada syndrome: a novel gene locus on chromosome 3. *Circulation* 105, 707–713. doi: 10.1161/hc0602.103618

Wilde, A. A. M., Postema, P. G., Di Diego, J. M., Viskin, S., Morita, H., Fish, J. M., et al. (2010). The pathophysiological mechanism underlying Brugada syndrome: depolarization versus repolarization. *J. Mol. Cell. Cardiol.* 49, 543–553. doi: 10.1016/j.yjmcc.2010.07.012

Wilders, R., and Verkerk, A. O. (2010). Role of the R1135H KCNH2 mutation in Brugada syndrome. *Int. J. Cardiol.* 144, 149–151. doi: 10.1016/j.ijcard.2008.12.177

Yan, G. X., and Antzelevitch, C. (1999). Cellular basis for the Brugada syndrome and other mechanisms of arrhythmogenesis associated with ST-segment elevation. *Circulation* 100, 1660–1666. doi: 10.1161/01.CIR.100.15.1660

Conflict of Interest Statement: The authors declare that the research was conducted in the absence of any commercial or financial relationships that could be construed as a potential conflict of interest.

Received: 29 April 2013; accepted: 24 June 2013; published online: 15 July 2013.

*Citation: Nielsen MW, Holst AG, Olesen S-P and Olesen MS (2013) The genetic component of Brugada syndrome. Front. Physiol. **4**:179. doi: 10.3389/fphys.2013.00179*

This article was submitted to Frontiers in Cardiac Electrophysiology, a specialty of Frontiers in Physiology.

frontiers in PHYSIOLOGY

ORIGINAL RESEARCH ARTICLE
published: 26 June 2013
doi: 10.3389/fphys.2013.00153

Characterization of N-terminally mutated cardiac Na^+ channels associated with long QT syndrome 3 and Brugada syndrome

Christian Gütter, Klaus Benndorf and Thomas Zimmer*

Institute of Physiology II, University Hospital Jena, Friedrich Schiller University Jena, Jena, Germany

Edited by:
Christopher Huang, University of Cambridge, UK

Reviewed by:
Christopher Huang, University of Cambridge, UK
Ming Lei, University of Manchester, UK

****Correspondence:***
Thomas Zimmer, Institute of Physiology II, University Hospital Jena, Friedrich Schiller University Jena, Kollegiengasse 9, 07743 Jena, Germany
e-mail: thomas.zimmer@mti.uni-jena.de

Mutations in *SCN5A*, the gene encoding the cardiac voltage-gated Na^+ channel $hNa_v1.5$, can result in life-threatening arrhythmias including long QT syndrome 3 (LQT3) and Brugada syndrome (BrS). Numerous mutant $hNa_v1.5$ channels have been characterized upon heterologous expression and patch-clamp recordings during the last decade. These studies revealed functionally important regions in $hNa_v1.5$ and provided insight into gain-of-function or loss-of-function channel defects underlying LQT3 or BrS, respectively. The N-terminal region of $hNa_v1.5$, however, has not yet been investigated in detail, although several mutations were reported in the literature. In the present study we investigated three mutant channels, previously associated with LQT3 (G9V, R18W, V125L), and six mutant channels, associated with BrS (R18Q, R27H, G35S, V95I, R104Q, K126E). We applied both the two-microelectrode voltage clamp technique, using cRNA-injected *Xenopus* oocytes, and the whole-cell patch clamp technique using transfected HEK293 cells. Surprisingly, four out of the nine mutations did not affect channel properties. Gain-of-function, as typically observed in LQT3 mutant channels, was observed only in R18W and V125L, whereas loss-of-function, frequently found in BrS mutants, was found only in R27H, R104Q, and K126E. Our results indicate that the $hNa_v1.5$ N-terminus plays an important role for channel kinetics and stability. At the same time, we suggest that additional mechanisms, as e.g., disturbed interactions of the Na^+ channel N-terminus with other proteins, contribute to severe clinical phenotypes.

Keywords: cardiac sodium channel, cardiac arrhythmia, *SCN5A* channelopathies, electrophysiology, Long QT syndrome, Brugada syndrome, N-terminus

INTRODUCTION

Voltage-gated sodium (Na^+) channels are responsible for the rapid upstroke of the action potential in electrically excitable cells. The tetrodotoxin (TTX) resistant isoform $hNa_v1.5$, encoded by the *SCN5A* gene, is the predominant isoform in the human heart (Gellens et al., 1992; Blechschmidt et al., 2008; Zimmer, 2010; Rook et al., 2012; Savio-Galimberti et al., 2012). A broad spectrum of mutations in *SCN5A* were related to a variety of inherited cardiac diseases, such as long QT syndrome type 3 (LQT3), Brugada syndrome (BrS), cardiac conduction disease (CCD), or sick sinus syndrome (SSS) (Zimmer and Surber, 2008; Gui et al., 2010). Heterologous expression of respective mutant $hNa_v1.5$ channels revealed important insight into the mechanisms underlying these cardiac diseases. In LQT3, mutant channels are characterized by gain-of-function features, like faster recovery from the inactivated state (Chandra et al., 1998; Clancy et al., 2003), inactivation defects (Bennett et al., 1995; Chandra et al., 1998), or dispersed reopenings from the inactivated state (Dumaine et al., 1996). Such defects are believed to result in an action potential widening and consequently, in the observed QT prolongation. In BrS or CCD, mutant channels often show loss-of-function features, like reduced channel availability at the resting membrane potential (Rivolta et al., 2001), a positive shift of steady-state activation (Vatta et al., 2002a; Potet et al., 2003), impaired trafficking to the plasma membrane (Baroudi et al., 2001; Valdivia et al., 2004), or the inability to conduct Na^+ (Kyndt et al., 2001; Zhang et al., 2008). Such defects can explain cardiac conduction abnormalities and the observed ST segment elevation (Alings and Wilde, 1999; Yan and Antzelevitch, 1999). These genotype-phenotype associations in *SCN5A* channelopathies are not only important for clinicians regarding the management of genotype-positive patients and symptom-free family members. Functional data on mutant channels also extended our knowledge about important structural elements in the cardiac Na^+ channel, like the DIII-DIV linker as the inactivation gate (Bennett et al., 1995) or position 1053 for ankyrin-G binding (Mohler et al., 2004).

Currently, however, we are faced with a growing number of mutations that are not yet characterized by electrophysiological measurements. The lack of functional data makes it difficult for clinicians to interpret the results of genetic testing, because a rare deviation from the published *SCN5A* sequence could be malign or even benign. For example, only 20% of the BrS patients are *SCN5A*-positive cases, and the majority of BrS-causative mutations or factors still remain obscure (Kapplinger et al., 2010). Consequently, the same yet unknown factors could

be also crucial for the manifestation of the disease in *SCN5A*-positive BrS patients, in particular when mutant channels were either not characterized or electrophysiologically indiscernible from wild-type $hNa_v1.5$.

The present study focuses on nine arrhythmia-causing missense mutations localized to the N-terminus of $hNa_v1.5$ that have not yet been characterized by electrophysiological techniques (**Figure 1**). We selected all three published LQT3 mutations and six out of seventeen BrS mutations reported in the online database of Drs. Priori and Napolitano (http://www.fsm.it/cardmoc/). The aim of this project was to establish respective genotype-phenotype correlations and to get more insight into the role of the intracellularly exposed N-terminus for channel gating. This region has not yet been investigated in detail in terms of structure-function relationships. Therefore, it was challenging for us to search for possible inactivation defects in the LQT3 mutant channels, and for loss-of-function features caused by the BrS missense mutations. All mutant channels were expressed in both HEK293 cells and *Xenopus* oocytes. We performed electrophysiological measurements in both heterologous hosts to identify or exclude cell-specific effects.

MATERIAL AND METHODS

RECOMBINANT DNA PROCEDURES

Generation of the expression plasmid pTSV40G-$hNa_v1.5$, coding for wild-type $hNa_v1.5$, was described previously (Walzik et al., 2011). The original hH1 cDNA (accession number M77235) was kindly provided by Dr. A. L. George (Gellens et al., 1992). Mutations at amino acid positions 9, 18, 27, 35, 95, 104, 125, and 126 were introduced using the recombinant PCR technique and the following internal primer pairs:

5′-TTACCTCGGGTCACCAGCAGCTTCCGCAGG-3′ and
5′-GGAAGCTGCTGGTGACCCGAGGTAATAGGAA GTTTG-3′ to obtain G9V,
5′-GCAGGTTCACACTGGGAGTCCCTGGCAGCCATC-3′ and
5′-CCAGGGACTCCCATGTGAACCTGCGGAAGCTG-3′ to obtain R18W,
5′-GCAGGTTCACACAGGAGTCCCTGGCAGCCATC-3′ and
5′-CCAGGGACTCCTGTGTGAACCTGCGGAAGCTG-3′ to obtain R18Q,
5′-CATCGAGAAGCACATGGCGGAGAAGCAAGCCC-3′ and
5′-CTTCTCCGCCATGTGCTTCTCGATGGCTGCCAGG-3′ to obtain R27H,
5′-AAGCAAGCCCGCAGCTCAACCACCTTGCAGGAG-3′ and
5′-GGTGGTTGAGCTGCGGGCTTGCTTCTCCGCCATG-3′ to obtain G35S,
5′-AAGACTTTCATCATACTGAATAAAGGCAAGACCA-3′ and
5′-CCTTTATTCAGTATGATGAAAGTCTTTTGGGTG-3′ to obtain V95I,
5′-ACCATCTTCCAGTTCAGTGCCACCAACGCCTT-3′ and
5′-TGGCACTGAACTGGAAGATGGTCTTGCCTTTA-3′ to obtain R104Q,
5′-AGAGCGGCTTTGAAGATTCTGGTTCACTCG-3′ and
5′-GAACCAGAATCTTCAAAGCCGCTCTCCGGATGGG GTGG-3′ to obtain V125L, and
5′-CGGCTGTGGAGATTCTGGTTCACTCGCTCTT-3′ and
5′-AGTGAACCAGAATCTCCACAGCCGCTCTCCGGAT GGGGT-3′

to obtain K126E. The recombinant PCR products were inserted as *Age*I/*Hind*III fragments into the corresponding sites of pTSV40G-$hNa_v1.5$. A thermostable DNA polymerase with proofreading activity was used for all PCR reactions (Pfu DNA polymerase, Promega, Madison, USA). The correctness of PCR-derived sequences was confirmed by DNA sequencing. Construction of the control plasmid encoding ΔKPQ channels was previously described (Surber et al., 2008). All channel variants were placed under the control of the SV40 promoter in expression plasmid pTSV40G, a derivative of pTracerSV40 (Invitrogen) (Camacho et al., 2006). Vector pTSV40G contains the T7 promoter and, in a separate expression cassette, the coding region of the enhanced green fluorescent protein (EGFP; Clontech) to allow for cRNA preparation and for selection of transfected HEK293 cells, respectively.

HETEROLOGOUS EXPRESSION IN HEK293 CELLS

Heterologous expression in mammalian cells was done as previously described (Zimmer et al., 2002b). Human embryonic kidney cells (HEK293 cell line, ATCC number CRL-1573) were cultured in Dulbecco's Modified Eagle Medium (DMEM; GibcoBRL), supplemented with 2 mM glutamine, 10% fetal bovine serum, 100 μg/ml streptomycin, 100 U/ml penicillin, and 0.25 μg/ml amphotericin B. HEK293 cells were transfected by a standard calcium phosphate precipitation method using 1.0 μg plasmid DNA per transfection dish (60 mm diameter). After an incubation time of 24 h, the transfection mixture was removed. Cells were seeded onto poly-L-lysine coated glass cover slips and cultured in fresh growth medium. Na^+ currents were investigated 24–48 h after transfection.

PATCH-CLAMP MEASUREMENTS

Electrophysiological recordings were performed, as previously described (Surber et al., 2008; Walzik et al., 2011). We used an inverted microscope (Axiovert 100, Carl Zeiss Jena GmbH, Germany) and an Axopatch 200B amplifier (Axon-Instruments, Foster City, USA). All measurements were carried out at room temperature (19–22°C). The bath solution contained (mM): 140.0 NaCl, 1.8 $CaCl_2$, 1.0 $MgCl_2$, 10.0 glucose, 10.0 HEPES, pH 7.4 (CsOH). The pipette solution contained (mM): 10.0 NaCl, 130.0 CsCl, 10.0 EGTA, 10.0 HEPES, pH 7.3 (CsOH). Currents were elicited by test potentials from −80 mV to 40 mV in 5 or 10 mV increments at a pulsing frequency of 1.0 Hz (holding potential −120 mV). Cells that produced a peak current amplitude >6 nA were excluded from data analysis. Steady-state activation (m_∞) was evaluated by fitting the Boltzmann equation $m_\infty = \{1 + \exp[-(V - V_m)/s]\}^{-1}$ to the normalized conductance as function of voltage. Steady-state inactivation (h_∞) was determined with a double-pulse protocol consisting of 500 ms prepulses to voltages between −140 and −30 mV followed by a constant test pulse of 10 ms duration to −20 mV at a pulsing frequency of 0.5 Hz. The amplitude of peak I_{Na} during the test pulse was normalized to the maximum peak current and

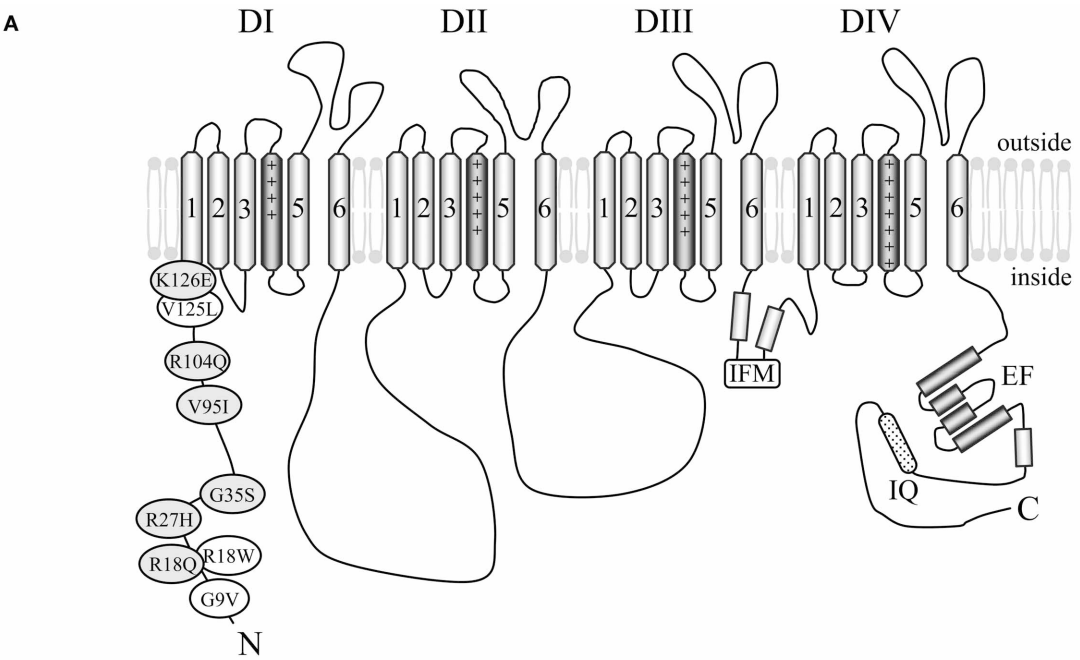

B

```
                          G9V       R18W
                                    R18Q        R27H      G35S
hNav1.1    1 MEQT---VLVPPGPDSFNFFTRESLAAIERRIAEEKAKNPKPD---KKD-DDENGPKPNSDLEAGKNLPF
hNav1.2    1 MAQS---VLVPPGPDSFRFFTRESLAAIEQRIAEEKAKRPKQE---RKDEDDENGPKPNSDLEAGKSLPF
hNav1.3    1 MAQA---LLVPPGPESFRLFTRESLAAIEKRAAEEKAKKPKKE---Q-DNDDENKPKPNSDLEAGKNLPF
hNav1.4    1 MARPSLCTLVPLGPECLRPFTRESLAAIEQRAVEEEARLQRN----KQMEIEEPERKPRSDLEAGKNLPM
hNav1.5    1 MAN----FLLPRGTSSFRRFTRESLAAIEKRMAEKQARGSTTLQESREGLPEEEAPRPQLDLQASKKLPD
hNav1.6    1 MAAR---LLAPPGPDSFKPFTPESLANIERRIAESKLKKPPKADGSHREDDEDSKPKPNSDLEAGKSLPF
hNav1.7    1 M--A---MLPPPGPQSFVHFTKQSLALIEQRIAERKSKEPKEE---KKDDDEE-APKPSSDLEAGKQLPF
hNav1.8    1 MEFP----IGSLETNNFRRFTPESLVEIEKQIAAKQGTK-KAREKHREQKDQEEKPRPQLDLKACNQLPK
hNav1.9    1 MDDRCYPVIFP-DERNFRPFTSDSLAAIEKRIAIQKEKK-----KSKDQTGEVPQPRPQLDLKASRKLPK

                                                                  V125L
                                        V95I      R104Q                   K126E   DI-S1
hNav1.1   64 IYGDIPPEMVSEPLEDLDPYYINKKTFIVLNKGKAIFRFSATSALYILTPFNPLRKIAIKILVHSLFSML
hNav1.2   65 IYGDIPPEMVSVPLEDLDPYYINKKTFIVLNKGKAISRFSATPALYILTPFNPIRKLAIKILVHSLFNML
hNav1.3   64 IYGDIPPEMVSEPLEDLDPYYINKKTFIVMNKGKAIFRFSATSALYILTPLNPVRKIAIKILVHSLFSML
hNav1.4   67 IYGDPPPEVIGIPLEDLDPYYSNKKTFIVLNKGKAIFRFSATPALYLLSPFSVVRRGAIKVLIHALFSMF
hNav1.5   67 LYGNPPQELIGEPLEDLDPFYSTQKTFIVLNKGKTIFRFSATNALYVLSPFHPVRRAAVKILVHSLFNML
hNav1.6   68 IYGDIPQGLVAVPLEDFDPYYLTQKTFVVLNRGKTLFRFSATPALYILSPFNLIRRIAIKILIHSVFSMI
hNav1.7   62 IYGDIPPGMVSEPLEDLDPYYADKKTFIVLNKGKTIFRFNATPALYMLSPFSPLRRISIKILVHSLFSML
hNav1.8   66 FYGELPAELIGEPLEDLDPFYSTHRTFMVLNKGRTISRFSATRALWLFSPFNLIRRTAIKVSVHSWFSLF
hNav1.9   65 LYGDIPRELIGKPLEDLDPFYRNHKTFMVLNRKRTIYRFSAKHALFIFGPFNSIRSLAIRVSVHSLFSMF
```

FIGURE 1 | Schematic representation of $hNa_v1.5$ and the N-terminal mutations investigated in this study. (A) Proposed $hNa_v1.5$ topology. Affected residues are indicated in white (LQT3) and light grey (BrS). The schematic structure also highlights some important structural features (DI to DIV—domain I to IV, IFM—residues isoleucine, phenylalanine, and methionine of the inactivation gate, IQ—calmodulin binding motif, EF—Ca^{++} binding EF hand domain). **(B)** Alignment of the N-terminal sequences of human Nav1.1—Nav1.9. Mutations associated with LQT3 or BrS are underlined or indicated in italics, respectively. Most of the eight affected residues are conserved among the Na_v1 subfamily. Residues at position 35 are variable, and position 125 is occupied by isoleucine in all other human Na^+ channels. All eight residues affected by a *SCN5A* mutation are identical in $Na_v1.5$ of human, rat, mouse, and dog (not shown). The N-terminal region of the first putative membrane spanning segment DI-S1 is indicated in light grey. References: G9V (Millat et al., 2006), R18W (Tester et al., 2005), R18Q (Kapplinger et al., 2010), R27H (Priori et al., 2002), G35S (Levy-Nissenbaum et al., 2001), V95I (Liang et al., 2006), R104Q (Levy-Nissenbaum et al., 2001), V125L (Tester et al., 2005), K126E (Vatta et al., 2002a).

plotted as function of the prepulse potential. Data were fitted to the Boltzmann equation $h_\infty = \{1 + \exp[(V - V_h)/s]\}^{-1}$. V is the test potential, V_m and V_h are the mid-activation and mid-inactivation potentials, respectively, and s the slope factor in mV. Glass pipettes were pulled from borosilicate glass. Glass tips were heat polished by microforge MF 830 (Narishige, Japan). The pipette resistance was between 1.4 and 2.6 MΩ. Series resistance compensation was adjusted so that any oscillations were avoided leaving at most 25% of the series resistance uncompensated. Currents were on-line filtered with a cut-off frequency of 10 kHz (4-pole Bessel). Recording and analysis of the data was performed on a personal computer with the ISO3 software (MFK, Niedernhausen, Germany). The sampling rate was 50 kHz. Student's *t*-test was used to test for statistical significance. Statistical significance was assumed for $P < 0.05$.

EXPRESSION IN *Xenopus Laevis* OOCYTES

Preparation of *Xenopus laevis* oocytes, *in vitro* transcription, and cRNA injection was done as previously described (Zimmer et al., 2002a). Fluorescence intensities of the cRNA bands were measured using the gel documentation system from Herolab (Wiesloch, Germany). Concentrations of the cRNA variants were adjusted to ∼ 0.01 μg/μl, before injecting about 50–80 nl cRNA per oocyte. After 3 days incubation at 18°C in Barth medium, the peak current amplitude of the whole-cell Na^+ current was between 0.5 and 8.0 μA, depending on the quality of the oocyte batch. Cells producing currents larger than 5 μA were not selected for data evaluation. Measurements were performed in at least four different batches of oocytes. For the measurements of persistent Na^+ currents we injected undiluted cRNA preparations (∼ 0.2 μg/μl) in order to increase this small current fraction. This resulted in transient Na^+ currents >8 μA in 96 mM external Na^+.

TWO-MICROELECTRODE VOLTAGE-CLAMP TECHNIQUE

Whole-cell Na^+ currents were recorded with the two-microelectrode voltage-clamp technique, similarly as previously described (Zimmer et al., 2002a). For all recordings we used the amplifier TEC-05-S (npi electronic GmbH, Tamm, Germany). For the determination of peak current amplitudes, steady-state activation, steady-state inactivation and recovery from inactivation, the following bath solution was used (in mM): 96 NaCl, 2 KCl, 1.8 $CaCl_2$, 1 $MgCl_2$, 10 HEPES/KOH, pH 7.4. The persistent current fraction was determined as previously described (Surber et al., 2008): First, we measured the inward current at the end of a 200 ms test pulse that could be blocked by 10 μM TTX in 96 mM external Na^+ ($I_{persistent}$). Then, we reduced the extracellular Na^+ concentration to 20 mM in order to insure adequate voltage control also for the first few milliseconds of the test pulse and determined the peak current amplitude in the same oocyte ($I_{transient}$). The following bath solution was used (in mM): 20 NaCl, 78 KCl, 1.8 $CaCl_2$, 1 $MgCl_2$, 10 HEPES/KOH, pH 7.4. Currents were elicited by 200 ms test potentials from −80 to 40 mV in 5 mV or 10 mV increments (holding potential −120 mV, pulsing frequency 1.0 Hz).

RESULTS

PROPERTIES OF LQT3 MUTANT CHANNELS (G9V, R18W, V125L)

All three mutant channels associated with LQT3 generated whole-cell currents comparable to those observed for $hNa_v1.5$ (**Table 1**, **Figure 2A**). No significant differences were observed in the peak current density when expressing G9V, R18W and V125L in HEK293 cells or in *Xenopus* oocytes. Also, the persistent current fraction was not increased in both expression systems (**Table 1**, **Figure 2B**), which is in contrast to mutant ΔKPQ channels that were included as a positive control. When analyzing channel inactivation by fitting the Na^+ current decay using a

Table 1 | Peak current densities and persistent currents in HEK293 and *Xenopus laevis* oocytes.

Channel	HEK239 cells				*Xenopus laevis* oocytes				
	Peak current density		$I_{persistent}/I_{transient}$		Normalized peak current		$I_{persistent}/I_{transient}$[a]		
	at −25 mV (pA/pF)	*n*	at −20 mV (%)	*n*	at −20 mV	*n*	at −30 mV (%)	at −10 mV (%)	*n*
CONTROL									
$hNa_v1.5$	193 ± 12	90	0.22 ± 0.09	5	1.00 ± 0.04	92	0.83 ± 0.10	1.27 ± 0.23	18
LQT3									
G9V	200 ± 33	11	0.25 ± 0.15	4	1.29 ± 0.23	26	1.45 ± 0.30	1.88 ± 0.29	12
R18W	260 ± 36	14	0.19 ± 0.07	4	0.84 ± 0.07	27	1.52 ± 0.70	1.20 ± 0.40	4
V125L	161 ± 28	21	0.08 ± 0.05	4	1.08 ± 0.16	36	1.28 ± 0.36	1.10 ± 0.38	6
BrS									
R18Q	175 ± 21	19	n.d.	–	1.26 ± 0.18	23	n.d.	n.d.	–
R27H	159 ± 20	18	n.d.	–	1.51 ± 0.36	19	n.d.	n.d.	–
G35S	224 ± 35	11	n.d.	–	1.09 ± 0.12	20	n.d.	n.d.	–
V95I	205 ± 15	20	n.d.	–	0.88 ± 0.15	23	n.d.	n.d.	–
R104Q	No current	10	n.d.	–	0.29 ± 0.02*	45	n.d.	n.d.	–
K126E	172 ± 20	24	n.d.	–	1.13 ± 0.09	36	n.d.	n.d.	–

[a] *$I_{persistent}/I_{transient}$ ratios in ΔKPQ channels: 10.4 ± 2.1 % at −30 mV, 12.8 ± 2.9 % at −10 mV (n = 8).*

** indicates $p < 0.05$ vs. $hNa_v1.5$.*

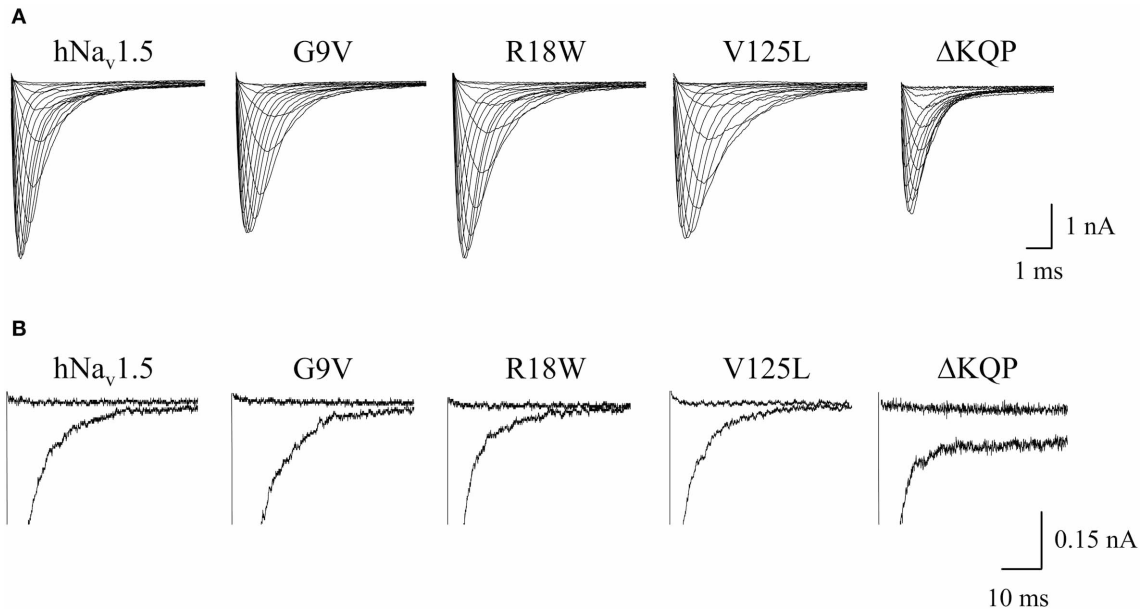

FIGURE 2 | Whole-cell Na^+ currents upon expression in HEK293 of hNa$_v$1.5 mutant channels associated with LQT3. (A) Current families. Currents were elicited by test potentials from −80 mV to various test pulses in 5 or 10 mV increments at a pulsing frequency of 1.0 Hz. **(B)** Persistent currents at −20 mV. The non-inactivating current fraction was similarly small in both wild-type and mutant hNa$_v$1.5 channels. For individual values see **Table 1**. Mutant ΔKQP channels were used as a positive control.

mono-exponential function, we observed a slower inactivation at more negative test potentials in R18W and V125L (**Figure 3A**). Respective inactivation time constants τ_h were significantly increased at −50 mV (R18W: $\tau_h = 11.5 \pm 2.2$, $n = 12$; V125L: $\tau_h = 9.9 \pm 1.4$, $n = 14$; hNa$_v$1.5: $\tau_h = 6.3 \pm 0.4$, $n = 55$).

Steady-state activation remained unchanged in all LQT3 mutant channels. Mid-activation potentials V_m were not significantly different from hNa$_v$1.5 values in HEK293 cells and *Xenopus* oocytes (**Tables 2**, **3**). Similarly, no differences were observed in channel availability, except for V125L in HEK293 cells (**Table 2**, **Figure 3B**). The respective mid-inactivation potential V_h was shifted by 3.1 mV into depolarized direction, when compared to wild-type channels. As a consequence, the window current resulting from the small overlap of the steady-state activation and steady-state inactivation curves should be increased in V125L (**Figure 3C**). Interestingly, this effect was not seen in the oocyte system: Mid-inactivation potentials were neither altered in V125L nor in the other two LQT3 mutant channels G9V and R18W (**Table 3**). When analyzing the recovery from inactivation in HEK293 cells using a double pulse protocol we noticed an accelerated recovery in V125L (**Figure 3D**). The fast time constant τ_f was significantly smaller and the corresponding amplitude A_f was increased (**Table 2**). This effect of the mutation at position 125 on recovery from inactivation was not observed in the oocyte system: Recovery time constants and the corresponding amplitudes were similar in all three LQT3 mutant channels, when compared to hNa$_v$1.5 data (**Table 3**).

In conclusion, G9V channels were indistinguishable from wild-type hNa$_v$1.5. R18W showed a decelerated current decay, similarly as seen in some other LQT3 mutant channels (see section Discussion). V125L was characterized by the most severe defects (slower inactivation, increased window current and faster recovery from inactivation). Moreover, our data show that the gain-of-function defects in V125L, typically seen in LQT3 mutant channels, became manifest only in the mammalian expression system.

PROPERTIES OF BrS MUTANT CHANNELS (R18Q, R27H, G35S, V95I, R104Q, K126E)

Expression of a great number of mutated Na^+ channel variants, associated with BrS, results either in a significant peak current reduction or even in non-functional channels. Surprisingly, when expressing the six N-terminally mutated variants in HEK293 cells, we did not observe a current reduction in five of them (**Table 1**, **Figure 4**). R18Q, R27H, G35S, V95I, and K126E generated whole-cell currents that were comparable to those observed for hNa$_v$1.5. Expression of R104Q did not result in functional channels in HEK293 cells (**Figure 4**). Interestingly, when injecting *Xenopus* oocytes with cRNA for this mutant variant, typical Na^+ inward currents were observed, but peak currents were reduced to 29% compared to hNa$_v$1.5 (**Table 1**).

In HEK293 cells, two out of the five functional mutant channels were characterized by a positive shift of the steady-state activation relationship. In R27H and K126E, the mid-activation potential V_m was shifted by 4.0 mV and 2.8 mV, respectively, and in R27H, the slope was significantly increased (**Table 2**, **Figure 5**). This shift in R27H and K126E was accompanied by a respectively slower channel inactivation at less depolarized membrane potentials (**Figure 5A**). Steady-state activation and inactivation time constants in R18Q, G35S and V95I were unchanged compared

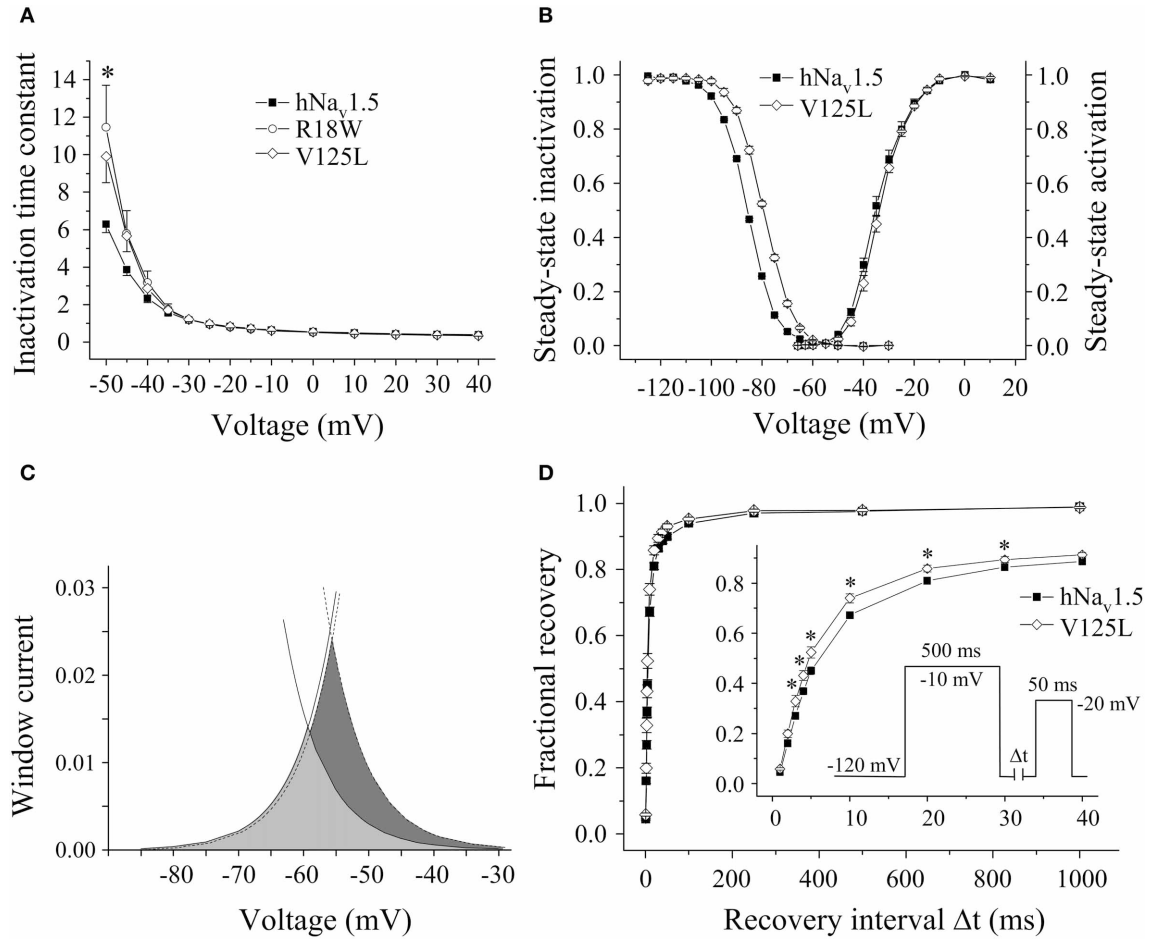

FIGURE 3 | Electrophysiological properties in HEK293 cells of mutant $hNa_v1.5$ channels associated with LQT3. (A) Inactivation time constants τ_h (ms) as function of voltage. At −50 mV both R18W and V125L channels inactivated more slowly compared to $hNa_v1.5$ (*indicates $p < 0.05$). G9V channel inactivation was indistinguishable from $hNa_v1.5$ (data not shown). **(B)** Steady-state activation and inactivation in V125L channels. The figure shows the mean of 4 representative measurements for each. **(C)** Window current in $hNa_v1.5$ (grey area, solid lines) and V125L (dark grey area, dotted lines). **(D)** Recovery from inactivation was accelerated in V125L (* indicates $p < 0.05$ vs. $hNa_v1.5$). For individual values see **Table 2**.

Table 2 | Electrophysiological properties of mutant $hNa_v1.5$ channels in HEK293 cells.

Channel	Steady-state activation			Steady-state inactivation			Recovery from inactivation				
	s (mV)	V_m (mV)	n	s (mV)	V_h (mV)	n	τ_f (ms)	A_f	τ_s (ms)	A_s	n
CONTROL											
$hNa_v1.5$	5.7 ± 0.1	−35.1 ± 0.4	88	5.9 ± 0.1	−84.3 ± 0.6	68	5.8 ± 0.3	0.84 ± 0.01	110 ± 17	0.16 ± 0.04	40
LQT3											
G9V	5.7 ± 0.4	−33.8 ± 1.3	11	6.0 ± 0.1	−84.2 ± 2.0	8	5.4 ± 0.7	0.81 ± 0.04	60.0 ± 9	0.19 ± 0.03	6
R18W	5.6 ± 0.3	−35.3 ± 2.2	13	5.6 ± 0.2	−83.0 ± 2.4	9	4.8 ± 0.5	0.83 ± 0.05	70.0 ± 24	0.17 ± 0.04	5
V125L	5.6 ± 0.2	−34.4 ± 1.0	21	5.6 ± 0.1	−81.2 ± 0.9*	20	4.8 ± 0.3*	0.88 ± 0.01*	128 ± 22	0.12 ± 0.01*	18
BrS											
R18Q	5.7 ± 0.2	−34.6 ± 1.1	18	5.7 ± 0.2	−82.1 ± 1.0	16	5.0 ± 0.5	0.82 ± 0.04	52.0 ± 6	0.18 ± 0.03	10
R27H	6.8 ± 0.2*	−31.1 ± 1.0*	18	5.8 ± 0.2	−84.7 ± 1.2	14	6.4 ± 0.6	0.77 ± 0.03*	111 ± 26	0.23 ± 0.03*	12
G35S	5.4 ± 0.4	−36.8 ± 1.5	10	5.4 ± 0.1	−86.1 ± 1.3	9	4.7 ± 0.4	0.85 ± 0.01	91.0 ± 23	0.15 ± 0.01	7
V95I	6.0 ± 0.2	−33.9 ± 0.9	20	5.5 ± 0.1	−83.3 ± 1.3	15	5.7 ± 0.6	0.83 ± 0.02	60.0 ± 11	0.17 ± 0.02	9
K126E	5.9 ± 0.3	−32.3 ± 1.1*	21	5.9 ± 0.1	−80.9 ± 0.9*	21	5.2 ± 0.5	0.86 ± 0.02	91.0 ± 23	0.14 ± 0.02	13

** indicates $p < 0.05$ vs. $hNa_v1.5$.*

Table 3 | Electrophysiological properties of mutant $hNa_v1.5$ channels in *Xenopus laevis* oocytes.

Channel	Steady-state activation			Steady-state inactivation			Recovery from inactivation				
	s (mV)	V_m (mV)	n	s (mV)	V_h (mV)	n	τ_f (ms)	A_f	τ_s (ms)	A_s	n
CONTROL											
$hNa_v1.5$	3.6 ± 0.1	−33.5 ± 0.4	82	5.4 ± 0.1	−71.2 ± 0.7	28	3.8 ± 0.1	0.93 ± 0.01	399 ± 50	0.07 ± 0.006	48
LQT3											
G9V	3.5 ± 0.2	−33.4 ± 0.6	6	5.2 ± 0.2	−71.3 ± 0.9	9	3.9 ± 0.3	0.93 ± 0.02	339 ± 64	0.07 ± 0.012	12
R18W	3.6 ± 0.2	−33.8 ± 1.0	6	4.9 ± 0.1	−72.1 ± 1.2	5	4.4 ± 0.4	0.94 ± 0.01	281 ± 48	0.06 ± 0.008	13
V125L	3.8 ± 0.2	−32.9 ± 0.6	25	5.2 ± 0.2	−74.5 ± 1.9	8	3.9 ± 0.3	0.93 ± 0.04	283 ± 64	0.07 ± 0.011	9
BrS											
R18Q	3.8 ± 0.1	−32.3 ± 1.6	12	5.5 ± 0.1	−70.6 ± 1.1	11	3.4 ± 0.3	0.93 ± 0.02	236 ± 53	0.07 ± 0.013	11
R27H	3.6 ± 0.1	−32.5 ± 0.9	26	5.5 ± 0.2	−72.2 ± 1.1	6	3.8 ± 0.6	0.91 ± 0.05	505 ± 182	0.09 ± 0.018	5
G35S	3.7 ± 0.2	−33.8 ± 0.8	10	5.2 ± 0.1	−73.3 ± 1.0	9	4.2 ± 0.2	0.92 ± 0.01	452 ± 97	0.08 ± 0.013	14
V95I	3.8 ± 0.3	−31.6 ± 2.4	6	5.1 ± 0.1	−71.6 ± 1.1	11	3.3 ± 0.1	0.90 ± 0.01	134 ± 35	0.10 ± 0.009	5
R104Q	3.9 ± 0.2	−34.0 ± 0.8	7	5.6 ± 0.3	−73.8 ± 0.5*	6	4.6 ± 0.1*	0.92 ± 0.02	344 ± 125	0.08 ± 0.012	12
K126E	3.7 ± 0.1	−32.9 ± 0.8	24	4.9 ± 0.1	−70.0 ± 0.8	9	3.1 ± 0.2	0.91 ± 0.04	105 ± 32	0.09 ± 0.009	6

** indicates $p < 0.05$ vs. $hNa_v1.5$.*

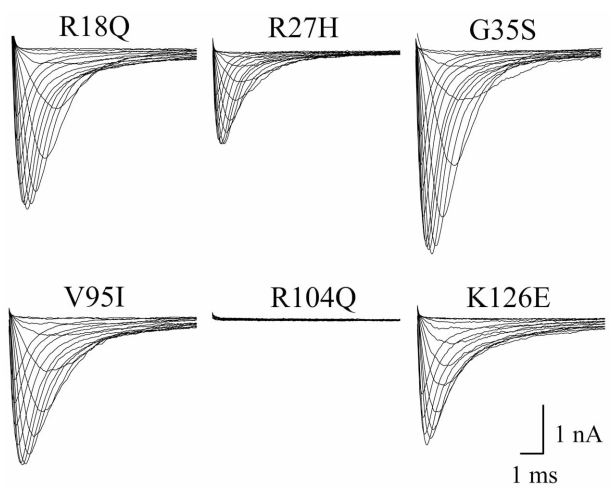

FIGURE 4 | Whole-cell Na^+ currents upon expression in HEK293 of $hNa_v1.5$ mutant channels associated with BrS. Currents were elicited from −80 mV to various test pulses in 5 or 10 mV increments at a pulsing frequency of 1.0 Hz (holding potential −120 mV). For average peak current densities see **Table 1**. Expression of R104Q did not result in functional channels in the mammalian expression system.

to $hNa_v1.5$ (**Table 2**). Analyzing steady-state inactivation in the mammalian expression system, we observed only an increased availability in K126E: The corresponding mid-inactivation potential V_h was by 3.4 mV more positive compared to $hNa_v1.5$ (**Table 2**, **Figure 5B**). Time constants for recovery from inactivation were not significantly altered in the BrS mutant channels. We only noticed a decreased amplitude of the fast recovery time constant and an increased amplitude of the slow recovery time constant in R27H.

When analyzing our oocyte recordings with the BrS mutant channels, we were very surprised that the electrophysiological parameters for steady-state activation, steady-state inactivation, and recovery from inactivation were statistically indistinguishable from those seen in $hNa_v1.5$ (**Table 3**). None of the loss-of-function defects, observed in R27H and K126E channels in HEK293 cells, were observed in the oocyte expression system.

Functional expression of R104Q in *Xenopus* oocytes allowed us to determine the electrophysiological properties of these mutant channels (**Table 3**). In addition to reduced peak current densities, we observed a significant reduction in channel availability (**Figure 6**). The mid-inactivation potential was shifted by 2.6 mV into the hyperpolarized direction (see V_h values in **Table 3**). At the same time, recovery from inactivation was decelerated in R104Q (**Table 3**, **Figure 6C**). Steady-state activation and inactivation time constants remained unchanged when compared to the corresponding $hNa_v1.5$ data.

In conclusion, expression of R18Q, G35S, and V95I in HEK293 and *Xenopus* oocytes did not reveal any of the loss-of-function features typically observed in BrS mutant channels. In HEK293 cells, R27H and K126E were characterized by positively shifted steady-state activation curves, a result that is in agreement with a BrS phenotype (Clancy and Kass, 2002). R104Q was not functional in HEK293 cells, whereas in *Xenopus* oocytes we found functional expression but the current amplitude was significantly diminished and the recovery from inactivation was slowed. So it seems that, similarly to the LQT3 mutants, channel defects are more pronounced in the mammalian than in the oocyte expression system.

DISCUSSION

Our study on the nine N-terminally mutated cardiac Na^+ channels revealed three main results: First, three mutations produced gain-of-function or loss-of-function defects that are most likely associated with LQT3 (V125L) or BrS (R104Q, R27H), respectively. Second, most of the heterologously expressed channels were either indistinguishable from wild-type $hNa_v1.5$ or characterized by only marginally altered electrophysiological properties. And third, in order to detect alterations of the electrophysiological

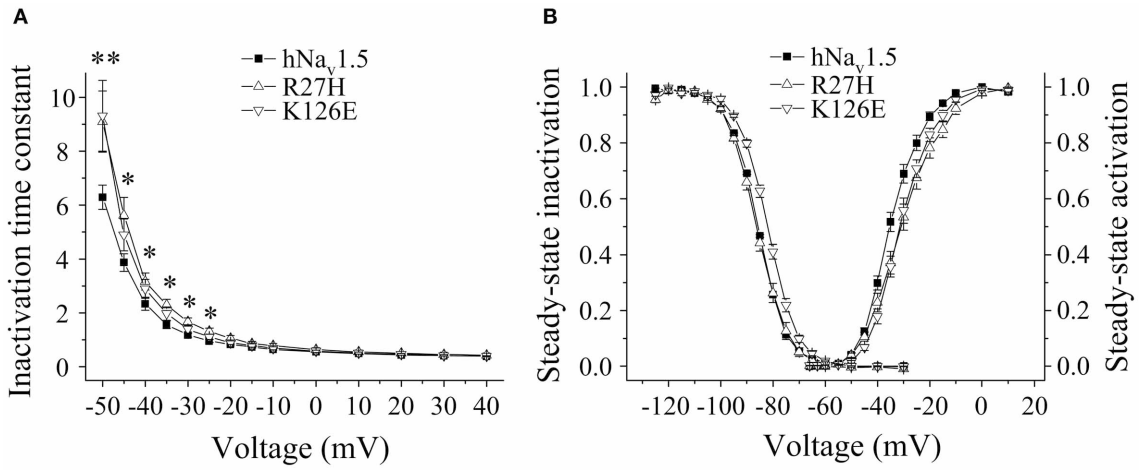

FIGURE 5 | Electrophysiological properties in HEK293 cells of mutant hNa$_v$1.5 channels associated with BrS. (A) Inactivation time constants τ_h (ms) as function of voltage. K126E channels inactivated more slowly at −50 mV (**), R27H inactivated more slowly from −50 to −25 mV (*), when compared to hNa$_v$1.5. R18Q, G35S, and V95I channels were indistinguishable from hNa$_v$1.5 (data not shown). **(B)** Steady-state activation and steady-state inactivation curves. Mid-activation potentials (V_m) were significantly shifted towards depolarized potentials in both R27H and K126E. Mid-inactivation potential V_h was shifted only in K126E. The figure was drawn using the mean of 4 representative measurements for each. V_m and V_h of the other mutant channels, R18Q, G35S and V95I, were indistinguishable from the respective hNa$_v$1.5 values. For data and statistics see **Table 2**.

properties in mutant channels mammalian cells were superior to *Xenopus* oocytes.

GENOTYPE-PHENOTYPE CORRELATIONS FOR LQT3 MUTANTS

Among the three LQT3 mutant channels investigated, the most pronounced gain-of-function features were noticed in V125L. Despite the absence of an increased persistent current fraction, three other channel defects were observed (**Figure 3**). These defects may synergistically prolong the cardiac action potential and explain QTc interval prolongation in the patients (Tester et al., 2005). In R18W we found only a slowing of open-state inactivation at less depolarized membrane potentials. It is doubtful that such a rather mild effect is sufficient to cause LQT3. A similar genotype-phenotype disassociation was previously reported in case of P1332L, a mutation that produced only mild channel defects, similarly as R18W (Ruan et al., 2007). P1332L was found in two independent studies and all index patients were kids with QTc values of up to 760 ms (Kehl et al., 2004). At the same time, other mutant channels characterized by a slower current decay also produced a significant persistent current fraction, like Y1795C channels (Rivolta et al., 2001), but patients did not present such extremely prolonged QT intervals. It is further noteworthy that R18W was identified in another study on BrS as a rare control, but not as a mutation causing LQT3 (Kapplinger et al., 2010). Together these observations strongly suggest that additional yet unknown mechanisms contribute to the ECG alteration in R18W and P1332L carriers. G9V mutant channels were even indistinguishable from wild-type hNa$_v$1.5. This was the most surprising result, because glycine is highly conserved at this position (**Figure 1**). One explanation for this obvious discrepancy between our results and clinical data is that the 69 years old patient also presented a homozygous *KCNH2* polymorphism (T897 instead of K897) (Millat et al., 2006). Future studies may answer the question whether or not this rare polymorphism is capable of modulating the cardiac action potential in G9V mutant carriers.

GENOTYPE-PHENOTYPE CORRELATIONS FOR BrS MUTANTS

Among the six BrS mutant channels investigated in this study, the most pronounced loss-of-function features were seen in R104Q. Expression in HEK293 cells did not result in functional channels suggesting *SCN5A* haploinsufficiency in R104Q carriers. Similar results were obtained in a recent study on R104W (Clatot et al., 2012). It is interesting to note that even successful expression in *Xenopus* oocytes resulted in significant channel loss-of-function (**Figure 6**). These data together suggest that position 104 is crucial for Na^+ channel expression and kinetics. The molecular mechanism leading to loss-of-function in R104Q is still unknown. The lack of a Na^+ current in R104Q-transfected cells could be due to incorrect folding in the endoplasmic reticulum, impaired post-translational modification, disturbed trafficking, enhanced degradation, or defective gating and permeation in otherwise correctly targeted channels. In R27H and K126E channels, we observed a positive shift of the steady-state activation curve, similarly as seen in other BrS mutants like A735V (Vatta et al., 2002b). Such a shift is expected to decelerate upstroke velocity and cardiac conduction, and thus may explain the observed ECG alterations (Clancy and Kass, 2002; Priori et al., 2002). In K126E, this loss-of-function feature was accompanied by an increased steady-state availability, and thus by a potential gain-of-function feature, suggesting additional yet unknown factors that contribute to BrS in K126E carriers. Nevertheless, we think that the K126E is indeed the primary cause of the disease. First, K126 is a conserved residue and the mutation caused an exchange of a positive charge by a negative amino acid. Second, K126E was detected in two unrelated patients (Vatta et al., 2002a; Kapplinger et al., 2010). And third, a concomitant shift of both steady-state activation and

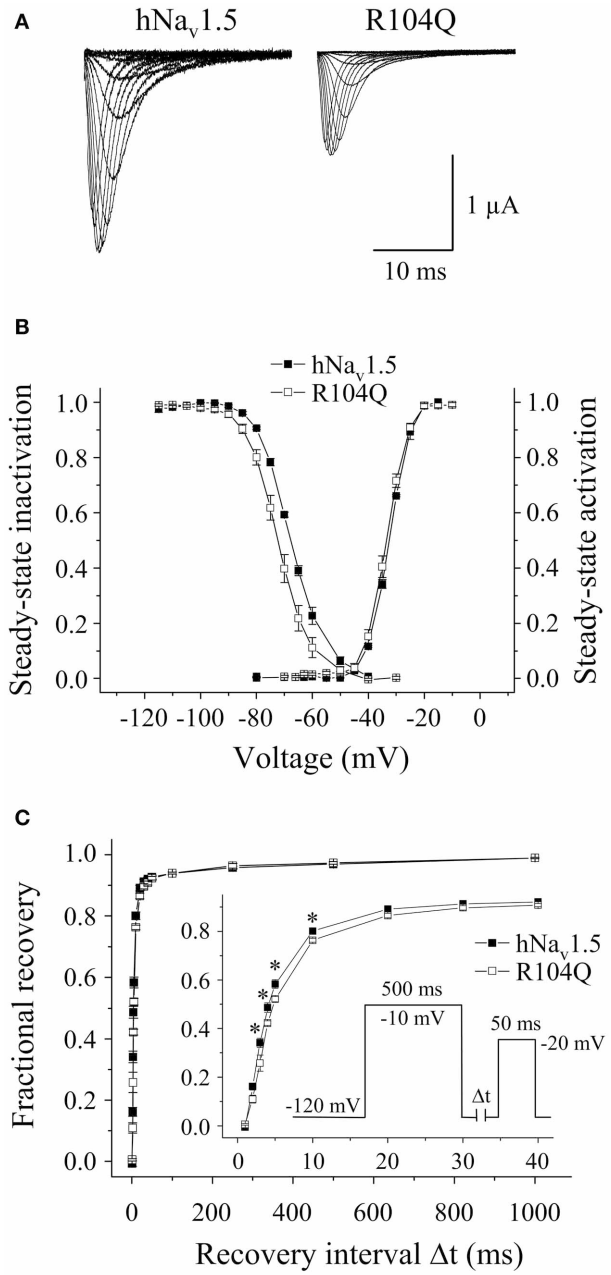

FIGURE 6 | Electrophysiological properties of R104Q in *Xenopus* oocytes. (A) Whole-cell Na^+ currents. Peak current amplitudes were significantly reduced in R104Q (see **Table 1**). Currents were elicited from −80 mV to various test pulses in 5 or 10 mV increments at a pulsing frequency of 1.0 Hz (holding potential −120 mV). **(B)** Steady-state activation and inactivation curves. In R104Q, steady-state availability was significantly reduced. **(C)** Recovery from inactivation was slower in R104Q (* indicates $p < 0.05$ vs. hNa$_v$1.5). For individual values see **Table 3**.

inactivation curves was also reported for other BrS mutant channels, like N406S (Itoh et al., 2005) and delK1479 (Zhang et al., 2007).

In R18Q, G35S, and V95I we could not detect any functional defect (**Tables 2**, **3**), and the pathogenic mechanism leading to BrS remains to be investigated. At least V95 is highly conserved, and it is reasonable to assume that the mutation at this position is correlated to the observed clinical phenotype (Liang et al., 2006). G35 is only conserved among the *SCN5A* orthologs, but not within the Na$_v$1 subfamily (**Figure 1**), which may suggest that G35S is a variant rather than a mutation. However, G35S was not found in 100 controls and, paradoxically, the clinical features of the respective patient were more severe than those seen in case of R104Q carriers (Levy-Nissenbaum et al., 2001).

POSSIBLE REASONS FOR THE OBSERVED GENOTYPE-PHENOTYPE DISASSOCIATIONS

When analyzing the N-terminally mutated cardiac Na^+ channels, we noticed dramatic differences between both expression systems. Channel defects were mainly seen in the mammalian system, but not in frog oocytes. Such expression system differences have been occasionally reported (Baroudi et al., 2000). However, it seems that this is rather the exception than the rule, and despite technical limitations of the oocyte system, like variations in oocyte quality and clamp properties, similar data have been observed for most of the hNa$_v$1.5 mutant channels. For example, an increased persistent current in ΔKPQ channels can be easily detected in both *Xenopus* oocytes and HEK293 cells (see **Table 1**). Moreover, in a previous study on nine SSS-related mutant channels, loss-of-function features were similarly detected in both expression systems (Gui et al., 2010). In some cases, even more severe loss-of-function properties were associated with the oocyte system. Interestingly, none of the SSS-related mutations localized to the hNa$_v$1.5 N-terminus.

We suggest that the expression system differences in the present study point to important cellular mechanisms or factors in cardiomyocytes that specifically control or modulate the Na^+ channel N-terminus. It has been shown that the cytoplasmic N-terminal domain of Na$_v$1.6 is required for intracellular transport to the plasma membrane, a process that is facilitated by microtubule-associated protein Map1b (Sharkey et al., 2009; O'Brien et al., 2012). *Xenopus* oocytes may not be equipped with respective protein quality control mechanisms, in contrast to HEK293 cells that may accommodate some of those molecular components. To provide evidence for this hypothesis, the N-terminally mutated variants have to be expressed in cardiomyocytes, similarly as done for D1275N channels by Watanabe and co-workers recently (Watanabe et al., 2011). The authors found near-normal currents upon heterologous expression of D1275N, but striking *in vivo* effects in mice carrying one D1275N allele. Similarly, E1053K channels were efficiently targeted to the plasma membrane in HEK293 cells and produced robust currents. The ankyrin-binding motif abolished by this mutation was not required for a successful expression in this cellular system. In cardiomyocytes, however, mutant channels were nearly absent from T-tubules and intercalated discs, and expression at the cell surface was strongly reduced (Mohler et al., 2004).

Other pathogenic mechanisms in monogenetic ion channel diseases, apart from defective trafficking or ankyrin binding, could be an acidic intracellular pH (Wang et al., 2007), increased temperature (Keller et al., 2005), or impaired channel expression from the wild-type and/or the mutated allele

(Shang and Dudley, 2005; Leoni et al., 2010; Atack et al., 2011). Moreover, we and others have demonstrated that the cellular splicing machinery is a player affecting genotype-phenotype correlations in cardiac diseases (Shang et al., 2007; Walzik et al., 2011; Murphy et al., 2012). It is possible that some mutant channels investigated in this study show normal electrophysiological features in the background of the wild-type sequence, but altered properties upon an alternative splicing event, similarly as shown previously for T1620K (Walzik et al., 2011). Genetic testing for the diagnosis of *SCN5A* channelopathies does not include analysis of the patients' mRNA, and consequently, possible splicing alterations can not be detected. It is intriguing to speculate that an abnormal splicing could be caused by a pathological alteration of the splicing machinery itself, leading to an excision of important *SCN5A* exons, to the alternative usage of neonatal exon 6a instead of adult exon 6b, or even to an alternative exon usage in another cardiac ion channel. This could result in ion channel defects also in the absence of any ion channel mutation, and thus explain why nearly 80% of all BrS patients are *SCN5A*-negative cases. We think that this is a fascinating idea worth to be tested in the future.

ACKNOWLEDGMENTS

The authors would like to thank Karin Schoknecht for her excellent contribution to the electrophysiological measurements and to Sandra Bernhardt for excellent technical assistance.

REFERENCES

Alings, M., and Wilde, A. (1999). "Brugada" syndrome: clinical data and suggested pathophysiological mechanism. *Circulation* 99, 666–673. doi: 10.1161/01.CIR.99.5.666

Atack, T. C., Stroud, D. M., Watanabe, H., Yang, T., Hall, L., Hipkens, S. B., et al. (2011). Informatic and functional approaches to identifying a regulatory region for the cardiac sodium channel. *Circ. Res.* 109, 38–46. doi: 10.1161/CIRCRESAHA.110.235630

Baroudi, G., Carbonneau, E., Pouliot, V., and Chahine, M. (2000). SCN5A mutation (T1620M) causing Brugada syndrome exhibits different phenotypes when expressed in *Xenopus oocytes* and mammalian cells. *FEBS Lett.* 467, 12–16. doi: 10.1016/S0014-5793(00)01099-1

Baroudi, G., Pouliot, V., Denjoy, I., Guicheney, P., Shrier, A., and Chahine, M. (2001). Novel mechanism for Brugada syndrome: defective surface localization of an SCN5A mutant (R1432G). *Circ. Res.* 88, E78–E83. doi: 10.1161/hh1201.093270

Bennett, P. B., Yazawa, K., Makita, N., and George, A. L. Jr. (1995). Molecular mechanism for an inherited cardiac arrhythmia. *Nature* 376, 683–685. doi: 10.1038/376683a0

Blechschmidt, S., Haufe, V., Benndorf, K., and Zimmer, T. (2008). Voltage-gated Na+ channel transcript patterns in the mammalian heart are species-dependent. *Prog. Biophys. Mol. Biol.* 98, 309–318. doi: 10.1016/j.pbiomolbio.2009.01.009

Camacho, J. A., Hensellek, S., Rougier, J. S., Blechschmidt, S., Abriel, H., Benndorf, K., et al. (2006). Modulation of Nav1.5 channel function by an alternatively spliced sequence in the DII/DIII linker region. *J. Biol. Chem.* 281, 9498–9506. doi: 10.1074/jbc.M509716200

Chandra, R., Starmer, C. F., and Grant, A. O. (1998). Multiple effects of KPQ deletion mutation on gating of human cardiac Na+ channels expressed in mammalian cells. *Am. J. Physiol.* 274, H1643–1654.

Clancy, C. E., and Kass, R. S. (2002). Defective cardiac ion channels: from mutations to clinical syndromes. *J. Clin. Invest.* 110, 1075–1077.

Clancy, C. E., Tateyama, M., Liu, H., Wehrens, X. H., and Kass, R. S. (2003). Non-equilibrium gating in cardiac Na+ channels: an original mechanism of arrhythmia. *Circulation* 107, 2233–2237. doi: 10.1161/01.CIR.0000069273.51375.BD

Clatot, J., Ziyadeh-Isleem, A., Maugenre, S., Denjoy, I., Liu, H., Dilanian, G., et al. (2012). Dominant-negative effect of SCN5A N-terminal mutations through the interaction of Na(v)1.5 alpha-subunits. *Cardiovasc. Res.* 96, 53–63. doi: 10.1093/cvr/cvs211

Dumaine, R., Wang, Q., Keating, M. T., Hartmann, H. A., Schwartz, P. J., Brown, A. M., et al. (1996). Multiple mechanisms of Na+ channel–linked long-QT syndrome. *Circ. Res.* 78, 916–924. doi: 10.1161/01.RES.78.5.916

Gellens, M. E., George, A. L. Jr., Chen, L. Q., Chahine, M., Horn, R., Barchi, R. L., et al. (1992). Primary structure and functional expression of the human cardiac tetrodotoxin-insensitive voltage-dependent sodium channel. *Proc. Natl. Acad. Sci. U.S.A.* 89, 554–558. doi: 10.1073/pnas.89.2.554

Gui, J., Wang, T., Jones, R. P., Trump, D., Zimmer, T., and Lei, M. (2010). Multiple loss-of-function mechanisms contribute to SCN5A-related familial sick sinus syndrome. *PLoS ONE* 5:e10985. doi: 10.1371/journal.pone.0010985

Itoh, H., Shimizu, M., Takata, S., Mabuchi, H., and Imoto, K. (2005). A novel missense mutation in the SCN5A gene associated with Brugada syndrome bidirectionally affecting blocking actions of antiarrhythmic drugs. *J. Cardiovasc. Electrophysiol.* 16, 486–493. doi: 10.1111/j.1540-8167.2005.40711.x

Kapplinger, J. D., Tester, D. J., Alders, M., Benito, B., Berthet, M., Brugada, J., et al. (2010). An international compendium of mutations in the SCN5A-encoded cardiac sodium channel in patients referred for Brugada syndrome genetic testing. *Heart Rhythm.* 7, 33–46. doi: 10.1016/j.hrthm.2009.09.069

Kehl, H. G., Haverkamp, W., Rellensmann, G., Yelbuz, T. M., Krasemann, T., Vogt, J., et al. (2004). Images in cardiovascular medicine. Life-threatening neonatal arrhythmia: successful treatment and confirmation of clinically suspected extreme long QT-syndrome-3. *Circulation* 109, e205–e206. doi: 10.1161/01.CIR.0000128874.43908.CA

Keller, D. I., Rougier, J. S., Kucera, J. P., Benammar, N., Fressart, V., Guicheney, P., et al. (2005). Brugada syndrome and fever: genetic and molecular characterization of patients carrying SCN5A mutations. *Cardiovasc. Res.* 67, 510–519. doi: 10.1016/j.cardiores.2005.03.024

Kyndt, F., Probst, V., Potet, F., Demolombe, S., Chevallier, J. C., Baro, I., et al. (2001). Novel SCN5A mutation leading either to isolated cardiac conduction defect or *Brugada syndrome* in a large French family. *Circulation* 104, 3081–3086. doi: 10.1161/hc5001.100834

Leoni, A. L., Gavillet, B., Rougier, J. S., Marionneau, C., Probst, V., Le Scouarnec, S., et al. (2010). Variable Na(v)1.5 protein expression from the wild-type allele correlates with the penetrance of cardiac conduction disease in the Scn5a(+/–) mouse model. *PLoS ONE* 5:e9298. doi: 10.1371/journal.pone.0009298

Levy-Nissenbaum, E., Eldar, M., Wang, Q., Lahat, H., Belhassen, B., Ries, L., et al. (2001). Genetic analysis of *Brugada syndrome* in Israel: two novel mutations and possible genetic heterogeneity. *Genet Test* 5, 331–334. doi: 10.1089/109065701753617480

Liang, P., Liu, W. L., Hu, D. Y., Li, C. L., Tao, W. H., and Li, L. (2006). [Novel SCN5A gene mutations associated with *Brugada syndrome*: V95I, A1649V and delF1617]. *Zhonghua Xin Xue Guan Bing Za Zhi* 34, 616–619.

Millat, G., Chevalier, P., Restier-Miron, L., Da Costa, A., Bouvagnet, P., Kugener, B., et al. (2006). Spectrum of pathogenic mutations and associated polymorphisms in a cohort of 44 unrelated patients with long QT syndrome. *Clin. Genet.* 70, 214–227. doi: 10.1111/j.1399-0004.2006.00671.x

Mohler, P. J., Rivolta, I., Napolitano, C., Lemaillet, G., Lambert, S., Priori, S. G., et al. (2004). Nav1.5 E1053K mutation causing *Brugada syndrome* blocks binding to ankyrin-G and expression of Nav1.5 on the surface of cardiomyocytes. *Proc. Natl. Acad. Sci. U.S.A.* 101, 17533–17538. doi: 10.1073/pnas.0403711101

Murphy, L. L., Moon-Grady, A. J., Cuneo, B. F., Wakai, R. T., Yu, S., Kunic, J. D., et al. (2012). Developmentally regulated SCN5A splice variant potentiates dysfunction of a novel mutation associated with severe fetal arrhythmia. *Heart Rhythm* 9, 590–597. doi: 10.1016/j.hrthm.2011.11.006

O'Brien, J. E., Sharkey, L. M., Vallianatos, C. N., Han, C., Blossom,

J. C., Yu, T., et al. (2012). Interaction of voltage-gated sodium channel Nav1.6 (SCN8A) with microtubule-associated protein Map1b. *J. Biol. Chem.* 287, 18459–18466. doi: 10.1074/jbc.M111.336024

Potet, F., Mabo, P., Le Coq, G., Probst, V., Schott, J. J., Airaud, F., et al. (2003). Novel brugada SCN5A mutation leading to ST segment elevation in the inferior or the right precordial leads. *J. Cardiovasc. Electrophysiol.* 14, 200–203. doi: 10.1046/j.1540-8167.2003.02382.x

Priori, S. G., Napolitano, C., Gasparini, M., Pappone, C., Della Bella, P., Giordano, U., et al. (2002). Natural history of *Brugada syndrome*: insights for risk stratification and management. *Circulation* 105, 1342–1347. doi: 10.1161/hc1102.105288

Rivolta, I., Abriel, H., Tateyama, M., Liu, H., Memmi, M., Vardas, P., et al. (2001). Inherited Brugada and long QT-3 syndrome mutations of a single residue of the cardiac sodium channel confer distinct channel and clinical phenotypes. *J. Biol. Chem.* 276, 30623–30630. doi: 10.1074/jbc.M104471200

Rook, M. B., Evers, M. M., Vos, M. A., and Bierhuizen, M. F. (2012). Biology of cardiac sodium channel Nav1.5 expression. *Cardiovasc. Res.* 93, 12–23. doi: 10.1093/cvr/cvr252

Ruan, Y., Liu, N., Bloise, R., Napolitano, C., and Priori, S. G. (2007). Gating properties of SCN5A mutations and the response to mexiletine in long-QT syndrome type 3 patients. *Circulation* 116, 1137–1144. doi: 10.1161/CIRCULATIONAHA.107.707877

Savio-Galimberti, E., Gollob, M. H., and Darbar, D. (2012). Voltage-gated sodium channels: biophysics, pharmacology, and related channelopathies. *Front. Pharmacol.* 3:124. doi: 10.3389/fphar.2012.00124

Shang, L. L., and Dudley, S. C. Jr. (2005). Tandem promoters and developmentally regulated 5′- and 3′-mRNA untranslated regions of the mouse Scn5a cardiac sodium channel. *J. Biol. Chem.* 280, 933–940. doi: 10.1074/jbc.M409977200

Shang, L. L., Pfahnl, A. E., Sanyal, S., Jiao, Z., Allen, J., Banach, K., et al. (2007). Human heart failure is associated with abnormal C-terminal splicing variants in the cardiac sodium channel. *Circ. Res.* 101, 1146–1154. doi: 10.1161/CIRCRESAHA.107.152918

Sharkey, L. M., Cheng, X., Drews, V., Buchner, D. A., Jones, J. M., Justice, M. J., et al. (2009). The ataxia3 mutation in the N-terminal cytoplasmic domain of sodium channel Na(v)1.6 disrupts intracellular trafficking. *J. Neurosci.* 29, 2733–2741. doi: 10.1523/JNEUROSCI.6026-08.2009

Surber, R., Hensellek, S., Prochnau, D., Werner, G. S., Benndorf, K., Figulla, H. R., et al. (2008). Combination of cardiac conduction disease and long QT syndrome caused by mutation T1620K in the cardiac sodium channel. *Cardiovasc. Res.* 77, 740–748. doi: 10.1093/cvr/cvm096

Tester, D. J., Will, M. L., Haglund, C. M., and Ackerman, M. J. (2005). Compendium of cardiac channel mutations in 541 consecutive unrelated patients referred for long QT syndrome genetic testing. *Heart Rhythm* 2, 507–517. doi: 10.1016/j.hrthm.2005.01.020

Valdivia, C. R., Tester, D. J., Rok, B. A., Porter, C. B., Munger, T. M., Jahangir, A., et al. (2004). A trafficking defective, *Brugada syndrome*-causing SCN5A mutation rescued by drugs. *Cardiovasc. Res.* 62, 53–62. doi: 10.1016/j.cardiores.2004.01.022

Vatta, M., Dumaine, R., Antzelevitch, C., Brugada, R., Li, H., Bowles, N. E., et al. (2002a). Novel mutations in domain I of SCN5A cause Brugada syndrome. *Mol. Genet. Metab.* 75, 317–324. doi: 10.1016/S1096-7192(02)00006-9

Vatta, M., Dumaine, R., Varghese, G., Richard, T. A., Shimizu, W., Aihara, N., et al. (2002b). Genetic and biophysical basis of sudden unexplained nocturnal death syndrome (SUNDS), a disease allelic to Brugada syndrome. *Hum. Mol. Genet.* 11, 337–345. doi: 10.1093/hmg/11.3.337

Walzik, S., Schroeter, A., Benndorf, K., and Zimmer, T. (2011). Alternative splicing of the cardiac sodium channel creates multiple variants of mutant T1620K channels. *PLoS ONE* 6:e19188. doi: 10.1371/journal.pone.0019188

Wang, D. W., Desai, R. R., Crotti, L., Arnestad, M., Insolia, R., Pedrazzini, M., et al. (2007). Cardiac sodium channel dysfunction in sudden infant death syndrome. *Circulation* 115, 368–376. doi: 10.1161/CIRCULATIONAHA.106.646513

Watanabe, H., Yang, T., Stroud, D. M., Lowe, J. S., Harris, L., Atack, T. C., et al. (2011). Striking *in vivo* phenotype of a disease-associated human SCN5A mutation producing minimal changes *in vitro*. *Circulation* 124, 1001–1011. doi: 10.1161/CIRCULATIONAHA.110.987248

Yan, G. X., and Antzelevitch, C. (1999). Cellular basis for the Brugada syndrome and other mechanisms of arrhythmogenesis associated with ST-segment elevation. *Circulation* 100, 1660–1666. doi: 10.1161/01.CIR.100.15.1660

Zhang, Y., Wang, T., Ma, A., Zhou, X., Gui, J., Wan, H., et al. (2008). Correlations between clinical and physiological consequences of the novel mutation R878C in a highly conserved pore residue in the cardiac Na+ channel. *Acta Physiol. (Oxf.)* 194, 311–323. doi: 10.1111/j.1748-1716.2008.01883.x

Zhang, Z. S., Tranquillo, J., Nepliouева, V., Bursac, N., and Grant, A. O. (2007). Sodium channel kinetic changes that produce *Brugada syndrome* or progressive cardiac conduction system disease. *Am. J. Physiol. Heart Circ. Physiol.* 292, H399–H407. doi: 10.1152/ajpheart.01025.2005

Zimmer, T. (2010). Effects of tetrodotoxin on the mammalian cardiovascular system. *Mar. Drugs* 8, 741–762. doi: 10.3390/md8030741

Zimmer, T., Biskup, C., Bollensdorff, C., and Benndorf, K. (2002a). The beta1 subunit but not the beta2 subunit colocalizes with the human heart Na+ channel (hH1) already within the endoplasmic reticulum. *J. Membr. Biol.* 186, 13–21. doi: 10.1007/s00232-001-0131-0

Zimmer, T., Biskup, C., Dugarmaa, S., Vogel, F., Steinbis, M., Bohle, T., et al. (2002b). Functional expression of GFP-linked human heart sodium channel (hH1) and subcellular localization of the a subunit in HEK293 cells and dog cardiac myocytes. *J. Membr. Biol.* 186, 1–12. doi: 10.1007/s00232-001-0130-1

Zimmer, T., and Surber, R. (2008). SCN5A channelopathies–an update on mutations and mechanisms. *Prog. Biophys. Mol. Biol.* 98, 120–136. doi: 10.1016/j.pbiomolbio.2008.10.005

Conflict of Interest Statement: The authors declare that the research was conducted in the absence of any commercial or financial relationships that could be construed as a potential conflict of interest.

Received: 26 April 2013; paper pending published: 19 May 2013; accepted: 10 June 2013; published online: 26 June 2013.

Citation: Gütter C, Benndorf K and Zimmer T (2013) Characterization of N-terminally mutated cardiac Na^+ channels associated with long QT syndrome 3 and Brugada syndrome. Front. Physiol. 4:153. doi: 10.3389/fphys.2013.00153

This article was submitted to Frontiers in Cardiac Electrophysiology, a specialty of Frontiers in Physiology.

frontiers in PHYSIOLOGY

REVIEW ARTICLE
published: 28 June 2013
doi: 10.3389/fphys.2013.00154

Determinants of myocardial conduction velocity: implications for arrhythmogenesis

James H. King[1], Christopher L.-H. Huang[1,2] and James A. Fraser[1]*

[1] *Physiological Laboratory, Department of Physiology, Development and Neuroscience, University of Cambridge, Cambridge, UK*
[2] *Department of Biochemistry, University of Cambridge, Cambridge, UK*

Edited by:
Ian N. Sabir, King's College, London, UK

Reviewed by:
Ruben Coronel, Academic Medical Center, Netherlands
Rob Gourdie, Medical University of South Carolina, USA

***Correspondence:**
James A. Fraser, Physiological Laboratory, University of Cambridge, Downing Street, CB2 3EG, Cambridge, UK
e-mail: jaf21@cam.ac.uk

Slowed myocardial conduction velocity (θ) is associated with an increased risk of re-entrant excitation, predisposing to cardiac arrhythmia. θ is determined by the ion channel and physical properties of cardiac myocytes and by their interconnections. Thus, θ is closely related to the maximum rate of action potential (AP) depolarization [$(dV/dt)_{max}$], as determined by the fast Na^+ current (I_{Na}); the axial resistance (r_a) to local circuit current flow between cells; their membrane capacitances (c_m); and to the geometrical relationship between successive myocytes within cardiac tissue. These determinants are altered by a wide range of pathophysiological conditions. Firstly, I_{Na} is reduced by the impaired Na^+ channel function that arises clinically during heart failure, ischemia, tachycardia, and following treatment with class I antiarrhythmic drugs. Such reductions also arise as a consequence of mutations in *SCN5A* such as those occurring in Lenègre disease, Brugada syndrome (BrS), sick sinus syndrome, and atrial fibrillation (AF). Secondly, r_a, may be increased due to gap junction decoupling following ischemia, ventricular hypertrophy, and heart failure, or as a result of mutations in *CJA5* found in idiopathic AF and atrial standstill. Finally, either r_a or c_m could potentially be altered by fibrotic change through the resultant decoupling of myocyte–myocyte connections and coupling of myocytes with fibroblasts. Such changes are observed in myocardial infarction and cardiomyopathy or following mutations in *MHC403* and *SCN5A* resulting in hypertrophic cardiomyopathy (HCM) or Lenègre disease, respectively. This review defines and quantifies the determinants of θ and summarizes experimental evidence that links changes in these determinants with reduced myocardial θ and arrhythmogenesis. It thereby identifies the diverse pathophysiological conditions in which abnormal θ may contribute to arrhythmia.

Keywords: conduction velocity, arrhythmia, sodium channel, gap junction, fibrosis

INTRODUCTION

Impaired myocardial action potential (AP) conduction can predispose to arrhythmogenesis through the formation of slow conducting re-entry circuits. Re-entry was first defined by Mines in the early twentieth century as a persisting electrical impulse that reactivates an area of previously activated myocardial tissue that is no longer refractory, resulting in a circus movement of activation (Mines, 1914). Subsequent studies suggest that sustained arrhythmia requires an ectopic AP triggering event to occur within such a substrate capable of generating self-sustaining re-entry processes (Mandapati et al., 2000; Zou et al., 2005). Thus, a triggered electrical impulse must enter a perpetuating electrical circuit containing a unidirectional conduction block along one of its two pathways. Such re-entry within the circuit is more likely to occur following reductions in conduction velocity (θ) and/or the effective refractory period (*ERP*). As shown in **Figure 1**, this could result in a reduction in the wavelength of excitation (λ), given by the product of θ and *ERP*, to values smaller than the dimensions of the available circuits (Mines, 1914; Wiener and Rosenblueth, 1946; Wakili et al., 2011). Alternatively if the site of slowed conduction is such that it prevents propagation of the triggered AP into the circuit, it may discourage re-entry.

This review describes the generation and propagation of the cardiac AP and defines the determinants of θ. It summarizes experimental evidence that links changes in these determinants with reduced myocardial θ and arrhythmogenesis, thereby identifying the diverse pathophysiological conditions in which abnormal θ may contribute to arrhythmogenesis.

THE GENERATION OF THE ACTION POTENTIAL

Cardiac APs are time-dependent voltage waveforms that propagate along excitable tissues. AP generation arises from specific changes in membrane permeability resulting in a sequence of selective ion fluxes through their contained ion channels down their electrochemical gradients. Cardiac AP waveforms have been divided into five phases. The AP is initiated by transmembrane potential depolarization beyond an "activation threshold" at which inward currents exceed outward currents. This results in a Na^+ influx through voltage-sensitive Na^+ channels that show a regenerative increase to result in large depolarizing Na^+ currents (I_{Na}) (of order 400 μA μF^{-1}). These generate the initial rapid ($\sim$400 V s^{-1}) phase 0 upstroke of the AP. The maximum rate of AP depolarization [$(dV/dt)_{max}$] in an isolated cell is thus directly proportional to the total

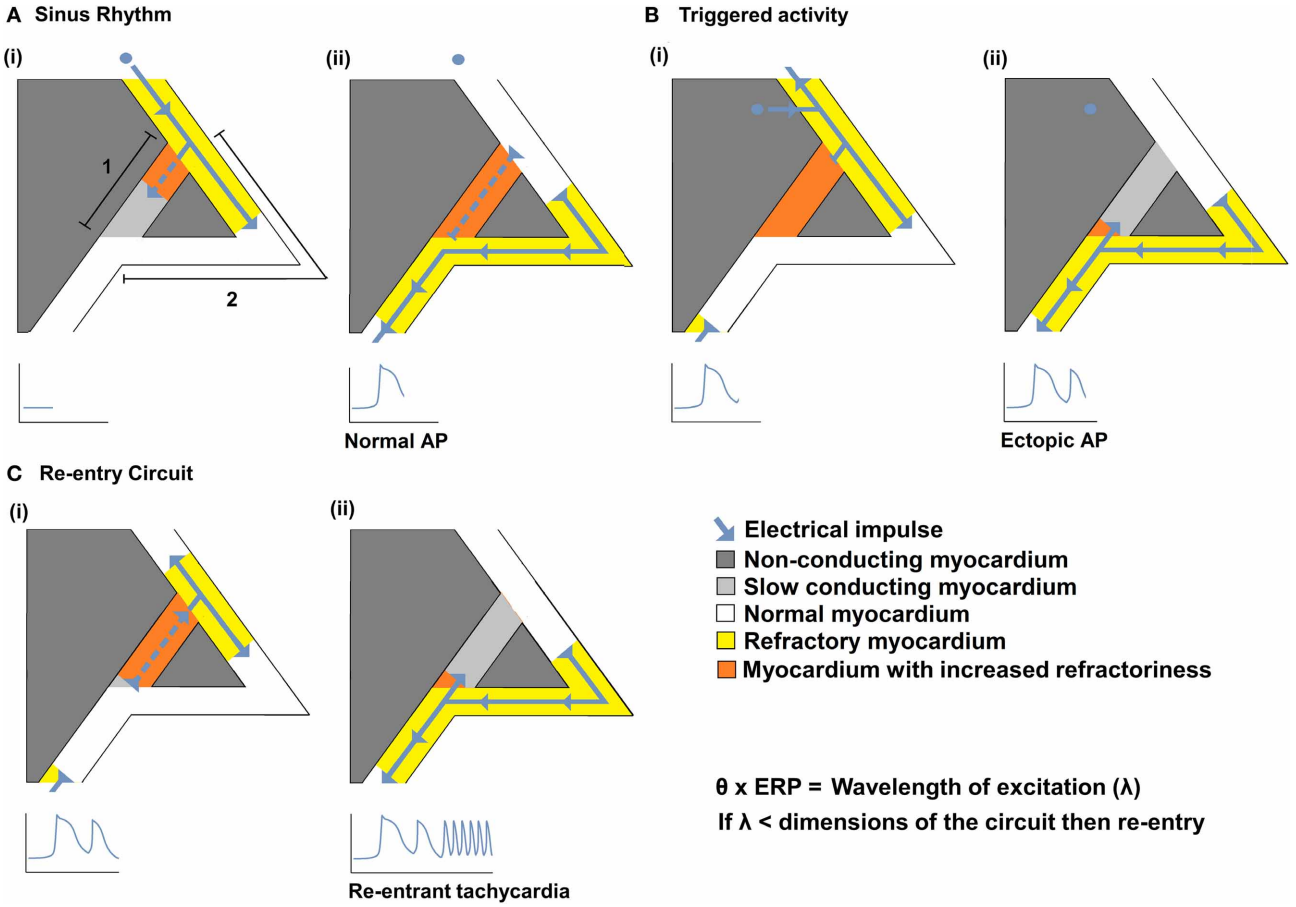

FIGURE 1 | The relationships between θ and re-entrant arrhythmia. A diagram illustrating a typical re-entry circuit, consisting of a pathway of slow conducting myocardium [**A**(i) path 1, light gray] passing through non-conducting myocardium (dark gray), bordered by a second pathway of normal myocardium [**A**(i) path 2, white]. **(A)** An electrical impulse (blue arrow) originating from the SAN, (i) propagates along path 2 (white) and path 1 (light gray) pathways. As the impulse conducts, the myocardium becomes refractory (yellow in path 2 or orange in path 1) (ii) The impulse that travels along path 2 reaches the end of the circuit resulting in a normal AP. The impulse that conducts along 1 cannot exit the circuit as it collides with the refractory tissue of path 2. **(B)** An abnormal impulse originating from an ectopic focus is triggered immediately following the sinus impulse (i). It cannot conduct down path 1 which remains refractory; it therefore conducts along path 2. (ii) When the impulse reaches the distal end of path 2 it splits, conducting retrogradely along path 1 and orthogradely along path 2. **(C)** The impulse conducting retrogradely along path 1 then activates the beginning of path 2 (i) without the need of any further stimuli, thereby creating a self-perpetuating re-entrant rhythm (ii). Such re-entry is more likely to occur following reductions in conduction velocity (θ) and/or the effective refractory period (*ERP*) that reduce the wavelength of excitation (λ), given by the product of the θ and *ERP*, to values smaller than the dimensions of the available circuits.

ionic current across the cell membrane (I_i) (Hodgkin and Katz, 1949).

As I_{Na} is the major transmembrane current in phase 0, $(dV/dt)_{max}$ is therefore often used as an index of I_{Na}. Having reached its peak amplitude, I_{Na} quickly inactivates in less than 1 ms, and requires an ERP to elapse before any further excitation. The succeeding brief rapid repolarization (phase 1) is additionally driven by the rapid activation and inactivation of K^+ channels carrying the fast and slow transient outward currents, $I_{to,f}$, and $I_{to,s}$, respectively. This is then followed by a plateau phase (phase 2) during which inward Ca^{2+} currents (I_{CaL}) through the L-type Ca^{2+} channels are balanced by I_{NCX}, resulting from $3Na^+/Ca^{2+}$ exchanger (NCX) activity, the ATP-activated K^+ current (I_{KATP}), and progressively activating I_{ks} and I_{kr},: the slow and rapid components of the delayed outward rectifying K^+ current. Finally the outward currents, particularly I_{Kr}, terminate the AP during phase 3 rapid repolarization. The resting membrane potential during the final, phase 4, electrical diastole, is primarily set by inward-rectifier currents (I_{K1}), fixing the resting membrane potential close to the K^+ equilibrium potential of about −80 to −90 mV.

The resting membrane potential persists until the next appropriately-initiated AP unless there is ectopic activity. Ectopic APs can be triggered by two types of afterdepolarization phenomena: early afterdepolarizations (EADs), or delayed afterdepolarizations (DADs). EADs are repolarization abnormalities characterized by oscillations in the membrane potential during phase 2 or 3 of the AP. They result from abnormalities in I_{Na}

inactivation, reductions in the outward K^+ currents (I_{K1}, I_{Ks}, and I_{to}), or increases in inward I_{CaL}, that then allow reactivation of I_{Na}, a persistent late Na^+ current, I_{NaL}, or both, thereby compromising the net outward current required to repolarize the myocyte. In contrast, DADs are formed during phase 3 or 4 of the AP when Ca^{2+} released by an abnormal diastolic sarcoplasmic reticulum (SR) Ca^{2+} discharge is exchanged for extracellular Na^+ via the NCX. Since NCX removes only 1 Ca^{2+} for every 3 Na^+ entering, it causes a net inward current and depolarization of the cell. If the resulting afterdepolarization is large enough to displace the membrane voltage beyond the activation threshold, an extrasystole is induced.

ACTION POTENTIAL PROPAGATION AND ITS DETERMINANTS

The magnitude of I_{Na} also plays a major role in the subsequent propagation of the cardiac impulse to its neighboring cells. In a simple model of AP propagation, an axial current flows along a linear cellular structure, or cable, from one depolarized myocyte to its quiescent neighbor via intercellular channels known as gap junctions (Rohr, 2004). If this axial current is sufficient to depolarize the neighboring cell beyond its activation threshold, voltage sensitive Na^+ channels will create transmembrane currents capable of propagating the AP. The axial resistance (r_a) to such local circuit currents arises from the resistances of the cytosol and the gap junctions between adjacent cells. Thus, in addition to Na^+ channels, gap junctions play a critical role in AP propagation and influence its velocity.

The determinants of θ can be identified using the nonlinear cable equation (Plonsey and Barr, 2007; Keener and Sneyd, 2009). This incorporates circuit elements each made up of a capacitance of unit fiber length, c_m, ($\mu F\ cm^{-1}$) in parallel with both a linear membrane resistance of unit fiber length r_m ($k\Omega$ cm) and nonlinear conductance elements responsible for individual ion channel properties. Together these generate a total current i_i in unit fiber length, x, as a function of time, t. Successive circuit elements are connected by elements reflecting cytoplasmic and gap junction resistances intervening between cells. These give rise to the effective intracellular r_a of unit fiber length, r_a, In classical cable theory, r_a is assumed constant. The membrane potential, V, across any given capacitative element depends on the charging of its unit length by currents traversing the local membrane conductance elements, i_i, as well as the axial current flow, i_a, arising from neighboring regions along the length, x, of the element in question. Thus,

$$\frac{1}{r_a}\left(\frac{d^2V}{dx^2}\right) = c_m\left(\frac{dV}{dt}\right) + i_i$$

At constant conduction velocity $\theta = dx/dt$, and so:

$$\frac{1}{\theta^2 r_a}\left(\frac{d^2V}{dt^2}\right) = c_m\left(\frac{dV}{dt}\right) + i_i$$

This simplest version of the cable equation clearly identifies the key determinants of θ as r_a, c_m, and i_i. However, several of its terms are interdependent, as will be discussed below, precluding its analytic solution. Furthermore, it is a stiff equation, requiring a good estimate of θ to be made before numerical solutions may be obtained (Jack et al., 1983) However, it is possible to derive simple relationships between θ and the parameters identified by this equation using a computer model of electrical conduction in a muscle fiber (Fraser et al., 2011). Although this model simulates skeletal rather than cardiac muscle, the insights that it provides into cable properties have general validity for any system in which fast sodium currents dominate the AP upstroke.

Thus, **Figure 2** demonstrates the empirical influences of r_a, c_m, and i_i upon θ and AP waveform in a computer model of AP propagation. It confirms that i_i is principally determined by I_{Na} during the AP upstroke, and demonstrates that $i_{Na(max)}$ α $\log[P_{Na(max)}]$ ($R^2 = 0.9965$), where $P_{Na(max)}$ is the maximum permeability of the fast Na^+ channels. Several important relationships then emerge that allow measurements of the AP waveform to be used to investigate relative changes in $i_{Na(max)}$ and c_m.

First, (**Figure 2A**) r_a does not influence the AP waveform [**Figure 2A**(i)] and thus does not influence dV/dt [**Figure 2A**(ii)] or d^2V/dt^2 (not shown). Consequently, θ^2 α $1/r_a$ ($R^2 = 1.0000$) [**Figure 2A**(iii)] as predicted from the cable equation. This simple relationship emerges because r_a influences only the AP waveform as a function of distance, not as a function of time. The effect is similar if r_a is unevenly distributed, as in cardiac myocytes connected by gap junctions (data not shown). Simulations show that, although uneven distribution of r_a produces small increases in AP amplitude and $(dV/dt)_{max}$ immediately before high resistance areas and small decreases in these parameters immediately after, θ and distance-averaged values of AP amplitude and $(dV/dt)_{max}$ are influenced as for evenly-distributed increases in r_a.

Second, (**Figure 2B**) increases in c_m influence the AP waveform [**Figure 2B**(i)], slowing the voltage excursions [**Figure 2B**(ii)] and producing a reduction in θ. Interestingly, θ^2 α $1/c_m$ ($R^2 = 0.9996$) [**Figure 2B**(iii)], as it appears in the cable equation, despite the influence of c_m on dV/dt and d^2V/dt^2 (not shown). These relationships have good empirical approximations: $(dV/dt)_{max}$ α $\log(c_m)$ ($R^2 = 0.9977$) and $(d^2V/dt^2)_{max}$ α $1/c_m$ ($R^2 = 1.0000$).

Finally, (**Figure 2C**), the relationship between $i_{Na(max)}$ and θ is difficult to derive from the cable equation because of the very large influence of $i_{Na(max)}$ upon AP waveform [**Figure 2C**(i)] and $(dV/dt)_{max}$ [**Figure 2C**(ii)] and d^2V/dt^2 (not shown). Nevertheless, the resultant empirical relationship for the range of values depicted in **Figure 2C** is straightforward: θ α $i_{Na(max)}$ ($R^2 = 1.0000$) [**Figure 2C**(iii)]. The AP waveform is influenced by $i_{Na(max)}$ as follows: $(dV/dt)_{max}$ α $\sqrt{i_{Na(max)}{}^3}$ ($R^2 = 0.9996$); and $(d^2V/dt^2)_{max}$ α $i_{Na(max)}{}^3$ ($R^2 = 0.9996$).

The cable equation can be extended from geometrically well-defined cylinders to cardiac tissue consisting of a continuous network of electrically-coupled cells. In doing so the analysis above becomes extended to one that determines conduction velocity resulting from the match between current and load (Kucera et al., 1998). Such an approach has been used to describe the macroscopic passive electrical properties of cardiac muscle (Weidmann, 1970; Kléber and Riegger, 1987), the relationship between dV/dt and macroscopic (>1 mm) propagation (Buchanan et al., 1985) and changes in cell to cell coupling.

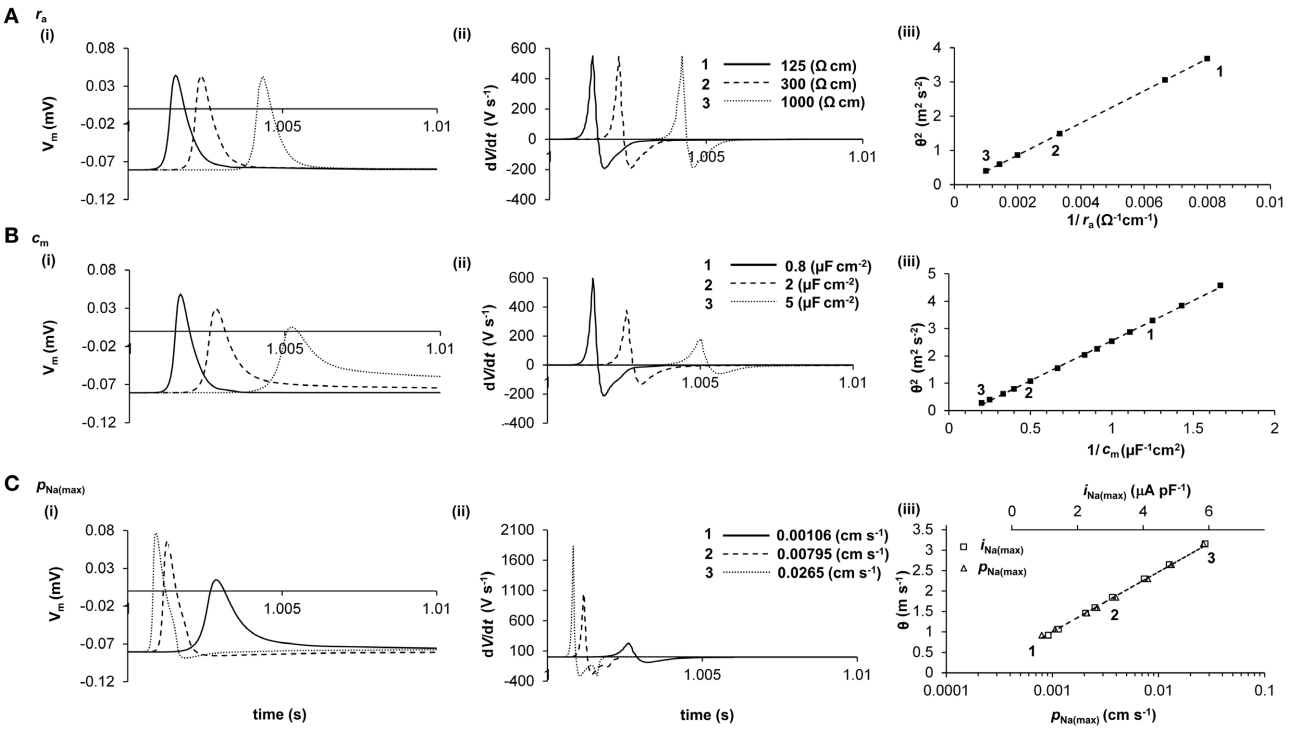

FIGURE 2 | Quantification of the determination of θ in a computer model. The cable equation identifies r_a, c_m, and i_i as the determinants of θ, but does not clearly demonstrate the magnitudes of their influences. Computer modeling of a skeletal muscle fiber (Fraser et al., 2011) shows the influence of r_a (panel **A**), c_m (panel **B**), and $i_{Na(max)}$ (panel **C**) on AP waveform (i), dV/dt (ii), and θ (iii). In panels i and ii, three representative APs are shown, each stimulated at 1 s and recorded 2.5 mm further along the cable, such that increased times to the AP peaks denote slowed conduction. In panel iii, the velocities of these APs are labeled 1, 2, and 3. It will be noted that r_a influences θ but not AP waveform, whereas c_m and $i_{Na(max)}$ each influence AP waveform and θ. Note that in panel **C**(iii), θ is plotted against both $i_{Na(max)}$ (upper scale, squares) and $P_{Na(max)}$ (lower scale, triangles). The simple quantitative relationships between these parameters that emerge from this analysis are given in the text.

As summarized in **Figure 3**, experimental studies have suggested a range of mechanisms through which changes in AP propagation leading to increased arrhythmic tendency can take place. They have been attributed to alterations in Na^+ channel and gap junction function, as well as to the consequences of fibrotic change. These could potentially alter the major determinants of θ: transmembrane current (i_i), cell to cell coupling (r_a), and cell capacitance (c_m), outlined in the quantitative analysis above.

THE Na^+ CHANNEL AND ITS RELATIONSHIP TO I_{Na}

Na^+ channels are transmembrane proteins responsible for a rapid, voltage-dependent, influx of Na^+ ions. They are located within the surface and transverse (t)-tubular membranes (Cohen, 1996) mainly concentrating in the perinexus region near gap junctions (Lin et al., 2011; Rhett et al., 2012). Na^+ channels consist of a principal α-subunit composed of four homologous domains each containing six, S1–S6, transmembrane segments. The function of the α-subunit is modulated by one or two associated ancillary β-subunits (Bezzina, 2001).

Several, $Na_v1.1$, $Na_v1.3$, $Na_v1.5$, $Na_v1.6$, α-subunits, are known to be expressed in the mammalian heart. Of these, $Na_v1.5$, encoded by the *SCN5A* gene is the most abundant. It is a large 260 KDa glycosylated protein that forms the pore component of the channel and has very high selective permeability for Na^+ (permeability ratio: Na^+:K^+ = 100.1) (Gellens et al., 1992; Wang et al., 1996). Na^+ influx and the resulting current flow through the open Na^+ channel (I_{Na}) are responsible for the initial rapid (phase 0) AP depolarization and drives its propagation. It is consequently a key determinant of θ.

ABNORMALITIES IN Na^+ CHANNEL FUNCTION

Abnormalities in conduction can arise from functional mutations in *SCN5A* that alter I_{Na} [**Figure 3A**(i)]. Of these the *SCN5a-1795insD* mutation is associated with an overlap syndrome with features of bradycardia, impaired conduction, LQT3, and Brugada syndrome (BrS) (Bezzina et al., 1999). Whilst mice homozygous for the mutation die *in utero*, the heterozygous *Scn5a*$^{1798insD/+}$ mouse shows sinus node dysfunction, conduction slowing, and QT prolongation replicating the phenotype in humans (Remme et al., 2006).

Acquired abnormalities can also lead to changes in Na^+ channel function. Abnormalities in AP depolarization were first described by Gelband and Bassett who recorded decreased values of $(dV/dt)_{max}$ and depolarized resting membrane potentials in experimental models of heart failure (Gelband and Bassett, 1973). Subsequent studies have also associated heart failure with reductions in peak I_{Na}

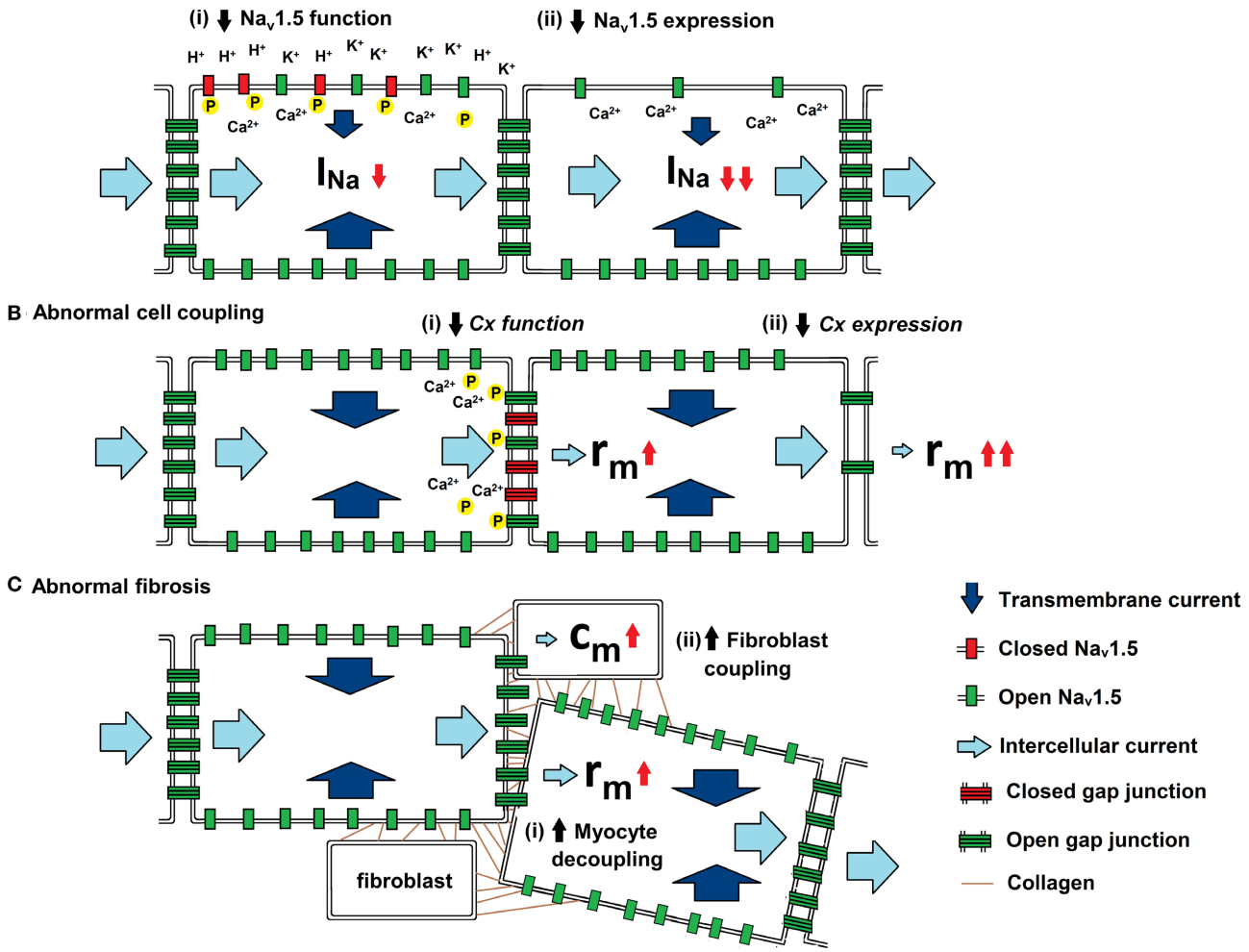

FIGURE 3 | Physiological influences on the determinants of θ. Three diagrams illustrating the mechanisms by which (a) membrane excitability, (b) cell coupling and (c) fibrotic change influence current. Transmembrane current (dark blue arrow) enters through open $Na_v1.5$ (green rectangle) and intercellular current (light blue arrow) passes through open Cxs (green ladder). **(A)** Abnormal membrane excitability results from reductions in either (i) $Na_v1.5$ function through increases in extracellular $[K^+]$ and pH and by increases in $[Ca^{2+}]_i$ and phosphorylation, or (ii) $Na_v1.5$ expression by mutations in *SCN5A* (Brugada syndrome) and through Ca^{2+} mediated down regulation of the channel. **(B)** Abnormal cell coupling results from reductions in either (i) Cx function through increases in $[Ca^{2+}]_i$ and dephosphorylation or (ii) Cx expression by mutations in either *CJA1 or CJA5* (idiopathic AF). **(C)** Abnormal fibrosis produces either (i) increased myocyte-myocyte decoupling, resulting in increased r_a,. or (ii) Cx-mediated myocyte-fibroblast coupling, resulting in increased c_m.

(Kuryshev et al., 1999; Ufret-Vincenty et al., 2001) through a number of mechanisms including reduced $Na_v1.5$ glycosylation (Ufret-Vincenty et al., 2001). Pathophysiological reductions in Na^+ channel availability have been additionally described during the acute phase of ischemia (Downar et al., 1977; Janse et al., 1986; Kleber et al., 1986; Kabell, 1989), tachycardia (Veenstra et al., 1987; Gaspo et al., 1997) and following treatment with class I anti-arrhythmic drugs (Sheldon et al., 1989).

Acute ischemia is pro-arrhythmogenic due to changes in intracellular and extracellular ionic concentrations, leading to reduced AP amplitudes, upstroke velocities (Downar et al., 1977; Janse et al., 1986) and conduction delays (Kleber et al., 1986; Kabell, 1989). Ischemic extracellular changes including: increases in $[K^+]$, decreases in pH, and hypoxia have been associated with modulation of Na^+ channel function (Corr and Yamada, 1995). Microelectrode studies in hypoxic guinea pig papillary muscle demonstrated a decrease in $(dV/dt)_{max}$ and depolarization of the resting membrane potential that was accentuated by increases in $[K^+]$ (Kodama et al., 1984). Subsequent studies in canine Purkinje fibers similarly showed a 8% decrease in θ in raised $[K^+]$ and a 4% decrease in θ following acidosis (Veenstra et al., 1987).

In addition to the extracellular effects, increases in intracellular cyclic adenosine monophosphate (cAMP) and cytosolic Ca^{2+} concentrations $[(Ca^{2+})_i]$ have also been reported in acute ischemia. Stimulation of β-adrenergic receptors is thought to produce adenylate cyclase-mediated increases in intracellular

cAMP, leading to phosphokinase A (PKA) activation (Bers, 2002). Modulation of $Na_v1.5$ by PKA occurs via phosphorylation at serine 525 and 528 within the DI–DII linker (Murphy et al., 1996). Following PKA activation, $Na_v1.5$ redistributes to the plasma membrane of HEK293 cells (Hallaq et al., 2006). This may explain the increases in I_{Na} reported following PKA activation with dibutyryl cAMP in rabbit and canine myocytes (Matsuda et al., 1992; Baba et al., 2004).

However, further experimental studies variously show that treatment with isoproterenol either increases (Matsuda et al., 1992) or decreases (Ono et al., 1989; Schubert et al., 1990) I_{Na}. Furthermore, when rabbit myocytes were treated with both a PKA inhibitor and isoproterenol, I_{Na} remained elevated suggesting that β-adrenergic stimulation produces an additional, PKA-independent modulation of the Na^+ channel. Myocytes treated with a GTP analog and stimulatory G protein subunit showed increased I_{Na} implicating involvement of a G protein regulatory pathway (Matsuda et al., 1992).

In contrast to PKA activation, Ca^{2+}-dependent activation of the protein phosphatase calcineurin has also been shown to strongly reduce I_{Na}, This has been variously attributed to activation of protein kinase-C (PKC) or modulation of Na^+ channel trafficking (Abriel, 2007). PKC also directly modulates $Na_v1.5$ by phosphorylation at serine 1505 in the DIII–DIV inactivation gate, significantly reducing I_{Na} (Qu et al., 1996).

Changes in intracellular Ca^{2+} may also exert direct regulatory effects on the Na^+ channel. Indeed the C-terminal region of Na^+ channel constructs contain two Ca^{2+}-sensitive regions: a calmodulin binding, IQ, domain, and a Ca^{2+} binding, EF-hand, motif (Wingo et al., 2004; Chagot et al., 2009). Thus, increases in CaMKII activity have been variously reported to increase (Aiba et al., 2010) or decrease (Wagner et al., 2006) peak I_{Na}. Alternatively, intracellular Ca^{2+} has been shown to directly inhibit I_{Na} without affecting channel gating through a permeation block. Indeed, reductions in I_{Na} density and $(dV/dt)_{max}$ have been reported following increases in $[Ca^{2+}]_i$ brought about by changing the Ca^{2+} concentration in the pipette solution in patch-clamped WT myocytes (Casini et al., 2009). Furthermore, reductions in $(dV/dt)_{max}$, θ and increased incidences of arrhythmia have been shown in both homozygous gain of function *RyR2-P2328S* ($RyR2^{S/S}$) and caffeine-treated WT hearts that have abnormal diastolic SR Ca^{2+} release (King et al., 2013b). Both immunohistochemical and biophysical studies subsequently attributed these abnormalities to the effects of Ca^{2+} homeostasis on I_{Na} function (King et al., 2013a).

Finally, treatment with class I anti-arrhythmic drugs modulates Na^+ channel function. Thus, lidocaine, mexiletine, tocainide, and aprindine have been shown to block Na^+ channels in the inactivated state whilst quinidine and disopyramide block the open channel (Kodama et al., 1986; Sheldon et al., 1989). Furthermore, lidocaine has been associated with impaired conduction and the induction of ventricular tachyarrythmias in experimental models (Anderson et al., 1990).

ABNORMALITIES IN Na^+ CHANNEL EXPRESSION

Abnormalities in AP depolarization could also arise from an alteration in $Na_v1.5$ expression [**Figure 3A**(ii)]. Knockout mutations in the *SCN5A* gene decrease I_{Na} and are associated with cardiac conduction diseases including Lenègre disease (Schott et al., 1999), BrS (Gussak et al., 1999), sick sinus syndrome (Benson et al., 2003) and atrial fibrillation (AF) (Laitinen-Forsblom et al., 2006; Ellinor et al., 2008).

Of these, BrS is associated with a high incidence of ventricular tachyarrhythmias and sudden cardiac death (Gussak et al., 1999). Although the exact pathophysiological mechanism is not yet known (Hoogendijk et al., 2010), mutations in 17 genes have been associated with BrS of which *SCN5A* mutations account for a significant proportion (Tan et al., 2001). Furthermore, BrS patients with Na^+ channel mutations show significantly longer conduction intervals than those without *SCN5A* mutations (Smits et al., 2002). In addition, class I anti-arrhythmic drugs have been used to unmask the BrS ECG pattern by exacerbating pre-existing conduction abnormalities (Gasparini et al., 2003).

Conduction alterations in BrS have been studied using a murine model with knock-out mutations in *Scn5a* (Papadatos et al., 2002). The homozygous embryos die *in utero* with severe defects in ventricular morphogenesis. Heterozygous mice ($Scn5a^{+/-}$) haploinsufficient for $Na_v1.5$ show normal survival with several cardiac conduction defects including decreased atrial, ventricular and atrioventricular conduction and increased susceptibility to pacing-induced ventricular arrhythmias (Papadatos et al., 2002).

The expression of $Na_v1.5$ has also been shown to be regulated by changes in intracellular ion concentrations, including Ca^{2+}. Thus, $Na_v1.5$ mRNA and $Na_v1.5$ protein expression increased following treatment with the Ca^{2+} channel blocker, verapamil, and decreased following treatment with the Ca^{2+} ionophore calcimycin in rat cardiomyocytes (Offord and Catterall, 1989; Taouis et al., 1991; Duff et al., 1992). Similarly, Na^+ current densities increased following elevations of $[Ca^{2+}]_i$ brought about by increased extracellular $[Ca^{2+}]$. It decreased following reductions of $[Ca^{2+}]_i$ produced by BAPTA-AM in patch-clamped cultured neonatal rat myocytes (Chiamvimonvat et al., 1995).

Such changes in the expression of Na^+ channels have been reported in experimental models of atrial tachycardia that are associated with increased $[Ca^{2+}]_i$ (Sun et al., 2001). Thus, atrial tachypacing decreased $Na_v1.5$ mRNA, I_{Na}, and θ over several weeks in canine models (Gaspo et al., 1997; Yue et al., 1999). In contrast, the development of AF does not further reduce atrial I_{Na} (Yagi et al., 2002) or $Na_v1.5$ mRNA (van der Velden et al., 2000) in canine and goat models, respectively.

GAP JUNCTIONS AND THEIR RELATIONSHIP TO r_a

Gap junctions are non-selective membrane channels that form low resistance cell-to-cell connections that permit intercellular currents, as well as the transfer of ions, amino acids, and nucleotides. Their distribution within the cell membrane is tissue-specific and helps determine the magnitude and anisotropy of conduction. In general, cardiac cells express gap junctions near Na^+ channels and at higher densities toward the ends of cells rather than their lateral margins, resulting in lower r_a and hence faster conduction in the longitudinal direction (Kumar and Gilula, 1996).

Gap junction channels are composed of a family of proteins known as connexins (Cx). Adjacent cells each contribute a hemichannel, made up of 6 Cxs, to the junction. There are 15 known Cxs defined by their molecular weight, each with different channel properties and gating mechanisms. Four main variants, Cxs 30.2, 40, 43, and 45, have been described in mammalian cardiac tissue (Davis et al., 1994). The type and distribution of these Cxs determines the properties of passive conduction throughout the heart. Cx43 is the most abundant and is expressed throughout the ventricular and atrial myocardium (Beyer et al., 1987), whilst Cx40 is limited to atrial tissue and the His Purkinje system (Gourdie et al., 1993a,b). Cx30.2 is only found in the atrioventricular node (AVN) (Kreuzberg et al., 2006) and Cx45 is variously reported to be expressed in the specialized conducting system (Coppen et al., 1998, 2001). Cx43 has a moderate conductance of ∼110 pS and compared to other cardiac Cx is relatively insensitive to changes in transjunctional voltage (Moreno et al., 1994; Veenstra, 1996). Cx40 conductances are similar to Cx43, ∼160 pS, but they have higher sensitivities to transjunctional voltage (Beblo et al., 1995; Bukauskas et al., 1995). In contrast, Cx45 has a much lower conductance at ∼30 ps and is extremely sensitive to transjunctional voltage (Veenstra et al., 1994; Veenstra, 1996). These conductances are heavily regulated in healthy and pathophysiological myocardium. The resistance of gap junctions makes up approximately half of the longitudinal resistance in rat atria (Fry et al., 2012). Thus, the conductance of Cxs and therefore gap junctions help determine the magnitude of r_a and are an important determinant of θ.

ABNORMALITIES IN GAP JUNCTION FUNCTION

Mutations in the genes encoding Cxs can change gap junction function [**Figure 3B**(i)] and thereby reduce cell to cell coupling. Loss-of-function somatic mutations of the *CJA5* gene that expresses Cx40 have been shown to result in idiopathic AF (Firouzi et al., 2004) and when combined with a *SCN5A* mutation, atrial standstill (Groenewegen, 2002). Heterozygous somatic missense mutations and polymorphisms within the gene's regulatory region have also been linked to conduction delays and AF (Gollob et al., 2006; Hauer et al., 2006). Other mutations of the Cx43 gene, such as *GJA1,* which affects phosphorylation sites, have been associated with cardiac structural abnormalities (Britz-Cunningham et al., 1995; Dasgupta et al., 2001) but without reported conduction abnormalities.

Acquired functional modifications of Cx [**Figure 3B**(i)] have been shown to arise during both heart failure and myocardial ischemia. Heart failure is associated with increased c-Src tyrosine-mediated tyrosine phosphorylation of Cx43 leading to decreased conductance (Toyofuku et al., 1999), conduction abnormalities and arrhythmia (Laurita et al., 2003).

During ischemia there are pathological decreases in the conductance of gap junctions following increases in $[Ca^{2+}]_i$ (Smith et al., 1995; De Groot et al., 2001), intracellular acidification (Yan and Kléber, 1992) and through changes in catecholamine-induced increases in cellular cAMP, which in turn modulate levels of phosphorylation. Acute increases in $[Ca^{2+}]_i$ occur in ischemic rabbit models (Dekker et al., 1996) and are associated with gap junctional uncoupling (De Mello, 1975; Smith et al., 1995) and decreased conductance (Kirchhoff et al., 1998; Gutstein et al., 2001). Such changes result in conduction slowing and conduction block (Dekker et al., 1996) that is exacerbated by increases in intracellular pH (Kleber et al., 1986). Myocardial ischemia also causes Cx43 to rapidly dephosphorylate (Huang et al., 1999; Beardslee et al., 2000) leading to its lateralization, transfer from the intercalated disks to intracellular pools and electrical uncoupling (Smith et al., 1991; Matsushita et al., 1999; Beardslee et al., 2000; Lampe et al., 2000). Dephosphorylation of Cxs may also be involved in lateralization of gap junctions resulting in conduction abnormalities in AF (Dobrev et al., 2012). However, other studies have reported that protein kinase C-dependent phosphorylation of Cx43 at serine 368 is associated with decreased gap junctional communication (Lampe et al., 2000) and conductance (Moreno et al., 1994; Kwak et al., 1995).

ABNORMALITIES IN CONNEXIN EXPRESSION

Abnormalities in AP propagation also arise from changes in the total number of Cxs [**Figure 3B**(ii)]. Such abnormalities have been extensively modeled experimentally by using genetically modified mice with altered Cx 40, 43, and 45 expression.

Cx45 knockout mice (Kumai et al., 2000) show normal contraction with atrioventricular conduction block and die *in utero* at day 10, consistent with studies showing Cx45 is uniquely expressed in the atrioventricular canal (Coppen et al., 1999, 2001). The homozygous Cx40 knockout mouse model shows slowed conduction and a partial atrioventricular block (Leaf et al., 2008); however arrhythmia was only observed in one study (Kirchhoff et al., 1998). The homozygote Cx43 knockout mouse ($Cx43^{-/-}$) dies from neonatal pulmonary outflow obstruction (Reaume et al., 1995) but electrocardiography and optical mapping have been used successfully to measure θ in mice haploid insufficient for Cx43 ($Cx43^{+/-}$). The first of these studies suggested slowed conduction (Guerrero et al., 1997) but later work contradicted these findings, showing no significant change in θ (Kirchhoff et al., 2000; Thomas et al., 2003). However, ischemic $Cx43^{+/-}$ hearts have shown conduction abnormalities and higher incidences of spontaneous ventricular arrhythmias compared to WT (Lerner et al., 2000).

A cardiac-restricted homozygote knockout of Cx43 model was used to prevent the neonatal lethal structural defects in $Cx43^{-/-}$. Such mice have a 90% reduction in Cx43 with normal heart structure and contractile function. Epicardial optical mapping showed that both longitudinal and transverse ventricular θ was reduced by 40–50%. In addition, Cx43 conditional knockout mice had high incidences of spontaneous ventricular arrhythmias and sudden cardiac death (Gutstein et al., 2001). These latter findings were supported by recent modeling suggesting that in non-ischemic conditions a 90% reduction in gap junctions is required to decrease θ by 50% (Jongsma and Wilders, 2000; Spach et al., 2000).

Interestingly, recent studies have proposed an additional, non-canonical method of cardiac conduction whereby the intercellular transfer of charge does not only occur by the passive flow of current through gap junctions. These studies suggest a role for extracellular space in modulating θ (Veeraraghavan et al.,

2012) and that connexins actively augment current propagation by the accumulation of functional sodium channels at the perinexus of the intercalated disc and by the maintenance of narrow intercellular distances (Agullo-Pascual and Delmar, 2012; Rhett et al., 2013). Such a mechanism is supported by experimental evidence in cardiac restricted $Cx43^{+/-}$ knockout mice that associates reduced Cx43 expression with reduced $Na_v1.5$ expression and I_{Na} (Jansen et al., 2012). These findings highlight one of the limitations of using simple cable theory and help explain why decreases in connexin expression that are classically thought to increase r_a do not result in proportional decreases in θ.

Acquired changes in Cx expression have also been associated with a number of cardiac conditions including ventricular hypertrophy, heart failure and AF. During the early stages of ventricular hypertrophy there were increases in Cx expression and myocyte coupling. Thus, neonatal rat ventricular myocytes cultured in cAMP (Darrow et al., 1996) or angiotensin II (Dodge et al., 1998), both mediators of hypertrophy, showed increases in Cx43 expression and θ. More recent studies have shown a 100% increase in Cx43 expression and resulting θ in neonatal ventricular myocytes cultured with a mechanical load (Zhuang et al., 2000). θ typically increases in the acute phases of hypertrophy due to both increases in Cx43 expression and cell size that decrease intercellular and longitudinal resistance, respectively (Wiegerinck et al., 2006). Over prolonged periods of hypertrophy θ starts to decrease, as seen in chronic arrhythmic conditions (Cooklin et al., 1997) where Cx43 shows 25–50% downregulation (Kaprielian et al., 1998). The expression of Cx43 is downregulated in experimental (Akar et al., 2004; Ai and Pogwizd, 2005) and clinical (Dupont et al., 2001; Kostin et al., 2004) studies of heart failure through recruitment of mitogen-activated protein kinase C-Jun NH2- terminal kinase (Petrich et al., 2002). Clinical heart failure studies showed Cx45 (Yamada et al., 2003) and Cx40 (Dupont et al., 2001) are up-regulated, possibly as a compensatory mechanism.

There are inconsistent clinical and experimental reports regarding changes in Cx expression during atrial tachyarrhythmias such as AF. Thus, experimental studies show up regulation of Cx43 in an atrial tachypaced canine model (Elvan et al., 1996; Sakabe et al., 2004), increased heterogeneity of Cx40 expression in tachypaced goat models with no changes in overall Cx expression (van der Velden et al., 1998). Whilst clinical studies support experimental findings of increased Cx expression on lateral cell surfaces (Smith et al., 1991; Polontchouk et al., 2001; Kostin et al., 2002) and increased heterogeneity (Dupont et al., 2001; Kostin et al., 2004) there is no consensus on changes in overall Cx expression. Studies show both increases (Dupont et al., 2001; Polontchouk et al., 2001) and decreases (Kostin et al., 2002; Nao et al., 2003) in Cx40 and Cx43 expression. However, conduction abnormalities are consistently described in experimental (Gaspo et al., 1997) and clinical studies of AF (Konings et al., 1994).

Such findings suggest changes in gap junction conductance do influence θ and arrhythmic susceptibility but only when the majority of gap junctions are impaired. Instead, reductions in membrane excitability and anatomical disruption are likely to have greater roles in most pathologies.

FIBROSIS AND ITS RELATIONSHIP TO r_a AND c_m

Fibroblasts make up 75% of the cells in the myocardium (Banerjee et al., 2006). Indeed, sequential contraction of the atria and ventricles is dependent on the annulus fibrosus cordis to electrically insulate the two structures. In normal wound healing they undergo apoptosis after having produced a mixture of cross-linked collagen and other extracellular matrix (ECM) (Gurtner et al., 2008).

However, in certain fibrotic conditions such as myocardial infarction and cardiomyopathy, fibroblasts do not apoptose and instead proliferate, migrate, and differentiate into myofibroblasts (Weber et al., 1994). Fibroblast and myofibroblasts then continue to increase ECM deposition between layers of neighboring cardiomyocytes unabated (Manabe et al., 2002). This results in altered tissue architecture that in turn reduces myocyte-myocyte coupling as well as results in the formation of fibroblast-myocyte couplings (Camelliti et al., 2004). Such changes could in turn alter r_a or c_m, respectively slowing conduction.

DISRUPTION OF CELL-TO CELL COUPLING AND ALTERATIONS IN r_a

When healthy myocardium is disrupted by insulating connective tissue, the current provided by cells preceding the disruption may disperse along alternative branches, giving rise to a local conduction delay. Such current to load mismatches are found in fibrotic myocardium (Spach et al., 1988; De Bakker et al., 1993) and have been shown to impair conduction (Mendez et al., 1970; Spach et al., 1982).

Experimental canine models of fibrosis have shown how the deposition of insulating ECM and the decoupling of myocytes [**Figure 3C**(i)] lead to the interruption of both longitudinal and transverse cardiomyocyte-bundle continuity, producing zigzag conduction patterns (Spach and Boineau, 1997; Burstein et al., 2009). Such changes lead to conduction delays that predispose to re-entry arrhythmias in both experimental (De Bakker et al., 1993) and clinical studies (Spach, 2007).

COUPLING OF CARDIOMYOCYTES TO FIBROBLASTS AND ALTERATIONS IN c_m

Fibroblasts have been shown to electrically couple with cardiomyocytes through Cx43 and Cx45 binding [**Figure 3C**(ii)] (Camelliti et al., 2004; Chilton et al., 2007). Fibroblasts lack ion channels associated with excitation. They also have depolarized resting membrane potentials (Kamkin et al., 1999) and would therefore modulate the membrane potential of the myocytes to which they are coupled, potentially inactivating Na^+ channels. In addition, the coupling of fibroblasts to myocytes produces a net increase in cell capacitance, c_m (Miragoli et al., 2006).

Both these features resulted in a slowing of conduction and re-entrant events in cardiomyocytes co-cultured with fibroblasts (Maleckar et al., 2009; Xie et al., 2009). The magnitude of these effects on conduction appeared to be determined by the number of fibroblasts coupled to each cardiomyocyte, with significant changes observed when 10–30 fibroblasts were coupled per cardiomyocyte (Jacquemet and Henriquez, 2008; Maleckar et al., 2009; Sachse et al., 2009).

MURINE MODELS OF FIBROSIS

Experimental studies in mice have supported the association between impaired conduction and fibrosis. However, most murine models of fibrosis have concurrent pathological processes that may additionally contribute to abnormal conduction, making interpretation of their findings difficult. Thus, mutations in sarcomere protein genes cause hypertrophic cardiomyopathy (HCM), a congenital condition associated with myocyte enlargement and increased myocardial fibrosis, heart failure, and arrhythmia (Lu et al., 2013). Experimental murine models that carry mutations in the α- myosin heavy chain gene, *MHC403*, show fibrosis, conduction abnormalities, and increased incidence of inducible arrhythmia (Berul et al., 1998). Mutations in *SCN5A* are associated with both BrS and Lenègre disease (Schott et al., 1999). The latter condition produces progressive cardiac fibrosis and conduction abnormalities that lead to complete atrioventricular block and episodes of cardiac syncope. *Scn5a*$^{+/-}$ hearts demonstrate similar age-related fibrosis and deterioration in conduction resembling the clinical phenotype of both Lenègre's disease (Lenegre and Moreau, 1963) and BrS (Coronel et al., 2005). Finally, age-related upregulation of transforming growth factor-β1 (TGF-β1) associated with increased measures of fibrosis have been reported in *Scn5a*$^{+/-}$ hearts (Hao et al., 2011).

TGF-β1 mediated myocardial fibrosis also directly plays an important role in atrial arrhythmogenesis, including AF (Nattel et al., 2005). Experimental studies suggest that mice with increased expression of TGF-β1 have higher incidences of AF and conduction abnormalities as a result of raised levels of atrial fibrosis (Verheule et al., 2004). Furthermore, atrial fibroblasts appear more sensitive to the actions of TGF-β than their ventricular counterparts (Nakajima et al., 2000). TGF-β1 polymorphisms are also thought to be involved in inducing congenital heart block as a result of fibrosis, leading to a predisposition to AF (Clancy et al., 2003).

SUMMARY AND CONCLUSIONS

This review defines the determinants of θ as I_{Na}; r_a and c_m and summarizes the mechanistic evidence that links changes in these determinants with reduced myocardial θ and arrhythmogenesis. Thus, firstly, $(dV/dt)_{max}$ is reduced by impaired Na^+ channel function that arises clinically during heart failure, ischemia, tachycardia, and following treatment with class I anti-arrhythmic drugs. Such reductions also arise as a consequence of mutations in *SCN5A* such as those in Lenègre disease, BrS, sick sinus syndrome and AF. Secondly, r_a may be increased due to decreased gap junction coupling following ischemia, ventricular hypertrophy, and heart failure, or as a result of mutations in *CJA5* found in idiopathic AF and atrial standstill. Finally, either r_a or c_m could potentially be altered by fibrotic change through its effects upon decoupling myocyte-myocyte connections and through myocyte-fibroblast coupling. Such changes are observed in myocardial infarction and cardiomyopathy or following mutations in *MHC403* and *SCN5A* resulting in HCM or Lenègre disease, respectively. The review thereby identifies the diverse pathophysiological conditions in which abnormal θ may contribute to arrhythmogenesis. Such findings provide insight into the mechanisms of arrhythmogenesis in common arrhythmias not usually attributed to impaired conduction such as those associated with abnormal Ca^{2+} homeostasis.

ACKNOWLEDGMENTS

We thank the Biotechnology and Biological Sciences Research Council (BBSRC), Medical Research Council (MRC) and the Raymond and Beverly Sackler foundation for their generous financial support. James A. Fraser holds a David Phillips Fellowship from the BBSRC.

REFERENCES

Abriel, H. (2007). Roles and regulation of the cardiac sodium channel Na v 1.5: recent insights from experimental studies. *Cardiovasc. Res.* 76, 381–389. doi: 10.1016/j.cardiores.2007.07.019

Agullo-Pascual, E., and Delmar, M. (2012). The noncanonical functions of Cx43 in the heart. *J. Membr. Biol.* 245, 477–482. doi: 10.1007/s00232-012-9466-y

Ai, X., and Pogwizd, S. M. (2005). Connexin 43 downregulation and dephosphorylation in nonischemic heart failure is associated with enhanced colocalized protein phosphatase type 2A. *Circ. Res.* 96, 54–63. doi: 10.1161/01.RES.0000152325.07495.5a

Aiba, T., Hesketh, G. G., Liu, T., Carlisle, R., Villa-Abrille, M. C., O'Rourke, B., et al. (2010). Na+ channel regulation by Ca2+/calmodulin and Ca2+/calmodulin-dependent protein kinase II in guinea-pig ventricular myocytes. *Cardiovasc. Res.* 85, 454–463. doi: 10.1093/cvr/cvp324

Akar, F. G., Spragg, D. D., Tunin, R. S., Kass, D. A., and Tomaselli, G. F. (2004). Mechanisms underlying conduction slowing and arrhythmogenesis in nonischemic dilated cardiomyopathy. *Circ. Res.* 95, 717–725. doi: 10.1161/01.RES.0000144125.61927.1c

Anderson, K. P., Walker, R., Lux, R. L., Ershler, P. R., Menlove, R., Williams, M. R., et al. (1990). Conduction velocity depression and drug-induced ventricular tachyarrhythmias. Effects of lidocaine in the intact canine heart. *Circulation* 81, 1024–1038. doi: 10.1161/01.CIR.81.3.1024

Baba, S., Dun, W., and Boyden, P. A. (2004). Can PKA activators rescue Na+ channel function in epicardial border zone cells that survive in the infarcted canine heart. *Cardiovasc. Res.* 64, 260–267. doi: 10.1016/j.cardiores.2004.06.021

Banerjee, I., Yekkala, K., Borg, T. K., and Baudino, T. A. (2006). Dynamic interactions between myocytes, fibroblasts, and extracellular matrix. *Ann. N.Y. Acad. Sci.* 1080, 76–84. doi: 10.1196/annals.1380.007

Beardslee, M. A., Lerner, D. L., Tadros, P. N., Laing, J. G., Beyer, E. C., Yamada, K. A., et al. (2000). Dephosphorylation and intracellular redistribution of ventricular connexin43 during electrical uncoupling induced by ischemia. *Circ. Res.* 87, 656–662. doi: 10.1161/01.RES.87.8.656

Beblo, D. A., Wang, H. Z., Beyer, E. C., Westphale, E. M., and Veenstra, R. D. (1995). Unique conductance, gating, and selective permeability properties of gap junction channels formed by connexin40. *Circ. Res.* 77, 813–822. doi: 10.1161/01.RES.77.4.813

Benson, D. W., Wang, D. W., Dyment, M., Knilans, T. K., Fish, F. A., Strieper, M. J., et al. (2003). Congenital sick sinus syndrome caused by recessive mutations in the cardiac sodium channel gene (SCN5A). *J. Clin. Invest.* 112, 1019–1028.

Bers, D. M. (2002). Cardiac excitation-contraction coupling. *Nature* 415, 198–205. doi: 10.1038/415198a

Berul, C. I., Christe, M. E., Aronovitz, M. J., Maguire, C. T., Seidman, C. E., Seidman, J. G., et al. (1998). Familial hypertrophic cardiomyopathy mice display gender differences in electrophysiological abnormalities. *J. Interv. Card. Electrophysiol.* 2, 7–14. doi: 10.1023/A:1009700404218

Beyer, E. C., Paul, D. L., and Goodenough, D. A. (1987). Connexin43: a protein from rat heart homologous to a gap junction protein from liver.

J. Cell Biol. 105, 2621–2629. doi: 10.1083/jcb.105.6.2621

Bezzina, C. (2001). Cardiac sodium channel and inherited arrhythmia syndromes. *Cardiovasc. Res.* 49, 257–271.

Bezzina, C., Veldkamp, M. W., Van den Berg, M. P., Postma, A. V., Rook, M. B., Viersma, J.-W., et al. (1999). A single Na+ channel mutation causing both long-QT and Brugada syndromes. *Circ. Res.* 85, 1206–1213.

Britz-Cunningham, S. H., Shah, M. M., Zuppan, C. W., and Fletcher, W. H. (1995). Mutations of the Connexin43 gap-junction gene in patients with heart malformations and defects of laterality. *N. Engl. J. Med.* 332, 1323–1329. doi: 10.1056/NEJM199505183322002

Buchanan, J. W., Saito, T., and Gettes, L. S. (1985). The effects of antiarrhythmic drugs, stimulation frequency, and potassium-induced resting membrane potential changes on conduction velocity and dV/dtmax in guinea pig myocardium. *Circ. Res.* 56, 696–703.

Bukauskas, F. F., Elfgang, C., Willecke, K., and Weingart, R. (1995). Biophysical properties of gap junction channels formed by mouse connexin40 in induced pairs of transfected human HeLa cells. *Biophys. J.* 68, 2289–2298. doi: 10.1016/S0006-3495(95)80411-X

Burstein, B., Comtois, P., Michael, G., Nishida, K., Villeneuve, L., Yeh, Y.-H., et al. (2009). Changes in connexin expression and the atrial fibrillation substrate in congestive heart failure. *Circ. Res.* 105, 1213–1222. doi: 10.1161/CIRCRESAHA.108.183400

Camelliti, P., Green, C. R., LeGrice, I., and Kohl, P. (2004). Fibroblast network in rabbit sinoatrial node: structural and functional identification of homogeneous and heterogeneous cell coupling. *Circ. Res.* 94, 828–835. doi: 10.1161/01.RES.0000122382.19400.14

Casini, S., Verkerk, A. O., Van Borren, M. M. G. J., Van Ginneken, A. C. G., Veldkamp, M. W., De Bakker, J. M. T., et al. (2009). Intracellular calcium modulation of voltage-gated sodium channels in ventricular myocytes. *Cardiovasc. Res.* 81, 72–81. doi: 10.1093/cvr/cvn274

Chagot, B., Potet, F., Balser, J. R., and Chazin, W. J. (2009). Solution NMR structure of the C-terminal EF-hand domain of human cardiac sodium channel NaV1.5. *J. Biol. Chem.* 284, 6436–6445. doi: 10.1074/jbc.M807747200

Chiamvimonvat, N., Kargacin, M. E., Clark, R. B., and Duff, H. J. (1995). Effects of intracellular calcium on sodium current density in cultured neonatal rat cardiac myocytes. *J. Physiol.* 483(Pt 2), 307–318.

Chilton, L., Giles, W. R., and Smith, G. L. (2007). Evidence of intercellular coupling between co-cultured adult rabbit ventricular myocytes and myofibroblasts. *J. Physiol.* 583, 225–236. doi: 10.1113/jphysiol.2007.135038

Clancy, R. M., Backer, C. B., Yin, X., Kapur, R. P., Molad, Y., and Buyon, J. P. (2003). Cytokine polymorphisms and histologic expression in autopsy studies: contribution of TNF-alpha and TGF-beta 1 to the pathogenesis of autoimmune-associated congenital heart block. *J. Immunol.* 171, 3253–3261.

Cohen, S. A. (1996). Immunocytochemical localization of rH1 sodium channel in adult rat heart atria and ventricle: presence in terminal intercalated disks. *Circulation* 94, 3083–3086. doi: 10.1161/01.CIR.94.12.3083

Cooklin, M., Wallis, W. R., Sheridan, D. J., and Fry, C. H. (1997). Changes in cell-to-cell electrical coupling associated with left ventricular hypertrophy. *Circ. Res.* 80, 765–771. doi: 10.1161/01.RES.80.6.765

Coppen, S. R., Dupont, E., Rothery, S., and Severs, N. J. (1998). Connexin45 expression is preferentially associated with the ventricular conduction system in mouse and rat heart. *Circ. Res.* 82, 232–243. doi: 10.1161/01.RES.82.2.232

Coppen, S. R., Gourdie, R. G., and Severs, N. J. (2001). Connexin45 is the first connexin to be expressed in the central conduction system of the mouse heart. *Exp. Clin. Cardiol.* 6, 17–23.

Coppen, S. R., Severs, N. J., and Gourdie, R. G. (1999). Connexin45 (alpha 6) expression delineates an extended conduction system in the embryonic and mature rodent heart. *Dev. Genet.* 24, 82–90.

Coronel, R., Casini, S., Koopmann, T. T., Wilms-Schopman, F. J. G., Verkerk, A. O., De Groot, J. R., et al. (2005). Right ventricular fibrosis and conduction delay in a patient with clinical signs of Brugada syndrome: a combined electrophysiological, genetic, histopathologic, and computational study. *Circulation* 112, 2769–2777. doi: 10.1161/CIRCULATIONAHA.105.532614

Corr, P. B., and Yamada, K. A. (1995). Selected metabolic alterations in the ischemic heart and their contributions to arrhythmogenesis. *Herz* 20, 156–168.

Darrow, B. J., Fast, V. G., Kléber, A. G., Beyer, E. C., and Saffitz, J. E. (1996). Functional and structural assessment of intercellular communication. Increased conduction velocity and enhanced connexin expression in dibutyryl cAMP-treated cultured cardiac myocytes. *Circ. Res.* 79, 174–183. doi: 10.1161/01.RES.79.2.174

Dasgupta, C., Martinez, A. M., Zuppan, C. W., Shah, M. M., Bailey, L. L., and Fletcher, W. H. (2001). Identification of connexin43 (alpha1) gap junction gene mutations in patients with hypoplastic left heart syndrome by denaturing gradient gel electrophoresis (DGGE). *Mutat. Res.* 479, 173–186. doi: 10.1016/S0027-5107(01)00160-9

Davis, L. M., Kanter, H. L., Beyer, E. C., and Saffitz, J. E. (1994). Distinct gap junction protein phenotypes in cardiac tissues with disparate conduction properties. *J. Am. Coll. Cardiol.* 24, 1124–1132. doi: 10.1016/0735-1097(94)90879-6

De Bakker, J. M., Van Capelle, F. J., Janse, M. J., Tasseron, S., Vermeulen, J. T., De Jonge, N., et al. (1993). Slow conduction in the infarcted human heart. "Zigzag" course of activation. *Circulation* 88, 915–926. doi: 10.1161/01.CIR.88.3.915

De Groot, J. R., Wilms-Schopman, F. J., Opthof, T., Remme, C. A., and Coronel, R. (2001). Late ventricular arrhythmias during acute regional ischemia in the isolated blood perfused pig heart. Role of electrical cellular coupling. *Cardiovasc. Res.* 50, 362–372. doi: 10.1016/S0008-6363(01)00222-X

Dekker, L. R. C., Fiolet, J. W. T., VanBavel, E., Coronel, R., Opthof, T., Spaan, J. A. E., et al. (1996). Intracellular Ca2+, intercellular electrical coupling, and mechanical activity in ischemic rabbit papillary muscle: effects of preconditioning and metabolic blockade. *Circ. Res.* 79, 237–246.

De Mello, W. C. (1975). Effect of intracellular injection of calcium and strontium on cell communication in heart. *J. Physiol.* 250, 231–245.

Dobrev, D., Carlsson, L., and Nattel, S. (2012). Novel molecular targets for atrial fibrillation therapy. *Nat. Rev. Drug Discov.* 11, 275–291. doi: 10.1038/nrd3682

Dodge, S. M., Beardslee, M. A., Darrow, B. J., Green, K. G., Beyer, E. C., and Saffitz, J. E. (1998). Effects of angiotensin II on expression of the gap junction channel protein connexin43 in neonatal rat ventricular myocytes. *J. Am. Coll. Cardiol.* 32, 800–807. doi: 10.1016/S0735-1097(98)00317-9

Downar, E., Janse, M. J., and Durrer, D. (1977). The effect of "ischemic" blood on transmembrane potentials of normal porcine ventricular myocardium. *Circulation* 55, 455–462. doi: 10.1161/01.CIR.55.3.455

Duff, H. J., Offord, J., West, J., and Catterall, W. A. (1992). Class I and IV antiarrhythmic drugs and cytosolic calcium regulate mRNA encoding the sodium channel alpha subunit in rat cardiac muscle. *Mol. Pharmacol.* 42, 570–574.

Dupont, E., Matsushita, T., Kaba, R. A., Vozzi, C., Coppen, S. R., Khan, N., et al. (2001). Altered connexin expression in human congestive heart failure. *J. Mol. Cell. Cardiol.* 33, 359–371. doi: 10.1006/jmcc.2000.1308

Ellinor, P. T., Nam, E. G., Shea, M. A., Milan, D. J., Ruskin, J. N., and MacRae, C. A. (2008). Cardiac sodium channel mutation in atrial fibrillation. *Heart Rhythm* 5, 99–105. doi: 10.1016/j.hrthm.2007.09.015

Elvan, A., Wylie, K., and Zipes, D. P. (1996). Pacing-induced chronic atrial fibrillation impairs sinus node function in dogs. Electrophysiological remodeling. *Circulation* 94, 2953–2960. doi: 10.1161/01.CIR.94.11.2953

Firouzi, M., Ramanna, H., Kok, B., Jongsma, H. J., Koeleman, B. P. C., Doevendans, et al. (2004). Association of human connexin40 gene polymorphisms with atrial vulnerability as a risk factor for idiopathic atrial fibrillation. *Circ. Res.* 95, e29–e33. doi: 10.1161/01.RES.0000141134.64811.0a

Fraser, J. A., Huang, C. L.-H., and Pedersen, T. H. (2011). Relationships between resting conductances, excitability, and t-system ionic homeostasis in skeletal muscle. *J. Gen. Physiol.* 138, 95–116. doi: 10.1085/jgp.201110617

Fry, C. H., Salvage, S. C., Manazza, A., Dupont, E., Labeed, F. H., Hughes, M. P., et al. (2012). Cytoplasm resistivity of mammalian atrial myocardium determined by dielectrophoresis and impedance methods. *Biophys. J.* 103, 2287–2294. doi: 10.1016/j.bpj.2012.10.023

Gasparini, M., Priori, S. G., Mantica, M., Napolitano, C., Galimberti, P., Ceriotti, C., et al. (2003). Flecainide

test in Brugada syndrome: a reproducible but risky tool. *Pacing Clin. Electrophysiol.* 26, 338–341. doi: 10.1046/j.1460-9592.2003.00045.x

Gaspo, R., Bosch, R. F., Bou-Abboud, E., and Nattel, S. (1997). Tachycardia-induced changes in Na+ current in a chronic dog model of atrial fibrillation. *Circ. Res.* 81, 1045–1052. doi: 10.1161/01.RES.81.6.1045

Gelband, H., and Bassett, A. L. (1973). Depressed transmembrane potentials during experimentally induced ventricular failure in cats. *Circ. Res.* 32, 625–634. doi: 10.1161/01.RES.32.5.625

Gellens, M. E., George, A. L., Chen, L. Q., Chahine, M., Horn, R., Barchi, R. L., et al. (1992). Primary structure and functional expression of the human cardiac tetrodotoxin-insensitive voltage-dependent sodium channel. *Proc. Natl. Acad. Sci. U.S.A.* 89, 554–558.

Gollob, M. H., Jones, D. L., Krahn, A. D., Danis, L., Gong, X.-Q., Shao, Q., et al. (2006). Somatic mutations in the connexin 40 gene (GJA5) in atrial fibrillation. *N. Engl. J. Med.* 354, 2677–2688. doi: 10.1056/NEJMoa052800

Gourdie, R. G., Green, C. R., Severs, N. J., Anderson, R. H., and Thompson, R. P. (1993a). Evidence for a distinct gap-junctional phenotype in ventricular conduction tissues of the developing and mature avian heart. *Circ. Res.* 72, 278–289.

Gourdie, R. G., Severs, N. J., Green, C. R., Rothery, S., Germroth, P., and Thompson, R. P. (1993b). The spatial distribution and relative abundance of gap-junctional connexin40 and connexin43 correlate to functional properties of components of the cardiac atrioventricular conduction system. *J. Cell. Sci.* 105(Pt 4), 985–991.

Groenewegen, W. A. (2002). A cardiac sodium channel mutation cosegregates with a rare connexin40 genotype in familial atrial standstill. *Circ. Res.* 92, 14–22.

Guerrero, P. A., Schuessler, R. B., Davis, L. M., Beyer, E. C., Johnson, C. M., Yamada, K. A., et al. (1997). Slow ventricular conduction in mice heterozygous for a connexin43 null mutation. *J. Clin. Invest.* 99, 1991–1998. doi: 10.1172/JCI119367

Gurtner, G. C., Werner, S., Barrandon, Y., and Longaker, M. T. (2008). Wound repair and regeneration. *Nature* 453, 314–321. doi: 10.1038/nature07039

Gussak, I., Antzelevitch, C., Bjerregaard, P., Towbin, J. A, and Chaitman, B. R. (1999). The Brugada syndrome: clinical, electrophysiologic and genetic aspects. *J. Am. Coll. Cardiol.* 33, 5–15. doi: 10.1016/S0735-1097(98)00528-2

Gutstein, D. E. E., Morley, G. E. E., Tamaddon, H., Vaidya, D., Schneider, M. D. D., Chen, J. J., et al. (2001). Conduction slowing and sudden arrhythmic death in mice with cardiac-restricted inactivation of connexin43. *Circ. Res.* 88, 333–339. doi: 10.1161/01.RES.88.3.333

Hallaq, H., Yang, Z., Viswanathan, P. C., Fukuda, K., Shen, W., Wang, D. W., et al. (2006). Quantitation of protein kinase A-mediated trafficking of cardiac sodium channels in living cells. *Cardiovasc. Res.* 72, 250–261. doi: 10.1016/j.cardiores.2006.08.007

Hao, X., Zhang, Y., Zhang, X., Nirmalan, M., Davies, L., Konstantinou, D., et al. (2011). TGF-β1-mediated fibrosis and ion channel remodeling are key mechanisms in producing the sinus node dysfunction associated with SCN5A deficiency and aging. *Circ. Arrhythm. Electrophysiol.* 4, 397–406. doi: 10.1161/CIRCEP.110.960807

Hauer, R. N. W., Groenewegen, W. A., Firouzi, M., Ramanna, H., and Jongsma, H. J. (2006). Cx40 polymorphism in human atrial fibrillation. *Adv. Cardiol.* 42, 284–291. doi: 10.1159/000092579

Hodgkin, A. L., and Katz, B. (1949). The effect of sodium ions on the electrical activity of giant axon of the squid. *J. Physiol.* 108, 37–77.

Hoogendijk, M. G., Opthof, T., Postema, P. G., Wilde, A. A. M., De Bakker, J. M. T., and Coronel, R. (2010). The Brugada ECG pattern: a marker of channelopathy, structural heart disease, or neither. Toward a unifying mechanism of the Brugada syndrome. *Circ. Arrhythm. Electrophysiol.* 3, 283–290. doi: 10.1161/CIRCEP.110.937029

Huang, X. D., Sandusky, G. E., and Zipes, D. P. (1999). Heterogeneous loss of connexin43 protein in ischemic dog hearts. *J. Cardiovasc. Electrophysiol.* 10, 79–91. doi: 10.1111/j.1540-8167.1999.tb00645.x

Jack, J., Noble, D., and Tsien, R. (1983). *Electric Current Flow in Excitable Cells.* Oxford: Oxford University Press.

Jacquemet, V., and Henriquez, C. S. (2008). Loading effect of fibroblast-myocyte coupling on resting potential, impulse propagation, and repolarization: insights from a microstructure model. *Am. J. Physiol. Heart Circ. Physiol.* 294, H2040–H2052.

Janse, M., Kleber, A., Capucci, A., Coronel, R., and Wilmsschopman, F. (1986). Electrophysiological basis for arrhythmias caused by acute ischemia. Role of the subendocardium. *J. Mol. Cell. Cardiol.* 18, 339–355.

Jansen, J. A., Noorman, M., Musa, H., Stein, M., De Jong, S., Van der Nagel, R., et al. (2012). Reduced heterogeneous expression of Cx43 results in decreased Nav1.5 expression and reduced sodium current that accounts for arrhythmia vulnerability in conditional Cx43 knockout mice. *Heart Rhythm* 9, 600–607. doi: 10.1016/j.hrthm.2011.11.025

Jongsma, H. J., and Wilders, R. (2000). Gap junctions in cardiovascular disease. *Circ. Res.* 86, 1193–1197. doi: 10.1161/01.RES.86.12.1193

Kabell, G. (1989). Ischemia-induced conduction delay and ventricular arrhythmias: comparative electropharmacology of bethanidine sulfate and bretylium tosylate. *J. Cardiovasc. Pharmacol.* 13, 471–482. doi: 10.1097/00005344-198903000-00017

Kamkin, A., Kiseleva, I., Wagner, K. D., Lammerich, A., Bohm, J., Persson, P. B., et al. (1999). Mechanically induced potentials in fibroblasts from human right atrium. *Exp. Physiol.* 84, 347–356. doi: 10.1017/S0958067099017947

Kaprielian, R. R., Gunning, M., Dupont, E., Sheppard, M. N., Rothery, S. M., Underwood, R., et al. (1998). Downregulation of immunodetectable connexin43 and decreased gap junction size in the pathogenesis of chronic hibernation in the human left ventricle. *Circulation* 97, 651–660. doi: 10.1161/01.CIR.97.7.651

Keener, J., and Sneyd, J. (2009). *Mathematical Physiology: I: Cellular Physiology (Interdisciplinary Applied Mathematics), 2nd Edn.* New York, NY: Springer.

King, J. H., Wickramarachchi, C., Kua, K., Du, Y., Jeevaratnam, K., Matthews, H. R., et al. (2013a). Loss of Nav1.5 expression and function in murine atria containing the RyR2-P2328S gain-of-function mutation. *Cardiovasc. Res.* doi: 10.1093/cvr/cvt141. [Epub ahead of print].

King, J., Zhang, Y., Lei, M., Grace, A., Huang, C.-H., and Fraser, J. (2013b). Atrial arrhythmia, triggering events and conduction abnormalities in isolated murine RyR2-P2328S hearts. *Acta Physiol.* 207, 308–323.

Kirchhoff, S., Kim, J. S., Hagendorff, A., Thönnissen, E., Krüger, O., Lamers, W. H., et al. (2000). Abnormal cardiac conduction and morphogenesis in connexin40 and connexin43 double-deficient mice. *Circ. Res.* 87, 399–405. doi: 10.1161/01.RES.87.5.399

Kirchhoff, S., Nelles, E., Hagendorff, A., Krüger, O., Traub, O., and Willecke, K. (1998). Reduced cardiac conduction velocity and predisposition to arrhythmias in connexin40-deficient mice. *Curr. Biol.* 8, 299–302. doi: 10.1016/S0960-9822(98)70114-9

Kleber, A. G., Janse, M. J., Wilms-Schopmann, F. J., Wilde, A. A., and Coronel, R. (1986). Changes in conduction velocity during acute ischemia in ventricular myocardium of the isolated porcine heart. *Circulation* 73, 189–198. doi: 10.1161/01.CIR.73.1.189

Kléber, A. G., and Riegger, C. B. (1987). Electrical constants of arterially perfused rabbit papillary muscle. *J. Physiol.* 385, 307–324.

Kodama, I., Toyama, J., and Yamada, K. (1986). Open and inactivated sodium channel block by class-I antiarrhythmic drugs. *Jpn. Heart J.* 27(Suppl. 1), 83–89.

Kodama, I., Wilde, A., Janse, M. J., Durrer, D., and Yamada, K. (1984). Combined effects of hypoxia, hyperkalemia and acidosis on membrane action potential and excitability of guinea-pig ventricular muscle. *J. Mol. Cell. Cardiol.* 16, 247–259. doi: 10.1016/S0022-2828(84)80591-X

Konings, K. T., Kirchhof, C. J., Smeets, J. R., Wellens, H. J., Penn, O. C., and Allessie, M. A. (1994). High-density mapping of electrically induced atrial fibrillation in humans. *Circulation* 89, 1665–1680. doi: 10.1161/01.CIR.89.4.1665

Kostin, S., Dammer, S., Hein, S., Klovekorn, W. P., Bauer, E. P., and Schaper, J. (2004). Connexin 43 expression and distribution in compensated and decompensated cardiac hypertrophy in patients with aortic stenosis. *Cardiovasc. Res.* 62, 426–436. doi: 10.1016/j.cardiores.2003.12.010

Kostin, S., Klein, G., Szalay, Z., Hein, S., Bauer, E. P., and Schaper, J. (2002). Structural correlate of atrial fibrillation in human patients. *Cardiovasc. Res.* 54, 361–379. doi: 10.1016/S0008-6363(02)00273-0

Kreuzberg, M. M., Schrickel, J. W., Ghanem, A., Kim, J.-S., Degen, J., Janssen-Bienhold, U., et al. (2006).

Connexin30.2 containing gap junction channels decelerate impulse propagation through the atrioventricular node. *Proc. Natl. Acad. Sci. U.S.A.* 103, 5959–5964.

Kucera, J. P., Kléber, A. G., and Rohr, S. (1998). Slow conduction in cardiac tissue, II: effects of branching tissue geometry. *Circ. Res.* 83, 795–805. doi: 10.1161/01.RES.83.8.795

Kumai, M., Nishii, K., Nakamura, K., Takeda, N., Suzuki, M., and Shibata, Y. (2000). Loss of connexin45 causes a cushion defect in early cardiogenesis. *Development* 127, 3501–3512.

Kumar, N. M., and Gilula, N. B. (1996). The gap junction communication channel. *Cell* 84, 381–388. doi: 10.1016/S0092-8674(00)81282-9

Kuryshev, Y. A., Brittenham, G. M., Fujioka, H., Kannan, P., Shieh, C.-C., Cohen, S. A., et al. (1999). Decreased sodium and increased transient outward potassium currents in iron-loaded cardiac myocytes: implications for the arrhythmogenesis of human siderotic heart disease. *Circulation* 100, 675–683. doi: 10.1161/01.CIR.100.6.675

Kwak, B. R., Hermans, M. M., De Jonge, H. R., Lohmann, S. M., Jongsma, H. J., and Chanson, M. (1995). Differential regulation of distinct types of gap junction channels by similar phosphorylating conditions. *Mol. Biol. Cell* 6, 1707–1719.

Laitinen-Forsblom, P. J., Makynen, P., Makynen, H., Yli-Mayry, S., Virtanen, V., Kontula, K., et al. (2006). SCN5A mutation associated with cardiac conduction defect and atrial arrhythmias. *J. Cardiovasc. Electrophysiol.* 17, 480–485. doi: 10.1111/j.1540-8167.2006.00411.x

Lampe, P. D., TenBroek, E. M., Burt, J. M., Kurata, W. E., Johnson, R. G., and Lau, A. F. (2000). Phosphorylation of connexin43 on serine368 by protein kinase C regulates gap junctional communication. *J. Cell Biol.* 149, 1503–1512. doi: 10.1083/jcb.149.7.1503

Laurita, K. R., Chuck, E. T., Yang, T., Dong, W.-Q., Kuryshev, Y. A., Brittenham, G. M., et al. (2003). Optical mapping reveals conduction slowing and impulse block in iron-overload cardiomyopathy. *J. Lab. Clin. Med.* 142, 83–89. doi: 10.1016/S0022-2143(03)00060-X

Leaf, D. E., Feig, J. E., Vasquez, C., Riva, P. L., Yu, C., Lader, J. M., et al. (2008). Connexin40 imparts conduction heterogeneity to atrial tissue. *Circ. Res.* 103, 1001–1008. doi: 10.1161/CIRCRESAHA.107.168997

Lenegre, J., and Moreau, P. (1963). [Chronic auriculo-ventricular block. Anatomical, clinical and histological study]. *Arch. Mal. Coeur Vaiss.* 56, 867–888.

Lerner, D. L., Yamada, K. A., Schuessler, R. B., and Saffitz, J. E. (2000). Accelerated onset and increased incidence of ventricular arrhythmias induced by ischemia in Cx43-deficient mice. *Circulation* 101, 547–552. doi: 10.1161/01.CIR.101.5.547

Lin, X., Liu, N., Lu, J., Zhang, J., Anumonwo, J. M. B., Isom, L. L., et al. (2011). Subcellular heterogeneity of sodium current properties in adult cardiac ventricular myocytes. *Heart Rhythm* 8, 1923–1930. doi: 10.1016/j.hrthm.2011.07.016

Lu, Q.-W., Wu, X.-Y., and Morimoto, S. (2013). Inherited cardiomyopathies caused by troponin mutations. *J. Geriatr. Cardiol.* 10, 91–101.

Maleckar, M. M., Greenstein, J. L., Giles, W. R., and Trayanova, N. A. (2009). Electrotonic coupling between human atrial myocytes and fibroblasts alters myocyte excitability and repolarization. *Biophys. J.* 97, 2179–2190. doi: 10.1016/j.bpj.2009.07.054

Manabe, I., Shindo, T., and Nagai, R. (2002). Gene expression in fibroblasts and fibrosis: involvement in cardiac hypertrophy. *Circ. Res.* 91, 1103–1113. doi: 10.1161/01.RES.0000046452.67724.B8

Mandapati, R., Skanes, A., Chen, J., Berenfeld, O., and Jalife, J. (2000). Stable microreentrant sources as a mechanism of atrial fibrillation in the isolated sheep heart. *Circulation* 101, 194–199. doi: 10.1161/01.CIR.101.2.194

Matsuda, J. J., Lee, H., and Shibata, E. F. (1992). Enhancement of rabbit cardiac sodium channels by beta-adrenergic stimulation. *Circ. Res.* 70, 199–207.

Matsushita, T., Oyamada, M., Fujimoto, K., Yasuda, Y., Masuda, S., Wada, Y., et al. (1999). Remodeling of cell-cell and cell-extracellular matrix interactions at the border zone of rat myocardial infarcts. *Circ. Res.* 85, 1046–1055. doi: 10.1161/01.RES.85.11.1046

Mendez, C., Mueller, W. J., and Urguiaga, X. (1970). Propagation of impulses across the Prukinje fiber-muscle junctions in the dog heart. *Circ. Res.* 26, 135–150. doi: 10.1161/01.RES.26.2.135

Mines, G. R. (1914). On circulating excitations in heart muscles and their possible relation to tachycardia and fibrillation. *Trans. R. Soc. Can.* 8, 43–52.

Miragoli, M., Gaudesius, G., and Rohr, S. (2006). Electrotonic modulation of cardiac impulse conduction by myofibroblasts. *Circ. Res.* 98, 801–810. doi: 10.1161/01.RES.0000214537.44195.a3

Moreno, A. P., Saez, J. C., Fishman, G. I., and Spray, D. C. (1994). Human connexin43 gap junction channels. Regulation of unitary conductances by phosphorylation. *Circ. Res.* 74, 1050–1057.

Murphy, B. J., Rogers, J., Perdichizzi, A. P., Colvin, A. A., and Catterall, W. A., (1996). cAMP-dependent phosphorylation of two sites in the alpha subunit of the cardiac sodium channel. *J. Biol. Chem.* 271, 28837–28843.

Nakajima, H., Nakajima, H. O., Salcher, O., Dittie, A. S., Dembowsky, K., Jing, S., et al. (2000). Atrial but not ventricular fibrosis in mice expressing a mutant transforming growth factor- 1 transgene in the heart. *Circ. Res.* 86, 571–579.

Nao, T., Ohkusa, T., Hisamatsu, Y., Inoue, N., Matsumoto, T., Yamada, J., et al. (2003). Comparison of expression of connexin in right atrial myocardium in patients with chronic atrial fibrillation versus those in sinus rhythm. *Am. J. Cardiol.* 91, 678–683. doi: 10.1016/S0002-9149(02)03403-3

Nattel, S., Shiroshita-Takeshita, A., Brundel, B. J., and Rivard, L. (2005). Mechanisms of atrial fibrillation: lessons from animal models. *Prog. Cardiovasc. Dis.* 48, 9–28. doi: 10.1016/j.pcad.2005.06.002

Offord, J., and Catterall, W. A. (1989). Electrical activity, cAMP, and cytosolic calcium regulate mRNA encoding sodium channel alpha subunits in rat muscle cells. *Neuron* 2, 1447–1452. doi: 10.1016/0896-6273(89)90190-6

Ono, K., Kiyosue, T., and Arita, M. (1989). Isoproterenol, DBcAMP, and forskolin inhibit cardiac sodium current. *Am. J. Physiol.* 256, C1131–C1137.

Papadatos, G. A., Wallerstein, P. M. R., Head, C. E. G., Ratcliff, R., Brady, P. A, Benndorf, K., et al. (2002). Slowed conduction and ventricular tachycardia after targeted disruption of the cardiac sodium channel gene Scn5a. *Proc. Natl. Acad. Sci. U.S.A.* 99, 6210–6215.

Petrich, B. G., Gong, X., Lerner, D. L., Wang, X., Brown, J. H., Saffitz, J. E., et al. (2002). c-Jun N-terminal kinase activation mediates downregulation of connexin43 in cardiomyocytes. *Circ. Res.* 91, 640–647. doi: 10.1161/01.RES.0000035854.11082.01

Plonsey, R., and Barr, R. (2007). *Bioelectricity: A Quantitative Approach, 3rd Edn.* New York, NY: Springer.

Polontchouk, L., Haefliger, J. A., Ebelt, B., Schaefer, T., Stuhlmann, D., Mehlhorn, U., et al. (2001). Effects of chronic atrial fibrillation on gap junction distribution in human and rat atria. *J. Am. Coll. Cardiol.* 38, 883–891. doi: 10.1016/S0735-1097(01)01443-7

Qu, Y., Rogers, J. C., Tanada, T. N., Catterall, W. A, and Scheuer, T. (1996). Phosphorylation of S1505 in the cardiac Na+ channel inactivation gate is required for modulation by protein kinase C. *J. Gen. Physiol.* 108, 375–379. doi: 10.1085/jgp.108.5.375

Reaume, A. G., De Sousa, P. A., Kulkarni, S., Langille, B. L., Zhu, D., Davies, T. C., et al. (1995). Cardiac malformation in neonatal mice lacking connexin43. *Science* 267, 1831–1834.

Remme, C. A., Verkerk, A. O., Nuyens, D., Van Ginneken, A. C. G., Van Brunschot, S., Belterman, C. N. W., et al. (2006). Overlap syndrome of cardiac sodium channel disease in mice carrying the equivalent mutation of human SCN5A-1795insD. *Circulation* 114, 2584–2594. doi: 10.1161/CIRCULATIONAHA.106.653949

Rhett, J. M., Ongstad, E. L., Jourdan, J., and Gourdie, R. G. (2012). Cx43 associates with Na(v)1.5 in the cardiomyocyte perinexus. *J. Membr. Biol.* 245, 411–422. doi: 10.1007/s00232-012-9465-z

Rhett, J. M., Veeraraghavan, R., Poelzing, S., and Gourdie, R. G. (2013). The perinexus: sign-post on the path to a new model of cardiac conduction. *Trends Cardiovasc. Med.* doi: 10.1016/j.tcm.2012.12.005. [Epub ahead of print].

Rohr, S. (2004). Role of gap junctions in the propagation of the cardiac action potential. *Cardiovasc. Res.* 62, 309–322. doi: 10.1016/j.cardiores.2003.11.035

Sachse, F. B., Moreno, A. P., Seemann, G., and Abildskov, J. A. (2009). A model of electrical conduction in cardiac tissue including fibroblasts. *Ann. Biomed. Eng.* 37, 874–389. doi: 10.1007/s10439-009-9667-4

Sakabe, M., Fujiki, A., Nishida, K., Sugao, M., Nagasawa, H., Tsuneda, T., et al. (2004). Enalapril prevents perpetuation of atrial fibrillation by suppressing atrial fibrosis and over-expression of

connexin43 in a canine model of atrial pacing-induced left ventricular dysfunction. *J. Cardiovasc. Pharmacol.* 43, 851–859. doi: 10.1097/00005344-200406000-00015

Schott, J. J., Alshinawi, C., Kyndt, F., Probst, V., Hoorntje, T. M., Hulsbeek, M., et al. (1999). Cardiac conduction defects associate with mutations in SCN5A. *Nat. Genet.* 23, 20–21. doi: 10.1038/12618

Schubert, B., Vandongen, A. M., Kirsch, G. E., and Brown, A. M. (1990). Inhibition of cardiac Na+ currents by isoproterenol. *Am. J. Physiol.* 258, H977–H982.

Sheldon, R. S., Hill, R. J., and Duff, H. J. (1989). Antiarrhythmic drugs and the cardiac sodium channel: current models. *Clin. Chem.* 35, 748–754.

Smith, J. H., Green, C. R., Peters, N. S., Rothery, S., and Severs, N. J. (1991). Altered patterns of gap junction distribution in ischemic heart disease. An immunohistochemical study of human myocardium using laser scanning confocal microscopy. *Am. J. Pathol.* 139, 801–821.

Smith, W. T., Fleet, W. F., Johnson, T. A., Engle, C. L., and Cascio, W. E. (1995). The Ib phase of ventricular arrhythmias in ischemic *in situ* porcine heart is related to changes in cell-to-cell electrical coupling. Experimental Cardiology Group, University of North Carolina. *Circulation* 92, 3051–3060. doi: 10.1161/01.CIR.92.10.3051

Smits, J. P. P., Eckardt, L., Probst, V., Bezzina, C. R., Schott, J. J., Remme, C. A., et al. (2002). Genotype-phenotype relationship in Brugada syndrome: electrocardiographic features differentiate SCN5A-related patients from non-SCN5A-related patients. *J. Am. Coll. Cardiol.* 40, 350–356. doi: 10.1016/S0735-1097(02)01962-9

Spach, M. S. (2007). Mounting evidence that fibrosis generates a major mechanism for atrial fibrillation. *Circ. Res.* 101, 743–745. doi: 10.1161/CIRCRESAHA.107.163956

Spach, M. S., and Boineau, J. P. (1997). Microfibrosis produces electrical load variations due to loss of side-to-side cell connections: a major mechanism of structural heart disease arrhythmias. *Pacing Clin. Electrophysiol.* 20, 397–413. doi: 10.1111/j.1540-8159.1997.tb06199.x

Spach, M. S., Dolber, P. C., and Heidlage, J. F. (1988). Influence of the passive anisotropic properties on directional differences in propagation following modification of the sodium conductance in human atrial muscle. A model of reentry based on anisotropic discontinuous propagation. *Circ. Res.* 62, 811–832. doi: 10.1161/01.RES.62.4.811

Spach, M. S., Heidlage, J. F., Dolber, P. C., and Barr, R. C. (2000). Electrophysiological effects of remodeling cardiac gap junctions and cell size: experimental and model studies of normal cardiac growth. *Circ. Res.* 86, 302–311. doi: 10.1161/01.RES.86.3.302

Spach, M. S., Miller, W. T., Dolber, P. C., Kootsey, J. M., Sommer, J. R., and Mosher, C. E. (1982). The functional role of structural complexities in the propagation of depolarization in the atrium of the dog. Cardiac conduction disturbances due to discontinuities of effective axial resistivity. *Circ. Res.* 50, 175–191. doi: 10.1161/01.RES.50.2.175

Sun, H., Chartier, D., Leblanc, N., and Nattel, S. (2001). Intracellular calcium changes and tachycardia-induced contractile dysfunction in canine atrial myocytes. *Cardiovasc. Res.* 49, 751–761. doi: 10.1016/S0008-6363(00)00294-7

Tan, H. L., Bink-Boelkens, M. T., Bezzina, C. R., Viswanathan, P. C., Beaufort-Krol, G. C., Van Tintelen, P. J., et al. (2001). A sodium-channel mutation causes isolated cardiac conduction disease. *Nature* 409, 1043–1047. doi: 10.1038/35059090

Taouis, M., Sheldon, R. S., and Duff, H. J. (1991). Upregulation of the rat cardiac sodium channel by *in vivo* treatment with a class I antiarrhythmic drug. *J. Clin. Invest.* 88, 375–378. doi: 10.1172/JCI115313

Thomas, S. P., Kucera, J. P., Bircher-Lehmann, L., Rudy, Y., Saffitz, J. E., and Kléber, A. G. (2003). Impulse propagation in synthetic strands of neonatal cardiac myocytes with genetically reduced levels of connexin43. *Circ. Res.* 92, 1209–1216. doi: 10.1161/01.RES.0000074916.41221.EA

Toyofuku, T., Yabuki, M., Otsu, K., Kuzuya, T., Tada, M., and Hori, M. (1999). Functional role of c-Src in gap junctions of the cardiomyopathic heart. *Circ. Res.* 85, 672–681. doi: 10.1161/01.RES.85.8.672

Ufret-Vincenty, C. A., Baro, D. J., Lederer, W. J., Rockman, H. A, Quinones, L. E., and Santana, L. F. (2001). Role of sodium channel deglycosylation in the genesis of cardiac arrhythmias in heart failure. *J. Biol. Chem.* 276, 28197–28203. doi: 10.1074/jbc.M102548200

van der Velden, H., van der Zee, L., Wijffels, M. C., van Leuven, C., Dorland, R., Vos, M. A., et al. (2000). Atrial fibrillation in the goat induces changes in monophasic action potential and mRNA expression of ion channels involved in repolarization. *J. Cardiovasc. Electrophysiol.* 11, 1262–1269. doi: 10.1046/j.1540-8167.2000.01262.x

van der Velden, H. M., Van Kempen, M. J., Wijffels, M. C., Van Zijverden, M., Groenewegen, W. A., Allessie, M. A., et al. (1998). Altered pattern of connexin40 distribution in persistent atrial fibrillation in the goat. *J. Cardiovasc. Electrophysiol.* 9, 596–607. doi: 10.1111/j.1540-8167.1998.tb00940.x

Veenstra, R. D. (1996). Size and selectivity of gap junction channels formed from different connexins. *J. Bioenerg. Biomembr.* 28, 327–337. doi: 10.1007/BF02110109

Veenstra, R. D., Joyner, R. W., Wiedmann, R. T., Young, M. L., and Tan, R. C. (1987). Effects of hypoxia, hyperkalemia, and metabolic acidosis on canine subendocardial action potential conduction. *Circ. Res.* 60, 93–101. doi: 10.1161/01.RES.60.1.93

Veenstra, R. D., Wang, H. Z., Beyer, E. C., and Brink, P. R. (1994). Selective dye and ionic permeability of gap junction channels formed by connexin45. *Circ. Res.* 75, 483–490.

Veeraraghavan, R., Salama, M. E., and Poelzing, S. (2012). Interstitial volume modulates the conduction velocity-gap junction relationship. *Am. J. Physiol. Heart Circ. Physiol.* 302, H278–H286.

Verheule, S., Sato, T., Everett, T., Engle, S. K., Otten, D., Rubart-von der Lohe, M., et al. (2004). Increased vulnerability to atrial fibrillation in transgenic mice with selective atrial fibrosis caused by overexpression of TGF-beta1. *Circ. Res.* 94, 1458–1465. doi: 10.1161/01.RES.0000129579.59664.9d

Wagner, S., Dybkova, N., Rasenack, E. C. L., Jacobshagen, C., Fabritz, L., Kirchhof, P., et al. (2006). Ca2+/calmodulin-dependent protein kinase II regulates cardiac Na+ channels. *J. Clin. Invest.* 116, 3127–3138. doi: 10.1172/JCI26620

Wakili, R., Voigt, N., Kääb, S., Dobrev, D., and Nattel, S. (2011). Recent advances in the molecular pathophysiology of atrial fibrillation. *J. Clin. Invest.* 121, 2955–2968. doi: 10.1172/JCI46315

Wang, Q., Li, Z., Shen, J., and Keating, M. T. (1996). Genomic organization of the human SCN5A gene encoding the cardiac sodium channel. *Genomics* 34, 9–16. doi: 10.1006/geno.1996.0236

Weber, K. T., Sun, Y., Tyagi, S. C., and Cleutjens, J. P. (1994). Collagen network of the myocardium: function, structural remodeling and regulatory mechanisms. *J. Mol. Cell. Cardiol.* 26, 279–292. doi: 10.1006/jmcc.1994.1036

Weidmann, S. (1970). Electrical constants of trabecular muscle from mammalian heart. *J. Physiol.* 210, 1041–1054.

Wiegerinck, R. F., Verkerk, A. O., Belterman, C. N., Van Veen, T. A. B., Baartscheer, A., Opthof, T., et al. (2006). Larger cell size in rabbits with heart failure increases myocardial conduction velocity and QRS duration. *Circulation* 113, 806–813. doi: 10.1161/CIRCULATIONAHA.105.565804

Wiener, N., and Rosenblueth, A. (1946). The mathematical formulation of the problem of conduction of impulses in a network of connected excitable elements, specifically in cardiac muscle. *Arch. Instit. Cardiol. Méx.* 16, 205–265.

Wingo, T. L., Shah, V. N., Anderson, M. E., Lybrand, T. P., Chazin, W. J., and Balser, J. R. (2004). An EF-hand in the sodium channel couples intracellular calcium to cardiac excitability. *Nat. Struct. Mol. Biol.* 11, 219–225. doi: 10.1038/nsmb737

Xie, Y., Garfinkel, A., Camelliti, P., Kohl, P., Weiss, J. N., and Qu, Z. (2009). Effects of fibroblast-myocyte coupling on cardiac conduction and vulnerability to reentry: a computational study. *Heart Rhythm* 6, 1641–1649.

Yagi, T., Pu, J., Chandra, P., Hara, M., Danilo, P., Rosen, M. R., et al. (2002). Density and function of inward currents in right atrial cells from chronically fibrillating canine atria. *Cardiovasc. Res.* 54, 405–415. doi: 10.1016/S0008-6363(02)00279-1

Yamada, K. A., Rogers, J. G., Sundset, R., Steinberg, T. H., and Saffitz, J. E. (2003). Up-regulation of connexin45 in heart failure. *J. Cardiovasc. Electrophysiol.* 14, 1205–1212. doi: 10.1046/j.1540-8167.2003.03276.x

Yan, G. X., and Kléber, A. G. (1992). Changes in extracellular and intracellular pH in ischemic rabbit papillary muscle. *Circ. Res.* 71, 460–470. doi: 10.1161/01.RES.71.2.460

Yue, L., Melnyk, P., Gaspo, R., Wang, Z., and Nattel, S. (1999). Molecular mechanisms underlying ionic remodeling in a dog model of atrial fibrillation. *Circ. Res.* 84, 776–784. doi: 10.1161/01.RES.84.7.776

Zhuang, J., Yamada, K. A., Saffitz, J. E., and Kléber, A. G. (2000). Pulsatile stretch remodels cell-to-cell communication in cultured myocytes. *Circ. Res.* 87, 316–322. doi: 10.1161/01.RES.87.4.316

Zou, R., Kneller, J., Leon, L. J., and Nattel, S. (2005). Substrate size as a determinant of fibrillatory activity maintenance in a mathematical model of canine atrium. *Am. J. Physiol. Heart Circ. Physiol.* 289, H1002–H1012.

Conflict of Interest Statement: The authors declare that the research was conducted in the absence of any commercial or financial relationships that could be construed as a potential conflict of interest.

Received: 30 April 2013; accepted: 10 June 2013; published online: 28 June 2013.

*Citation: King JH, Huang CL-H and Fraser JA (2013) Determinants of myocardial conduction velocity: implications for arrhythmogenesis. Front. Physiol. **4**:154. doi: 10.3389/fphys.2013.00154*

This article was submitted to Frontiers in Cardiac Electrophysiology, a specialty of Frontiers in Physiology.

frontiers in
PHYSIOLOGY

MINI REVIEW ARTICLE
published: 25 June 2013
doi: 10.3389/fphys.2013.00150

Abnormal Ca^{2+} homeostasis, atrial arrhythmogenesis, and sinus node dysfunction in murine hearts modeling *RyR2* modification

***Yanmin Zhang*[1,2]*, *Gareth D. K. Matthews*[3], *Ming Lei*[2†] *and Christopher L.-H. Huang*[3,4†]**

[1] *Department of Paediatrics, Institute of Shaanxi Province Children's Cardiovascular Diseases, The Shaanxi Provincial People's Hospital of Xi'an Jiaotong University, Xi'an, PR of China*
[2] *Faculty of Medicine and Human Sciences, Institute of Cardiovascular Sciences, University of Manchester, Manchester, UK*
[3] *Physiological Laboratory, Faculty of Biology, University of Cambridge, Cambridge, UK*
[4] *Department of Biochemistry, University of Cambridge, Cambridge, UK*

Edited by:
Ian N. Sabir, King's College London, UK

Reviewed by:
Henggui Zhang, The University of Manchester, UK
Søren P. Olesen, University of Copenhagen, Denmark

***Correspondence:**
Yanmin Zhang, Institute of Cardiovascular Sciences, University of Manchester, CTF Building, 46 Grafton Street, Manchester M13 9NT, UK
e-mail: yanmin.zhang@manchester.ac.uk
† Joint senior authors for this paper.

Ryanodine receptor type 2 (*RyR2*) mutations are implicated in catecholaminergic polymorphic ventricular tachycardia (CPVT) thought to result from altered myocyte Ca^{2+} homeostasis reflecting inappropriate "leakiness" of RyR2-Ca^{2+} release channels arising from increases in their basal activity, alterations in their phosphorylation, or defective interactions with other molecules or ions. The latter include calstabin, calsequestrin-2, Mg^{2+}, and extraluminal or intraluminal Ca^{2+}. Recent clinical studies additionally associate *RyR2* abnormalities with atrial arrhythmias including atrial tachycardia (AT), fibrillation (AF), and standstill, and sinus node dysfunction (SND). Some *RyR2* mutations associated with CPVT in mouse models also show such arrhythmias that similarly correlate with altered Ca^{2+} homeostasis. Some examples show evidence for increased Ca^{2+}/calmodulin-dependent protein kinase II (CaMKII) phosphorylation of RyR2. A homozygotic *RyR2-P2328S* variant demonstrates potential arrhythmic substrate resulting from reduced conduction velocity (CV) in addition to delayed afterdepolarizations (DADs) and ectopic action potential (AP) firing. Finally, one model with an increased RyR2 activity in the sino-atrial node (SAN) shows decreased automaticity in the presence of Ca^{2+}-dependent decreases in $I_{Ca,L}$ and diastolic sarcoplasmic reticular (SR) Ca^{2+} depletion.

Keywords: *RyR2*, mutation, sinus node dysfunction, atrial arrhythmias, mouse models

INTRODUCTION

Catecholaminergic polymorphic ventricular tachycardia (CPVT) is one of the most malignant cardiac channelopathies. It is characterized by episodic, life-threatening, arrhythmias provoked by stress and emotion in individuals with otherwise structurally normal hearts (Swan et al., 1999; Priori et al., 2001; Priori and Chen, 2011). Two genes have been implicated in CPVT. One, transmitted as an autosomal dominant trait, is caused by mutations in the ryanodine receptor type 2 (*RyR2*) gene (Laitinen et al., 2001; Priori et al., 2001). It accounts for 50–55% of the CPVT cases attributable to genetic abnormalities (Priori et al., 2002). The other, less common, recessive variant results from mutations in the cardiac-specific isoform of calsequestrin type 2 gene (*CASQ2*) (Lahat et al., 2001). There are currently more than 150 known pathological allelic variants involving *RyR2* that are associated with CPVT (Priori and Chen, 2011). Ventricular arrhythmia has been attributed in such cases to altered myocyte Ca^{2+} homeostasis. This results in an inappropriate "leakiness" of RyR2-Ca^{2+} release channels owing to increases in their basal activity, altered phosphorylation status or defective interactions with other molecules or ions, including calstabin (FKBP12.6) (Lehnart et al., 2004b), CASQ2, or Mg^{2+}, or abnormal activation by extra- or intraluminal Ca^{2+} (Wehrens et al., 2004). This in turn results in spontaneous Ca^{2+} waves of Ca^{2+}-induced Ca^{2+} release (CICR) in turn producing the delayed afterdepolarisation (DADs) thought to be the major cause of RyR2-associated CPVT (George et al., 2007; Mohamed et al., 2007; Priori and Chen, 2011). Seven *RyR2* mutations are additionally associated with atrial arrhythmic disorders that include atrial tachycardia (AT), fibrillation (AF), and standstill as well as sinus node dysfunction (SND) (Laitinen et al., 2001; Bhuiyan et al., 2007; Sumitomo et al., 2007; Beery et al., 2009; Marjamaa et al., 2009; Kazemian et al., 2011). RyR mutations can thus affect function in cardiac regions including sino-atrial node (SAN), atria, and atrioventricular (AV) node in addition to ventricular myocardium. This review surveys atrial arrhythmias and SNDs related to *RyR2* mutations as revealed by investigations in genetically modified murine cardiac models.

FEATURES OF Ca^{2+} HOMEOSTASIS IN SINO-ATRIAL AND ATRIAL CELLS HAVE IMPLICATIONS FOR RHYTHM ABNORMALITIES

Atrial myocytes show differences from ventricular cells in their Ca^{2+} homeostasis in some important respects, with implications

for the physiological consequences of alterations in their RyR2 function. Thus, atrial myocytes of small mammals lack extensive T-tubules (Mackenzie et al., 2001, 2004; Brette and Orchard, 2003). These are replaced by prominent, transversely-orientated, sarcoplasmic reticular (SR), Z-tubular, elements. Junctional RyR2–L-type Ca^{2+} channel (LTCC) clusters are confined to the cell peripheries in contrast to their dense distribution throughout the more extensive ventricular tubular system (Mackenzie et al., 2001). However, an abundant corbular SR contains non-junctional RyR2s (Jorgensen et al., 1993). Atrial activation is thus likely initiated by CICR following voltage-sensitive extracellular Ca^{2+} entry at the peripheral T-SR junctional elements. This initiates a centripetal propagation of this CICR process thereby increasing open probabilities in the corbular RyR2-Ca^{2+} release channels in the cell interior (Bootman et al., 2001; Mackenzie et al., 2001, 2004; Blatter et al., 2003; Sheehan and Blatter, 2003).

The detailed mechanisms leading to AF are poorly understood. Nevertheless, increasing evidence implicates alterations in intracellular Ca^{2+} signaling in its associated focal firing, substrate evolution and remodeling processes (Hove-Madsen et al., 2004; Vest et al., 2005; Dobrev and Nattel, 2008; Liang et al., 2008; Qi et al., 2008; Chelu et al., 2009; Dobrev, 2010). Acute atrial arrhythmogenesis in intact hearts in turn is related to diastolic Ca^{2+} events in atrial myocytes. These depend upon finite SR Ca^{2+} stores and diastolic CICR processes both of which ultimately depend upon extracellular Ca^{2+} entry. Thus, ectopic activity results from afterdepolarisation and triggered activity, whether arising from increased action potential duration (APD) resulting in early afterdepolarisation (EAD) or SR Ca^{2+} release resulting in DAD phenomena, and may trigger re-entrant activity or drive atrial rhythm at rapid rate resulting in fibrillatory conduction. However, reentry requires a vulnerable substrate, likely determined by the balance of conduction velocity (CV) and refractory period (Comtois et al., 2005; Dobrev and Nattel, 2008; Nattel et al., 2008).

Atrial myocytes from chronic AF patients similarly show increased frequencies of pro-arrhythmic spontaneous Ca^{2+} release events (Hove-Madsen et al., 2004; Vest et al., 2005). These took place despite reduced L-type voltage-dependent Ca^{2+} currents (Bosch et al., 1999; Van Wagoner et al., 1999; Workman et al., 2001; Christ et al., 2004) and have accordingly been attributed to increased RyR2-mediated Ca^{2+} release activity (De Bakker et al., 2002; Vest et al., 2005). Thus, RyR2-single-channel open probabilities were increased in canine hearts with persistent AF. AF is also associated with increased protein kinase A (PKA)-mediated RyR2 phosphorylation at S2808 and decreased calstabin binding to RyR2 (Vest et al., 2005). Such changes would be expected to cause a failure of RyR2 channel closure resulting in a potentially arrhythmogenic Ca^{2+} leak from the SR (Wehrens et al., 2004; Balasubramaniam et al., 2005; Chelu and Wehrens, 2007). However, the extent to which such a mechanism might be directly applicable to AF remains under discussion (Venetucci et al., 2007; Eckstein et al., 2008).

These general principles are likely to be applicable to atria in murine hearts, which have previously also provided useful models for studies of ventricular arrhythmic phenomena. Introduction of caffeine transiently induced diastolic Ca^{2+} waves in regularly stimulated atrial myocytes. This could result either from RyR2 sensitization to cytosolic Ca^{2+} or increased intracellular cAMP levels resulting from phosphodiesterase inhibition (Daly, 2007). However, this effect was inhibited by prior inhibition of either Ca^{2+}-ATPase activity by cyclopiazonic acid or of extracellular Ca^{2+} entry by nifedipine. These latter findings in turn directly correlated with the induction of atrial arrhythmic tendency or its inhibition by the same agents in intact hearts (Zhang et al., 2009, 2011).

Possible roles for RyR2-Ca^{2+} release channels in normal SAN pacemaker activity remain under discussion (Mangoni and Nargeot, 2008; Lakatta and Difrancesco, 2009). The SAN contains both RyR2 and RyR3 as well as SR Ca^{2+} stores (Masumiya et al., 2003). Release of intracellularly stored Ca^{2+} tends to activate depolarizing inward Na^+/Ca^{2+} exchange current (Rubenstein and Lipsius, 1989; Ju and Allen, 1998; Terrar and Rigg, 2000; Bogdanov et al., 2001; Lakatta et al., 2010). Should this occur at the end of diastolic depolarization it could potentially facilitate action potential (AP) firing. Such findings have given rise to suggestions for a "Ca^{2+} clock" (Bogdanov et al., 2001; Vinogradova et al., 2004). Certainly, SAN cells show high basal levels of cAMP that could increase PKA-dependent RyR2 phosphorylation modulating its release of Ca^{2+} and thereby potentially influencing SAN pacemaker function (Vinogradova et al., 2006). Ryanodine-mediated RyR2 block indeed reduces SAN beating frequency (Rubenstein and Lipsius, 1989; Ju and Allen, 1998; Bogdanov et al., 2001). However, others have suggested that such SR Ca^{2+} release is not a predominant factor in normal SAN pacemaker activity (Honjo et al., 2003; Mangoni and Nargeot, 2008; Lakatta and Difrancesco, 2009; Himeno et al., 2011).

RyR2 MUTATIONS ARE ASSOCIATED WITH CLINICAL ATRIAL ARRHYTHMIC AND SND PHENOTYPES

A number of *RyR2* mutations associated with CPVT are also associated with atrial arrhythmias and SND (**Table 1**). However, there have been no reported cases of lone AF or SAN dysfunction in the absence of CPVT. Large deletions encompassing exon 3 in RyR2 NH_2-terminal regions are relatively frequent. This may reflecting their containing *Alu* repeats predisposing to deletions resulting from large *Alu* repeat–mediated genomic rearrangements resulting from polymerase slippage (Gu et al., 2008). *Alu* sequences occur in intron 2, 190 bp upstream from exon 3 and also 536 bp downstream in intron 3. They are related to the 1.1 kb deletion containing part of intron 2, exon 3, and part of intron 3, with a *Alu-Alu* recombination in which exon 2 is recombined with exon 4 and exon 3 is completely deleted (Bhuiyan et al., 2007; Marjamaa et al., 2009; Medeiros-Domingo et al., 2009). However, crystal structure studies revealed that exon 3 deletion causes a structural rescue whereby a flexible loop inserts itself into the β trefoil domain. This increases the thermal stability of the RyR2 channel. As a result the mutation is neither lethal nor confers loss of function (Lobo et al., 2011). In the HEK293 expression system, it results in a marked reduction in the luminal Ca^{2+} threshold at which Ca^{2+} release terminates thereby increasing fractional Ca^{2+} release (Tang et al., 2012). The RyR2 NH_2-terminal region may thus be an important determinant for termination of Ca^{2+} release, abnormalities in which are common

Table 1 | Summary of RyR2 mutations associated with atrial and/or sinoatrial node dysfunction.

Nucleotide	Amino acid change	Mutation	Location	Exon	Phenotype	References
1.1 kb deletion	Exon 3 deletion	Deletion	Amino terminal domain	3	CPVT, SND, AV nodal block, AF, and atrial standstill, DCM	Bhuiyan et al., 2007; Marjamaa et al., 2009; Medeiros-Domingo et al., 2009
C6982T	P2328S	Missense	FKBP binding domain	46	CPVT, AT, Normal heart structure	Laitinen et al., 2001
-No information	G3946A	Missense	Cytosol	88	CPVT, AT, AF, Normal heart structure	Pizzale et al., 2008
T12056G	M4109R	Missense	Domain II	90	CPVT, AF, transient QT prolongation during AF, and postpacing, Normal heart structure	Nof et al., 2011
A12457C	S4153R	Missense	Domain II	90	CPVT, AF, Normal heart structure	Kazemian et al., 2011
-No information	W4645R	Missense	Transmembrane domain	96	CPVT, AF, Normal heart structure	Beery et al., 2009
-No information	A7420G	Missense	C-Terminal domain	105	CPVT, AF, Normal heart structure	Sumitomo et al., 2007

in RyR2-associated cardiomyopathies (Gu et al., 2008; Tang et al., 2012).

A large exon 3 *deletion* has been reported in a number of unrelated families. It has been associated with a broad range of atrial, ventricular and SND phenotypes. Thus, several unrelated families showed a large deletion encompassing part of intron 2, exon 3, and part of intron 3, expected to result in an in-frame deletion of 35 amino acids (p.Asn57-Gly91) (NM-001035) (Bhuiyan et al., 2007; Marjamaa et al., 2009; Medeiros-Domingo et al., 2009). This deletion was associated with a spectrum of phenotypes including SND, AF, atrioventricular block (AVB), decreased left ventricular function, increased trabeculation, CPVT, and dilated cardiomyopathy (DCM). Two further families showing CPVT with large deletions in the region did not show the association with DCM (Marjamaa et al., 2009). Mutation carriers in one of these families showed CPVT, AF, sinus bradycardia, and AV conduction abnormalities without structural cardiovascular abnormalities. Patients from the other family showed increased left ventricular trabeculation suggestive of non-compaction cardiomyopathy (Marjamaa et al., 2009). An additional report of a large large 3.6 Kb exon 3 deletion was not accompanied by a description of the corresponding patient phenotype (Medeiros-Domingo et al., 2009).

Some single CPVT-associated *RyR2* mutations are also associated with atrial arrhythmias. Two such families, including one with *RyR-P2328S*, contained 14 CPVT patients (Swan et al., 1999; Laitinen et al., 2001). All carriers showed polymorphic ventricular tachycardia (PVT) and/or ventricular fibrillation (VF) of which three patients also showed non-sustained AT. Three further case reports described a further three *RyR2* mutations all of which showed AT and/or AF in addition to CPVT without abnormalities in cardiac structure (Sumitomo et al., 2007; Pizzale et al., 2008; Kazemian et al., 2011). Thus, a patient with the *RyR2-G3946A* variant who had an implantable cardioverter defibrillator (ICD) for CPVT showed AT/AF both during exercise and on ambulatory electrocardiographic (ECG) recording (Pizzale et al., 2008). The *RyR2-S4153R* variant was identified in a women presenting with a cardiac arrest due to VF; she showed AF on 12-lead ECG immediately following emergency defibrillation. Over a 12 month follow-up period, in addition to experiencing three ICD shocks related to appropriately detected PVTs, she showed several exercise-induced self-terminating episodes of AF with rapid ventricular responses (Kazemian et al., 2011). Finally, a *RyR2-A7420G* variant was identified in a patient with both clinical and induced AF as well as frequent episodes of paroxysmal AF during walking or with mental stress despite normal sinus node recovery times (SNRT) and cardiac structure (Sumitomo et al., 2007).

In a further clinical situation, a preceding rapid AF could initiate CPVT, after a marked transient QT prolongation following a long RR interval that in turn followed a sequence of short R-R beats. This was associated with two heterozygous nucleotide substitutions, *RyR2-M4109R* and *RyR2-I406T*. All the *RyR2-M4109R* but none of the *RyR2-I606T* carriers showed prominent postpacing QT prolongation during electrophysiological study, although both showed normal QT intervals during regular rhythm (Nof et al., 2011). Finally, VT and AT could be induced by isoproterenol infusion, an effect blocked by propranolol administration, in a mother and son both having a *RyR2-W4645R* mutation and clinical diagnoses of PVT and AT in an absence of detectable significant underlying cardiac disease (Beery et al., 2009).

ATRIAL ARRHYTHMIC AND Ca^{2+} HOMEOSTATIC ABNORMALITIES IN MOUSE MODELS HARBORING RyR2 MUTATIONS

Increased diastolic Ca^{2+} release has been implicated in generation of ventricular arrhythmias in genetically modified mouse models harboring CPVT-related *RyR2* mutations (Cerrone et al., 2005; Kannankeril et al., 2006; Goddard et al., 2008; Lehnart et al., 2008; Suetomi et al., 2011). Recently, a few mouse models have similarly shown atrial arrhythmias and SND and similarly demonstrated evidence for diastolic SR Ca^{2+} release through "leaky" RyR2s

(Chelu et al., 2009; Suetomi et al., 2011; Zhang et al., 2011; Neco et al., 2012; Shan et al., 2012).

RyR2-R176Q/+ mice (Kannankeril et al., 2006) did not show spontaneous AF but nevertheless showed increased vulnerabilities to AF during rapid atrial pacing when compared to wild-type (WT). This was associated with increased Ca^{2+}/calmodulin-dependent protein kinase II (CaMKII) phosphorylation of RyR2. Conversely, pharmacological inhibition of CaMKII prevented this AF inducibility. So did genetic inhibition of CaMKII-mediated RyR2 phosphorylation in *RyR2-S2814A* mice studied in a vagotonic AF model. Atrial biopsies from mice with atrial enlargement and spontaneous AF, goats with lone AF, and patients with chronic AF similarly showed increased CaMKII phosphorylation of RyR2. These findings implicate a RyR2-dependent Ca^{2+} release resulting from increased CaMKII activity in susceptibility to AF (Chelu et al., 2009).

The *RyR2-P2328S* mutation has been clinically related to atrial in addition to ventricular arrhythmic phenotypes (Swan et al., 1999; Laitinen et al., 2001). Heterozygotic and homozygotic *RyR2-P2328S* mouse atria both showed acute arrhythmogenic properties in the absence of structural abnormalities with a severity related to gene dose, consistent with previous results in expression systems (Lehnart et al., 2004a). Intact anaesthetized hetero- or homozygotic *RyR2-P2328S* showed normal electrocardiographic parameters both before and after isoproterenol addition apart from increased heart rates. Nevertheless, bipolar electrogram and monophasic AP recordings from either regular or programmed stimulation demonstrated higher atrial arrhythmogenic incidences in isolated perfused homozygotic but not heterozygotic *RyR2-P2328S* relative to WT. Isoproterenol increased these incidences in all three groups despite unchanged AP durations at 90% recovery (APD_{90}) and atrial effective refractory periods (AERP) (**Figure 1A**). These findings correlated with occurrences of diastolic Ca^{2+} release phenomena in regularly stimulated, isolated, fluo-3-loaded $RyR2^{S/S}$, but not $RyR2^{+/S}$ or WT, atrial myocytes, whose frequency was increased by isoproterenol (**Figure 1B**) (Zhang et al., 2011). Finally, microelectrode recordings in isolated perfused homozygotic *RyR2-P2328S* atria showed DADs and ectopic APs not found in WT that could potentially result from such Ca^{2+} release phenomena (King et al., 2013). These also further implicated atrial arrhythmic substrate resulting from reduced CV in agreement with similar results bearing on ventricular conduction (Zhang et al., 2013). This was reflected in their increased interatrial conduction delays, reduced

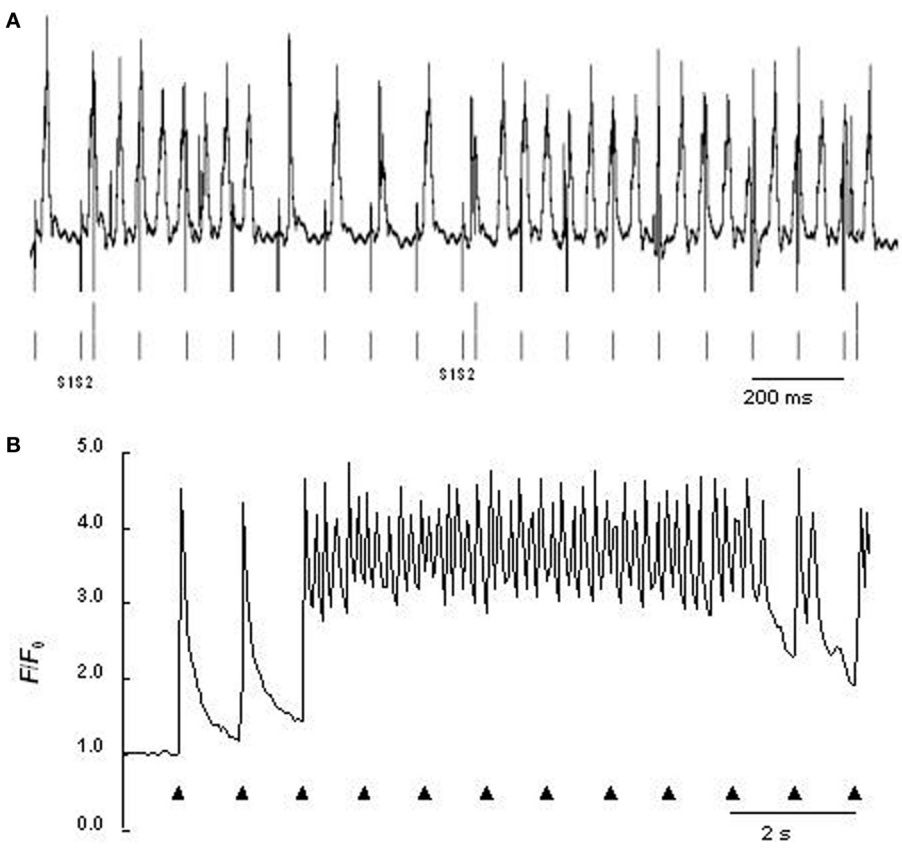

FIGURE 1 | (A) Atrial monophasic action potential recording of arrhythmic events provoked by programmed electrical stimulation involving extrasystolic S2 stimulation (long vertical bars beneath trace) following series of pacing S1 stimuli (short vertical bars beneath trace) from isolated perfused homozygotic *RyR2-P2328S* heart. **(B)** Ca^{2+} transients from regularly stimulated fluo-3-loaded *RyR2-P2328S* atrial myocytes under confocal microscopy, both following introduction of isoproterenol [From Figures 5D, 6F of Zhang et al. (2011)].

epicardial CVs and reduced maximum rates of AP depolarization [$(dV/dt)_{max}$], despite similar effective refractory periods, AP durations and AP amplitudes.

Finally, AF could be induced by an intra-esophageal burst pacing protocol in mice harboring the *RyR2-R2474S+/−*, *RyR2-N2386I+/−*, and *RyR2-L433P+/−* mutations known to be associated with human CPVT. Their isolated atrial myocytes showed significant diastolic SR Ca^{2+} leaks. Atrial RyR2s from *RyR2-R2474S+/−* mice were oxidized and their RyR2 complexes depleted of the calstabin2 unit known to stabilize the RyR2 closed state. The Rycal agent S107, known to stabilize RyR2-calstabin2 interactions and inhibit the oxidation/phosphorylation-induced dissociation of calstabin2 from the channel, rescued the resulting increase in Ca^{2+} release, and prevented burst pacing–induced AF *in vivo*. It did not do so in calstabin2-deficient mice, implicating calstabin2 in these arrhythmic properties (Shan et al., 2012).

PARADOXICAL SINUS NODE DISORDER IN MOUSE MODELS HARBORING RyR2 MUTATIONS

In contrast to experimental evidence implicating a Ca^{2+} clock involving RyR2 in pacemaker activity (see section on Features of Ca^{2+} homeostasis in sino-atrial and atrial cells have implications for rhythm abnormalities), CPVT is associated with high incidences of SAN dysrhythmia in the form of *reduced* SAN automaticity resulting in basal bradycardia, sinus pauses, and impaired chronotropic responses to β-adrenergic stimulation (Leenhardt et al., 1995; Sumitomo et al., 2003; Postma et al., 2005; Katz et al., 2009). Although they do not show a basal bradycardia, *RyR2-R4496C* mice studied using *in vivo* telemetric recordings similarly showed sinus pauses overcome by atrial and junctional escapes triggered by catecholamines, and impaired SAN automaticity following isoproterenol injection. These features paralleled post-exercise findings in CPVT patients (Neco et al., 2012). Measurements of spontaneous $[Ca^{2+}]_i$ transients reflecting pacemaker activity in SAN cells by confocal microscopy correspondingly demonstrated slower pacemaker activity and impaired chronotropic responses to β-adrenergic stimulation, and sinus pauses in 75% of the cases. These changes were associated with 50% reductions in L-type Ca^{2+} current ($I_{Ca,\,L}$) density in whole-cell patch-clamped *RyR2-R4496C* SAN cells. Isoproterenol dramatically increased the frequency of Ca^{2+} sparks and Ca^{2+} waves by ∼5 and ∼10-fold (Neco et al., 2012).

CONCLUSION

Enhanced RyR2 activity associated with *RyR2* mutations can be associated with atrial arrhythmic tendency and SND. This is potentially attributable to increased RyR2-mediated release of intracellularly stored, SR, Ca^{2+} release and altered interactions with CaMKII and calstabin2. Increased RyR2 activity in the SAN leads to an unanticipated decrease in its automaticity accompanied by a Ca^{2+}-dependent decrease of $I_{Ca,\,L}$ and diastolic SR Ca^{2+} depletion.

FUNDING SOURCE

This work was supported by the Medical Research Council, Wellcome Trust, British Heart Foundation, the Biotechnology and Biological Sciences Research Council, and Natural Science Foundation of China (30371571, 30830051, and 30672209).

REFERENCES

Balasubramaniam, R., Chawla, S., Grace, A. A., and Huang, C. L. (2005). Caffeine-induced arrhythmias in murine hearts parallel changes in cellular Ca2+ homeostasis. *Am. J. Physiol. Heart Circ. Physiol.* 289, H1584–H1593. doi: 10.1152/ajpheart.01250.2004

Beery, T. A., Shah, M. J., and Benson, D. W. (2009). Genetic characterization of familial CPVT after 30 years. *Biol. Res. Nurs.* 11, 66–72. doi: 10.1177/1099800409333369

Bhuiyan, Z. A., Van Den Berg, M. P., Van Tintelen, J. P., Bink-Boelkens, M. T., Wiesfeld, A. C., Alders, M., et al. (2007). Expanding spectrum of human RYR2-related disease: new electrocardiographic, structural, and genetic features. *Circulation* 116, 1569–1576. doi: 10.1161/CIRCULATIONAHA.107.711606

Blatter, L. A., Kockskamper, J., Sheehan, K. A., Zima, A. V., Huser, J., and Lipsius, S. L. (2003). Local calcium gradients during excitation-contraction coupling and alternans in atrial myocytes. *J. Physiol.* 546, 19–31. doi: 10.1113/jphysiol.2002.025239

Bogdanov, K. Y., Vinogradova, T. M., and Lakatta, E. G. (2001). Sinoatrial nodal cell ryanodine receptor and Na+-Ca2+ exchanger: molecular partners in pacemaker regulation. *Circ. Res.* 88, 1254–1258. doi: 10.1161/hh1201.092095

Bootman, M. D., Collins, T. J., Peppiatt, C. M., Prothero, L. S., Mackenzie, L., De Smet, P., et al. (2001). Calcium signalling–an overview. *Semin. Cell Dev. Biol.* 12, 3–10. doi: 10.1006/scdb.2000.0211

Bosch, R. F., Zeng, X., Grammer, J. B., Popovic, K., Mewis, C., and Kuhlkamp, V. (1999). Ionic mechanisms of electrical remodeling in human atrial fibrillation. *Cardiovasc. Res.* 44, 121–131. doi: 10.1016/S0008-6363(99)00178-9

Brette, F., and Orchard, C. (2003). T-tubule function in mammalian cardiac myocytes. *Circ. Res.* 92, 1182–1192. doi: 10.1161/01.RES.0000074908.17214.FD

Cerrone, M., Colombi, B., Santoro, M., Di Barletta, M. R., Scelsi, M., Villani, L., et al. (2005). Bidirectional ventricular tachycardia and fibrillation elicited in a knock-in mouse model carrier of a mutation in the cardiac ryanodine receptor. *Circ. Res.* 96, e77–e82. doi: 10.1161/01.RES.0000169067.51055.72

Chelu, M. G., Sarma, S., Sood, S., Wang, S., Van Oort, R. J., Skapura, D. G., et al. (2009). Calmodulin kinase II-mediated sarcoplasmic reticulum Ca2+ leak promotes atrial fibrillation in mice. *J. Clin. Invest.* 119, 1940–1951.

Chelu, M. G., and Wehrens, X. H. (2007). Sarcoplasmic reticulum calcium leak and cardiac arrhythmias. *Biochem. Soc. Trans.* 35, 952–956. doi: 10.1042/BST0350952

Christ, T., Boknik, P., Wohrl, S., Wettwer, E., Graf, E. M., Bosch, R. F., et al. (2004). L-type Ca2+ current downregulation in chronic human atrial fibrillation is associated with increased activity of protein phosphatases. *Circulation* 110, 2651–2657. doi: 10.1161/01.CIR.0000145659.80212.6A

Comtois, P., Kneller, J., and Nattel, S. (2005). Of circles and spirals: bridging the gap between the leading circle and spiral wave concepts of cardiac reentry. *Europace* 7(Suppl. 2), 10–20. doi: 10.1016/j.eupc.2005.05.011

Daly, J. W. (2007). Caffeine analogs: biomedical impact. *Cell. Mol. Life Sci.* 64, 2153–2169. doi: 10.1007/s00018-007-7051-9

De Bakker, J. M., Ho, S. Y., and Hocini, M. (2002). Basic and clinical electrophysiology of pulmonary vein ectopy. *Cardiovasc. Res.* 54, 287–294. doi: 10.1016/S0008-6363(01)00532-6

Dobrev, D. (2010). Atrial Ca2+ signaling in atrial fibrillation as an antiarrhythmic drug target. *Naunyn Schmiedebergs Arch. Pharmacol.* 381, 195–206. doi: 10.1007/s00210-009-0457-1

Dobrev, D., and Nattel, S. (2008). Calcium handling abnormalities in atrial fibrillation as a target for innovative therapeutics. *J. Cardiovasc. Pharmacol.* 52, 293–299. doi: 10.1097/FJC.0b013e318171924d

Eckstein, J., Verheule, S., De Groot, N. M., Allessie, M., and Schotten, U. (2008). Mechanisms of perpetuation of atrial fibrillation in chronically dilated atria. *Prog. Biophys. Mol. Biol.* 97, 435–451. doi: 10.1016/j.pbiomolbio.2008.02.019

George, C. H., Jundi, H., Thomas, N. L., Fry, D. L., and Lai, F. A. (2007). Ryanodine receptors and ventricular arrhythmias: emerging trends in mutations,

mechanisms and therapies. *J. Mol. Cell. Cardiol.* 42, 34–50. doi: 10.1016/j.yjmcc.2006.08.115

Goddard, C. A., Ghais, N. S., Zhang, Y., Williams, A. J., Colledge, W. H., Grace, A. A., et al. (2008). Physiological consequences of the P2328S mutation in the ryanodine receptor (RyR2) gene in genetically modified murine hearts. *Acta Physiol. (Oxf.)* 194, 123–140. doi: 10.1111/j.1748-1716.2008.01865.x

Gu, W., Zhang, F., and Lupski, J. R. (2008). Mechanisms for human genomic rearrangements. *Pathogenetics* 1, 4. doi: 10.1186/1755-8417-1-4

Himeno, Y., Toyoda, F., Satoh, H., Amano, A., Cha, C. Y., Matsuura, H., et al. (2011). Minor contribution of cytosolic Ca2+ transients to the pacemaker rhythm in guinea pig sinoatrial node cells. *Am. J. Physiol. Heart Circ. Physiol.* 300, H251–H261. doi: 10.1152/ajpheart.00764.2010

Honjo, H., Inada, S., Lancaster, M. K., Yamamoto, M., Niwa, R., Jones, S. A., et al. (2003). Sarcoplasmic reticulum Ca2+ release is not a dominating factor in sinoatrial node pacemaker activity. *Circ. Res.* 92, e41–e44. doi: 10.1161/01.RES.0000055904.21974.BE

Hove-Madsen, L., Llach, A., Bayes-Genis, A., Roura, S., Rodriguez Font, E., Aris, A., et al. (2004). Atrial fibrillation is associated with increased spontaneous calcium release from the sarcoplasmic reticulum in human atrial myocytes. *Circulation* 110, 1358–1363. doi: 10.1161/01.CIR.0000141296.59876.87

Jorgensen, A. O., Shen, A. C., Arnold, W., McPherson, P. S., and Campbell, K. P. (1993). The Ca2+-release channel/ryanodine receptor is localized in junctional and corbular sarcoplasmic reticulum in cardiac muscle. *J. Cell. Biol.* 120, 969–980. doi: 10.1083/jcb.120.4.969

Ju, Y. K., and Allen, D. G. (1998). Intracellular calcium and Na+-Ca2+ exchange current in isolated toad pacemaker cells. *J. Physiol.* 508, 153–166. doi: 10.1111/j.1469-7793.1998.153br.x

Kannankeril, P. J., Mitchell, B. M., Goonasekera, S. A., Chelu, M. G., Zhang, W., Sood, S., et al. (2006). Mice with the R176Q cardiac ryanodine receptor mutation exhibit catecholamine-induced ventricular tachycardia and cardiomyopathy. *Proc. Natl. Acad. Sci. U.S.A.* 103, 12179–12184. doi: 10.1073/pnas.0600268103

Katz, G., Arad, M., and Eldar, M. (2009). Catecholaminergic polymorphic ventricular tachycardia from bedside to bench and beyond. *Curr. Probl. Cardiol.* 34, 9–43. doi: 10.1016/j.cpcardiol.2008.09.002

Kazemian, P., Gollob, M. H., Pantano, A., and Oudit, G. Y. (2011). A novel mutation in the RYR2 gene leading to catecholaminergic polymorphic ventricular tachycardia and paroxysmal atrial fibrillation: dose-dependent arrhythmia-event suppression by beta-blocker therapy. *Can. J. Cardiol.* 27, 870.e7–870.e10. doi: 10.1016/j.cjca.2011.02.003

King, J. H., Zhang, Y., Lei, M., Grace, A. A., Huang, C. L., and Fraser, J. A. (2013). Atrial arrhythmia, triggering events and conduction abnormalities in isolated murine RyR2-P2328S hearts. *Acta Physiol. (Oxf.).* 207, 308–323. doi: 10.1111/apha.12006

Lahat, H., Pras, E., Olender, T., Avidan, N., Ben-Asher, E., Man, O., et al. (2001). A missense mutation in a highly conserved region of CASQ2 is associated with autosomal recessive catecholamine-induced polymorphic ventricular tachycardia in Bedouin families from Israel. *Am. J. Hum. Genet.* 69, 1378–1384. doi: 10.1086/324565

Laitinen, P. J., Brown, K. M., Piippo, K., Swan, H., Devaney, J. M., Brahmbhatt, B., et al. (2001). Mutations of the cardiac ryanodine receptor (RyR2) gene in familial polymorphic ventricular tachycardia. *Circulation* 103, 485–490. doi: 10.1161/01.CIR.103.4.485

Lakatta, E. G., and Difrancesco, D. (2009). What keeps us ticking: a funny current, a calcium clock, or both. *J. Mol. Cell. Cardiol.* 47, 157–170. doi: 10.1016/j.yjmcc.2009.03.022

Lakatta, E. G., Maltsev, V. A., and Vinogradova, T. M. (2010). A coupled SYSTEM of intracellular Ca2+ clocks and surface membrane voltage clocks controls the timekeeping mechanism of the heart's pacemaker. *Circ. Res.* 106, 659–673. doi: 10.1161/CIRCRESAHA.109.206078

Leenhardt, A., Lucet, V., Denjoy, I., Grau, F., Ngoc, D. D., and Coumel, P. (1995). Catecholaminergic polymorphic ventricular tachycardia in children. a 7-year follow-up of 21 patients. *Circulation* 91, 1512–1519. doi: 10.1161/01.CIR.91.5.1512

Lehnart, S. E., Mongillo, M., Bellinger, A., Lindegger, N., Chen, B. X., Hsueh, W., et al. (2008). Leaky Ca2+ release channel/ryanodine receptor 2 causes seizures and sudden cardiac death in mice. *J. Clin. Invest.* 118, 2230–2245. doi: 10.1172/JCI35346

Lehnart, S. E., Wehrens, X. H., Laitinen, P. J., Reiken, S. R., Deng, S. X., Cheng, Z., et al. (2004a). Sudden death in familial polymorphic ventricular tachycardia associated with calcium release channel (ryanodine receptor) leak. *Circulation* 109, 3208–3214. doi: 10.1161/01.CIR.0000132472.98675.EC

Lehnart, S. E., Wehrens, X. H., and Marks, A. R. (2004b). Calstabin deficiency, ryanodine receptors, and sudden cardiac death. *Biochem. Biophys. Res. Commun.* 322, 1267–1279. doi: 10.1016/j.bbrc.2004.08.032

Liang, X., Xie, H., Zhu, P. H., Hu, J., Zhao, Q., Wang, C. S., et al. (2008). Ryanodine receptor-mediated Ca2+ events in atrial myocytes of patients with atrial fibrillation. *Cardiology* 111, 102–110. doi: 10.1159/000119697

Lobo, P. A., Kimlicka, L., Tung, C. C., and Van Petegem, F. (2011). The deletion of exon 3 in the cardiac ryanodine receptor is rescued by beta strand switching. *Structure* 19, 790–798. doi: 10.1016/j.str.2011.03.016

Mackenzie, L., Bootman, M. D., Berridge, M. J., and Lipp, P. (2001). Predetermined recruitment of calcium release sites underlies excitation-contraction coupling in rat atrial myocytes. *J. Physiol.* 530, 417–429. doi: 10.1111/j.1469-7793.2001.0417k.x

Mackenzie, L., Roderick, H. L., Berridge, M. J., Conway, S. J., and Bootman, M. D. (2004). The spatial pattern of atrial cardiomyocyte calcium signalling modulates contraction. *J. Cell Sci.* 117, 6327–6337. doi: 10.1242/jcs.01559

Mangoni, M. E., and Nargeot, J. (2008). Genesis and regulation of the heart automaticity. *Physiol. Rev.* 88, 919–982. doi: 10.1152/physrev.00018.2007

Marjamaa, A., Laitinen-Forsblom, P., Lahtinen, A. M., Viitasalo, M., Toivonen, L., Kontula, K., et al. (2009). Search for cardiac calcium cycling gene mutations in familial ventricular arrhythmias resembling catecholaminergic polymorphic ventricular tachycardia. *BMC Med. Genet.* 10:12. doi: 10.1186/1471-2350-10-12

Masumiya, H., Yamamoto, H., Hemberger, M., Tanaka, H., Shigenobu, K., Chen, S. R., et al. (2003). The mouse sinoatrial node expresses both the type 2 and type 3 Ca2+ release channels/ryanodine receptors. *FEBS Lett.* 553, 141–144. doi: 10.1016/S0014-5793(03)00999-2

Medeiros-Domingo, A., Bhuiyan, Z. A., Tester, D. J., Hofman, N., Bikker, H., Van Tintelen, J. P., et al. (2009). The RYR2-encoded ryanodine receptor/calcium release channel in patients diagnosed previously with either catecholaminergic polymorphic ventricular tachycardia or genotype negative, exercise-induced long QT syndrome: a comprehensive open reading frame mutational analysis. *J. Am. Coll. Cardiol.* 54, 2065–2074. doi: 10.1016/j.jacc.2009.08.022

Mohamed, U., Napolitano, C., and Priori, S. G. (2007). Molecular and electrophysiological bases of catecholaminergic polymorphic ventricular tachycardia. *J. Cardiovasc. Electrophysiol.* 18, 791–797. doi: 10.1111/j.1540-8167.2007.00766.x

Nattel, S., Burstein, B., and Dobrev, D. (2008). Atrial remodeling and atrial fibrillation: mechanisms and implications. *Circ. Arrhythm. Electrophysiol.* 1, 62–73. doi: 10.1161/CIRCEP.107.754564

Neco, P., Torrente, A. G., Mesirca, P., Zorio, E., Liu, N., Priori, S. G., et al. (2012). Paradoxical effect of increased diastolic Ca2+ release and decreased sinoatrial node activity in a mouse model of catecholaminergic polymorphic ventricular tachycardia. *Circulation* 126, 392–401. doi: 10.1161/CIRCULATIONAHA.111.075382

Nof, E., Belhassen, B., Arad, M., Bhuiyan, Z. A., Antzelevitch, C., Rosso, R., et al. (2011). Postpacing abnormal repolarization in catecholaminergic polymorphic ventricular tachycardia associated with a mutation in the cardiac ryanodine receptor gene. *Heart Rhythm* 8, 1546–1552. doi: 10.1016/j.hrthm.2011.05.016

Pizzale, S., Gollob, M. H., Gow, R., and Birnie, D. H. (2008). Sudden death in a young man with catecholaminergic polymorphic ventricular tachycardia and paroxysmal atrial fibrillation. *J. Cardiovasc. Electrophysiol.* 19, 1319–1321. doi: 10.1111/j.1540-8167.2008.01211.x

Postma, A. V., Denjoy, I., Kamblock, J., Alders, M., Lupoglazoff, J. M., Vaksmann, G., et al. (2005). Catecholaminergic polymorphic ventricular tachycardia: RYR2 mutations, bradycardia, and follow up of the patients. *J. Med. Genet.* 42, 863–870. doi: 10.1136/jmg.2004.028993

Priori, S. G., and Chen, S. R. (2011). Inherited dysfunction

of sarcoplasmic reticulum Ca2+ handling and arrhythmogenesis. *Circ. Res.* 108, 871–883. doi: 10.1161/CIRCRESAHA.110.226845

Priori, S. G., Napolitano, C., Memmi, M., Colombi, B., Drago, F., Gasparini, M., et al. (2002). Clinical and molecular characterization of patients with catecholaminergic polymorphic ventricular tachycardia. *Circulation* 106, 69–74. doi: 10.1161/01.CIR.0000020013.73106.D8

Priori, S. G., Napolitano, C., Tiso, N., Memmi, M., Vignati, G., Bloise, R., et al. (2001). Mutations in the cardiac ryanodine receptor gene (hRyR2) underlie catecholaminergic polymorphic ventricular tachycardia. *Circulation* 103, 196–200. doi: 10.1161/01.CIR.103.2.196

Qi, X. Y., Yeh, Y. H., Xiao, L., Burstein, B., Maguy, A., Chartier, D., et al. (2008). Cellular signaling underlying atrial tachycardia remodeling of L-type calcium current. *Circ. Res.* 103, 845–854. doi: 10.1161/CIRCRESAHA.108.175463

Rubenstein, D. S., and Lipsius, S. L. (1989). Mechanisms of automaticity in subsidiary pacemakers from cat right atrium. *Circ. Res.* 64, 648–657. doi: 10.1161/01.RES.64.4.648

Shan, J., Xie, W., Betzenhauser, M., Reiken, S., Chen, B. X., Wronska, A., et al. (2012). Calcium leak through ryanodine receptors leads to atrial fibrillation in 3 mouse models of catecholaminergic polymorphic ventricular tachycardia. *Circ. Res.* 111, 708–717. doi: 10.1161/CIRCRESAHA.112.273342

Sheehan, K. A., and Blatter, L. A. (2003). Regulation of junctional and non-junctional sarcoplasmic reticulum calcium release in excitation-contraction coupling in cat atrial myocytes. *J. Physiol.* 546, 119–135. doi: 10.1113/jphysiol.2002.026963

Suetomi, T., Yano, M., Uchinoumi, H., Fukuda, M., Hino, A., Ono, M., et al. (2011). Mutation-linked defective interdomain interactions within ryanodine receptor cause aberrant Ca2+release leading to catecholaminergic polymorphic ventricular tachycardia. *Circulation* 124, 682–694. doi: 10.1161/CIRCULATIONAHA.111.023259

Sumitomo, N., Harada, K., Nagashima, M., Yasuda, T., Nakamura, Y., Aragaki, Y., et al. (2003). Catecholaminergic polymorphic ventricular tachycardia: electrocardiographic characteristics and optimal therapeutic strategies to prevent sudden death. *Heart* 89, 66–70. doi: 10.1136/heart.89.1.66

Sumitomo, N., Sakurada, H., Taniguchi, K., Matsumura, M., Abe, O., Miyashita, M., et al. (2007). Association of atrial arrhythmia and sinus node dysfunction in patients with catecholaminergic polymorphic ventricular tachycardia. *Circ. J.* 71, 1606–1609. doi: 10.1253/circj.71.1606

Swan, H., Piippo, K., Viitasalo, M., Heikkila, P., Paavonen, T., Kainulainen, K., et al. (1999). Arrhythmic disorder mapped to chromosome 1q42-q43 causes malignant polymorphic ventricular tachycardia in structurally normal hearts. *J. Am. Coll. Cardiol.* 34, 2035–2042. doi: 10.1016/S0735-1097(99)00461-1

Tang, Y., Tian, X., Wang, R., Fill, M., and Chen, S. R. (2012). Abnormal termination of Ca2+ release is a common defect of RyR2 mutations associated with cardiomyopathies. *Circ. Res.* 110, 968–977. doi: 10.1161/CIRCRESAHA.111.256560

Terrar, D., and Rigg, L. (2000). What determines the initiation of the heartbeat. *J. Physiol.* 524, 316. doi: 10.1111/j.1469-7793.2000.00316.x

Van Wagoner, D. R., Pond, A. L., Lamorgese, M., Rossie, S. S., McCarthy, P. M., and Nerbonne, J. M. (1999). Atrial L-type Ca2+ currents and human atrial fibrillation. *Circ. Res.* 85, 428–436. doi: 10.1161/01.RES.85.5.428

Venetucci, L. A., Trafford, A. W., and Eisner, D. A. (2007). Increasing ryanodine receptor open probability alone does not produce arrhythmogenic calcium waves: threshold sarcoplasmic reticulum calcium content is required. *Circ. Res.* 100, 105–111. doi: 10.1161/01.RES.0000252828.17939.00

Vest, J. A., Wehrens, X. H., Reiken, S. R., Lehnart, S. E., Dobrev, D., Chandra, P., et al. (2005). Defective cardiac ryanodine receptor regulation during atrial fibrillation. *Circulation* 111, 2025–2032. doi: 10.1161/01.CIR.0000162461.67140.4C

Vinogradova, T. M., Lyashkov, A. E., Zhu, W., Ruknudin, A. M., Sirenko, S., Yang, D., et al. (2006). High basal protein kinase A-dependent phosphorylation drives rhythmic internal Ca2+ store oscillations and spontaneous beating of cardiac pacemaker cells. *Circ. Res.* 98, 505–514. doi: 10.1161/01.RES.0000204575.94040.d1

Vinogradova, T. M., Zhou, Y. Y., Maltsev, V., Lyashkov, A., Stern, M., and Lakatta, E. G. (2004). Rhythmic ryanodine receptor Ca2+ releases during diastolic depolarization of sinoatrial pacemaker cells do not require membrane depolarization. *Circ. Res.* 94, 802–809. doi: 10.1161/01.RES.0000122045.55331.0F

Wehrens, X. H., Lehnart, S. E., Reiken, S. R., Deng, S. X., Vest, J. A., Cervantes, D., et al. (2004). Protection from cardiac arrhythmia through ryanodine receptor-stabilizing protein calstabin2. *Science* 304, 292–296. doi: 10.1126/science.1094301

Workman, A. J., Kane, K. A., and Rankin, A. C. (2001). The contribution of ionic currents to changes in refractoriness of human atrial myocytes associated with chronic atrial fibrillation. *Cardiovasc. Res.* 52, 226–235. doi: 10.1016/S0008-6363(01)00380-7

Zhang, Y., Fraser, J. A., Jeevaratnam, K., Hao, X., Hothi, S. S., Grace, A. A., et al. (2011). Acute atrial arrhythmogenicity and altered Ca2+ homeostasis in murine RyR2-P2328S hearts. *Cardiovasc. Res.* 89, 794–804. doi: 10.1093/cvr/cvq229

Zhang, Y., Schwiening, C., Killeen, M. J., Ma, A., Lei, M., Grace, A. A., et al. (2009). Pharmacological changes in cellular Ca2+ homeostasis parallel initiation of atrial arrhythmogenesis in murine Langendorff-perfused hearts. *Clin. Exp. Pharmacol. Physiol.* 36, 969–980. doi: 10.1111/j.1440-1681.2009.05170.x

Zhang, Y., Wu, J., Jeevaratnam, K., King, J. H., Guzadhur, L., Ren, X., et al. (2013). Conduction slowing contributes to spontaneous ventricular arrhythmias in intrinsically active murine RyR2-P2328S hearts. *J. Cardiovasc. Electrophysiol.* 24, 210–218. doi: 10.1111/jce.12015

Conflict of Interest Statement: The authors declare that the research was conducted in the absence of any commercial or financial relationships that could be construed as a potential conflict of interest.

Received: 21 April 2013; accepted: 05 June 2013; published online: 25 June 2013.

*Citation: Zhang Y, Matthews GDK, Lei M and Huang CL-H (2013) Abnormal Ca^{2+} homeostasis, atrial arrhythmogenesis, and sinus node dysfunction in murine hearts modeling RyR2 modification. Front. Physiol. **4**:150. doi: 10.3389/fphys.2013.00150*

This article was submitted to Frontiers in Cardiac Electrophysiology, a specialty of Frontiers in Physiology.

frontiers in PHYSIOLOGY

ORIGINAL RESEARCH ARTICLE
published: 17 October 2013
doi: 10.3389/fphys.2013.00282

Carbon monoxide effects on human ventricle action potential assessed by mathematical simulations

Beatriz Trenor[1], Karen Cardona[1], Javier Saiz[1], Sridharan Rajamani[2], Luiz Belardinelli[2] and Wayne R. Giles[3]*

[1] Instituto Interuniversitario de Investigación en Bioingeniería y Tecnología Orientada al Ser Humano, Universitat Politècnica de València, Valencia, Spain
[2] Cardiovascular Therapeutic Area, Gilead Sciences, Foster City, CA, USA
[3] Faculty of Kinesiology, University of Calgary, Calgary, AB, Canada

Edited by:
Christopher Huang, University of Cambridge, UK

Reviewed by:
Gareth D. K. Matthews, University of Cambridge, UK
Christopher Huang, University of Cambridge, UK

***Correspondence:**
Wayne R. Giles, Faculty of Kinesiology, University of Calgary, 2500 University Drive, Calgary AB T2N 1N4, Canada
e-mail: wgiles@ucalgary.ca

Carbon monoxide (CO) that is produced in a number of different mammalian tissues is now known to have significant effects on the cardiovascular system. These include: (i) vasodilation, (ii) changes in heart rate and strength of contractions, and (iii) modulation of autonomic nervous system input to both the primary pacemaker and the working myocardium. Excessive CO in the environment is toxic and can initiate or mediate life threatening cardiac rhythm disturbances. Recent reports link these ventricular arrhythmias to an increase in the slowly inactivating, or "late" component of the Na^+ current in the mammalian heart. The main goal of this paper is to explore the basis of this pro-arrhythmic capability of CO by incorporating changes in CO-induced ion channel activity with intracellular signaling pathways in the mammalian heart. To do this, a quite well-documented mathematical model of the action potential and intracellular calcium transient in the human ventricular myocyte has been employed. *In silico* iterations based on this model provide a useful first step in illustrating the cellular electrophysiological consequences of CO that have been reported from mammalian heart experiments. Specifically, when the Grandi et al. model of the human ventricular action potential is utilized, and after the Na^+ and Ca^{2+} currents in a single myocyte are modified based on the experimental literature, early after-depolarization (EAD) rhythm disturbances appear, and important elements of the underlying causes of these EADs are revealed/illustrated. Our modified mathematical model of the human ventricular action potential also provides a convenient digital platform for designing future experimental work and relating these changes in cellular cardiac electrophysiology to emerging clinical and epidemiological data on CO toxicity.

Keywords: carbon monoxide (CO), late sodium current ($I_{Na\text{-}L}$), action potential (AP), early after-depolarizations (EADs), S-nitrosylation

INTRODUCTION

It is now well known that carbon monoxide (CO) has significant physiological and pathophysiological effects in a number of different organ systems in mammals (Wu and Wang, 2005). This paper considers CO induced ventricular rhythm disturbances in the human heart. Recently, attention has been drawn to the fact that CO can induce cardiac arrhythmias. This is based on a number of studies in animal models and literature regarding emergency hospital admissions due to life-threatening cardiac rhythm disturbances triggered by increases in ambient levels of CO (Goldstein, 2008; Bell et al., 2009; Dallas et al., 2012). More generally, substances somewhat similar to CO, including nitric oxide (NO), and hydrogen sulfide (H_2S) are now often referred to in the neurophysiological literature as gaseous transmitters (Leffler et al., 2006). These compounds are receiving increased attention as (i) mediators or modulators of significant, sometimes acute pathophysiological challenges, and as (ii) potential targets for therapeutic interventions (Motterlini and Otterbein, 2010).

The ability of CO to alter electrophysiological activity in the heart and nervous system has led to quite broad-ranging examinations of the ability of CO to regulate specific ion channels (Wilkinson and Kemp, 2011). These effects can occur either as direct actions of CO, or (and more commonly) CO effects on closely related intracellular signaling pathways, often involving nitric oxide signaling, metabolism, and/or downstream targets for chemical modifications of individual amino acids in functional proteins. In the cardiovascular system, specific attention has been drawn to S-nitrosylation of, specific ion channel residues (Jaffrey et al., 2001; Haldar and Stamler, 2013).

In this paper, our focus will be on the cellular electrophysiological effects of NO and related S-nitrosylation of specific sites on ion channels, ion transporters, or directly related signaling molecules (Jaffrey et al., 2001; Tamargo et al., 2010; Haldar and Stamler, 2013). This is because many cellular effects initiated by increased CO levels are mediated by downstream changes in NO and ultimately through targeted nitrosylation of defined sites (residues). At present, it is known that NO/S-nitrosylation can:

(i) increase the background K^+ current that generates the resting potential in heart (Gómez et al., 2009) (ii) activate ATP sensitive K^+ channels in neurons (Kawano et al., 2009), and (iii) reduce a major repolarizing current ($K_v1.5$) in mammalian atria (Núñez et al., 2006). In addition, a similar CO and/or NO induced reaction mechanism, as S-nitrosylation, can modulate (iv) Na^+/K^+ ATPase turn over in the hypoxic heart (Yakushev et al., 2012), and (v) alter release of Ca^{2+} from the sarcoplasmic reticulum (SR) by targeting the ryanodine receptor complex in heart and skeletal membranes (Gonzalez et al., 2010; Wang et al., 2010). There is also evidence that NO can increase the slowly inactivating or late Na^+ current in nerve, muscle and heart preparations (Ahern et al., 2000; Evans and Bielefeldt, 2000).

Two recent papers (Abramochkin et al., 2011; Dallas et al., 2012) have reported CO induced changes in electrical activity and contractions, as well as induction of cardiac arrhythmias in a rat ventricle model. Evidence that a major ion channel mediated effect is an augmentation of slow inactivation of the cardiac Na^+ current is provided. These results also emphasize an essential involvement of NO as a second messenger of this CO-induced effect. CO-induced increases in this late Na^+ current, I_{Na-L}, can significantly lengthen the action potential (AP) and result in abnormal electrical activity (early after-depolarization, EADs) characterized by repetitive firing, even after application of only one stimulus (Dallas et al., 2012). This arrhythmia can be reduced substantially following superfusion of this experimental preparation with the compound ranolazine (Dallas et al., 2012). Ranolazine, originally developed as a coronary vasodilator, is now known to be a potent and quite selective inhibitor of the I_{Na-L} in a number of different mammalian preparations (Makielski and Valdivia, 2006; Zaza et al., 2008), and also in human ventricle (Moss et al., 2008). Ranolazine effects are significant in the settings of stable angina and also in heart failure where, in both cases, it is known that I_{Na-L} is increased (c.f. Trenor et al., 2012).

The main goal of our mathematical simulations is to illustrate, using a current mathematical model of the AP in human ventricle, the consequences of a CO induced: (i) increase in I_{Na-L}, (ii) NO-S-nitrosylation induced changes in I_{Ca-L}, and (iii) this combination. For this purpose, CO-induced changes in I_{Na-L} that are similar to those reported in the primary experimental data (Dallas et al., 2012) were introduced into two different models of the ventricular AP and the consequences were explored systematically.

METHODS

HUMAN VENTRICULAR MYOCYTE MODELS

To simulate the electrical activity of human ventricular myocytes, two relatively recent AP models were evaluated. The Grandi et al. model (Grandi et al., 2010) is perhaps the most detailed mathematical model that is available, when judged in terms of its comprehensive ionic current portfolio and inclusion of mathematical expressions for the Ca^{2+} transient and Ca^{2+} homeostasis in the human ventricle. For the purpose of simulating some aspects of heart failure we have previously modified and utilized the original Grandi et al. model (Trenor et al., 2012). In this paper, the slowly inactivating component of I_{Na}, which is denoted I_{Na-L}, was reformulated based on experimental data. In the simulations presented here, we have made use of this code: specifically the Grandi model was employed after (i) modifying the Na^+ current as in (Trenor et al., 2012), (ii) changing the L-type Ca^{2+} current, I_{Ca-L}, or (iii) both.

Early in this study, some simulations were carried out using the latest human ventricular AP model published by O'Hara et al. (2011). This model is based on experimental data taken from 140 healthy human hearts; it encompasses the formulation of 18 ionic currents and carrier-mediated fluxes and a detailed formulation of steady-state and transient ion concentrations, including intracellular Ca^{2+} transients. This model reproduces many aspects of the electrophysiological behavior of human ventricular myocytes with high fidelity, and can simulate some AP alterations due to drug effects. However, it appears *not* to be able to generate/exhibit any EADs in response to the reported, CO induced, changes in I_{Na} or I_{Ca} or their combination. We have not explored the reasons for this in detail; however, it is likely that the net current at the level of the plateau of the AP is an area for further examination/modification.

SIMULATION OF CO EFFECTS

As reported in (Dallas et al., 2012), CO can reduce peak transient inward I_{Na} by as much as 50%, shift the inactivation curve in hyperpolarizing direction, and significantly increase the late sodium current I_{Na-L}. Thus, in our simulation CO effects on the fast component of I_{Na} were modeled by introducing a 50% decrease in I_{Na} maximum conductance and a 5 mV shift in the hyperpolarizing direction of the two Na^+ current inactivation relationships h_∞ and j_∞ (see Equation 1). In addition, I_{Na-L} was increased 2-fold compared to its values in the original Grandi et al. model (Trenor et al., 2012).

$$h_{\infty\_shifted} = j_{\infty\_shifted} = \frac{1}{\left(1 + e^{\frac{V_m + 71.55 + 5}{7.43}}\right)^2} \quad (1)$$

V_m is the membrane potential.

CO is known to elevate NO levels (Dallas et al., 2012), and this "second messenger" can have important effects on L-type Ca^{2+} current, I_{Ca-L}, in the mammalian (ferret) heart, as documented in the detailed studies of Campbell et al. (1996). These investigators reported a significant increase in I_{Ca-L} (30–50%) under conditions of NO induced S-nitrosylation of this Ca^{2+} channel α-subunit. In addition, this paper also reported a nitrosylation induced change in I_{Ca-L} gating—specifically a small but significant change in the voltage dependent activation relationship—an approximately 6.5 mV shift in the hyperpolarizing direction. To reproduce these effects using the Grandi et al. model (Grandi et al., 2010), we have made a number of changes in these parameters. The most favorable/realistic results were obtained when the maximum conductance for I_{Ca-L} was increased by 20% and its activation gate was shifted 3 mV in the hyperpolarizing direction (see Equation 2). The changes applied were slightly smaller than the ones reported experimentally, but were sufficient to trigger EADs, as shown in **Figure 2**.

$$d_{\infty\_shifted} = \frac{1}{1 + e^{\frac{V_m + 5 + 3}{6}}} \quad (2)$$

V_m is the membrane potential.

SIMULATION OF RANOLAZINE EFFECTS

The effects of ranolazine, at an assumed plasma level of 5–10 μM, were simulated by decreasing the maximum $I_{Na\text{-}L}$ conductance by 50% (see **Figure 4**) (cf. Trenor et al., 2013). This maneuver was based on the fact that the recommended adult dosage level for ranolazine is in the 3–8 μM range (Belardinelli et al., 2006).

STIMULATION PROTOCOLS

AP simulations were conducted at a stimulation rate of 1 Hz. Measurements were taken on stimulated output data only after achieving steady-state conditions.

NUMERICAL IMPLEMENTATION

All model equations were taken from Grandi et al. (2010), and were implemented in Matlab (Mathworks Inc., Natick, MA, USA). Differential equations were solved numerically using a variable order solver (ode15s) (Shampine and Reichelt, 1997). As indicated, some simulations were performed using O'Hara et al. model, which was also implemented in Matlab. These model equations were downloaded from http://rudylab.wustl.edu, and the rapid integration methods provided in the Supplemental Materials from O'Hara et al. (2011) and one of our previous papers (Trenor et al., 2012) were used.

RESULTS

The initial set of computations was done for the purpose of illustrating the consequences of the CO induced changes in mammalian heart Na^+ current, I_{Na} that were described in a primary experimental study. This paper (Dallas et al., 2012) reported that CO acting through an intracellular NO-mediated signaling cascade can (i) reduce peak I_{Na} by as much as 50% while also (ii) shifting the inactivation curve for the large transient component of I_{Na} in hyperpolarizing direction, and (iii) significantly increasing the slowly inactivating component of I_{Na} (which is denoted $I_{Na\text{-}L}$).

The two superimposed human ventricular APs in **Figure 1A** illustrate the control AP waveform at 1 Hz, and the AP elicited following the changes in I_{Na} and $I_{Na\text{-}L}$ described above. For these computations, the steady-state inactivation curve was shifted in the hyperpolarizing direction by 5 mV and $I_{Na\text{-}L}$ was increased 2-fold. **Figure 1B** shows the changes in $I_{Na\text{-}L}$; **Figure 1C** illustrates the indirect effects on $I_{Ca\text{-}L}$; that is, the AP waveform lengthened, and this changed the $I_{Ca\text{-}L}$; and **Figure 1D** shows the computed intracellular Ca^{2+} transient, $[Ca^{2+}]_i$.

In summary the reported changes in I_{Na} and $I_{Na\text{-}L}$, when combined, result in predictable decreases in AP rate-of-rise (not shown) and small increase in AP duration. However, these changes fail to elicit spontaneous firing (EADs on DADs) or produce any correlates of arrythmogenesis. Although this pattern of results was somewhat unexpected, it is important to recall that the primary experimental data on CO were obtained in rat hearts (Ahern et al., 2000; Dallas et al., 2012), and not from human ventricular tissue or myocytes. We therefore, continued to attempt to illustrate and further understand the electrophysiological effects of CO on the human ventricular myocardium by considering additional variables.

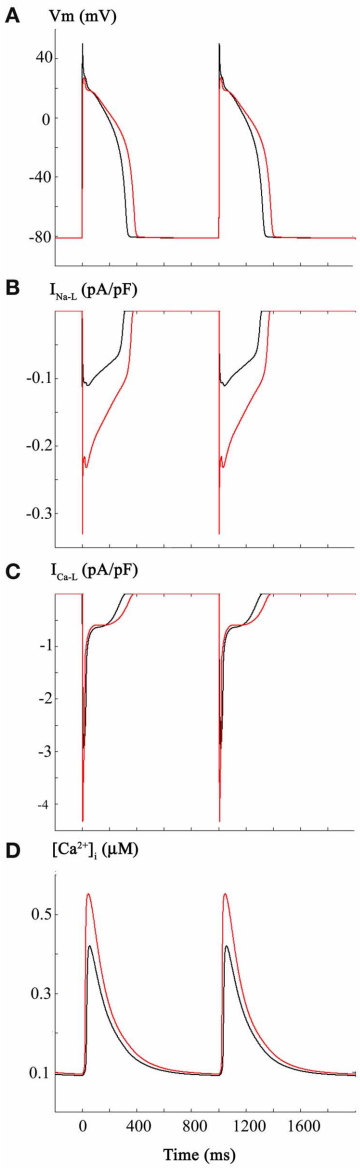

FIGURE 1 | Effects of carbon monoxide (CO) induced changes in Na^+ current on the action potential in a human ventricular myocyte. In this and all subsequent Figures, the Grandi et al. mathematical model of the human ventricular action potential was employed (see Methods). Control simulations are shown as black traces and simulations generated by selected changes in model parameters are shown in red. Panel **(A)** consists of control action potentials (black, 1 Hz., steady state) together with superimposed action potentials (red) that were elicited by the same stimulus parameters after: (i) reducing peak Na^+ current by 50%, (ii) shifting the steady state inactivation relationship 5 mV in the hyperpolarizing direction, and (iii) altering the mathematical descriptors that govern the slowly inactivating or late sodium current, $I_{Na\text{-}L}$, such that its size was increased 2-fold. As expected, these changes reduced excitability and decreased the dV/dt of the action potential upstroke as well as lengthening the AP at both APD-30 and APD-90. $I_{Na\text{-}L}$ records are shown in Panel **(B)**. In Panels **(C,D)** the corresponding L-type Ca^{2+} current, $I_{Ca\text{-}L}$, and intracellular calcium transient, $[Ca^{2+}]_i$ are illustrated. Note that these changes are indirect, i.e., they result from the changes in APD waveform and the intrinsic biophysical properties of $I_{Ca\text{-}L}$ and the Ca^{2+}-induced Ca^{2+} release (CICR) mechanisms.

In fact, studies of NO-mediated effects in heterologous expression systems utilizing the alpha subunit of the human heart Na^+ channel, $Na_v1.5$ (Ueda et al., 2008), reveal a somewhat different pattern of results. These include (i) an (approximately 30%) increase in peak inward Na^+ current, a (ii) small hyperpolarizing shift in the steady-state inactivation curve for I_{Na}, (iii) a marked enhancement (approximately 2-fold) in $I_{Na\text{-}L}$ and (iv) an essential NO-induced S-nitrosylation of a defined residue on $Na_v1.5$. These changes, when introduced into the Grandi model, also failed to result in increased arrhythmogenesis (results not shown).

We were aware of the detailed studies of Campbell et al. (1996) on the effects of NO on $I_{Ca\text{-}L}$, in the mammalian (ferret) heart. These investigators reported a significant increase in $I_{Ca\text{-}L}$ (30–50%) under conditions of NO induced S-nitrosylation of this Ca^{2+} channel α-subunit. Importantly, this paper also reported a nitrosylation-induced change in $I_{Ca\text{-}L}$ gating, specifically, a small but significant shift in the voltage dependent activation relationship—approximately 6 mV in the hyperpolarizing direction. The superimposed APs in **Figure 2** illustrate the consequences of introducing these changes into the original Grandi et al. model (Grandi et al., 2010). Panel **(A)** shows the AP waveforms (black, baseline, or control) (red, following $I_{Ca\text{-}L}$ changes). $I_{Na\text{-}L}$ and $I_{Ca\text{-}L}$ records are shown in Panels **(B,C)**, respectively. The L-type Ca^{2+} current is shown in Panel **(C)**. As shown in Panel **(D)**, these changes in $I_{Ca\text{-}L}$ also resulted in a large increase in $[Ca^{2+}]_i$, and the $[Ca^{2+}]_i$ exhibited pronounced frequency dependence or alternans (see Discussion and Clark et al., 1996; Bouchard et al., 2004).

Detailed inspection of **Figure 2** and comparison of this pattern of results with those in **Figure 1** reveal (Panel **B**) that $I_{Na\text{-}L}$ now shows pronounced changes in peak amplitude, even in response to the fixed stimulus rate at 1 Hz. Presumably, this arises from the markedly prolonged AP and intrinsic voltage-dependence of reactivation of $I_{Na\text{-}L}$ (see Discussion).

The third set of computations in this study combined the reported CO induced changes in I_{Na} and $I_{Na\text{-}L}$ (**Figure 1**), with those for $I_{Ca\text{-}L}$ (**Figure 2**). The resulting very significant changes in AP duration (Panel **A**), $I_{Na\text{-}L}$ (Panel **B**), $I_{Ca\text{-}L}$ (Panel **C**), and $[Ca^{2+}]_i$ (Panel **D**) are shown in **Figure 3**. This pattern of results was similar to, but not identical with **Figure 2**. In particular, the majority of the APs elicited at a physiological stimulus rate (1 Hz) exhibited marked prolongation (approximately 100%), with the appearance of an EAD late in the prolonged plateau phase. Note that under these starting conditions, the combined inward currents due to $I_{Na\text{-}L}$ and $I_{Ca\text{-}L}$ "held" the membrane potential of the plateau near 0 mV in contrast with the approximately −10 mV plateau level in **Figure 2**.

The pattern of changes shown in **Figure 3** is not surprising. It is now well known that abnormal, slow depolarizations, which are denoted EADs, can be elicited by changes in $I_{Ca\text{-}L}$ (Marban et al., 1986; January and Riddle, 1989, for review see Clusin, 2003). In fact, in rabbit ventricle a recent report from the Weiss laboratory (Madhvani et al., 2011) has illustrated in detail ways in which even very small changes in the voltage dependence of the activation of $I_{Ca\text{-}L}$ can give rise to EADs. This is mainly, but not entirely due to the fact that there is an increased inward current at or very

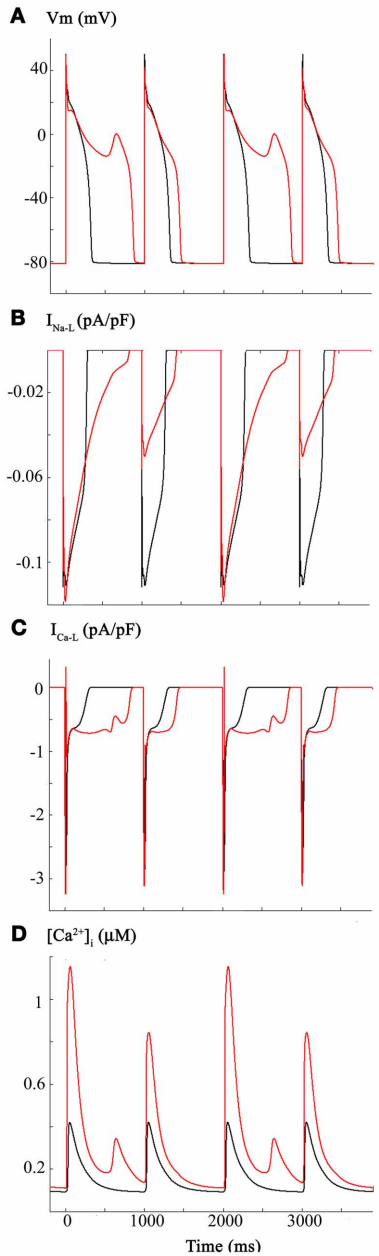

FIGURE 2 | Effects of CO-induced changes in L-type Ca^{2+} current on the human ventricular myocyte. Based on the work of Campbell et al., $I_{Ca\text{-}L}$ was increased 50% and the voltage dependence for the activation curve was shifted in the depolarizing direction by 3 mV. As shown in Panel **(A)** these changes resulted in a lengthening of the action potential plateau and appearance of associated oscillatory potentials or early after depolarizations (EADs). Panel **(B)** shows the changes in $I_{Na\text{-}L}$. The longer APD results in a protracted $I_{Na\text{-}L}$; the alterations in amplitude of this current are due to the voltage dependence of its reactivation. As shown in Panel **(C)**, these changes in the biophysical parameters that regulate $I_{Ca\text{-}L}$ resulted in a change in peak amplitude and perhaps more importantly a significant alteration in its time course of inactivation. $I_{Ca\text{-}L}$ also reactivates under these conditions. Panel **(D)** shows the control Ca^{2+} transient and the computed changes in $[Ca^{2+}]_i$ that occur as a consequence of alterations in the $I_{Ca\text{-}L}$.

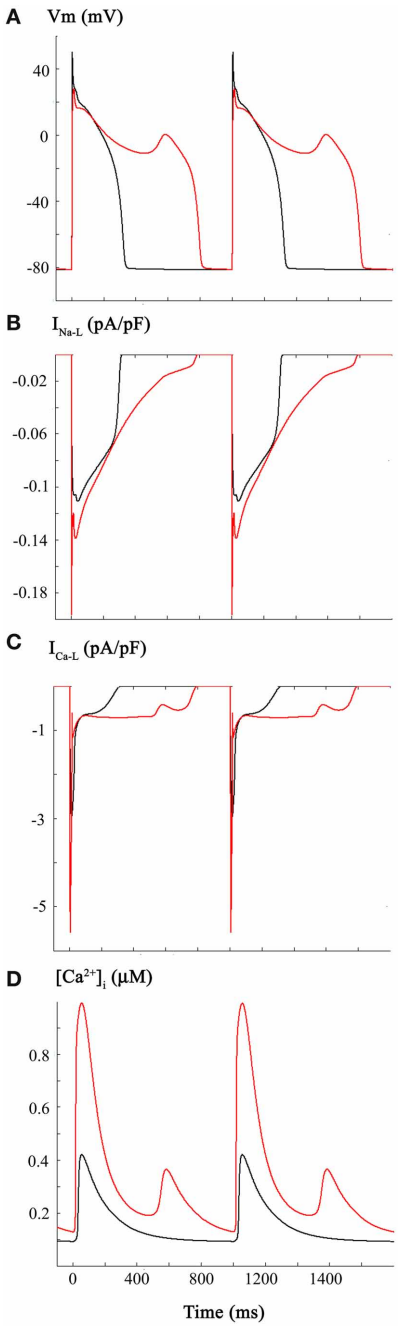

FIGURE 3 | Changes in the human ventricular action potential as a consequence of CO-induced changes in both I_{Na} and I_{Ca-L}. The layout and color-coding of this Figure is identical to that described for **Figures 1**, **2**. As shown in Panel **(A)** when the CO-induced changes in Na^+ and Ca^{2+} currents are combined there is marked lengthening of the action potential and a significantly increased incidence and frequency of EADs occurring during the somewhat depolarized plateau phase of the action potential. I_{Na-L} records are shown in Panel **(B)**. Panels **(C,D)** show the changes in I_{Ca-L} and $[Ca^{2+}]_i$. Note that the changes in I_{Ca-L} differ from those in **Figure 2** as a result of the alterations in action potential waveform caused by the combined changes in I_{Na} and I_{Ca-L}.

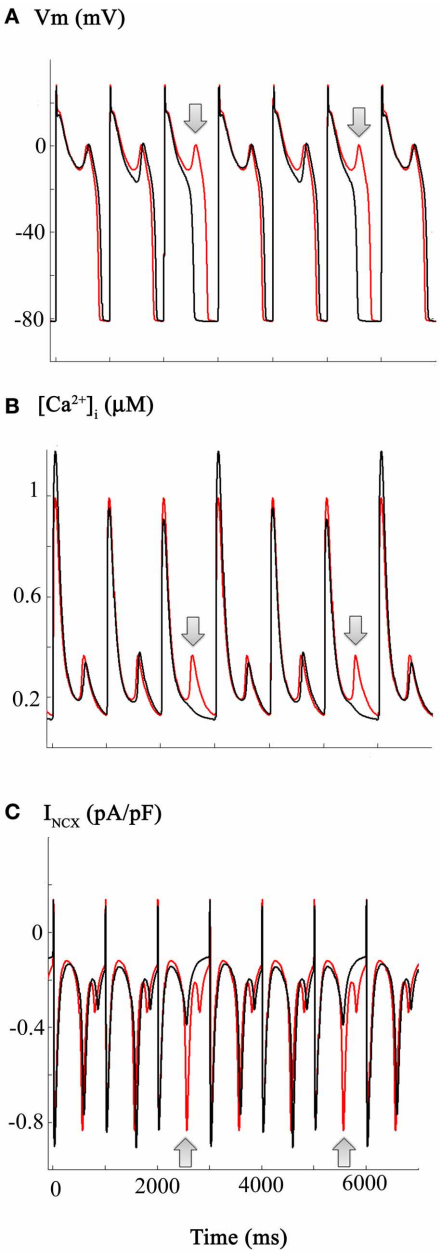

FIGURE 4 | Estimation and illustration of the effects of ranolazine on CO-induced changes in the action potential and underlying I_{Na-L}, I_{Ca-L}, and Na^+/Ca^{2+} exchange currents (I_{NCX}) in human ventricle. The effects of ranolazine (shown in black) were modeled as a selective 50% reduction in the I_{Na-L}. Note that this reduces action potential, duration of every 3rd action potential, as well as decreasing the incidence and the frequency of EADs. However, these changes are complex. APD (Panel **A**) as well as $[Ca^{2+}]_i$ and I_{NCX} records all show variations or alternans, even at this fixed stimulus rate (1 Hz). Panel **(C)** illustrates the corresponding ranolazine-induced changes in the I_{NCX}. Note that in the action potential traces showing a ranolazine-induced shortening of APD, there is no spontaneous inward I_{NCX} current (see also **Figure 5** and Results). The arrows denote the "extra" EADs (Panel **A**), and underlying $[Ca^{2+}]_i$ transient (Panel **B**), and I_{NCX} (Panel **C**) records.

near the range of membrane potentials of the plateau of the normal or prolonged AP. The underlying biophysical mechanism(s) involves the non-linear interactions of the small overlapping Ca^{2+} channel—and Na^+/Ca^{2+}—exchanger mediated currents in this range of membrane potentials (Madhvani et al., 2011, for review see Fink et al., 2006). The altered AP waveform and related pro- or anti-arrhythmic effects are sometimes described in terms of an altered "repolarization reserve" at defined time-points of early or late repolarization (Wu et al., 2009; Varró and Baczkó, 2011; Trenor et al., 2013).

If environmental or tissue-derived CO can induce life-threatening ventricular rhythm disturbances through a mechanism involving enhancement of $I_{Na\text{-}L}$, it is plausible that, as mentioned in the Introduction, ranolazine could be effective in Critical Care settings (Dallas et al., 2012, cf. Belardinelli et al., 2006; Bell et al., 2009). The mathematical simulations shown in **Figure 4** address this possibility by illustrating the effects of ranolazine "*in silico*." These computations were carried out under starting conditions (i.e., an initial parameter set) almost identical to those for **Figure 3**. However, for these computations it was assumed that ranolazine actions would be the equivalent of a 50% reduction of the CO induced increase in $I_{Na\text{-}L}$ (see **Figure 1**). The results show that if ranolazine (at an assumed plasma level of 5 μM) did block approximately 50% of $I_{Na\text{-}L}$, it could shorten the AP elicited by a 1 Hz train of stimuli. Note, however, that this partial block of $I_{Na\text{-}L}$ reduced APD only (approximately) every 3rd AP in this 1 Hz AP train. An additional effect is also apparent: reducing $I_{Na\text{-}L}$ changes the (i) waveform and (ii) the most negative membrane potential in some repolarizing components within this train of AP's. This primary "effect" appears to be linked functionally to the approximately normal repolarization of the next AP. In summary, when ranolazine is introduced *in silico*, the resulting AP waveforms show complex alternating patterns. However, there is an increased number of (i) near normal AP waveforms and (ii) monotonic $[Ca^{2+}]_i$ records. The incidence of EADs is also reduced, consistent with the previously described actions of this drug in the settings of free radical challenge, genetic abnormalities in Na^+ channel biophysics, hypoxia, or global ischemia/heart failure (Fink et al., 2006; Trenor et al., 2012).

The simulations in **Figure 5** address and attempt to illustrate some of the underlying causative factors for EAD generation within the framework/limitations of this model of the human ventricle AP. EAD generation requires the membrane potential to be relatively depolarized, so that L-type Ca^{2+} channels can be activated and contribute a small but significant inward Ca^{2+} current. We note that the main interacting (or overlapping) ion channel mediated currents at the plateau of the AP are: (i) $I_{Na\text{-}L}$, (ii) $I_{Ca\text{-}L}$, (iii) I_{K1}, a time-independent or background inwardly rectifying current, and (iv) the delayed rectifier K^+ current, I_{K-R} (Trenor et al., 2013). In the presence of an enhanced $I_{Na\text{-}L}$ the AP plateau is somewhat depolarized and the AP tends to be prolonged. In addition, under these conditions I_{NCX} generated by the Na^+/Ca^{2+} exchange mechanism can be functionally important. A key question is: are the pronounced changes in $[Ca^{2+}]_i$ the cause or the consequence of the EAD/CO-induced pro-arrhythmic substrate. A plausible answer can be obtained by consideration of the results in Panels (**A–F**) of **Figure 5**.

Panel (**A**) shows two superimposed pairs of APs, each elicited at steady state (1 Hz) before (black) and after (red) introducing the changes shown in **Figure 3**. Panels (**B,C**) show the corresponding $I_{Na\text{-}L}$ and $I_{Ca\text{-}L}$ records. Although this information is redundant with that in **Figure 3**: here, it provides a means for direct comparison with the new data: Panel (**D**), $[Ca^{2+}]_i$ records; Panel (**E**), I_{NCX}; and Panel (**F**), the Ca^{2+} content of the SR.

Taken together, these results suggest that in this model the CO/NO-induced changes in $I_{Ca\text{-}L}$ are critical. With each stimulus, a large "extra" Ca^{2+} influx prolongs the plateau and results in enhanced Ca^{2+} release and a much larger increase in $[Ca^{2+}]_i$. This change in $[Ca^{2+}]_i$ can stimulate the I_{NCX}. Perhaps more importantly, however, this time-dependent and cumulative change in myocyte Ca^{2+} homeostasis results in markedly increased Ca^{2+} in the SR. Eventually, this causes anomalous Ca^{2+} release from the SR, and the Na^+/Ca^{2+} exchanger (denoted by arrows) responds by generating an inward current that gives rise to the EAD. Under these conditions, approximately every second AP is associated with spontaneous release at the steady-state stimulus rate of 1 Hz.

This scheme/scenario seems plausible, since similar patterns of changes have been described experimentally. However, it may not be readily apparent how ranolazine, acting only on $I_{Na\text{-}L}$ could be anti-arrhythmic (see Discussion). In brief, the answer appears to be that ranolazine, by blocking $I_{Na\text{-}L}$, can shorten the AP. This reduction in APD results in reduced Ca^{2+} influx through $I_{Ca\text{-}L}$ during each AP and thus, there is less Ca^{2+}-loading of the SR. The end result is that SR Ca^{2+} content does *not* reach the abnormal levels required for anomalous and spontaneous Ca^{2+} release. Hence, there is no intracellular Ca^{2+} "trigger" for the electrogenic I_{NCX}, that has an important role in initiating the EAD in this model (Houser, 2000; Clusin, 2003).

DISCUSSION

SUMMARY OF MAIN FINDINGS

Our mathematical modeling illustrates one set of conditions under which human ventricle myocytes can respond to a significant CO induced challenge (environmental or intrinsic) by generating an aberrant cellular electrophysiological pattern of responses, denoted EADs.

When using a modified Grandi et al. modeling framework (Grandi et al., 2010), the reported (Dallas et al., 2012) changes in Na^+ current following CO exposure were *not* sufficient to provide the required pro-arrhythmic substrate. Additional changes in $I_{Na\text{-}L}$ parameters may have given rise to EAD waveforms. However, we evaluated the possibility that other ion channel targets were involved in EAD initiation. Accordingly, our analyses of CO-induced EADs include changes in $I_{Na\text{-}L}$ and $I_{Ca\text{-}L}$. As shown in **Figure 2**, even very small changes in $I_{Ca\text{-}L}$ can produce EAD generation. Although this pattern of results has not been reported when CO is used as the "toxic" stimulus; it is known that NO is a primary mediator of CO-induced pro-arrhythmic events in the heart (Dallas et al., 2012). Campbell et al. (1996) have established that NO driven S-nitrosylation can modify $I_{Ca\text{-}L}$. We adopted this approach and were guided by this comprehensive biophysical/molecular pharmacological data set.

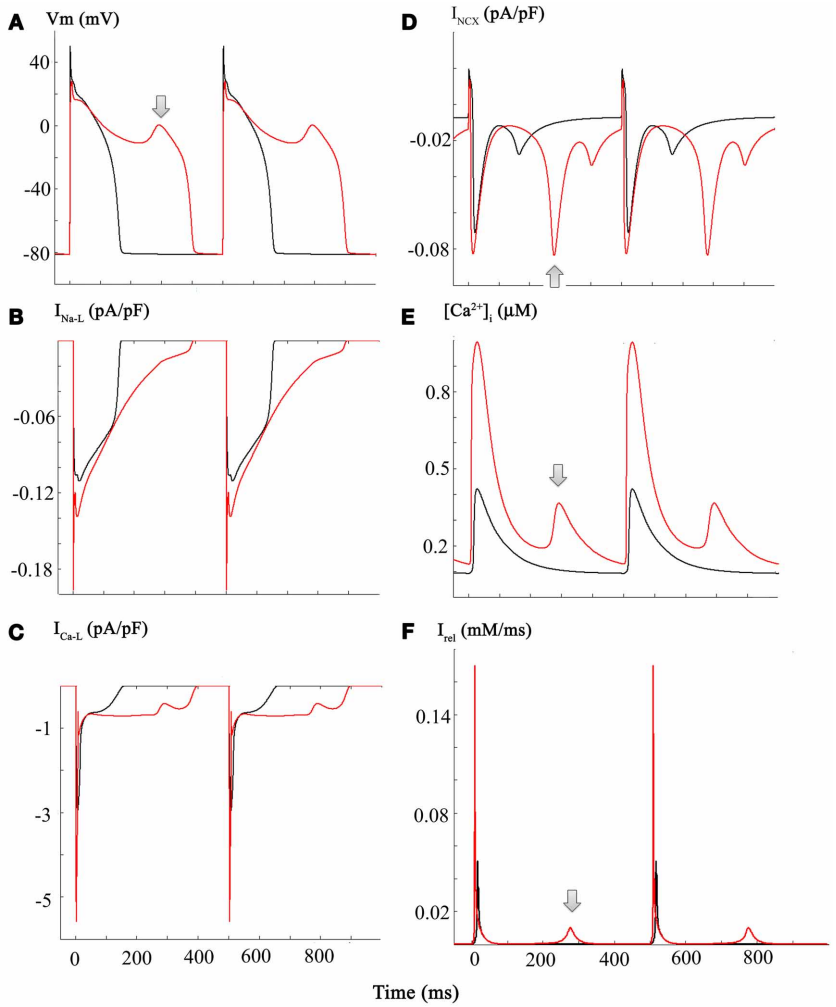

FIGURE 5 | Diagram illustrating a plausible mechanism for generation of EADs in our modified Grandi model of the human ventricular action potential. Panels **(A** through **C)** each consist of a pair of superimposed records for the AP, I_{Na-L}, and I_{Ca-L} records, respectively. Those in black correspond to control or baseline conditions, and the CO-induced changes are shown in red. Important new information is illustrated in the corresponding (i) I_{NCX} currents, Panel **(D)**; (ii) $[Ca^{2+}]_I$ data, Panel **(E)**; and the current generated by Ca^{2+} release from the sarcoplasmic reticulum I_{rel}, Panel **(F)**. The arrows denote the EAD (Panel **A**) and underlying spontaneous Ca^{2+} release from the SR (Panel **F**), and I_{NCX} current driven by the increase in $[Ca^{2+}]_i$ (Panel **E**). Refer to Results and Discussion sections for further details and explanation.

It is interesting that in spite of an apparent "double hit" being required for the initiation of EADs, *in silico*, reduction of only one of these contributing factors, a 50% decrease of I_{Na-L}, resulted in a reduction in the EAD incidence (see **Figure 4**). This is consistent with the experimental observation that selective pharmacological inhibition of I_{Na-L} can serve as an antidote to CO-induced rhythm disturbances in rat ventricle (Dallas et al., 2012).

MECHANISTIC INSIGHTS

Some aspects of the cellular/biophysical mechanism(s) responsible for EAD generation can be deduced/confirmed by careful inspection of the new data from our simulations. EADs are slow, small depolarizations that arise in the ventricle (and in Purkinje tissue) within a transmembrane voltage range corresponding to the plateau of the ventricular AP (approximately −10 to +10 mV). A net inward current is required, and the work from the Marban (Marban et al., 1986) and January (January and Riddle, 1989) Laboratories has established that there is an obligatory requirement for activation of I_{Ca-L}. In fact, I_{Ca-L}, in most cases, must reactivate. That is, a small fraction of the same I_{Ca-L} channels that have opened previously in the AP to produce the distinctive plateau of the human ventricular AP open again. This produces a "pedestal" or apparently non-inactivating I_{Ca-L} component (Corrias et al., 2011). Our simulations are interesting in this regard. Detailed inspection of **Figures 2–4** in fact show that EAD generation in this model occurs at a time when the I_{Ca-L} pedestal shows a small, transient *decrease*. In the Grandi et al. model, this is due to the specific mathematical expression of $[Ca^{2+}]_i$ dependent inactivation that is employed.

However, the non-inactivating component of $I_{Ca\text{-}L}$ and the inward current due to $I_{Na\text{-}L}$ markedly prolong the AP, and this change in APD waveform results in a significant increase in Ca^{2+} influx since $I_{Ca\text{-}L}$ does not fully inactivate. This extra Ca^{2+} influx, results in a time-dependent and marked increase in SR Ca^{2+} content. Eventually this causes a spontaneous and intermittent (anomalous) pattern of SR Ca^{2+} release. Each of these increases in $[Ca^{2+}]_i$ gives rise to a significant "new" inward current generated by the sarcolemmal Na^+/Ca^{2+} exchanger mechanism.

It is worth noting that during CO challenge (intoxication and recovery) or in any setting involving stress, the known effects of stimulation of the sympathetic nervous system would be expected to augment both Na^+ and Ca^{2+} currents. These changes, alone or in combination, would enhance $I_{Ca\text{-}L}$ and perhaps $I_{Na\text{-}L}$, both of which would contribute a net inward current at the plateau level of the ventricular AP. The Koren Laboratory (Liu et al., 2012) has recently developed a robust model of EAD induced arrhythmias based on genetically targeted malfunction of distinct repolarizing K^+ currents in adult rabbit ventricle. Their findings provide interesting insights into underlying mechanisms of pro-arrhythmic impulse generation at relatively depolarized (AP plateau) levels in the ventricular myocardium. Specifically, they have reported enhanced EAD activity either (i) following augmentation of $I_{Ca\text{-}L}$ with isoproterenol, or (ii) a reduction of repolarizing K^+ current(s) during hypokalemic conditions. Both of these maneuvers can alter the net current at the plateau of the AP and thus, change the repolarization reserve during the early repolarization phase of the AP (cf. Fink et al., 2006; Sarkar and Sobie, 2011; Trenor et al., 2012). Further insights into the ionic mechanisms responsible for EAD initiation and maintenance requires definition of, and agreement on, the range of membrane potentials at which those small oscillating events occur (Gaur et al., 2009).

FUTURE DIRECTIONS

As indicated in the Introduction, there are a number of additional targets or sites, at which CO or CO-generated signaling molecules are known to act. Perhaps the most important of these are the K^+ currents that are expressed throughout the mammalian heart, and have important roles in setting the resting potential and modulating repolarization. The Tamargo Group (Gómez et al., 2009) has shown that the K^+ conductance which underlies the resting potential in atrium and ventricle, $K_{ir}2.1$ or I_{K1}, is a target for S-nitrosylation. This chemical modification of this current results in increased I_{K1}. Although I_{K1} is non-linear, it increases the repolarization reserve during final repolarization, and may cause a small (1–3 mV) hyperpolarization of the resting potential (cf. Fink et al., 2006). More detailed studies of CO effects should include this target of CO-mediated channel effects.

Tamargo et al. (Núñez et al., 2006) have also reported that a prominent repolarizing current in the atrium of most mammalian species, $K_v1.5$, can be altered by S-nitrosylation. $K_v1.5$ is decreased by S-nitrosylation, and this would be pro-arrhythmic. We note however, that $K_v1.5$ is a small current in human ventricle (cf. Fink et al., 2006; Grandi et al., 2010).

As noted in the Introduction, the Makielski Group (Ueda et al., 2008) has reported that NO and an associated S-nitrosylation modification of I_{Na} can result in a significantly enhanced $I_{Na\text{-}L}$. In fact, however, their investigation focused on NO effects on I_{Na} in the setting of an identified mutation in syntrophin that results in one variant of a pattern of ventricular rhythm disturbances, denoted the long Q-T syndrome (cf. Moss et al., 2008; Thomas et al., 2008).

It has been proposed (Dallas et al., 2012) that consideration should be given to utilization of ranolazine or ranolazine-like compounds in clinical settings (Emergency or Critical Care Medicine) that involve documented CO poisoning and involve ventricular rhythm disturbances. Improved clinical interventions directed toward minimizing cardiac risk during the required recovery period from CO intoxication are much needed (Goldstein, 2008; Motterlini and Otterbein, 2010). In principle, and as illustrated, ranolazine or ranolazine-like compounds could be considered for this purpose (Belardinelli et al., 2006; Kinobe et al., 2008; Saint, 2008; Wu et al., 2009). Ranolazine quite selectively targets $I_{Na\text{-}L}$. However, the net current change that is the direct result of ranolazine interaction with Na^+ channel, is integrated in the overall cardiac electrophysiological system (biophysical mechanism) for maintenance and generation of the plateau of the AP, in a way that involves complex, often non-linear interactions of a number of different currents (Fink et al., 2006). Thus, a monotonic dose-response relationship for ranolazine effects is not anticipated in this type of clinical/therapeutic setting/application and individual differences in the electrophysiological substrate are expected to/need to continue to be considered (Sarkar et al., 2012).

The computations presented in this paper have all been carried out assuming that the CO target is a single ventricular myocyte. Although this is a valid starting point, it is known that the isolated single human ventricular myocyte has electrophysiological characteristics somewhat different than the same myocyte functionally joined to other myocytes through gap junction or "placed" in a syncytium consisting of many other similar or identical myocytes. Often, the AP waveform in the syncytium is slightly but significantly different than that in a single cell. For example, the plateau "height" is less depolarized in the syncytium. Intracellular current flow, and other factors, such as intrinsic electrophysiological heterogeneity of the myocytes, can also result in the AP of a myocyte within a syncytium having a more stable resting potential together with much less intrinsic action APD variability (Huelsing et al., 2000; Zaniboni et al., 2000; Spitzer et al., 2006). In addition, it is now known that in both the ventricular and the atrial myocardium the fibroblast/myofibroblast cell population (Wu and Wang, 2005) may produce significant electrotonic effects (Maleckar et al., 2009, cf. Baudino et al., 2006). It is possible that either CO or its immediate downstream signaling molecules could alter fibroblast electrophysiology/paracrine function. One or more of these factors may alter the pattern of response which we have observed in our *in silico* investigation of CO effects.

LIMITATIONS

We are aware that as presented our analysis of CO effects on the human ventricle is incomplete. Primary reasons for this include:

1. The computational platform that we have used is comprehensive and has been tested in terms of its ability to illustrate the functional roles of many of the individual ion channel currents that underlie the AP. However, it and most other such models have limitations. In this paper, we illustrate pronounced effects on AP waveforms and pro-arrhythmic patterns of response that arise from very small current changes that would be consistent with CO effects. The Grandi model (Grandi et al., 2010) can be relied on as a computational platform for human ventricular myocytes when exploring problems that can be addressed with semi-quantitative endpoints. However, caution is warranted when the input data suggests only e.g., a 1–3 mV shift in an activation parameter (cf. Terkildsen et al., 2008).
2. It is apparent that simulation of CO-mediated electrophysiological effects requires detailed understanding of each major component of Ca^{2+} homeostasis in the human ventricular myocyte. Recent publications show that S-nitrosylation can alter ryanodine receptor function and change Ca^{2+}-induced Ca^{2+} release (Ahern et al., 2000; Wang et al., 2010; Cutler et al., 2012). Our work does not address this possibility. In fact, in the Grandi et al. modeling environment (Grandi et al., 2010) detailed studies of the consequences of changes in Ca^{2+}-induced Ca^{2+} release (CICR) are not possible since many of the known subcellular details of CICR release are not included in this computational platform. After this model is developed further and e.g., the existing electrophysiological components are integrated with known properties of E-C coupling and mechanical activation (Tao et al., 2011), further insights into CO-mediated effects may be able to be obtained and Ca^{2+}-pump (SERCA 2) mediated relaxation.
3. Detailed studies of CO-mediated alterations of mammalian cardiac electrophysiological phenomena are relatively recent. At present, there is incomplete information on clinically relevant plasma levels, interspecies variations, and specific intracellular signaling cascades. This information is essential for more extensive simulations that could address cellular or molecular mechanisms for CO-I_{Na}-NO interactions (Ueda et al., 2008), including those arising from ion channel mutations (Thomas et al., 2008) or changes in intercellular coupling (Haas and Landisman, 2011), identification or selection of therapeutic agents, and improvement of Systems Biology (Winslow et al., 2011) approaches to human cardiac sudden death in humans.
4. Our work is not intended to detract from or replace well-established principles of CO generation or action (Maines, 1997) based on the heme oxygenase system. However, two points are noteworthy. (i) It is now known that an essential site of action of CO in resistance vessels is a reduced heme moiety that is co-localized with the Ca^{2+}-activated K^+ channels that modulate CO-induced vasodilation (Jaggar et al., 2005). (ii) CO challenge results in compromised haemoglobin function and pronounced hypoxia. Hypoxia is an established condition that results in augmented $I_{Na\text{-}L}$ in the myocardium (Ju et al., 1996). A recent paper advances an interesting plausible scenario in which micro-anatomical integration, that is co-expression of Na^+ channels, NO synthase isoform and G proteins are co-localized in caveolae (Besse et al., 2011).
5. Our approach to the pro-arrhythmic effects of CO challenge has placed an emphasis on EAD initiation. We acknowledge that alterations in micro- or macroscopic conduction patterns or velocities; and/or I_{Na}, $I_{Na\text{-}L}$, and $I_{Ca\text{-}L}$ dependent changes in AP waveform have *not* been ruled out as plausible pro-arrhythmic elements. These, along with the S-nitosylation induced change in mammalian heart K^+ currents (Gómez et al., 2009; Tamargo et al., 2010), could form the basis of a more comprehensive study, after sufficient data from one mammalian species, preferably human, is obtained.

AUTHOR CONTRIBUTIONS

Doctors Trenor, Saiz and Giles shared responsibilities for study design. Computations were performed at Universidad Politécnica de Valencia by Doctors Cardona and Trenor, Dr. Giles wrote this manuscript. All authors contributed to final editing and the R-1 revisions.

ACKNOWLEDGMENTS

In Valencia, this work was supported by: (i) VI Plan Nacional de Investigación Científica, Desarrollo e Innovación Tecnológica from the Ministerio de Economía y Competitividad of Spain (TIN2012-37546-C03-01) and the European Commission (European Regional Development Funds—ERDF—FEDER)., (ii) Plan Avanza en el marco de la Acción Estratégica de Telecomunicaciones y Sociedad de la Información del Ministerio de Industria Turismo y Comercio of Spain (TSI-020100-2010-469), (iii) Programa deApoyo a la Investigación y Desarrollo (PAID-06-11-2002) de la Universitat Politècnica de València, (iv) Programa Prometeo (PROMETEO/2012/030) de la Consellería d'Educació Formació I Ocupació, Generalitat Valenciana, and (v) GileadSciences, Ltd. Wayne Giles acknowledges receipt of financial support in the form of a salary award (Medical Scientist) from Alberta Innovates-Health Solutions, and operating funding from the Canadian Institutes for Health Research and the Heart and Stroke Foundation of Alberta.

REFERENCES

Abramochkin, D. V., Haertdinov, N. N., Porokhnya, M. V., Zefirov, A. L., and Sitdikova, G. F. (2011). Carbon monoxide affects electrical and contractile activity of rat myocardium. *J. Biomed. Sci.* 18:40. doi: 10.1186/1423-0127-18-40

Ahern, G. P., Hsu, S. F., Klyachko, V. A., and Jackson, M. B. (2000). Induction of persistent sodium current by exogenous and endogenous nitric oxide. *J. Biol. Chem.* 275, 28810–28815. doi: 10.1074/jbc.M003090200

Baudino, T., Carver, W., Giles, W., and Borg, T. K. (2006). Cardiac fibroblasts: friend or foe? *Am. J. Physiol. Heart Circ. Physiol.* 291, H1015–H1026. doi: 10.1152/ajpheart.00023.2006

Belardinelli, L., Shryock, J. C., and Fraser, H. (2006). Inhibition of the late sodium current as a potential cardioprotective principle: effects of the late sodium current inhibitor ranolzaine. *Heart* 92(Suppl. 4), iv6–iv14. doi: 10.1136/hrt.2005.078790

Bell, M. L., Peng, R. D., Dominici, F., and Samet, J. M. (2009). Emergency hospital admissions for cardiovascular diseases and ambient levels of carbon monoxide: results for 126 United States urban counties, 1999–2005. *Circulation* 120, 949–955. doi: 10.1161/CIRCULATIONAHA.109.851113

Besse, I. A., Mitchell, C. C., Hund, T. J., and Shibata, E. F. (2011). A computational investigation of cardiac caveolae as a source of persistent sodium current. *Front. Physiol.* 2:87. doi: 10.3389/fphys.2011.00087

Bouchard, R., Clark, R. B., Juhasz, A. E., and Giles, W. R. (2004). Changes in extracellular K^+ concentration modulate contractility of rat and rabbit cardiac myocytes via the inward rectifier K+ current I_{K1}. *J. Physiol.* 556(pt 3), 773–790. doi: 10.1113/jphysiol.2003.058248

Campbell, D. L., Stamler, J. S., and Strauss, H. C. (1996). Redox modulation of L-type calcium channels in ferret ventricular myocytes. Dual mechanism regulation by nitric oxide and S-nitrosothiols. *J. Gen. Physiol.* 108, 277–293. doi: 10.1085/jgp.108.4.277

Clark, R. B., Bouchard, R. A., and Giles, W. R. (1996). Action potential duration modulates calcium influx, Na^+-Ca^{2+} exchange, and intracellular calcium release in rat ventricular myocytes. *Ann. N.Y. Acad. Sci.* 779, 417–429. doi: 10.1111/j.1749-6632.1996.tb44817.x

Clusin, W. T. (2003). Calcium and cardiac arrhythmias: DADs, EADs, and alternans. *Crit. Rev. Clin. Lab. Sci.* 40, 337–375. doi: 10.1080/713609356

Corrias, A., Giles, W., and Rodiguez, B. (2011). Ionic mechnisms of elctrophysiological properties and repolarization abnormalities in rabbit Purkinje fibers. *Am. J. Physiol. Heart Circ. Physiol.* 300, H1806–H1813. doi: 10.1152/ajpheart.01170.2010

Cutler, M. J., Plummer, B. N., Wan, X., Sun, Q. A., Hess, D., Liu, H., et al. (2012). Aberrant S-nitrosylation mediates calcium-triggered ventricular arrhythmia in the intact heart. *Proc. Natl. Acad. Sci. U.S.A.* 109, 18186–18191. doi: 10.1073/pnas.1210565109

Dallas, M. L., Yang, Z., Boyle, J. P., Boycott, H. E., Scragg, J. L., Milligan, C. J., et al. (2012). Carbon monoxide induces cardiac arrhythmia via induction of the late Na^+ current. *Am. J. Respir. Crit. Care Med.* 186, 648–656. doi: 10.1165/rccm.201204-0688OC.

Evans, J. R., and Bielefeldt, K. (2000). Regulation of sodium currents through oxidation and reduction of thiol residues. *Neuroscience* 101, 229–236. doi: 10.1016/S0306-4522(00)00367-5

Fink, M., Giles, W. R., and Noble, D. (2006). Contributions of inwardly rectifying K^+ currents to repolarization assessed using mathematical models of human ventricular myocytes. *Philos. Trans. A Math. Phys. Eng. Sci.* 364, 1207–1222. doi: 10.1098/rsta.2006.1765

Gaur, N., Rudy, Y., and Hool, L. (2009). Contributions of ion channel currents to ventricular action potential changes and induction of early afterdepolarizations during acute hypoxia. *Circ. Res.* 105, 1196–1203. doi: 10.1161/CIRCRESAHA.109.202267

Goldstein, M. (2008). Carbon monoxide poisoning. *J. Emerg. Nurs.* 34, 538–542. doi: 10.1016/j.jen.2007.11.014

Gómez, R., Caballero, R., Barana, A., Amorós, I., Calvo, E., López, J. A., et al. (2009). Nitric oxide increases cardiac I_{K1} by nitrosylation of cysteine 76 of Kir2.1 channels. *Circ. Res.* 105, 383–392. doi: 10.1161/CIRCRESAHA.109.197558

Gonzalez, D. R., Treuer, A. V., Castellanos, J., Dulce, R. A., and Hare, J. M. (2010). Impaired S-nitrosylation of the ryanodine receptor caused by xanthine oxidase activity contributes to calcium leak in heart failure. *J. Biol. Chem.* 285, 28938–28945. doi: 10.1074/jbc.M110.154948

Grandi, E., Pasqualini, F. S., and Bers, D. M. (2010). A novel computational model of the human ventricular action potential and Ca transient. *J. Mol. Cell. Cardiol.* 48, 112–121. doi: 10.1016/j.yjmcc.2009.09.019

Haas, J. S., and Landisman, C. E. (2011). State-dependent modulation of gap junction signaling by the persistent sodium current. *Front. Cell. Neurosci.* 5:31. doi: 10.3389/fncel.2011.00031

Haldar, S. M., and Stamler, J. S. (2013). S-nitrosylation: integrator of cardiovascular performance and oxygen delivery. *J. Clin. Invest.* 123, 101–110. doi: 10.1172/JCI62854

Houser, S. R. (2000). When does spontaneous sarcoplasmic reticulum Ca^{2+} release cause a triggered arrythmia? Cellular versus tissue requirements. *Circ. Res.* 87, 725–727. doi: 10.1161/01.RES.87.9.725

Huelsing, D. J., Spitzer, K. W., and Pollard, A. E. (2000). Electrotonic suppression of early afterdepolarization in isolated rabbit Purkinje myocytes. *Am. J. Physiol. Heart Circ. Physiol.* 279, H250–H259.

Jaffrey, S. R., Erdjument-Bromage, H., Ferris, C. D., Tempst, P., and Snyder, S. H. (2001). Protein S-nitrosylation: a physiological signal for neuronal nitric oxide. *Nat. Cell Biol.* 3, 193–197. doi: 10.1038/35055104

Jaggar, J. H., Li, A., Parfenova, H., Liu, J., Umstot, E. S., Dopico, A. M., et al. (2005). Heme is a carbon monoxide receptor for large-conductance Ca^{2+}-activated K^+ channels. *Circ. Res.* 97, 805–812. doi: 10.1161/01.RES.0000186180.47148.7b

January, C. T., and Riddle, J. M. (1989). Early afterdepolarizations: mechanism of induction and block. A role for L-type Ca^{2+} current. *Circ. Res.* 64, 977–990. doi: 10.1161/01.RES.64.5.977

Ju, Y. K., Saint, D. A., and Gage, P. W. (1996). Hypoxia increases persistent sodium current in rat ventricular myocytes. *J. Physiol.* 497, 337–347.

Kawano, T., Zoga, V., Kimura, M., Liang, M. Y., Wu, H. E., Gemes, G., et al. (2009). Nitric oxide activates ATP-sensitive potassium channels in mammalian sensory neurons: action by direct S-nitrosylation. *Mol. Pain* 5, 12. doi: 10.1186/1744-8069-5-12

Kinobe, R. T., Dercho, R. A., and Nakatsu, K. (2008). Inhibitors of the heme oxygenase—carbon monoxide system: on the doorstep of the clinic? *Can. J. Physiol. Pharmacol.* 86, 577–599. doi: 10.1139/Y08-066

Leffler, C. W., Parfenova, H., Jaggar, J. H., and Wang, R. (2006). Carbon monoxide and hydrogen sulfide: gaseous messengers in cerebrovascular circulation. *J. Appl. Physiol.* 100, 1065–1076. doi: 10.1152/japplphysiol.00793.2005

Liu, G. X., Choi, B. R., Ziv, O., Li, W., de Lange, E., Qu, Z., et al. (2012). Differential conditions for early after-depolarizations and triggered activity in cardiomyocytes derived from transgenic LQT1 and LQT2 rabbits. *J. Physiol.* 590, 1171–1180. doi: 10.1113/jphysiol.2011.218164

Madhvani, R. V., Xie, Y., Pantazis, A., Garfinkel, A., Qu, Z., Weiss, J. N., et al. (2011). Shaping a new Ca^{2+} conductance to suppress early afterdepolarizations in cardiac myocytes. *J. Physiol.* 589, 6081–6092. doi: 10.1113/jphysiol.2011.219600

Maines, M. D. (1997). The heme oxygenase system: a regulator of second messenger gases. *Annu. Rev. Pharmacol. Toxicol.* 37, 517–554. doi: 10.1146/annurev.pharmtox.37.1.517

Makielski, J. C., and Valdivia, C. R. (2006). Ranolazine and late cardiac sodium current–a therapeutic target for angina, arrhythmia and more? *Br. J. Pharmacol.* 148, 4–6. doi: 10.1038/sj.bjp.0706713

Maleckar, M. M., Greenstein, J. L., Giles, W. R., and Trayanova, N. A. (2009). Electrotonic coupling between human atrial myocytes and fibroblasts alters myocyte excitability and repolarization. *Biophys. J.* 97, 2179–2190. doi: 10.1016/j.bpj.2009.07.054

Marban, E., Robinson, S. W., and Wier, W. G. (1986). Mechanisms of arrhythmogenic delayed and early afterdepolarizations in ferret ventricular muscle. *J. Clin. Invest.* 78, 1185–1192. doi: 10.1172/JCI112701

Moss, A. J., Zareba, W., Schwarz, K. Q., Rosero, S., McNitt, S., and Robinson, J. L. (2008). Ranolazine shortens repolarization in patients with sustained inward sodium current due to type-3 long-QT syndrome. *J. Cardiovasc. Electrophysiol.* 19, 1289–1293. doi: 10.1111/j.1540-8167.2008.01246.x

Motterlini, R., and Otterbein, L. E. (2010). The therapeutic potential of carbon monoxide. *Nat. Rev. Drug Discov.* 9, 728–743. doi: 10.1038/nrd3228

Núñez, L., Vaquero, M., Gómez, R., Caballero, R., Mateos-Cáceres, P., Macaya, C., et al. (2006). Nitric oxide blocks hKv1.5 channels by S-nitrosylation and by a cyclic GMP-dependent mechanism. *Cardiovasc. Res.* 72, 80–89. doi: 10.1016/j.cardiores.2006.06.021

O'Hara, T., Virag, L., Varro, A., and Rudy, Y. (2011). Simulation of the undiseased human cardiac ventricular action potential: model formulation and experimental validation. *PLoS Comput. Biol.* 7:e1002061. doi: 10.1371/journal.pcbi.1002061

Saint, D. A. (2008). The cardiac persistent sodium current: an appealing therapeutic target? *Br. J. Pharmacol.* 153, 1133–1142. doi: 10.1038/sj.bjp.0707492

Sarkar, A. X., Christini, D. J., and Sobie, E. A. (2012). Exploiting mathematical models to illuminate electrophysiological variability between individuals. *J. Physiol.* 590(pt 11), 2555–2567. doi: 10.1113/jphysiol.2011.223313

Sarkar, A. X., and Sobie, E. A. (2011). Quantification of repolarization reserve to understand interpatient variability in the response to proarrhythmic drugs: a computational analysis. *Heart Rhythm* 8, 1749–1755. doi: 10.1016/j.hrthm.2011.05.023

Shampine, L. F., and Reichelt, M. W. (1997). The MATLAB ODE suite. *SIAM J. Sci. Comput.* 18, 1–22. doi: 10.1137/S1064827594276424

Spitzer, K. W., Pollard, A. E., Yang, L., Zaniboni, M., Cordeiro, J. M., and Huelsing, D. J. (2006). Cell-to-cell electrical interactions during early and late repolarization. *J. Cardiovasc. Electrophysiol.* 17(Suppl. 1), S8–S14. doi: 10.1111/j.1540-8167.2006.00379.x

Tamargo, J., Caballero, R., Gómez, R., and Delpón, E. (2010). Cardiac

electrophysiological effects of nitric oxide. *Cardiovasc. Res.* 87, 593–600. doi: 10.1093/cvr/cvq214

Tao, T., Paterson, D. J., and Smith, J. P. (2011). A model of cellular cardiac-neutral coupling that captures the sympathetic control of sinoatrial node excitability in normotensive and hypertensive rats. *Biophys. J.* 101, 594–602. doi: 10.1016/j.bpj.2011.05.069

Terkildsen, J. R., Niederer, S., Crampin, E. J., Hunter, P., and Smith, N. P. (2008). Using Physiome standards to couple cellular functions for rat cardiac excitation-contraction. *Exp. Physiol.* 93, 919–929. doi: 10.1113/expphysiol.2007.041871

Thomas, G., Killeen, M. J., Grace, A. A., and Huang, C. L. (2008). Pharmacological separation of early afterdepolarizations from arrhythmogenic substrate in DeltaKPQ Scn5a murine hearts modelling human long QT 3 syndrome. *Acta Physiol.* 192, 505–517. doi: 10.1111/j.1748-1716.2007.01770.x

Trenor, B., Cardona, K., Gomez, J. F., Rajamani, S., Ferrero, J. M., Belardinelli, L., et al. (2012). Simulation and mechanistic investigation of the arrhythmogenic role of the late sodium current in human heart failure. *PLoS ONE* 7:e32659. doi: 10.1371/journal.pone.0032659

Trenor, B., Gomis-Tena, J., Cardona, K., Romero, L., Rajamani, S., Belardinelli, L., et al. (2013). *In silico* assessment of drug safety in human heart applied to late sodium current blockers. *Channels (Austin)* 7, 1–14. doi: 10.4161/chan.24905

Ueda, K., Valdivia, C., Medeiros-Domingo, A., Tester, D. J., Vatta, M., Farrugia, G., et al. (2008). Syntrophin mutation associated with long QT syndrome through activation of the nNOS-SCN5A macromolecular complex. *Proc. Natl. Acad. Sci. U.S.A.* 105, 9355–9360. doi: 10.1073/pnas.0801294105

Varró, A., and Baczkó, I. (2011). Cardiac ventricular repolarization reserve: a principle for understanding drug-related proarrhythmic risk. *Br. J. Pharmacol.* 164, 14–36. doi: 10.1111/j.1476-5381.2011.01367.x

Wang, H., Viatchenko-Karpinski, S., Sun, J., Györke, I., Benkusky, N. A., Kohr, M. J., et al. (2010). Regulation of myocyte contraction via neuronal nitric oxide synthase: role of ryanodine receptor S-nitrosylation. *J. Physiol.* 588(pt 15), 2905–2917. doi: 10.1113/jphysiol.2010.192617

Wilkinson, W. J., and Kemp, P. J. (2011). Carbon monoxide: an emerging regulator of ion channels. *J. Physiol.* 589, 3055–3062. doi: 10.1113/jphysiol.2011.206706

Winslow, R. L., Cortassa, S., O'Rourke, B., Hashambhoy, Y. L., Rice, J. J., and Greenstein, J. L. (2011). Integrative modeling of the cardiac ventricular myocyte. *Wiley Interdiscip. Rev. Syst. Biol. Med.* 3, 392–413. doi: 10.1002/wsbm.122

Wu, L., Rajamani, S., Li, H., January, C. T., Shryock, J. C., and Belardinelli, L. (2009). Reduction of repolarization reserve unmasks the proarrhythmic role of endogenous late Na^+ current in the heart. *Am. J. Physiol. Heart Circ. Physiol.* 297, H1048–H1057. doi: 10.1152/ajpheart.00467.2009

Wu, L., and Wang, R. (2005). Carbon monoxide: endogenous production, physiological functions, and pharmacological applications. *Pharmacol. Rev.* 57, 585–630. doi: 10.1124/pr.57.4.3

Yakushev, S., Band, M., Tissot van Patot, M. C., Gassmann, M., Avivi, A., and Bogdanova, A. (2012). Cross talk between S-nitrosylation and S-glutathionylation in control of the Na,K-ATPase regulation in hypoxic heart. *Am. J. Physiol. Heart Circ. Physiol.* 303, H1332–H1343. doi: 10.1152/ajpheart.00145.2012

Zaniboni, M., Pollard, A. E., Yang, L., and Spitzer, K. W. (2000). Beat-to-beat repolarization variability in ventricular myocytes and its suppression by electrical coupling. *Am. J. Physiol. Heart Circ. Physiol.* 278, SH677–SH687.

Zaza, A., Belardinelli, L., and Shryock, J. C. (2008). Pathophysiology and pharmacology of the cardiac "late sodium current." *Pharmacol. Ther.* 119, 326–339. doi: 10.1016/j.pharmthera.2008.06.001

Conflict of Interest Statement: The authors declare that the research was conducted in the absence of any commercial or financial relationships that could be construed as a potential conflict of interest.

Received: 30 July 2013; paper pending published: 14 August 2013; accepted: 18 September 2013; published online: 17 October 2013.

*Citation: Trenor B, Cardona K, Saiz J, Rajamani S, Belardinelli L and Giles WR (2013) Carbon monoxide effects on human ventricle action potential assessed by mathematical simulations. Front. Physiol. **4**:282. doi: 10.3389/fphys.2013.00282*

This article was submitted to Cardiac Electrophysiology, a section of the journal Frontiers in Physiology.

frontiers in PHYSIOLOGY

ORIGINAL RESEARCH ARTICLE
published: 05 July 2013
doi: 10.3389/fphys.2013.00166

In silico investigation of the short QT syndrome, using human ventricle models incorporating electromechanical coupling

Ismail Adeniran[1], Jules C. Hancox[2] and Henggui Zhang[1,3]*

[1] Computational Biology, Biological Physics Group, School of Physics and Astronomy, The University of Manchester, Manchester, UK
[2] School of Physiology and Pharmacology, and Cardiovascular Research Laboratories, School of Medical Sciences, University of Bristol, Bristol, UK
[3] School of Computer Science and Technology, Harbin Institute of Technology, Harbin, China

Edited by:
Christopher Huang, University of Cambridge, UK

Reviewed by:
Christopher Huang, University of Cambridge, UK
James A. Fraser, University of Cambridge, UK

***Correspondence:**
Henggui Zhang, Biological Physics Group, School of Physics and Astronomy, The University of Manchester, Room 3.07, Schuster Building, Brunswick Street, Oxford Road, Manchester, M13 9PL, UK
e-mail: henggui.zhang@manchester.ac.uk

Introduction: Genetic forms of the Short QT Syndrome (SQTS) arise due to cardiac ion channel mutations leading to accelerated ventricular repolarization, arrhythmias and sudden cardiac death. Results from experimental and simulation studies suggest that changes to refractoriness and tissue vulnerability produce a substrate favorable to re-entry. Potential electromechanical consequences of the SQTS are less well-understood. The aim of this study was to utilize electromechanically coupled human ventricle models to explore electromechanical consequences of the SQTS.

Methods and Results: The Rice et al. mechanical model was coupled to the ten Tusscher et al. ventricular cell model. Previously validated K^+ channel formulations for SQT variants 1 and 3 were incorporated. Functional effects of the SQTS mutations on $\left[Ca^{2+}\right]_i$ transients, sarcomere length shortening and contractile force at the single cell level were evaluated with and without the consideration of stretch-activated channel current (I_{sac}). Without I_{sac}, at a stimulation frequency of 1Hz, the SQTS mutations produced dramatic reductions in the amplitude of $\left[Ca^{2+}\right]_i$ transients, sarcomere length shortening and contractile force. When I_{sac} was incorporated, there was a considerable attenuation of the effects of SQTS-associated action potential shortening on Ca^{2+} transients, sarcomere shortening and contractile force. Single cell models were then incorporated into 3D human ventricular tissue models. The timing of maximum deformation was delayed in the SQTS setting compared to control.

Conclusion: The incorporation of I_{sac} appears to be an important consideration in modeling functional effects of SQT 1 and 3 mutations on cardiac electro-mechanical coupling. Whilst there is little evidence of profoundly impaired cardiac contractile function in SQTS patients, our 3D simulations correlate qualitatively with reported evidence for dissociation between ventricular repolarization and the end of mechanical systole.

Keywords: short QT syndrome, stretch-activated channel, mechanical contraction, 3D model, human ventricles

INTRODUCTION

The short QT syndrome (SQTS) was first recognized as a distinct clinical entity in 2000 (Gussak et al., 2000). It is characterized by an abnormally short QT interval on the ECG with a QT_C interval of ~320 ms or less, tall and peaked T-waves, and increased $T_{peak}-T_{end}$ width (Anttonen et al., 2009; Patel and Pavri, 2009; Couderc and Lopes, 2010; Cross et al., 2011; Gollob et al., 2011). Patients usually have structurally normal hearts and affected families tend to exhibit histories of syncope, abbreviated atrial and ventricular refractory periods, as well as increased susceptibility to atrial and ventricular arrhythmias and sudden death (Gaita et al., 2003; Schimpf et al., 2005; Giustetto et al., 2006; Hancox et al., 2011).

There are currently six identified forms of the genetic SQTS (SQT1–SQT6). SQT1-3 result from *gain-of-function* mutations to K^+ channel subunits. For SQT1, these mutations are to the *KCNH2* (*hERG*) gene encoding the α-subunit of the rapidly-activating delayed rectifier K^+ channel I_{Kr} (Brugada et al., 2004; Hong et al., 2005a; Sun et al., 2011). The SQT2 variant arises from mutations to the *KCNQ1* gene encoding the α-subunit of the slowly-activating delayed rectifier K^+ channel I_{Ks} (Bellocq et al., 2004; Hong et al., 2005b), whilst SQT3 involves mutations to the *KCNJ2* gene encoding the Kir 2.1 protein, which underlie the inwardly-rectifying K^+ current I_{K1} (Priori et al., 2005; Hattori et al., 2011; Deo et al., 2013). SQT4–SQT6 are due, respectively, to *loss-of-function* mutations to the *CACNA1C*, *CACNB2b* (Antzelevitch et al., 2007) and *CACNA2D1* (Templin et al., 2011) genes encoding the α1C, β2b, and α2δ-1- subunits of the L-type Ca^{2+} channel.

Pro-arrhythmic mechanisms in the SQTS have been investigated through the application of K^+ channel openers to left ventricular wedge preparations (e.g., Extramiana and Antzelevitch,

2004; Patel and Antzelevitch, 2008). Data from these experiments have been suggestive of a role for amplified transmural dispersion of repolarization and abbreviation of effective refractory period in the arrhythmogenic substrate in the SQTS (e.g., Extramiana and Antzelevitch, 2004; Patel and Antzelevitch, 2008). However, at present there are no phenotypically accurate animal models of the SQTS, making *in silico* approaches attractive for exploring the consequences of identified SQTS mutations. Computer models have reproduced QT interval shortening produced by K^+ channel mutations in the syndrome (Zhang and Hancox, 2004; Priori et al., 2005; Weiss et al., 2005; Zhang et al., 2008; Adeniran et al., 2011, 2012; Deo et al., 2013). Using a Markov-model of the N588K-hERG SQT1 mutation based on experimental data from recombinant wild-type and N588K-hERG channels, we have recently shown that this SQT1 mutation reduces substrate size and increases tissue vulnerability to premature stimuli in order to facilitate and maintain re-entrant excitation waves in 2D and 3D tissue. We have also shown that the SQT3 D172N Kir2.1 mutation increases tissue vulnerability, alters excitability, stabilizes and accelerates re-entry (Adeniran et al., 2012).

Although the SQTS is an electrical disorder, the heart is both an electrical and mechanical organ and it is feasible, at least in principle, that abbreviated repolarization in the syndrome might influence the mechanical function of the heart. In SQTS patients, there is some evidence of significant dissociation between ventricular repolarization and the end of mechanical systole (Schimpf et al., 2008). All modeling studies to-date that have investigated arrhythmogenesis in the SQTS have utilized ventricular cell and tissue electrical models that do not consider mechanical properties (Zhang and Hancox, 2004; Priori et al., 2005; Weiss et al., 2005; Zhang et al., 2008; Adeniran et al., 2011, 2012; Deo et al., 2013). Through mechano-electric feedback, the heart is able to regulate its electrical activity in response to changes in contractility or volume load (Lab, 1982, 1996; Franz, 1996). This regulation is believed to occur through the activation of stretch-activated channels (SACs) (Taggart, 1996; Bett and Sachs, 1997; Hu and Sachs, 1997; Youm et al., 2005). As potential electromechanical consequences of the SQTS are incompletely understood, the present study was conducted in order: (1) to investigate the potential functional consequences of the SQTS on ventricular contraction at the single cell, tissue and organ levels in the presence and absence of a stretch-activated current (I_{sac}) and (2) to evaluate the relationship between ventricular repolarization and mechanical systole in the setting of the SQTS. In order to address these aims, established models of the SQT1 and SQT3 K^+-channel-linked SQTS variants (Adeniran et al., 2011, 2012) were coupled to a validated mechanical model (Rice et al., 2008).

MATERIALS AND METHODS

SQT1 (I_{Kr}) AND SQT3 (I_{K1}) FORMULATIONS

For SQT1, we used a biophysically-detailed Markov chain model formulation which incorporates the experimentally observed kinetic properties of wild-type (WT) and N588K-mutated hERG/I_{Kr} channel current at 37°C (Adeniran et al., 2011). For SQT3, we employed a biophysically-detailed Hodgkin-Huxley model formulation (Adeniran et al., 2012), which also incorporates the experimentally observed kinetic properties of the D172N-mutant Kir 2.1 channel at 37°C.

ELECTROMECHANICAL MODEL

For electrophysiology, we utilized the ten Tusscher and Panfilov (TP) human ventricular single cell model (Ten Tusscher and Panfilov, 2006), which recapitulates human ventricular cell electrical and membrane channel properties and the transmural heterogeneity of ventricular action potential (AP) across the ventricular wall (Ten Tusscher et al., 2004; Ten Tusscher and Panfilov, 2006). The TP model was modified and updated in 2006 to incorporate newly available experimental data (Xia et al., 2006); these modifications were also employed in the present study. This approach mirrors that used in our recent studies of electrical consequences of the SQT1 and SQT3 mutations (Adeniran et al., 2011, 2012).

We used the Rice et al. myocyte contraction model (Rice et al., 2008) to describe the mechanics of a cardiac myocyte. This model was chosen as it is based on the cross-bridge cycling model of cardiac muscle contraction and is able to replicate a wide range of experimental data including steady-state force-sarcomere length (F-SL), force-calcium and sarcomere length-calcium relations (Rice et al., 2008).

The intracellular calcium concentration $\left[Ca^{2+}\right]_i$ from the electrophysiology model (EP) was used as the coupling link to the myofilament mechanics model (MM). $\left[Ca^{2+}\right]_i$ produced as dynamic output from the EP model during the time course of the AP served as input to the MM model from which the amount bound to troponin is calculated. The formulation of the myoplasmic Ca^{2+} concentration in the EP model is:

$$\frac{dCa_i}{dt} = Ca_{\text{ibufc}}\left(\frac{V_{\text{sr}}}{V_c}\left(I_{\text{leak}} - I_{\text{up}}\right) + I_{\text{xfer}}\right) - C_m\frac{I_{\text{bca}} + I_{\text{pca}} - 2I_{\text{NaCa}}}{2V_cF} \quad (1)$$

where Ca_{ibufc} is the total cytoplasmic buffer concentration, V_{sr} is the sarcoplasmic reticulum (SR) volume, V_c is the cytoplasmic volume, I_{leak} is the SR Ca^{2+} leak current, I_{up} is the SR Ca^{2+} pump current, I_{xfer} is the diffusive Ca^{2+} current current between dyadic Ca^{2+} subspace and bulk cytoplasm, C_m is the membrane cell capacitance per unit surface area, I_{bCa} is the background Ca^{2+} current, I_{pCa} is the plateau Ca^{2+} current, I_{NaCa} is the Na^+/Ca^{2+} exchanger and F is the Faraday constant.

The flux of the binding of Ca^{2+} to troponin was incorporated into Equation 1 as follows:

$$\frac{dCa_i}{dt} = Ca_{\text{ibufc}}\left(\frac{V_{\text{sr}}}{V_c}\left(I_{\text{leak}} - I_{\text{up}}\right) + I_{\text{xfer}}\right) - C_m\frac{I_{\text{bCa}} + I_{\text{pCa}} - 2I_{\text{NaCa}}}{2V_cF} - \frac{dTropTot_{\text{Ca}}}{dt} \times \frac{1}{1000} \quad (2)$$

where $\frac{dTropTot_{\text{Ca}}}{dt}$ is the rate of Ca^{2+} binding to troponin. The combination of all state variables from the EP model with the MM model and the substitution of (Equation 2) for (Equation 1) yielded a human ventricular myocyte electromechanical cell model.

STRETCH-ACTIVATED CURRENT

In accord with previous studies (Kohl and Sachs, 2001; Panfilov et al., 2005; Youm et al., 2005; Kuijpers, 2008; Lunze et al., 2010), we incorporated a stretch-activated current (I_{sac}) into the electromechanics model using the following formulation:

$$I_{sac} = G_{sac} \times P_m \times (V_m - E_{sac}) \tag{3}$$

where G_{sac} and E_{sac} are the maximum channel conductance and reversal potential of the SAC, respectively. In the electromechanics model, E_{sac} was typically set to 1 mV and describes the experimentally observed depolarizing effect of the channel (Kohl et al., 1999; Trayanova et al., 2004). V_m is the membrane potential and P_m is the channel's open probability modeled as:

$$P_m = \frac{1.0}{1 + e^{-\left(\frac{\varepsilon - \varepsilon_{1/2}}{k_e}\right)}} \tag{4}$$

where ε and $\varepsilon_{1/2}$ are the strain (with an explicit dependence on the sarcomere length) and half-activation strain, respectively, $K_e = 0.02$ (Zabel et al., 1996; Youm et al., 2005; Lunze et al., 2010) is the activation slope.

The SAC is assumed to be permeable to Na^+, K^+ and Ca^{2+} (Kamkin et al., 2000; Youm et al., 2005; Kuijpers, 2008) with I_{sac} therefore defined as:

$$I_{sac} = I_{sac,\,Na} + I_{sac,\,K} + I_{sac,\,Ca} \tag{5}$$

where $I_{sac,\,Na}$, $I_{sac,\,K}$, and $I_{sac,\,Ca}$ are the contributions of Na^+, K^+ and Ca^{2+} to I_{sac}. To evaluate the effects of the permeability of the SAC to Na^+, K^+, and Ca^{2+}, two permeability ratio cases were considered in the single cell simulations: $P_{Na} : P_K : P_{Ca} = 1{:}1{:}0$ and $P_{Na} : P_K : P_{Ca} = 1{:}1{:}1$ where P_{Na}, P_K, and P_{Ca} are the relative permeabilities of the channel to Na^+, K^+ and Ca^{2+}, respectively.

TISSUE MECHANICS MODEL

We modeled cardiac tissue mechanics within the theoretical framework of non-linear elasticity (Marsden and Hughes, 1994; Holzapfel, 2000) as an inhomogeneous, anisotropic, nearly incompressible non-linear material similar to previous studies (Hunter et al., 1997; Costa et al., 2001; Whiteley et al., 2007; Niederer and Smith, 2008; Pathmanathan and Whiteley, 2009). We used a two-field variational principle with the deformation u and the hydrostatic pressure p as the two fields (Lions and Ciarlet, 1994; Holzapfel, 2000; Bonet and Wood, 2008). p is utilized as the Lagrange multiplier to enforce the near incompressibility constraint. Thus, the total potential energy functional Π for the mechanics problem is formulated as:

$$\Pi(u, p) = \Pi_{int}(u, p) + \Pi_{ext}(u) \tag{6}$$

where $\Pi_{int}(u, p)$ is the internal potential energy or total strain energy of the body and $\Pi_{ext}(u)$ is the external potential energy or potential energy of the external loading of the body. With the axes of the geometry aligned to the underlying tissue microstructure (Seemann et al., 2006; Legrice et al., 1997), the second Piola-Kirchhoff stress tensor S, obtained from the directional derivative of Equation 6 in the direction of an arbitrary virtual displacement and which relates a stress to a strain measure (Holzapfel, 2000; Bonet and Wood, 2008) is defined as:

$$S = \frac{1}{2}\left(\frac{\partial W}{\partial E_{MN}} + \frac{\partial W}{\partial E_{NM}}\right) - pC_{MN}^{-1} + S_{ActiveTension} \tag{7}$$

where W is a strain energy function that defines the constitutive behavior of the material, E is the Green-Lagrange strain tensor that quantifies the length changes in a material fiber and angles between fiber pairs in a deformed solid, C is the Right-Cauchy green strain tensor, p is a Lagrange multiplier (referred to as the hydrostatic pressure in the literature) used to enforce incompressibility of the cardiac tissue, $S_{ActiveTension}$ is a stress tensor incorporating active tension from the electromechanics cell model and enables the reproduction of the three physiological movements of the ventricular wall: longitudinal shortening, wall thickening and rotational twisting (MacGowan et al., 1997; Lorenz et al., 2000; Tseng et al., 2000; Bogaert and Rademakers, 2001; Cheng et al., 2008; Coppola and Omens, 2008; Lilli et al., 2013).

For the strain energy function W, we used the Guccione constitutive law (Guccione et al., 1991) given by:

$$W = C_1 e^Q \tag{8}$$

Where

$$Q = C_2 E_{11}^2 + C_3\left(E_{22}^2 + E_{33}^2 + 2E_{23}^2\right) + 2C_4(E_{12}E_{21} + E_{13}E_{31}) \tag{9}$$

following previous work (Land et al., 2012), $C_1 = 0.831$ kPa, $C_2 = 14.31$, $C_3 = 4.49$, $C_4 = 10$. E_{ij} are the components of the Green-Lagrange strain tensor.

TISSUE ELECTROPHYSIOLOGY MODEL

The monodomain representation (Colli Franzone et al., 2005; Potse et al., 2006; Keener and Sneyd, 2008) of cardiac tissue was used for the electrophysiology model with a modification (the incorporation of the Right Cauchy Green deformation tensor $\boldsymbol{C}$), which allows the monodomain equation to take into account the effect of the deforming tissue, similar to previous studies (Nash and Panfilov, 2004; Whiteley et al., 2007; Pathmanathan and Whiteley, 2009):

$$C_m \frac{dV}{dt} = -(I_{ion} + I_{stim}) + \nabla \times (DC^{-1}\nabla V) \tag{10}$$

where C_m is the cell capacitance per unit surface area, V is the membrane potential, I_{ion} is the sum of all transmembrane ionic currents from the electromechanics single cell model, I_{stim} is an externally applied stimulus and D is the diffusion tensor. In simulations, intracellular conductivities in the fiber, cross-fiber and sheet directions were set to 3.0, 1.0, and 0.31525 ms mm^{-1}, respectively. These gave a conduction velocity of 65 cm s^{-1} in the

fiber direction along multiple cells, which is close to the value 70 cm s^{-1} observed in the fiber direction in human myocardium (Taggart et al., 2000).

COMPUTATIONAL METHODS

Geometry and meshes

The 3D simulations were carried out on a DT-MRI reconstructed anatomical human ventricle geometry, incorporating anisotropic fiber orientation, from a healthy 34-year-old male. This had a spatial resolution of 0.2 mm and approximately 24.2 million nodes in total and was segmented into distinct ENDO (25%), MCELL (35%), and EPI (40%) regions. The chosen cell proportion in each region is similar to those used in other studies (Gima and Rudy, 2002; Zhang et al., 2008; Adeniran et al., 2011, 2012). The conditional activation sites were determined empirically across the ventricle wall and were validated by reproducing the activation sequence and QRS complex in the measured 64-channel ECG (Keller et al., 2009) of that person.

Solving the electromechanics problem

The electromechanics problem consists of two sub-problems: the electrophysiology problem and the mechanics problem. The electrophysiology problem (Equation 10) was solved with a Strang splitting method (Sundnes et al., 2005) ensuring that the solution is second-order accurate. It was discretized in time using the Crank-Nicholson method (Burnett, 1987), which is also second-order accurate and discretized in space with Finite Elements (Burnett, 1987; Braess, 2007; Brenner and Scott, 2010; Ern and Guermond, 2010). I_{ion} in (Equation 10) represents the single cell electromechanics model from which the active tension input to the Tissue mechanics model for contraction is obtained. The system of ordinary differential equations (ODE) composing I_{ion} was solved with a combination of the Rush-Larsen scheme (Rush and Larsen, 1978) and the CVODE solver (Cohen et al., 1996; Hindmarsh et al., 2005).

The mechanics problem (Equation 6) was also solved using the Finite element Method using the automated scientific computing library, FEniCS (Logg et al., 2012). The resulting non-linear system of equations was solved iteratively using the Newton method to determine the equilibrium configuration of the system. The value of the Right Cauchy Green Tensor C was then used to update the diffusion coefficient tensor in Equation 10. Over a typical finite element domain, P_2 elements (Braess, 2007; Brenner and Scott, 2010; Ern and Guermond, 2010) were used to discretize the displacement variable u, while the pressure variable p was discretized with P_1 elements (Braess, 2007; Brenner and Scott, 2010; Ern and Guermond, 2010). This P_2–P_1 mixed finite element has been proven to ensure stability (Chamberland et al., 2010; Haga et al., 2012; Logg et al., 2012) and an optimal convergence rate (Hughes, 2000; Chamberland et al., 2010; Ern and Guermond, 2010).

The algorithm for solving the full electromechanics problem is as follows:

1. Determine the initial deformation and obtain the value of the Right Cauchy Green Tensor C.
2. While time $< t_{end}$:
   a. Solve the electrophysiology problem for $\Delta t_{mechanics} =$ 1 ms with C as input and active tension T_a as output ($\Delta t_{electrophysiology} = 0.01$ ms).
   b. Project T_a from the electrophysiology mesh onto the mechanics mesh.
   c. Solve the mechanics problem with T_a as input and C as output.

RESULTS

SINGLE CELL ELECTROMECHANICAL SIMULATIONS

Simulations without incorporation of I_{sac}

Initial simulations, in the absence of I_{sac}, were performed using the coupled electromechanics model for the WT condition for each of ENDO, MCELL, and EPI conditions. **Figure 1** shows the electrophysiological consequences of the SQT1 and SQT3 mutations in EPI, MCELL, and ENDO cell types at a stimulation frequency of 1 Hz (**Figures 1Ai–Ci**). For the EPI cell, action potential duration at 90% repolarization (APD_{90}) was 317 ms under WT conditions and was shortened to 212 ms and 283 ms respectively under SQT1 and SQT3 conditions. For the MCELL, WT APD_{90} was 441 ms, whilst it was 232 and 382 ms under SQT1 and SQT3 conditions, respectively. For the ENDO cell model, WT APD_{90} was 317 ms, whilst it was 211 and 284 ms under SQT1 and SQT3 respectively. The observed APD shortening was more extensive for SQT1 than SQT3 and this is explicable on the basis of the relative timings and roles of I_{Kr} and I_{K1} during ventricular AP repolarization. As shown in **Figures 1Aii–Cii**, the SQT1 N588K mutation produced a large increase in I_{Kr} together with a change in the current's profile that resulted in a significant augmentation of I_{Kr} and shift in timing of maximal current to be earlier during the AP plateau (see also Adeniran et al., 2011). The D172N mutation significantly increased I_{K1} magnitude (**Figures 1 Aiii–Ciii**), but as I_{K1} contributes to terminal AP repolarization, the consequence of the mutation for APD shortening was less extensive than that for the SQT1 mutation. The electrophysiological consequences of the SQT1 and SQT3 mutations in these simulations are comparable to those reported previously from non-mechanically coupled ventricular cell models (Adeniran et al., 2011, 2012).

To validate the electromechanics model, we simulated force-frequency relationship (FFR) by stimulating the single cell at different frequencies for 1000 beats until steady state, recorded the maximum force developed and plotted it against frequency and compared it to experimental data (Mulieri et al., 1992). The results are shown in **Figure 2**. In the frequency range, 1–2 Hz, the electromechanics model produced an FFR which is qualitatively comparable to experimental data (vertical dashed lines) (Mulieri et al., 1992) and showed the Bowditch staircase or Treppe effect (Woodworth, 1902; Mulieri et al., 1992; Lakatta, 2004). All subsequent simulations in this study were carried out at 1 Hz. We then proceeded to characterize the calcium and contractile properties of the electromechanically coupled WT cell models. **Figure 3** shows the action potential (AP), $\left[Ca^{2+}\right]_i$ transient, sarcomere length shortening (SLs): EPI (**Figures 3Ai–Aiv**), MCELL (**Figures 3Bi–Biv**), and ENDO (**Figures 3Ci–Civ**). The larger $\left[Ca^{2+}\right]_i$ transient (and hence contraction) of the MCELL compared to EPI and ENDO cells is consistent with experimental data (McIntosh et al., 2000).

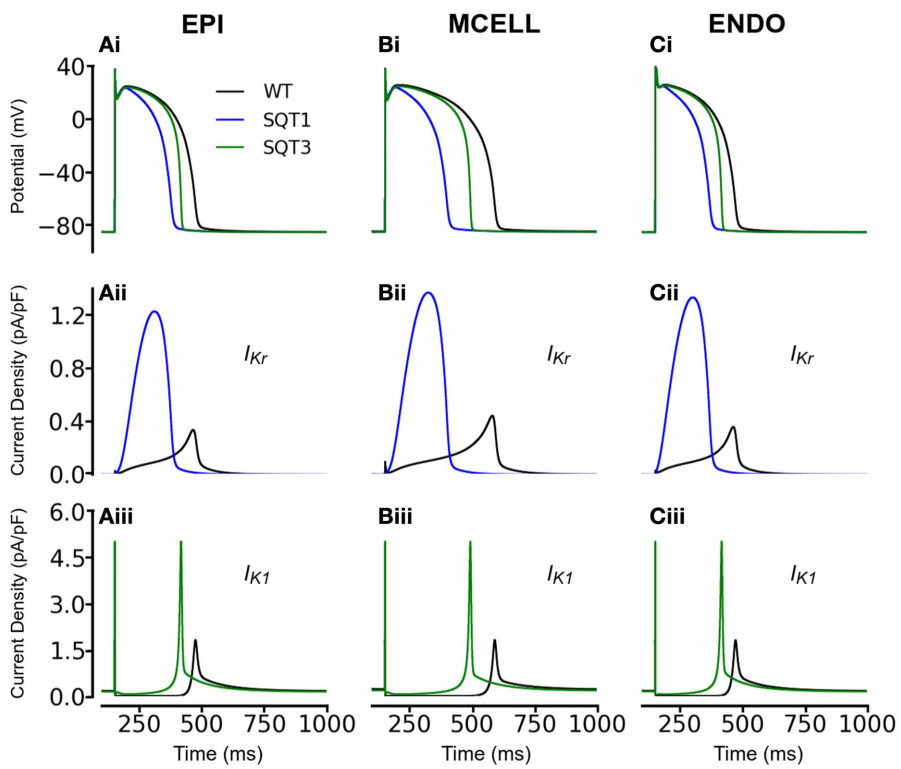

FIGURE 1 | Simulation of ventricular action potentials and the time course of I_{Kr} and I_{K1}. (Ai–Ci) Steady state (at a stimulation frequency of 1 Hz) action potentials for EPI **(Ai)**, MCELL **(Bi)**, and ENDO **(Ci)** cells under wild-type (WT; black), SQT1 (blue) and SQT3 (green) conditions. **(Aii–Cii)** Corresponding I_{Kr} current profiles for EPI **(Aii)**, MCELL **(Bii)**, and ENDO **(Cii)** cells under the WT (black) and SQT1 (blue) conditions. **(Aiii–Ciii)** Corresponding I_{K1} current profiles for EPI **(Aiii)**, MCELL **(Biii)**, and ENDO **(Ciii)** cells under the WT (black) and SQT1 (blue) conditions.

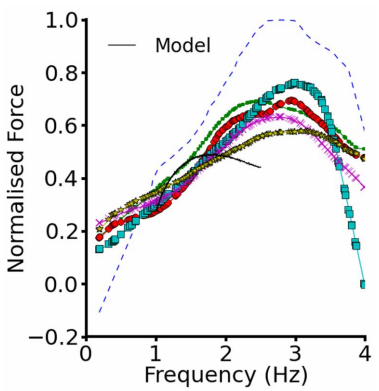

FIGURE 2 | Force-frequency relationship. Plot of steady state normalized active force vs. heart rate using the EPI cell model. Black continuous line represents the WT electromechanics model while symbols represent experimental data from non-failing control preprarations of human myocardium. Experimental data from Mulieri et al. (1992).

Figure 3 also shows the effects of incorporating the SQT1 and SQT3 mutations on the AP, $[Ca^{2+}]_i$ transient, SL shortening and active force in the coupled electromechanics single cell models. Both mutations shortened the AP (**Figures 3Ai–Ci**), reduced the amplitude of $[Ca^{2+}]_i$ (**Figures 3Aii–Cii**) and SL shortening (**Figures 3Aiii–Ciii**) in each of the EPI, MCELL, and ENDO cell models. These effects led to the attenuation of contractility (percentage of WT) in all the cell types (**Figures 3Aiv–Civ**) (SQT1 EPI 30%; SQT3 EPI 76%; SQT1 MCELL 44%; SQT3 MCELL 83%; SQT1 ENDO 41%; SQT3 ENDO 78%). As identified in **Figure 1**, the effects for the SQT3 mutation were not as pronounced as the SQT1 mutation because of the relative timing of I_{Kr} and I_{K1} during the AP, with the SQT3 mutation influencing only terminal repolarization and consequently giving rise to longer APDs across the ventricular wall.

The observed reduction in the active force under the mutation conditions in **Figure 3** was profound, particularly in the case of SQT1. In order to elucidate the mechanism causing such a decrease in contractile force, we performed a simulated "AP clamp" experiment on the WT electromechanics model (**Figure 4**), using two different AP profiles—one AP of a normal duration and the other AP with an abbreviated duration. In this experiment, WT I_{Kr} and I_{K1} formulations were used, therefore any observed alterations to $[Ca^{2+}]_i$ and contractile force would relate to APD *per se*. **Figure 4A** shows the two AP clamp commands used. **Figure 4B** shows the AP-evoked I_{CaL} whilst **Figures 4C–E** respectively show $[Ca^{2+}]_i$, active force, and the difference in steady state level of free calcium concentration in the sarcoplasmic reticulum (CaSR). The results of these simulations

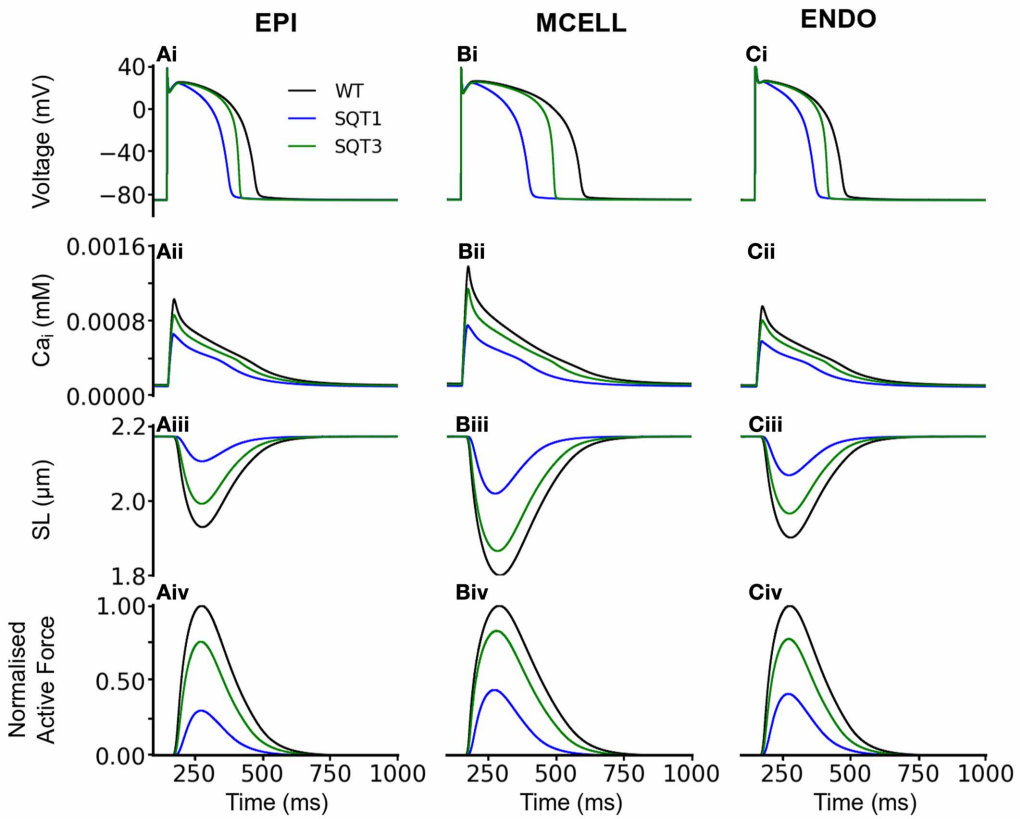

FIGURE 3 | Single cell effects of the SQT1 and SQT3 mutations (without I_{sac}). (Ai–Ci) WT (black), SQT1 (blue) and SQT3 (green) action potentials in the EPI **(Ai)**, MCELL **(Bi)**, and ENDO **(Ci)** cell models. **(Aii–Cii)** WT (black), SQT1 (blue) and SQT3 (green) intracellular calcium concentration and Ca^{2+} transients in the EPI **(Aii)**, MCELL **(Bii)**, and ENDO **(Cii)** cell models. **(Aiii–Ciii)** WT (black), SQT1 (blue) and SQT3 (green) sarcomere length (SL) in the EPI **(Aiii)**, MCELL **(Biii)**, and ENDO **(Ciii)** cell models. **(Aiv–Civ)** WT (black), SQT1 (blue) and SQT3 (green) active force in the EPI **(Aiv)**, MCELL **(Biv)**, and ENDO **(Civ)** cell models. Values are normalized to WT maximum active force for each cell type.

showed that though the shorter AP did not alter notably the peak amplitude of I_{CaL}, it reduced the amplitude of the $\left[Ca^{2+}\right]_i$ transient, SL shortening and the active force and—notably—SR calcium content (CaSR). These effects are similar to the results shown in **Figure 3** for the SQT models. However, in the AP clamp simulation, any observed reduction in amplitude of $\left[Ca^{2+}\right]_i$, SL shortening, CaSR and the active force can be attributed solely to consequences of application of the shorter AP waveform. This suggests that the key reason for the reduced active force in the SQTS setting (**Figure 3**) is the indirect effect of the SQT mutation-linked AP shortening on Ca^{2+} handling (and on SR content in particular).

To investigate further the functional impact of AP duration on the loading of SR calcium content at the steady state, we applied conditioning trains containing one of two different AP clamp commands (one with a longer and the other with a shorter AP duration) to the WT electromechanics model; the conditioning train was followed by an identical single square voltage command to +10 mV for 300 ms (**Figure 5A**). With the conditioning train of APs comprised of the longer duration AP, it was observed that the +10 mV square pulse command produced a larger $\left[Ca^{2+}\right]_i$ transient than that when conditioning trains of shorter duration APs were applied. Results are shown in **Figure 5C**. With the conditioning AP trains of different durations, the square pulse elicited an identical I_{CaL} (**Figure 5B**), but a smaller $\left[Ca^{2+}\right]_i$ amplitude (**Figure 5C**) and active force (**Figure 5D**) for the shorter duration AP. These simulations also showed that prior to the square pulse command, the SR was filled to a greater level with the longer duration conditioning APs than with those of shorter duration,(as illustrated by the steady state CaSR in **Figure 5E**). This further validates the notion that the attenuation of $\left[Ca^{2+}\right]_i$ amplitude and contractility with the SQT mutations was consequent upon reduced SR content associated with abbreviation of AP duration.

Incorporation of I_{sac}

We then performed comparable simulations with the incorporation of I_{sac}. **Figures 6**, **7** show the results with the SAC assumed to be permeable to Na^+, K^+ and Ca^{2+} in the ratio 1:1:0 (**Figure 6**) and 1:1:1 (**Figure 7**). The resting potential for EPI, MCELL and ENDO decreased from −86 to −76 mV (I_{sac} at 1:1:0 permeability ratio) and to −79 mV (I_{sac} at 1:1:1 permeability ratio) for the WT

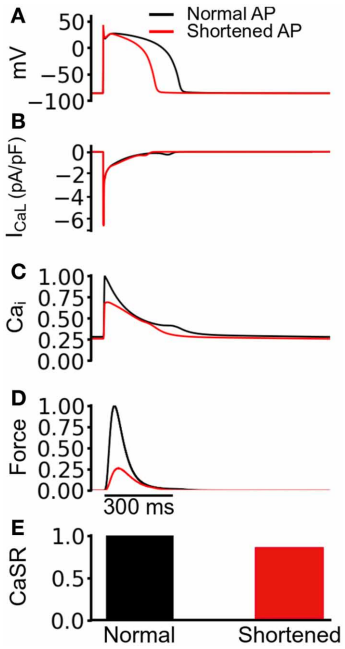

FIGURE 4 | Simulated AP clamp using the WT electromechanics model without I_{sac}. (A) The normal (black) and shortened (red) AP waveforms applied as voltage clamp commands to the WT electromechanics model. **(B)** I_{CaL} elicited by the two AP waveforms in **(A)**. **(C)** Normalized $\left[Ca^{2+}\right]_i$ elicited by the two AP waveforms in **(A)**. Values are normalized to maximum $\left[Ca^{2+}\right]_i$ for the "normal" AP waveform. **(D)** Normalized SL shortening elicited by the two AP waveforms in **(A)**. Values are normalized to maximum SL shortening for the normal AP waveform. **(E)** Normalized contractile force elicited by the two AP waveforms in **(A)**. Values are normalized to maximum active force for the normal AP waveform.

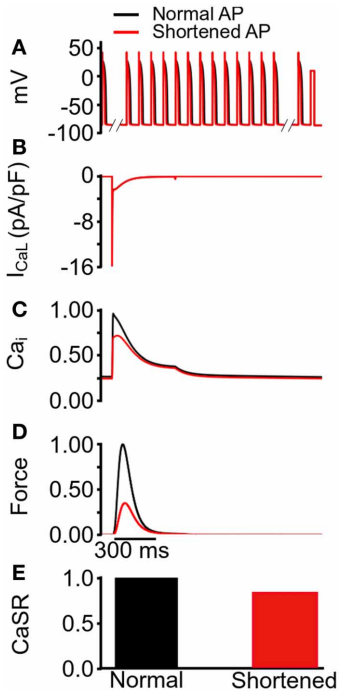

FIGURE 5 | Changes in steady state SR content induced by conditioning trains of action potentials of differing duration. (A) Protocol used to determine steady state SR content, comprised of train of 100 normal (black) and shortened (red) AP clamp commands followed by a 300 ms square command voltage pulse to +10 mV. **(B)** I_{CaL} elicited by the +10 mV voltage command. Peak I_{CaL} is equal with the two AP waveforms in **(A)**. **(C)** Normalized $\left[Ca^{2+}\right]_i$ elicited by the by the +10 mV voltage command. Values are normalized to maximum $\left[Ca^{2+}\right]_i$ for the "normal" AP waveform. **(D)** Normalized active force elicited by the +10 mV voltage command. Values are normalized to maximum active force for the normal AP waveform. **(E)** Normalized maximum SR Ca^{2+} content prior to the application of +10 mV voltage command in **(A)**. Values are normalized to maximum SR Ca^{2+} for the normal AP waveform.

and SQT1 conditions respectively. Depolarization of the membrane potential is an effect of SACs, which has been observed experimentally (Boland and Troquet, 1980; Franz et al., 1992; Kamkin et al., 2000). The resting membrane potential remained unchanged under the SQT3 condition because the increase in outward I_{K1} caused by the mutation counteracted the depolarizing effect of I_{sac}. Similar to the situation without I_{sac}, the incorporation of SQT1 and SQT3 mutations abbreviated the AP in all three cell types (**Figures 6Ai–Ci**, **7Ai–Ci**). The most significant consequences of inclusion of I_{sac} were upon $\left[Ca^{2+}\right]_i$ and contractile activity. Thus, the results shown in **Figures 6**, **7** indicate that incorporation of I_{sac} attenuated the reduction caused by the SQT1 and SQT3 mutations shown in **Figure 3** on $\left[Ca^{2+}\right]_i$ (**Figures 6Aii–Cii**, **7Aii–Cii**), SLs (**Figures 6Aiii–Ciii**, **7Aiii–Ciii**) and active force (**Figures 6Aiv–Civ**, **7Aiv–Civ**). I_{sac} incorporated at 1:1:1 permeability ratio (i.e., incorporating Ca^{2+} permeability) produced the greater effect, with contractility across the ventricular wall being approximately 85% of control under the SQT1 mutation and 92% of control under the SQT3 mutation. In contrast, with I_{sac} incorporated at a permeability ratio of 1:1:0, on average across the ventricular wall, the contractile force was 62% of control under the SQT1 condition and 82% of control under the SQT3 condition.

In order to investigate how I_{sac} attenuated the effects of the SQT1 and SQT3 mutations on $\left[Ca^{2+}\right]_i$ and cell contractility, a side-by-side comparison was made between the effects of the SQT1 and SQT3 mutations on AP duration, $\left[Ca^{2+}\right]_i$ and force production, in the absence of I_{sac} and with I_{sac} incorporated at the two permeability ratios (**Figure 8**). **Figures 8Ai–Ci** shows that the incorporation of I_{sac} at both permeability ratios reduced the APDs under the WT, SQT1 or SQT3 conditions,with a greater APD reduction in the case of permeability ratio of 1:1:1 than that of 1:1:0 as shown in **Table 1**. There was a greater $\left[Ca^{2+}\right]_i$ transient amplitude under both SQTS mutation conditions with the incorporation of I_{sac}; the greatest amplitude being at the 1:1:1 permeability ratio (**Figures 8Aii–Cii**). From **Figures 8Aiii–Ciii**, it is clear to see the increase in the $\left[Ca^{2+}\right]_i$ produced a greater SL shortening (relative to WT) on incorporation of I_{sac}, which consequently led to greater cell contractility in the SQT1 and SQT3 mutations particularly with a permeability ratio of 1:1:1 (**Figures 8Aiv–Civ**).

We then investigated how the incorporation of I_{sac} led to better maintenance of the $[Ca^{2+}]_i$ transient magnitude. **Figure 9** shows

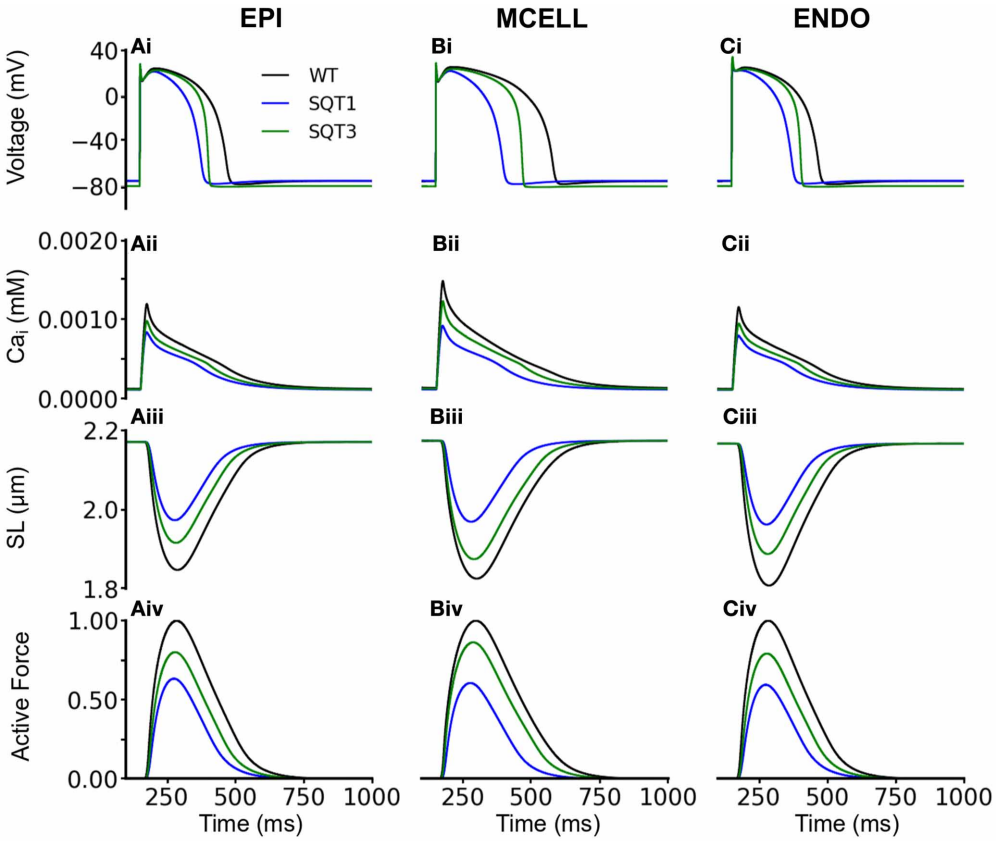

FIGURE 6 | Effects of I_{sac} on the WT, SQT1, and SQT3 electromechanics model. (Ai–Ci) WT (black), SQT1 (blue) and SQT3 (green) action potentials in the EPI **(Ai)**, MCELL **(Bi)**, and ENDO **(Ci)** cell models. **(Aii–Cii)** WT (black), SQT1 (blue) and SQT3 (green) intracellular calcium concentration and Ca^{2+} transients in the EPI **(Aii)**, MCELL **(Bii)**, and ENDO **(Cii)** cell models. **(Aiii–Ciii)** WT (black), SQT1 (blue) and SQT3 (green) sarcomere length (SL) in the EPI **(Aiii)**, MCELL **(Biii)**, and ENDO **(Ciii)** cell models. **(Aiv–Civ)** WT (black), SQT1 (blue) and SQT3 (green). SAC in these simulations were permeable to Na^+, K^+, and Ca^{2+} in the ratio 1:1:0.

the computed APs (**Figures 9Ai–Ci**), I_{CaL} (**Figures 9Aii–Cii**), $[Na^+]_i$ (**Figures 9Aiii–Ciii**), $[Ca^{2+}]_i$ (**Figures 9Aiv–Civ**), CaSR (**Figures 9 Av–Cv**) and I_{NaCa} (**Figures 9 Avi–Cvi**) with and without I_{sac} (permeability ratio 1:1:1) in the WT, SQT1 and SQT2 conditions. Under the WT, SQT1 and SQT3 conditions, it was shown that incorporation of I_{sac} did not produce a noticeable change in the amplitude of I_{CaL}, but elevated $[Na^+]_i$, $[Ca^{2+}]_i$, and CaSR. These changes in the intracellular Na^+ and Ca^{2+} concentrations were associated with an altered I_{NaCa} as shown in **Figures 9Avi–Cvi**. In the case when I_{sac} was absent, during the initial depolarization phase of the AP, I_{NaCa} operated briefly in its reverse-mode that brought Ca^{2+} into the cytoplasmic space, producing an outward I_{NaCa}. During the plateau and early repolarization phases, I_{NaCa} remained almost zero for a period before switching to a forward mode to extrude Ca^{2+} out of cell cytoplasmic space, producing an inward I_{NaCa} current in the late repolarization phase. However, in the case with I_{sac}, the activation of I_{sac} brought more Na^+ into the cell cytoplasmic space (as it is permeable to Na^+) producing an elevated level of $\left[Na^+\right]_i$ (**Figures 9Aiii–Ciii**) as compared to the case when I_{sac} was absent. Consequently, I_{NaCa} operated longer in a reverse-mode during the AP phase before it reverted to a normal mode in late repolarization phase. This led to a greater I_{NaCa} amplitude in both the reverse and forward modes (**Figures 9 Avi–Cvi**). A greater I_{NaCa} in the reverse-mode brought more Ca^{2+} into the cell cytoplasmic space, resulting in a higher systolic level of $\left[Ca^{2+}\right]_i$ (**Figures 9 Aiv–Civ**) and a greater level of the CaSR (**Figures 9Av–Cv**). Though this observation was *qualitatively* similar for the WT (**Figure 9Avi**), SQT1 (**Figure 9Bvi**) and SQT3 conditions (**Figure 9Cvi**), in *quantitative* terms the increase in the $\left[Ca^{2+}\right]_i$ was more dramatic in the SQT1 and 3 than WT settings. Thus, incorporation of I_{sac} into the simulations increased $\left[Ca^{2+}\right]_i$ by 88% under the WT condition, but by 153% under the SQT1 condition and by 94% under the SQT3 setting. The greater increase of $\left[Ca^{2+}\right]_i$ under the SQT simulation conditions provides an explanation for the maintenance of the Ca^{2+} transient by I_{sac}. Our simulated elevation of $\left[Na^+\right]_i$ by I_{sac} is consistent with previous experimental studies (Alvarez et al., 1999; Isenberg et al., 2003; Youm et al., 2005) that have shown an increase in cytosolic and total $\left[Na^+\right]_i$ by a mechanical stretch in human, mouse and ventricular myocytes, which has been attributed to the reverse-mode of I_{NaCa} during the rising phase of APs (Gannier et al., 1996;

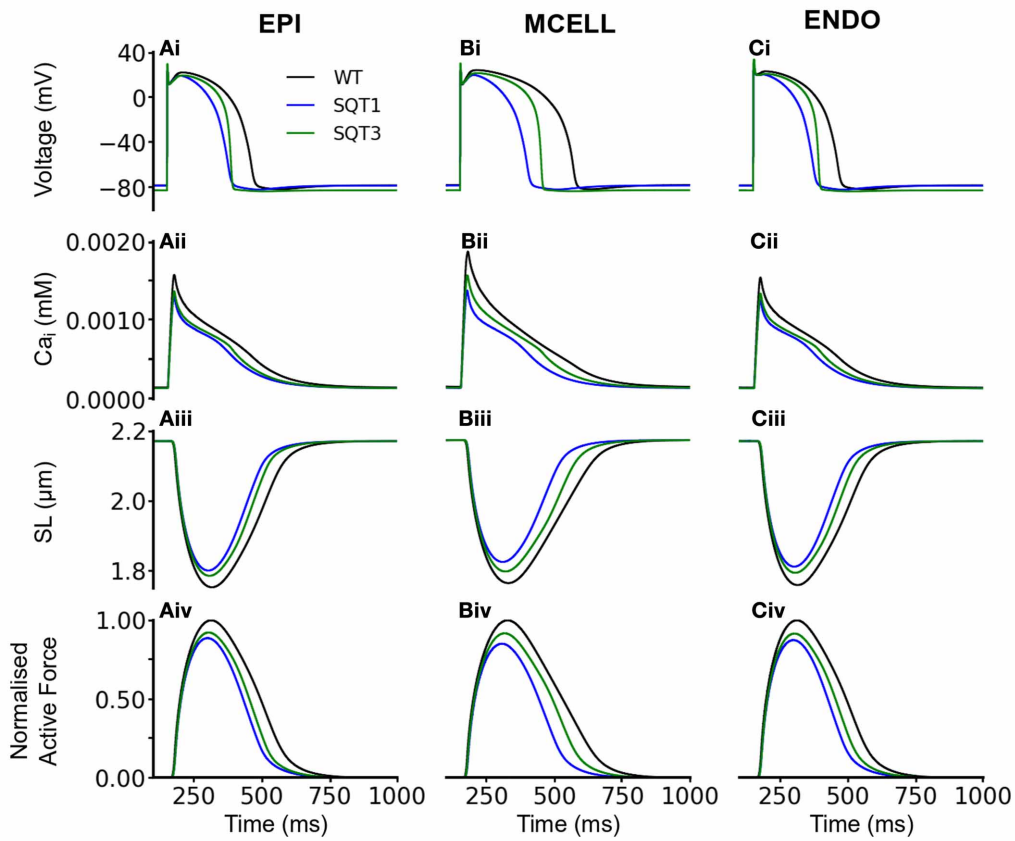

FIGURE 7 | Effects of I_{sac} on the WT, SQT1, and SQT3 electromechanics model. (Ai–Ci) WT (black), SQT1 (blue) and SQT3 (green) action potentials in the EPI **(Ai)**, MCELL **(Bi)**, and ENDO **(Ci)** cell models. **(Aii–Cii)** WT (black), SQT1 (blue) and SQT3 (green) intracellular calcium concentration and Ca^{2+} transients in the EPI **(Aii)**, MCELL **(Bii)**, and ENDO **(Cii)** cell models. **(Aiii–Ciii)** WT (black), SQT1 (blue) and SQT3 (green) sarcomere length (SL) in the EPI **(Aiii)**, MCELL **(Biii)**, and ENDO **(Ciii)** cell models. **(Aiv–Civ)** WT (black), SQT1 (blue) and SQT3 (green). SAC in these simulations were permeable to Na^+, K^+, and Ca^{2+} in the ratio 1:1:1.

Alvarez et al., 1999; Calaghan and White, 1999; Kamkin et al., 2000, 2003; Calaghan et al., 2003; Youm et al., 2005).

3D SIMULATIONS

Results from single cell models cannot be translated automatically to the intact tissue situation due to intercellular electrical coupling and mechanical deformation of tissue. Schimpf et al. (2008) observed a dissociation between ventricular repolarization and the end of mechanical systole in SQT patients. Consequently, to investigate this observation, we implemented a multi-cellular 3D tissue model of the human ventricles that considered the intercellular electrical coupling and mechanical deformation of tissue. Simulation results using the human ventricle 3D model are shown in **Figure 10**. **Figure 10A** shows the ventricles during diastole before contraction, whilst **Figure 10B** shows deformation under the WT condition; maximum deformation occurred at 230 ms. Maximum deformation occurred at 200 ms and 210 ms under the SQT1 (**Figure 10C**) and SQT3 (**Figure 10D**) conditions respectively but in contrast to WT, repolarization had already advanced significantly, particularly under the SQT1 condition. The vertical lines show that contraction was greatest in the WT condition (**Figure 10B**) and least in the SQT1 setting (**Figure 10C**) but due to the incorporation of I_{sac}, contractility was not significantly impaired in either mutation condition, which agrees with available clinical evidence (Schimpf et al., 2008).

DISCUSSION

SUMMARY OF MAJOR FINDINGS

Electromechanical coupling in the heart is an active area of research and an important mechanism that couples electrical and mechanical processes is the presence of cardiac ion channels activated by mechanical stimuli such as changes in cell volume or cell stretch (Morris, 1990; Bustamante et al., 1991; Hagiwara et al., 1992; Van Wagoner, 1993; Suleymanian et al., 1995). In the present study, we have developed a family of multi-physical scale models for simulating the electromechanical coupling in the human ventricle at cellular and tissue levels under both WT and SQTS mutation conditions. Using these models we investigated the functional impact of AP abbreviation due to the SQT1 and SQT3 mutations on human ventricular mechanical dynamics. In the heart, SACs transduce mechanical energy into

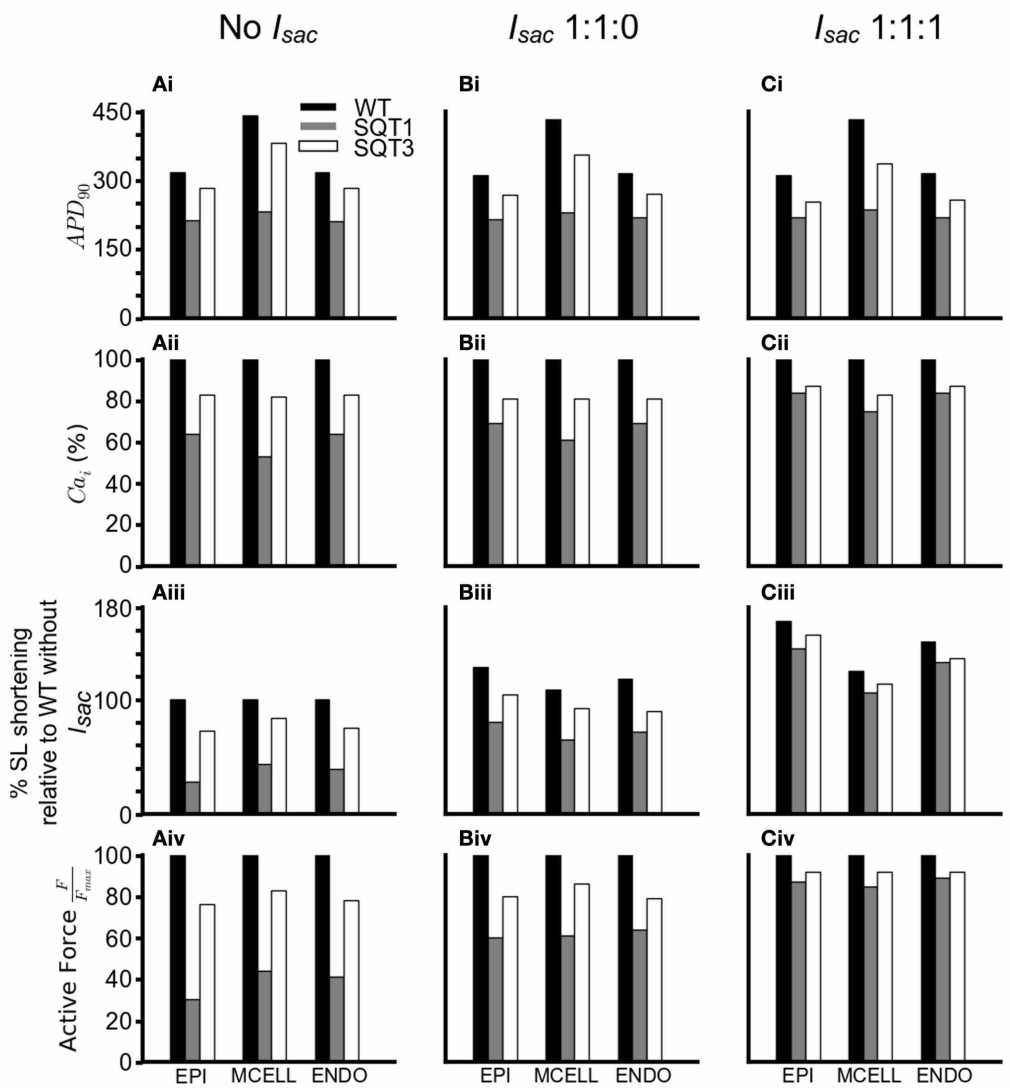

FIGURE 8 | Summary of effects of SQTS mutations on APD_{90}, $\left[Ca^{2+}\right]_i$, SL shortening and active force under different simulation conditions. (Ai–Ci) Changes in APD_{90} under the WT (black), SQT1 (gray) and SQT3 (white) in the EPI, MCELL and ENDO cell types without I_{sac} **(Ai)**, with I_{sac} at a permeability ratio of 1:1:0 **(Bi)** and with I_{sac} at a permeability ratio of 1:1:1 **(Ci)**. **(Aii–Cii)** Percentage changes in $\left[Ca^{2+}\right]_i$ under the WT (black), SQT1 (gray) and SQT3 (white) in the EPI, MCELL and ENDO cell types without I_{sac} **(Aii)**, with I_{sac} at a permeability ratio of 1:1:0 **(Bii)** and with I_{sac} at a permeability ratio of 1:1:1 **(Cii)**. **(Aiii–Ciii)** Percentage sarcomere length shortening under the WT (black), SQT1 (gray) and SQT3 (white) in the EPI, MCELL, and ENDO cell types without I_{sac} **(Aiii)**, with I_{sac} at a permeability ratio of 1:1:0 **(Biii)** and with I_{sac} at a permeability ratio of 1:1:1 **(Ciii)**. Values are relative to WT without I_{sac} **(Aiii)**. **(Aiv–Civ)** Normalized active force under the WT (black), SQT1 (gray) and SQT3 (white) in the EPI, MCELL and ENDO cell types without I_{sac} **(Aiv)**, with I_{sac} at a permeability ratio of 1:1:0 **(Biv)** and with I_{sac} at a permeability ratio of 1:1:1 **(Civ)**.

cellular responses and can carry considerable currents (Franz et al., 1992; Alvarez et al., 1999; Calaghan and White, 1999; Calaghan et al., 2003; Youm et al., 2005). Consequently, we incorporated a stretch-activated channel current (I_{sac}) into our single cell models to investigate the consequences of its inclusion under WT and SQTS mutation conditions. Our simulations suggest that: (i) at least *in silico*, abbreviated repolarization in the SQTS has the potential to reduce ventricular mechanical function; (ii) the inclusion of (I_{sac}) in the model acts to maintain the normal amplitude of the contractile force (**Figures 6–8**); and (iii) there is a dissociation between ventricular repolarization and the end of mechanical systole in 3D SQTS simulations (**Figure 10**), which matches clinical observations by Schimpf et al. (2008). Several aspects of our findings merit more detailed discussion.

MECHANISTIC INSIGHTS

The results of simulated AP clamp experiments utilizing longer and shorter duration APs in the WT electromechanics model (**Figure 4**) provide mechanistic insight into the cause of the

profound reduction and effects on contractility under simulated SQT1 and SQT3 conditions. In these simulations it was shown that markedly reduced contractility was attributable to reduced SR Ca^{2+} loading. AP shortening alters cellular electrical dynamics and provides less time for SR Ca^{2+} loading and therefore SR Ca^{2+} content is compromised. This leads to a reduced SR Ca^{2+} release and, consequently, cell shortening. These observations are somewhat similar to previously reported effects of K-ATP channel openers. For example, K-ATP channel activation with lemakalim has been reported to reduce ventricular myocyte Ca^{2+} transients and contraction (Jiang et al., 1994), whilst a second K-ATP channel opener HOE 234 produced a negative inotropic effect on papillary muscle preparations (Kocić and Siluta, 1995).

Table 1 | Changes in APD in the EPI, MCELL, and EDO cells with I_{sac}.

		APD (ms)		
		No I_{sac}	I_{sac} (Permeability 1:1:0)	I_{sac} (Permeability 1:1:1)
WT	EPI	317	310	306
	MCELL	441	433	420
	ENDO	317	314	310
SQT1	EPI	212	214	218
	MCELL	232	230	237
	ENDO	211	218	218
SQT3	EPI	283	269	253
	MCELL	382	355	336
	ENDO	284	270	257

Our simulation data are suggestive that the presence of SACs attenuates the reduced ventricular cell contractility arising from SQTS K channel mutations. This can be ascribed to the effects of I_{sac} on SR Ca^{2+} loading and therefore the amplitude of $[Ca^{2+}]_i$ transients as shown in **Figure 8**. With I_{sac}, with a Na:K:Ca ratio of either 1:1:0 or 1:1:1, there was a greater $[Ca^{2+}]_i$ transient amplitude and higher SR Ca^{2+} content, resulting in a greater shortening of the SL and active force as compared to the case when I_{sac} was absent. Such an effect of I_{sac} on the intracellular Ca^{2+} handling is due to two factors. First, during the depolarization phase of the AP, I_{NaCa} operates in a reverse mode that brings Ca^{2+} into the cytoplasmic space due to Na^{+} influx. As I_{sac} is permeable to

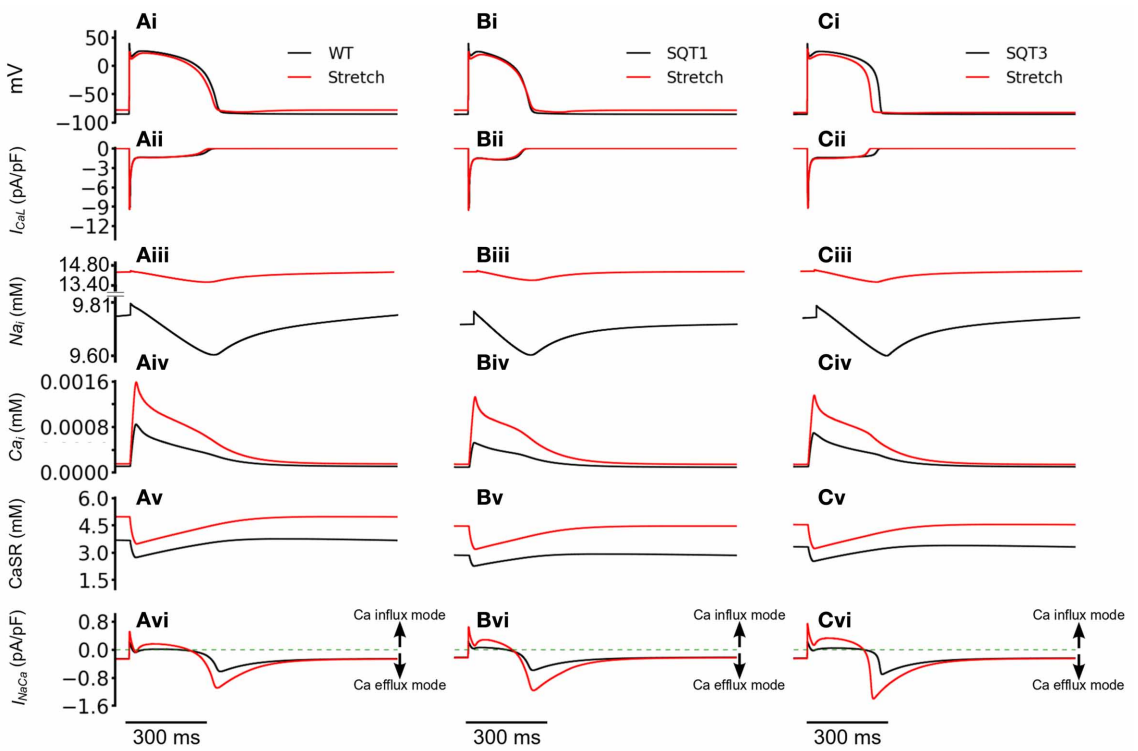

FIGURE 9 | Reverse mode operation of NCX with the incorporation of SAC. (Ai–Ci) Action potentials of WT **(Ai)**, SQT1 **(Bi)**, and SQT3 **(Ci)** without stretch (black) and with stretch (red). **(Aii–Cii)** $[Na^{+}]_i$ for WT **(Aii)**, SQT1 **(Bii)**, and SQT3 **(Cii)** without stretch (black) and with stretch (red). **(Aiii–Ciii)** Action potentials of WT **(Aiii)**, SQT1 **(Biii)**, and SQT3 **(Ciii)** without stretch (black) and with stretch (red). As the SAC is permeable to Na^{+}, it is of higher amplitude under stretch conditions. **(Aiv–Civ)** $[Ca^{2+}]_i$ for WT **(Aiv)**, SQT1 **(Biv)**, and SQT3 **(Civ)** without stretch (black) and with stretch (red). **(Av–Cv)** SR Ca^{2+} release under WT **(Av)**, SQT1 **(Bv)** and SQT3 **(Cv)** without stretch (black) and with stretch (red). The SR is refilled to a greater level prior to AP initiation under stretch conditions. **(Avi–Cvi)** I_{NaCa} of WT **(Avi)**, SQT1 **(Bvi)** and SQT3 **(Cvi)** without stretch (black) and with stretch (red).

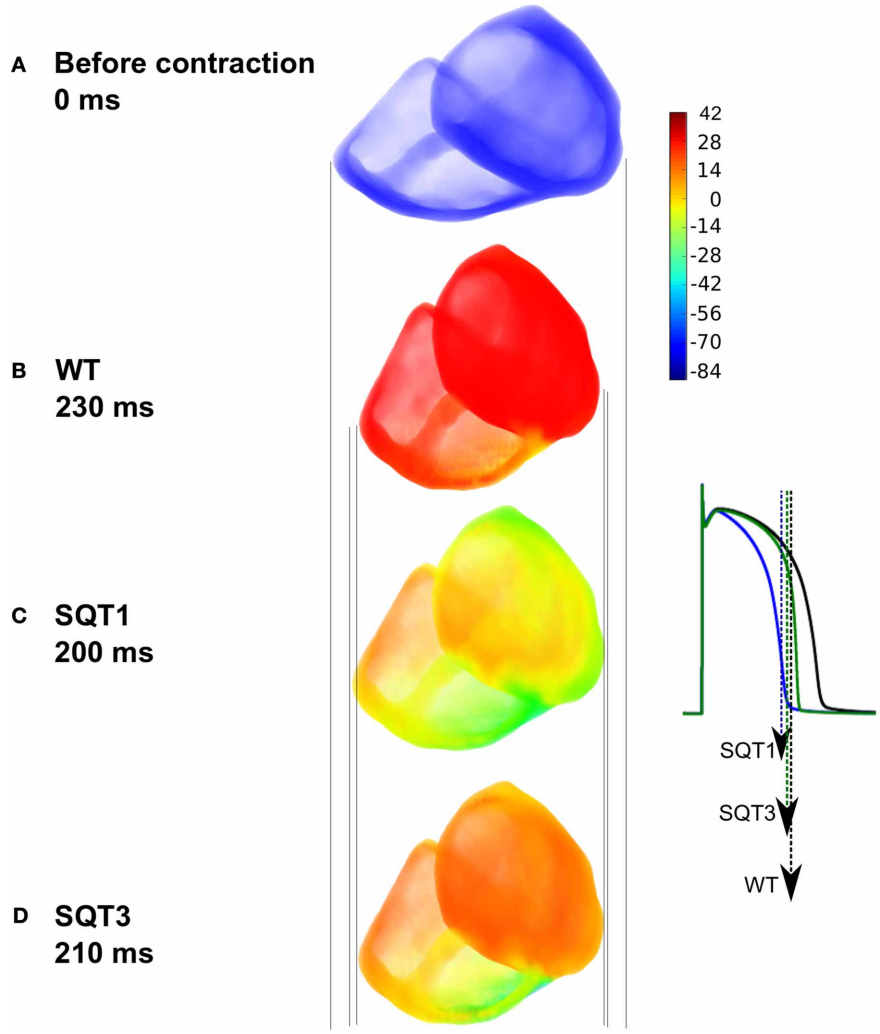

FIGURE 10 | Electromechanical coupling in 3D ventricle model under the SQT1 and SQT3 mutations with I_{sac}. (A) Resting position of the ventricles prior to electrical stimulation. **(B)** Snapshot of maximum deformation occurring at 230 ms under the WT condition just at the onset of repolarization (black AP). **(C)** Snapshot of maximum deformation occurring at 200 ms under the SQT1 condition. Repolarization is already significantly advanced (blue AP). **(D)** Snapshot of maximum deformation occurring at 210 ms under the SQT3 condition. Repolarization is already in progress (green AP). Vertical lines show a comparison of the degree of contraction of the ventricles between the different conditions. Color bar represents the membrane potentials of cells in the ventricles ranging from –86 to 42 mV. The APs shown in the inset are from a left ventricular cell under the WT, SQT1 and SQT3 conditions. Arrows indicate the snapshot time shown in the main figure for each condition corresponding to the repolarization time at which maximal deformation occurs.

Na^+, the activation of I_{sac} elevates $[Na^+]_i$, consequentially produces a greater reversed I_{NaCa} that elevates the $[Ca^{2+}]_i$ (**Figure 9**). The elevation of $[Na^+]_i$ leading to the reverse-mode of I_{NaCa} have been reported by previous studies (Bassingthwaighte et al., 1976; Eisner et al., 1983; Hume and Uehara, 1986; Barcenas-Ruiz et al., 1987; Gannier et al., 1996; Alvarez et al., 1999; Calaghan and White, 1999; Kamkin et al., 2000, 2003; Calaghan et al., 2003; Youm et al., 2005). Secondly, the increased $[Ca^{2+}]_i$ and the Ca^{2+} entry via I_{NaCa} in its reversed mode can both lead to more Ca^{2+} being pumped back to the SR, contributing to a greater CaSR, and trigger more SR Ca^{2+} release (Leblanc and Hume, 1990; Levesque et al., 1991; Litwin et al., 1996; Bers, 2001), thereby elevating $[Ca^{2+}]_i$ (**Figure 10**).

The dissociation between ventricular repolarization and the end of mechanical systole reflects the difference time course of the two processes. Our simulation data show that relative to ongoing mechanical contraction, ventricular repolarization terminates significantly earlier in SQTS conditions. Thus, accelerated repolarization in the SQTS exacerbates differences between electrical and mechanical events. By way of illustration, in our 3D anatomical human ventricle simulations, at the point of maximum deformation, repolarization was already underway in the SQT1 and SQT3 conditions (**Figure 10**) whereas it had not begun under the WT condition.

RELEVANCE TO PREVIOUS STUDIES

Our simulation data suggest that I_{sac} plays an important role in modulating cardiac electromechanical coupling. This is consistent with previous findings (Hirabayashi et al., 2008; Keldermann et al., 2010). In their study, Keldermann developed a coupled

electromechanical model for the left human ventricle, and used the model to investigate possible functional roles of I_{sac} on the re-entrant electrical wave conductions. It was found that mechanoelectrical feedback via I_{sac} can induce the deterioration of an otherwise stable spiral wave into turbulent wave patterns similar to that of ventricular fibrillation. A similar role for I_{sac} has also been observed in the study of (Hirabayashi et al., 2008). Findings from the present study add to these previous studies, in demonstrating the important role of I_{sac} in cardiac electromechanical dynamics.

In relation to the SQTS, Gaita et al. (2003) performed echocardiography, cardiac MRI and stress tests on the two families in which the SQTS was first reported (Gaita et al., 2003) and found no evident structural abnormalities. In subsequent work on mechanical function in the SQTS by Schimpf et al. (2008), no significant difference was seen between control subjects and SQTS patients in end systolic volume, end diastolic volume and ejection fraction. However, a dissociation between ventricular repolarization and the end of mechanical systole was observed. Our 3D simulations (**Figure 10**) qualitatively match and substantiate this clinical finding (Schimpf et al., 2008).

LIMITATIONS

In addition to acknowledged limitations of both the TP electrophysiology model (Ten Tusscher and Panfilov, 2006) and the Rice et al. (2008) mechanics model, although our coupled electromechanics model exhibited the Bowditch staircase or Treppe effect (Woodworth, 1902; Mulieri et al., 1992; Lakatta, 2004), it was only qualitatively able to reproduce experimental force-frequency characteristics. In simulations at increased pacing rates from 1.5 to 4 Hz, we observed APD shortening with an increase in the pacing rate, but due to reduced time for Ca^{2+} extrusion and SR accumulation between successive APs, there was an increase in the amplitude of the $[Ca^{2+}]_i$ transient and the active force in both WT and SQT settings. This was particularly the case at the faster rates examined, where there was insufficient time for restoration of Ca^{2+} dynamics between successive APs. These modeling observations require further validation and, if necessary, improvement in Ca^{2+} dynamics when experimental data become available. However, over the frequency range of 1–2 Hz our data matched reasonably experimental force-frequency data (**Figure 2**) and all simulations of the effects of SQT mutations presented here were conducted at 1 Hz. In the ventricular electrophysiology cell models, we did not consider the effects of β-adrenergic stimulation or more physiologically-detailed Ca^{2+} handling mechanisms as implemented in some recently published models (Grandi et al., 2010; O'Hara et al., 2011). These effects may affect quantitatively the simulation results (Puglisi et al., 2013). Additionally, due to lack of experimental data on the I_{sac} in human ventricular myocytes, I_{sac} density was based on the study of (Panfilov et al., 2005; Youm et al., 2005; Kuijpers, 2008; Kohl and Sachs, 2001; Lunze et al., 2010). Whilst we have investigated the effects of I_{sac} on attenuation of force reduction in the SQTS setting, it is possible that alternative mechanisms may be involved such as calcium transport controlled by feedback of SR filling via store-operated Ca^{2+} channels (SOC) (Kusters et al., 2005; Kowalewski et al., 2006; Berna-Erro et al., 2012). Consequently, in additional simulations (data not shown), we have incorporated into the model a SOC channel current based on the Kuster et al. model (Kusters et al., 2005). In contrast to our findings with I_{sac}, with I_{SOC} incorporation no significant attenuation (<6%) of the force reduction in the SQTS settings was observed for the maximal SOC channel conductance varying from 0.2 to 20 pS/pF. Whilst it is important that these potential limitations are stated, they do not fundamentally alter the principal conclusions of this study.

CONCLUSION

Our tissue simulations qualitatively reproduce and provide a possible explanation for dissociation between the end of mechanical systole and ventricular repolarization (Schimpf et al., 2008): accelerated repolarization under SQTS conditions exacerbates differences in time-course between mechanical and electrical events. The results of the simulations in this study also raise a question as to whether electromechanical coupling involving I_{sac} offsets a negative inotropic effect of ventricular action potential abbreviation that might otherwise occur for K^+-channel linked SQTS. If, *in vivo*, I_{sac} does not execute such a role, then it is possible that other compensatory changes exist in SQTS patients as accelerated repolarization might otherwise result in altered SR Ca^{2+} loading and a reduction in contractile activity.

ACKNOWLEDGMENTS

This work was supported by project grants from Engineering and Physical Science Research Council UK (EP/J00958X/1; EP/I029826/1), the British Heart Foundation (FS/08/021), the Natural Science Foundation of China (61179009) and the University of Manchester.

REFERENCES

Adeniran, I., El Harchi, A., Hancox, J. C., and Zhang, H. (2012). Proarrhythmia in KCNJ2-linked short QT syndrome - insights from modelling. *Cardiovasc. Res.* 94, 66–76. doi: 10.1093/cvr/cvs082

Adeniran, I., McPate, M. J. W., Witchel, H. J., Hancox, J. C., and Zhang, H. (2011). Increased vulnerability of human ventricle to re-entrant excitation in hERG-linked variant 1 short QT syndrome. *PLoS Comput. Biol.* 7:e1002313. doi: 10.1371/journal.pcbi.1002313

Alvarez, B. V., Pérez, N. G., Ennis, I. L., Camilión de Hurtado, M. C., and Cingolani, H. E. (1999). Mechanisms underlying the increase in force and Ca(2+) transient that follow stretch of cardiac muscle: a possible explanation of the Anrep effect. *Circ. Res.* 85, 716–722. doi: 10.1161/01.RES.85.8.716

Anttonen, O., Junttila, J., Giustetto, C., Gaita, F., Linna, E., Karsikas, M., et al. (2009). T-Wave morphology in short QT syndrome. *Ann. Noninvasive Electrocardiol.* 14, 262–267. doi: 10.1111/j.1542-474X.2009.00308.x

Antzelevitch, C., Pollevick, G. D., Cordeiro, J. M., Casis, O., Sanguinetti, M. C., Aizawa, Y., et al. (2007). Loss-of-function mutations in the cardiac calcium channel underlie a new clinical entity characterized by ST-segment elevation, short QT intervals, and sudden cardiac death. *Circulation* 115, 442–449. doi: 10.1161/CIRCULATIONAHA.106.668392

Barcenas-Ruiz, L., Beuckelmann, D. J., and Wier, W. G. (1987). Sodium-calcium exchange in heart: membrane currents and changes in [Ca2+]$_i$. *Science* 238, 1720–1722. doi: 10.1126/science.3686010

Bassingthwaighte, J. B., Fry, C. H., and McGuigan, J. A. (1976). Relationship between internal calcium and outward current in mammalian ventricular muscle; a mechanism for the control of the action potential duration. *J. Physiol. (Lond.)* 262, 15–37.

Bellocq, C., van Ginneken, A. C. G., Bezzina, C. R., Alders, M., Escande, D., Mannens, M. M. A.

M., et al. (2004). Mutation in the KCNQ1 gene leading to the short QT-interval syndrome. *Circulation* 109, 2394–2397. doi: 10.1161/01.CIR.0000130409.72142.FE

Berna-Erro, A., Redondo, P. C., and Rosado, J. A. (2012). Store-operated Ca(2+) entry. *Adv. Exp. Med. Biol.* 740, 349–382. doi: 10.1007/978-94-007-2888-2_15

Bers, D. (2001). *Excitation-Contraction Coupling and Cardiac Contractile Force. 2nd Edn.* Dordrecht: Springer. doi: 10.1007/978-94-010-0658-3

Bett, G. C., and Sachs, F. (1997). Cardiac mechanosensitivity and stretch-activated ion channels. *Trends Cardiovasc. Med.* 7, 4–8. doi: 10.1016/S1050-1738(96)00119-3

Bogaert, J., and Rademakers, F. E. (2001). Regional nonuniformity of normal adult human left ventricle. *Am. J. Physiol. Heart Circ. Physiol.* 280, H610–H620.

Boland, J., and Troquet, J. (1980). Intracellular action potential changes induced in both ventricles of the rat by an acute right ventricular pressure overload. *Cardiovasc. Res.* 14, 735–740. doi: 10.1093/cvr/14.12.735

Bonet, J., and Wood, R. D. (2008). *Nonlinear Continuum Mechanics for Finite Element Analysis, 2nd Edn.* New York, NY: Cambridge University Press. doi: 10.1017/CBO9780511755446

Braess, D. (2007). *Finite Elements: Theory, Fast Solvers, and Applications in Solid Mechanics, 3rd Edn.* New York, NY: Cambridge University Press. doi: 10.1017/CBO9780511618635

Brenner, S. C., and Scott, R. (2010). *The Mathematical Theory of Finite Element Methods. Softcover Reprint of Hardcover, 3rd Edn. 2008*. New York, NY: Springer.

Brugada, R., Hong, K., Dumaine, R., Cordeiro, J., Gaita, F., Borggrefe, M., et al. (2004). Sudden death associated with short-QT syndrome linked to mutations in HERG. *Circulation* 109, 30–35. doi: 10.1161/01.CIR.0000109482.92774.3A

Burnett, D. S. (1987). *Finite Element Analysis: From Concepts to Applications, 1st Edn.* Reading, MA: Addison Wesley.

Bustamante, J. O., Ruknudin, A., and Sachs, F. (1991). Stretch-activated channels in heart cells: relevance to cardiac hypertrophy. *J. Cardiovasc. Pharmacol.* 17(Suppl. 2), S110–S113. doi: 10.1097/00005344-199117002-00024

Calaghan, S. C., Belus, A., and White, E. (2003). Do stretch-induced changes in intracellular calcium modify the electrical activity of cardiac muscle. *Prog. Biophys. Mol. Biol.* 82, 81–95. doi: 10.1016/S0079-6107(03)00007-5

Calaghan, S. C., and White, E. (1999). The role of calcium in the response of cardiac muscle to stretch. *Prog. Biophys. Mol. Biol.* 71, 59–90. doi: 10.1016/S0079-6107(98)00037-6

Chamberland, í., Fortin, A., and Fortin, M. (2010). Comparison of the performance of some finite element discretizations for large deformation elasticity problems. *Comput. Struct.* 88, 664–673.

Cheng, A., Nguyen, T. C., Malinowski, M., Daughters, G. T., Miller, D. C., and Ingels, N. B. Jr. (2008). Heterogeneity of left ventricular wall thickening mechanisms. *Circulation* 118, 713–721. doi: 10.1161/CIRCULATIONAHA.107.744623

Cohen, S., Alan, and Hindmarsh, C. (1996). "Cvode, a stiff/nonstiff ode solver in, C.," in *C. Computers in Physics*, ed L. M. Holmes (New York, NY: American Institute of Physics Inc.), 138–143.

Colli Franzone, P., Pavarino, L. F., and Taccardi, B. (2005). Simulating patterns of excitation, repolarization and action potential duration with cardiac bidomain and monodomain models. *Math. Biosci.* 197, 35–66. doi: 10.1016/j.mbs.2005.04.003

Coppola, B. A., and Omens, J. H. (2008). Role of tissue structure on ventricular wall mechanics. *Mol. Cell. Biomech.* 5, 183–196.

Costa, K. D., Holmes, J. W., and Mcculloch, A. D. (2001). Modelling cardiac mechanical properties in three dimensions. *Phil. Trans. R. Soc. Lond. A* 359, 1233–1250. doi: 10.1098/rsta.2001.0828

Couderc, J.-P., and Lopes, C. M. (2010). Short and long QT syndromes: does QT length really matter. *J. Electrocardiol.* 43, 396–399. doi: 10.1016/j.jelectrocard.2010.07.009

Cross, B., Homoud, M., Link, M., Foote, C., Garlitski, A., Weinstock, J., et al. (2011). The short QT syndrome. *J. Int. Cardiac Electrophysiol.* 31, 25–31. doi: 10.1007/s10840-011-9566-0

Deo, M., Ruan, Y., Pandit, S. V., Shah, K., Berenfeld, O., Blaufox, A., et al. (2013). KCNJ2 mutation in short QT syndrome 3 results in atrial fibrillation and ventricular proarrhythmia. *Proc. Natl. Acad. Sci. U.S.A.* 110, 4291–4296. doi: 10.1073/pnas.1218154110

Eisner, D. A., Lederer, W. J., and Vaughan-Jones, R. D. (1983). The control of tonic tension by membrane potential and intracellular sodium activity in the sheep cardiac Purkinje fibre. *J. Physiol. (Lond.)* 335, 723–743.

Ern, A., and Guermond, J.-L. (2010). *Theory and Practice of Finite Elements. Softcover reprint of Hardcover, 1st Edn., 2004*. New York, NY: Springer.

Extramiana, F., and Antzelevitch, C. (2004). Amplified transmural dispersion of repolarization as the basis for arrhythmogenesis in a canine ventricular-wedge model of short-QT syndrome. *Circulation* 110, 3661–3666. doi: 10.1161/01.CIR.0000143078.48699.0C

Franz, M. R. (1996). Mechano-electrical feedback in ventricular myocardium. *Cardiovasc. Res.* 32, 15–24.

Franz, M. R., Cima, R., Wang, D., Profitt, D., and Kurz, R. (1992). Electrophysiological effects of myocardial stretch and mechanical determinants of stretch-activated arrhythmias. *Circulation* 86, 968–978. doi: 10.1161/01.CIR.86.3.968

Gaita, F., Giustetto, C., Bianchi, F., Wolpert, C., Schimpf, R., Riccardi, R., et al. (2003). Short QT Syndrome: a familial cause of sudden death. *Circulation* 108, 965–970. doi: 10.1161/01.CIR.0000085071.28695.C4

Gannier, F., White, E., Garnier, and Le Guennec, J. Y. (1996). A possible mechanism for large stretch-induced increase in $[Ca2+]_i$ in isolated guinea-pig ventricular myocytes. *Cardiovasc. Res.* 32, 158–167.

Gima, K., and Rudy, Y. (2002). Ionic current basis of electrocardiographic waveforms: a model study. *Circ. Res.* 90, 889–896. doi: 10.1161/01.RES.0000016960.61087.86

Giustetto, C., Di Monte, F., Wolpert, C., Borggrefe, M., Schimpf, R., Sbragia, P., et al. (2006). Short QT syndrome: clinical findings and diagnostic-therapeutic implications. *Eur. Heart J.* 27, 2440–2447. doi: 10.1093/eurheartj/ehl185

Gollob, M. H., Redpath, C. J., and Roberts, J. D. (2011). The short QT syndrome: proposed diagnostic criteria. *J. Am. Coll. Cardiol.* 57, 802–812. doi: 10.1016/j.jacc.2010.09.048

Grandi, E., Pasqualini, F. S., and Bers, D. M. (2010). A novel computational model of the human ventricular action potential and Ca transient. *J. Mol. Cell. Cardiol.* 48, 112–121. doi: 10.1016/j.yjmcc.2009.09.019

Guccione, J. M., McCulloch, A. D., and Waldman, L. K. (1991). Passive material properties of intact ventricular myocardium determined from a cylindrical model. *J. Biomech. Eng.* 113, 42–55. doi: 10.1115/1.2894084

Gussak, I., Brugada, P., Brugada, J., Wright, R. S., Kopecky, S. L., Chaitman, B. R., et al. (2000). Idiopathic short QT interval: a new clinical syndrome. *Cardiology* 94, 99–102. doi: 10.1159/000047299

Haga, J. B., Osnes, H., and Langtangen, H. P. (2012). On the causes of pressure oscillations in low-permeable and low-compressible porous media. *Int. J. Num. Anal. Methods Geomech.* 36, 1507–1522. doi: 10.1002/nag.1062

Hagiwara, N., Masuda, H., Shoda, M., and Irisawa, H. (1992). Stretch-activated anion currents of rabbit cardiac myocytes. *J. Physiol. (Lond.)* 456, 285–302.

Hancox, J. C., McPate, M. J., Harchi, A., Duncan, R. S., Dempsey, C. E., Witchel, H. J., et al. (2011). "The Short QT Syndrome," in *Heart Rate and Rhythm*, eds. O. N. Tripathi, U. Ravens, and M. C. Sanguinetti (Berlin, Heidelberg: Springer Berlin Heidelberg), 431–449. Available online at: http://www.springerlink.com/content/m8l86l8n3h81w43m/ [Accessed July 10, 2011].

Hattori, T., Makiyama, T., Akao, M., Ehara, E., Ohno, S., Iguchi, M., et al. (2011). A novel gain-of-function KCNJ2 mutation associated with short QT syndrome impairs inward rectification of Kir2.1 currents. *Cardiovas. Res.* 666–673. doi: 10.1093/cvr/cvr329

Hindmarsh, A. C., Brown, P. N., Grant, K. E., Lee, S. L., Serban, R., Shumaker, D. E., et al. (2005). SUNDIALS: suite of nonlinear and differential/algebraic equation solvers. *ACM Trans. Math. Softw.* 31, 363–396. doi: 10.1145/1089014.1089020

Hirabayashi, S., Inagaki, M., and Hisada, T. (2008). Effects of wall stress on the dynamics of ventricular fibrillation: a simulation study using a dynamic mechanoelectric model of ventricular tissue. *J. Cardiovasc. Electrophysiol.* 19, 730–739. doi: 10.1111/j.1540-8167.2008.01099.x

Holzapfel, G. A. (2000). *Nonlinear Solid Mechanics: A Continuum Approach for Engineering, 1st Edn.* Chichester: Wiley.

Hong, K., Bjerregaard, P., Gussak, I., and Brugada, R. (2005a). Short QT syndrome and atrial fibrillation caused by mutation in KCNH2.

J. Cardiovasc. Electrophysiol 16, 394–396. doi: 10.1046/j.1540-8167.2005.40621.x

Hong, K., Piper, D. R., Diaz-Valdecantos, A., Brugada, J., Oliva, A., Burashnikov, E., et al. (2005b). De novo KCNQ1 mutation responsible for atrial fibrillation and short QT syndrome *in utero*. *Cardiovasc. Res*. 68, 433–440. doi: 10.1016/j.cardiores.2005.06.023

Hu, H., and Sachs, F. (1997). Stretch-activated ion channels in the heart. *J. Mol. Cell. Cardiol.* 29, 1511–1523. doi: 10.1006/jmcc.1997.0392

Hughes, T. J. R. (2000). *The Finite Element Method: Linear Static and Dynamic Finite Element Analysis.* New Jersey, NJ: Dover Publications.

Hume, J. R., and Uehara, A. (1986). "Creep currents" in single frog atrial cells may be generated by electrogenic Na/Ca exchange. *J. Gen. Physiol.* 87, 857–884. doi: 10.1085/jgp.87.6.857

Hunter, P. J., Nash, M. P., and Sands, G. B. (1997). "Computational Mechanics of the Heart," in *Computational Biology of the Heart,* eds. A. V. Panfilov and A. V. Holden (West Sussex: Wiley), 345–407.

Isenberg, G., Kazanski, V., Kondratev, D., Gallitelli, M. F., Kiseleva, I., and Kamkin, A. (2003). Differential effects of stretch and compression on membrane currents and [Na+]c in ventricular myocytes. *Prog. Biophys. Mol. Biol.* 82, 43–56. doi: 10.1016/S0079-6107(03)00004-X

Jiang, C., Mochizuki, S., Poole-Wilson, P. A., Harding, S. E., and MacLeod, K. T. (1994). Effect of lemakalim on action potentials, intracellular calcium, and contraction in guinea pig and human cardiac myocytes. *Cardiovasc. Res.* 28, 851–857. doi: 10.1093/cvr/28.6.851

Kamkin, A., Kiseleva, I., and Isenberg, G. (2000). Stretch-activated currents in ventricular myocytes: amplitude and arrhythmogenic effects increase with hypertrophy. *Cardiovasc. Res.* 48, 409–420. doi: 10.1016/S0008-6363(00)00208-X

Kamkin, A., Kiseleva, I., and Isenberg, G. (2003). Ion selectivity of stretch-activated cation currents in mouse ventricular myocytes. *Pflugers Arch.* 446, 220–231.

Keener, J., and Sneyd, J. (2008). *Mathematical Physiology: II: Systems Physiology, 2nd Edn.* New York, NY: Springer.

Keldermann, R. H., Nash, M. P., Gelderblom, H., Wang, V. Y., and Panfilov, A. V. (2010). Electromechanical wavebreak in a model of the human left ventricle. *Am. J. Physiol. Heart Circ. Physiol.* 299, H134–H143. doi: 10.1152/ajpheart.00862.2009

Keller, D. U. J., Kalayciyan, R., Dössel, O., and Seemann, G. (2009). "Fast creation of endocardial stimulation profiles for the realistic simulation of body surface ECGs," in *IFMBE Proceedings,* 145–148. Available online at: http://www.scopus.com/inward/record.url?eid=2-s2.0-77950134835andpartnerID=40andmd5=2db2b89cc19de5e28ec01ebbf0dffff0 [Accessed July 20, 2011]. doi: 10.1007/978-3-642-03882-2_37

Kocić, I., and Siluta, W. (1995). Cardiopharmacological profile of HOE 234, the new activator of ATP-sensitive K+ channels in the guinea pig heart. *Pol. J. Pharmacol.* 47, 457–460.

Kohl, P., Hunter, P., and Noble, D. (1999). Stretch-induced changes in heart rate and rhythm: clinical observations, experiments and mathematical models. *Prog. Biophys. Mol. Biol.* 71, 91–138. doi: 10.1016/S0079-6107(98)00038-8

Kohl, P., and Sachs, F. (2001). Mechanoelectric feedback in cardiac cells. *Phil. Trans. R. Soc. Lond. A* 359, 1173–1185. doi: 10.1098/rsta.2001.0824

Kowalewski, J. M., Uhlén, P., Kitano, H., and Brismar, H. (2006). Modeling the impact of store-operated Ca2+ entry on intracellular Ca2+ oscillations. *Math. Biosci.* 204, 232–249. doi: 10.1016/j.mbs.2006.03.001

Kuijpers, N. H. L. (2008). *Cardiac Electrophysiology and Mechanoelectric Feedback*. PhD thesis. Eindhoven: Eindhoven University of Technology.

Kusters, J. M. A. M., Dernison, M. M., van Meerwijk, W. P. M., Ypey, D. L., Theuvenet, A. P. R., and Gielen, C. C. A. M. (2005). Stabilizing role of calcium store-dependent plasma membrane calcium channels in action-potential firing and intracellular calcium oscillations. *Biophys. J.* 89, 3741–3756. doi: 10.1529/biophysj.105.062984

Lab, M. J. (1982). Contraction-excitation feedback in myocardium. *Physiol. Basis Clin. Relevance. Circ. Res.* 50, 757–766. doi: 10.1161/01.RES.50.6.757

Lab, M. J. (1996). Mechanoelectric feedback (transduction) in heart: concepts and implications. *Cardiovasc. Res.* 32, 3–14.

Lakatta, E. G. (2004). Beyond Bowditch: the convergence of cardiac chronotropy and inotropy. *Cell Calcium* 35, 629–642. doi: 10.1016/j.ceca.2004.01.017

Land, S., Niederer, S. A., and Smith, N. P. (2012). Efficient computational methods for strongly coupled cardiac electromechanics. *IEEE Trans. Biomed. Eng.* 59, 1219–1228. doi: 10.1109/TBME.2011.2112359

Leblanc, N., and Hume, J. R. (1990). Sodium current-induced release of calcium from cardiac sarcoplasmic reticulum. *Science* 248, 372–376. doi: 10.1126/science.2158146

Legrice, I. J., Hunter, P. J., and Smaill, B. H. (1997). Laminar structure of the heart: a mathematical model. *Am. J. Physiol.* 272, H2466–H2476.

Levesque, P. C., Leblanc, N., and Hume, J. R. (1991). Role of reverse-mode Na(+)-Ca2+ exchange in excitation-contraction coupling in the heart. *Ann. N.Y. Acad. Sci.* 639, 386–397. doi: 10.1111/j.1749-6632.1991.tb17327.x

Lilli, A., Baratto, M. T., Meglio, J. D., Chioccioli, M., Magnacca, M., Talini, E., et al. (2013). Left ventricular rotation and twist assessed by four-dimensional speckle tracking echocardiography in healthy subjects and pathological remodeling: a single center experience. *Echocardiography* 30, 171–179. doi: 10.1111/echo.12026

Lions, J. L., and Ciarlet, P. G. (1994). *Handbook of Numerical Analysis; Vol.3, Techniques of Scientific Computing (part 1); Numerical methods for solids (part 1); Solution of equations in R(n) (part 2)*. London: North-Holland Available online at: http://catalogue.library.manchester.ac.uk/items/815424 [Accessed April 25, 2013].

Litwin, S., Kohmoto, O., Levi, A. J., Spitzer, K. W., and Bridge, J. H. (1996). Evidence that reverse Na-Ca exchange can trigger SR calcium release. *Ann. N.Y. Acad. Sci.* 779, 451–463. doi: 10.1111/j.1749-6632.1996.tb44820.x

Logg, A., Mardal, K.-A., and Wells, G. eds. (2012). *Automated Solution of Differential Equations by the Finite Element Method: The FEniCS Book. 2012th Edn*. Heidelberg: Springer.

Lorenz, C. H., Pastorek, J. S., and Bundy, J. M. (2000). Delineation of normal human left ventricular twist throughout systole by tagged cine magnetic resonance imaging. *J. Cardiovasc. Magn. Reson.* 2, 97–108. doi: 10.3109/10976640009148678

Lunze, K., Stålhand, J., and Leonhardt, S. (2010). "Modeling of stretch-activated sarcolemmal channels in smooth muscle cells," in *World Congress on Medical Physics and Biomedical Engineering, September 7 - 12 2009, Munich, Germany IFMBE Proceedings*, eds O. Dössel and W. C. Schlegel (Springer Berlin Heidelberg), 740–743. Available online at: http://www.springerlink.com/content/k3052r8670832k70/abstract/ [Accessed September 20, 2012].

MacGowan, G. A., Shapiro, E. P., Azhari, H., Siu, C. O., Hees, P. S., Hutchins, G. M., et al. (1997). Noninvasive measurement of shortening in the fiber and cross-fiber directions in the normal human left ventricle and in idiopathic dilated cardiomyopathy. *Circulation* 96, 535–541. doi: 10.1161/01.CIR.96.2.535

Marsden, J. E., and Hughes, T. J. R. (1994). *Mathematical Foundations of Elasticity.* New Jersey, NJ: Dover Publications.

McIntosh, M. A., Cobbe, S. M., and Smith, G. L. (2000). Heterogeneous changes in action potential and intracellular Ca2+ in left ventricular myocyte sub-types from rabbits with heart failure. *Cardiovasc. Res.* 45, 397–409. doi: 10.1016/S0008-6363(99)00360-0

Morris, C. E. (1990). Mechanosensitive ion channels. *J. Membr. Biol.* 113, 93–107. doi: 10.1007/BF01872883

Mulieri, L. A., Hasenfuss, G., Leavitt, B., Allen, P. D., and Alpert, N. R. (1992). Altered myocardial force-frequency relation in human heart failure. *Circulation* 85, 1743–1750. doi: 10.1161/01.CIR.85.5.1743

Nash, M. P., and Panfilov, A. V. (2004). Electromechanical model of excitable tissue to study reentrant cardiac arrhythmias. *Prog. Biophys. Mol. Biol.* 85, 501–522. doi: 10.1016/j.pbiomolbio.2004.01.016

Niederer, S. A., and Smith, N. P. (2008). An improved numerical method for strong coupling of excitation and contraction models in the heart. *Prog. Biophys. Mol. Biol.* 96, 90–111. doi: 10.1016/j.pbiomolbio.2007.08.001

O'Hara, T., Virág, L., Varró, A., and Rudy, Y. (2011). Simulation of the undiseased human cardiac ventricular action potential: model formulation and experimental validation. *PLoS Comput. Biol.* 7: e1002061. doi: 10.1371/journal.pcbi.1002061

Panfilov, A. V., Keldermann, R. H., and Nash, M. P. (2005). Self-organized pacemakers in a coupled reaction-diffusion-mechanics system. *Phys.*

Rev. Lett. 95, 258104. doi: 10.1103/PhysRevLett.95.258104

Patel, C., and Antzelevitch, C. (2008). Cellular basis for arrhythmogenesis in an experimental model of the SQT1 form of the short QT syndrome. *Heart Rhythm* 5, 585–590. doi: 10.1016/j.hrthm.2008.01.022

Patel, U., and Pavri, B. B. (2009). Short QT syndrome: a review. *Cardiol. Rev.* 17, 300–303. doi: 10.1097/CRD.0b013e3181c07592

Pathmanathan, P., and Whiteley, J. P. (2009). A numerical method for cardiac mechanoelectric simulations. *Ann. Biomed. Eng.* 37, 860–873. doi: 10.1007/s10439-009-9663-8

Potse, M., Dubé, B., Richer, J., Vinet, A., and Gulrajani, R. M. (2006). A comparison of monodomain and bidomain reaction-diffusion models for action potential propagation in the human heart. *IEEE Trans. Biomed. Eng.* 53, 2425–2435. doi: 10.1109/TBME.2006.880875

Priori, S. G., Pandit, S. V., Rivolta, I., Berenfeld, O., Ronchetti, E., Dhamoon, A., et al. (2005). A novel form of short QT syndrome (SQT3) is caused by a mutation in the KCNJ2 gene. *Circ. Res* 96, 800–807. doi: 10.1161/01.RES.0000162101.76263.8c

Puglisi, J. L., Negroni, J. A., Chen-Izu, Y., and Bers, D. M. (2013). The force-frequency relationship: insights from mathematical modeling. *Adv. Physiol. Educ.* 37, 28–34. doi: 10.1152/advan.00072.2011

Rice, J. J., Wang, F., Bers, D. M., and de Tombe, P. P. (2008). Approximate model of cooperative activation and crossbridge cycling in cardiac muscle using ordinary differential equations. *Biophys. J.* 95, 2368–2390. doi: 10.1529/biophysj.107.119487

Rush, S., and Larsen, H. (1978). A practical algorithm for solving dynamic membrane equations. *IEEE Trans. Biomed. Eng.* 25, 389–392. doi: 10.1109/TBME.1978.326270

Schimpf, R., Antzelevitch, C., Haghi, D., Giustetto, C., Pizzuti, A., Gaita, F., et al. (2008). Electromechanical coupling in patients with the short QT syndrome: further insights into the mechanoelectrical hypothesis of the U wave. *Heart Rhythm* 5, 241–245. doi: 10.1016/j.hrthm.2007.10.015

Schimpf, R., Wolpert, C., Gaita, F., Giustetto, C., and Borggrefe, M. (2005). Short QT syndrome. *Cardiovasc. Res* 67, 357–366. doi: 10.1016/j.cardiores.2005.03.026

Seemann, G., Keller, D. U. J., Weiss, D. L., and Dössel, O. (2006). "Modeling human ventricular geometry and fiber orientation based on diffusion tensor MRI," in *Computers in Cardiology*, 801–804. Available online at: http://www.scopus.com/inward/record.url?eid=2-s2.0-38049006338andpartnerID=40andmd5=d7c99be0309654b17513e9b39ee96029 [Accessed July 20, 2011].

Suleymanian, M. A., Clemo, H. F., Cohen, N. M., and Baumgarten, C. M. (1995). Stretch-activated channel blockers modulate cell volume in cardiac ventricular myocytes. *J. Mol. Cell. Cardiol.* 27, 721–728. doi: 10.1016/S0022-2828(08)80062-4

Sun, Y., Quan, X.-Q., Fromme, S., Cox, R. H., Zhang, P., Zhang, L., et al. (2011). A novel mutation in the KCNH2 gene associated with short QT syndrome. *J. Mol. Cell. Cardiol.* 50, 433–441. doi: 10.1016/j.yjmcc.2010.11.017

Sundnes, J., Lines, G. T., and Tveito, A. (2005). An operator splitting method for solving the bidomain equations coupled to a volume conductor model for the torso. *Math. Biosci.* 194, 233–248. doi: 10.1016/j.mbs.2005.01.001

Taggart, P. (1996). Mechano-electric feedback in the human heart. *Cardiovasc. Res.* 32, 38–43.

Taggart, P., Sutton, P. M., Opthof, T., Coronel, R., Trimlett, R., Pugsley, W., et al. (2000). Inhomogeneous transmural conduction during early ischaemia in patients with coronary artery disease. *J. Mol. Cell. Cardiol* 32, 621–630. doi: 10.1006/jmcc.2000.1105

Templin, C., Ghadri, J.-R., Rougier, J.-S., Baumer, A., Kaplan, V., Albesa, M., et al. (2011). Identification of a novel loss-of-function calcium channel gene mutation in short QT syndrome (SQTS6). *Eur. Heart J.* 32, 1077–1088. doi: 10.1093/eurheartj/ehr076

Trayanova, N., Li, W., Eason, J., and Kohl, P. (2004). Effect of stretch-activated channels on defibrillation efficacy. *Heart Rhythm* 1, 67–77. doi: 10.1016/j.hrthm.2004.01.002

Tseng, W.-Y. I., Reese, T. G., Weisskoff, R. M., Brady, T. J., and Wedeen, V. J. (2000). Myocardial fiber shortening in humans: Initial results of MR imaging. *Radiology* 216, 128–139.

Ten Tusscher, K. H. W. J., Noble, D., Noble, P. J., and Panfilov, A. V. (2004). A model for human ventricular tissue. *Am. J. Physiol. Heart Circ. Physiol* 286, H1573–H1589. doi: 10.1152/ajpheart.00794.2003

Ten Tusscher, K. H. W. J., and Panfilov, A. V. (2006). Alternans and spiral breakup in a human ventricular tissue model. *Am. J. Physiol. Heart Circ. Physiol* 291, H1088–H1100. doi: 10.1152/ajpheart.00109.2006

Van Wagoner, D. R. (1993). Mechanosensitive gating of atrial ATP-sensitive potassium channels. *Circ. Res.* 72, 973–983. doi: 10.1161/01.RES.72.5.973

Weiss, D. L., Seemann, G., Sachse, F. B., and Dössel, O. (2005). Modelling of short QT syndrome in a heterogeneous model of the human ventricular wall. *Europace* 7(Suppl. 2), 105–117. doi: 10.1016/j.eupc.2005.04.008

Whiteley, J. P., Bishop, M. J., and Gavaghan, D. J. (2007). Soft tissue modelling of cardiac fibres for use in coupled mechano-electric simulations. *Bull. Math. Biol.* 69, 2199–2225. doi: 10.1007/s11538-007-9213-1

Woodworth, R. S. (1902). Maximal contraction, "staircase" contraction, refractory period, and compensatory pause, of the heart. *Am. J. Physiol.* 8, 213–249.

Xia, L., Zhang, Y., Zhang, H., Wei, Q., Liu, F., and Crozier, S. (2006). Simulation of Brugada syndrome using cellular and three-dimensional whole-heart modeling approaches. *Physiol. Meas.* 27, 1125–1142. doi: 10.1088/0967-3334/27/11/006

Youm, J. B., Han, J., Kim, N., Zhang, Y.-H., Kim, E., Leem, C. H., et al. (2005). "role of stretch-activated channels in the heart: action potential and Ca2+ transients - mechanosensitivity in cells and tissues - NCBI bookshelf," in eds A. Kamkin and I. Kiseleva (Moscow: Academia). Available online at: http://www.ncbi.nlm.nih.gov/books/NBK7490/ [Accessed September 15, 2012].

Zabel, M., Koller, B. S., Sachs, F., and Franz, M. R. (1996). Stretch-induced voltage changes in the isolated beating heart: importance of the timing of stretch and implications for stretch-activated ion channels. *Cardiovasc. Res.* 32, 120–130.

Zhang, H., and Hancox, J. C. (2004). *In silico* study of action potential and QT interval shortening due to loss of inactivation of the cardiac rapid delayed rectifier potassium current. *Biochem. Biophys. Res. Commun.* 322, 693–699. doi: 10.1016/j.bbrc.2004.07.176

Zhang, H., Kharche, S., Holden, A. V., and Hancox, J. C. (2008). Repolarisation and vulnerability to re-entry in the human heart with short QT syndrome arising from KCNQ1 mutation–a simulation study. *Prog. Biophys. Mol. Biol* 96, 112–131. doi: 10.1016/j.pbiomolbio.2007.07.020

Conflict of Interest Statement: The authors declare that the research was conducted in the absence of any commercial or financial relationships that could be construed as a potential conflict of interest.

Received: 25 April 2013; paper pending published: 14 May 2013; accepted: 14 June 2013; published online: 05 July 2013.

*Citation: Adeniran I, Hancox JC and Zhang H (2013) In silico investigation of the short QT syndrome, using human ventricle models incorporating electromechanical coupling. Front. Physiol. **4**:166. doi: 10.3389/fphys.2013.00166*

This article was submitted to Frontiers in Cardiac Electrophysiology, a specialty of Frontiers in Physiology.

frontiers in PHYSIOLOGY

ORIGINAL RESEARCH ARTICLE
published: 04 September 2013
doi: 10.3389/fphys.2013.00213

Bridging the gap between computation and clinical biology: validation of cable theory in humans

Malcolm C. Finlay[1†], Lei Xu[2†], Peter Taggart[1], Ben Hanson[2] and Pier D. Lambiase[1]*

[1] *Department of Cardiac Electrophysiology, The Heart Hospital, Institute of Cardiovascular Science, University College London, London, UK*
[2] *Department of Mechanical Engineering, University College London, London, UK*

Edited by:
Ian N. Sabir, King's College, London, UK

Reviewed by:
Ming Lei, University of Manchester, UK
Matthew Killeen, Massachusetts General Hospital, USA

****Correspondence:***
Pier D. Lambiase, Reader in Cardiology, Institute of Cardiovascular Science, The Heart Hospital, University College London, 16-18 Westmoreland St., London W1G 8PH, UK
e-mail: pier.lambiase@uclh.nhs.uk
[†] These authors have contributed equally to this work.

Introduction: Computerized simulations of cardiac activity have significantly contributed to our understanding of cardiac electrophysiology, but techniques of simulations based on patient-acquired data remain in their infancy. We sought to integrate data acquired from human electrophysiological studies into patient-specific models, and validated this approach by testing whether electrophysiological responses to sequential premature stimuli could be predicted in a quantitatively accurate manner.

Methods: Eleven patients with structurally normal hearts underwent electrophysiological studies. Semi-automated analysis was used to reconstruct activation and repolarization dynamics for each electrode. This S_2 extrastimuli data was used to inform individualized models of cardiac conduction, including a novel derivation of conduction velocity restitution. Activation dynamics of multiple premature extrastimuli were then predicted from this model and compared against measured patient data as well as data derived from the ten-Tusscher cell-ionic model.

Results: Activation dynamics following a premature S_3 were significantly different from those after an S_2. Patient specific models demonstrated accurate prediction of the S_3 activation wave, (Pearson's $R^2 = 0.90$, median error 4%). Examination of the modeled conduction dynamics allowed inferences into the spatial dispersion of activation delay. Further validation was performed against data from the ten-Tusscher cell-ionic model, with our model accurately recapitulating predictions of repolarization times ($R^2 = 0.99$).

Conclusions: Simulations based on clinically acquired data can be used to successfully predict complex activation patterns following sequential extrastimuli. Such modeling techniques may be useful as a method of incorporation of clinical data into predictive models.

Keywords: conduction velocity restitution, computational modeling, action potential duration, patient specific modeling, cardiac arrhythmia

INTRODUCTION

Computerized simulations of cardiac activity have significantly contributed to our understanding of cardiac electrophysiology (Carusi et al., 2012). The recent leaps in raw processing power and access to supercomputing by research organizations has allowed proof-in-principle of many theories of cardiac conduction, from the cellular action potential to the generation of arrhythmia in heterogenous systems (e.g., in inherited arrhythmia syndromes such as Brugada or LQT syndromes). Though simulation has been very successful at bridging a knowledge gap between basic research findings and understanding of arrhythmia, efforts have principally concentrated on the "forward" solution, i.e., production of computer models that inform us of the behavior expected from our mathematical knowledge of cardiac physiology (Trayanova, 2011; Krummen et al., 2012). Few studies have attempted to broach a reverse solution, i.e., the construction of an accurate simulation based on patient-acquired data. There have been attempts to use patient anatomical data, such as those acquired from cardiac MRI, to fit a pre-existing cellular model, and some early work has attempted to fit clinically acquired data to a simulation (Relan et al., 2011). There remains some distance between computational modeling and clinical appreciation of arrhythmia generation, and computational approaches have not as yet found a clinical role.

Recently work has illustrated an approach by which electrophysiological data may be incorporated into simulations. Gilmour's group has concentrated on examination of one-dimensional conduction models, and has shown how sequential close-coupled activations may result in functional block "at-a-distance" from the stimulation site i.e., how an activating wavefront may impinge upon a prior wave of activation (Gilmour et al., 2007; Otani, 2007). Such functional block and wavebreak appear to be necessary events in triggering and sustaining the development of chaotic human arrhythmias, particularly VF. These frameworks incorporate both action potential duration

Abbreviations: ARI, Activation Recovery Interval; APD, Action potential duration; CV, Conduction Velocity; AT, Activation Time; ECG, Electrocardiogram; S1, S2, S3, Stimulus, Extrastimulus, Second Extrastimulus; ERP, Effective Refractory Period; RT, Repolarization Time; MRI, Magnetic Resonance Imaging; VT, Ventricular Tachycardia; VF, Ventricular Fibrillation.

(APD) restitution and conduction velocity restitution, and are founded on the cable theory principles originating in the work of Hodgkin and Huxley (Noble, 1962). In brief, this concept embodies cardiac conduction as a syncytium; strips of cardiac muscle are considered to act as uniform cables, allowing conduction in all directions. Unlike the squid giant axon, the cable properties of cardiac cells span many different cells, but they may still be represented as a two syncytial domains: intracellular and extracellular, and conduction properties depend on the properties of the cell membranes, ionic concentrations and cellular geometric arrangements. This concept can be developed to higher dimensions e.g., Spach et al., 1979, and/or simplified into descriptions of pure propagation of activation and repolarization e.g., Nolasco and Dahlen, 1968. These latter coupled-map models are easy to deal with both analytically and numerically and avoid the large complexities of high-dimensional, non-linear models of cardiac conduction. Further iterations of these models have clarified mathematical descriptions of conduction block at-a-distance in one-dimensional fiber (Fox, 2002; Fox et al., 2003).

Such a model underwent a qualitative validation in a canine model by Gelzer et al. (2008), where it was used to predict the initiation of VF by combinations of up to 5 extrastimuli. This work was notable in that the computer model had incorporated biologically-acquired data (action potential restitution measured from the interventricular septum). Thus, it represented a proof-of-concept of animal-specific electrophysiological models in the prediction of VF induction by extrastimuli, and has begun to bridge the gap between theoretical electrophysiological modeling and clinical application. But whether such models can be applied to the human heart, particularly in the investigation of cardiac risk, remains unproven.

A major limitation to closing the gap between ionic cardiac models and clinical implementation is the iterative process required to be undertaken to fit the model to the data (Clayton et al., 2011). The great number of variables in cardiac ionic models precludes accurately fitting of clinical data with confidence (Zaniboni et al., 2010). Previous attempts have concentrated on anatomical approaches to fit data to the individual, relying on "generic" models of the electrophysiology itself (Trayanova, 2011). Recognizing this, we have endeavored to describe observed cardiac electrophysiology at the tissue level using simple parameters.

This paper describes the approach we have taken to derive computer models from clinical data in our attempt to close the gap from theoretical modeling. The mathematical foundation of our work remains that of the one-dimensional model, which is itself a manifestation of cable theory. Thus, this work incorporating observed clinical parameters into a predictive model, and the validation of this method, in itself acts as a validation-step to the relevance of cable theory to human arrhythmogenisis.

We hypothesized that individual human restitution dynamics could be described by a one-dimensional model incorporating both conduction velocity restitution and action potential restitution. We tested this by incorporating patient-acquired data into individualized one-dimensional models (Hand and Griffith, 2010). These models were used to predict activation time (AT) dynamics following a second extrastimulus, and predictions were compared to experimental results.

METHODS

PATIENT POPULATION AND ELECTROPHYSIOLOGICAL STUDIES

Studies were performed in patients undergoing cardiac electrophysiological studies with a view to diagnosis and ablation of supraventricular tachycardia. All patients gave prior informed consent. Studies were performed under minimal conscious sedation in the post-absorptive state. Antidysrhythmic drugs were discontinued for 5 days prior to the study. The study protocol had local ethics committee approval and conformed to the standards set by the Declaration of Helsinki. Decapolar catheters were placed in an epicardial coronary vein via the coronary sinus, at the RV apex and retrogradely within the LV cavity adjacent to the epicardial catheter (St Jude Pathfinder). A reference anodal electrode was placed in the inferior vena cava. Further catheters were placed according to clinical requirements (**Figure 1**). Electrograms were digitized and recorded at 1000 Hz (Bard Clearsign, MN, USA). If no arrhythmia was initiated by ventricular pacing during the initial clinical study, restitution studies were performed prior to further clinical testing.

STUDY PROTOCOL

Following 3 min of steady-state pacing at the RV apex at a cycle length of 600 ms, a drivetrain of 10 beats was followed by an extrastimulus (S_2). The S_1S_2 interval was decremented by 20 to 300 ms, thereafter in 5 ms intervals until ERP was reached. The ERP was found by increasing CIs by 8 ms and then decrementing by further 2 ms intervals. In patients undergoing second extrastimuli (S_3) studies, the S_2 extrastimulus was set at 10 ms

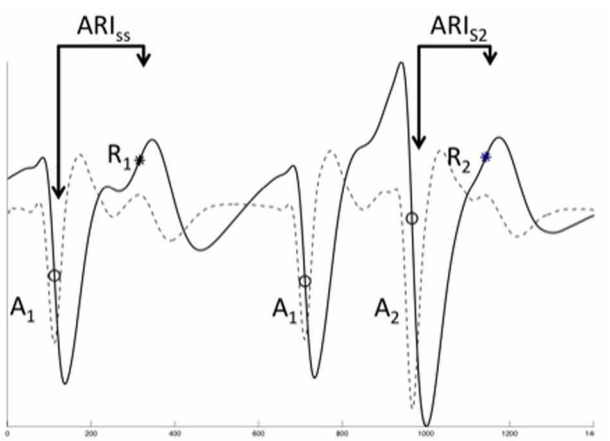

FIGURE 1 | Unipolar EGM analysis. The three final of a restitution train are shown, typical unipolar electrograms (solid line) and their differential (dashed line). Local activation was defined as the most rapid downstroke (dVdtmin, circles, A_1, A_2) of the activation inscription, repolarization was defined using the classical (Wyatt) method as dVdtmax of the T-wave (asterisks, R_1, R_2). Activation time was defined as the time from pacing stimulus (not shown) to local activation, ARI as time from local activation to repolarization. It was not possible to reliably measure the diastolic interval for close coupled beats, therefore DI was taken as A_1A_2—ARI$_{ss}$.

above the observed refractory period, and an S_3 was delivered at CIs progressively decrementing to a minimum of 180 ms.

WAVEFORM ANALYSIS

All electrogram analysis was performed using custom semi-automated software running in Matlab r2009b (The Mathworks Inc, MA, USA). Local AT and repolarization time (RT) were identified using an algorithm and manually checked. Filter settings of 0.1–150 Hz band-pass (for AT) and 40 Hz low-pass (RT) were used. Any electrogram in which the T-wave morphology was either inconsistent throughout the drivetrains or inadequately defined was excluded from analysis.

The electrograms of the ultimate 2 beats of each drive train and subsequent S_2 were exported and analyzed. It is technically challenging to measure action potentials in humans at more than one site simultaneously. However, the activation-repolarization index (ARI), i.e., the time from local activation to local repolarization as calculated from a unipolar electrogram signal, is a well-validated surrogate for the APD. Techniques for derivation of ARI analysis from unipolar electrograms have been well-described (Franz et al., 1987; Yue et al., 2004; Hanson et al., 2009). Briefly, AT was defined at the steepest negative slope of the activation waveform (**Figure 1**), and local repolarization time defined as the steepest positive slope of the T-wave (**Figure 1**), as supported by in-depth analysis (Yue et al., 2004; Yue, 2006; Potse et al., 2007, 2009). The diastolic interval (DI) preceding S_2 was calculated using measured values taken from steady state data. Similarly, the DI prior to a S_3 beat was estimated using a restitution model previously obtained for each electrode location. AT and repolarization time (RT) were measured from the stimulus time (defined as $t = 0$). The ARI of each beat is defined as the time difference from AT to RT, such that the repolarization time RT = AT + ARI.

ARI was plotted against DI to give standard ARI restitution curves. AT was plotted against coupling interval to illustrate conduction delay. These graphs were used for model creation. All electrogram analysis was performed using custom semi-automated software running in Matlab r2009b (The Mathworks Inc, MA, USA). AT and RT were identified using an algorithm and manually checked. Filter settings of 0.1–150 Hz band-pass (for AT) and 40 Hz low-pass (RT) were used. Any electrogram in which the T-wave morphology was inconsistent throughout the drivetrains or inadequately defined was excluded from analysis.

ONE-DIMENSIONAL CONDUCTION MODEL AND CV RESTITUTION MODELING

We derived a novel method whereby conduction velocity restitution can be quantified from biologically acquired data using a linear cell fiber model. Arbitrary length of cells of 0.1 mm was used for model derivation. Each cell within a fiber was assumed to have homogenous CV and APD restitution properties. Both of these factors were described by exponential functions.

If the length of a tissue unit (e.g., a myocyte) is assumed as Δx, and the conduction velocity within tissue as CV, the AT and repolarization time of a cell x_i can be calculated as:

$$\text{Activation time: } AT_n(x_i) = AT_n(x_{i-1}) + \frac{\Delta x}{CV_n(x_i)} \quad (1)$$

$$\text{Repolarization time: } RT_n(x_i) = AT_n(x_i) + ARI_n(x_i) \quad (2)$$

Where: AT and RT are the AT and repolarization time; ARI is the activation recovery interval; n is the number of beat.

Hence, the AT and recovery time at cell x_i can be expressed as:

$$AT_n(x_i) = AT_n(x_0) + \sum_{j=0}^{i} \frac{\Delta x}{CV_n(x_j)} \quad (3)$$

$$RT_n(x_i) = AT_n(x_0) + \sum_{j=0}^{i} \frac{\Delta x}{CV_n(x_j)} + ARI_n(x_i) \quad (4)$$

Where: x_0 represents the site of stimulation.

Thus, the period between activation n and activation $n + 1$ for site x_i can be calculated as:

$$AT_{n+1}(x_i) - AT_n(x_i) = AT_{n+1}(x_0) - AT_{n+1}(x_0) + \sum_{j=0}^{i}\left(\frac{\Delta x}{CV_{n+1}(x_i)} - \frac{\Delta x}{CV_n(x_i)}\right) \quad (5)$$

Here, the period between activation n and activation $n + 1$ for site x_0 equals to the coupling interval (CI_{n+1}) applied at site x_0

$$AT_{n+1}(x_0) - AT_n(x_0) = CI_{n+1} \quad (6)$$

The period between activation n and activation $n + 1$ for site x_i can also be calculated as:

$$AT_{n+1}(x_i) - AT_n(x_i) = ARI_n(x_i) + DI_{n+1}(x_i) \quad (7)$$

Combining equation 5, 6, and 7, the basic equation for one-dimensional conduction model can be expressed as:

$$DI_{n+1}(x_i) = CI_{n+1} + \sum_{j=0}^{i}\left(\frac{\Delta x}{CV_{n+1}(x_j)} - \frac{\Delta x}{CV_n(x_j)}\right) - ARI_n(x_i) \quad (8)$$

The conduction velocity $CV(x_i)$ is assumed to be a function of its preceding DI:

$$CV(x_i) = CV_{SS} - B_{CV} \cdot e^{C_{CV} \cdot DI} \quad (9)$$

where CV_{SS} is the steady-state conduction velocity, a constant defined to be 0.72 (Fox, 2002); B_{CV} and C_{CV} are two constants determining the steepness of CV restitution curve. This derivation is summarized in **Figure 2**.

Referring to the experimental data, $DI_{n+1}(x_i)$ is the DI of premature beat S_2, ARI_n is the ARI of the steady-state activation following S_1 ($ARI_n = ARI_{SS}$), CI_{n+1} is the S_1S_2 coupling interval. These three parameters were directly obtained from experimental data. $CV_n(x_i)$ is the conduction velocity of a steady-state activation, i.e., is equal to CV_{SS}.

For each investigated site, the activation conduction pathway from the pacing site to the investigated site was assumed to be an independent one-dimensional conduction pathway with uniform restitution properties. From the experimental

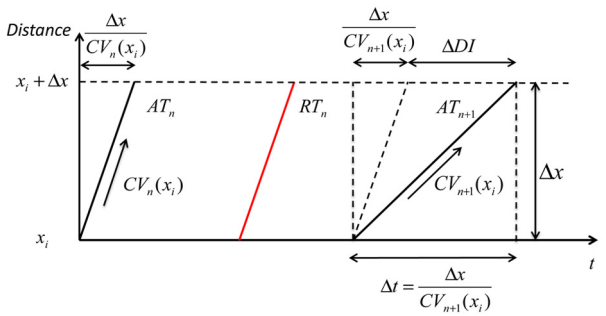

FIGURE 2 | Geometry relationship based on CV restitution. A geometric relationship based on the CV restitution model is shown. x_i is the position along a conduction path, ΔDI is the change in diastolic interval, Δt is the time that an activation wave takes to travel the distance Δx. AT_n: steady-state activation time with long DI; RT_n: steady-state repolarization time; AT_{n+1}: activation time of an early beat with shorter pacing interval and consequently showing some CV decrease (CV_{n+1} (x_i), but as the distance over which this operates (Δx) is very small this can be considered as a straight line.

data, an assumed length of the conduction pathway (given the assumed steady state conduction velocity) can be calculated by the product of steady-state conduction velocity and the steady-state conduction time, $AT_{SS}(x_i)$, from the pacing site to the investigated site:

$$L(x_i) = CV_{SS} \cdot AT_{SS}(x_i) \tag{10}$$

Hence, the number of cells included in the conduction pathway is $i = \frac{L(x_i)}{\Delta x}$.

Equation 8 can be rearranged into the following form, which allows its solution using experimental data:

$$DI_{S2}(x_i) + ARI_{SS}(x_i) - CI_{S2} + AT_{SS}(x_i) = \sum_{j=0}^{i} \frac{\Delta x}{CV_{S2}(x_j)} \tag{11}$$

All the dynamics in the left hand side of equation 11 are those obtained from experimental data. For each investigated site, the one-dimensional conduction model and CV restitution model can be fitted with its dynamics from experimental data. An iterative approach was taken, adjusting B_{CV} and C_{CV} in equation 9, and a minimum least-squares error method was employed to select optimum parameters.

INCORPORATION OF PATIENT DATA INTO ONE DIMENSIONAL MODELS

Data acquired from patient studies was applied to the model, and a separate (and independent) model was created for each electrode site. ARI restitution was modeled using a mono-exponential equation of the form specified in equation 13.

A standard value of 0.72 ms-1 was assumed as baseline conduction velocity, changing this absolute value by ±0.2 ms did not significantly affect derived CV dynamics. Despite model fitting being computationally intense, the use of simplified exponential dynamics allowed modern desktop machines to derive CV parameters reasonably quickly. For a typical patient, 100–2000 cells were included, depending on the distance of the conduction pathway. For example, if the steady-state conduction time was 100 ms at the investigated site, assuming the steady-state conduction velocity to be 0.72 ms-1 and cell length to be 100 μm, the number of cells included in the conduction model was 720.

Validation of our method was performed in two ways, comparison with ionic cellular model system and comparison with experimentally acquired patient data.

Once both ARI and CV restitution parameters had been derived from patient data, the cell fiber model was used to predict conduction dynamics of a second extrastimuli (S_3) introduced following a short S_1S_2 coupling interval. Modeling of sequential beats was only attempted if the r^2 for fitting to S_2 data was >0.7 at that electrode site, and sites where electrograms were of poor quality were excluded. ATs following the S_3 beat obtained experimentally were quantatively compared to those obtained from the cell fiber model.

COMPARING THE EXPONENTIAL MODEL OF REPOLARIZATION DYNAMICS AGAINST DATA IONIC CELLULAR SIMULATION

At short S_2S_3 coupling intervals, the QRS complex of the unipolar electrogram following an S_3 can widen to fuse with the repolarization complex. This precludes using unipolar electrograms to validate our simple model for prediction of repolarization times. We thus performed preliminary validation of our model for prediction of S_3 repolarization times against data taken from an ionic cellular model. The ion channel model is obtained from ten Tusscher et al. from their studies of human ventricular tissue (ten Tusscher et al., 2009).

The ten Tusscher human ventricular ionic model includes 16 types of currents, and 30 ionic gate variables. It is practically impossible with current technology to obtain detailed information of each type of ion current or gate variables on an individual patient. However, the experimental data provides information on key cellular properties such as APD, AT, and repolarization time. These three interdependent properties were fitted with the restitution models, which is then used to simulate interactions of activation and repolarization.

The ten Tusscher human ventricular model can be summarized in a general form below (the forward Euler method was used to integrate the model). Initial conditions for ionic values and conductances are given in **Table 1**:

$$\frac{\partial V}{\partial t} = -\frac{I_{ion} + I_{stim}}{C_m} \tag{12}$$

Where: V is voltage,
t is time,
I_{ion} is the sum of all transmembrane ionic currents,
I_{stim} is the stimulus current,
C_m is cell capacitance per unit surface area.

Action potential duration (APD) is defined to be action potential duration at 90% repolarization (APD_{90}).

Diastolic interval (DI) equals to the coupling interval of S2 minus APD from steady-state beat (APD_{ss}).

Table 1 | Initial conditions for state variables in human ventricular ionic model.

V	−87.84 mV	$[Na^+]_i$	7.23 mM	$[Na^+]_{ss}$	7.23 mM
$[K^+]_i$	143.79 mM	$[K^+]_{ss}$	143.79 mM	$[Ca^{2+}]_i$	$8.54 \bullet 10^{-5}$ mM
$[Ca^{2+}]_{ss}$	$8.43 \bullet 10^{-5}$ mM	$[Ca^{2+}]_{nsr}$	1.61 mM	$[Ca^{2+}]_{jsr}$	1.56 mM
m	0.0074621	h_{fast}	0.692591	h_{slow}	0.692574
j	0.692574	$h_{CaMK,slow}$	0.448501	j_{CaMK}	0.692413
m_L	0.000194015	h_L	0.496116	$h_{L,CaMK}$	0.265885
a	0.00101185	i_{fast}	0.999542	i_{slow}	0.589579
a_{CaMK}	0.000515567	$i_{CaMK,fast}$	0.999542	$i_{CaMK,slow}$	0.641861
d	$2.43015 \bullet 10^{-9}$	f_{fast}	1	f_{slow}	0.910671
$f_{Ca,fast}$	1	$f_{Ca,slow}$	0.99982	j_{Ca}	0.999977
n	0.00267171	$f_{CaMK,fast}$	1	$f_{Ca,CaMK,fast}$	1
$x_{r,fast}$	$8.26608 \bullet 10^{-6}$	$x_{r,slow}$	0.453268	x_{s1}	0.270492
x_{s2}	0.0001963	x_{K1}	0.996801	$J_{rel,NP}$	$2.53943 \bullet 10^{-5}$ mM/ms
$J_{rel,CaMK}$	$3.17262 \bullet 10^{-7}$ mM/ms	$CaMK_{trap}$	0.0124065		

Where: V, membrane voltage; $[Na^+]_i$, intracellular sodium ion concentration; $[Na^+]_{ss}$, concentration of sodium ion, in subspace compartment; $[K^+]_i$, intracellular potassium ion concentration; $[K^+]_{ss}$, concentration of potassium ion, in subspace compartment; $[Ca^{2+}]_i$, intracellular calcium ion concentration; $[Ca^{2+}]_{ss}$, concentration of calcium ion, in subspace compartment; $[Ca^{2+}]_{nsr}$, concentration of calcium ion, in network SR compartment; $[Ca^{2+}]_{jsr}$, concentration of calcium ion, in junctional SR compartment; m, activation gate for fast Na^+ current I_{Na}; h_{fast}, fast development of inactivation gate for fast Na^+ current I_{Na}; h_{slow}, slow development of inactivation gate for fast Na^+ current I_{Na}; j, recovery from inactivation gate for fast Na^+ current I_{Na}; $h_{CaMK,slow}$, slow development of inactivation gate for CaMK phosphorylated fast Na^+ current I_{Na}; j_{CaMK}, recovery from inactivation gate for CaMK phosphorylated fast Na^+ current I_{Na}; m_L, activation gate for late Na^+ current I_{Na}; h_L, inactivation gate for late Na^+ current I_{Na}; $h_{L,CaMK}$, inactivation gate for CaMK phosphorylated Na^+ current I_{Na}; a, activation gate for transient outward K^+ current I_{to}; i_{fast}, fast inactivation gate for transient outward K^+ current I_{to}; i_{slow}, slow inactivation gate for transient outward K^+ current I_{to}; a_{CaMK}, activation gate for CaMK phosphorylated transient outward K^+ current I_{to}; $i_{CaMK,fast}$, fast inactivation gate for CaMK phosphorylated transient outward K^+ current I_{to}; $i_{CaMK,slow}$, slow inactivation gate for CaMK phosphorylated transient outward K^+ current I_{to}; d, activation gate for Ca^{2+} current through the L-type Ca^{2+} channel I_{CaL}; f_{fast}, fast voltage dependent inactivation gate for Ca^{2+} current through the L-type Ca^{2+} channel I_{CaL}; f_{slow}, slow voltage dependent inactivation gate for Ca^{2+} current through the L-type Ca^{2+} channel I_{CaL}; $f_{Ca,fast}$, fast development of Ca^{2+} dependent inactivation gate for Ca^{2+} current through the L-type Ca^{2+} channel I_{CaL}; $f_{Ca,slow}$, slow development of Ca^{2+} dependent inactivation gate for Ca^{2+} current through the L-type Ca^{2+} channel I_{CaL}; j_{Ca}, recovery from Ca^{2+} dependent inactivation gate for Ca^{2+} current through the L-type Ca^{2+} channel I_{CaL}; n, fraction in Ca^{2+} dependent inactivation mode for Ca^{2+} current through the L-type Ca^{2+} channel I_{CaL}; $f_{CaMK,fast}$, fast development of Ca^{2+} dependent inactivation gate for CaMK phosphorylated I_{CaL}; $f_{Ca,CaMK,fast}$, slow development of Ca^{2+} dependent inactivation gate for CaMK phosphorylated I_{CaL}; $x_{r,fast}$, fast activation/deactivation gate for rapid delayed rectifier K^+ current I_{Kr}; $x_{r,slow}$, slow activation/deactivation gate for rapid delayed rectifier K^+ current I_{Kr}; x_{s1}, activation gate for slow delayed rectifier K^+ current I_{Ks}; x_{s2}, deactivation gate for slow delayed rectifier K^+ current I_{Ks}; x_{K1}, inactivation gate for inward rectifier K^+ current I_{K1}; $J_{rel,NP}$, non-phosphorylated Ca^{2+} release, via ryanodine receptors, from jsr to myoplasm; $J_{rel,CaMK}$, CaMK phosphorylated Ca^{2+} release, via ryanodine receptors, from jsr to myoplasm; $CaMK_{trap}$, fraction of autonomous CaMK binding sites with trapped calmodulin.

The form of exponential model tested against data acquired from the ionic cellular model was:

$$APD = APD_{ss} - B \bullet e^{C \bullet DI} \tag{13}$$

The pacing protocols applied to ion channel model were the same as those used clinically (i.e., a sequential extrastimulus study). Data acquired from the ion channel model was compared against S_3 repolarization times modeled using our simple exponential-based approach.

STATISTICS

Data is presented as mean ± standard deviation unless otherwise stated. Comparative statistics were calculated within R. An individual simulation was performed for each measured site, thus each patient had multiple simulations performed. Multilevel regression enabled appreciation of the statistical reliability of predictions without inappropriate prejudice or favor regarding the grouped and leveled nature of measurements (i.e., incorporating both within-subject and between-subject variances). These calculations were performed using the lmer package (Pinheiro et al., 2009), single-level comparisons of normally-distributed continuous variables were performed using Student's T-test. A p-value of less than 0.05 was taken as significant. Correlation coefficients involving model comparisons were performed with Matlab.

RESULTS

PATIENT DEMOGRAPHICS

Eleven patients were enrolled in the study, aged 29 ± 10 years, 7 females. All patients had structurally normal hearts on echocardiography, and underwent EP studies for symptoms consistent with paroxysmal supraventricular tachycardia. Final diagnoses were atrioventricular re-entrant tachycardia (5 patients), paroxysmal atrial fibrillation (1). No arrhythmia was induced in 5 patients. Six of these patients underwent S_3 studies and were included in the S_3 validation.

ACTIVATION TIME, ARI RESTITUTION AND REPOLARIZATION CURVES

The dynamics of how AT, ARI, repolarization time (RT) and DI varied with the coupling interval of the first extrastimulus were examined. This is illustrated in **Figure 3**. As coupling interval decreases from steady state, ARI restitution is observed, and

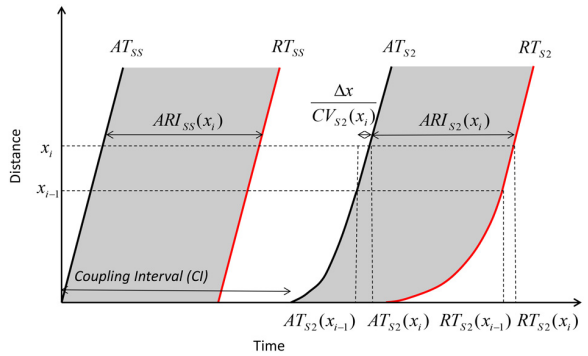

FIGURE 3 | Geometry relationship and derivation of modulation of dispersion. A premature extrastimulus results in conduction velocity restitution. Consequently, ATs are delayed, but this delay allows resumption toward steady state conduction velocities over the course of the activation path. The modulation of activation dispersion is amplified via ARI restitution on the repolarization wavefront, and dispersion of repolarization increases further.

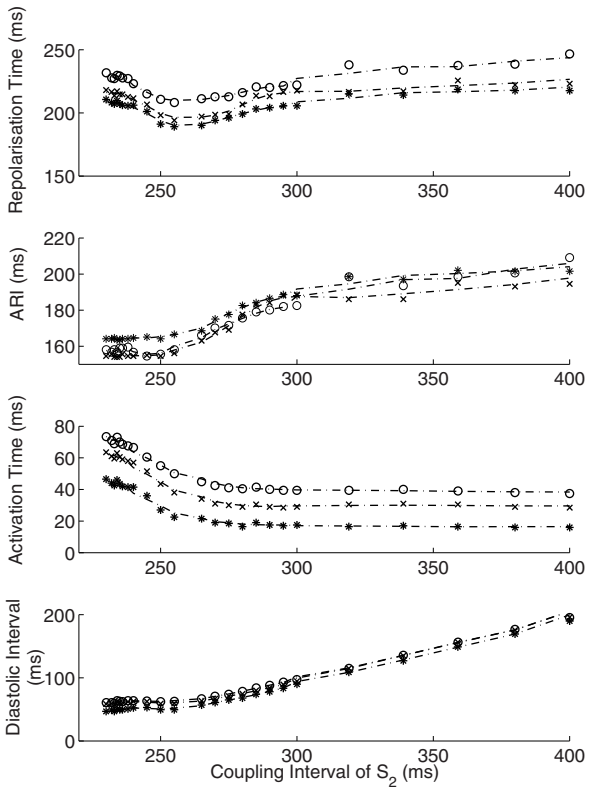

FIGURE 4 | Interactions of activation and ARI leading to repolarization time change. The response of diastolic interval (DI), activation time and ARI to shortening coupling interval are shown, with the overall repolarization time dynamic shown in the top panel. As paced intervals decrease, diastolic intervals decrease initially in a linear fashion (**Bottom** panel). The reduction in DI is associated with a non-linear reduction in ARI (restitution). As coupling intervals become very short, activation time increases due to the effect of conduction velocity restitution acting between the stimulus site and the recording electrode. Activation time increases prevent further reduction of local diastolic interval (**Bottom** panel), which is seen to level off. ARI restitution is blunted at these short coupling intervals. Repolarization time thus increases as a result of increasing activation times. Representative patient data from RV (Star—early activating site, cross- mid activating site, circle- late activating site, dotted lines represent smoothed dynamics).

both ARI and repolarization time shorten. But as coupling intervals shortened further toward ERP, the effects of conduction velocity restitution became apparent (as illustrated by increasing ATs). This prevents further decrease in local DIs, and hence ARI restitution is restricted. The local repolarization time effectively represents the cumulative effect of ARI and conduction velocity restitution, together these produced a distinctive repolarization time curve illustrated in **Figure 4**.

MODEL FITTING TO S_2 DATA

One-dimensional models were fitted to clinically acquired S_2 data in all 11 patients. ARI restitution curves were accurately described by a simple exponential model (Coefficient of determination, $r^2 = 0.966$ [95% CI 0.963–0.968], $p < 0.0001$). AT curves were similarly accurately reproduced following our derivations of conduction velocity restitution, ($r^2 = 0.993$ [0.992–0.993], $p < 0.0001$).

ACTIVATION TIMES FOLLOWING SEQUENTIAL PREMATURE STIMULI

To show that prediction of ATs following sequential extrastimuli was a reasonable standard by which to assess the accuracy of our model, we compared the activation dynamics following S_2 and S_3 stimuli. At similar coupling intervals, AT following a premature S_3 was significantly shorter than after an S_2 [AT normalized to steady state: 1.1 following S_3 (95% confidence interval 1.1–1.2) vs. 1.6 following S_2 (1.5–1.7), $p < 0.0001$]. ERP of S_3 was shorter than ERP of S_2 ($<186 \pm 8$ vs. 222 ± 25 ms, $p < 0.0001$). More activation delay existed after an S_3 pre-ERP than after an S_2 (39 ± 28 vs. 33 ± 16 ms, $p = 0.0003$). Activation dynamics were thus significantly different following S_2 and S_3 stimuli, with the ERP of an S_2 considerably shorter than that following the steady state beats.

VALIDATION OF 1D MODELS

We tested whether the one-dimensional model, incorporating both ARI and CV restitution, could explain and predict the observed variation in activation dynamics following S_2 and S_3 stimuli. This serves as a quantative validation of the 1D model incorporating CV and ARI restitution. Validation was performed using data from 6 patients who underwent S_3 protocol. The coefficient of determination (predicted values vs. measured), R^2, was 0.902 [95% CI: 0.890–0.911] ($p < 0.0001$, **Figure 5**). The high predictive accuracy possible with this method serves as a quantitative validation of this one-dimensional model of cardiac activation in human hearts.

SIMULATING MODULATION OF DISPERSION OF REPOLARIZATION

Simulations based on patient data enable examination of electrophysiology which otherwise remains impenetrable through traditional experimental methods. We examined how dispersion of repolarization varied with shortening of S_2 coupling interval. True dispersion of repolarization, the difference from the earliest

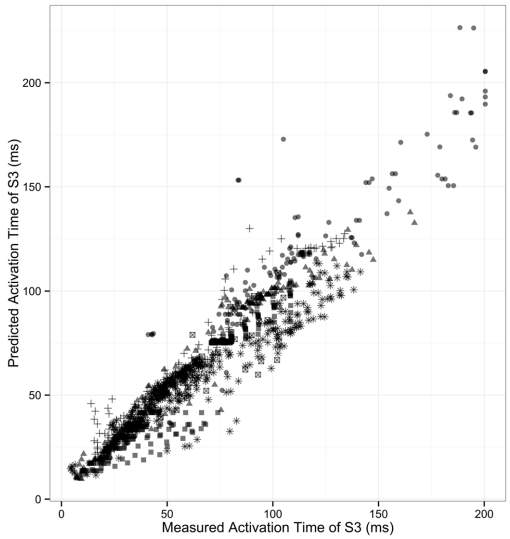

FIGURE 5 | Correlation of measured and predicted AT of second extrastimulus. The correlation of modeled S_3 activation time with measured S_3 activation is shown. Each patient is represented by individual symbols. $r^2 = 0.90$.

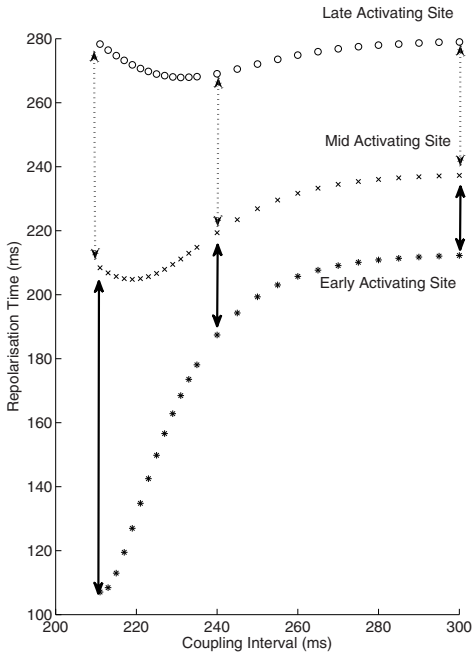

FIGURE 6 | Increase in dispersion of repolarization with reducing coupling intervals. Repolarization times from 3 sites are shown against coupling intervals. The early activating site can be considered to be equivalent to the stimulus site, and is not measured clinically due to artifact. This early site is exposed to only minimal activation time increase at short coupling intervals, thus the repolarization time is approximately equal to the ARI at this site. The mid and late activating sites do exhibit an increase in dispersion of repolarization (broken arrows), but this is minor in comparison to the increase from the early to mid site (solid arrows). Thus, there is a marked spatial increase in the repolarization gradient near the stimulus site following premature extrastimuli.

repolarization to the latest repolarization, has both a spatial and temporal component. It is very hard to measure repolarization time accurately very close to the stimulus site due to stimulus artifact. But the most significant repolarization gradients will be close to the stimulus site following a close-coupled S_2; the area immediately at the stimulus site is exposed to very little delay prior to activation, whereas further sites only a very short distance away experience significant activation delay. A patient-based simulation allows appreciation of these gradients (**Figure 6**). In the example shown the dispersion of repolarization increased from 41 to 70 ms between mid to late activating sites, yet increased 4-fold from 25 to 100 ms between earlier activating sites. Thus, the induction of repolarization gradients by premature stimuli occurs very close to the stimulus site.

VALIDATION OF REPOLARIZATION TIME PREDICTIONS AGAINST IONIC CELLULAR SIMULATIONS

For S_3 responses, there was close agreement between repolarization times determined from our model and repolarization times acquired using the ionic model (coefficient of determination, $r^2 = 0.997$ [95% CI 0.993–0.999], $p < 0.0001$). This supports the validity of our model in comparison to full ionic cellular models undergoing sequential premature extrastimuli.

DISCUSSION

Using a combination of physiological measurement and simulation, this study demonstrates that the complex dynamic interactions between activation and repolarization induced by sequential extrastimuli can approximated in terms of ARI (APD) and CV restitution. This serves as a strong validation of a personalized computational approach incorporating biologically acquired variables and it serves as an extension and validation in humans of previous animal work (Gilmour et al., 2007). Our technique provides a platform by which individual patient data may be incorporated into computerized simulations and serves as an example of a method by which the gap between fundamental cardiac simulation and clinical science can be bridged.

This study is the first to quantitatively validate a one-dimensional model of cardiac conduction in man. Such patient-based models provide a method by which physiologically acquired data may be interrogated in a computerized simulation. We have shown that endocardial physiology can be adequately modeled by simple mathematical descriptors of CV and ARI restitution curves, and confirm the relevance of one-dimensional conduction models incorporating both these features to human cardiac electrophysiology. Our validation of a straightforward one-dimension model can allow further in-depth examination of human physiology in a manner that would not be possible experimentally, for both ethical and practical reasons.

The presented modeling is founded on the work of Otani, Gilmour and Fox (Fox et al., 2003; Gilmour et al., 2007; Otani, 2007; Gelzer et al., 2008, 2010). Seminal work by this group, along with the single fiber models of Cherry and Fenton (2004, 2007), provided initial validation of the use of one-dimensional conduction simulation in biological systems. The ability of such a model to predict whether large variations of long-short CIs would

induce VF in normal and cardiomyopathic canines was a powerful demonstration of the physiological relevance of such simulations (Gelzer et al., 2008, 2010).

We have enhanced these models by fully deriving CV restitution; allowing better approximation to the actual behavior of the activation wavefront and observation of the heterogeneity introduced by sequential extrastimuli. This adds to our earlier description of the modulated dispersion of repolarization in humans (Hanson et al., 2009), and addresses questions raised from this work (Poelzing and Rosenbaum, 2009). CV restitution is often assumed to operate over the entire conduction path in a similar manner, obscuring the importance of the spatial differences in CV restitution. Our validation also sought a high fidelity correlation of ATs rather than a binary outcome. The large datasets acquired from the multiple recording electrodes used in each patient (rather than only one in the canine studies) enabled an accurate validation of this concept in humans.

The degree of latency has been described as being important in determining the initiation of VT or VF due to programmed electrical stimulation in earlier clinical studies (Avitall et al., 1992), yet the mechanism of this has been unclear. Our explanation of CV restitution, and of a mechanism by which cumulative interactions can set up conduction heterogeneities is consistent with these previous descriptions.

Knowledge of these timing dynamics may help determine susceptibility to arrhythmia in channelopathies (Lambiase et al., 2009; Nam et al., 2010) or a suspected cardiomyopathy. The demonstration that patient-specific modeling can predict initiation sites of clinical arrhythmia underlines the importance of ARI and CV interactions in human arrhythmogenisis.

STUDY LIMITATIONS

We used clinically acquired data to observe and explain the complex interactions seen following sequential extrastimuli. These are considered central to the initiation of cardiac arrhythmia. We did not expect to, nor did we induce arrhythmia in any patient undergoing prospective evaluation, and the contribution of these mechanisms in clinical arrhythmogenisis was not fully examined. Prospective patient data was acquired from contact electrodes; simultaneous mapping from the entire endo- and epicardial surface is unfeasible in conscious patients. However, as a result of lack of 3D geometry, conduction path distances were derived from timing data and knowledge of electrode spacings. The demonstration that these techniques can effectively predict wavebreak and arrhythmia initiation requires confirmation in prospective studies.

By design, our modeling and simulation was relatively simple and was limited to a one-dimensional system. This did not allow examination of wavebreak, arrhythmia development or re-entry, and observations are limited to assumptions of homogenous properties. The APD and CV restitution models used in this paper are in the form of exponential equations, this assumed behavior is based on the tendency of experimental data and on equations used in previous studies. Biological behavior would be expected to deviate from these simple exponential models, which in turn will result in discrepancies between simulation and clinical measurement. The use of derivations allowing direct fitting of ionic models to clinical results, perhaps by using an iterative approach, will improve the fidelity of such patient-derived simulations.

The success of our model at predicting local ATs following an S_3 stimulus makes it tempting to assume that it will retain predictive accuracy for S_4, S_5 and so on. This is unlikely. Though the principles demonstrated remain valid, our model did not include myocardial memory effects, post-repolarization refractoriness or anisotropy. These may have increasing importance with longer extrastimuli sequences, and ARI restitution dynamics may change significantly as a consequence of these (Kobayashi et al., 1992; Shimizu et al., 2000). Despite a very high agreement in predicting S_3 ARI restitution obtained from a complex ionic model, even these ionic models may still not fully reproduce these less studied phenomena. However, our model's simplicity made it accessible to the incorporation of clinical data, and the robust prediction and demonstration of S_3 wavefront dynamics (which do not require knowledge of S_3 ARI restitution) remains impressive.

FUTURE STUDIES

This study provides important information to assist electrophysiological characterization of myocardial diseases and phenotypes. Some of the techniques we describe may be applicable to clinical practice e.g., determining an individual patient heart's boundary conditions for functional block as a method for arrhythmic risk stratification. All data was acquired in patients with normal hearts under baseline conditions. Further studies should examine the modulation of changes in conduction/repolarization interactions under conditions of autonomic stress or drug interactions. More complicated models, such as those based on ionic cellular models could be applied to the data, possibly using our method as an intermediary step to allow parameter fitting. This could produce more detailed and realistic simulations, extending the described parameters into 3 dimensions. Furthermore, new technologies such as non-invasive body surface mapping may allow acquisition of whole heart activation and repolarization dynamic data.

Specific future uses of the described method may have an early application in patients at risk of inherited ventricular arrhythmias, particularly Brugada syndrome or arrhythmogenic right ventricular cardiomyopathy (ARVC). Both of these conditions have well-described changes in invasive electrophysiology, yet risk stratification is incomplete. Patient specific models could give valuable diagnostic information and help quantify the risk of arrhythmia in such patients. Pharmaceutical testing may also benefit from such analysis, as a method to determine arrhythmogenicity of subtle changes in electrophysiological responses after drug challenge. Furthermore, a bullish use of this method would be as an adjunct in early clinical assessments of new anti-arrhythmia agents, to lend support to an investigational compound's antiarrhythmic properties, or otherwise.

CONCLUSIONS

Conduction and repolarization interactions in humans can be described in terms of restitution of CV and APD. Simulations based on clinically acquired data can be used to successfully predict complex activation patterns following sequential extrastimuli. Such modeling techniques may be useful as a method of incorporation of clinical data into predictive models.

REFERENCES

Avitall, B., McKinnie, J., Jazayeri, M., Akhtar, M., Anderson, A. J., and Tchou, P. (1992). Induction of ventricular fibrillation versus monomorphic ventricular tachycardia during programmed stimulation. Role of premature beat conduction delay. *Circulation* 85, 1271–1278. doi: 10.1161/01.CIR.85.4.1271

Carusi, A., Burrage, K., and Rodriguez, B. (2012). Bridging experiments, models and simulations: an integrative approach to validation in computational cardiac electrophysiology. *Am. J. Physiol. Heart Circ. Physiol*. 303, H144–H155. doi: 10.1152/ajpheart.01151.2011

Cherry, E. M., and Fenton, F. H. (2004). Suppression of alternans and conduction blocks despite steep APD restitution: electrotonic, memory, and conduction velocity restitution effects. *Am. J. Physiol. Heart Circ. Physiol*. 286, H2332–H2341. doi: 10.1152/ajpheart.00955.2006

Cherry, E. M., and Fenton, F. H. (2007). A tale of two dogs: analyzing two models of canine ventricular electrophysiology. *Am. J. Physiol. Heart Circ. Physiol*. 292, H43–H55.

Clayton, R. H., Bernus, O., Cherry, E. M., Dierckx, H., Fenton, F. H., Mirabella, L., et al. (2011). Models of cardiac tissue electrophysiology: progress, challenges and open questions. *Prog. Biophys. Mol. Biol*. 104, 22–48. doi: 10.1016/j.pbiomolbio.2010.05.008

Fox, J. J. (2002). Spatiotemporal transition to conduction block in canine ventricle. *Circ. Res*. 90, 289–296. doi: 10.1088/1367-2630/5/1/401

Fox, J. J., Riccio, M. L., Drury, P., and Werthman, A., and Gilmour, R. F. Jr. (2003). Dynamic mechanism for conduction block in heart tissue. *New J. Phys*. 5, 101.1–101.14. doi: 10.1088/1367-2630/5/1/401

Franz, M. R., Bargheer, K., Rafflenbeul, W., Haverich, A., and Lichtlen, P. R. (1987). Monophasic action potential mapping in human subjects with normal electrocardiograms: direct evidence for the genesis of the T wave. *Circulation* 75, 379–386. doi: 10.1161/01.CIR.0000141734.43393.BE

Gelzer, A. R., Koller, M. L., Otani, N. F., Fox, J. J., Enyeart, M. W., Hooker, G. J., et al. (2008). Dynamic mechanism for initiation of ventricular fibrillation *in vivo*. *Circulation* 118, 1123–1129.

Gelzer, A. R. M., Otani, N. F., Koller, M. L., Enyeart, M. W., Moise, N. S., and Gilmour, R. F. (2010). Dynamically-induced spatial dispersion of repolarization and the development of VF in an animal model of sudden death. *Comput. Cardiol*. 2009, 309–312.

Gilmour, R. F. J., Gelzer, A. R., and Otani, N. F. (2007). Cardiac electrical dynamics: maximizing dynamical heterogeneity. *J. Electrocardiol*. 40, S51–S55.

Hand, P. E., and Griffith, B. E. (2010). Adaptive multiscale model for simulating cardiac conduction. *Proc. Natl. Acad. Sci. U.S.A*. 107, 14603–14608. doi: 10.1073/pnas.1008443107

Hanson, B., Sutton, P., Elameri, N., Gray, M., Critchley, H., Gill, J. S., et al. (2009). Interaction of activation-repolarization coupling and restitution properties in humans. *Circ. Arrhythm. Electrophysiol*. 2, 162–170.

Kobayashi, Y., Peters, W., Khan, S. S., Mandel, W. J., and Karagueuzian, H. S. (1992). Cellular mechanisms of differential action potential duration restitution in canine ventricular muscle cells during single versus double premature stimuli. *Circulation* 86, 955–967.

Krummen, D. E., Bayer, J. D., Ho, J., Ho, G., Smetak, M. R., Clopton, P., et al. (2012). Mechanisms for human atrial fibrillation initiation: clinical and computational studies of repolarization restitution and activation latency. *Circ. Arrhythm. Electrophysiol*. 5, 1149–1159. doi: 10.1161/CIRCEP.111.969022

Lambiase, P. D., Ahmed, A. K., Ciaccio, E. J., Brugada, R., Lizotte, E., Chaubey, S., et al. (2009). High-density substrate mapping in Brugada syndrome: combined role of conduction and repolarization heterogeneities in arrhythmogenesis. *Circulation* 120, 106–117, 1–4. doi: 10.1161/CIRCULATIONAHA.108.771401

Nam, G. B., Ko, K. H., Kim, J., Park, K. M., Rhee, K. S., Choi, K. J., et al. (2010). Mode of onset of ventricular fibrillation in patients with early repolarization pattern vs. Brugada syndrome. *Eur. Heart J*. 31, 330–339. doi: 10.1093/eurheartj/ehp423

Noble, D. A. (1962). Modification of the Hodgkin–Huxley equations applicable to Purkinje fibre action and pacemaker potentials. *J. Physiol*. 160, 317–352.

Nolasco, J. B., and Dahlen, R. W. (1968). A graphic method for the study of alternation in cardiac action potentials. *J. Appl. Physiol*. 25, 191–196.

Otani, N. F. (2007). Theory of action potential wave block at-a-distance in the heart. *Phys. Rev. E*. 75, 21910. doi: 10.1103/PhysRevE.75.021910

Pinheiro, J., Bates, D., DebRoy, S., Sarkar, D. and the R Core team. (2009). "nlme: linear and nonlinear mixed effects models," in *R package version 3.1-96. R Foundation for Statistical Computing*, Vienna.

Poelzing, S., and Rosenbaum, D. S. (2009). The modulated dispersion hypothesis confirmed in humans. *Circ. Arrhythm. Electrophysiol*. 2, 100–101. doi: 10.1161/CIRCEP.109.862227

Potse, M., Coronel, R., Opthof, T., and Vinet, A. (2007). The positive T wave. *Anadolu Kardiyol Derg*. 7(Suppl. 1), 164–167.

Potse, M., Vinet, A., Opthof, T., and Coronel, R. (2009). Validation of a simple model for the morphology of the T wave in unipolar electrograms. *Am. J. Physiol. Heart Circ. Physiol*. 297, H792–H801. doi: 10.1152/ajpheart.00064.2009

Relan, J., Chinchapatnam, P., Sermesant, M., Rhode, K., Ginks, M., Delingette, H., et al. (2011). Coupled personalization of cardiac electrophysiology models for prediction of ischaemic ventricular tachycardia. *Interface Focus* 1, 396–407. doi: 10.1098/rsfs.2010.0041

Shimizu, S., Kobayashi, Y., Miyauchi, Y., Ohmura, K., Atarashi, H., and Takano, T. (2000). Temporal and spatial dispersion of repolarization during premature impulse propagation in human intact ventricular muscle: comparison between single vs double premature stimulation. *Europace* 2, 201–206.

Spach, M., Miller, W. T., Miller-Jones, E., Warren, R., and Barr, R. C. (1979). Extracellular potentials related to intracellular action potentials during impulse conduction in anisotropic canine cardiac muscle. *Circ. Res*. 45, 188–204.

ten Tusscher, K. H., Mourad, A., Nash, M. P., Clayton, R. H., Bradley, C. P., Paterson, D. J., et al. (2009). Organization of ventricular fibrillation in the human heart: experiments and models. *Exp. Physiol*. 94, 553–562.

Trayanova, N. A. (2011). Whole-heart modeling: applications to cardiac electrophysiology and electromechanics. *Circ. Res*. 108, 113–128. doi: 10.1161/CIRCRESAHA.110.223610

Yue, A. M. (2006). Letter regarding article by Koller et al. : Altered dynamics of action potential restitution and alternans in humans with structural heart disease. *Circulation* 113:e462. doi: 10.1161/CIRCULATIONAHA.105.597310

Yue, A. M., Paisey, J. R., Robinson, S., Betts, T. R., Roberts, P. R., and Morgan, J. M. (2004). Determination of human ventricular repolarization by noncontact mapping: validation with monophasic action potential recordings. *Circulation* 110, 1343–1350.

Zaniboni, M., Riva, I., Cacciani, F., and Groppi, M. (2010). How different two almost identical action potentials can be: a model study on cardiac repolarization. *Math. Biosci*. 228, 56–70. doi: 10.1016/j.mbs.2010.08.007

Conflict of Interest Statement: The authors declare that the research was conducted in the absence of any commercial or financial relationships that could be construed as a potential conflict of interest.

Received: 13 May 2013; paper pending published: 02 June 2013; accepted: 25 July 2013; published online: 04 September 2013.

*Citation: Finlay MC, Xu L, Taggart P, Hanson B and Lambiase PD (2013) Bridging the gap between computation and clinical biology: validation of cable theory in humans. Front. Physiol. **4**:213. doi: 10.3389/fphys.2013.00213*

This article was submitted to Cardiac Electrophysiology, a section of the journal Frontiers in Physiology.

frontiers in
PHYSIOLOGY

REVIEW ARTICLE
published: 12 September 2013
doi: 10.3389/fphys.2013.00199

The investigation of sudden arrhythmic death syndrome (SADS)—the current approach to family screening and the future role of genomics and stem cell technology

Vishal Vyas*[1] *and Pier D. Lambiase*[2]*

[1] *Barnet and Chase Farm Hospitals NHS Trust, Medicine, Enfield, UK*
[2] *Cardiology, The Heart Hospital, University College Hospital and Institute of Cardiovascular Sciences, University College London, London, UK*

Edited by:
Christopher Huang, University of Cambridge, UK

Reviewed by:
Carol Ann Remme, University of Amsterdam, Netherlands
Christopher Huang, University of Cambridge, UK

****Correspondence:***
Pier D. Lambiase, Cardiology, The Heart Hospital, University College Hospital and Institute of Cardiovascular Sciences, University College London, 16-18 Westmoreland Street, London W1G 8PH, UK
e-mail: pier.lambiase@uclh.nhs.uk

SADS is defined as sudden death under the age of 40 years old in the absence of structural heart disease. Family screening studies are able to identify a cause in up to 50% of cases-most commonly long QT syndrome (LQTS), Brugada and early repolarization syndrome, and catecholaminergic polymorphic ventricular tachycardia (CPVT) using standard clinical screening investigations including pharmacological challenge testing. These diagnoses may be supported by genetic testing which can aid cascade screening and may help guide management. In the current era it is possible to undertake molecular autopsy provided suitable samples of DNA can be obtained from the proband. With the evolution of rapid sequencing techniques it is possible to sequence the whole exome for candidate genes. This major advance offers the opportunity to identify novel causes of lethal arrhythmia but also poses the challenge of managing the volume of data generated and evaluating variants of unknown significance (VUS). The emergence of induced pluripotent stem cell technology could enable evaluation of the electrophysiological relevance of specific ion channel mutations in the proband or their relatives and will potentially enable screening of idiopathic ventricular fibrillation survivors combining genetic and electrophysiological studies in derived myocytes. This also could facilitate the assessment of personalized preventative pharmacological therapies. This review will evaluate the current screening strategies in SADS families, the role of molecular autopsy and genetic testing and the potential applications of molecular and cellular diagnostic strategies on the horizon.

Keywords: sudden death, screening, ion channel, stem cell, SADS

INTRODUCTION

Of the 484,367 deaths registered in England and Wales in 2011, 29% were attributed to circulatory disorders (Births and Deaths in England and Wales, 2011). A report in 2009 found that sudden cardiac death was responsible for ∼60,000 deaths, with ischemic heart disease the major cause (Papadakis et al., 2009). In the younger population (1–35 years of age), sudden cardiac death is the most common cause of premature death (Tester and and Ackerman, 2012). Here, a thorough investigation including autopsy is critical in identifying a cause—for instance, structural abnormalities such as cardiomyopathies [e.g., hypertrophic cardiomyopathy (HCM)] may be identified at the point of autopsy. However, in a substantial proportion (reports ranging from 3–53% Tester and and Ackerman, 2012) despite extensive post-mortem examination, no structural cause of death may be identified. It is thought that ion channelopathies such as Long QT Syndrome (LQTS) may explain a significant number of these events. Cases of sudden death in patients between the ages of 1–40 years with no previous cardiac history, who are seen alive in the 12 hours preceding death and have a normal coroner's autopsy (confirmation of a normal heart by an expert cardiac pathologist) in addition to a negative toxicological screen are deemed to have sudden arrhythmic death syndrome (SADS; Nunn and Lambiase, 2011). It is this syndrome that will form the focus of the review.

EPIDEMIOLOGY

SADS is thought to be responsible for an estimated 0.24 deaths per 100,000 population according to an analysis of death certification data from England and Wales (Papadakis et al., 2009). This contrasts strongly with data available from north-east Thailand where it has been demonstrated that amongst men aged 20–49, the annual incidence of sudden unexplained death is 38 per 100,000 population per year (Tungsanga and Sriboonlue, 1993), with Brugada syndrome (BrS) thought to be the main cause for this dramatically higher rate of sudden death (Sangwatanaroj et al., 2001). Cardiac ion channelopathies such as LQTS, BrS, Catecholaminergic polymorphic ventricular tachycardia (CPVT) cannot be identified on conventional autopsy while certain cardiomyopathies including arrhythmogenic right ventricular cardiomyopathy (ARVC) and HCM may be missed at post-mortem due to subtle histological anomalies. The yield of

genetic screening varies considerably according to the syndrome in question—some forms of LQTS e.g., Timothy Syndrome have a diagnostic yield that is near 100% while in ARVC, for instance, only 30–40% of clinically diagnosed patients have desmosomal mutations which are thought to be the main cause of the condition (Priori and Napolitano, 2006).

ION CHANNELOPATHIES ASSOCIATED WITH A STRUCTURALLY NORMAL HEART

The inherited arrhythmia syndromes LQTS, CPVT, and BrS form a substantial proportion of fatal arrhythmia-associated sudden deaths on the background of a structurally normal heart. Here, the epidemiology, genetic basis of the syndromes, the characteristic clinical features as well as insights into how genotype may play a role in guiding management and prognosis will be discussed (a list of known genes involved in the various syndromes is outlined in **Table 1**).

Table 1 | Genetic basis of principal ion channelopathies [adapted from Table 1, Giudicessi and Ackerman (2013)].

Gene	Protein	Frequency
LQTS		
KCNQ1 (LQT1)	Kv7.1	30–35%
KCNH2 (LQT2)	Kv11.1	25–30%
SCN5A (LQT3)	Nav1.5	5–10%
ANKB (LQT4)	Ankyrin B	<1%
KCNE1 (LQT5)	MinK	<1%
KCNE2 (LQT6)	MiRP1	<1%
KCNJ2 (LQT7)	Kir2.1	<1%
CACNA1C (LQT8)	Cav1.2	<1%
CAV3 (LQT9)	Caveolin 3	<1%
SCN4B (LQT10)	Nav1.5 β4-subunit	<1%
AKAP9 (LQT11)	Yotiao	<1%
SNTA1 (LQT12)	Syntrophin- α1	<1%
KCNJ5 (LQT13)	Kir3.4	<1%
CPVT		
RYR2 (CPVT1)	Ryanodine receptor 2	50-60%
CASQ2 (CPVT2)	Calsequestrin 2	1–2%
KCNJ2 (CPVT3)	Kir2.1	10%
BrS		
SCN5A (BrS1)	Nav1.5	20–30%
GPD1L (BrS2)	Glycerol-3-phosphate dehydrogenase 1-like	<1%
CACNA1C (BrS3)	Cav1.2	6.6%
CACNB2 (BrS4)	Cav1.2 β2-subunit	<1%
SCN1B (BrS5)	Nav1.5 β1-subunit	<1%
KCNE3 (BrS6)	MiRP2	<1%
SCN3B (BrS7)	Nav1.5 β3-subunit	<1%
KCNJ8 (BrS8)	Kir6.1	2%
CACNA2D1 (BrS9)	Cav1.2 α2/∂1-subunit	<1%
KCND3 (BrS10)	Kv4.3	<1%
MOG1 (BrS11)	Mog1	<1%

Note the likely syndrome subtype recorded in parenthesis but no consensus on numerical nomenclature for minor syndrome subtypes.

LONG QT SYNDROME

LQTS is defined by delayed repolarization of the myocardium. Clinically, this corresponds to a prolonged heart rate-corrected QT interval (QTc). Such patients have an increased risk of syncope, seizures, and sudden death. Its incidence is thought be 1/2000 (Schwartz et al., 2009) and so far 13 LQTS-associated genes have been implicated in this disorder. However, 60–75% of patients with definite LQTS have mutations in one of the three major susceptibility genes (Giudicessi and Ackerman, 2013). The remaining 10 genes are thought to increase the yield by less than 5% and contribute to an increase in false positives (Giudicessi and Ackerman, 2013). Triggers associated with LQTS include exertion, swimming, emotion, auditory stimuli e.g., alarm ringing with such triggers potentially bringing about syncope, seizures and in 5% untreated cases sudden fatal arrhythmia (Lambiase, 2010). **Table 2** summarizes (Ackerman et al., 2011; Gollob et al., 2011; Tester and and Ackerman, 2012; Giudicessi and Ackerman, 2013) the key features of the three principle LQTS syndromes and **Figure 1** illustrates some typical ECG patterns.

Current management guidelines of the Heart Rhythm Society/European Heart Rhythm Association (Ackerman et al., 2011) state that comprehensive/targeted LQTS genetic testing is recommended for anyone where there is strong evidence to suggest LQTS based on the phenotype (history, family history, ECG findings). For relatives of the index patient, mutation-specific testing is recommended even if they are asymptomatic with a normal ECG. Genotyping has been helpful in directing therapy: for instance β-blockade has been shown to have similar effects in preventing cardiac events in LQT1 and LQT2 patients but not having the same degree of beneficial effect in LQT3 (Moss et al., 2000).

BRUGADA AND EARLY REPOLARIZATION ("J WAVE") SYNDROME

BrS is characterized by coved-type ST-segment elevation followed by a negative T-wave in right precordial leads V1–V3 (type 1 ECG pattern) or saddleback pattern in V1 (with ST-segment elevation) or V2 (without ST-segment elevation). However, only a type 1 pattern is diagnostic of the syndrome where there is ST-segment elevation in >1 precordial lead (standard/high position V1–V3) in the presence/absence of a sodium channel blocker (see **Figures 2**, **3**) in addition to either documented ventricular fibrillation (VF), polymorphic VT, family history of sudden cardiac death aged <45 years, coved-type ECG changes in family members, inducibility of VT with programmed electrical stimulation, syncope, or nocturnal agonal respiration (Haïssaguerre et al., 2008). The estimated prevalence is 1/2000 in Caucasians although the prevalence may be more in individuals of Asian descent (Antzelevitch et al., 2005). So far, mutations in at least 11 distinct susceptibility genes have been identified. The most common being mutations in the *SCN5A* gene (20–30% cases), while the other 10 genotypes identified so far are comparatively much rarer and thus only in BrS type 1 is gene testing for *SCN5A* mutations thought to be clinically useful at present, when there is a strong clinical suspicion of BrS based on clinical data (history, family history and ECG findings; Ackerman et al., 2011; Gollob et al., 2011). Cascade screening of relatives of the proband can follow thereafter. Patients are characteristically young males

Table 2 | Outline of the current genetic testing recommendations for the principal ion channelopathies.

Likely arrhythmia syndrome	Prevalence	Major clinical triggers	Characteristic ECG findings	Exercise testing	Pharmacological challenge testing	Recommended genetic testing
LQT1	Overall LQTS 1/2000	Exercise	Broad tented T wave	QTc fails to shorten particularly in the recovery phase of exercise	IV epinephrine prolongs QTc (epinephrine could be helpful in unmasking LQTS and thus identifying new pathogenic mutations where the QTc is normal at rest)	*KCNQ1, KCNH2*, and *SCN5A*. Routine clinical testing of rare genes (<1% detection rate) not recommended. If patients have a clear clinical phenotype but negative in genetic testing for the above genes, rare genes may be assessed on a case-by-case basis.
LQT2		Emotional stimuli	Bifid T wave			
LQT3		Sleep and rest without arousal	Late onset peaked/biphasic T wave	Prolongation of QTc at night (24 hour ECG thus of great importance)		
BrS	1/2000	Rest or sleep	Coved-type ST-segment elevation in right precordial leads (type 1 ECG pattern)		IV sodium channel blocker converting a type 2 or type 3 ECG pattern to a type 1 ECG pattern	*SCN5A* gene testing only.
CPVT	1/7000–10,000	Emotion/Exercise (high adrenaline states)	Baseline usually normal	Bidirectional VT/polymorphic VT	IV infusion of adrenergic agonist inducing bidirectional VT/polymorphic VT	*RYR2* gene; if *RYR2* gene screening negative despite high clinical suspicion then consider *CASQ2* screening.

aged about 40 when the arrhythmias first manifest, with sleep being a major trigger (Antzelevitch et al., 2005). However, the majority of families screened have normal or borderline/subtle changes in the J point. Hence, pharmacological challenge testing using a sodium channel blocker is key in unmasking the condition (**Figure 3**).

Until recently inducibility of VT at electrophysiological study was thought to be predictive of sudden death risk (Priori et al., 2002a). However, recent large series have shown that this is not consistent, meaning it has dropped to a class IIb level of evidence in the recent HRS/EHRA Consensus Statement on the assessment of ion channel disorders (Eckardt et al., 2002; Tester and Ackerman, 2011; Priori et al., 2012). Other parameters such as ventricular effective refractory period, signal averaged ECG and ST changes in recovery may play a role in the future.

Currently, as per the HRS/EHRA guidelines, only *SCN5A* genetic testing is useful when there is strong clinical/ECG data to suggest BrS in the index case with a view to identifying a causative mutation and thereby facilitating cascade screening of relatives. However, as yet there is no clear therapeutic or prognostic utility in genetic testing (Ackerman et al., 2011).

Recent attention has been focused on the potential arrhythmogenic risk of J waves or early repolarization on the resting 12 lead ECG. Haïssaguerre et al. (2008) and Rosso et al. (2008) have demonstrated a significantly higher prevalence of J point elevation in the infero-lateral leads in idiopathic ventricular fibrillation survivors vs. matched healthy controls, coupled with pronounced J point elevation preceding the development of VF. The precise mechanism of this early repolarization phenomenon in humans remains uncertain. Recently, a Finnish population study of over 10,000 unselected people with a mean follow up of 30 years found that the presence of J point elevation was associated with a higher rate of death from cardiac causes and arrhythmia (Tikkanen et al., 2009) further supporting the notion that J point elevation may indicate an increased susceptibility to lethal arrhythmia, acting as a modifying factor whatever the underlying pathology. Our group has identified a higher proportion of SADS relatives with J waves vs. the general population, this suggests that the heritable J point elevation could account for a proportion of SADS deaths caused by ion channel mutations in the K_{ATP} channel and L-type Calcium channel (Antzelevitch and Yan, 2010; Nunn et al., 2011).

CATECHOLAMINERGIC POLYMORPHIC VENTRICULAR TACHYCARDIA (CPVT)

CPVT is a disease of perturbed intracellular calcium homeostasis. Like LQTS, it is associated with a structurally normal heart however it usually displays a completely unremarkable resting

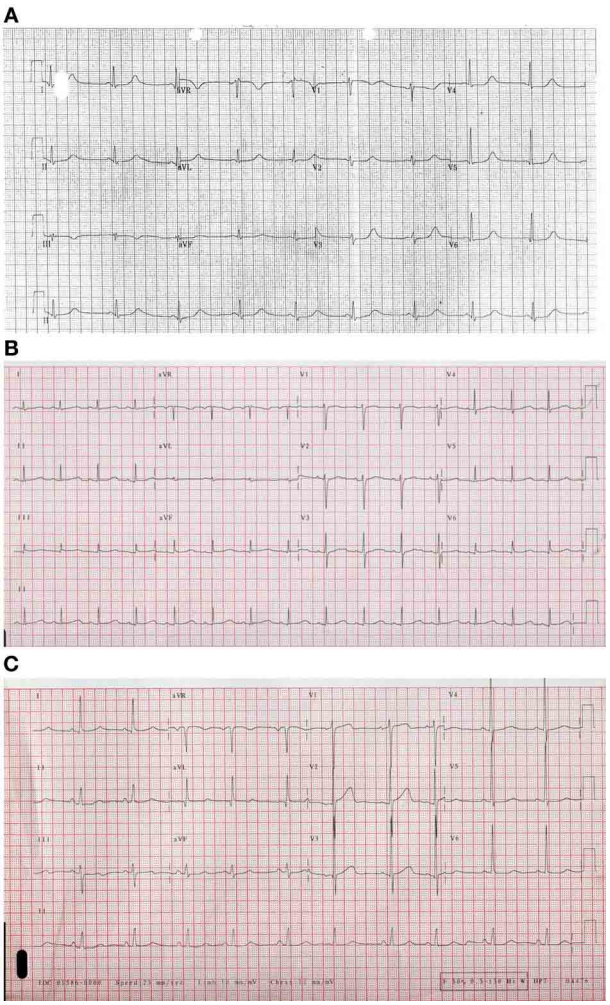

FIGURE 1 | Examples of ECGs for different forms of Long QT Syndrome (A). Long QT 1 **(B)** LQT2 illustrating bifid T wave morphology **(C)**. Long QT3 illustrating flat isoelectric segment with small symmetrical T wave particularly in lead III.

ECG (occasionally bradycardia and U waves) and is usually only unmasked (ventricular ectopy is seen) following exertion or catecholaminergic stress testing (Tester and Ackerman, 2011) (**Figure 4**). It is thought to affect 1/7000–10,000 individuals with three distinct CPVT-associated genes so far identified (Giudicessi and Ackerman, 2013). Sixty to sixty-five percent of CPVT cases are associated with a mutation in the *RYR2*-encoded cardiac ryanodine receptor/intracellular calcium channel—CPVT type 1 (CPVT1; Priori et al., 2002b). The remainder of the mutations in the other two susceptibility genes are found in fewer than 5% cases (Crotti et al., 2012). A rare autosomal recessive form of CPVT has been associated with mutations in calsequestrin (*CASQ2*; Lahat et al., 2001). Both *CASQ2* and *RYR2* encode proteins involved in intracellular calcium handling. Mutations may predispose to elevated calcium levels during cardiac diastole and thus increasing the risk of developing ventricular arrhythmias. Genetic testing is currently recommended for anyone where clinical features and ECG findings observed on exercise/catecholaminergic testing indicate CPVT (Ackerman et al., 2011). This of course facilitates mutation-specific cascade screening of family members and advice on avoidance of triggers i.e., exercise. Genotype however does not impact on management or risk stratification strategies at present (Eckardt et al., 2002), although there is some evidence to indicate prophylactic β-blockade in these individuals may be useful.

SHORT QT SYNDROME

This arrhythmia syndrome is comparatively infrequently encountered in clinical practice. It is however associated with a high incidence of syncope and sudden cardiac death, even in the younger patients and newborns. The defining electrocardiographic feature is QTc < 320 ms. Mutations in *KCNH2, KCNQ1,* and *KCNJ2* genes have been identified as associated with the condition. However, data is limited on the condition (a recent population screening study over 100,000 ECGs failed to identify a single case) and very little evidence is available to help guide genetic screening of this condition (Lambiase, 2010).

Having briefly overviewed the various arrhythmia syndromes, it is evident that a clinical diagnostic approach must first be followed in these scenarios and then targeted genetic screening if a clear phenotype is identified to maximize the yield of genetic screening in the family.

SCREENING

THE CLINICAL SCREENING APPROACH TO SADS FAMILIES

Screening of the 1st degree relatives in specialist clinics can diagnose an inherited cardiac condition in 22–53% of families. Behr et al. (2003) investigated 109 1st degree relatives of 32 people who died of SADS. Seven (22%) of the 32 families were diagnosed with an inherited cardiac disease. A subsequent more detailed evaluation of 57 consecutively referred families with SADS death identified 30 families (53%) with an inheritable heart disease (Giudicessi and Ackerman, 2013). Over half of those relatives affected received potentially lifesaving intervention with β-blockers and/or an ICD (Behr et al., 2008). Tan et al. (2005) investigated 43 consecutive families with >1 SADS victim who died at <40 years of age. Only 51% of probands underwent a post-mortem. 183 relatives were initially screened triggering the cascade screening of a further 150 relatives. A diagnosis was established in 17 of 43 families (40%) and revealed 151 pre-symptomatic disease carriers. Most recently, Wilde and colleagues (Van Der Werf et al., 2010) reported the assessment of 140 families with a sudden unexplained death (aged 1–50 years.) A diagnosis was established in 33% of families although a post mortem was performed in only 46% of cases. Strategies to increase the diagnostic yield include: ensuring all cases have a post-mortem, ideally with an expert cardiac pathologist review of the whole heart; reviewing as many 1st degree relatives in each family as possible; and carrying out a molecular autopsy where possible.

PRACTICAL CONSIDERATIONS OF CLINICAL SCREENING

Effective clinical screening of SADS families requires a comprehensive multidisciplinary team approach. Moreover, chapter 8

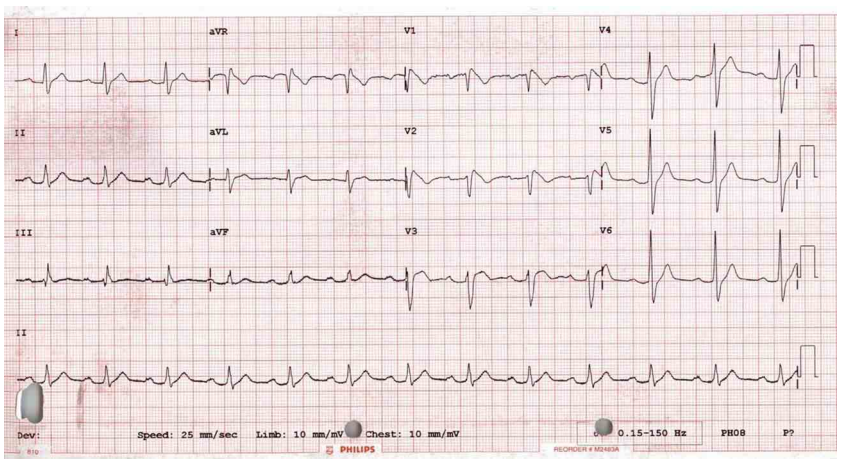

FIGURE 2 | A typical Brugada syndrome type 1 ECG showing coved ST elevation in leads V1 and V2.

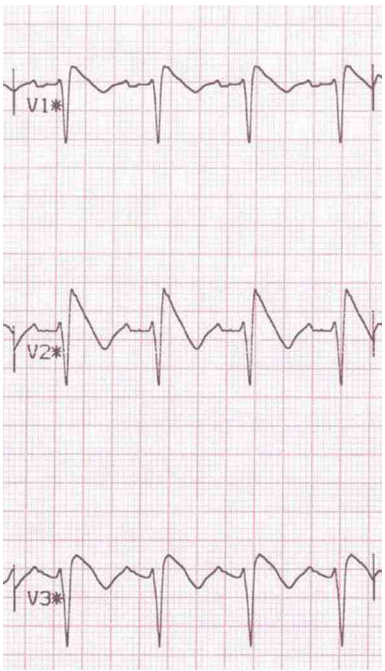

FIGURE 3 | Pharmacological challenge testing unmasking in Brugada phenotype. Type 1 response to ajmaline challenge test.

FIGURE 4 | Bidirectional VT in CPVT.

of the National Service Framework in the UK requires the National Health Service (NHS) to provide a dedicated clinic to assess families with appropriately trained staff (Department of Health, 2005). A dedicated clinic typically comprises cardiologists, physiologists, echocardiographers, specialist nurses, bereavement and genetic counselors, and clinical geneticists (Lambiase, 2010).

Prior to seeing families in a SADS clinic, as much background information as possible should be obtained about the index case. This should include specific clinical information such as previous clinical encounters with a family physician or visits to the emergency department, as this may yield useful diagnostic information such as previous ECGs. Additionally, a detailed post-mortem report should be obtained. Usually a specialist nurse will coordinate the clinic and liaise with families, the family physician as well as the coroner's office to obtain relevant background information including a copy of the post-mortem report. Moreover, tissue sections or ideally the whole heart should be reviewed by a specialist cardiac pathologist to identify any histopathological evidence of an underlying cardiomyopathic process. For instance, myocyte disarray suggestive of HCM or local fibrosis and fatty infiltration indicative of ARVC may be identified (Lambiase, 2010).

Importantly, prior to conducting any investigations on SADS families, appropriate counseling must be undertaken to ensure the implications of the screening tests are well-understood. Employment, insurance, effects on children and other family members as well as the psychological impact of test results must all be appropriately discussed. The outcomes of investigations can vary from inconclusive non-diagnostic findings, which require regular follow-up to the need for medical therapy (e.g., β-blockers) or even invasive procedures such as the insertion of an implantable cardioverter-defibrillator (ICD) device (Lambiase, 2010).

CONSULTATION WITH PHYSICIAN

HISTORY

Family screening should start with a detailed evaluation of the index case. The mode of death may provide useful information regarding etiology. For instance, long QT (LQT) 1 subtype (LQT1) and catecholaminergic polymorphic VT is associated with death while swimming (Tester and Ackerman, 2011). Syncope in the context of sudden loud noise or alarm is characteristic of LQT2 and death during sleep suggests the possibility of BrS and LQT3 (all three associated with an increased risk of arrhythmia during periods of increased cholinergic tone or bradycardia). Thus, a careful and systematic history from first-degree relatives can be great value in helping to determine the details prior to pre-syncopal or syncopal events as well as identifying other symptomatic family members.

Past medical history, previous accidents, prescribed/non-prescribed and recreational drugs e.g., cocaine use are all of relevance. Family history including any relatives who may have died under 40 years of age, family history of cardiac interventions e.g., pacemaker implantation, heart failure or any available death certification can all be invaluable. Certain markers in the history including syncope, 2 or more sudden deaths in the family at younger ($\leq$40 years) age are all thought to be predictive markers of a diagnosis in the family (Tan et al., 2005; Behr et al., 2008).

INVESTIGATIONS

A number of tests may be performed to aid in the screening process of SADS families. These will be at the physician's discretion and may vary between units. These can include a resting ECG, exercise ECG, VO_2 max tests, signal averaged ECG, transthoracic echocardiogram and ajmaline or flecainide challenge test (to unmask BrS when suspected; Lambiase, 2010).

THE ROLE OF GENETIC TESTING

There has been a steady advance in the potential for gene testing since the discovery of the channelopathy-causing genes in the 1990s. With an ever-burgeoning panel of commercially available diagnostic genetic tests available to the electrophysiologist, consensus guidance is clearly highly relevant in helping to determine when and which tests are indicated. The Heart Rhythm Society/European Heart Rhythm Association Consensus Statement published in 2011 (Ackerman et al., 2011) aptly summarizes the current recommendations for genetic screening. These have been outlined together with overviews of the principal genetic syndromes associated with SADS in the summary table [Ackerman et al., 2011; Gollob et al., 2011; Tester and and Ackerman, 2012; Giudicessi and Ackerman, 2013; above (**Table 2**)].

PRACTICAL CONSIDERATIONS OF GENETIC TESTING

Genetic testing is usually employed as a confirmatory tool primarily to facilitate cascade screening of the family. Only after a thorough clinical assessment (with likely diagnosis established based on family history, patient background, ECG and pharmacological testing) should genetic screening be used in clinical practice. Moreover, genetic counseling (to include a comprehensive discussion of the relative risks and benefits) is highly recommended prior to any testing (Ackerman et al., 2011). The benefits offered by testing are in identifying a specific genetic mutation, which may help, to determine both management and prognosis of affected family members, best illustrated in the case of LQTS (see below). Alternatively, where the clinical screening process does not yield sufficient information to make a diagnosis or may require a large number of first-degree relatives to be screened, a single genetic test may prove to be the most cost-effective method. Furthermore, genetic testing may assist in family planning or for prenatal diagnosis in a parent who carries a known mutation (Schwartz et al., 2009). However, the yield of genetic testing varies considerably among the channelopathies; from 20% in BrS to 75% for LQTS (Ackerman et al., 2011). Hence, a negative test does not rule out the presence of a particular disease. Furthermore, the diagnostic, therapeutic and prognostic benefit derived from a genetic test is also highly disease-specific. Hence, testing must always be considered in the context of relevant clinical data (Ackerman et al., 2011).

CLINICAL IMPACT OF GENETIC TESTING

Out of the channelopathies, LQTS testing has the highest yield as well as the maximum evidence for being able to guide diagnosis and management (Ackerman et al., 2011). Hence, this syndrome is well-placed to illustrate the clinical impact of genetic testing. Testing for the *KCNQ1, KCNH2,* and *SCN5A* genes, when LQTS is clinically suspected, should yield positive LQT1-3 causing mutations in 75% cases (Ackerman et al., 2011). However, as alluded to earlier negative testing does not exclude the disease where there is strong clinical suspicion. On the other hand, testing should not be performed without clinical suspicion, considering there is a substantial rate of rare variants of unknown significance (VUS) i.e., where there is insufficient evidence to label mutations as definitely disease-causing (discussed in detail later)—4–8% in the LQT1-3 genes (Kapa et al., 2009). Identifying a causative mutation in an index case of LQTS mandates mutation-specific cascade screening of all first-degree relatives (even when there is no clinical suspicion in that relative). Helpfully, in the absence of a clinical phenotype for LQTS in the relative, a negative genetic test will effectively exclude LQTS (Ackerman et al., 2011).

Genetic testing can additionally direct therapy in LQTS: β-blockers are highly protective in the case of LQT1 patients, moderately protective in LQT2 (Runa et al., 2008) while in LQT3 other agents such as mexiletine, flecainide, ranolazine, or

propranolol are indicated (Schwartz et al., 1998; Moss et al., 2005, 2008; Ackerman et al., 2011). Hence, gene-directed therapeutic options are highly significant here. Prognostically, genotype appears also to be very significant: for instance, LQT1 transmembrane-localizing missense mutations have a greater risk of an LQT1-triggered cardiac event compared to a C-terminal mutation (Shimizu et al., 2004). In LQT2, patients with pore-region mutations tend to have longer QTc and more severe clinical manifestations (Moss et al., 2002). For the other principal channelopathies—CPVT and BrS, while cascade screening of index cases is indicated, there is no clear genotype-dependent differential therapeutic approach nor does genotype influence prognosis as yet (Ackerman et al., 2011).

In summary, genetic testing serves a vital role in confirmatory testing of individuals with a robust clinical phenotype and facilitates cascade family screening of index cases. However, at present, it is only in LQTS that genotype helps to clearly direct therapy and inform prognosis.

MOLECULAR AUTOPSY: THE NEW FRONTIER

Molecular autopsy refers to the use of DNA extracted from tissue retained after the post-mortem, which can be utilized for confirmatory testing of a mutation identified in the relative (Lambiase, 2010). This approach facilitates post-mortem genetic testing of conditions that are known to cause SADS e.g., LQTS. The first reported case of the use of molecular autopsy to diagnose an inherited arrhythmia syndrome was by Ackerman et al. (1999). They found a 9 base pair deletion in the *KVLQT1* gene of a 19 year-old, previously fit and well lady, who had died after being resuscitated following a near-drowning experience. Subsequently, this same mutation had been found in the proband's other family members and appropriate therapy was then offered to the affected family members.

Only a handful of molecular autopsy series have been reported to date with one of the largest reported by Tester et al. (2012) who performed a comprehensive mutational analysis in 173 cases of the LQTS susceptibility genes as well a targeted analysis of the CPVT type 1-associated *RYR2* gene. Forty-five putative pathogenic mutations (25 novel mutations) were identified (26.0% yield). Correlation of genotype with phenotype demonstrated that females showing a higher yield than males (38.8 vs. 17.9%) and mutation-positive females were more likely to host an LQTS-associated mutation while mutation-positive males more likely to host a CPVT1-associated mutation. Exertion (34.8%) and sleep (18.6%) were also major triggers. Furthermore, 40.5% of cases (70/173) were found have a positive personal or family history of syncope, seizures, cardiac arrest, near drowning, or unexplained drowning (in a family member) or a known prolonged QT interval. This builds on their earlier study of 49 cases (Tester and Ackerman, 2007). Data from a series in Denmark (Larsen et al., 2013) found that in the 0–40 year old population, there was a yield of 8.3% in targeted *RYR2* gene sequencing. This follows-up from earlier series including that by Chugh et al. (2004), who showed in a cohort of 270 sudden death cases over a 13 year period that there were 12 autopsy negative cases of which 2 showed a mutation in the *KCNH2* gene. More recently, Skinner et al. (2011) found that in a prospective population-based long QT molecular autopsy study of 1–40 year-olds, 5/33 had rare possible LQTS-associated mutations.

PRACTICAL CONSIDERATIONS

In most autopsy studies, DNA extraction is typically based on formalin-fixed, paraffin-embedded tissue (FF-PET) due to the comparative ease of storing and transporting tissue (Basso et al., 2010). However, DNA extracted from this source is thought to be unreliable for molecular autopsy and usually inadequate for comprehensive post-mortem genetic testing (to detect a pathological mutation; Carturan et al., 2008). Indeed, a study by Doolan et al. (2008) found no putative pathogenic mutations in a series of 59 cases of sudden expected death when using DNA extracted from FF-PET. Optimal sources of intact DNA include blood collected in ethylenediaminetetraacetic acid (EDTA) or frozen heart, liver, or spleen tissue. Furthermore, 10–15 ml of EDTA blood or 5–10 g of fresh tissue should be obtained at autopsy and stored at −80°C to provide the ideal source of material for comprehensive genetic testing (Ackerman et al., 2001). In order to try and combat the limitations of material for autopsy, Gladding et al. (2010) used DNA extracted from Guthrie blood spots and used whole genome amplification prior to sequencing. They found out of 19 cases in their series, 4 had pathological mutations and all probands had at least one first-degree family member with the same mutation. This was followed-up by a Danish group (Winkel et al., 2012) who showed a yield of 11% for 3 major LQTS-associated genes amongst a cohort of 1–35 year-olds.

The advent of full exonic sequencing will mean that the whole patient exome can be sequenced. This significantly reduces the cost of gene testing but also generates enormous quantities of bioinformatic data with multiple genetic variants and potentially mutations in other non-cardiac genes being identified. At present, we only have a limited understanding of the etiology of recognized arrhythmic conditions. Hence, the interpretation of any additional genetic information must be carefully assessed and put into the context of the patient/family being screened. This is particularly important considering we are currently severely hampered by our limited ability to assess the pathogenicity of specific variants.

RECOMMENDATIONS

Most of the series published so far are a relatively small in size. Thus, larger studies and analyses are required to help better characterize the yield of mutation detection and also offer better phenotype/genotype correlations. For instance, helping to identify clinical correlations between genetic mutations and clinical characteristics such as age or gender. This would contribute to guiding the clinical evaluation of the proband's family members and improving the cost effectiveness of the current approach. At present a combined clinical diagnostic approach and molecular autopsy would be recommended, as mutation carriers may only have minor manifestations of disease and compound heterozygotes may have clinically milder or more severe forms of the condition depending upon the functionality of the complementary allele gene. For example, if the complementary gene is itself a polymorphism with a down-regulation in function to 30%, this cannot compensate for the effects of a non-functioning channel

and hence significantly reduces repolarization reserve in the case of LQTS (Crotti et al., 2005).

VARIANTS OF UNKNOWN SIGNIFICANCE

Another major question looms regarding VUS identified on gene testing. As briefly mentioned earlier, VUS refer to mutations where there is inadequate evidence to deem them as disease-causing; increasingly, this is becoming an issue with the declining costs of genetic screening allowing large sections of the genome or indeed the whole exome to be sequenced. Cotton and Scriver (1998) have outlined several criteria that help determine whether a mutation or variant is indeed a disease-causing mutation (when taken in context of the other clinical data). These include:

- non-sense/frameshift mutations leading to generation of stop codons or downstream stop codons, respectively
- insertion/deletion mutations leading to truncated protein products
- co-segregation of the variant with disease
- absence/rarity of the variant in control populations
- mutations in highly conserved amino acid residues/domains likely altering the gene product
- functional analysis of the gene product through *in vitro* expression analysis

Satisfying any one of the criteria above does not necessarily point toward a definitive designation as a pathogenic mutation. Moreover, if taken together the criteria above do not allow for a variant to be considered disease-causing, it is thereafter deemed a VUS until further analysis (including functional assessment) is used to confirm whether it is pathogenic. Moreover, the presence of a VUS should not be used to assist in the diagnosis of an index patient nor should it be used for cascade screening of relatives (Giudicessi and Ackerman, 2013).

In light of recent genome-wide association studies (GWAS), new insights have been gained into potential variants that may be associated with increased risk of sudden cardiac death. Arking et al. (2006) assessed the QT interval extremes in a cohort of German subjects. They identified *NOS1AP,* a regulator of neuronal nitric oxide synthase as a potential novel disease-causing gene modulating cardiac repolarization with one minor allele explaining up to 1.5% of QT interval variation. Further studies specifically assessed the effect of *NOS1AP* variants in known ion channelopathy populations. Crotti et al. (2009) assessed the clinical manifestations and symptom occurrence in a South African LQTS population (with a *KCNQ1* mutation). They found that LQTS individuals with the rs4657139 variant in *NOS1AP* had greater probability of cardiac arrest and sudden death and had a greater likelihood of having a more prolonged QT interval. Taken together these findings would indicate that variants in the *NOS1AP* gene could act as genetic modifiers with a potentially significant impact on electrical function. Tomas et al. (2010) findings supported the work of Crotti et al. (2009). They found in a LQTS1 cohort with mutations in 5-associated genes that alleles rs4657139 and rs16847548 were associated with an increased risk of cardiac events. This would add further evidence to the notion that specific variants in *NOS1AP* gene act as risk-modifiers in known LQTS patients.

Albert et al. (2010) demonstrated in a case-control study of 6 prospective cohorts that 2 common intronic variants in the *KCNQ1* and *SCN5A* genes were significantly associated with sudden death in individuals of European descent (after adjustment for cardiovascular risk factors). The alleles identified were the T-allele at rs22832222 in *KCNQ1* with a population frequency of 67 and 60% for the C-allele at rs11720523 in the *SCN5A* gene.

Finally, in the largest meta-analysis of GWAS to date, Arking et al. (2011) found that there is a strong association with sudden cardiac death at locus 2q24.2 including the *BAZ2B* gene, which is thought to increase risk of sudden cardiac death by >1.9 fold per allele in individuals of European descent.

While GWAS have opened an avenue to identifying novel VUS which may indeed go on to be causative or risk-modifying due to the impact on electrical function, caution must be exercised until further functional studies are performed to identify the risk of cardiac events. Hence, the presence of a VUS should not be used to assist in the diagnosis of an index patient nor should it be used for cascade screening of relatives at present and is therefore, as yet, generally not a realistic screening tool (Giudicessi and Ackerman, 2013).

THE POTENTIAL ROLE OF INDUCED PLURIPOTENT STEM CELL TECHNOLOGY IN FUNCTIONAL ION CHANNEL MUTATION TESTING AND CLINICAL EVALUATION

Since human embryonic stem cells (hESCs) were first isolated from blastocysts in 1998, it has become possible to produce human-induced pluripotent stem cells (hiPSCs) by reprogramming somatic cells with just four genetic factors (Thomson et al., 1998; Takahashi et al., 2007; Yu et al., 2007). This means that a skin biopsy can be taken from a patient or SADS index case and fibroblasts cultured and reprogrammed to create specific cell lines with cardiomyocytes being the most relevant in the context of SADS.

These cells can be characterized by techniques including patch clamping and multi-electrode array (MEA) to interrogate their electrophysiological behavior (Terrenoire et al., 2013) (**Figure 5**). Alterations in calcium handling can be visualized using real-time microscopy utilizing calcium sensitive dyes (Jung et al., 2011). There is now data from hiPSC lines carrying mutations that cause LQTS and CPVT which shows these cells not only recapitulate the clinical phenotypes but the response to drugs can be reproduced *in vitro* (**Figure 5**) (Matsa et al., 2011). This has an advantage over heterologous cell expression systems for testing individual ion channel mutations using human embryonic kidney (HEK) cells, and Chinese Hamster Ovary (CHO) cells which lack the ion channels and cofactors that are relevant to human cardiac electrophysiology. In the case of LQTS2, caused by mutations in the I_{Kr} channel, hiPSC-derived cardiomyocytes (hiPSC-CMs) developed arrhythmias when exposed to isoprenaline, a stressor used clinically to precipitate and diagnose the condition (Terrenoire et al., 2013). This effect could be reversed by applying the patient's own medication, nadolol (a β-blocker), dantrolene and roscovitin; drugs known to be beneficial in moderating calcium flux, stabilized ion flux in hiPSC models of the

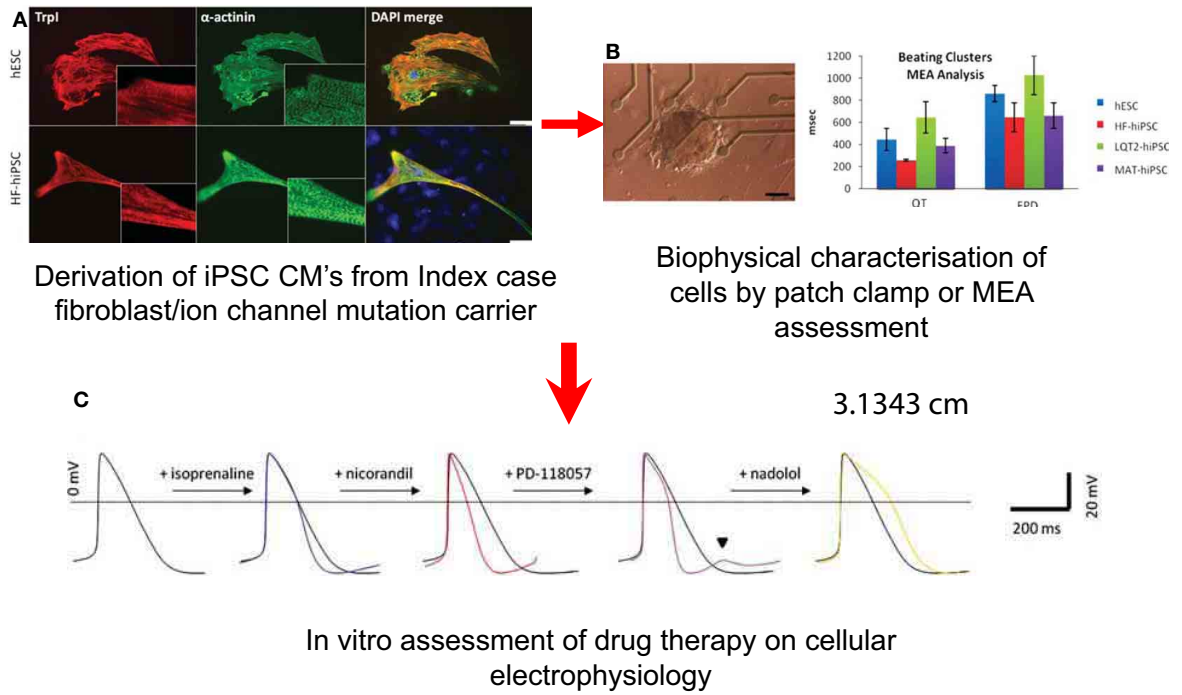

FIGURE 5 | Potential Uses of iPSC-CMs in the Investigation of SADS. Derivation of cells **(A)** Immunostaining for cardiac troponin I (TrpI) and a-actinin in myocytes derived from hESCs, HF–hiPSC, LQT2–hiPSC, and MAT–hiPSC, showing characteristic cardiac muscle striations. **(B)** Characterization of cellular electrophysiology: Image of an LQT2–hiPSC beating cluster mounted onto a multi-electrode array for electrophysiology analysis, and graph showing prolongation in QT interval and field potential duration in LQT2–hiPSC beaters relative to controls. (From Matsa et al., 2011). **(C)** Testing of drugs: (i) Averaged and (ii) raw action potential curves of LQT2–hiPSC myocytes showing isoprenaline-induced arrhythmogenesis (blue traces) and attenuation of this phenotype by nadolol (yellow trace) or propranolol (green trace).

calcium channel disorders, CPVT and Timothy syndrome (linked to LQT type 8), respectively (Matsa et al., 2011; Pasca et al., 2011; Yazawa et al., 2011).

However, this approach still requires significant refinement as there are a number of issues related to iPSC technology which will affect its application to the evaluation of specific ion channel mutations. The utilization of this technology and its pitfalls has been recently extensively reviewed in this journal (Hoekstra et al., 2012). Mixed cultures of atrial and ventricular myocytes are obtained affecting cellular electrophysiology and their response to specific drugs. These selected populations of the derived cells vary in their membrane potentials compared to other populations, which will affect the ion channel gating properties and thereby alter the behavior of a specific mutant ion channel under investigation. The cells often manifest a more immature electrophysiological phenotype. While I_{to1}, I_{K1}, and I_f are present in hiPSC-CMs (Ma et al., 2011), their contribution to the biophysics of the cell has not been verified. The presence of I_{NCX} has not been studied in detail but its functional presence can also be presumed since intact calcium handling has been demonstrated (Itzhaki et al., 2011; Lee et al., 2011). Currently, there is no evidence for the functional presence or absence of $I_{K,ACh}$. The functional presence of sarcoplasmic reticulum (SR), ryanodine receptors (RyRs), and the calcium-binding protein CASQ2 has been demonstrated (Itzhaki et al., 2011; Lee et al., 2011; Novak et al., 2012). However, due to the absence of t-tubulin in hiPSC-CMs, the coupling between calcium influx through L-type calcium channels and calcium release from the SR through RyRs is significantly reduced. Therefore, the use of hiPSC-CMs to study specific cardiac arrhythmia syndromes influenced by calcium handling e.g., CPVT and LQT8, has to be focused on the biophysical properties of the affected protein. Some of these issues can be addressed by generating and assessing more refined populations of iPSCs in order to ensure that they have more consistent electrophysiological profiles to faciliate mutant protein profiling and testing of drugs.

Taking into account the technical limitations and current caveats of utilizing iPSC technology, this approach has potential value in the field of SADS on a number of fronts. First of all in the case of an ion channel VUS, the behavior of that channel could be assessed in the patients' derived cardiomyocytes to assess the extent to which it causes significant alterations in ion channel function, trafficking and action potential duration. Furthermore, in SADS victims or idiopathic VF survivors where no known disease causing mutation has been identified, the function of specific ion channels and cellular electrophysiology could be interrogated to identify novel causes of lethal arrhythmia and new drug targets. The specific problem of compound heterozygosity where more than one VUS is inherited, which may only partially down-regulate ion channel function/trafficking can also be evaluated in

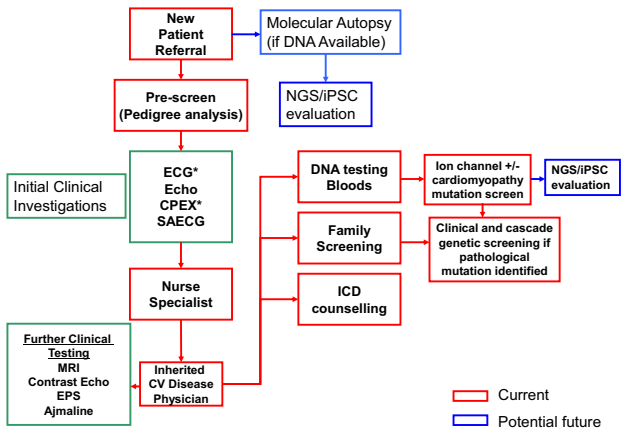

FIGURE 6 | Overview of the different strategies in the management of a SADS family. Abbreviations include: EPS, electrophysiological study; Echo, echocardiogram; CPEX, cardiopulmonary exercise testing; SAECG, signal averaged ECG; NGS, next-generation sequencing.

the individual patient. Therefore, one can assess if this particular combination of defects actually exerts important cellular electrophysiological abnormalities, which are pro-arrhythmic and not necessarily manifest on routine clinical testing. This information could be utilized to prescribe prophylactic drug therapy and protect against cardiac arrest in at-risk individuals. This concept has recently been illustrated when hiPSCs were produced from a healthy donor as well as from a mother and daughter, wherein the mother was clinically asymptomatic with a moderately prolonged QT interval and the daughter was symptomatic with an excessively prolonged QT interval (arrhythmias, syncope, and seizure episodes). Recording action potential durations from the different hiPSC-cardiomyocytes showed that the clinical profile was reflected *in vitro* (i.e., action potential longest in the daughter's cells, then the mother's, then the healthy control) and only hiPSC-cardiomyocytes produced from the daughter developed spontaneous arrhythmias (Terrenoire et al., 2013). The next decade should help establish whether *in vitro* to *in vivo* associations can be applied in other conditions with important mechanistic and therapeutic implications in this and other arenas.

CONCLUSIONS

The diagnosis and management of SADS families is evolving rapidly (**Figure 6** summarizes the current management approaches). Comprehensive clinical assessment is still the mainstay of screening families of SADS patients with highly specific recommendations for complementing clinical assessment with genetic screening options. Molecular autopsy adds another strategy in the armory of screening of SADS families and validating cases of SADS. However, with a limited understanding of the etiology of the heritable arrhythmic syndromes, careful interpretation of the added genetic information in the context of the family being screened is critical. VUS are as yet not a viable screening tool but provide a burgeoning data set to validate through functional studies. Finally, the new techniques of full exonic sequencing and iPSC technologies will certainly facilitate diagnosis and management. However, the clinical relevance of mutation screening and iPSC-derived information will need to be carefully translated back to the individual relatives, in order to ensure that any anomalies identified are clinically relevant and impact on the patient's well-being and arrhythmogenic risk.

REFERENCES

Ackerman, M. J., Priori, S. G., Willems, S., Berul, C., Brugada, R., Calkins, H., et al. (2011). HRS/EHRA expert consensus statement on the state of genetic testing for the channelopathies and cardiomyopathies: this document was developed as a partnership between the Heart Rhythm Society (HRS) and the European Heart Rhythm Association (EHRA). *Heart Rhythm* 8, 1308–1339. doi: 10.1016/j.hrthm.2011.05.020

Ackerman, M. J., Tester, D. J., and Driscoll, D. J. (2001). Molecular autopsy of sudden unexplained death in the young. *Am. J. Forensic Med. Pathol.* 22, 105–111. doi: 10.1097/00000433-200106000-00001

Ackerman, M. J., Tester, D. J., Porter, C. J., and Edwards, W. D. (1999). Molecular diagnosis of the inherited long QT syndrome in a woman who died after near-drowning. *N. Engl. J. Med.* 341, 1121–1125. doi: 10.1056/NEJM199910073411504

Albert, C. M., MacRae, C. A., Chasman, D. I., VanDenburgh, M., Buring, J. E., Manson, J. E., et al. (2010). Common variants in cardiac ion channel genes are associated with sudden cardiac death. *Circ. Arrhythm. Electrophysiol.* 3, 222–229. doi: 10.1161/CIRCEP.110.944934

Antzelevitch, C., and Yan, G. X. (2010). J wave syndromes. *Heart Rhythm* 7, 549–558. doi: 10.1016/j.hrthm.2009.12.006

Antzelevitch, C., Brugada, P., Borggrefe, M., Brugada, J., Brugada, R., Corrado, D., et al. (2005). Brugada syndrome: report of the second consensus conference – endorsed by the Heart Rhythm Society and the European Heart Rhythm Association. *Circulation* 111, 659–670. doi: 10.1161/01.CIR.0000152479.54298.51

Arking, D. E., Junttila, M. J., Goyette, P., Huertas-Vazquez, A., Eijgelsheim, M., Blom, M. T., et al. (2011). Identification of a sudden cardiac death susceptibility locus at 2q24.2 through genome-wide association in European ancestry individuals. *PLoS Genet.* 7:e1002158. doi: 10.1371/journal.pgen.1002158

Arking, D. E., Pfeufer, A., Post, W., Kao, W. H., Newton-Cheh, C., Ikeda, M., et al. (2006). A common genetic variant in the NOS1 regulator NOS1AP modulates cardiac repolarization. *Nat. Genet.* 38, 644–651. doi: 10.1038/ng1790

Basso, C., Carturan, E., Pilichou, K., Rizzo, S., Corrado, D., and Thiene, G. (2010). Sudden cardiac death with normal heart: molecular autopsy. *Cardiovasc. Pathol.* 19, 321–325. doi: 10.1016/j.carpath.2010.02.003

Behr, E. R., Dalageorgou, C., Christiansen, M., Syrris, P., Hughes, S., Tome Esteban, M. T., et al. (2008). Sudden arrhythmic death syndrome: familial evaluation identifies inheritable heart disease in the majority of families. *Eur. Heart J.* 29, 1670–1680. doi: 10.1093/eurheartj/ehn219

Behr, E. R., Wood, D. A., Wright, M., Syrris, P., Sheppard, M. N., Casey, A., et al. (2003). Cardiological assessment of first-degree relatives in sudden arrhythmic death syndrome. *Lancet* 362, 1457–1459. doi: 10.1016/S0140-6736(03)14692-2

Births and Deaths in England and Wales. (2011). *Births and Deaths in England and Wales.* Available online at: http://www.ons.gov.uk/ons/dcp171778283306.pdf (Accessed 5 February 2013).

Carturan, E., Tester, D. J., Brost, B. C., Basso, C., Thiene, G., and Ackerman, M. J. (2008). Postmortem genetic testing for conventional autopsy-negative sudden unexplained death: an evaluation of different DNA extraction protocols and the feasibility of mutational analysis from archival paraffin-embedded heart tissue. *Am. J. Clin. Pathol.* 129, 391–397. doi: 10.1309/VLA7TT9EQ05FFVN4

Chugh, S. S., Senashova, O., Watts, A., Tran, P. T., Zhou, Z., Gong, Q., et al. (2004). Postmortem molecular screening in unexplained sudden death. *J. Am. Coll. Cardiol.* 43, 1625–1629. doi: 10.1016/j.jacc.2003.11.052

Cotton, R. G., and Scriver, C. R. (1998). Proof of "disease-causing" mutation. *Hum. Mutat.* 12, 1–3.

Crotti, L., Lundquist, A. L., Insolia, R., Pedrazzini, M., Ferrandi, C., De Ferrari, G. M., et al. (2005). KCNH2-K897T is a genetic modifier of latent congenital long-QT syndrome. *Circulation* 112, 1251–1258. doi: 10.1161/CIRCULATIONAHA.105.549071

Crotti, L., Marcou, C. A., Tester, D. J., Castelletti, S., Giudicessi, J. R., Torrchio, M., et al. (2012). Spectrum and prevalence of mutations involving BrS1- through BrS12-susceptibility genes in a cohort of unrelated patients referred for Brugada syndrome genetic testing: implications for genetic testing. *J. Am. Coll. Cardiol.* 60, 1410–1418. doi: 10.1016/j.jacc.2012.04.037

Crotti, L., Monti, M. C., Insolia, R., Peljto, A., Goosen, A., Brink, P. A., et al. (2009). NOS1AP is a genetic modifier of the long-QT syndrome. *Circulation* 120, 1657–1663. doi: 10.1161/CIRCULATIONAHA.109.879643

Department of Health. (2005). *National Service Framework for Coronary Heart Disease. Chapter Eight: Arrhythmias and Sudden Cardiac Death*. Available online at: http://www.dh.gov.uk/prod_consum_dh/groups/dh_digitalassets/@dh/@en/documents/digitalasset/dh_4105280.pdf (Accessed 5 February 2013).

Doolan, A., Langlois, N., Chiu, C., Ingles, J., Lind, J. M., and Semsarian, C. (2008). Postmortem molecular analysis of KCNQ1 and SCN5A genes in sudden unexplained death in young Australians. *Int. J. Cardiol.* 127, 138–141. doi: 10.1016/j.ijcard.2007.05.001

Eckardt, L., Kirchhof, P., Schulze-Bahr, E., Rolf, S., Ribbling, M., Loh, P., et al. (2002). Electrophysiologic investigation in Brugada syndrome; yield of programmed ventricular stimulation at two ventricular sites with up to three premature beats. *Eur. Heart J.* 23, 1394–1401. doi: 10.1053/euhj.2002.3256

Giudicessi, J. R., and Ackerman, M. J. (2013). Genetic testing in heritable cardiac arrhythmia syndromes: differentiating pathogenic mutations from background genetic noise. *Curr. Opin. Cardiol.* 28, 63–71. doi: 10.1097/HCO.0b013e32835b0a41

Gladding, P. A., Evans, C. A., Crawford, J., Chung, S. K., Vaughan, A., Webster, D., et al. (2010). Posthumous diagnosis of long QT syndrome from neonatal screening cards. *Heart Rhythm* 7, 481–486. doi: 10.1016/j.hrthm.2009.12.023

Gollob, M. H., Blier, L., Brugada, R., Champagne, J., Chauhan, V., Connors, S., et al. (2011). Recommendations for the use of genetic testing in the clinical evaluation of inherited cardiac arrhythmias associated with sudden cardiac death: Canadian Cardiovascular Society/Canadian Heart Rhythm Society joint position paper. *Can. J. Cardiol.* 27, 232–245. doi: 10.1016/j.cjca.2010.12.078

Haïssaguerre, M., Derval, N., Sacher, F., Jesel, L., Deisenhofer, I., de Roy, L., et al. (2008). Sudden cardiac arrest associated with early repolarization. *N. Engl. J. Med.* 358, 2016–2023. doi: 10.1056/NEJMoa071968

Hoekstra, M., Mummery, C. L., Wilde, A. A., Bezzina, C. R., and Verkerk, A. O. (2012). Induced pluripotent stem cell derived cardiomyocytes as models for cardiac arrhythmias. *Front. Physiol.* 3:346. doi: 10.3389/fphys.2012.00346

Itzhaki, I., Rapoport, S., Huber, I., Mizrahi, I., Zwi-Dantsis, L., Arbel, G., et al. (2011). Calcium handling in human induced pluripotent stem cell derived cardiomyocytes. *PLoS ONE* 6:e18037. doi: 10.1371/journal.pone.0018037

Jung, C. B., Moretti, A., Mederos y Schnitzler, M., Iop, L., Storch, U., Bellin, M., et al. (2011). Dantrolene rescues arrhythmogenic RYR2 defect in a patient-specific stem cell model of catecholaminergic polymorphic ventricular tachycardia. *EMBO Mol. Med.* 4, 180–191. doi: 10.1002/emmm.201100194

Kapa, S., Tester, D. J., Salisbury, B. A., Harris-Kerr, C., Pungliya, M. S., Alders, M., et al. (2009). Genetic testing for long-QT syndrome: distinguishing pathogenic mutations from benign variants. *Circulation* 120, 1752–1760. doi: 10.1161/CIRCULATIONAHA.109.863076

Lahat, H., Pras, E., Olender, T., Avidan, N., Ben-Asher, E., Man, O., et al. (2001). A missense mutation in a highly conserved region of CASQ2 is associated with autosomal recessive catecholamine-induced polymorphic ventricular tachycardia in Bedouin families from Israel. *Am. J. Hum. Genet.* 69, 1378–1384. doi: 10.1086/324565

Lambiase, P. (2010). "The sudden arrhythmic death syndrome," in *Principles and Practice of Clinical Cardiovascular Genetics*, eds D. Kumar and P. Elliott (Oxford, UK: Oxford University Press), 483–494.

Larsen, M. K., Berge, K. E., Leren, T. P., Nissen, P. H., Hansen, J., Kristensen, I. B., et al. (2013). Postmortem genetic testing of the ryanodine receptor 2 (RYR2) gene in a cohort of sudden unexplained death cases. *Int. J. Legal Med.* 127, 139–144. doi: 10.1007/s00414-011-0658-2

Lee, Y. K., Ng, K. M., Lai, W. H., Chan, Y. C., Lau, Y. M., Lian, Q., et al. (2011). Calcium homeostasis in human induced pluripotent stem cell-derived cardiomyocytes. *Stem Cell Rev.* 7, 976–986. doi: 10.1007/s12015-011-9273-3

Ma, J., Guo, L., Fiene, S. J., Anson, B. D., Thomson, J. A., Kamp, T. J., et al. (2011). High purity human-induced pluripotent stem cell-derived cardiomyocytes: electrophysiological properties of action potentials and ionic currents. *Am. J. Physiol. Heart Circ. Physiol.* 301, H2006–H2017. doi: 10.1152/ajpheart.00694.2011

Matsa, E., Rajamohan, D., Dick, E., Young, L., Mellor, I., Staniforth, A., et al. (2011). Drug evaluation in cardiomyocytes derived from human induced pluripotent stem cells carrying a long QT syndrome type 2 mutation. *Eur. Heart J.* 32, 952–962. doi: 10.1093/eurheartj/ehr073

Moss, A. J., Windle, J. R., Hall, W. J., Zareba, W., Robinson, J. L., McNitt, S., et al. (2005). Safety and efficacy of flecainide in subject with Long QT-3 syndrome (DeltaKPQ mutation): a randomized, double-blind, placebo-controlled clinical trial. *Ann. Noninvasive Electrocardiol.* 10, 59–66. doi: 10.1111/j.1542-474X.2005.00077.x

Moss, A. J., Zareba, W., Hall, W. J., Schwartz, P. J., Crampton, R. S., Benhorin, J., et al. (2000). Effectiveness and limitations of betablocker therapy in congenital long-QT syndrome. *Circulation* 101, 616–623. doi: 10.1161/01.CIR.101.6.616

Moss, A. J., Zareba, W., Kaufman, E. S., Gartman, E., Peterson, D. R., Benhorin, J., et al. (2002). Increased risk of arrhythmic events in long-QT syndrome with mutations in the pore region of the human ether-a-go-go-related gene potassium channel. *Circulation* 105, 794–799. doi: 10.1161/hc0702.105124

Moss, A. J., Zareba, W., Schwarz, KQ Rosero, S., McNitt, S., and Robinson, J. L. (2008). Ranolazine shortens repolarization in patients with sustained inward sodium current due to type-3 long-QT syndrome. *J. Cardiovasc. Electrophysiol.* 19, 1289–1293. doi: 10.1111/j.1540-8167.2008.01246.x

Novak, A., Barad, L., Zeevi-Levin, N., Shick, R., Shtrichman, R., Lorber, A., et al. (2012). Cardiomyocytes generated from CPVTD307H patients are arrhythmogenic in response to beta-adrenergic stimulation. *J. Cell Mol. Med.* 16, 468–482. doi: 10.1111/j.1582-4934.2011.01476.x

Nunn, L. M., and Lambiase, P. D. (2011). Genetics and cardiovascular disease – causes and prevention of unexpected sudden adult death: the role of the SADS clinic. *Heart* 97, 1122–1127. doi: 10.1136/hrt.2010.218511

Nunn, L. M., Bhar-Amato, J., Lowe, M. D., Macfarlane, P. W., Rogers, P., McKenna, W. J., et al. (2011). Prevalence of J-point elevation in sudden arrhythmic death syndrome families. *J. Am. Coll. Cardiol.* 58, 286–290. doi: 10.1016/j.jacc.2011.03.028

Papadakis, M., Sharma, S., Cox, S., Sheppard, M. N., Panoulas, V. F., and Behr, E. R. (2009). The magnitude of sudden cardiac death in the young: a death certificate-based review in England and Wales. *Europace* 11, 1353–1358. doi: 10.1093/europace/eup229

Pasca, S. P., Portmann, T., Voineagu, I., Yazawa, M., Shcheglovitov, A., Paşca, A. M., et al. (2011). Using iPSC-derived neurons to uncover cellular phenotypes associated with Timothy syndrome. *Nat. Med.* 17, 1657–1662. doi: 10.1038/nm.2576

Priori, S. G., and Napolitano, C. (2006). Role of genetic analyses in cardiology: part I: mendelian diseases: cardiac channelopathies. *Circulation* 113, 1130–1135. doi: 10.1161/CIRCULATIONAHA.105.563205

Priori, S. G., Gasparini, M., Napolitano, C., Della Bella, P., Ottonelli, A. G., Sassone, B., et al. (2012). Risk stratification in Brugada syndrome: results of the PRELUDE (PRogrammed ELectrical stimULation preDictive valuE) registry. *J. Am. Coll. Cardiol.* 59, 37–45. doi: 10.1016/j.jacc.2011.08.064

Priori, S. G., Napolitano, C., Gasparini, Pappone, C., Della Bella, P., Giordano, U., et al. (2002a). Natural history of Brugada syndrome: insights for risk stratification and management. *Circulation* 105, 1342–1347. doi: 10.1161/hc1102.105288

Priori, S. G., Napolitano, C., Memmi, M., Colombi, B., Drago, F., Gasparini, M., et al. (2002b). Clinical and molecular characterization of patients with catecholaminergic polymorphic ventricular tachycardia. *Circulation* 106, 69–74. doi: 10.1161/01.CIR.0000020013.73106.D8

Rosso, R., Kogan, E., Belhassen, B., Rozovski, U., Scheinman, M. M., Zeltser, D., et al. (2008). J-point elevation in survivors of primary ventricular fibrillation and matched control subjects: incidence and clinical significance. *J. Am. Coll. Cardiol.* 52, 1231–1238. doi: 10.1016/j.jacc.2008.07.010

Runa, Y., Liu, N., Napolitano, C., and Priori, S. G. (2008). Therapeutic strategies for long-QT syndrome: does the molecular substrate matter? *Circ. Arrhythm. Electrophysiol.* 1, 290–297. doi: 10.1161/CIRCEP.108.795617

Sangwatanaroj, S., Prechawat, S., Sunsaneewitayakul, B., Sitthisook, S., Tosukhowong, P., and Tungsanga, K. (2001). New electrocardiographic leads and the procainamide test for the detection of the Brugada sign in sudden unexplained death syndrome survivors and their relatives. *Eur. Heart J.* 22, 2290–2296. doi: 10.1053/euhj.2001.2691

Schwartz, P. J., Priori, S. G., Locati, E. H., Napolitano, C., Cantù, K., Towbin, J. A., et al. (1998). Long QT syndrome patients with mutations of the SCN5A and HERG genes have differential responses to Na+ channel blockade and to increases in heart rate. Implications for gene-specific therapy. *Circulation* 92, 3381–3386. doi: 10.1161/01.CIR.92.12.3381

Schwartz, P. J., Stramba-Badiale, M., Crotti, L., Pedrazzini, M., Besana, A., Bosi, G., et al. (2009). Prevalence of the congenital long-QT syndrome. *Circulation* 120, 1761–1767. doi: 10.1161/CIRCULATIONAHA.109.863209

Shimizu, W., Horie, M., Ohno, S., Takenaka, K., Yamaguchi, M., Shimizu, M., et al. (2004). Mutation site-specific differences in arrhythmic risk and sensitivity to sympathetic stimulation in the LQT1 form of congenital long QT syndrome: multicenter study in Japan. *J. Am. Coll. Cardiol.* 44, 117–125. doi: 10.1016/j.jacc.2004.03.043

Skinner, J. R., Crawford, J., Smith, W., Aitken, A., Heaven, D., Evans, C. A., et al. (2011). Prospective, population-based long QT molecular autopsy study of postmortem negative sudden death in 1 to 40 year olds. *Heart Rhythm* 8, 412–419. doi: 10.1016/j.hrthm.2010.11.016

Takahashi, K., Tanabe, K., Ohnuki, M., Narita, M., Ichisaka, T., Tomoda, K., et al. (2007). Induction of pluripotent stem cells from adult human fibroblasts by defined factors. *Cell* 131, 861–872. doi: 10.1016/j.cell.2007.11.019

Tan, H. L., Hofman, N., van Langen, van der Wal, A. C., and Wilde, A. A. (2005). Sudden unexplained death: heritability and diagnostic yield of cardiological and genetic examination in surviving relatives. *Circulation* 112, 207–213. doi: 10.1161/CIRCULATIONAHA.104.522581

Terrenoire, C., Wang, K., Tung, K. W., Chung, W. K., Pass, R. H., Lu, J. T., et al. (2013). Induced pluripotent stem cells used to reveal drug actions in a long QT syndrome family with complex genetics. *J. Gen. Physiol.* 141, 61–72. doi: 10.1085/jgp.201210899

Tester, D. J., and Ackerman, M. J. (2007). Postmortem long QT syndrome genetic testing for sudden unexplained death in the young. *J. Am. Coll. Cardiol.* 49, 240–246. doi: 10.1016/j.jacc.2006.10.010

Tester, D. J., and Ackerman, M. J. (2011). Genetic testing for potentially lethal, highly treatable inherited cardiomyopathies/channelopathies in clinical practice. *Circulation* 123, 1021–1037. doi: 10.1161/CIRCULATIONAHA.109.914838

Tester, D. J., Medeiros-Domingo, A., Will, M. L., Haglund, C. M., and Ackerman, M. J. (2012). Cardiac channel molecular autopsy: insights from 173 consecutive cases of autopsy-negative sudden unexplained death referred for postmortem genetic testing. *Mayo Clin. Proc.* 87, 524–539. doi: 10.1016/j.mayocp.2012.02.017

Tester, D. J., and Ackerman, M. J. (2012). The molecular autopsy: should the evaluation continue after the funeral. *Pediatr. Cardiol.* 33, 461–470. doi: 10.1007/s00246-012-0160-8

Thomson, J. A., Itskovitz-Eldor, J., Shapiro, S. S., Waknitz, M. A., Swiergiel, J. J., Marshall, V. S., et al. (1998). Embryonic stem cell lines derived from human blastocysts. *Science* 282, 1145–1147. doi: 10.1126/science.282.5391.1145

Tikkanen, J. T., Anttonen, O., Junttila, J., Aro, A. L., Kerola, T., Rissanen, H. A., et al. (2009). Long-term outcome associated with early repolarisation on electrocardiography. *N. Engl. J. Med.* 361, 2529–2537. doi: 10.1056/NEJMoa0907589

Tomas, M., Napolitano, C., De Giuli, L., Bloise, R., Subirana, I., Malovini, A., et al. (2010). Polymorphisms in the NOS1AP gene modulate QT interval duration and risk of arrhythmias in the long QT syndrome. *J. Am. Coll. Cardiol.* 55, 2745–2752. doi: 10.1016/j.jacc.2009.12.065

Tungsanga, K., and Sriboonlue, P. (1993). Sudden unexplained death syndrome in northeast Thailand. *Int. J. Epidemiol.* 22, 81–87. doi: 10.1093/ije/22.1.81

Van Der Werf, C., Hofman, N., Tan, H. L., van Dessel, P. F., Alder, M., van der Wal, A. C., et al. (2010). Diagnostic yield in sudden unexplained death and aborted cardiac arrest in the young: the experience of a tertiary referral center in the Netherlands. *Heart Rhythm* 7, 1383–1389. doi: 10.1016/j.hrthm.2010.05.036

Winkel, B. G., Larsen, M. K., Berge, K. E., Leren, T. P., Nissen, P. H., Olesen, M. S., et al. (2012). The prevalence of mutations in KCNQ1, KCNH2, and SCN5A in an unselected national cohort of young sudden unexplained death cases. *J. Cardiovasc. Electrophysiol.* 23, 1092–1098. doi: 10.1111/j.1540-8167.2012.02371.x

Yazawa, M., Hsueh, B., Jia, X., Pasca, A. M., Bernstein, J. A., Hallmayer, J., et al. (2011). Using induced pluripotent stem cells to investigate cardiac phenotypes in Timothy syndrome. *Nature* 471, 230–234. doi: 10.1038/nature09855

Yu, J., Vodyanik, M. A., Smuga-Otto, K., Antosiewicz-Bourget, J., Frane, J. L., Tian, S., et al. (2007). Induced pluripotent stem cell lines derived from human somatic cells. *Science* 318, 1917–1920. doi: 10.1126/science.1151526

Conflict of Interest Statement: The authors declare that the research was conducted in the absence of any commercial or financial relationships that could be construed as a potential conflict of interest.

Received: 22 April 2013; paper pending published: 15 May 2013; accepted: 11 July 2013; published online: 12 September 2013.

*Citation: Vyas V and Lambiase PD (2013) The investigation of sudden arrhythmic death syndrome (SADS)—the current approach to family screening and the future role of genomics and stem cell technology. Front. Physiol. **4**:199. doi: 10.3389/fphys.2013.00199*

This article was submitted to Cardiac Electrophysiology, a section of the journal Frontiers in Physiology.

frontiers in PHYSIOLOGY

ORIGINAL RESEARCH ARTICLE
published: 13 June 2013
doi: 10.3389/fphys.2013.00130

Serum sphingolipids level as a novel potential marker for early detection of human myocardial ischaemic injury

Emmanuel E. Egom[1,2], Mamas A. Mamas[2,3], Sanoj Chacko[4], Sally E. Stringer[2], Valentine Charlton-Menys[2], Magdi El-Omar[3], Debora Chirico[3], Bernard Clarke[3], Ludwig Neyses[2,3], J. Kennedy Cruickshank[2], Ming Lei[2]*† and Farzin Fath-Ordoubadi[3]*†

[1] Department of Physiology and Biophysics, Faculty of Medicine, Dalhousie University, Halifax, NS, Canada
[2] Faculty of Medicine and Human Sciences, Institute of Cardiovascular Sciences, University of Manchester, Manchester, UK
[3] Biomedical Research Centre, Central Manchester NHS Foundation Trust, Manchester, UK
[4] Manchester Royal Infirmary, Manchester Heart Centre, Manchester, UK

Edited by:
Ian N. Sabir, King's College London, UK

Reviewed by:
Kaivan Khavandi, King's College London, UK
Lucia M. Li, Imperial College London, UK

***Correspondence:**
Ming Lei, Faculty of Medical and Human Sciences, University of Manchester, CFT Building, 46 Grafton Road, Manchester, M13 9NT, UK
e-mail: ming.lei@manchester.ac.uk; Farzin Fath-Ordoubadi, Manchester Heart Centre, Manchester Royal Infirmary, Manchester, M13 9WL, UK
e-mail: farzin.fath-ordoubadi@cmft.nhs.uk
† *Joint senior authors.*

Background: Ventricular tachyarrhythmias are the most common and often the first manifestation of coronary heart disease and lead to sudden cardiac death (SCD). Early detection/identification of acute myocardial ischaemic injury at risk for malignant ventricular arrhythmias in patients remains an unmet medical need. In the present study, we examined the sphingolipids level after transient cardiac ischaemia following temporary coronary artery occlusion during percutaneous coronary intervention (PCI) in patients and determined the role of sphingolipids level as a novel marker for early detection of human myocardial ischaemic injury.

Methods and Results: Venous samples were collected from either the coronary sinus ($n = 7$) or femoral vein ($n = 24$) from 31 patients aged 40–73 years-old at 1, 5 min, and 12 h, following elective PCI. Plasma sphingolipids levels were assessed by HPLC. At 1 min coronary sinus levels of sphingosine 1-phosphate (S1P), sphingosine (SPH), and sphinganine (SA) were increased by 314, 115, and 614%, respectively ($n = 7$), while peripheral blood levels increased by 79, 68, and 272% ($n = 24$). By 5 min, coronary sinus S1P and SPH levels increased further (720%, 117%), as did peripheral levels of S1P alone (792%). Where troponin T was detectable at 12 h (10 of 31), a strong correlation was found with peak S1P ($R^2 = 0.818$; $P < 0.0001$).

Conclusion: For the first time, we demonstrate the behavior of plasma sphingolipids following transient cardiac ischaemia in humans. The observation supports the important role of sphingolipids level as a potential novel marker of transient or prolonged myocardial ischaemia.

Keywords: sphingolipids, sphingosine 1-phosphate, ischaemia

INTRODUCTION

Despite recent advances in preventing sudden cardiac death (SCD) due to cardiac arrhythmia, its incidence in the population at large has remained unacceptably high. It is responsible for 50% of the mortality from cardiovascular disease in the developed countries and accounts for 300,000 to 400,000 deaths every year in the United States. About 80% of SCDs are caused by ventricular tachyarrhythmias that often occur without warning, leading to death within minutes in patients who do not receive prompt medical attention. It is the most common and often the first manifestation of coronary heart disease. Early detection/identification of acute myocardial ischaemia in patients at risk for lethal ventricular arrhythmias remains an unmet medical need. At *in vivo*, acute myocardial ischaemia is associated with dramatic electrophysiological alterations that may lead to malignant ventricular arrhythmias which occur within minutes of cessation of coronary flow and are rapidly reversible with reperfusion. This suggests that subtle and reversible biochemical and/or ionic alterations within or near the sarcolemma of myocardium during the early stage of acute ischaemic injury may contribute to the electrophysiological instability.

Sphingolipids are biologically active lipids (Alewijnse and Peters, 2008), whose serum sphingosine (SPH) levels were found to be elevated in animal models of myocardial infarction (MI; Zhang et al., 2001; Thielmann et al., 2002) and are thought to have an important cardioprotective role during the ischemic insult (Karliner et al., 2001). Sphingosine 1-phosphate (S1P) has been shown to be an important mediator of ischemic pre- and post-conditioning in both pharmacological and knockout animal studies (Karliner, 2009), with SIP receptors being expressed in the myocardium, endothelium, and platelets (Karliner, 2009). Deutschman et al. (2003) reported that sphingolipid levels are elevated in patients with coronary artery disease (CAD) and that S1P had a greater predictive value in detecting CAD, than traditional risk factors. It is not clear whether sphingolipids are markers of the inflammatory process associated with atherosclerotic CAD and/or are markers of cardiac ischaemia associated with flow obstructive coronary artery lesions. During coronary occlusion

and subsequent reperfusion such as occurs during treatment of MI with percutaneous coronary intervention (PCI), reactive oxygen species (ROS) are formed that mediate ischaemia-reperfusion injury based on oxidative stress (Nikolic-Heitzler et al., 2006). ROS regulate S1P levels through changes in the function of sphingosine kinase, the final rate limiting step in S1P synthesis (Maceyka et al., 2007). Using samples collected from humans before and after balloon occlusion of coronary arteries during PCI we have for the first time investigated whether sphingolipids are elevated during brief periods of coronary occlusion and therefore transient cardiac ischaemia, hence providing novel insight into pathophysiological mechanisms that occur during ischaemia reperfusion injury and determined whether change of their level can be a novel marker for early detection of human myocardial ischemic injury. To understand whether oxidative stress during this transient ischaemia may potentially account for changes in sphingolipids level we also evaluated changes in oxidized LDL (Ox-LDL) used here as an oxidative stress biomarker.

METHODS

STUDY PROTOCOL

This study complies with the Declaration of Helsinki, was approved by the North West 8 Research Ethics Committee of Greater Manchester East and all patients gave written informed consent before entry. Ethical approval was obtained from the National Research Ethics committee via the NRES committee-North West Greater Manchester Central, REC reference 07/H1008/162. Blood samples were obtained from 31 patients aged 40 to 73 years-old undergoing elective PCI to native coronary arteries at the Manchester Heart Centre, Manchester, UK. Procedures were performed via the femoral artery through standard 6Fr sheaths and peripheral venous samples were collected through a 6Fr femoral venous sheath. Coronary sinus sampling was performed using a 6Fr Amplatz Left-1 catheter (AL-1) during PCI. Control venous blood samples were obtained either from the coronary sinus (7 patients) or via the femoral venous sheath (24 patients) once the guide catheter and guide wire were in position prior to the PCI procedure. Balloon inflations of between 30 s and 1 min were performed to predilate the target lesions. Serial venous samples were then collected from either the coronary sinus or femoral vein at 1 and 5 min post-balloon inflation. PCI was then completed as per routine at our center. Twelve hour post-procedure samples to measure sphingolipid and troponin T levels were taken from a peripheral vein.

After PCI, blood samples were immediately dispensed into 3 ml ethylenediaminetetraacetic acid (EDTA) tubes with 2-chloroadenosine (0.05 mmol/liter) and procaine hydrochloride (0.154 mol/liter) and equilibrated at 4°C. All blood samples collected were centrifuged briefly to clarify and kept at 4°C. Once samples are derivatized, they were diluted into the mobile phase, kept at 0–4°C, and analyzed by HPLC as soon as possible. As an added precaution, standards were alternated with samples to detect (and correct for) losses over time.

Only patients with angiographic single vessel disease undergoing elective PCI participated in this study, and had documented normal left ventricular and renal function. Patients with history of coronary artery bypass graft (CABG), valvular heart disease, or MI/acute coronary syndrome (ACS) were excluded as were PCI procedures in patients with chronic total occlusions. Peripheral blood samples were also taken from 11 healthy controls with no history of CAD.

HIGH-PERFORMANCE LIQUID CHROMATOGRAPHY

S1P standards were purchased from Avanti Polar Lipids, Inc. (Delfzyl, The Netherlands). All other chemicals, including *o*-phthaldialdehyde (OPA), D-sphingosine, D-erythro-dihydrosphingosine, boric Acid, β-mercaptoethanol were purchased from Sigma-Aldrich (Dorset, UK). All solvents for high-performance liquid chromatography (HPLC) were purchased from Fisher Scientific (Leicestershire, UK). All blood samples collected into EDTA with 2-chloroadenosine and procaine during the procedure were centrifuged at 2056 g for 15 min at 4°C. Aliquots of plasma (0.5 ml) were stored at −80°C until analyzed by HPLC. Sphingolipids were extracted from samples and HPLC analysis of sphingolipids (S1P, SPH, and SA) levels were performed according to Caligan et al. (2000).

DETERMINATION OF TROPONIN T AND HIGH SENSITIVE TROPONIN T (hsTnT)

Troponin T level in peripheral vein at 12 h after post-PCI was measured by standard assay (Roche Troponin T). The level of high sensitive troponin T (hsTnT) in samples from both the coronary sinus and femoral vein at 1 and 5 min after post-PCI was also measured by High-Sensitive Troponin T assay (Roche Diagnostics; Helleskov Madsen et al., 2008). The lower detection limits of standard and hsTnT assays are 0.01 ug/l and 5 ng/l, respectively.

DETERMINATION OF Ox-LDL AND hsCRP

Ox-LDL was measured by a commercially available sandwich ELISA (Mercodia) with specific monoclonal antibody mAb-4E6 as described by Holvoet et al. (1998). A standard curve showing the binding range of Ox-LDL samples was prepared. Internal controls consisting of high and low standard plasma samples were included on each microtiter plate to detect potential variations between microtitration plates. Each sample was assayed in triplicate. The intra-assay coefficients of variation for all assays were 5–9%. High resolution CRP (hsCRP) was measured using a high-sensitivity assay with reagents and a BNII analyzer from Dade-Behring, Milton Keynes, UK. The intra- and inter-assay coefficient of variation for the hsCRP assay was 3.9 and 4.6%, respectively.

STATISTICAL ANALYSIS

All data are reported as means ± sem. Repeated measure One-Way ANOVA was used to compare values of measurements between groups. When analysis of variance revealed a significant difference among values, Tukey's test was applied to determine the significance of a difference between selected group means. $P < 0.05$ was taken to indicate statistical significance.

RESULTS

Blood samples were taken from total of 31 study participants undergoing routine elective PCI. Characteristics and coronary

lesion data of the study cohort are presented in **Table 1**. Pre-dilation of the target lesions was performed with angioplasty balloons inflated between 14 and 22 Atmospheres (mean 15 Atmospheres) for a period of between 28 and 40 s (mean 31.1 s). During balloon inflation ischemic ECG changes were noted in 20/31 patients (64.5%) with ST elevation in 13/31 patients (41.9%, mean ST elevation 0.5 mm) and ST depression in 7/31 patients (22.5%, mean ST depression 0.5 mm). In the remaining 11/31 patients (35.4%) no ECG changes were observed although all patients reported transient chest discomfort during this period.

Using HPLC we analysed plasma levels of sphingolipids in patients at baseline (pre-balloon inflation) and at different time course points after balloon inflation (1, 5 min, and 12 h). HPLC analysis revealed significant alterations in plasma levels of sphingolipids sampled from the coronary sinus from 7 patients and peripheral veins from 24 patients following induction of transient myocardial ischaemia by balloon occlusion of target lesion. Representative examples of isolation and detection of sphingolipids, at baseline and at different time course points after balloon inflation are shown in **Figures 1A,B**. Baseline concentrations of S1P measured from peripheral blood samples were more than 4-fold higher in patients with documented CAD undergoing PCI compared to healthy controls (1.29 ± 0.27 vs. 0.38 ± 0.05 μmol/liter; $n = 11$; $P < 0.001$; **Figure 1C**). As illustrated in **Table 2**, there was a significant increase in all three sphingolipid levels at 1 and 5 min, compared with baseline levels, both in coronary sinus blood (**Figures 2A**,**B**,**C**) and peripheral blood (**Figures 2D**,**E**,**F**). S1P showed the largest increase of the three sphingolipids, with its greatest level at 5 min (**Figures 2A,D**), whereas the levels of SPH and SA were highest at 1 min and began to decrease at 5 min (**Figures 2B**,**C**,**E**,**F**).

Table 1 | Characteristics and coronary lesion data of the study cohort ($n = 31$).

DEMOGRAPHICS	
Age (Years; mean ± SEM)	63 ± 9
Sex (% Male)	97
Caucasian (%)	87
% Normal LV function (EF > 60%)	100
% Normal renal function	100
RISK FACTORS	
Hypertension (%)	53
Diabetes (%)	15
Hyperlipidemia (%)	85
Smoking (%)	39
BMI (kg/m^2)	27.4 ± 4.8
MEDICATION	
Antiplatelet therapy (%)	100
B-Blockers (%)	82
ACEi (%)	65
Statins (%)	100
Nitrates (%)	22.5
Ca Blockers (%)	29.5
TARGET VESSEL	
LAD	21/37 (67.7%)
RCA	8/31 (25.8%)
Cx	2/31 (6.4%)
VESSEL DIAMETER	
2.5–2.99 mm	12/31 (38.7%)
3–3.49 mm	11/31 (35.4%)
3.5–3.99 mm	7/31 (22.5%)
4.5–4.99 mm	1/31 (3.2%)
LESION LENGTH	
10–14 mm	4/31 (12.9%)
15–19 mm	5/31 (16.1%)
20–24 mm	11/31 (35.4%)
25–30 mm	8/31 (25.8%)
>30 mm	8/31 (25.8%)
% STENOSIS	
50–74%	2/31 (6.4%)
75–94%	22/31 (70.9%)
>95%	7/31 (22.5%)

At 1 min following balloon inflation, in coronary sinus, levels of S1P, SPH, and SA increased by 314, 115 and 614%, respectively, compared with baseline levels ($n = 7$, all $P < 0.001$), whereas in peripheral blood, levels of S1P, SPH, and SA increased by 79, 68, and 272%, respectively, compared with baseline levels ($n = 24$, all $P < 0.001$). Peripheral sphingolipid levels at 1 min were consistently very much lower than coronary sinus levels. At 5 min after balloon inflation, in coronary sinus blood, levels of S1P, SPH, and SA increased by 720, 117, and 320% compared with baseline levels ($n = 7$, all $P < 0.001$), while in peripheral blood, levels of S1P, SPH, and SA increased by 792, 44, and 56% compared with baseline levels ($n = 24$, all $P < 0.001$). At 12 h following the PCI procedure, peripheral levels of S1P were much lower than that at 1 or 5 min, but were still elevated compared to baseline [S1P: by 88% ($n = 24$, all $P < 0.001$)]. Peripheral SPH and SA levels had declined to below baseline (decrease of SPH: 33% $n = 24$, all $P < 0.001$; SA: 51%, $n = 24$, all $P < 0.001$).

To determine whether the observed increase in sphingolipids following transient coronary occlusion was related to myocardial necrosis or cardiac ischaemia *per se*, serum troponin levels were measured. Elevated 12 h troponin T levels were detectable in only 10 of 31 study subjects (32.3%), following PCI (**Figure 3A**), whereas S1P concentrations were elevated in all subjects studied. **Figure 3B** shows 12 h troponin T levels plotted against peak S1P level in the study participants. For those individuals in whom troponin T was detectable at 12 h, a strong correlation was found between peak serum SIP levels and 12 h troponin T level ($R^2 = 0.818$; $P < 0.0001$). Furthermore no significant changes occurred in hsTnT levels in either the coronary sinus ($n = 6$) or peripheral blood ($n = 12$) at 1 and 5 min time points after transient coronary occlusion as shown in **Figures 3C,D**, respectively.

Oxidized LDL (OxLDL) was measured as a biomarker of oxidative stress in the serum samples obtained. OxLDL levels in coronary sinus and peripheral blood at different time points are shown in **Figures 4A,B**, respectively. At 1 min following balloon inflation, in coronary sinus, levels of OxLDL increased by 16%, compared with baseline levels ($n = 7$, $P = 0.29$), whereas in

Table 2 | Plasma levels of sphingolipids in coronary sinus and peripheral blood in patients who underwent PCI.

Time	Coronary sinus (μmol per liter) $n = 7$			Peripheral (μmol per liter) $n = 24$		
	S1P	SPH	SA	S1P	SPH	SA
Baseline	123.34 ± 7	27.19 ± 9	0.44 ± 0.28	1.23 ± 0.27†	0.31 ± 0.004†	0.0009 ± 0.0002†
1 min	509.13 ± 86*	58.45 ± 5*	3.14 ± 0.35*	2.31 ± 0.06*†	0.52 ± 0.002*†	0.0032 ± 0.001*†
5 min	1008.8 ± 152*	59 ± 1.08*	1.85 ± 0.14*	11.48 ± 2.70*†	0.45 ± 0.005*†	0.0013 ± 0.0001*†
12 h	N/A	N/A	N/A	2.42 ± 0.20*	0.21 ± 0.001	0.0004 ± 0.00004

Concentrations are shown for baseline (pre-balloon inflation) and at 1 and 5 min post-inflation both for coronary sinus and peripheral and also 12 h post-PCI for peripheral samples. Values are expressed as mean ± sem. N/A denotes not available.

** $P < 0.001$ for the comparison between the baseline vs. 1 and 5 min post-balloon inflation.*

† $P < 0.001$ for comparison between coronary sinus and peripheral levels.

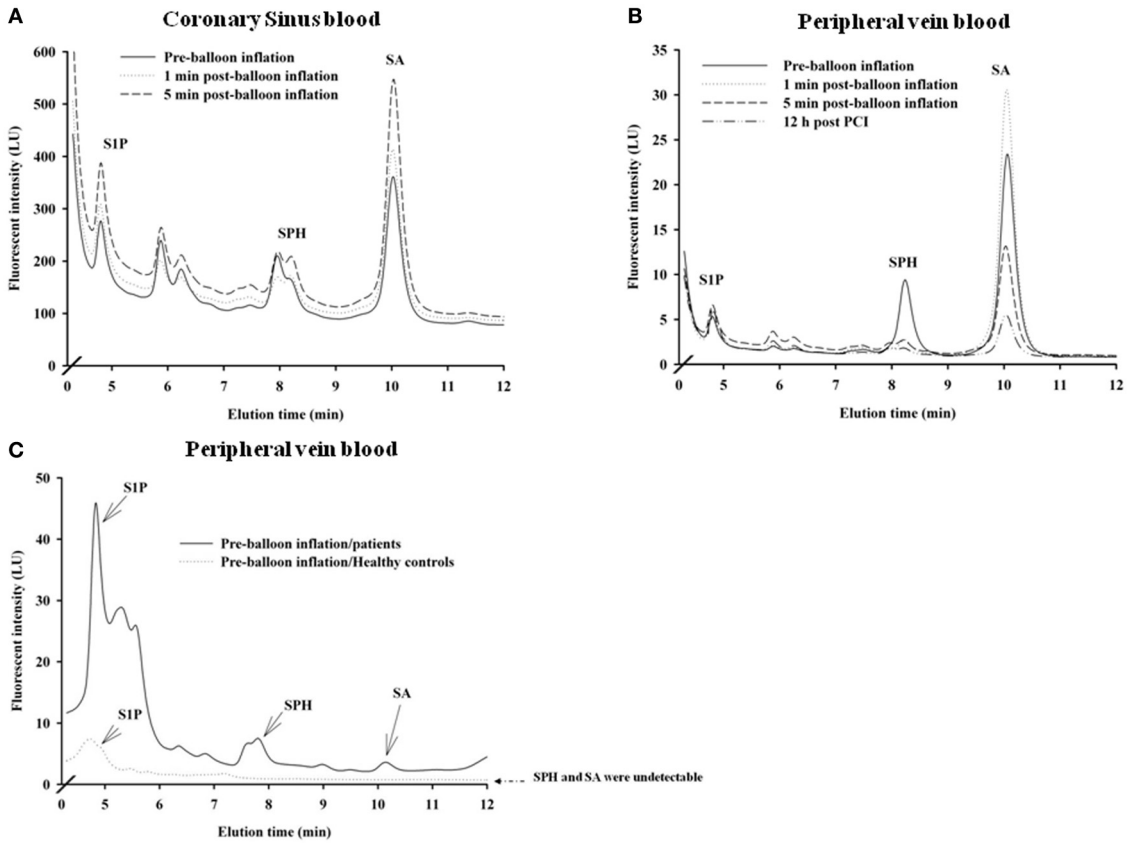

FIGURE 1 | Distribution of sphingolipids in coronary sinus blood (A; $n = 7$) and in peripheral blood (B; $n = 24$) in patients who underwent PCI. Also shown are comparative distributions of sphingolipids in peripheral blood at baseline (before balloon inflation in a patient) and in a blood sample from a healthy control (**C**; $n = 11$). Representative examples of relative plasma levels of sphingolipids as detected by HPLC at baseline and at different time points: 1, 5 min, and 12 h post-PCI are shown.

peripheral blood, levels increased by 29% compared with baseline ($n = 24$, all $P < 0.001$). Peripheral OxLDL levels were consistently lower than coronary sinus levels. At 5 min after balloon inflation, in coronary sinus blood, levels of OxLDL increased by 42% compared with baseline ($n = 7$, all $P < 0.001$), while in peripheral blood, levels of OxLDL increased by 60% compared with baseline ($n = 24$, all $P < 0.001$). At 12 h following the PCI procedure, levels of OxLDL increased by 82% compared with baseline ($n = 7$, all $P < 0.001$ 95% CI).

hsCRP levels were measured as a general marker of inflammation. No significant changes occurred in hsCRP levels in coronary sinus and peripheral blood at different time points as shown in **Figures 5A,B**, respectively.

DISCUSSION

This study demonstrated for the first time plasma sphingolipid behavior following transient cardiac ischaemia in humans, with dramatic increases in S1P, SPH, and SA. Levels were markedly

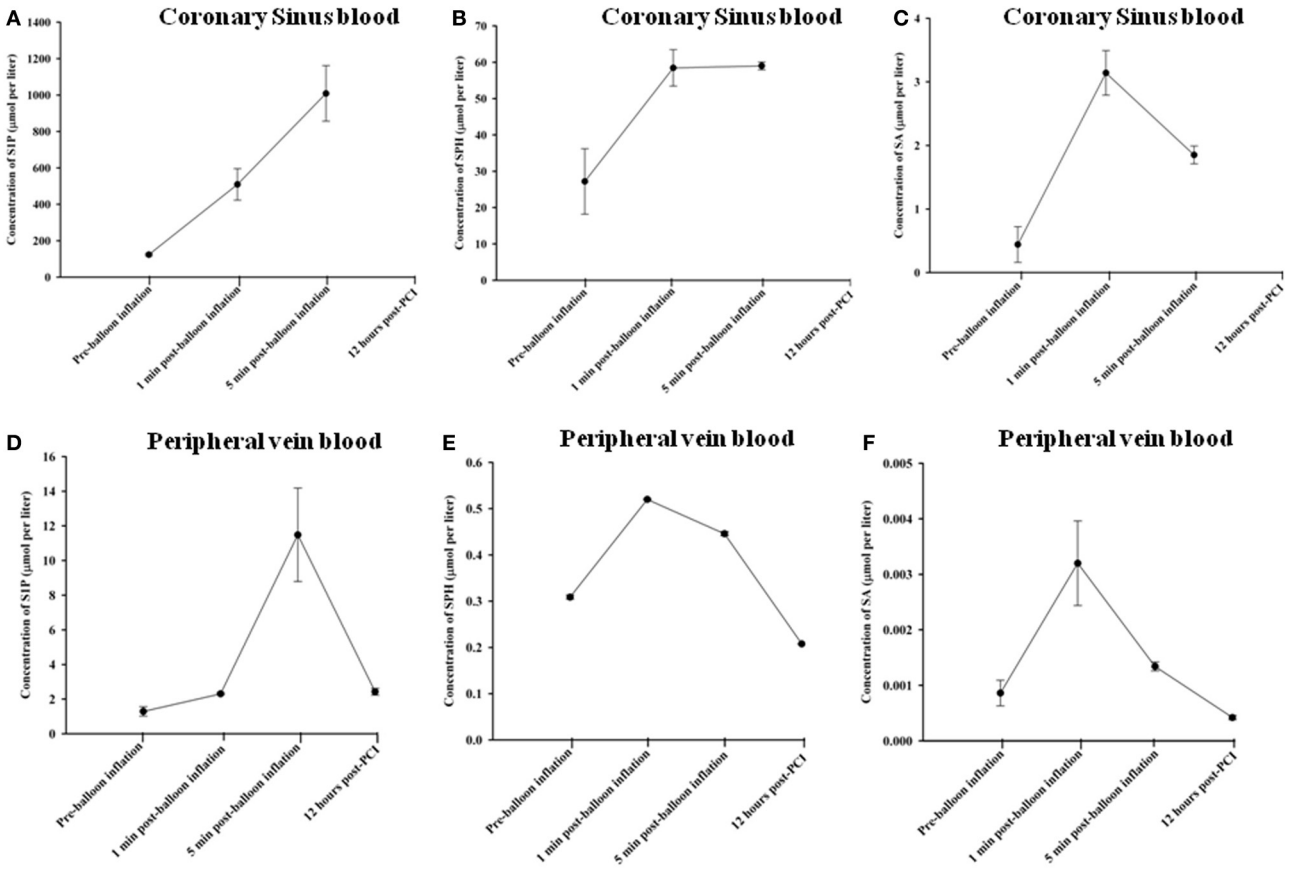

FIGURE 2 | Changes in sphingolipid concentrations in coronary sinus blood: S1P (A); SPH (B); and SA (C) and comparative concentrations in peripheral blood for S1P (D); SPH (E); and SA (F), at different time course points following balloon inflation.

increased in both the coronary sinus and peripherally within 1 min of transient ischaemia mediated by short periods of coronary vessel occlusion. To date, no biomarker used in clinical practice has the ability to detect such transient episodes of cardiac ischaemia as we observed with sphingolipids.

Cardiac biomarkers, such as cardiac troponins, have become the standard test in combination with clinical and electrocardiographic findings to diagnose and risk stratify patients with ACS. Recently two studies reported the early diagnosis of MI with high sensitive troponin assays, demonstrating this to be more accurate in diagnosing MI, compared to the conventional troponin test and other markers (Keller et al., 2009). These high sensitivity tropnin assays have high diagnostic specificity and sensitivity for the diagnosis of ACSs after only 2 or 3 h following the onset of chest pain (Keller et al., 2009; Bonaca et al., 2010). The enhancements in troponin assays have enabled resolution of the 99th percentile reference limit at progressively lower concentrations. However, the clinical significance of low-level increases with sensitive assays is still debated (Bonaca et al., 2010).

Plasma S1P, SPH, and SA levels are more sensitive markers of transient cardiac ischaemia in the subjects studied in this report compared to either hsTnT or regular TnT since we did not observe a significant elevation of hsTnT in coronary samples of the subjects at 1 and 5 mins following PCI despite marked changes in sphingolipid levels. Indeed, previous studies have shown that the greatest diagnostic utility of hsTnT is between 2 and 6 h following ischemic insult (Keller et al., 2009; Bonaca et al., 2010) which is several orders of magnitude longer than we have observed with our sphingolipid markers. Furthermore, elevated troponin T level was detectable at 12 h following PCI in 10 of 31 study subjects (32.3%).

Significant changes observed in oxidized LDL, a biomarker of oxidative stress, over the same time-course as the changes in sphingolipids may suggest a role for oxidative stress in the regulation of sphingolipid metabolism as described in animal studies (Maceyka et al., 2007). The peripheral baseline ox-LDL levels in our study are similar to those reported by Holvoet et al. (1998) in their comparison of ox-LDL levels between healthy controls and CAD patients. Tsimikas and co-workers found, in patients presenting at the Emergency Room with chest pain, that circulating ox-LDL specific markers strongly reflect the presence of ACS (Holvoet et al., 2006). Ehara et al. showed that plasma ox-LDL levels were significantly higher in AMI patients than in stable angina patients (Ehara et al., 2008) Interestingly, the magnitude of increase of ox-LDL observed in our study was much greater than those observed in AMI patients in Ehara et al.'s study suggesting

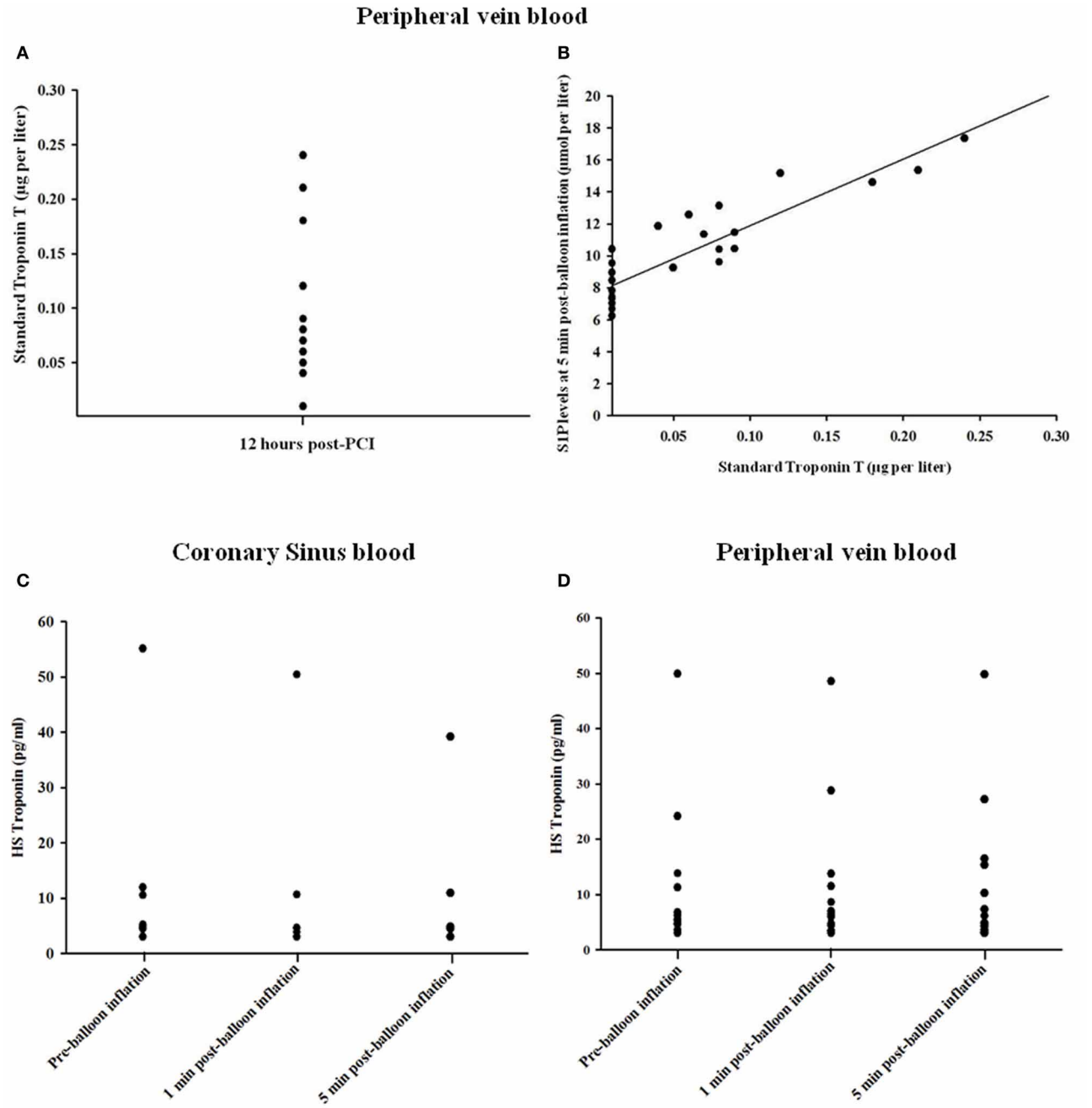

FIGURE 3 | Relationship between troponin T levels at 12 h (A) and peak S1P levels (B) in the study participants. In those cases where troponin T was detectable there was close correlation between troponin T and S1P levels ($R^2 = 0.818$; $P < 0.0001$). **(C,D)** Changes in hsTnT concentration in coronary sinus blood and peripheral blood.

that such an increase would be unlikely due to a rupture of unstable plaques. Buffon et al. (2000) have similarly observed transient (<15 min' duration) elevation of free lipid peroxides in the coronary sinus during balloon occlusion of the left anterior descending coronary artery. It is possible that ROS generated secondary to such ischemic insults may oxidize phospholipids in the vessel wall or even in plasma, which would then be subsequently detected as OxLDL in plasma. It is well-known that during the onset of hypoxia, ROS activates neutral sphingomyelinase, generating ceramide. Furthermore, ROS also leads to activation of Sphingosine Kinase 1 in a PKC-dependent manner (Jin et al., 2002), hence some of this ceramide may be metabolized to S1P thereby increasing S1P levels, in line with our observations. Indeed, the differences in sphingolipid response observed during cardiac ischaemia between our study and that of Knapp et al. (2009) in which they observed a decrease in S1P levels following

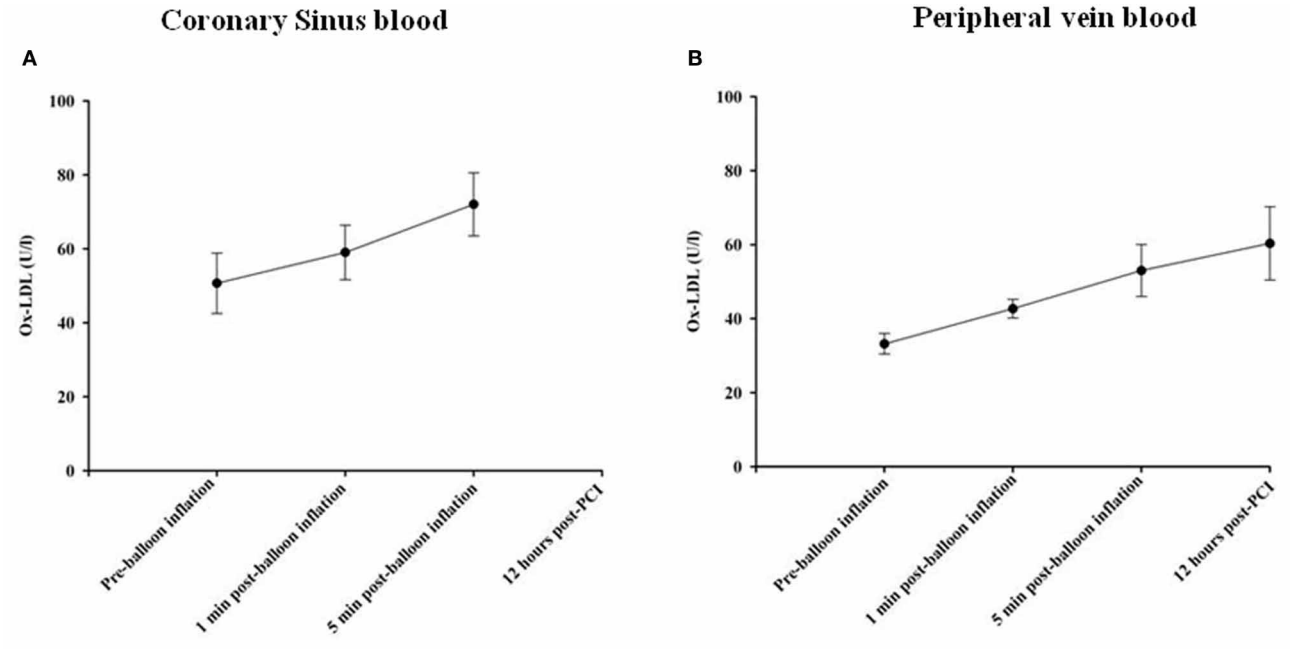

FIGURE 4 | Changes in Ox-LDL concentrations in coronary sinus (A) and peripheral (B) blood at different time course points following balloon inflation.

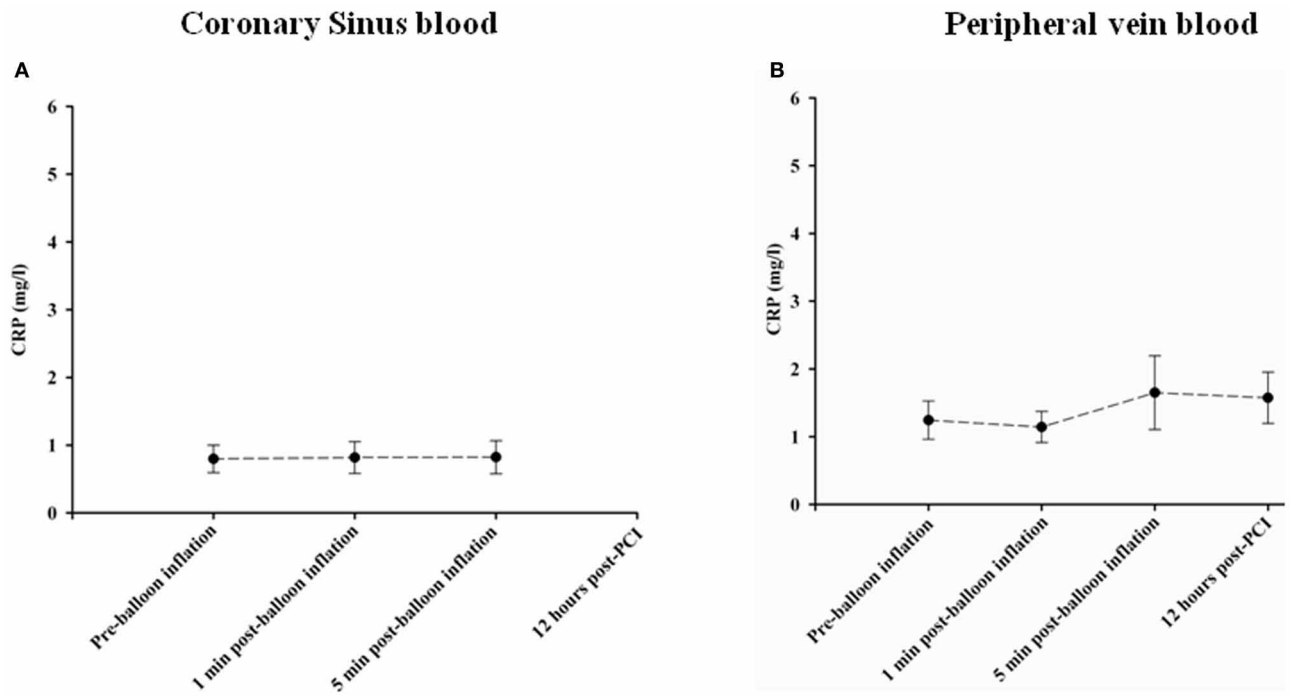

FIGURE 5 | Changes in CPR concentrations in Coronary sinus (A) and peripheral (B) blood at different time course points following balloon inflation.

MI may be due to the more prolonged ischaemia during MI resulting in degradation of sphingosine kinase 1 (Maceyka et al., 2007) and an inhibition of its activity mediated by ROS leading to decreased levels of S1P and its metabolites (Knapp et al., 2009).

Distinct changes in levels of S1P, SPH, and SA over the 12 h time course of sampling reflect the complex dynamic metabolism or inter-conversion of these three sphingolipids in the coronary and peripheral circulation. Yatomi et al. (1995) showed that about

50% of SPH was converted to S1P within 5 min in intact platelets and plasma. These results may explain why our SPH plasma levels tend to decrease and S1P increases after 5 min. S1P has been found to be metabolically stable for at least 2 h (Yatomi et al., 1995) so once released from cardiac myocytes is likely to circulate in the body, which could account for the 11% of the 5 min S1P peripheral blood levels that was still detectable at 12 h. Consistently, Sattler et al showed that S1P levels in plasma rise during the first 12 h of MI and decline thereafter. The authors demonstrated that in this setting plasma high density lipoprotein-C (HDL-C), but not other carriers, is the acceptor of S1P as mirrored by the increase in their S1P content to concentrations exceeding even those of healthy HDL (Sattler et al., 2010). The decrease in levels of SA may also be attributed to its very fast turnover (Yatomi et al., 1997).

Our study also indicates a potential role of sphingolipids in pathophysiological processes that occur during early cardiac ischaemia. Vessey and colleagues have demonstrated that sphingolipids are important endogenous cardioprotectants released by ischemic pre- and post-conditioning in experimental animal models (Vessey et al., 2009) and pre-treatment with exogenous S1P provides protection against cardiac I/R injury (Karliner, 2009). Kelly et al. have shown that ethanolamine, a metabolite of S1P protects the murine heart against I/R injury via activation of STAT-3 (Kelly et al., 2010). In addition, Theilmeier et al. have shown that the HDL and its constituent, S1P, acutely protect the heart against ischaemia/reperfusion injury *in vivo* via an S1P3-mediated and nitric oxide-dependent pathway, suggesting that a rapid therapeutic elevation of S1P-containing HDL plasma levels may be beneficial in patients at high risk of acute myocardial ischaemia (Theilmeier et al., 2006). Interestingly, Sattler et al. have recently shown that the amount of plasma S1P not bound to HDL and the ratio of non-HDL-bound and HDL-bound S1P in plasma are increased in patients with stable CAD and MI compared to healthy individuals and are correlated to the clinical severity of CAD symptoms (Sattler et al., 2010). In addition the authors also found that the amount of plasma S1P not bound to HDL is inversely associated with the S1P content of isolated HDL only in healthy individuals but not in patients with CAD, implying a functional alteration in the S1P exchange between HDL-bound and non-HDL-bound S1P plasma pools in CAD. We recently found that the S1P receptor agonist, FTY720, a new generation of S1P receptor modulator in phase III clinical trials as an immuno-suppressant agent for the treatment of auto-immune diseases and in organ transplantation (Budde et al., 2006), can prevent ischaemia-reperfusion damage in isolated heart and sino-atrial (SA) nodes in the rat (Egom et al., 2010a). We also showed that FTY720 reduces ischaemia-induced ventricular arrhythmias and SA nodal dysfunction via activation of p21-activated kinase (Pak1), a Ser/Thr kinase downstream of small G-proteins, and Akt (Egom et al., 2010a,b). FTY720 may also inhibit atherosclerosis by suppressing the machinery involved in monocyte/macrophage emigration to atherosclerotic lesions (Keul et al., 2007). In contrast to S1P receptors on lymphocytes, the authors also demonstrated that FTY720 did not desensitize vascular S1P receptors suggesting that S1P agonists that selectively target the vasculature and not the immune system may be promising new drugs against atherosclerosis (Keul et al., 2007). In addition, $S1P_3$ receptor may mediate the chemotactic effect of S1P in macrophages *in vitro* and *in vivo* and may play a causal role in atherosclerosis by promoting inflammatory monocyte/macrophage recruitment and altering smooth muscle cell behavior (Keul et al., 2011).

Recently, several novel biomarkers including hFABP (Colli et al., 2007) and cMyBP-C (Govindan et al., 2012) have been proposed. hFABP is a small soluble cytosolic protein involved in the transportation of long-chain fatty acids into the cardiomyocyte is released rapidly into the circulation in response to cardiomyocyte injury. Due to its solubility, hFABP can be released more rapidly than structurally bound molecules like cardiac troponins. Furthermore, it may enter the vascular system directly via endothelium because of its small size (15 kDA). Thus, hFABP is regarded as an early sensitive marker of AMI (Colli et al., 2007). Cardiac myosin binding protein-C (cMyBP-C) is a thick filament assembly protein that stabilizes sarcomeric structure and regulates cardiac function; however, the profile of cMyBP-C degradation after MI is unknown (Govindan et al., 2012).

Are sphingolipids mechanistically relevant to ischaemia-related arrhythmias? We have recently demonstrated that the S1P agonist FTY720 may reduce ischaemia-induced ventricular arrhythmias and SA nodal dysfunction via activation of Pak1, a Ser/Thr kinase downstream of small G-proteins, and Akt (Egom et al., 2010a). The detailed mechanisms underlying this protective effect is likely to be complex, and may involve primary effects on ion channels/transporters and secondary effect to protect cardiac myocytes from hypoxia-or ischemia-induced stress and cell death. Both S1P and FTY720 may have functional effect through $I_{K,ACh}$ as suggested by previous studies (Guo et al., 1999; Koyrakh et al., 2005).

The current study has number of limitations. Firstly, the study was conducted in a limited number of patients hence larger studies are needed to validate the value of serum sphingolipids level in the early detection of cardiac ischaemia. Secondly, transient balloon dilatation is a very different process from plaque rupture and thrombus/emboli occlusion in clinical situation. Therefore, the clinical implication of the findings in this study need to be further studied in larger number of cases of ACSs. Thirdly, since this was a prospective, observational study, we cannot quantify the clinical effect associated with the increase in early diagnostic accuracy. Fourthly, the specificity of serum sphingolipids in the early detection of cardiac ischaemia is uncertain, since it is possible that sphingolipids may also be elevated in other cardiovascular diseases as well as in situations such as sepsis and a variety of other inflammatory processes that evoke the release of inflammatory cytokines and involve the TNF pathway. However, hsTnT have also been shown to be elevated in aortic dissection, valvular heart disease and acute decompensated heart failure (Keller et al., 2009). Finally, it is still to be decided whether the elevation in Sphingolipids from these patients is derived from vascular trauma due to PCI or from myocardial ischaemia and/or necrosis, although the strong correlation with 12 h troponin levels would suggest that they are less likely to be derived from vascular trauma alone. In addition, there is no significant correlation between ECG changes (ischaemia phenotype) and plasma levels of S1P,

SPH, and SA, This may be due to a limited number of patients involved in this cohort. However, even in those patients who did not have ECG changes, ischemic symptoms were experienced.

In conclusion, we demonstrate the behavior of plasma sphingolipids level in transient cardiac ischaemia in humans produced by transient coronary vessel occlusion observed during PCI. The results show a dramatic increase in plasma S1P, SPH, and SA levels at very early stages of ischaemia, correlating strongly with Troponin levels 12 h post-PCI. These molecules therefore may become novel potentially robust early predictors of acute myocardial ischaemia presenting with ACS therefore provide a crucial timing window for treating this condition for preventing the occurrence of fatal ventricular arrhythmias. This study also raises the question of whether modulating the sphingolipid pathway may lead to potential therapeutic benefit both before and during an ischemic coronary event.

FUNDING SOURCES

This research was supported by the Wellcome Trust, MRC, and BHF (Ming Lei), Emmanuel E. Egom is a recipient of the Heart and Stroke Foundation of Canada Fellowship, British Heart Foundation (Ming Lei, Sally E. Stringer), The Biomedical Research Centre (Mamas A. Mamas, Ludwig Neyses, Farzin Fath-Ordoubadi). MHC coronary intervention research fund (Farzin Fath-Ordoubadi).

ACKNOWLEDGMENTS

We thank Mr. Andrew Hamilton for his assistance in HPLC assay.

REFERENCES

Alewijnse, A. E., and Peters, S. L. M. (2008). Sphingolipid signalling in the cardiovascular system: good, bad or both? *Eur. J. Pharmacol.* 585, 292–302. doi: 10.1016/j.ejphar.2008.02.089

Bonaca, M., Scirica, B., Sabatine, M., Dalby, A., Spinar, J., Murphy, S. A., et al. (2010). Prospective evaluation of the prognostic implications of improved assay performance with a sensitive assay for cardiac troponin i. *J. Am. Coll. Cardiol.* 55, 2118–2124. doi: 10.1016/j.jacc.2010.01.044

Budde, K., Schutz, M., Glander, P., Peters, H., Waiser, J., Liefeldt, L., et al. (2006). Fty720 (fingolimod) in renal transplantation. *Clin. Transplant.* 20(Suppl 17), 17–24. doi: 10.1111/j.1399-0012.2006.00596.x

Buffon, A., Santini, S. A., Ramazzotti, V., Rigattieri, S., Liuzzo, G., Biasucci, L. M., et al. (2000). Large, sustained cardiac lipid peroxidation and reduced antioxidant capacity in the coronary circulation after brief episodes of myocardial ischemia. *J. Am. Coll. Cardiol.* 35, 633–639.

Caligan, T. B., Peters, K., Ou, J., Wang, E., Saba, J., and Merrill, A. H. (2000). A high-performance liquid chromatographic method to measure sphingosine 1-phosphate and related compounds from sphingosine kinase assays and other biological samples. *Anal. Biochem.* 281, 36–44. doi: 10.1006/abio.2000.4555

Colli, A., Josa, M., Pomar, J. L., Mestres, C. A., and Gherli, T. (2007). Heart fatty acid binding protein in the diagnosis of myocardial infarction: where do we stand today? *Cardiology* 108, 4–10. doi: 10.1159/000095594

Deutschman, D. H., Carstens, J. S., Klepper, R. L., Smith, W. S., Page, M. T., Young, T. R., et al. (2003). Predicting obstructive coronary artery disease with serum sphingosine-1-phosphate. *Am. Heart J.* 146, 62–68. doi: 10.1016/S0002-8703(03)00118-2

Egom, E. E., Ke, Y., Musa, H., Mohamed, T. M., Wang, T., Cartwright, E., et al. (2010a). Fty720 prevents ischemia/reperfusion injury-associated arrhythmias in an ex vivo rat heart model via activation of pak1/akt signaling. *J. Mol. Cell. Cardiol.* 48, 406–414. doi: 10.1016/j.yjmcc.2009.10.009

Egom, E. E., Ke, Y., Solaro, R. J., and Lei, M. (2010b). Cardioprotection in ischemia/reperfusion injury: spotlight on sphingosine-1-phosphate and bradykinin signalling. *Prog. Biophys. Mol. Biol.* 103, 142–147. doi: 10.1016/j.pbiomolbio.2010.01.001

Ehara, S., Naruko, T., Shirai, N., Itoh, A., Hai, E., Sugama, Y., et al. (2008). Small coronary calcium deposits and elevated plasma levels of oxidized low density lipoprotein are characteristic of acute myocardial infarction. *J. Atheroscler. Thromb.* 15, 75–81.

Govindan, S., McElligott, A., Muthusamy, S., Nair, N., Barefield, D., Martin, J. L., et al. (2012). Cardiac myosin binding protein-C is a potential diagnostic biomarker for myocardial infarction. *J. Mol. Cell. Cardiol.* 52, 154–164. doi: 10.1016/j.yjmcc.2011.09.011

Guo, J., MacDonell, K. L., and Giles, W. R. (1999). Effects of sphingosine 1-phosphate on pacemaker activity in rabbit sino-atrial node cells. *Pflugers Arch.* 438, 642–648.

Helleskov Madsen, L., Ladefoged, S., Hildebrandt, P., and Atar, D. (2008). Comparison of four different cardiac troponin assays in patients with end-stage renal disease on chronic haemodialysis. *Acute Card. Care* 10, 173–180. doi: 10.1080/17482940802100279

Holvoet, P., Macy, E., Landeloos, M., Jones, D., Nancy, J. S., Van de Werf, F., et al. (2006). Analytical performance and diagnostic accuracy of immunometric assays for the measurement of circulating oxidized ldl. *Clin. Chem.* 52, 760–764. doi: 10.1373/clinchem.2005.064337

Holvoet, P., Vanhaecke, J., Janssens, S., Van de Werf, F., and Collen, D. (1998). Oxidized ldl and malondialdehyde-modified ldl in patients with acute coronary syndromes and stable coronary artery disease. *Circulation* 98, 1487–1494.

Jin, Z.-Q., Zhou, H.-Z., Zhu, P., Honbo, N., Mochly-Rosen, D., Messing, R. O., et al. (2002). Cardioprotection mediated by sphingosine-1-phosphate and ganglioside gm-1 in wild-type and pkcepsilon knockout mouse hearts. *Am. J. Physiol. Heart Circ. Physiol.* 282, H1970–H1977. doi: 10.1152/ajpheart.01029.2001

Karliner, J. S. (2009). Sphingosine kinase and sphingosine 1-phosphate in cardioprotection. *J. Cardiovasc. Pharmacol.* 53, 189–197. doi: 10.1097/FJC.0b013e3181926706

Karliner, J. S., Honbo, N., Summers, K., Gray, M. O., and Goetzl, E. J. (2001). The lysophospholipids sphingosine-1-phosphate and lysophosphatidic acid enhance survival during hypoxia in neonatal rat cardiac myocytes. *J. Mol. Cell. Cardiol.* 33, 1713–1717. doi: 10.1006/jmcc.2001.1429

Keller, T., Zeller, T., Peetz, D., Tzikas, S., Roth, A., Czyz, E., et al. (2009). Sensitive troponin i assay in early diagnosis of acute myocardial infarction. *N. Engl. J. Med.* 361, 868–877. doi: 10.1056/NEJMoa0903515

Kelly, R. F., Lamont, K. T., Somers, S., Hacking, D., Lacerda, L., Thomas, P., et al. (2010). Ethanolamine is a novel stat-3 dependent cardioprotective agent. *Basic Res. Cardiol.* 105, 763–770. doi: 10.1007/s00395-010-0125-0

Keul, P., Lucke, S., von Wnuck Lipinski, K., Bode, C., Graler, M., Heusch, G., et al. (2011). Sphingosine-1-phosphate receptor 3 promotes recruitment of monocyte/macrophages in inflammation and atherosclerosis. *Circ. Res.* 108, 314–323. doi: 10.1161/CIRCRESAHA.110.235028

Keul, P., Tolle, M., Lucke, S., von Wnuck Lipinski, K., Heusch, G., Schuchardt, M., et al. (2007). The sphingosine-1-phosphate analogue fty720 reduces atherosclerosis in apolipoprotein e-deficient mice. *Arterioscler. Thromb. Vasc. Biol.* 27, 607–613. doi: 10.1161/01.ATV.0000254679.42583.88

Knapp, M., Baranowski, M., Czarnowski, D., Lisowska, A., Zabielski, P., Górski, J., et al. (2009). Plasma sphingosine-1-phosphate concentration is reduced in patients with myocardial infarction. *Med. Sci. Monit.* 15, 490–493.

Koyrakh, L., Roman, M. I., Brinkmann, V., and Wickman, K. (2005). The heart rate decrease caused by acute FTY720 administration is mediated by the G protein-gated potassium channel I. *Am. J. Transplant* 5, 529–536. doi: 10.1111/j.1600-6143.2005.00754.x

Maceyka, M., Milstien, S., and Spiegel, S. (2007). Shooting the messenger: Oxidative stress regulates sphingosine-1-phosphate. *Circ. Res.* 100, 7–9. doi: 10.1161/01.RES.0000255895.19868.a3

Nikolic-Heitzler, V., Rabuzin, F., Tatzber, F., Vrkic, N., Bulj, N., Borovic, S., et al. (2006). Persistent oxidative stress after myocardial infarction treated by percutaneous

coronary intervention. *Tohoku J. Exp. Med.* 210, 247–255.

Sattler, K. J., Elbasan, S., Keul, P., Elter-Schulz, M., Bode, C., Graler, M. H., et al. (2010). Sphingosine 1-phosphate levels in plasma and hdl are altered in coronary artery disease. *Basic Res. Cardiol.* 105, 821–832. doi: 10.1007/s00395-010-0112-5

Theilmeier, G., Schmidt, C., Herrmann, J., Keul, P., Schafers, M., Herrgott, I., et al. (2006). High-density lipoproteins and their constituent, sphingosine-1-phosphate, directly protect the heart against ischemia/reperfusion injury in vivo via the s1p3 lysophospholipid receptor. *Circulation* 114, 1403–1409. doi: 10.1161/CIRCULATIONAHA.105.607135

Thielmann, M., Dorge, H., Martin, C., Belosjorow, S., Schwanke, U., van de Sand, A., et al. (2002). Myocardial dysfunction with coronary microembolization: Signal transduction through a sequence of nitric oxide, tumor necrosis factor-{alpha}, and sphingosine. *Circ. Res.* 90, 807–813.

Vessey, D. A., Li, L., Honbo, N., and Karliner, J. S. (2009). Sphingosine 1-phosphate is an important endogenous cardioprotectant released by ischemic pre- and postconditioning. *Am. J. Physiol. Heart Circ. Physiol.* 297, H1429–H1435. doi: 10.1152/ajpheart.00358.2009

Yatomi, Y., Igarashi, Y., Yang, L., Hisano, N., Qi, R., Asazuma, N., et al. (1997). Sphingosine 1-phosphate, a bioactive sphingolipid abundantly stored in platelets, is a normal constituent of human plasma and serum. *J. Biochem.* 121, 969–973.

Yatomi, Y., Ruan, F., Hakomori, S., and Igarashi, Y. (1995). Sphingosine-1-phosphate: A platelet-activating sphingolipid released from agonist-stimulated human platelets. *Blood* 86, 193–202.

Zhang, D. X., Fryer, R. M., Hsu, A. K., Zou, A. P., Gross, G. J., Campbell, W. B., et al. (2001). Production and metabolism of ceramide in normal and ischemic-reperfused myocardium of rats. *Basic Res. Cardiol.* 96, 267–274.

Conflict of Interest Statement: The authors declare that the research was conducted in the absence of any commercial or financial relationships that could be construed as a potential conflict of interest.

Received: 01 March 2013; paper pending published: 26 March 2013; accepted: 17 May 2013; published online: 13 June 2013.

*Citation: Egom EE, Mamas MA, Chacko S, Stringer SE, Charlton-Menys V, El-Omar M, Chirico D, Clarke B, Neyses L, Cruickshank JK, Lei M and Fath-Ordoubadi F (2013) Serum sphingolipids level as a novel potential marker for early detection of human myocardial ischaemic injury. Front. Physiol. **4**:130. doi: 10.3389/fphys.2013.00130*

This article was submitted to Frontiers in Cardiac Electrophysiology, a specialty of Frontiers in Physiology.

frontiers in PHYSIOLOGY

ORIGINAL RESEARCH ARTICLE
published: 31 May 2013
doi: 10.3389/fphys.2013.00127

The prevalence of electrocardiographic early repolarization in an adult cohort with chronic kidney disease and its impact upon all-cause mortality and progression to dialysis

Reza Hajhosseiny[1,2], Ronak Rajani[2], Kaivan Khavandi[2], Frédéric A. Sebag[2], Soudeh Mashayekhi[1], Matthew Wright[2] and David Goldsmith[1]*

[1] *MRC Centre for Transplantation and Renal Unit, Guy's and St. Thomas' NHS Foundation Trust, King's College Academic Health Partners, London, UK*
[2] *BHF Centre of Cardiovascular Excellence, Guy's and St. Thomas' NHS Foundation Trust, King's College Academic Health Partners, London, UK*

Edited by:
Ian N. Sabir, King's College, UK

Reviewed by:
Konstantinos Letsas, Evangelismos General Hospital of Athens, Greece
Jack R. Brownrigg, St. George's Hospital, UK
Padman Vamadevan, Harley Street at UCLH, UK

****Correspondence:***
David Goldsmith, Professor in Cardio-Renal Medicine, Department of Nephrology and Transplantation, 6th Floor, Borough Wing, Guy's Hospital, London, SE1 9RT, UK
e-mail: david.goldsmith@gstt.nhs.uk

Background: Electrocardiographic early repolarization (ER) occurring in <5% of general/atherosclerotic populations, is a marker of sudden cardiac death (SCD). The prevalence of ER in chronic kidney disease (CKD) patients, in whom SCD is common, is unknown. We aimed to determine the prevalence, contributing factors, and relationship of ER to all-cause mortality and progression to dialysis in CKD patients.

Methods: A retrospective study of 197 patients with stage 3–5 CKD. Full demographic data were collected including cardiovascular risk factors and history. All patients underwent a 12-lead ECG, analysed for the presence of ER and other ECG findings. ER was defined as elevation of the QRS-ST junction (J point) by at least 0.1 mV from baseline with slurring/notching of the QRS complex. The primary and secondary endpoints were all cause mortality and progression to dialysis respectively at 1 year. To control for the effects of CKD, we evaluated the ECGs of 39 healthy renal transplant donors (RTD).

Results: CKD patients had a mean age of 61.5 (±16.1). Prevalence of ER in pre-dialysis patients with CKD stage 4 and 5 was higher than in RTD (26.4 vs. 7.7%, $p = 0.02$). ER frequency increased with CKD stage (stage 3: 7.7%, stage 4: 29.7%, and pre-dialysis stage 5: 24.6%), but decreased in dialysis patients (13%). On multivariate analysis only the QRS duration was a significant independent predictor of ER (OR 0.97, 95% CI, 0.94–0.99, $p = 0.01$). At 1-year follow-up, there were 24 (12%) deaths in the patients with CKD of whom 5 (21%) had ER. ER was not a predictor of all cause mortality ($p = 1.00$) and had no effects on the rate of progression to dialysis ($p = 0.67$).

Conclusions: ER is more common in pre-dialysis CKD patients, compared to healthy RTD but is not associated with increased 1-year mortality or entry onto dialysis programs. Further longitudinal studies are indicated to determine whether this increased prevalence of ER is associated with the rate of SCD seen in this population.

Keywords: early repolarization, chronic kidney disease, sudden cardiac death, dialysis, mortality

INTRODUCTION

The renal and cardiovascular systems have a unique and intricate inter-relationship, with disease or dysfunction in one organ frequently leading to injury in the other. This complex interaction has led to the use of the term "cardio-renal syndrome" (Ronco et al., 2009; Hajhosseiny et al., 2013). Overall, for subjects with chronic kidney disease (CKD) stage 3, it is more likely that a patient will develop cardiovascular disease (CVD) than progress to dialysis-requiring renal failure (CKD stage 5D; Bleyer et al., 2006; Hajhosseiny et al., 2013). Sudden cardiac death (SCD) is particularly prevalent amongst patients with CKD, with estimates ranging from 25 to 60% (Herzog, 2003; Pun et al., 2009). In dialysis patients, the incidence of SCD is very high; eclipsing other causes of cardiac death, and rises with both the duration of time that the patient has been on a dialysis program, as well as the severity and frequency of dialysis-associated electrolyte imbalances (Karnik et al., 2001; Bleyer et al., 2006).

Until recently, electrocardiographic early repolarization (ER) was considered a benign finding on a patient's electrocardiogram (ECG). However, a number of recent studies have suggested that ER may represent an independent marker of sudden arrhythmic cardiac arrest in otherwise healthy individuals (Haissaguerre et al., 2008; Ghosh et al., 2010; Sinner et al., 2010; Tikkanen et al., 2012). Despite this, it is currently unknown whether or not there is a similar increased prevalence of ER in CKD patients in whom SCD is common. The aim of the current study was therefore to determine the prevalence of ER, possible contributory factors,

Abbreviations: CKD, chronic kidney disease; ECG, 12-lead electrocardiogram; ER, early repolarization; SCD, sudden cardiac death.

and whether or not ER is related to all-cause mortality and progression to dialysis in patients with CKD.

METHODS

PATIENTS

We retrospectively studied adults with stage 3–5 CKD referred to the Nephrology department at Guy's and St. Thomas' Hospital between March 2007 and December 2011. Our study population consisted of newly diagnosed patients with CKD, or patients with follow-up appointments. In addition, we also studied 39 adults without CKD to control for the effects of renal failure on ER. These controls were healthy renal transplant donors (RTD) with no documentation of structural heart disease or a history of syncope. Full demographic data pertaining to cardiovascular risk factors, prior cardiac history, current medications, and concurrent co-morbidities were recorded along with recent laboratory results (renal profile, serum calcium, and hs C-reactive protein levels). Cardiovascular risk factors were determined by pre-set defined criteria. Hypertension was defined as a systolic blood pressure of >140 mmHg, a diastolic blood pressure of >90 mmHg, or antihypertensive drug use. Smoking was defined as a current smoker or past heavy smoker (>20 package-years). Diabetes mellitus was defined as a previously established diagnosis, insulin, or oral hypoglycemic therapy, fasting glucose of >126 mg/dL, or non-fasting glucose of >200 mg/dL. Family history of coronary artery disease was defined as myocardial infarction, coronary revascularization, or SCD in a first-degree relative <65 years old. A 12-lead ECG was performed on all patients and the primary inclusion criteria were based on CKD severity and the availability of a recent adequate ECG recording in their clinical file. Patients with permanent pacemakers were excluded from the study. All patients were followed up for a minimum time period of 12-months from the data of the first ECG. Written informed consent was obtained from the 19 haemodialysis patients for obtaining an ECG before and after dialysis and the study was granted institutional ethics committee approval in accordance with the Helsinki Declaration (1964, amended in 1975 and in 1984).

ECG ACQUISITION AND ANALYSIS

All patients underwent a 12-lead ECG. These were fully interrogated by two electrophysiologists blinded to the clinical data for relevant electrical intervals (PR, QRS, and QTc durations), and for bundle branch block, the cardiac axis, left ventricular hypertrophy (LVH), and ER. The presence or absence of LVH was assessed according to the Sokolow–Lyon criteria and the QT interval was corrected for heart rate according to Bazett's formula. Early repolarization was defined as an elevation of the QRS-ST junction (J point) in at least two leads. The amplitude of J-point elevation had to be at least 1 mm (0.1 mV) above the baseline level either as QRS slurring (a smooth transition from the QRS segment to the ST segment—**Figure 1A**) or notching (a positive J deflection inscribed on the S wave—**Figure 1B**) in the inferior leads (II, III, and aVF), lateral leads (I, aVL, and V4–V6), or both. The anterior precordial leads (V1–V3) were excluded from the analysis to avoid the inclusion of patients with right ventricular dysplasia or Brugada syndrome. In order to account for the effects of dialysis on ER, we obtained an ECG recording from 19 patients on hemodialysis immediately prior to the start of their dialysis session, and followed this up with the acquisition of another ECG immediately after their dialysis session had finished.

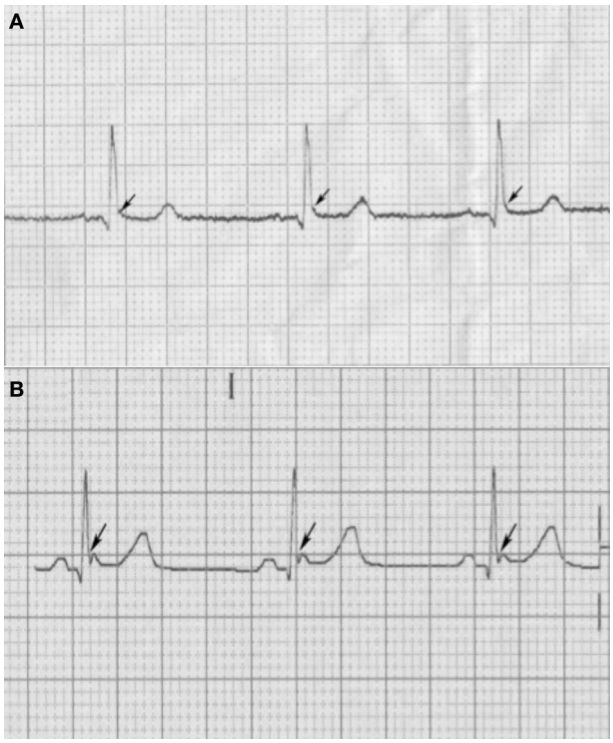

FIGURE 1 | The identification of ER from the 12-lead electrocardiogram. (A) Shows a typical example of a slurred patterned ER (arrows) while **(B)** shows the appearance of a notched ER (arrows).

FOLLOW UP

In order to investigate the prognostic and predictive value of ER, all patients (CKD and controls) were followed up for 12 months from the start of the study. The primary endpoint was all-cause mortality (all cause) and the secondary endpoint, the new commencement of dialysis.

STATISTICAL ANALYSIS

All continuous variables included in the analysis are presented as mean ± SD. Variables with non-normal distributions are presented as median with range. Univariate analyses were performed on continuous variables using the two-sample *t*-test for normally distributed variables and the Mann–Whitney U test for non-normally distributed data. Spearman's correlation coefficient was used to assess the relationship between continuous variables. Multivariable logistic regression was used to determine the predictors of ER using age, presence of COPD, mineralocorticoid receptor antagonist use, heart rate, PR interval, QRS interval, and dialysis as covariates. Statistical significance for all analyses was set at the 5% level. All data were collected and analyzed using SPSS for MAC (Version 19, IBM, Somers, NY, USA).

RESULTS

The baseline demographics of the population are given in **Table 1**. There were 202 patients with CKD stage 3–5 who were approached for inclusion into the study. Of these, 5 patients were excluded due to the presence of a permanent cardiac pacemaker. In the remaining cohort of 197 patients, the ethnic origin was Caucasian in 121 (61%), Afro-Caribbean in 60 (31%), and South Asian in 16 (8%). There was a prior cardiac history present in 62 (32%) patients [8 (4%) congestive cardiac failure, 47 (24%) coronary artery disease, 14 (16%) myocardial infarction, 8 (4%) valvular heart disease and 14 (7%) atrial fibrillation].

PREVALENCE OF EARLY REPOLARIZATION IN PATIENTS WITH AND WITHOUT CKD

Table 2 gives the comparison of baseline demographics between the 197 patients with CKD and the 39 healthy renal donors who represented the control group. The healthy renal donors were of a younger age and were predominantly Caucasian in ethnic origin. Although there was a tendency to an increased prevalence of ER in the CKD population (19.8%) compared with the renal donors (7.7%), this did not reach statistical significance ($P = 0.07$). There was no difference observed in the magnitude or distribution of J-point elevation. Prevalence of ER in pre-dialysis patients with CKD stage 4 and 5 was higher than in the RTD (26.4 vs. 7.7%, $p = 0.02$). Early repolarization frequency increased with CKD stage (stage 3: 7.7%, stage 4: 29.7%, and pre-dialysis stage 5: 24.6%), but decreased in dialysis patients (13%).

PREDICTORS OF EARLY REPOLARIZATION

In the CKD group of patients, age, gender, ethnicity, prior cardiac history, cardiovascular risk factors, eGFR, and CKD stage were unrelated to the presence of ER (**Table 3**). Similarly, there was no relationship to the use of cardiac medications or serum electrolytes and biochemistry. There were however a number of ECG predictors of ER. Patients with ER had lower heart rates (HR with ER 71 ± 15 BPM vs. 77 ± 17 without ER, $p = 0.03$), shorter QRS durations (QRS duration with ER 84 ± 11 vs. 94 ± 21 without ER, $p < 0.01$), and shorter QTc durations (QTc duration with ER 412 ± 22 vs. 427 ± 34 without ER, $p < 0.001$). On multivariate analysis (**Table 4**) with ER as the dependent variable and age, presence of COPD, mineralocorticoid receptor antagonist use, heart rate, PR interval, QRS interval, and dialysis as covariates, only the QRS duration remained a significant independent predictor of ER (OR 0.97, 95% CI, 0.94–0.99, $p = 0.01$).

EARLY REPOLARIZATION AS A PREDICTOR OF ALL-CAUSE MORTALITY AND PROGRESSION TO DIALYSIS

At 1-year follow-up, there were 24 deaths. There was no difference in mortality between those who had ER 13% (5 of 39 patients) to those who did not 12% (19 of 158 patients), $p = 1.0$ (**Figure 2**). From the 119 patients who were not already on dialysis at the study commencement, 56 (47%) patients progressed to either peritoneal or hemodialysis. Of the 29 patients with ER who were not yet on dialysis, 15 (52%) progressed to renal replacement therapy, compared with 41 (46%) of the 90 patients without ER ($p = 0.67$).

Table 1 | Baseline characteristics of patients with CKD.

	CKD (*N* = 197)
Age (years)	61.5 ± 16.1
Gender (male) *n* (%)	113 (57)
eGFR (mL/min/1.73 m^2)	14.0 (10.0–17.3)
CKD STAGE *n* (%)	
3	13 (6.6)
4	37 (18.8)
5 no dialysis	69 (35.0)
5 dialysis	78 (39.6)
Renal Transplant *n* (%)	16 (8.1)
Duration of CKD (months)	25 (12–54)
Stroke *n* (%)	19 (9.6)
COPD *n* (%)	11 (5.6)
CARDIOVASCULAR RISK FACTOR *n* (%)	
Diabetes	77 (39.1)
BMI (kg/m^2)	28.8 ± 6.6
Current smoker	4 (2)
Dyslipidaemia	33 (16.8)
Hypertension	133 (67.5)
Systolic blood pressure (mmHg)	145 ± 25
Diastolic blood pressure (mmHg)	75 ± 15
MEDICATIONS *n* (%)	
β blockers	73 (37.1)
Diuretics	72 (36.5)
Aldosterone antagonist	4 (2.0)
ACE inhibitors	53 (26.9)
ARB	49 (24.9)
CCB	4 (2.0)
Amiodarone	1 (0.5)
Statins	106 (53.8)
Erythropoietin	112 (56.9)
BIOCHEMICAL	
Potassium (mmol/L)	4.7 ± 0.7
Calcium (mmol/L)	2.3 ± 0.3
Phosphate (mmol/L)	1.4 ± 0.4
Parathormone (PTH)	191 (97–396)
CRP	6 (5–20)
Hemoglobin (g/dL)	10.8 ± 1.9
ELECTROCARDIOGRAM	
Heart rate (bpm)	76 ± 17
PR duration (ms)	162 ± 49
QRS duration (ms)	92 ± 20
QRS axis (°)	17.3 ± 41.5
Right BBB *n* (%)	11 (5.6)
Left BBB *n* (%)	6 (3.0)
Electrical LVH *n* (%)	33 (16.8)
QTc duration (ms)	424 ± 32

Abbreviations: ACE-I, angiotensin converting enzyme inhibitors; ARB, angiotensin receptor blockers; BMI, body mass index; CKD, chronic kidney disease; COPD, chronic obstructive pulmonary disease; CRP, C-reactive protein; PTH, parathyroid hormone.

DISCUSSION

The main finding of the current study is that there is an increased prevalence of ER in CKD patients (20%) when compared to healthy controls (8%). We also show that the presence of ER is

Table 2 | Comparison of baseline characteristics of patients with CKD vs. the renal transplant donors.

	CKD ($n = 197$)	Donors ($n = 39$)	p
Age (years)	61.5 ± 16.1	44.0 ± 11.6	<0.0001
ETHNICITY			
Caucasian *n* (%)	121 (61.4)	35 (89.7)	0.0001
Afro-Caribbean *n* (%)	60 (30.5)	1 (2.6)	
Asian *n* (%)	16 (8.1)	3 (7.7)	
Gender (male) *n* (%)	113 (57.4)	20 (51.3)	0.48
Height (cm)	167 ± 10	170 ± 9	0.04
Weight (kg)	81 ± 21	76 ± 13	0.13
eGFR (mL/min/1.73 m^2)	14 (10–20)	85 (79–92)	<0.0001
Early repolarization *n* (%)	39 (19.8)	3 (7.7)	0.07
PATTERN *n* (%)			
Slurred	26 (66.7)	2 (66.7)	1.00
Notch	13 (33.3)	1 (33.3)	
J POINT ELEVATION *n* (%)			
≥0.1 and <0.2 mV	38 (97.4)	3 (100.0)	1.00
≥0.2 mV	1 (2.6)	0 (0.0)	
LOCALIZATION *n* (%)			
Inferior	16 (41.0)	0 (0.0)	0.22
Lateral	14 (35.9)	3 (100.0)	
Inferior and lateral	9 (23.1)	0 (0.0)	

Abbreviations: eGFR, estimated glomerular filtration rate.

associated to a shorter QRS duration in patients with CKD but that this did not translate to an increased incidence of all-cause mortality or progression to dialysis at 1-year follow-up.

A number of prior studies have suggested a relationship between the presence of ER and SCD. Haissaguerre et al. (2008) conducted a multicentre study of 206 patients resuscitated after an episode of idiopathic ventricular fibrillation. The authors found that there was an increased prevalence of ER (31%) when compared to 412 age, gender, and race matched controls (5%), and that after a median follow-up of 61 months patients with ER had a significantly higher incidence of ventricular fibrillation than those cases without ER (HR 2.1, 95% CI 1.2–3.5, $p = 0.008$). In another study of 432 victims of a SCD from an acute coronary event Tikkanen et al. (2012), showed that there was an increased prevalence of ER (14.4%) when compared to 532 survivors of an acute coronary syndrome (7.9%). Finally, in a study of 1945 individuals aged between 35 and 74 years of age (Sinner et al., 2010), found a greater than 2-fold-increased risk of cardiac mortality in participants with ER compared to individuals without ER.

Although the exact mechanism of ER-induced arrhythmogenicity is still unclear, it has been hypothesized that this may be related to either an increased susceptibility or vulnerability to cardiac arrest in critical ischemic conditions such as acute coronary syndromes (Tikkanen et al., 2012), or to subtle changes in the cardiac action potential (Benito et al., 2010). Early repolarization in its simplest form occurs in Phase 1 of the cardiac action potential and is caused by the cardiac transient outward potassium current (I_{to}). If a situation arises where there is a reduced density of the

Table 3 | Comparison of baseline characteristics of adults with ER vs. those without ER.

	Overall ($N = 197$)	ER ($N = 39$)	No ER ($N = 158$)	p
Age (years)	61.5 ± 16.1	58.1 ± 17.1	62.3 ± 15.8	0.14
Male *n* (%)	113 (57.4)	22 (56.4)	91 (57.6)	0.89
ETHNICITY *n* (%)				
Caucasian *n* (%)	121(61.4)	74 (61.2)	47 (38.8)	0.91
Afro-Caribbean *n* (%)	60 (30.5)	31 (51.7)	29 (48.3)	
Asian *n* (%)	16 (8.1)	8 (50.0)	8 (50.0)	
CARDIAC HISTORY *n* (%)				
Congestive heart failure	8 (4.1)	2 (5.1)	6 (3.8)	0.66
Palpitations	1 (0.5)	1 (2.6)	0 (0)	0.20
Syncope	1 (0.5)	0 (0)	1 (0.6)	1.00
SCD	0 (0)	0 (0)	0 (0)	N/A
Coronary artery disease	47 (23.9)	8 (20.5)	39 (24.7)	0.58
Myocardial infarction	14 (16.1)	1 (2.6)	13 (8.2)	0.31
PCI	18 (9.1)	3 (7.7)	15 (9.5)	0.72
CABG	8 (4.1)	1 (2.6)	7 (4.4)	0.59
Other*	26 (13.2)	5 (12.8)	21 (13.3)	1.00
eGFR (mL/min/1.73m^2)	10.0 ± 7.2	12.0 ± 9.2	10 ± 7–17.0	0.38
CKD STAGE *n* (%)				
3	13 (6.6)	1 (2.6)	12 (7.6)	0.07
4	37 (18.8)	11 (28.2)	26 (16.5)	
5 no dialysis	69 (35.0)	17 (43.6)	52 (32.9)	
5 dialysis	78 (39.6)	10 (5.1)	68 (43.0)	
Renal dialysis *n* (%)	78 (39.6)	10 (25.6)	68 (43.0)	0.046
Renal transplant *n* (%)	16 (8.1)	3 (7.7)	13 (8.2)	0.91
CKD duration (months)	25 (12–54)	30 (11–57)	25 (12–64)	0.61
Stroke *n* (%)	19 (9.6)	3 (7.7)	16 (10.1)	0.77
COPD *n* (%)	11 (5.6)	0 (0)	11 (7.0)	0.13
CV RISK FACTORS *n* (%)				
Diabetes	77 (39.1)	16 (41.6)	61 (38.6)	0.78
BMI (kg/m^2)	29 ± 7	29 ± 7	29 ± 7	0.86
Current smoker	4 (2)	1 (2.6)	3 (1.9)	1.00
Dyslipidaemia	33 (16.8)	7 (17.9)	26 (16.5)	0.82
Hypertension	133 (67.5)	25 (64.1)	108 (68.4)	0.61
SBP (mmHg)	145 ± 25	141 ± 22	146 ± 26	0.35
DBP (mmHg)	75 ± 15	76 ± 13	75 ± 15	0.76
MEDICATIONS *n* (%)				
β blockers	73 (37.1)	16 (41.0)	57 (36.1)	0.56
Diuretics	72 (36.5)	17 (43.6)	55 (34.8)	0.31
MRA	4 (2.0)	2 (5.1)	2 (1.3)	0.17
ACE inhibitors	53 (26.9)	8 (20.5)	45 (28.5)	0.31
ARB	49 (24.9)	10 (25.6)	39 (24.7)	0.90
CCB	4 (2.0)	0 (0)	4 (2.5)	0.59
Amiodarone	1 (0.5)	0 (0)	1 (0.6)	1.00
Statins	106 (53.8)	19 (48.7)	87 (55.1)	0.48
Erythropoietin	112 (56.9)	18 (46.2)	94 (59.5)	0.13

(Continued)

Table 3 | Continued

	Overall (*N* = 197)	ER (*N* = 39)	No ER (*N* = 158)	*p*
BIOCHEMISTRY				
Potassium (mmol/L)	4.7 ± 0.7	4.8 ± 0.6	4.7 ± 0.8	0.34
Calcium (mmol/L)	2.3 ± 0.3	2.3 ± 0.2	2.3 ± 0.3	0.51
Phosphate (mmol/L)	1.4 ± 0.4	1.4 ± 0.4	1.4 ± 0.4	0.68
Parathormone (PTH)	191 (97–396)	221 (100–368)	183 (97–404)	0.92
CRP	6 (5–20)	6 (5–12)	6 (5–24)	0.30
Hemoglobin (g/dL)	10.8 ± 1.9	10.8 ± 1.9	10.7 ± 1.9	0.82
ELECTROCARDIOGRAM				
Heart Rate (bpm)	76 ± 17	71 ± 15	77 ± 17	0.03
PR duration (ms)	162 ± 49	172 ± 29	160 ± 52	0.18
QRS duration (ms)	92 ± 20	84 ± 11	94 ± 21	<0.01
QRS axis (°)	17.3 ± 41.5	27.0 ± 25.0	15.0 ± 44.4	0.03
Right BBB *n* (%)	11 (5.6)	1 (2.6)	10 (6.3)	0.70
Left BBB *n* (%)	6 (3.0)	0 (0)	6 (3.8)	0.60
Electrical LVH *n* (%)	33 (16.8)	5 (12.8)	28 (17.7)	0.46
QTc duration (ms)	424 ± 32	412 ± 22	427 ± 34	<0.001

Abbreviations: BBB, bundle branch block; CABG, coronary artery bypass graft; CCB, calcium channel blocker; DBP, diastolic blood pressure; ICD, implantable cardiac defibrillator; MRA, mineralocorticoid receptor antagonist; PCI, percutaneous coronary intervention; SBP, systolic blood pressure; SCD, sudden cardiac death.

**Atrial fibrillation, ICD, Valvular heart disease, Ventricular tachycardia.*

Table 4 | Multivariate logistic regression analyses for the predictors of ER.

	OR (95% CI)	*p*
Age	0.98 (0.96, 1.01)	0.20
COPD	0.00 (0.00, 0.00)	1.00
Anti-aldosterone	7.95 (0.40, 158.48)	0.18
Heart rate	0.98 (0.95, 1.00)	0.76
PR interval	1.01 (1.00, 1.02)	0.28
QRS duration	0.97 (0.94, 0.99)	0.01
Dialysis	0.55 (0.24, 1.27)	0.16

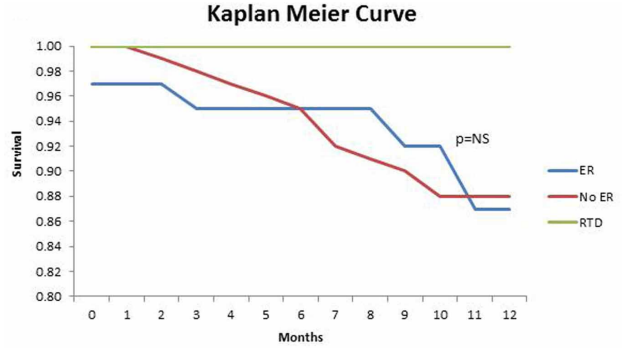

FIGURE 2 | Kaplan Meier Curve comparing 1-year survival in CKD patients with ER, without ER, and the renal transplant donors (RTD).

I_{to} channels in the endocardium compared with epicardium or mid-myocardium (Li et al., 2002), a large I_{to} current can occur that results in electrocardiographic ER and large voltage gradients that have the propensity to initiate life threatening arrhythmias (Li et al., 2002; Benito et al., 2010). In addition, an increase in transmural dispersion of ventricular repolarization, which is associated with ER (Karim Talib et al., 2012), has been demonstrated in patients with CKD (Tun et al., 1991; Saravanan and Davidson, 2010). This increase may partially explain the increased prevalence of ER in our CKD population.

In the current study, although we showed an increased prevalence of ER in patients with CKD, this was not associated with either all-cause mortality at 1-year or progression to dialysis. There are a number of potential explanations for this finding. The sample size in the current study was modest in comparison to prior studies and it is possible that any true effect of ER on mortality or progression to dialysis was concealed. It is also possible that CKD patients represent an entirely different cohort of patients to that previously studied and that the presence of ER may not be of prognostic importance. Further studies of larger cohorts of patients with CKD are indicated to clarify the findings of the current study.

Interestingly we also showed on univariate analysis that the presence of ER was related to a slower heart rate and shorter QRS and QTc durations. Although slower heart rates have been shown to be associated with ER (Li et al., 2002; Benito et al., 2010), potentially as a result of time-dependent recovery of I_{to} from inactivation (Antzelevitch and Yan, 2010; Benito et al., 2010), the finding of an association of a shorter QRS duration to an increased prevalence of ER is discrepant with prior studies. (Tikkanen et al., 2009, 2012) showed that ER was related to a slight increase in the QRS duration, while Haissaguerre et al. (2008) found no relationship between ER and QRS duration. It is possible that in the current study a broader QRS duration may have masked subtle J point elevation making the significance of this finding difficult to interpret. In keeping with prior reports (Haissaguerre et al., 2008; Watanabe et al., 2010) we also showed that a shorter QTc interval was associated to ER supporting the hypothesis that ER and short QT syndrome may share common cardiac channel genetic mutations (Watanabe et al., 2010).

If ER is shown to be prognostically important in CKD, there are potential therapeutical applications: antiarrhythmic drugs such as isoproterenol and quinidine have been shown to reduce ER or even restore normal ECG patterns (Haissaguerre et al., 2009). Further, this electrocardiographic marker could contribute to risk stratification tools to guide ICD therapy in high risk patients.

STUDY LIMITATIONS

There are a number of limitations to the current study. The sample size was relatively small with a low incidence of mortality and progression to dialysis. This may have concealed any potential adverse effects of having ER. The retrospective design of the study did not permit the demonstration of any potential temporal relationships between CKD and ER or adverse clinical events. There was a difference between the ethnic origin of the patients with CKD and the RTD that were used as controls. This may have

magnified the differences in prevalence of ER between the two groups with prior studies having shown an increased prevalence of ER in patients of Afro-Caribbean origin. Furthermore, a significant proportion of our cohort had a previous cardiac history, which has been associated with ER. Therefore, we may have overestimated the prevalence of ER in our population. However, on closer analysis of these patients, we found no significant association between previous cardiac history and the presence of ER. Finally owing to the study design, only a single ECG was available for analysis for each patient and it is unknown whether the presence of ER was a fixed or more dynamic electrocardiographic finding during the study period. Further studies are indicated to confirm our findings in a larger cohort of patients with CKD and also to assess for serial electrocardiographic changes.

CONCLUSIONS

Electrocardiographic early repolarization is more common in patients with pre-dialysis CKD compared to healthy RTD. However, this increased prevalence of ER was not associated with increased 1-year mortality or entry onto dialysis programs. Further longitudinal studies are indicated to determine whether this increased prevalence of ER is associated with the increased rate of SCD observed in this population.

REFERENCES

Antzelevitch, C., and Yan, G. X. (2010). J wave syndromes. *Heart Rhythm* 7, 549–558. doi: 10.1016/j.hrthm.2009.12.006

Benito, B., Guasch, E., Rivard, L., and Nattel, S. (2010). Clinical and mechanistic issues in early repolarization of normal variants and lethal arrhythmia syndromes. *J. Am. Coll. Cardiol.* 56, 1177–1186. doi: 10.1016/j.jacc.2010.05.037

Bleyer, A. J., Hartman, J., Brannon, P. C., Reeves-Daniel, A., Satko, S. G., and Russell, G. (2006). Characteristics of sudden death in hemodialysis patients. *Kidney Int.* 69, 2268–2273. doi: 10.1038/sj.ki.5000446

Ghosh, S., Cooper, D. H., Vijayakumar, R., Zhang, J., Pollak, S., Haissaguerre, M., et al. (2010). Early repolarization associated with sudden death: insights from noninvasive electrocardiographic imaging. *Heart Rhythm* 7, 534–537. doi: 10.1016/j.hrthm.2009.12.005

Haissaguerre, M., Derval, N., Sacher, F., Jesel, L., Deisenhofer, I., de Roy, L., et al. (2008). Sudden cardiac arrest associated with early repolarization. *N. Engl. J. Med.* 358, 2016–2023. doi: 10.1056/NEJMoa071968

Haissaguerre, M., Sacher, F., Nogami, A., Komiya, N., Bernard, A., Probst, V., et al. (2009). Characteristics of recurrent ventricular fibrillation associated with inferolateral early repolarization role of drug therapy. *J. Am. Coll. Cardiol.* 53, 612–619. doi: 10.1016/j.jacc.2008.10.044

Hajhosseiny, R., Khavandi, K., and Goldsmith, D. J. (2013). Cardiovascular disease in chronic kidney disease: untying the Gordian knot. *Int. J. Clin. Pract.* 67, 14–31. doi: 10.1111/j.1742-1241.2012.02954.x

Herzog, C. A. (2003). Cardiac arrest in dialysis patients: approaches to alter an abysmal outcome. *Kidney Int. Suppl.* 84, S197–S200. doi: 10.1046/j.1523-1755.63.s84.17.x

Karim Talib, A., Sato, N., Sakamoto, N., Tanabe, Y., Takeuchi, T., Saijo, Y., et al. (2012). Enhanced transmural dispersion of repolarization in patients with J wave syndromes. *J. Cardiovasc. Electrophysiol.* 23, 1109–1114. doi: 10.1111/j.1540-8167.2012.02363.x

Karnik, J. A., Young, B. S., Lew, N. L., Herget, M., Dubinsky, C., Lazarus, J. M., et al. (2001). Cardiac arrest and sudden death in dialysis units. *Kidney Int.* 60, 350–357. doi: 10.1046/j.1523-1755.2001.00806.x

Li, G. R., Lau, C. P., Ducharme, A., Tardif, J. C., and Nattel, S. (2002). Transmural action potential and ionic current remodeling in ventricles of failing canine hearts. *Am. J. Physiol. Heart Circ. Physiol.* 283, H1031–H1041. doi: 10.1152/ajpheart.00105.2002

Pun, P. H., Smarz, T. R., Honeycutt, E. F., Shaw, L. K., Al-Khatib, S. M., and Middleton, J. P. (2009). Chronic kidney disease is associated with increased risk of sudden cardiac death among patients with coronary artery disease. *Kidney Int.* 76, 652–658. doi: 10.1038/ki.2009.219

Ronco, C., Chionh, C. Y., Haapio, M., Anavekar, N. S., House, A., and Bellomo, R. (2009). The cardiorenal syndrome. *Blood Purif.* 27, 114–126. doi: 10.1159/000167018

Saravanan, P., and Davidson, N. C. (2010). Risk assessment for sudden cardiac death in dialysis patients. *Circ. Arrhythm. Electrophysiol.* 3, 553–559. doi: 10.1161/CIRCEP.110.937888

Sinner, M. F., Reinhard, W., Muller, M., Beckmann, B. M., Martens, E., Perz, S., et al. (2010). Association of early repolarization pattern on ECG with risk of cardiac and all-cause mortality: a population-based prospective cohort study (MONICA/KORA). *PLoS Med.* 7:e1000314. doi: 10.1371/journal.pmed.1000314

Tikkanen, J. T., Anttonen, O., Junttila, M. J., Aro, A. L., Kerola, T., Rissanen, H. A., et al. (2009). Long-term outcome associated with early repolarization on electrocardiography. *N. Engl. J. Med.* 361, 2529–2537. doi: 10.1056/NEJMoa0907589

Tikkanen, J. T., Wichmann, V., Junttila, M. J., Rainio, M., Hookana, E., Lappi, O. P., et al. (2012). Association of early repolarization and sudden cardiac death during an acute coronary event. *Circ. Arrhythm. Electrophysiol.* 5, 714–718. doi: 10.1161/CIRCEP.112.970863

Tun, A., Khan, I. A., Wattanasauwan, N., Win, M. T., Hussain, A., Hla, T. A., et al. (1991). Increased regional and transmyocardial dispersion of ventricular repolarization in end-stage renal disease. *Can. J. Cardiol.* 15, 53–56.

Watanabe, H., Makiyama, T., Koyama, T., Kannankeril, P. J., Seto, S., Okamura, K., et al. (2010). High prevalence of early repolarization in short QT syndrome. *Heart Rhythm* 7, 647–652. doi: 10.1016/j.hrthm.2010.01.012

Conflict of Interest Statement: The authors declare that the research was conducted in the absence of any commercial or financial relationships that could be construed as a potential conflict of interest.

Received: 04 April 2013; paper pending published: 26 April 2013; accepted: 14 May 2013; published online: 31 May 2013.

Citation: Hajhosseiny R, Rajani R, Khavandi K, Sebag FA, Mashayekhi S, Wright M and Goldsmith D (2013) The prevalence of electrocardiographic early repolarization in an adult cohort with chronic kidney disease and its impact upon all-cause mortality and progression to dialysis. Front. Physiol. ***4****:127. doi: 10.3389/fphys.2013.00127*

This article was submitted to Frontiers in Cardiac Electrophysiology, a specialty of Frontiers in Physiology.